Modelling Nutrient Utilization in Farm Animals

McNamara
France
Beever

CABI

Modelling Nutrient Utilization in Farm Animals

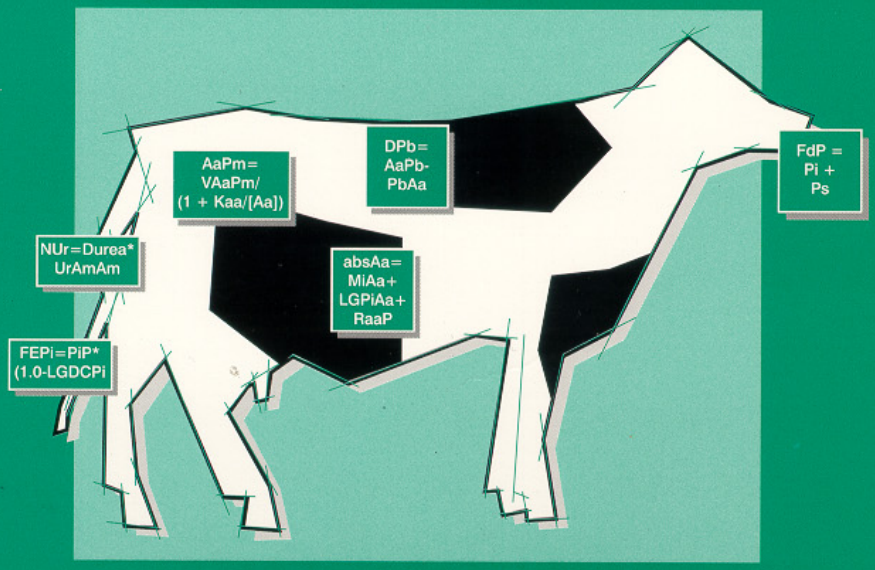

Edited by J.P. McNamara,
J. France and D. Beever

CABI Publishing

Modelling Nutrient Utilization in Farm Animals

Edited by

J.P. McNamara
Department of Animal Sciences
Washington State University
Pullman
USA

and

J. France and D.E. Beever
Department of Agriculture
University of Reading
Reading
UK

CABI *Publishing*

CABI *Publishing* is a division of CAB *International*

CABI Publishing
CAB International
Wallingford
Oxon OX10 8DE
UK

Tel: +44 (0)1491 832111
Fax: +44 (0)1491 833508
Email: cabi@cabi.org
Web site: http://www.cabi.org

CABI Publishing
10 E 40th Street
Suite 3203
New York, NY 10016
USA

Tel: +1 212 481 7018
Fax: +1 212 686 7993
Email: cabi-nao@cabi.org

A catalogue record for this book is available from the British Library, London, UK.

Library of Congress Cataloging-in-Publication Data
Modelling nutrient utilization in farm animals / edited by J.P. McNamara, J. France and E.E. Beever.
p. cm.
Includes bibliographical references (p.)
ISBN 0-85199-449-0 (alk. paper)
1. Ruminants--Feed utilization efficiency--Mathematical models. 2. Feeds--Evaluation--Mathematical models. I. McNamara, J.P. (John P.) II. France, J. III. Beever, D.E.

SF95.M663 2000
636.2′085--dc21 00-023729

ISBN 0 85199 449 0

Typeset by Columns Design Ltd, Reading.
Printed and bound in the UK by Biddles Ltd, Guildford and King's Lynn.

Contents

Session 6: Production and Evaluation Models
Session Chair: *J.P. McNamara*

Contributors

J. Agabriel, Unité de Recherche sur les Herbivores, INRA, 63122 Saint Genès Champanelle, France
R. Allison, ADAS Bridgets, Martyr Worthy, Winchester SO21 1AP, UK
R.L. Baldwin, Department of Animal Science, University of California, One Shields Avenue, Davis, CA 95616, USA
A. Bannink, Institute for Animal Science and Health (ID-Lelystad), ID TNO Animal Nutrition, PO Box 65, 8200 AB Lelystad, The Netherlands
D.E. Beever, Centre for Dairy Research, Department of Agriculture, University of Reading, Earley Gate, PO Box 236, Reading RG6 6AT, UK
B.J. Bequette, Rowett Research Institute, Greenburn Road, Bucksburn, Aberdeen AB21 9SB, UK
J.F. Bernier, Université Laval, Département des Sciences Animales, Pavillon Paul-Comtois, Ste Foy, Quebec G1K 7P4, Canada
F. Blanc, ENSAM-INRA, Productions Animales, 9 Place Viala, 34060 Montpellier Cedex 1, France
S. Boisen, Danish Institute of Agricultural Sciences, Research Centre Foulum, PO Box 50, DK-8830 Tjele, Denmark
R.C. Boston, University of Pennsylvania, Kennett Square, PA 19348, USA
C.C. Calvert, Department of Animal Science, University of California, One Shields Avenue, Davis, CA 95616, USA
A. Cannas, Dipartimento di Scienze Zootecniche, University of Sassari, 07100 Sassari, Sardinia, Italy
W. Chalupa, Department of Clinical Studies, NBC, School of Veterinary Medicine, University of Pennsylvania, PA 19348, USA
A. Chudy, Forschunginstitut für die Biologie Landwirtschaftlicher Nutziere, Dummerstorf, Forschungsbereich Ernährungspysiologie 'OSKAR

KELLNER', Justus-von-Liebig-Weg 2, D-18059 Rostock, Germany
L.A. Crompton, Department of Agriculture, University of Reading, Earley Gate, Reading RG6 6AT, UK
A. Danfær, Danish Institute of Agricultural Sciences, Research Centre Foulum, PO Box 50, 8830 Tjele, Denmark
M.S. Dhanoa, Institute of Grassland and Environmental Research, Plas Gogerddan, Aberystwyth SY23 3EB, UK
J. Dijkstra, Animal Nutrition Group, Wageningen Institute of Animal Sciences (WIAS), Wageningen University, Marijkeweg 40, 6709 PG Wageningen, The Netherlands
R.A. Dynes, CSIRO Animal Production, Private Mail Bag, PO, Wembley, WA 6014, Australia
D.G. Fox, Department of Animal Science, Cornell University, Ithaca, NY 14853, USA
J. France, Department of Agriculture, University of Reading, Earley Gate, Reading RG6 6AT, UK
W.J.J. Gerrits, Animal Nutrition Group, Wageningen Institute of Animal Sciences, PO Box 338, 6700 AH, Wageningen, The Netherlands
G.L.R. Gordon, CSIRO Animal Production, Locked Bag 1, Delivery Centre, Blacktown, NSW 2148, Australia
B.D. Hahn, Department of Mathematics and Applied Mathematics, University of Cape Town, Rondebosch 7701, South Africa
M.D. Hanigan, Purina Mills Inc., St Louis, MO 63144, USA
E. Hasting, Department of Animal Science, University of California, Davis, CA 95616, USA
T. Hoch, Unité de Recherche sur les Herbivores, INRA Centre de Clermont-Theix, 63122 Saint Genès Champanelle, France
E. Janczewski, Department of Clinical Studies, NBC, School of Veterinary Medicine, University of Pennsylvania, PA 19348, USA
P. Jean dit Bailleul, Agriculture and AgriFood Canada, CP 90, 2000 Road 108 East, Lennoxville, Quebec J1M 1Z3, Canada
H.A. Johnson, Department of Animal Science, University of California, Davis, CA 95616, USA
E. Kebreab, Centre for Dairy Research, Department of Agriculture, University of Reading, Earley Gate, PO Box 236, Reading RG6 6AT, UK
J. Kogut, ID-Lelystad, Department of Animal Nutrition, PO Box 65, 8200 AB Lelystad, The Netherlands
R.A. Kohn, University of Maryland, College Park, MD 20742, USA
G.E. Lobley, Rowett Research Institute, Bucksburn, Aberdeen AB21 9SB, UK
M.A. Lomax, Department of Agriculture, University of Aberdeen, 581 King Street, Aberdeen AB24 5UA, UK
S. López, Departamento de Producción Animal, Universidad de León, E-24007 León, Spain
P.A. Lovatto, Laboratoire INRA–INAPG de Nutrition et Alimentation, INAPG, 16 rue Claude Bernard, 75231 Paris Cedex 05, France

M. McMahon, McMahon's EZ Acres, Homer, NY 13077, USA
P. McMahon, McMahon's EZ Acres, Homer, NY 13077, USA
J.P. McNamara, Department of Animal Science and the Nutrition Program, Washington State University, PO Box 646351, Pullman, WA 99164-6351, USA
J.A. Maas, Department of Agriculture, University of Reading, Earley Gate, PO Box 236, Reading RG6 6AT, UK
R. Mansbridge, ADAS Bridgets, Martyr Worthy, Winchester SO21 1AP, UK
R. Munson, Department of Clinical Studies, NBC, School of Veterinary Medicine, University of Pennsylvania, PA 19348, USA
B.N. Nagorcka, CSIRO Animal Production, PO Box 1600, Canberra, ACT 2600, Australia
J. Noblet, Station de Recherches Porcines, Institut National de la Recherche Agronomique, 35590 Saint-Gilles, France
V.H. Oddy, NSW Agriculture, Cattle and Beef Cooperative Research Center, University of New England, Armidale, New South Wales 2351, Australia
J.W. Oltjen, Department of Animal Science, University of California, Davis, CA 95616, USA
G.J. Phillips, Department of Animal Sciences, Washington State University, Pullman, WA 99164-6351, USA
A.B. Pleasants, Ag Research, Ruakura Research Centre, Hamilton, New Zealand
C. Pomar, Agriculture and AgriFood Canada, CP 90, 2000 Road 108 East, Lennoxville, Quebec J1M 1Z3, Canada
F.D. Richardson, Department of Mathematics and Applied Mathematics, University of Cape Town, Rondebosch 7701, South Africa
B. Robson, Applied Management and Computing Division, PO Box 84, Lincoln University, Canterbury, New Zealand
K. Russell, Waltham Centre for Pet Nutrition, Freeby Lane, Waltham on the Wolds, Melton Mowbray, Leicestershire LE14 4RT, UK
P. Sabatier, ENV Lyon, 1 avenue Bourgelat, 69280 Marcy l'Etoile, France
R.D. Sainz, Department of Animal Science, University of California, Davis, CA 95616, USA
D. Sauvant, Laboratoire INRA–INAPG de Nutrition et Alimentation, INAPG, 16 rue Claude Bernard, 75231 Paris Cedex 05, France
S.J. Schoeman, Department of Animal Science, University of Stellenbosch, Stellenbosch 7600, South Africa
C. Sniffen, W.H. Miner Agricultural Research Institute, Chazy, NY 12921, USA
T.K. Soboleva, Ag Research, Ruakura Research Centre, Hamilton, New Zealand
S. Tamminga, Animal Nutrition Group, Wageningen Institute of Animal Sciences (WIAS), Wageningen University, Marijkeweg 40, 6709 PG Wageningen, The Netherlands
T.P. Tylutki, Department of Animal Science, Cornell University, Ithaca, NY 14853, USA

P. Udén, Department of Animal Nutrition and Management, Swedish University of Agricultural Sciences, Box 7024, 750 07 Uppsala, Sweden
P.L. van der Togt, Animal Nutrition Group, Wageningen Institute of Animal Sciences, PO Box 338, 6700 AH Wageningen, The Netherlands
J. van Milgen, Station de Recherches Porcines, Institut National de la Recherche Agronomique, 35590 Saint Gilles, France
P.J. Van Soest, Department of Animal Science, Cornell University, Ithaca, NY 14853, USA
A.M. van Vuuren, ID-Lelystad, Department of Animal Nutrition, PO Box 65, 8200 AB Lelystad, The Netherlands
M. Vlieg, Applied Management and Computing Division, PO Box 84, Lincoln University, Canterbury, New Zealand
G.Q. Witten, Department of Mathematics and Applied Mathematics, University of Cape Town, Rondebosch 7701, South Africa
G. Zuur, Biomathematics and Statistics Scotland, Rowett Research Institute, Bucksburn, Aberdeen AB21 9SB, UK

Preface

This book presents edited and revised versions of papers presented at the Fifth International Workshop on Modelling Nutrient Utilization in Farm Animals, held at the University of Cape Town, Cape Town, South Africa, 25–28 October 1999. The purpose of this workshop was to bring together active experimentalists and modellers interested in research into and the application of nutritional principles in food-producing animals. This was the fifth such workshop, which has been held every 5 years since 1979. Dr Baldwin's Introduction to this book contains a brief history and the purpose of the workshop and modelling efforts in his laboratory and others over the last three decades, so that will not be provided here. This preface is simply the chair's thoughts about this workshop and suggestions for research and application models for the future. This is the first time that the proceedings of this workshop have been published beyond distribution to participants. It is my hope, and I can speak for all the Workshop Committee and participants, that, because of this publication, readers will be challenged to continue or increase specific efforts in the development, testing and application of research and applied models in the area of food-producing animals.

It is our belief that the human population has much to benefit from the utilization of food-producing animals. Food animals in general are well-managed and fed and the efficiency of food production is impressively high, given the systems involved. However, in spite of increasing concerns about resource availability, animal welfare issues and concern about the environment, the research emphasis on animal nutrition and metabolism has paradoxically waned. In large part, this is in common with the lackadaisical interest in agricultural research by well-fed societies in general, and in part this is because of the movement of biological research more and more toward molecular areas. I think in

part it is the very complexity of the biochemical interactions in animals themselves, as well as the interactions of animals with their environments, which has limited enthusiasm for research in complex systems. Most scientists are not trained to think quantitatively and about multiple simultaneous and continuous variables. Also 'modelling' is viewed by some animal nutritionists and physiologists either as 'theoretical' or as solely applied research and thus not exciting. Our colleagues in areas such as protein biochemistry and biophysics, where models are a necessity, may disagree with this view. In any case, the complexity of animal biochemistry is daunting, has limited growth of understanding in recent years and necessitates a biomathematical approach to problem-solving in this field.

Yet, at the same time, demand for quantitative, dynamic approaches to research is growing. There is an increasing amount of interest by governmental and private funding agencies in model systems in many areas of biology. I think this is in recognition, over the last several years, that the great body of knowledge that has been accumulated on nutrient requirements, feed practices and metabolic regulation has not been as effectively utilized as it might have been, had more people had the insight of Dr Baldwin and the other founders of this workshop. Partial evidence is the increased number of model papers in animal science society meetings; the recent meeting of the International Society for Ruminant Physiology, held just prior to this workshop, is one example. Several scientists there spoke on their research on models of various kinds and the need for more models to handle the increased complexity. Partial evidence is also provided by this very workshop, which was held somewhat 'off the beaten track', in a year full of other important conferences in subject-matters under research by the attendees, and yet this was the biggest yet of the five workshops in terms of number of papers presented. New contributors to the field (those not in attendance at one or more previous modelling workshops) made up the majority of the participants.

The research areas presented in this book cover the thermodynamic to the full ecosystem. I would unabashedly say that my favourite was presented by Professor David Richardson (see Chapter 20) of the University of Capetown on a model of the South African ecosystem. Complexity is exemplified by the combination of the rumen ecosystem of the cattle themselves, the amount of grass and other feed available to them, the effect of long-term rainfall patterns on grass availability and the interactions of goats with the types of plants (i.e. without goat browsers, woody plants eventually take over). In this total system, there are represented several levels of biological organization with dynamic time frames, spanning from minutes (rumen) to dozens of years (rainfall patterns and browsing). Yet, at each level, Dr Richardson and colleagues have provided a systematic set of hypotheses and model equations pertinent to the level being modelled. For the reader interested in any one of these general areas, this chapter provides a realistic and elegant framework for how systems interact and how research on complex systems could be conducted. In addition, Professor Richardson's love of his work and enthusiasm showed through during the

workshop, and it was a joy for me to interact with him and learn from him. I should like to extend my personal and professional thanks for his help in putting on this workshop.

The workshop was set up to flow generally from lower levels of organization (rumen, thermodynamics, feed chemistry), through higher levels (tissue metabolism) to even higher levels (animals, production systems and ecosystems). In general, that format was a success, as participants could see how the concepts build from the (relatively) simple to the more complex. Each level of organization provides its own challenges to the scientist, and in our area of endeavour we are always striving to work the complexities of one level into a simple and practical management system at increasingly higher levels. This I view as our challenge for the next several years.

Dr Boston's presentation near the end of the conference (see Chapter 28) on the development of commercial software for model systems embodied this quite well. Moving from the need of animal nutritionists for a fact-based, validated and yet simple and practical decision-making tool, Dr Boston and colleagues at several universities have developed model systems in animal nutrition for a practical application. Through several iterations of research, model construction and testing and field testing, two things have been brought out: the first is the absolute possibility and increasing likelihood that cooperative efforts among scientists, software developers and industry can result in useful model systems; and the second is that, with each new round of testing, a need for greater detail (mechanistic elements) in the models is recognized and research is designed to supply them. This, I think, embodies the very nature of our effort: as we study and apply more, the modelling approach forces efficient and focused research, which continually improves our knowledge and ability to apply it.

The needs of the human population, the absolute requirement to sustain our natural environment and the health and welfare of our food-producing animals demand an efficient and effective programme of research and application of knowledge. The complexity involved demands a strict, logical, mathematical approach to effectively identify key limitations in our knowledge, the most important research areas and the best management practices.

I should also like to take this opportunity to thank the Workshop Committee for all their help in making the workshop a success. This effort is not an official event of any society, nor is it subsidized by any society. Its existence is only the result of the need recognized by its participants. We hope this effort continues to grow. We thank CAB *International* for agreeing to publish these proceedings at no cost to the workshop; this helped our financial outcome and made the workshop a possibility. We also specifically thank Agribrands International, ADM, BioProducts and Purina Mills, Inc. and their representatives for their financial support.

The reader is asked to remember that these are the proceedings of an informal workshop, which was organized neither to impress the participants with great wisdom nor to pad out the contributor's curriculum vitae, but to allow a group of interested scientists to gather to present cutting-edge research and

application models and experiments. Thus, the chapters in this book are not to be viewed and referenced as final summations or research reviews. However, they should be read as works in progress, and referenced as contributions which, while making important findings, also raise many questions and, most importantly, point out the still significant lacks of understanding in the areas presented. This embodies the quantitative approach, which is meant to identify the key inadequacies in our knowledge to make our research and practical efforts meaningful.

Workshop Committee

Introduction: History and Future of Modelling Nutrient Utilization in Farm Animals

R.L. Baldwin

Department of Animal Science, University of California, One Shields Avenue, Davis, CA 95616, USA

Abstract

A brief, abridged commentary on past workshops on the modelling of farm animal digestion and metabolism is presented. This is followed by a discussion of changes in feeding system models that have occurred over the past 40 years or so. Changes discussed include addition of adjustments to accommodate differences in efficiencies of metabolizable energy (ME) use for various functions attributable to the energy density (ME kg^{-1}) of feeds; explicit consideration of factors influencing amino acid availability to ruminant animals including diet proteins which pass from the rumen undigested and variable microbial growth yields; and, explicit consideration of the dynamics of utilization of chemical as opposed to proximate entities by rumen microbes and animals.

This is recorded as the fifth of our series of meetings on modelling nutrient utilization in farm animals. The first workshop was held in Hurley, England, during the week between the Fifth Symposium on Digestive Physiology and Metabolism in Ruminants, held in Clermont-Ferrand, France (Ruckebusch and Thivend, 1980), and the Eighth Symposium on Energy Metabolism, held in Cambridge, England (Mount, 1980). As a contrast, the modelling workshop was sandwiched between these well-established venues for ruminant nutrition, which had been ongoing for 25 and 24 years, respectively.

Our first meeting was truly a workshop and a beginning. There were no anointed leaders in the field to offer sage advice. We were simply a group of scientists gathered together to try to figure out how to integrate and utilize the ever-increasing knowledge of digestive physiology, rumen microbial metabolism,

 Modelling Nutrient Utilization in Farm Animals (eds J.P. McNamara, J. France and D.E. Beever)

animal and tissue metabolism, metabolic regulation and animal energetics, as exemplified in the two symposia, in a quantitative fashion. This was to better explain and utilize the data and concepts presented to advance animal science and agriculture. We had all recognized that research thrusts at that time – learning more and more about less and less and documenting the many sources of variance in whole-animal energy expenditures – were nice and rewarding in the sense that excellent, astute, word descriptions of progress in the several specific areas of enquiry could be and were presented at the symposia but that quantitative integration of our data and concepts was lacking. Organizers of both symposia recognized this and that modelling was the means by which this goal could be realized by incorporating several modelling papers. These papers depicted a field in its infancy. At the workshop, we were attempting to bring the field to its childhood. We discussed modelling philosophy, terminology and methods as best we could and illustrated our diversity by dividing into work groups to address modelling approaches to specific problems, with variable and limited success. Deliberations of this workshop are unrecorded – who wants to record baby talk? – but we learned.

Five years later, the workshop was reconvened at Davis, California. Development of the field is illustrated in the proceedings of that workshop (Baldwin and Bywater, 1984). Unifying philosophy, terminology and context, since adopted by most, were developed through the presentations of Thornley and France, Matis, Ramberg and the discussion edited by Bywater and Pond. In subsequent sessions, specific models, modelling analyses, concepts, problems and challenges were addressed and discussed at length. The field had clearly advanced through its childhood and was advancing toward puberty. This process of maturation continued through the two subsequent workshops (Robson and Poppi, 1989; Danfær and Lescoat, 1995). Aspects of philosophy were reiterated, restated and discussed at each meeting, partly for the purpose of educating new participants entering the field. The breadth and depth of models presented and discussed continuously expanded as our knowledge of animal functions improved, along with improvements in our modelling skills and computer science and technology. The results of this continuing development of the field are evident in this current workshop. One might even venture the opinion that modelling is now a mature discipline within the animal sciences. We can point to relatively sophisticated models of physiological and metabolic functions at the tissue and animal levels, to models currently in practical use in support of animal agriculture and to farming system models that incorporate mechanistic animal elements to an extent not previously realized; many of these models are represented in this workshop. There have been a number of books on modelling animal systems, including those authored or edited by participants in these workshops, such as France and Thornley (1984), Forbes and France (1993) and Baldwin (1995), numerous chapters in symposia and other books addressing animal physiology, nutrition and production, and hundreds of original papers. However, this appearance of maturity should not be interpreted as indicating that the discipline has attained fruition.

Tremendous progress has been made. However, I suggest that we still have a long way to go. I am a firm believer in the defender : challenger concept in model evaluations. This view holds that, in order to replace a currently accepted (defender) model, new (challenger) models must be proved superior. When the model challenged fails in some regard, it behoves the investigator conducting the evaluation to identify specific elements within the defender model which led to the errors detected and to explain how deficiencies in the model were, could be or should be addressed in the challenged model. Similarly, the challenger model can be improved. It is not adequate to simply conclude that a given model fails to predict a specific output adequately. This does not advance animal science.

This is the process that was followed during the development of our current feeding systems. For example, it was observed – indeed, I was taught in class during the 1950s – that total digestible nutrients (TDN) from concentrate (grain) diets was superior to TDN from forage diets. The speculation was that fermentation products from the digestion of concentrate feeds were utilized more efficiently for productive functions than were the products of forage digestion. This led to experimentation, which resulted in the development of equations that defined relationships between the metabolizable energy (ME) density (ME kg^{-1}) of diets and efficiency of use for differing functions. The starch equivalent system assigned a value to feedstuffs relative to starch, based upon the energy deposited as fat when a kilogram of that feedstuff or starch was fed above maintenance requirements to an adult steer. Recognition of the fact that efficiencies of ME use by animals differed, dependent upon whether the products of digestion of a feedstuff were used to support maintenance, growth, fattening or lactation, led to the development of net energy (NE) systems in the USA (dairy cattle: NRC, 1989; beef cattle: NRC, 1996), wherein values were assigned to feedstuffs based upon the amount of body energy spared by a feed in animals fed below maintenance (NE_m) and feed energy recovered as energy in gain (NE_g) or milk (NE_l) when that feedstuff was fed to producing animals. Similarly, in the UK (ARC, 1980), ME-based systems were developed wherein efficiencies of ME use for alternative functions were defined using equations relating efficiencies of ME use to the ME kg^{-1} of feeds.

Concurrently with the adoption of the NRC (National Research Council) (1989, 1996) and ARC (Agricultural Research Council) (1980) systems, concern arose regarding the adequacy of crude protein (CP) as an index of the values of rations as related to the availability of amino acids to producing animals. This led the NRC to appoint a committee to evaluate the problem and suggest how the problem should be addressed. This committee concluded that resistance of proteins to hydrolysis in the rumen leading to passage of proteins undigested from the rumen be defined as rumen-undigested protein (RUP). This suggestion was addressed in the 1989 NRC publication on the nutrient requirements of dairy cattle and at Cornell in the development of the Cornell Net Carbohydrate and Protein System (CNCPS), currently in common use in the USA. The RUP concept is incorporated in the CNCPS and, in addition, the

concept that rumen microbial growth yields can vary was addressed by including mechanistic equations to predict rumen microbial growth, so that amino acids available to producing animals could be better defined.

During this period, investigators at the University of California at Davis were concerned about the fact that microbes ferment and animals utilize specific chemicals, and that these are converted to different products utilized at differing efficiencies by different animals. In order to better define the products formed from the several carbohydrates fermented by rumen microbes, Murphy *et al*. (1982) formulated an analytical model based upon known pathways and stoichiometries of fermentation by the several rumen microbes and used literature data on feed composition and molar proportions of acetate, propionate, butyrate and valerate along with the model to deduce stoichiometric coefficients defining the proportions of volatile fatty acids (VFA) formed from diet-soluble carbohydrates, starch, hemicellulose, cellulose and protein. Evaluations indicated systematic errors in predicting amounts of acetate and propionate formed in the rumen when the deduced stoichiometric coefficients were used. These systematic errors were found to be attributable to percentages of fermentable carbohydrates in concentrate diets and amounts of insoluble ash in forage rations, respectively. Equations for correcting these systematic errors were developed (Murphy *et al*., 1982). Deduced stoichiometric coefficients for protein fermentation were found to be non-unique, as were those for butyrate and valerate formation (Murphy *et al*., 1982). As no underlying reasons for differences in butyrate formation were evident, no remedy for errors in predicting butyrate was identified or proposed. Subsequent workers (Dijkstra *et al*., 1992) have specifically noted failures in predicting butyrate using the deduced stoichiometric coefficients. However, no mechanistic approaches to resolution of this problem have been offered to date.

Subsequent to the work of Murphy *et al*. (1982), it was proposed that the systematic errors attributed to percentage concentrate in the ration by Murphy *et al*. (1982) may have been due to differences in pH values in the rumens of cattle fed the several diets. Equations for estimating pH in dynamic models of ruminant digestion and for adjusting the stoichiometric coefficients dependent upon pH were incorporated into a ruminant digestion model and improved performance of the digestive element of the model (Argyle and Baldwin, 1988).

As noted above, concern arose about potential errors associated with the use of constant efficiencies of ME utilization as an aggregate term to estimate energy from digestion of feed available to an animal. This was apposed to considering amounts of individual nutrients (chemical entities) absorbed by an animal which contribute to ME estimates. Theoretical analyses based upon known pathways of nutrient utilization strongly reinforced the view that the utilization of individual nutrients should be considered explicitly when it was calculated that the biochemical efficiencies of conversion of acetate and absorbed fatty acids to body and milk fat differ significantly, at 78–80% and 95–97%, respectively. It was proposed that biochemical differences such as these would help explain why relationships between efficiencies of ME use vary as a function of

energy densities of feeds. Thus, in our models of ruminant metabolism, the uses of specific absorbed nutrients are depicted explicitly and in accord with known biochemical pathways.

Another long-standing concern with the models upon which the several feeding systems are based was with differences in the coefficients used to estimate so-called maintenance requirements assigned animals, based upon whether they are growing, pregnant or lactating, independent of rate of growth or stage of lactation. For example, the coefficients used to calculate the ME requirement of growing and lactating animals for maintenance ranging from 0.48 to 0.56 MJ $W^{-0.75}$ have been used for ruminants (Reid, 1974; NRC, 1989; Baldwin, 1995). Speculation was widespread regarding reasons for these differences. Smith and Baldwin (1974), Webster (1981) and Canas *et al.* (1982) suggested that the differences could be attributed, in part, to increases in the relative weights of visceral organs with high-energy expenditures per unit mass due to high feed intakes. Koong and associates (Koong *et al.*, 1983; Ferrell, 1984) confirmed this supposition. Milligan and his associates (Milligan, 1971; McBride and Milligan, 1985; Milligan and McBride, 1985; Summers *et al.*, 1988) suggested that energy expenditures per unit mass of organs increased at high feed intakes due to increases in the activity of the Na^+K^+ ATPase involved in nutrient transport across membranes. In formulating the animal element of their model, Baldwin *et al.* (1985) incorporated the concept that energy expenditures due to membrane transport vary, dependent upon energy intake. This resulted in the responses depicted in Fig. I.1. Gill *et al.* (1989) adopted a similar approach. Thus, the treatment of 'maintenance' as a constant function of body weight, independent of physiological state and rate of production, was replaced by equations recognizing variable energy expenditures in functions conventionally associated with maintenance and which vary as colinear components of estimated costs of production in multiple regression analyses (Baldwin, 1995).

Johnson *et al.* (1999) and McNamara (2000) reported that provisions for computing energy expenditures in the Baldwin *et al.* (1985) model were inadequate, in that systematic errors in simulations of experimental data on lactating cows resulted in body fat gains exceeding observed values by 2–4 Mcal day^{-1} during lactation. Adjustment of parameter values defining effects of energy intake upon energy costs of membrane transport corrected this systematic error in simulated as compared with observed fat gains (Fig. I.2) during lactation.

Broster and Broster (1984) evaluated long-term effects of plane of nutrition on performance in lactating dairy cattle and documented the residual effect high planes of nutrition have upon later performance. This led Baldwin (1995) to suggest that such effects should be accommodated in feeding system models and, further, that such 'carry-over' effects could only be accommodated in dynamic, mechanistic models. The model of Baldwin *et al.* (1985) had the property of simulating residual effects of high planes of nutrition upon subsequent performance (Baldwin, 1995).

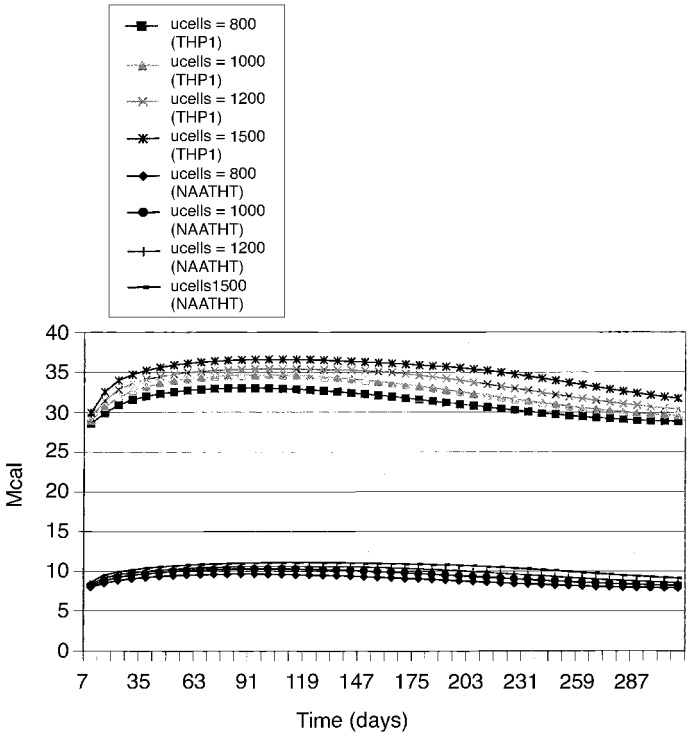

Fig. I.1. Simulated total energy expenditure (THP1, Mcal day^{-1}) and energy costs associated with membrane transport (Na^+K^+ ATPase; NAATHT) during the lactation cycle in cows with differing genetic potentials (ucells) for milk production.

Previewing the future is always an equivocal process. Based upon the past, we are confident that mechanistic models of metabolic processes will continue to evolve as our knowledge of regulatory mechanisms improve and that modelling analyses will continue to be a valuable means of placing advances in our knowledge in context with overall aspects of ruminant digestion and metabolism and productive functions in growing and lactating animals. Through this process, our models of digestion and metabolism in ruminants will continue to improve and provide insights. We also anticipate that the value of mechanistic, dynamic models will become more widely recognized and, further, that they will slowly replace the empirical, factorial models used in current feeding system models. Such adoption will probably take the form of strategic elements used to define diets that provide for optimal animal performance throughout growth periods and lactation, according to cost efficiency and environmental constraints. The diets and feeding strategies thus defined will, in turn, be utilized in the specification of inputs used in the formulation of rations, using least-cost linear programmes.

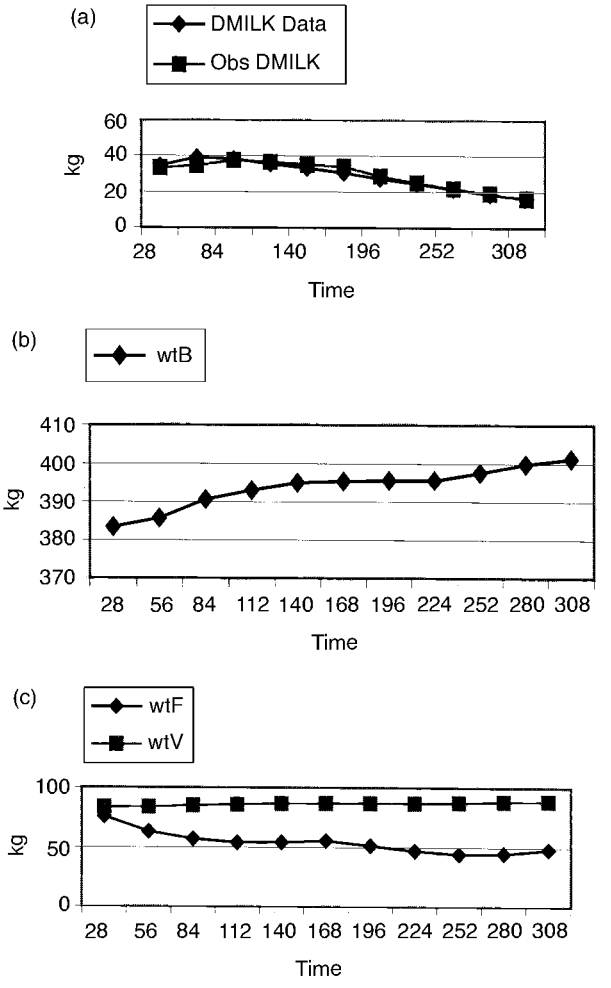

Fig. I.2. (a) Simulated daily milk yields (DMILK) and (b) weights of carcass (wtB), (c) adipose tissue (wtF) and viscera (wtV) during lactation. Monthly feed intakes for cows milked three times a day in a full lactation study by DePeters *et al.* (1998).

References

ARC (Agriculture Research Council) (1980) *The Nutrient Requirements of Ruminant Livestock*. Commonwealth Agricultural Bureaux, Farnham Royal, Surrey, UK, 351 pp.

Argyle, J.L. and Baldwin, R.L. (1988) Modeling of rumen water kinetics and effects of rumen pH changes. *Journal of Dairy Science* 71, 1178–1188.

Baldwin, R.L. (1995) *Modelling Ruminant Digestion and Metabolism*. Chapman & Hall, London, UK, 578 pp.

Baldwin, R.L. and Bywater, A.C. (1984) *Modeling Ruminant Digestion and Metabolism: Proceedings of the Second International Workshop*. Department of Animal Science, University of California, Davis, California, 138 pp.

Baldwin, R.L., Forsberg, N.E. and Hu, C.Y. (1985) Potential for altering energy partition in the lactating cow. *Journal of Dairy Science* 68, 3394–3402.

Broster, W.H. and Broster, V.J. (1984) Reviews of the progress of dairy science: long term effects of plane of nutrition on performance of the dairy cow. *Journal of Dairy Research* 51, 149–196.

Canas, R., Romero, J.J. and Baldwin, R.L. (1982) Maintenance energy requirements during lactation in rats. *Journal of Nutrition* 112, 1876–1880.

Danfær, A. and Lescoat, P. (1995) *Modelling Nutrient Utilisation in Farm Animals: Proceedings of IVth International Workshop*. National Institute of Animal Science, Foulum, Denmark, 195 pp.

DePeters, E.J., Perez-Monti, H., Taylor, S.J., Wyckoff, J.A. and Zinn, R.A. (1998) Tallow and grease as sources of supplemental dietary fat for dairy cattle during early lactation. *Journal of Dairy Science* 81 (Suppl. 1), 352.

Dijkstra, J., Neal, H.D.St C., Beever, D.E. and France, J. (1992) Simulation of nutrient digestion, absorption and outflow of the rumen: model description. *Journal of Nutrition* 122, 2239–2256.

Ferrell, C.L. (1984) Sources of variation in animal energy expenditures. In: Baldwin, R.L. and Bywater, A.C. (eds) *Modeling Ruminant Digestion and Metabolism: Proceedings of the Second International Workshop*. Department of Animal Science, University of California, Davis, California, pp. 100–105.

Forbes, J.M. and France, J. (1993) *Quantitative Aspects of Ruminant Digestion and Metabolism*. CAB International, Wallingford, UK, 515 pp.

France, J. and Thornley, J.H.M. (1984) *Mathematical Models in Agriculture*. Butterworths, London, UK, 335 pp.

Gill, M., France, J., Summer, M., McBride, B.W. and Milligan, L.P. (1989) Simulation of the energy cost associated with protein turnover and Na^+, K^+ ATPase transport in growing lambs. *Journal of Nutrition* 119, 1287–1299.

Johnson, H.A., DePeters, E.J. and Baldwin, R.L. (1999) Evaluation of Molly, a dynamic, metabolic model of a dairy cow for predicting milk production. *Journal of Dairy Science* 82 (Suppl. 1), 103.

Koong, L.J., Nienaber, J.A. and Mersmann, H.J. (1983) Effects of plane of nutrition on organ size and fasting heat production in genetically obsese and lean pigs. *Journal of Nutrition* 113, 1626–1631.

McBride, B.W. and Milligan, L.P. (1985) Influence of feed intake and starvation on the magnitude of Na^+, K^+, ATPase-dependent respiration in duodenal mucosa of sheep. *British Journal of Nutrition* 53, 605–613.

McNamara, J.P. (2000) Computer simulation of nutrient digestion and metabolism in lactating dairy cattle. *Journal of Dairy Science* 83, 128–143.

Milligan, L.P. (1971) Energetic efficiency and metabolic transformation. *Federation Proceedings* 30, 1454–1458.

Milligan, L.P. and McBride, B.W. (1985) Symposium: shifts in animal energy requirements across physiological and alimentation states. *Journal of Nutrition* 115, 1374–1382.

Mount, L.E. (1980) *Energy Metabolism: Proceedings of the Eighth Symposium on Energy Metabolism*. Butterworths, London, UK, 484 pp.

Murphy, M.R., Baldwin, R.L. and Koong, L.J. (1982) Estimation of stoichiometric para-

meters for rumen fermentation of roughage and concentrate diets. *Journal of Animal Science* 55, 411–421.

NRC (National Research Council) (1989) *Nutrient Requirements of Domestic Animals: Nutrient Requirements of Dairy Cattle,* 6th edn. National Academy Press, Washington, DC, 157 pp.

NRC (National Research Council) (1996) *Nutrient Requirements of Domestic Animals: Nutrient Requirements of Beef Cattle,* 7th edn. National Academy Press, Washington, DC, 242 pp.

Reid, J.T. (1974) Energy metabolism of the whole animal. In: Sink, J.D. (ed.) *The Control of Metabolism*. Pennsylvania State University Press, University Park, Pennsylvania, pp. 113–151.

Robson, A.B. and Poppi, D.P. (1989) *Modelling Digestion and Metabolism in Farm Animals: Proceedings of the Third International Workshop*. Lincoln University, Canterbury, New Zealand, 360 pp.

Ruckebusch, Y. and Thivend, P. (1980) *Digestive Physiology and Metabolism in Ruminants: Proceedings of the 5th International Symposium on Ruminant Physiology*. MTP Press, Lancaster, UK, 854 pp.

Smith, N.E. and Baldwin, R.L. (1974) Effects of breed, pregnancy, and lactation on weights of organs and tissues in dairy cattle. *Journal of Dairy Science* 57, 1055–1060.

Summers, M., McBride, B.W. and Milligan, L.P. (1988) Components of basal energy expenditure. In: Dobson, A. and Dobson, M.J. (eds) *Aspects of Digestive Physiology in Ruminants*. Comstock Publishing Associates, Ithaca, New York, pp. 257–285.

Webster, A.J.F. (1981) The energetic efficiency of metabolism. *Proceedings of Nutrition Society* 40, 121–128.

1

The Role of Thermodynamics in Controlling Rumen Metabolism

R.A. Kohn[1] and R.C. Boston[2]

[1] *University of Maryland, College Park, MD 20742, USA;*
[2] *University of Pennsylvania, Kennett Square, PA 19348, USA*

Abstract

Chemical reactions are controlled either thermodynamically or kinetically. Most mechanistic biological models assume kinetic control of metabolism pathways. The profile of products formed depends on substrate concentrations and enzyme activities, which control the rates of synthesis for competing pathways. Thermodynamic control occurs when reactants are sufficiently limited relative to products for the reactions not to be able to proceed, according to the second law of thermodynamics. Under these circumstances, thermodynamics controls which pathway branches are available and the final concentration of products. This chapter investigates the possibility of thermodynamic control of ruminal fermentation. Ruminal pH is buffered by bicarbonate in a system that is near equilibrium. This is a clear example of thermodynamic control. Rates of acetate, propionate and methane synthesis also appear to be controlled by thermodynamics, but these reactions do not approach equilibrium. These reactions proceed until the change in Gibbs free energy (ΔG) approaches a negative value, representing the inherent inefficiency of the system. A dynamic model of glucose fermentation was developed that incorporated thermodynamic limits to volatile fatty acid (VFA) and gas production. Incorporation of thermodynamic limits was achieved by including fractional rate constants for reverse reactions. These reverse rate constants were determined from published thermodynamic data for the reactants and products. This model predicted realistic steady-state concentrations of major VFA and gases. Incorporation of factors that decrease the efficiency of certain reactions (i.e. low pH or use of ionophores) would shift the fermentation in directions similar to those observed in the rumen.

© CAB *International* 2000. *Modelling Nutrient Utilization in Farm Animals*
(eds J.P. McNamara, J. France and D.E. Beever)

Introduction

Ruminal fermentation initially results in the degradation of starch, fibre and protein to short-term intermediates, such as sugars and amino acids. The kinetics of these initial degradation steps are frequently discussed, as they are considered rate-limited processes, which are dependent on substrate level and enzyme specific activity, and are in turn affected by the microbial population and ruminal environment (Baldwin *et al.*, 1987; Dijkstra *et al.*, 1992). The products of this initial degradation are readily metabolized to microbial mass and carbon dioxide (CO_2), methane (CH_4), ammonia (NH_3) and volatile fatty acids (VFA) – primarily acetate, propionate and butyrate – and, to a lesser degree, branched-chain VFA and occasionally lactate (Prins, 1977). Baker and Dijkstra (1999) extensively reviewed what is known about the control of this secondary degradation, but much remains to be discovered.

Murphy *et al.* (1982) developed a mathematical model based on the stoichiometry of major pathways in the rumen to predict relative proportions of VFA, CH_4 and CO_2 from digestible feed fractions: soluble carbohydrate, starch, hemicellulose, cellulose and protein. This model has since been used for many efforts of dynamic modelling (Baldwin *et al.*, 1987; Dijkstra *et al.*, 1992), with inconsistent levels of success (Neal *et al.*, 1992; Kohn *et al.*, 1995). The prediction is based on a principal component analysis of the data set, and not on a fundamental understanding of the factors that may alter VFA profiles. For this reason, although the model has been an essential element of whole-animal modelling, it has not been flexible enough to predict VFA profiles of feeds that differ substantially from those in the data sets from which coefficients were derived. In addition, this approach provides little information as to how the ruminal fermentation may be manipulated by dietary factors other than those considered in the model's development and provides little insight into other regulators of microbial growth, such as ionophores.

A more mechanistic approach to predict profiles of VFA and gases from rumen fermentation requires an understanding of the control mechanisms of metabolism. Chemical reactions are controlled either thermodynamically or kinetically (Chang, 1981). If reactants are sufficiently limited relative to products, the reactions cannot proceed, according to the second law of thermodynamics. Under these circumstances, thermodynamics controls which pathway branches are available. On the other hand, if the rates of utilization of a substrate control the pathways for product formation where all of the reactions are thermodynamically favourable, the reactions are kinetically controlled. These rates may depend on substrate and/or enzyme concentrations.

Consider a system in which key intermediates are found in very low concentrations relative to products. For example, one would not expect to find appreciable concentrations of glucose in the rumen, where fermentation occurs rapidly. This expectation results from our understanding that glucose is rapidly metabolized to other compounds. If the very moment a glucose molecule is released into solution it is a candidate for metabolism, whether that molecule

becomes acetate, propionate, butyrate or lactate would depend on the speed of the respective reactions or at least on how quickly the reactions can remove the molecule from solution. If the end-products build up, however, the VFA may inhibit the reaction from occurring at all, based on the second law of thermodynamics. The second law of thermodynamics requires that Gibbs free energy (G) be released for a process to occur spontaneously. If the concentration of precursor becomes small enough relative to product, the forward reaction will not proceed. In this case, the precursor may be used to produce a different product, and there may be a shift from one VFA or gas to another. Equilibrium thermodynamic principles were recently integrated into kinetic models explaining reaction shifts in anaerobic digesters (Hoh, 1996).

The objective of the present chapter is to demonstrate the potential for thermodynamic control of ruminal fermentation. This approach will allow determination of the possibilities for manipulating gas and VFA profiles and which pathway branches may control their production.

The Second Law of Thermodynamics

The first law of thermodynamics (that energy cannot be created or destroyed but can be converted from one form to another) has been applied to animal biology since the late 18th century. The first law of thermodynamics is applied when energy balance trials are conducted. The energy of faecal matter, urine, heat increment, maintenance, growth and milk secretion is equal to the energy consumed in feed. The first law of thermodynamics is used to describe how much energy is in a feed and thus how much work can be done or how much milk and meat can be produced. The second law of thermodynamics has been central to the fields of physics and chemistry, but, for the most part, has not been incorporated into mathematical models of biological systems or explanations of occurrences in biology. The second law deals with how the energy will be used and whether or not the work will be done or whether the energy will be used for milk production, growth or heat.

The second law of thermodynamics is: entropy of the universe increases in an irreversible process or remains unchanged in a reversible process (Chang, 1981). Entropy is defined as 'randomness' and a reversible process is defined as an infinitely slow one with an infinite number of steps. In fact, most reactions are irreversible and so the entropy of the universe increases or heat is released from the system to the surroundings. Stated mathematically, the second law is as follows:

$$dS_u \geqslant 0 \quad (1)$$

where dS_u represents the change in entropy of the universe. This change in entropy can be divided between that of any given system (dS_{system}) and the surroundings of the system ($dS_{surroundings}$); therefore:

$$dS_u = dS_{system} + dS_{surroundings} \quad (2)$$

In a system that is imperfect, heat is generated while work is done. That heat is dissipated from the system to the surroundings. The system can be defined to include all changes in chemical composition of products and reactants. Thus only heat loss from the system needs to be considered as a loss to the surroundings. This heat loss ($-dH_{system}$) must equal the change in entropy of the system when corrected for temperature in kelvin (T):

$$dS_{surroundings} = -dH_{system}/T \quad (3)$$

By substituting the right-hand side of equation 3 into equation 2, a new definition of the change in entropy of the universe is derived:

$$dS_u = dS_{system} - dH_{system}/T \quad (4)$$

Substituting the right-hand side of equation 4 into equation 1 reminds us that the change in entropy of the universe must be greater than or equal to 0:

$$0 \leqslant dS_{system} - dH_{system}/T \quad (5)$$

Multiplying both sides by ($-T$) provides the relation:

$$0 \geqslant dH_{system} - TdS_{system} \quad (6)$$

This negative value is the definition of the change in Gibbs free energy (ΔG). Thus, ΔG of a system is negative when heat is lost from the system to the surroundings. The more inefficient the system is in using available energy, or the more heat lost, the more negative the ΔG must be. This relationship will be important to understanding shifts in ruminal metabolism associated with lower efficiency of fermentation and greater heat increment.

Integration of the second law of thermodynamics with the ideal gas law provides a mathematical relationship that is especially useful to chemistry and biology. Under constant pressure, the change in free energy of a reaction is a function of the activity of the products and reactants:

$$\Delta G = \Delta G^\circ + RT \ln\{[\text{Products}]/[\text{Reactants}]\} \quad (7)$$

where [x] represents activity of x (or pressure in atmospheres of x for ideal gases and molarity of x for ideal solutes), R is the gas constant and equals 8.314 J K^{-1} mol^{-1}, K represents the temperature in kelvin and ΔG° represents the change in free energy for the reaction under standard conditions. These conditions are 278.15 K, one unit of activity for all solutes and 1 atmosphere of pressure for all gases. If a reaction goes to equilibrium, the ΔG is equal to zero. Therefore, the ΔG° can be determined by measuring the concentration of products and reactants. Once this value is determined, it can be used with other similar values to determine the ΔG of other reactions contained within these reactions. The amount of free energy of a material is intrinsic to that material. Furthermore, once the G is determined for potential reactants and products, the equilibrium constant for those reactions can be easily calculated. Setting ΔG to 0 in equa-

tion 7 represents equilibrium. Using book values for the $\Delta G°$ enables determination of the equilibrium constant (K_{eq}) as follows:

$$K_{eq} = e^{-\Delta G/RT} \quad (8)$$

Ruminal pH

One of the most obvious examples of thermodynamic control of ruminal metabolism is the control of pH by the bicarbonate ion (HCO_3^-). The bicarbonate system includes two major ionic forms: HCO_3^- and CO_3^{2-}. The HCO_3^- ion is of primary importance to buffering because it may be protonated to H_2CO_3. The equilibrium constant for weak acid dissociation can be derived from setting ΔG for the reaction to 0 and solving for the concentration of products over reactants. This value can be expressed as the negative log of the equilibrium constant, pK_a, to convert it to a more convenient form. The pK_a of this acid is only 3.80 at 37°C and 0.15 M ionic strength (Segel, 1976). However, H_2CO_3 may establish an equilibrium with dissolved CO_2 and H_2O:

$$CO_2 + H_2 \rightleftharpoons H_2CO_3 \rightleftharpoons HCO_3^- + H^+$$

The equilibrium constant (K_{eq}) for the two steps of the reaction combined is the product of the individual equilibrium constants:

$$K_{eq} = (k_1 k_2)(k_{-1} k_{-2}) = ([HCO_3^-]\,[H^+])/([CO_2]\,[H_2O]) \quad (9)$$

where k_1 and k_2 = fractional rate constants for each forward reaction, and k_{-1} and k_{-2} = fractional rate constants for each reverse reaction. Considering both steps in equilibrium, the effective pK_a for the system (pK_a') is 6.1 for solutions of 0.15 M ionic strength at 37°C (Segel, 1976). Ruminal gases and liquids are in close contact, so that an equilibrium between soluble and evolved gas may be attained. The overall equilibrium constant for the ruminal system is therefore the product of three equilibrium constants for each of the reactions in which CO_2 gas is converted to HCO_3^-. The effective pK_a when determining $[HCO_3^-]$ for the rumen compared with the partial pressure of CO_2 in atmospheres (PCO_2) is 7.74. Thus the Henderson–Hasselbalch equation is as follows:

$$pH_{rumen} = 7.74 + \log([HCO_3^-]/PCO_2) \quad (10)$$

The pH of ruminal fluid is clearly dependent on the concentration of HCO_3^- and the pressure of CO_2. Some have argued that the rumen is saturated with CO_2 and so both of these variables are unchanging and uncontrollable. Kohn and Dunlap (1998) used equation 10 to demonstrate that changes in ruminal fluid pH result from one of three sources: (i) changes in strong ion (e.g. Na^+, Cl^-) concentrations; (ii) changes in VFA concentrations; and (iii) changes in PCO_2. Strong ion concentrations could be affected by diet, contribution from saliva or even hot weather (ion excretion). VFA concentrations may result from different fermentation rates. Finally, the pressure of CO_2 in the rumen has been

shown to vary substantially for fistulated cows (Barry *et al.*, 1977). The rumen contains a large percentage of N_2, particularly after feeding, which reduces the Pco_2 and increases pH. You could argue that the large percentage of nitrogen in rumen gases results from leakage around the fistula. None the less, pH measurements do not usually account for the effect of Pco_2 on pH, despite the large differences in pH these changing pressures have.

Methanogenesis and Reductive Acetogenesis

A second application of the second law of thermodynamics is in the prediction of the feasibility of methane generation or synthesis of acetate from CO_2 and H_2. It is well understood that H_2 is used by methanogens to produce CH_4, which is thought to be a waste product of metabolism. If this H_2 could be used instead to generate acetate from CO_2, greater energy could be preserved for production. What is the feasibility of methanogenesis or reductive acetogenesis in the rumen under typical conditions? The balanced reactions of interest in this case are:

$$CO_2(aq) + 4\,H_2 \rightarrow CH_4 + 2\,H_2O$$

$$CO_2(aq) + 4\,H_2 \rightarrow C_2H_3O_2^- + H^+ + 2\,H_2O$$

If the total gas pressure in the rumen approximates 1 atm and CO_2 comprises 70% of that pressure, the Pco_2 would be 0.7 atm. Multiplied by the solubility constant (Segel, 1976) for this ionic strength, temperature and pressure (0.0229 mol atm^{-1}), this Pco_2 would provide 0.016 M of dissolved (aq) CO_2 at equilibrium. The H_2 concentration can be calculated, using the Nerst equation, from the reducing potential and pH (Segel, 1976):

$$\Delta E = \Delta E^\circ + RT/(nF) \times \ln\left([H^+]^2/[H_2]_g\right) \qquad (11)$$

where ΔE is the reducing potential in volts, measured using an appropriate electrode, ΔE° is the change in reducing potential for the reaction under standard conditions, which is equal to zero for the H^+ to H_2 half-reaction, R is the gas constant (8.3145 J K^{-1} mol^{-1}), T is the temperature in K, n is the number of moles reduced (2) and F is Faraday's constant (9.6487×10^4 C mol^{-1}), which converts ΔE from ΔG. The solution for $[H_2]_g$ in this case yields the concentrations under equilibrium conditions for the H_2 half-reaction. Typical ruminal conditions are $E = -0.315$ V and pH = 6.5 (Barry *et al.*, 1977). Thus, $[H_2]_g$ would be 1.6×10^{-3} atm. For this example, let us assume that the partial pressure of CH_4 is 0.3 atm. Multiplied by its solubility constant (2×10^{-5}) (Fogg and Gerrard, 1985) yields a concentration of 6×10^{-6} mol l^{-1}. The molecular weight of water is 18 g mol^{-1} with 1000 g l^{-1}. Therefore, the molarity of pure water is 55.6 mol l^{-1}. Assuming 10% dry matter of the ruminal solvent yields a molarity of approximately 50 mol l^{-1} for rumen liquid, typical ruminal conditions allow for at least 0.05 mol l^{-1} of acetate. Thus the concentrations of all products and reactants for a particular set of ruminal conditions have been defined.

Table 1.1 shows key thermodynamic data under standard conditions for these reactants and products, as well as some other important ruminal metabolites. These values represent the free energy of formation (ΔG_f°) and enthalpy of formation (ΔH_f°) of the metabolites from the elements (e.g. H_2, O_2, graphite). Free energy under standard conditions and concentrations, ΔG°, can be determined from these tabular values for each reaction of interest (Chang, 1981):

$$\Delta G^\circ = \Delta G^\circ_f \text{ of products} - \Delta G^\circ_f \text{ reactants} \quad (12)$$

Adjustment to each ΔG_f° for temperature can be made using a transformation of the vant Hoff equation (Chang, 1981) and enthalpy of formation, ΔH_f°, where T_1 and T_2 are the initial and final temperatures respectively, and $\Delta G^\circ_{T_1}$ and $\Delta G^\circ_{T_2}$ are the respective standard free energy values:

$$\Delta G^\circ_{T_2} = T_2/T_1[\Delta G^\circ_{T_1} - \Delta H^\circ(T_2 - T_1)/T_2] \quad (13)$$

Table 1.2 shows the resulting standard change in free energy (ΔG°) calculated for several reactions important to ruminal metabolism under standard conditions and adjusted for 311 K.

Now it is possible to use equation 7 to determine the ΔG of methanogenesis and acetogenesis under the ruminal conditions that were just described. For methanogenesis:

$$\Delta G = \Delta G^\circ + RT \ln\{ [CH_4]_{aq} [H_2O]^2/([CO_2]_{aq} [H_2]_g^{\,4}) \} \quad (14)$$

$$\Delta G = -134.9 + 0.008314 \times 311 \ln \{(6 \times 10^{-6})(50^2)/ [(0.016)(1.6 \times 10^{-3})^4] \} \quad (15)$$

$$\Delta G = -68.5 \text{ kJ mol}^{-1} \quad (16)$$

Table 1.1. Standard free energy of formation and enthalpy of formation in kJ mol^{-1} of key rumen metabolites at 298.15 K and 1 atm.

Metabolite	ΔG°_f	ΔH°_f
α,β-D-Glucose (aq) ($C_6H_{12}O_6$)	−916.97	−1263.78
Acetate (aq)	−376.89	−485.6
Propionate (aq)	−373.82	−511.70
Butyrate (aq)	−372.04	−535.55
Lactate (aq)	−516.72	−686.64
Methane (aq)	−50.79	−74.85
Carbon dioxide (aq)	−386.23	−412.92
Water (l)	−237.19	−285.84
Hydrogen (g)	0.0	0.0

Data are not adjusted to pH 7 and are from Chang (1981) except for propionate (CRC, 1991). Standard conditions are 1 M concentration of each soluble reactant and product, 1 atm of all gases and 298.15 K.
aq, Dissolved; l, liquid; g, gas.

Table 1.2. Key reactions in the rumen: standard change in enthalpy in kJ mol^{-1} ($\Delta H°$), standard change in free energy at 298 K in kJ mol^{-1} ($\Delta G°_{298}$) and standard change in free energy at 311 K in kJ mol^{-1} ($\Delta G°_{311}$).

Reaction	Formula	$\Delta H°$	$\Delta G°_{298}$	$\Delta G°_{311}$
Glucose to acetate	$C_6H_{12}O_6 + 2H_2O \rightarrow 2C_2H_3O_2 + 2H^+ + 4H_2(g) + 2CO_2(aq)$	38.4	−134.9	−142.4
Glucose to propionate	$C_6H_{12}O_6 + 2H_2 \rightarrow 2C_3H_5O_2 + 2H^+ + 2H_2O$	−331.3	−305.0	−303.9
Glucose to butyrate	$C_6H_{12}O_6 \rightarrow C_4H_7O_2 + H^+ + 2H_2(g) + 2CO_2(aq)$	−97.6	−227.5	−233.1
Glucose to lactate	$C_6H_{12}O_6 \rightarrow 2C_3H_5O_3 + 2H^+$	−109.5	−116.5	−116.8
Lactate to propionate	$C_3O_3H_5 + H_2 \rightarrow C_3H_5O_2 + H_2O$	−110.9	−94.3	−93.6
Methanogenesis	$CO_2(aq) + 4H_2 \rightarrow CH_4(aq) + 2H_2O$	−233.6	−138.9	−134.9
Acetogenesis	$2CO_2 + 4H_2 \rightarrow C_2H_3O_2 + H^+ + 2H_2O$	−231.4	−78.8	−72.2
ATP generation	$ADP + P_i + H^+ \rightarrow ATP + H_2O$	24.3	−9.0	−10.4

Data are calculated from values in Table 1.1, except for ATP, which is from Rekharsky *et al.* (1986). Data are not adjusted to pH 7.
g, Gas; aq, dissolved.

The ΔG for this reaction is negative, so the reaction is feasible. Now consider the ΔG for the use of H_2 for acetate production under the same ruminal conditions:

$$\Delta G = \Delta G^\circ + RT \ln\{ [C_3H_3O_2^-] [H^+] [H_2O]^2/([CO_2]_{aq}{}^2 [H_2]^4) \quad (17)$$

$$\Delta G = -72.2 + 0.008314 \times 311 \ln \{0.050 (1 \times 10^{-6.5}) 50^2 / [(0.016)^2(1.6 \times 10^{-3})^4] \} \quad (18)$$

$$\Delta G = -10.4 \text{ kJ mol}^{-1} \quad (19)$$

The ΔG is negative so the reaction is feasible under these conditions. However, the production of ATP was not considered for these reactions. In fact, including energy for ATP production would have shifted the equilibrium, so that more reducing conditions would be needed for acetogenesis.

Thermodynamic Efficiency

For reactions that are very fast and inexpensive to catalyse (i.e. no complex enzyme systems are needed), the reactions can approach equilibrium. The pH buffers discussed earlier represent this type of reaction. However, complex biological pathways have built-in inefficiencies, so that it is not feasible for the reactions to proceed all the way to equilibrium. The efficiency of ATP synthesis can be determined from the concentrations of reactants and products. For example, the efficiencies of some key reactions in the rumen under typical conditions are shown in Table 1.3.

Table 1.3. Free energy of key reactions in the rumen in kJ mol^{-1} under typical ruminal conditions.

Reaction	No. ATP	ΔG_{rxn}	ΔG_{ATP}	ΔG_{Total}	$-\Delta G_{ATP}/\Delta G_{rxn}$
Glucose to acetate	4	−317.7	177.5	−140.2	0.559
Glucose to propionate	4	−321.8	177.5	−144.3	0.552
Glucose to butyrate	3	−312.0	133.1	−178.9	0.427
Glucose to lactate	2	−206.1	88.8	−117.3	0.431
Methanogenesis	1	−67.9	44.4	−23.5	0.653
Acetogenesis	0.2	−8.7	8.9	0.1	1.015
ADP to ATP	1	44.4	–	–	–

Data are calculated from values in Table 1.3 and assuming the following ruminal conditions: [glucose] = 0.1 mmol l^{-1}, [acetate] = 80 mmol l^{-1}, [propionate] = 30 mmol l^{-1}, [butyrate] = 30 mmol l^{-1}, [lactate] = 1 mmol l^{-1}, [CH_4] = 0.3 atm, [CO_2] = 0.7 atm, [H_2O] = 50 mmol l^{-1}, [H_2] = 0.00152 atm, [ATP] = 1 mmol l^{-1}, [ADP][P_i] = 0.002 mmol l^{-1}, and pH = 6.5.

As expected, the efficiency for methanogenesis is higher than that for VFA production. Methane production is a simpler process than VFA formation, so we should not be surprised to learn that less free energy is lost from carrying it out. Methanogenesis can occur at pH 7 and −0.33 V or more negative reducing potential (Wolfe and Higgins, 1979). An equivalent H_2 concentration would be observed at pH 6.5 and –0.30 V reducing potential. Thus, the conditions where methanogenesis can begin to occur are quite similar to the conditions in the rumen, and methanogenesis appears to be thermodynamically limited.

The observed efficiencies for acetate and propionate production are probably near the maximal efficiencies that are feasible, allowing for the necessary losses of heat from fermentation. Thus, the concentrations of acetate and propionate are probably limited by thermodynamics. On the other hand, maximal butyrate efficiency is probably higher than observed. Therefore, this pathway is probably not approaching the concentrations that would be infeasible and it is probably not dependent on product concentration. An efficiency greater than 1.0 is not possible even from the least complex of reactions; therefore reductive acetogenesis would not occur under these ruminal conditions.

The efficiency of lactate production is lower than that of acetate and propionate. Only two ATP are generated via lactate production, and the lactate pathway to produce propionate is thought to produce less ATP than the direct pathway. These less efficient reactions are likely to proceed faster than the more efficient alternatives (Jou and Llebot, 1990). However, they would not be able to proceed at all unless the concentration of reactants relative to products was high. Thus, it is likely that lactate cannot be produced even at the low efficiencies shown here and would not exist under these conditions. If the glucose and VFA concentrations increased (due to a momentary increase in fermentable energy or inhibition of pathways by low pH), lactate synthesis would play a role in rapidly using the available nutrients. Once the microbial population adapted, more propionate producers could compete and reduce glucose levels to again limit lactate production.

Use of Thermodynamics in Dynamic Models

Judging from the previous analysis of the efficiencies of VFA production, it seems appropriate to incorporate thermodynamics into kinetic and dynamic models of fermentation. Acetate, propionate, methane and lactate all seem to be limited by thermodynamics at some time. Dynamic models need to account for these limits so that infeasible concentrations are not predicted. Including thermodynamics will make the models more stable.

Previously, we calculated the efficiencies of free energy utilization for specific metabolite concentrations. Development of dynamic models using thermodynamics requires estimation of the maximum potential efficiencies. The actual efficiency may be lower unless the reactions approach thermodynamic limits. The ΔG at the maximum efficiency is called the threshold free energy

(ΔG_T). It is the ΔG of a reaction when that reaction is as close as it can ever get to zero, but for reactions with built-in inefficiency it is always negative. The ΔG_T is equivalent to the unavoidable losses in free energy (i.e. heat loss from a system) and it can be calculated from a modification of equation 7:

$$\Delta G_T = \Delta G^\circ + RT \ln \{[\text{Products}]_T / [\text{Reactants}]_T\} \quad (20)$$

where $[X]_T$ represents the concentrations of reactant or product X when the system approaches its threshold. When a reaction approaches the threshold ΔG, the forward reaction rate equals the reverse reaction:

$$k_{rxn} [\text{Reactants}] = k_{-rxn} [\text{Products}] \quad (21)$$

where k_{rxn} and k_{-rxn} represent the fractional rate constants. Combining equations 20 and 21 yields a ratio that is analogous to an equilibrium constant for reactions that never obtain equilibrium, due to the inherent inefficiencies and complexities of the system:

$$k_{rxn} / k_{-rxn} = e^{(\Delta G^\circ - \Delta G^\circ T) RT} \quad (22)$$

A dynamic model of glucose fermentation was developed assuming the stochiometry shown in Fig. 1.1 and assuming 56% efficiency of glucose fermentation to acetate, propionate or butyrate and 70% efficiency of methane production. These efficiencies were used to represent the highest efficiencies typically observed for the rumen. The ΔG_T was determined from these assumed efficiencies, and from these values the k_{rxn}/k_{-rxn} was determined for each reaction. Initial concentrations of each metabolite were set to approximate values that were similar to those observed in the rumen. Forward rate constants were set to values such that, when multiplied by each of the reactant concentrations, the resulting fluxes were realistic. The reverse rate constants were calculated as the k_{rxn} (as set previously) divided by the k_{rxn}/k_{-rxn}. Glucose was infused continuously into this system at a rate of 25 mmol h^{-1} l^{-1} and VFA were removed at a fractional rate of 0.40 h^{-1}. As gas pressures exceeded 1 atm, CO_2 and CH_4 were allowed to escape in the proportions that they were predicted to represent in the gas phase.

The results of the simulation to steady state are shown in Table 1.4. Using fermentation balances, Wolin (1960) showed that the stoichiometry of the rumen is balanced, but this solution did not explain the unique combination of metabolites in the rumen. For example, a fermentation of only butyrate and methane can be balanced stoichiometrically, but such a fermentation does not exist. The inclusion of thermodynamics explains the proportions of each VFA and gas that are observed.

The dynamic model can be used to show how ionophores affect ruminal fermentation patterns. Ionophores result in reduced methane, increased propionate and higher pH. They permit ions to penetrate Gram-negative bacteria, such as the acetate producers (Russell and Strobel, 1989). This effect should increase the cost of acetate production by causing the Gram-negative organisms to expend ATP to repair internal ion concentrations. This cost would directly

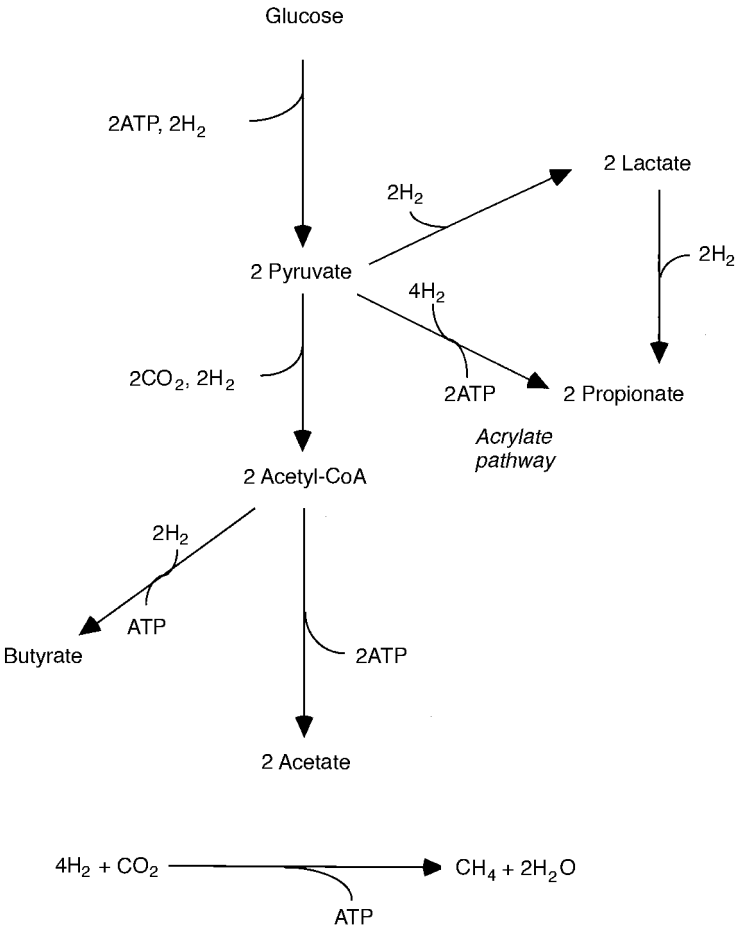

Fig. 1.1. Major fermentation pathways in the rumen (adapted from Prins, 1977).

decrease the threshold ΔG (make it more negative) for acetate and would shift the equilibrium against acetate production. The glucose spared from this shift would further increase propionate production, which would decrease H_2 available for methane.

As the energy density of the diet increases, acetate-to-propionate ratio and methane production decline while H_2 concentration increases. Since methane does not increase in response to the increased H_2, the calculated efficiency for methanogenesis would decrease. This change suggests that the ruminal conditions of high-energy diets make it more energetically expensive to produce methane, causing the efficiency to decline. This change would favour propionate production over methane production. Therefore, the thermodynamics suggest that methanogenesis is inhibited on high-energy diets, thus causing the

Table 1.4. Predicted steady-state concentrations and fluxes for a mathematical model incorporating thermodynamic and kinetic elements.

Metabolite	Concentration
Glucose, mmol l^{-1}	0.15
Acetate, mmol l^{-1}	59.1
Propionate, mmol l^{-1}	38.6
Butyrate, mmol l^{-1}	13.8
CH_4, atm	0.31
CO_2, atm	0.69
H_2, atm	1.3×10^{-3}
Acetate/propionate	1.5

	Flux (mmol substrate used per hour)		
Reaction	Forward	Reverse	Net
Glucose → 2 acetate	15.2	3.6	11.6
Glucose → 2 propionate	11.9	4.2	7.7
Glucose → butyrate	5.4	10^{-16}	5.4
$CO_2 \rightarrow CH_4$	14.4	3.6	10.8

Model assumed 56% maximal free energy efficiency for acetate, propionate and butyrate formation, and 70% maximal efficiency for methane formation, pH 6.5, glucose infusion at 25 mmol l^{-1} h^{-1}, fatty acid removal at 0.40 h^{-1} and gas removal as accumulated in proportion to partial pressures.

shift to propionate (Kohn and Boston, 1995). Recent research supports this hypothesis by suggesting that methanogenesis appears to be inhibited by low pH (Russell, 1998), which could result from rapid fermentation. However, another mechanism could also explain the shift in equilibrium toward propionate. The efficiency of acetate production could also decrease, along with the efficiency of methanogenesis, which would also shift the fermentation toward propionate.

Up until now, microbiologists have preferred to use anthropomorphic explanations to explain fermentation shifts. For example, certain organisms are thought to prefer certain substrates and make certain products. But these explanations do not explain why certain organisms would shift their fermentation or thrive in certain environments. The use of the second law of thermodynamics explains these shifts more systematically, as being caused by changes in the ruminal environment.

References

Baker, S.K. and Dijkstra, J. (1999) Dynamic aspects of the microbial ecosystem of the reticulo-rumen. In: Jung, H.G. and Fahey, G.C. Jr (eds) *Nutritional Ecology of*

Herbivores: Proceedings Vth International Symposium on Nutrition of Herbivores. American Society of Animal Science, Savoy, USA, pp. 261–311.

Baldwin, R.L., Thornley, J.H.M. and Beever, D.E. (1987) Metabolism of the lactating cow. II. Digestive elements of a mechanistic model. *Journal of Dairy Research* 54, 107–131.

Barry, T.N., Thompson, A. and Armstrong, D.G. (1977) Rumen fermentation studies on two contrasting diets. *Journal of Agricultural Science, Cambridge* 89, 183–195.

Chang, R. (1981) The second law of thermodynamics. In: *Physical Chemistry with Applications to Biological Systems,* 2nd edn. Macmillan, New York, pp. 129–163.

CRC (1991) In: *CRC Handbook of Chemistry and Physics*, 71st edn. CRC Press, Cleveland, pp. 5/28–5/55.

Dijkstra, J., Neal, H.D.C., Beever, D.E. and France, J. (1992) Simulation of nutrient digestion, absorption and outflow in the rumen: model description. *Journal of Nutrition* 122, 2239–2256.

Fogg, P.G.T. and Gerrard, W. (1985) In: *Solubility of Gases in Liquids: A Critical Evaluation of Gas/Liquid Systems in Theory and Practice*. John Wiley & Sons, Chichester, pp. 113–127.

Hoh, C. (1996) Modelling of reaction kinetics in anaerobic ecosystems with considerations of thermodynamic principles. PhD dissertation, Murdoch University, Australia.

Jou, D. and Llebot, J.E. (1990) *Introduction to the Thermodynamics of Biological Processes.* Prentice Hall, Englewood Cliffs.

Kohn, R.A. and Boston, R.C. (1995) The feasibility of methanogenesis and acetogenesis in the rumen. *Journal of Dairy Science* Suppl. 445 (Abstr.).

Kohn, R.A. and Dunlap, T.F. (1998) Calculation of the buffering capacity of bicarbonate in the rumen and *in vitro*. *Journal of Animal Science* 76, 1702–1709.

Kohn, R.A., Boston, R.C., Ferguson, J.D. and Chalupa, W. (1995) The integration and comparison of dairy cow models. In: Danfær, A. and Lescoat, P. (eds) *Proceedings of the IVth International Workshop on Modelling Nutrient Utilization in Farm Animals, 3–5 October, 1994, Viborg, Denmark*. Tiele, Denmark.

Murphy, M.R., Baldwin, R.L. and Koong, L.J. (1982) Estimation of stoichiometric parameters for rumen fermentation of roughage and concentrate diets. *Journal of Animal Science* 55, 411–421.

Neal, H.D.C., Dijkstra, J. and Gill, M. (1992) Simulation of nutrient digestion, absorption and outflow in the rumen: model evaluation. *Journal of Nutrition* 122, 2257–2272.

Prins, R.A. (1977) Biochemical activities of gut micro-organisms. In: Clarke, R.T.J. and Bauchop, T. (eds) *Microbial Ecology of the Gut.* Academic Press, New York, pp. 73–184.

Rekharsky, M.V., Galchenko, G.L., Egorov, A.M. and Berenzin, I.V. (1986) Thermodynamics of enzymatic reactions. In: Hinz, H.-J. (ed.) *Thermodynamic Data for Biochemistry and Biotechnology*. Springer-Verlag, Berlin, pp. 431–444.

Russell, J.B. (1998) The importance of pH in the regulation of ruminal acetate to propionate ratio and methane production *in vitro*. *Journal of Dairy Science* 81, 3222–3230.

Russell, J.B. and Strobel, H.J. (1989) Effect of ionophores on ruminal fermentation. *Applied Environmental Microbiology* 55, 1–6.

Segel, I.H. (1976) *Biochemical Calculations*, 2nd edn. John Wiley & Sons, New York.

Wolfe, R.S. and Higgins, I.J. (1979) Microbial biochemistry of methane – a study in contrasts. *Microbial Biochemistry* 21, 267–353.

Wolin, M.J. (1960) A theoretical rumen fermentation balance. *Journal of Dairy Science* 40, 1452–1459.

2

Modelling Lipid Metabolism in the Rumen

Jan Dijkstra,[1] Walter J.J. Gerrits,[1] Andre Bannink[2] and James France[3]

[1]*Animal Nutrition Group, Wageningen Institute of Animal Sciences (WIAS), Wageningen University, Marijkeweg 40, 6709 PG Wageningen, The Netherlands;* [2]*ID-Lelystad, Department of Animal Nutrition, PO Box 65, 8200 AB Lelystad, The Netherlands;* [3]*Department of Agriculture, University of Reading, Earley Gate, Reading RG6 6AT, UK*

Abstract

Nutritional manipulation through fat supplementation of diets is of interest because of the large energy requirements of high-producing ruminants, and because of human health concerns about saturated long-chain fatty acids (LCFA) in ruminant products. High dietary fat levels may adversely affect microbial activity and nutrient degradation in the rumen. Mathematical models of the rumen fermentation process have been developed and applied to quantify the profile of nutrients available for absorption. However, the representation of lipid dynamics is limited in these rumen models. Therefore, an extant rumen model was modified to represent the effects of LCFA on microbial metabolism and nutrient digestion. The primary objective of the model currently being developed is to integrate LCFA metabolism with microbial metabolism of other substrates in the rumen, and to predict the effect of amount and composition of dietary fat upon the profile of nutrients available for absorption.

In the modified model, there are three rumen lipid pools: unhydrolysed lipid (Li), saturated free LCFA (Fs) and unsaturated free LCFA (Fu). Inputs to these pools are from the feed and outputs are flows to the duodenum. The rate of biohydrogenation is dependent on the amount of fibre and of unsaturated LCFA in the rumen. The unsaturated LCFA are considered to inhibit fibrolytic bacterial metabolism, but not amylolytic bacterial metabolism, whilst saturated LCFA are assumed not to affect bacterial metabolism. Protozoal metabolism is assumed to be inhibited by both saturated and unsaturated LCFA. The rates of biohydrogenation and inhibition of bacterial metabolism are represented by sigmoidal Michaelis–Menten equations, with

 Modelling Nutrient Utilization in Farm Animals (eds J.P. McNamara, J. France and D.E. Beever)

parameters derived from *in vitro* and *in vivo* data. Preliminary results of sensitivity analyses suggest that the model responds appropriately to perturbations in dietary inputs. The degradation of fibre in the rumen was reduced when the amount of unsaturated LCFA in the diet was raised, but the reduction in fibre degradation was far more pronounced with a low forage diet in comparison to a high forage diet. In all cases, the efficiency of microbial growth was increased upon an increase in dietary LCFA content because of a reduction in protozoal numbers and consequently in microbial recycling within the rumen. Decreasing the forage proportion of the diet decreases the degree of saturation of LCFA flowing to the duodenum. A decrease in acetate to propionate ratio in rumen fluid was only apparent when a diet high in unsaturated LCFA was fed. Such responses are related to the effects of unsaturated LCFA and saturated LCFA on metabolism of amylolytic and fibrolytic bacteria and of protozoa, and consequently on nutrient degradation in the rumen.

Introduction

Long-chain fatty acids (LCFA) are a potentially useful energy source for cattle. However, dietary fat levels should not exceed some 50–70 g kg^{-1} dry matter (DM) (reviewed by Palmquist and Jenkins, 1980), as higher levels may adversely affect microbial activity and nutrient degradation in the rumen. The magnitude of this negative effect depends, amongst other things, on the degree of saturation of the LCFA. Unsaturated LCFA have been shown to inhibit fermentation more than saturated LCFA (Henderson, 1973; Maczulak *et al.*, 1981). In the rumen, extensive biohydrogenation of unsaturated LCFA occurs, but biohydrogenation may be reduced when the amount of dietary fibre is small or the amount of unsaturated LCFA is high (reviewed by Harfoot and Hazlewood, 1997). These events in the rumen have a profound effect on the type of LCFA subsequently presented to the small intestine for digestion and ultimately on the LCFA composition of fat in milk and meat. The degree of saturation of LCFA in milk and meat has implications for human health, including cardiovascular diseases (Grundy, 1990) and cancer (Parodi, 1997).

Despite the impact of dietary LCFA on rumen metabolism, its representation has received only limited attention in extant mechanistic models of rumen fermentation. Lipid has not been included in the rumen models of Baldwin *et al.* (1970), France *et al.* (1982) and Lescoat and Sauvant (1995). Other models have a crude representation of lipid metabolism in the rumen, representing input from the diet, outflow to the duodenum and incorporation of LCFA into microbial lipid (Black *et al.*, 1981; Baldwin *et al.*, 1987; Danfær, 1990; Dijkstra *et al.*, 1992, 1996; Dijkstra, 1994). Biohydrogenation of unsaturated LCFA has been represented in the model of Baldwin *et al.* (1977) during computation of methane production, but mathematical equations or any further details were not provided. The model of Baldwin (1995) is the only one that represents the inhibition of fibre degradation and the enhanced microbial growth efficiency by

added fat, though independent of the degree of LCFA saturation. Baldwin (1995) admitted that the empirical representation of these effects is tentative and that further modelling research is required.

The present chapter describes relevant parts of a rumen model currently being developed that mathematically represents LCFA biohydrogenation and incorporation of LCFA into microbial lipids and inhibition of substrate degradation by LCFA in the rumen. This model is based upon the rumen model developed and evaluated by Dijkstra *et al.* (1992). The primary objective of the model currently being developed is to integrate LCFA metabolism with microbial metabolism of other substrates in the rumen, and to predict the effect of amount and composition of dietary fat on the profile of nutrients available for absorption, including the degree of saturation of LCFA flowing to the duodenum. Preliminary results of simulations will be presented as well.

Description of the Model

General structure

The model is modified from the mechanistic, dynamic rumen model described by Dijkstra *et al.* (1992). The original model comprised 17 state variables, representing nitrogen, carbohydrate, lipid, microbial and volatile fatty acid (VFA) pools in the rumen. A single differential equation for each state variable described the rate of change of pool size (Q_i) with time, dQ_i/dt. The differential equations were integrated numerically for given initial conditions and parameter values, assuming a continuous input of nutrients. The concentration of each rumen entity (C_i) is calculated as the pool size divided by rumen volume.

The original model included a crude representation of LCFA dynamics by a lipid pool that receives input from the feed and from lipid released upon the death of microbes in the rumen, and with a single output of lipids being washed out from the rumen. In evaluation of this model, Neal *et al.* (1992) noticed that the model was not suitable for evaluating high-lipid diets, because of the absence of an inhibitory effect of lipid on fibre degradation in the rumen. In the present model, the original lipid pool is replaced by three pools: unhydrolysed lipid (Li), saturated free LCFA (Fs) and unsaturated free LCFA (Fu) in the rumen. These pools and the associated fluxes are shown in Fig. 2.1. The pools are expressed in moles and molecular masses of lipid and free LCFA, assumed to be 675 and 284 g, respectively. In addition to the nutrient inputs of the original model, inputs related to amount and saturation of fat have to be specified, namely, the dietary concentration of Li, Fs and Fu, and the amount of Fs and Fu in dietary Li. In contrast to the original model, the present model also includes a representation of the inhibitory effect of LCFA on microbial metabolism and fibre degradation in the rumen.

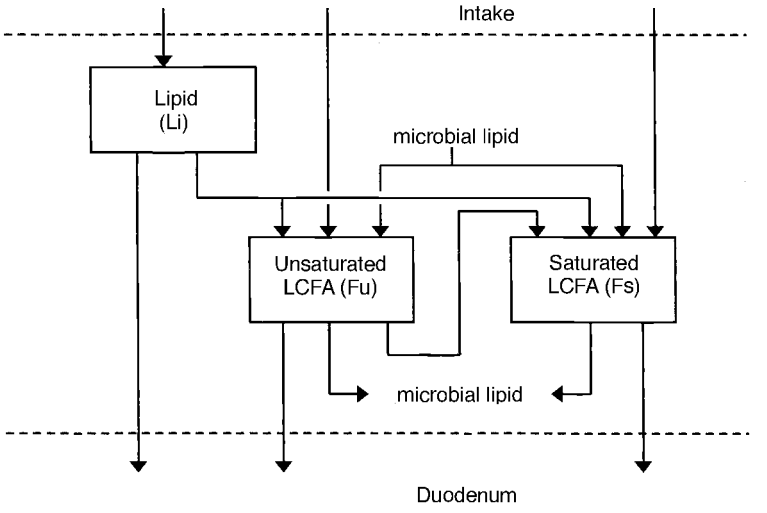

Fig. 2.1. Diagrammatic representation of the lipid and free LCFA pools of the modified rumen model. Boxes enclosed by solid lines indicate state variables and arrows indicate fluxes.

Lipid pool, Q_{Li}

The only input to the rumen lipid pool is from the feed. Upon the death and lysis of microbes in the rumen, microbial lipids will be released into the rumen fluid as well. However, in line with the assumptions made in the original model with respect to the instantaneous hydrolysis of microbial protein and storage polysaccharides, it is assumed that these lipids are immediately hydrolysed and are input to the Fs and Fu pool. There are two outputs from the Li pool: hydrolysis of lipid to free LCFA (Fs and Fu) and outflow to the duodenum with the solid material. The corresponding flux equations are described by mass-action forms. The hydrolysis of unprotected feed lipids by microbial enzymes is extensive (Jenkins, 1993; Harfoot and Hazlewood, 1997). The fractional hydrolysis rate is assumed to be nine times the fractional solid passage rate, which will result in a predicted extent of lipid hydrolysis of 90% of the total outflow. If protected lipid is included in the diet, the fractional hydrolysis rate will have to be adjusted. For example, when extruded fat is included, the fractional hydrolysis rate may be set at 2.3 times the fractional solid passage rate, resulting in 70% lipid hydrolysis, as observed (Ashes *et al.*, 1997).

Saturated free LCFA pool, Q_{Fs}

There are four inputs to this pool. These are Fs arising from free LCFA in the diet, from hydrolysis of dietary lipid, from biohydrogenation of unsaturated LCFA and from LCFA released upon the death and lysis of microbes in the rumen. The lipid content of the polysaccharide-free microbial DM is assumed constant (0.143 g g^{-1} DM; Dijkstra *et al.*, 1992). The LCFA fraction (0.70 g g^{-1} microbial lipid; Reichl and Baldwin, 1975) and the saturated LCFA fraction (0.80 g g^{-1} microbial LCFA; Harfoot and Hazlewood, 1997) are also assumed to be constant. Although the amount and composition of supplemental dietary fat may affect the lipid composition of microbial DM (Bauchart *et al.*, 1990; O'Kelly and Spiers, 1991), a fixed composition has been chosen, since it is unknown what proportion of the microbial LCFA is adherent as opposed to incorporated. Details on the biohydrogenation of unsaturated LCFA are described in the Fu pool section.

The two outputs from this pool represent incorporation of saturated LCFA into microbial lipid for growth purposes and outflow from the rumen with the solid material. The LCFA requirements per unit microbial growth have been calculated based on the lipid composition of microbial DM described previously and on the assumption that 20% of the microbial LCFA result from the uptake of preformed LCFA (Harfoot and Hazlewood, 1997). To ensure that microbial uptake of Fs and Fu is smaller than the amount available, Fu and Fs affinity constants, which are assigned low values, were added to those Michaelis–Menten equations in the model that represent the uptake of hexose for microbial growth.

Unsaturated free LCFA pool, Q_{Fu}

There are three inputs to this pool: Fu arising from free LCFA in the diet, from hydrolysis of dietary lipid and from LCFA released upon the death and lysis of microbes in the rumen, with assumptions and parameter values described in the Fs pool section. The three outputs from this pool represent incorporation of unsaturated LCFA into microbial lipid for growth purposes, biohydrogenation to saturated LCFA and outflow from the rumen with the solid material.

Generally, unsaturated LCFA are rapidly hydrogenated by microbes (Jenkins, 1993; Harfoot and Hazlewood, 1997). As in the Li pool, the maximal rate of biohydrogenation is assumed to be nine times the fractional solid passage rate, which will result in a predicted maximum extent of biohydrogenation of 90% of total unsaturated LCFA flux. Most of biohydrogenation occurs on food particles (Harfoot *et al.*, 1973). The results of *in vitro* experiments indicate that, in contrast to readily fermentable carbohydrate sources, the amount of fibre positively affects rate of biohydrogenation (Latham *et al.*, 1972; Gerson *et al.*, 1985). Whilst many bacterial species are capable of hydrogenating polyunsaturated LCFA to monounsaturated LCFA, only a few species can hydrogenate the monounsaturated LCFA to saturated LCFA (reviewed by Harfoot and Hazlewood, 1997). These differences in hydrogenation help to explain that

increases in the concentration of polyunsaturated LCFA increase the formation of monounsaturated LCFA, but decrease the formation of saturated LCFA (Noble *et al.*, 1974; Fellner *et al.*, 1995). In the model, biohydrogenation is represented by a Michaelis–Menten-type equation, in which the concentration of fibre in the rumen non-sigmoidally stimulates the biohydrogenation rate, and the concentration of unsaturated LCFA inhibits the biohydrogenation rate in a sigmoidal way (Fig. 2.2). The parameters of this function are estimated using data on duodenal flows of fibre, microbial N, saturated and unsaturated LCFA (Klusmeyer and Clark, 1991; Doreau *et al.*, 1993; Ferlay *et al.*, 1993; Klusmeyer *et al.*, 1993; Pantoja *et al.*, 1994, 1996; Kalscheur *et al.*, 1997a, b), applying the assumptions related to maximal rate of biohydrogenation and microbial composition as described previously and a proper solid passage rate. Note that it is assumed that all unsaturated LCFA are equally susceptible to biohydrogenation and that incomplete hydrogenation of unsaturated LCFA is not represented in the model.

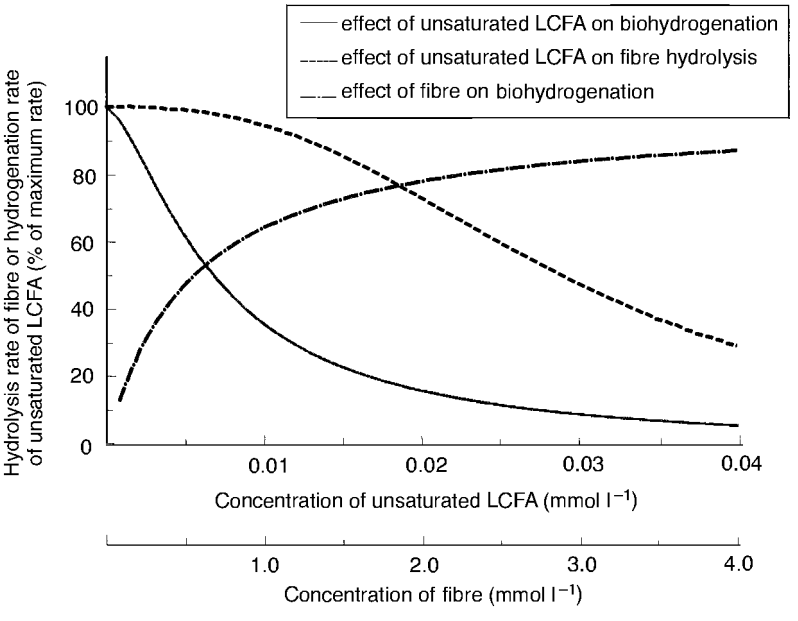

Fig. 2.2. Effect of the concentration of unsaturated LCFA and of fibre on rate of biohydrogenation of unsaturated LCFA and of the concentration of unsaturated LCFA on hydrolysis of fibre as adopted in the modified model.

Inhibitory effect of LCFA on microbial metabolism

The inhibitory effect of LCFA on microbial metabolism depends on the type of LCFA and the microbial species. In general, unsaturated LCFA are far more detrimental to bacterial growth than saturated LCFA, and fibrolytic bacteria and protozoa are more affected by LCFA than amylolytic bacteria (see reviews of Jenkins, 1993; Doreau and Ferlay, 1995; Harfoot and Hazlewood, 1997). Therefore, in the model it is assumed that LCFA inhibit the growth of fibrolytic bacteria and of protozoa, but not that of amylolytic bacteria.

With respect to the fibrolytic bacteria, unsaturated LCFA (but not saturated LCFA) are assumed to inhibit the hydrolysis rate of potentially degradable fibre. This inhibition is represented using a sigmoidal Michaelis–Menten equation, to ensure that at low concentrations of unsaturated LCFA metabolism is only slightly reduced, whereas at higher concentrations metabolism will be progressively reduced (see Fig. 2.2). The inhibition constant and steepness parameter are estimated by non-linear regression from an *in vitro* experiment (Maczulak *et al.*, 1981), using the data on growth of fibrolytic bacterial species expressed as a fraction of the uninhibited growth, in response to variations in oleic acid additions to the medium. The effect of oleic acid is assumed to be representative for all unsaturated LCFA, because the effects of chain length and of the number of double bonds of the LCFA on fibrolytic growth are variable and controversial (reviewed by Doreau and Ferlay, 1995). *In vivo*, the presence of feed particles permits much higher concentrations of unsaturated LCFA than *in vitro* (reviewed by Harfoot and Hazlewood, 1997) and the inhibition constant calculated based on the *in vitro* data is multiplied by an arbitrarily chosen value of 270, to be applied in the model.

Fat addition decreases protozoal populations, but no clear differences have been found due to degree of LCFA saturation or chain length (reviewed by Doreau and Ferlay, 1995). Therefore, in the model it is assumed that both saturated and unsaturated LCFA inhibit protozoal metabolism. This inhibition is represented by a linear reduction of the fraction of protozoa in the amylolytic microbial pool with increased dietary LCFA contents when dietary LCFA exceed 40 g kg^{-1} DM. The slope of the equation is estimated based on the observed protozoal concentrations in cattle (as a percentage of the control), as summarized by Doreau and Ferlay (1995).

Results and Discussion

The behaviour of the model being developed was examined with respect to the roughage proportion of the diet, the dietary lipid content and the degree of saturation of the dietary LCFA. The diets consisted of various amounts of hay and concentrate (in a DM ratio of 80 : 20 and 33 : 67, respectively), fed continuously at 17 kg DM day^{-1} for a dairy cow. The contents of the hay were (in g kg^{-1} DM): neutral detergent fibre (NDF), 520; starch, 0; soluble sugars, 100; N, 22. The

contents of the concentrate were (in g kg^{-1} DM): NDF, 200; starch, 350; soluble sugars, 100; N, 28. The lipid content of the diets was set at an average and a high level (40 and 80 g kg^{-1} DM, respectively), with corresponding LCFA contents of 28 and 62 g kg^{-1} DM. The degree of saturation of dietary LCFA was set at a low (20%) and a high (80%) level. Some preliminary results are presented in Table 2.1.

The simulations showed a pronounced effect of the dietary lipid content on rumen fermentation and nutrient outflow. However, in line with general observations (see reviews by Jenkins, 1993; Doreau and Ferlay, 1995), the effect was dependent on the roughage proportion of the diet and the degree of saturation of dietary LCFA. Upon a doubling of the lipid content from 40 to 80 g kg^{-1} DM and at a low degree of dietary LCFA saturation (20%), ruminal NDF degradation was substantially reduced with the low-roughage diet (from 55.3 to 50.0%) but less so with the high-roughage diet (from 66.6 to 65.0%). In contrast to a low degree of dietary LCFA saturation, an increase of dietary lipid that contained a high proportion of saturated LCFA resulted in a small increase of ruminal NDF degradation. This increase is a result of the assumption in the model that only unsaturated LCFA inhibit fibrolytic bacterial metabolism, but both unsaturated and saturated LCFA inhibit protozoal metabolism. The reduced protozoal metabolism decreases the engulfment of bacteria, giving rise to a higher amount of fibrolytic bacteria and, in turn, higher NDF degradation. In line with observations (Doreau and Ferlay, 1995), the efficiency of microbial protein synthesis is increased as well, as can be seen from the much larger relative decrease in NDF degradation than in microbial N flow upon an increase in unsaturated LCFA content. The acetate-to-propionate ratio in rumen fluid did not vary in response to changes in dietary lipid and degree of saturation when the high roughage diet was fed. The ratio was slightly smaller when the high-lipid diet with a low degree of LCFA saturation was fed.

The apparent degree of saturation of duodenal LCFA was reduced upon an increase in dietary unsaturated LCFA. This result is qualitatively in line with observations and is caused by the inhibitory effect of excess unsaturated LCFA on biohydrogenation (Noble *et al.*, 1974; Fellner *et al.*, 1995; Kalscheur *et al.*, 1997b). The high-roughage diet resulted in an elevated concentration of fibre in rumen fluid compared with the low-roughage diet and, since the presence of fibre promotes biohydrogenation of unsaturated LCFA (Latham *et al.*, 1972; Gerson *et al.*, 1985), the apparent degree of duodenal LCFA saturation also increased upon an increase in roughage proportion of the diet. The simulated effect of dietary roughage on the biohydrogenation of unsaturated LCFA was similar to that observed by Pantoja *et al.* (1996), in which the observed rumen fluid pH was not changed (Pantoja *et al.*, 1994), but was less pronounced than that observed by Kalscheur *et al.* (1997a), in which pH was observed to be lower with the low-forage diet. A reduced pH may lower the rate of hydrolysis of dietary lipid and thus may increase the protection against biohydrogenation (reviewed by Jenkins, 1993), but this effect was not represented in the model. The simulated apparent biohydrogenation of unsaturated LCFA was relatively

Table 2.1. Simulated degradation of neutral detergent fibre (NDF) and ratio of acetic to propionic acid in the rumen, flow of lipid and microbial non-ammonia nitrogen (NAN) to the duodenum, apparent degree of saturation of LCFA flowing to the duodenum, and biohydrogenation of unsaturated LCFA of cows fed low-roughage (33% hay, 67% concentrate on DM basis) or high-roughage (80% hay, 20% concentrate on DM basis) diets that contained 40 or 80 g lipid kg^{-1} DM and with 20 or 80% of dietary LCFA being saturated.

	Diet							
	Low roughage: dietary lipid content				High roughage: dietary lipid content			
	40 (g kg^{-1} DM): degree of LCFA saturation		80 (g kg^{-1} DM): degree of LCFA saturation		40 (g kg^{-1} DM): degree of LCFA saturation		80 (g kg^{-1} DM): degree of LCFA saturation	
	20%	80%	20%	80%	20%	80%	20%	80%
Ruminal NDF degradation (%)	55.3	55.5	50.0	56.5	66.6	66.6	65.0	66.8
Ratio of acetic to propionic acid in rumen	2.4	2.4	2.3	2.4	4.7	4.7	4.7	4.7
Duodenal flow of:								
Lipid (g day^{-1})	890	890	1489	1499	911	912	1514	1520
Microbial N (g day^{-1})	251.4	251.8	249.6	260.6	289.1	289.2	290.0	295.6
Apparent degree of duodenal LCFA saturation (%)	71.9	88.8	61.7	90.4	72.8	88.5	62.7	90.5
Biohydrogenation of unsaturated LCFA (%)	64.9	43.9	52.2	52.1	66.0	42.2	53.4	52.5

small when the diet contained little unsaturated LCFA, because of the assumption in the model that unsaturated LCFA are incorporated in microbial lipids in a fixed saturated-to-unsaturated LCFA ratio.

Conclusions

The modified model of rumen fermentation simulates the effects of amount and degree of saturation of dietary LCFA on nutrient degradation and biohydrogenation of LCFA in the rumen. Preliminary simulation results indicate that the model responds properly to changes in dietary roughage proportion, lipid content and LCFA saturation. Such responses are related to the respective effects of saturated and unsaturated LCFA on fibrolytic and amylolytic bacterial and protozoal metabolism. After further evaluation, the model may be used to help devise diets that will result in a desired degree of saturation of LCFA in duodenal contents and in milk or meat, beneficial to the animal and to the consumer.

References

Ashes, J.R., Gulati, S.K. and Scott, T.W. (1997) Potential to alter the content and composition of milk fat through nutrition. *Journal of Dairy Science* 80, 2204–2212.

Baldwin, R.L. (1995) *Modelling Ruminant Digestion and Metabolism*. Chapman & Hall, London, 578 pp.

Baldwin, R.L., Lucas, H.L. and Cabrera, R. (1970) Energetic relationships in the formation and utilization of fermentation end-products. In: Phillipson, A.T., Annison, E.F., Armstrong, D.G., Balch, C.C., Comline, R.S., Hardy, R.S., Hobson, P.N. and Keynes, R.D. (eds) *Physiology of Digestion and Metabolism in the Ruminant*. Oriel Press, Newcastle upon Tyne, pp. 319–334.

Baldwin, R.L., Koong, L.J. and Ulyatt, M.J. (1977) A dynamic model of ruminant digestion for evaluation of factors affecting nutritive value. *Agricultural Systems* 2, 255–288.

Baldwin, R.L., Thornley, J.H.M. and Beever, D.E. (1987) Metabolism of the lactating cow. II. Digestive elements of a mechanistic model. *Journal of Dairy Research* 54, 107–131.

Bauchart, D., Legay-Carmier, F., Doreau, M. and Gaillard, B. (1990) Lipid metabolism of liquid-associated and solid-associated bacteria in rumen contents of dairy cows offered lipid-supplemented diets. *British Journal of Nutrition* 63, 563–578.

Black, J.L., Beever, D.E., Faichney, G.J., Howarth, B.R. and Graham, N.McC. (1981) Simulation of the effects of rumen function on the flow of nutrients from the stomach of sheep: part 1 – description of a computer program. *Agricultural Systems* 6, 195–219.

Danfær, A. (1990) A dynamic model of nutrient digestion and metabolism in lactating dairy cows. PhD thesis, National Institute of Animal Science, Foulum, Denmark.

Dijkstra, J. (1994) Simulation of the dynamics of protozoa in the rumen. *British Journal of Nutrition* 72, 679–699.

Dijkstra, J., Neal, H.D.StC., Beever, D.E. and France, J. (1992) Simulation of nutrient

digestion, absorption and outflow in the rumen: model description. *Journal of Nutrition* 122, 2239–2256.
Dijkstra, J., France, J., Neal, H.D.StC., Assis, A.G., Aroeira, L.J.M. and Campos, O.F. (1996) Simulation of digestion in cattle fed sugar cane: model development. *Journal of Agricultural Science, Cambridge* 127, 231–246.
Doreau, M. and Ferlay, A. (1995) Effect of dietary lipids on nitrogen metabolism in the rumen: a review. *Livestock Production Science* 43, 97–110.
Doreau, M., Ferlay, A. and Elmeddah, Y. (1993) Organic matter and nitrogen digestion by dairy cows fed calcium salts of rapeseed oil fatty acids or rapeseed oil. *Journal of Animal Science* 71, 499–504.
Fellner, V., Sauer, F.D. and Kramer, J.K.G. (1995) Steady-state rates of linoleic acid biohydrogenation by ruminal bacteria in continuous culture. *Journal of Dairy Science* 78, 1815–1823.
Ferlay, A., Chabrot, J., Elmeddah, Y. and Doreau, M. (1993) Ruminal lipid balance and intestinal digestion by dairy cows fed calcium salts of rapeseed oil fatty acids or rapeseed oil. *Journal of Animal Science* 71, 2237–2245.
France, J., Thornley, J.H.M. and Beever, D.E. (1982) A mathematical model of the rumen. *Journal of Agricultural Science, Cambridge* 99, 343–353.
Gerson, T., John, A. and King, A.S.D. (1985) The effects of dietary starch and fibre on the *in vitro* rates of lipolusis and hydrogenation by sheep rumen digesta. *Journal of Agricultural Science, Cambridge* 105, 27–30.
Grundy, S.M. (1990) *Trans* monounsaturated fatty acids and serum cholesterol levels. *New England Journal of Medicine* 323, 480–481.
Harfoot, C.G. and Hazlewood, G.P. (1997) Lipid metabolism in the rumen. In: Hobson, P.N. and Stewart, C.S. (eds) *The Rumen Microbial Ecosystem,* 2nd edn. Blackie Academic & Professional, London, pp. 382–426.
Harfoot, C.G., Noble, R.C. and Moore, J.H. (1973) Food particles as a site for biohydrogenation of unsaturated fatty acids in the rumen. *Biochemical Journal* 132, 829–832.
Henderson, C. (1973) The effects of fatty acids on pure cultures of rumen bacteria. *Journal of Agricultural Science, Cambridge* 81, 107–112.
Jenkins, T.C. (1993) Lipid metabolism in the rumen. *Journal of Dairy Science* 76, 3851–3863.
Kalscheur, K.F., Teter, B.B., Piperova, L.S. and Erdman, R.A. (1997a) Effect of dietary forage concentration on duodenal flow of *trans*-C18:1 fatty acids and milk fat production in dairy cows. *Journal of Dairy Science* 80, 2104–2114.
Kalscheur, K.F., Teter, B.B., Piperova, L.S. and Erdman, R.A. (1997b) Effect of fat source on duodenal flow of *trans*-C18:1 fatty acids and milk fat production in dairy cows. *Journal of Dairy Science* 80, 2115–2126.
Klusmeyer, T.H. and Clark, J.H. (1991) Effects of dietary fat and protein on fatty acid flow to the duodenum and in milk produced by dairy cows. *Journal of Dairy Science* 74, 3055–3067.
Klusmeyer, T.H., Lynch, G.L., Clark, J.H. and Nelson, D.R. (1993) Effects of calcium salts of fatty acids and protein source on ruminal fermentation and nutrient flow to duodenum of cows. *Journal of Dairy Science* 74, 2206–2219.
Latham, M.J., Storry, J.E. and Sharpe, M.E. (1972) Effect of low-roughage diets on the microflora and lipid metabolism in the rumen. *Applied Microbiology* 24, 871–877.
Lescoat, P. and Sauvant, D. (1995) Development of a mechanistic model for rumen digestion validated using the duodenal flux of amino acids. *Reproduction Nutrition Développement* 35, 45–70.

Maczulak, A.E., Dehority, B.A. and Palmquist, D.L. (1981) Effects of long-chain fatty acids on growth of rumen bacteria. *Applied and Environmental Microbiology* 42, 856–862.

Neal, H.D.StC., Dijkstra, J. and Gill, M. (1992) Simulation of nutrient digestion, absorption and outflow in the rumen: model evaluation. *Journal of Nutrition* 122, 2257–2272.

Noble, R.C., Moore, J.H. and Harfoot, C.G. (1974) Observations on the pattern of biohydrogenation of esterified and unesterified linoleic acid in the rumen. *British Journal of Nutrition* 31, 99–108.

O'Kelly, J.C. and Spiers, W.G. (1991) Influence of host diet on the concentrations of fatty acids in rumen bacteria from cattle. *Australian Journal of Agricultural Research* 42, 243–252.

Palmquist, D.L. and Jenkins, T.C. (1980) Fat in lactation rations: a review. *Journal of Dairy Science* 63, 1–14.

Pantoja, J., Firkins, J.L., Eastridge, M.L. and Hull, B.L. (1994) Effects of fat saturation and source of fibre on site of nutrient digestion and milk production by lactating dairy cows. *Journal of Dairy Science* 77, 2341–2356.

Pantoja, J., Firkins, J.L., Eastridge, M.L. and Hull, B.L. (1996) Fatty acid digestion in lactating dairy cows fed fats varying in degree of saturation and different fiber sources. *Journal of Dairy Science* 79, 575–584.

Parodi, P.W. (1997) Cows' milk fat components as potential anticarcinogenic agents. *Journal of Nutrition* 127, 1055–1060.

Reichl, J.R. and Baldwin, R.L. (1995) Rumen modelling: rumen input-output models. *Journal of Dairy Science* 58, 879–890.

3

Towards a More Accurate Representation of Fermentation in Mathematical Models of the Rumen

B.N. Nagorcka,[1] G.L.R. Gordon[2] and R.A. Dynes[3]

[1]*CSIRO Animal Production, PO Box 1600, Canberra, ACT 2600, Australia;* [2]*CSIRO Animal Production, Locked Bag 1, Delivery Centre, Blacktown, NSW 2148, Australia;* [3]*CSIRO Animal Production, Private Mail Bag, PO, Wembley, WA 6014, Australia*

Abstract

Most mathematical models of the rumen make use of empirical stoichiometric equations to predict the production of fermentation products in the rumen. These models are based on a one, two and three microbial group representation of the total rumen microbial population. The prediction of total VFA concentration by these models is considered to be satisfactory but the predictions of the molar proportions of different VFAs are considered to be inaccurate. A number of possible reasons for this have been suggested, including an inadequate representation of VFA absorption and the effects of pH. We believe the main reason for this lies in the fact the fermentation stoichiometries used by all the models are dependent only on substrate and are otherwise independent of the different microbial groups. Therefore we attempted to improve the predictions of the VFA proportions by developing a new set of fermentation stoichiometries which are dependent both on substrate and the different fermentation pathways characterizing the different microbial groups.

We collected information from the literature concerning the range of substrates and biochemical pathways for fermentation, by 16 different microbial groups present in the rumen. This information was used to define the preferred substrates and a stoichiometry for fermentation for each group. A weighted combination of these stoichiometries was then formed using information about their cellular size and relative numbers in the total microbial population to finally obtain stoichiometries representing the fermentation of a range of substrates by three microbial groups,

 Modelling Nutrient Utilization in Farm Animals (eds J.P. McNamara, J. France and D.E. Beever)

namely, the amylolytic bacteria, cellulolytic bacteria and protozoa. The rumen model of Dijkstra was then modified to incorporate a new submodel for fermentation. Input parameters to classify diets as roughage, concentrate or mixed are no longer used. We evaluated the modified model using several of published data sets. The fermentation submodel resulted in an immediate and significant improvement in the predictions of the VFA proportions.

Introduction

The organic matter which undergoes fermentation in the rumen is converted into a range of products, including volatile fatty acids (VFAs), carbon dioxide (CO_2), hydrogen (H_2), and ammonia. Almost all the hydrogen is subsequently converted into methane and expelled. A substantial amount of the digestible energy is absorbed, in the form of VFAs produced during fermentation, from the rumen and the small intestine (Sutton, 1985). The proportions of the VFAs in the form of acetic, propionic and butyric acid are also important in determining both the amount and the composition of milk produced (reviewed by Sutton, 1985; Thomas and Martin, 1988). The ammonia produced as a result of fermentation becomes available for the growth of the rumen microbes. The importance of all the fermentation products means that mathematical models of the rumen must be able to predict accurately their rate of production in the rumen.

The performance of rumen models has been reviewed by Dijkstra and France (1996). Mathematical models of the rumen, such as those of Baldwin *et al.* (1987) and Dijkstra *et al.* (1992), have been demonstrated to provide useful predictions of the total VFAs produced (mean square prediction error (MSPE) between 10% and 15%). The model by Dijkstra *et al.* (1992) has also been shown to give reasonable predictions of methane production, while that by Baldwin *et al.* (1987) significantly overestimates the production of methane, according to the estimates of Benchaar *et al.* (1998). The predictions of the different proportions of VFAs and of ammonia, on the other hand, have been poor in virtually all models (Neal *et al.*, 1992; Dijkstra, 1994a; Dijkstra and France, 1996). In this chapter, we wish to reconsider the capacity of these models, in particular that by Dijkstra *et al.* (1992), to predict the products of fermentation. Although Dijkstra (1994a) has identified a number of areas which may be the source of the unsatisfactory performance, in this chapter we will focus on the fermentation stoichiometry, which will be derived using the quantitative structure chosen to represent the microbial population in the rumen.

Representation of the Total Microbial Population in the Rumen

There are hundreds of different microbial species and strains making up the total population of microbes in the rumen (Hungate, 1966). Some of the main

microbial species in the total population have been listed by Baldwin and Allison (1983) and classified according to their primary substrate. Most of the species listed are able to ferment two or more substrates and there is competition between species for substrates. Some of the major metabolic pathways involved in fermentation of the substrates have been identified. In general, the pathways involved will depend on the substrate and the combination of enzymes that characterize the microbial species (Baldwin, 1995).

Other important differences exist between species, such as their capacity to attach to feed particles, their nutrient requirements for growth, their capacity to prey (via engulfment) on other species and their dependencies on other species. Ideally, all of these aspects of the total population should be represented in a quantitative description. In practice, a minimum level of approximation to meet the required goals is always sought. The desired goals for most rumen models designed for practical use are to predict with reasonable accuracy the rate at which digestible degraded and digestible undegraded nutrients reach the lower gut, as well as the rate at which nutrients are absorbed from the rumen.

The early efforts to develop a mathematical model of the rumen considered the microbial population as a single mass (state variable) (Baldwin *et al.*, 1977a; Black *et al.*, 1981; France *et al.*, 1982). Although Baldwin *et al.* (1987) also considered the microbial mass as a single variable, they introduced a differential attachment of microbes to large and small feed particles, as well as different outflow rates for the attached and unattached components. More recent models (Dijkstra *et al.*, 1992; Russell *et al.*, 1992; Lescoat and Sauvant, 1995) divide the total microbial mass into two components. One component contains all the microbial species that digest either starch or sugar as their primary substrate. The second component contains all the microbial species that digest holocellulose as their primary substrate. The first microbial group therefore includes both the amylolytic bacteria and protozoa, while the second includes all the fibrolytic species of bacteria. Subsequently, Dijkstra (1993) separated the amyloytic species and the protozoa in order to represent better the interaction between protozoa, bacteria and dietary characteristics (Dijkstra, 1994b; Dijkstra and Tamminga, 1995). The division of the microbial mass into three components reflects the current level of approximation in models of the rumen. Other, more complex, representations of the microbial population have been presented (Reichl and Baldwin, 1975), but these were designed for research purposes only and will not be considered here.

Modelling Fermentation in the Rumen

The energy requirements for growth and maintenance of the rumen microbes are obtained from fermentation of nutrients in the rumen. Equations calculating the rate of growth are often chosen to be Michaelis–Menten in form, but may be modified to include a dependence on more than one substrate and/or an inhibitory effect. Fermentation of both structural and non-structural

carbohydrates is often considered to be Michaelis–Menten in form. The proportion of the microbes attached to feed particles containing the substrate may be a modifying factor. If the microbial population is represented by two or more groups, equations defining the rate of fermentation of each substrate used by each microbial group must be specified. Thus the amount of each substrate fermented per unit time by each microbial group is calculated.

In principle, there may be a different metabolic pathway and hence a different stoichiometry associated with each substrate fermented by each microbial group. In fact, almost all rumen models published to date associate a particular stoichiometry only with a particular substrate, regardless of the number of microbial groups chosen to represent the microbial population. Examples are the stoichiometries published by Murphy (1984), based on the work of Murphy *et al.* (1982), who used a statistical fit of a range of observed rumen VFA concentrations to the dietary components to determine the dependence of fermentation on dietary component. The Murphy (1984) stoichiometric coefficients, shown in Table 3.1, are frequently used in current rumen models (Baldwin *et al.*, 1987; Dijkstra *et al.*, 1992; Dijkstra, 1993) to calculate the VFAs produced. It can be seen in Table 3.1 that separate fits were made in the case of diets containing predominantly roughage and diets containing predominantly concentrates, yielding two different sets of stoichiometries.

Predictions of Fermentation Products (VFAs) Using Existing Models of the Rumen

Neal *et al.* (1992) have evaluated the rumen model proposed by Dijkstra *et al.* (1992) by simulating rumen function using a range of high-fibre, high-starch and high-protein diets. After comparing the model predictions with observations they concluded that the predicted duodenal flows of neutral detergent fibre (NDF), total non-ammonia nitrogen (NAN) and total VFA were 'satisfactory'.

Table 3.1. Estimated stoichiometric coefficients* for rumen fermentation (from Murphy, 1984).

	Acetate		Propionate		Butyrate		Valerate	
Substrate	R	C	R	C	R	C	R	C
Soluble carbohydrate	1.38	0.90	0.41	0.42	0.10	0.30	0.00	0.04
Starch	1.19	0.80	0.28	0.60	0.20	0.20	0.06	0.10
Hemicellulose	1.13	1.12	0.36	0.51	0.21	0.11	0.05	0.07
Cellulose	1.32	1.58	0.17	0.12	0.23	0.06	0.03	0.09
Protein	0.40	0.36	0.13	0.16	0.08	0.08	0.33	0.33

* Moles of VFA produced per mole of substrate fermented.
R, proportion of roughage ⩾ 60%; C, proportion of concentrate ⩾ 60%.

However, the performance of the model was found to be 'unsatisfactory' when it came to predictions of two components of NAN, namely, microbial and non-microbial NAN, and the predictions of the proportions of different VFAs in the rumen. We shall focus here on the latter problem.

We have repeated the calculations of Neal *et al.* (1992), using exactly the same inputs describing some of the diets they considered, which were very kindly provided for us by Dr Jan Dijkstra. The predictions of the total VFA concentration, and the proportions of acetate, propionate and butyrate in the total using the Dijkstra *et al.* (1992) model are shown in Fig. 3.1 (open symbols). It

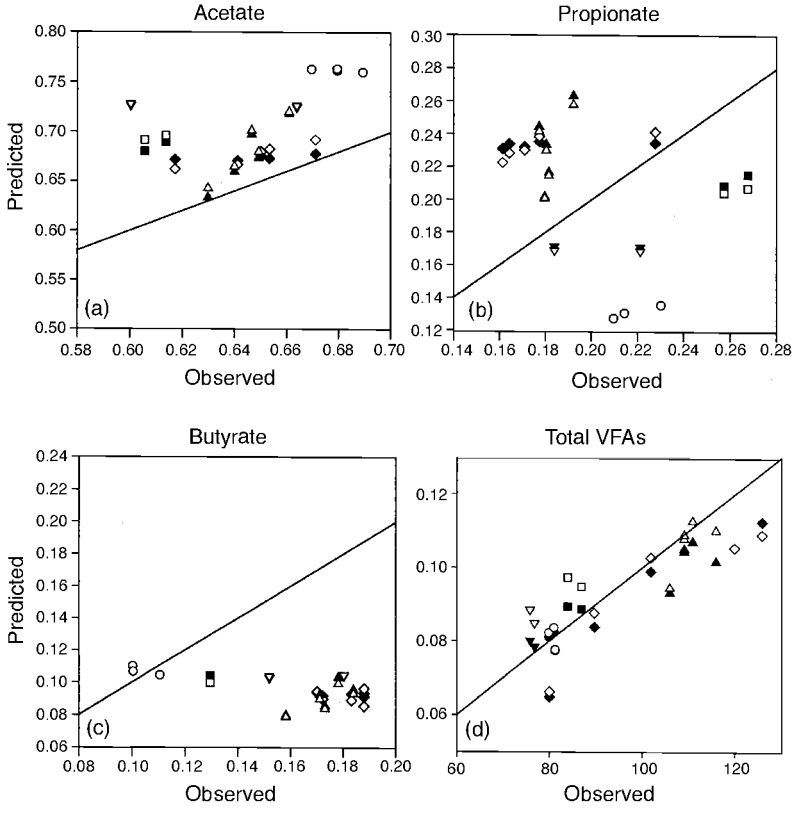

Fig. 3.1. The proportions of (a) acetate, (b) propionate, (c) butyrate and (d) total VFAs predicted by the rumen model of Dijkstra *et al.* (1992) (open symbols) and the rumen model of Dijkstra (1993) (solid symbols) compared with experimental observations (horizontal axis). The experimental diets used in these calculations are those of Horner *et al.* (1988) (▽, ▼), Robinson *et al.* (1987), intake level (◇, ◆) and starch level (△, ▲), Robinson and Kennelly (1990) (□, ■) and Beever *et al.* (1990) (○, ●). These results should be compared with those of Neal *et al.* (1992). Where symbols overlap, as they frequently do, the open symbols dominate.

is clear from the results (open symbols) in Fig. 3.1 (and the results in Figure 4 by Neal *et al.* (1992)) that there is a tendency for the model to consistently overpredict the proportion of acetate and to underpredict the proportion of butyrate in the total concentration. In fact, there is also a lack of variation in the predicted proportion of butyrate (Fig. 3.1c, open symbols), which is completely inconsistent with observations. There is also considerable scatter in the predicted proportion of propionate compared with observations (Fig. 3.1b, open symbols). It is for these reasons that the capacity of the model to predict VFAs was considered unsatisfactory by Neal *et al.* (1992) and by Dijkstra (1994a). It is also important to note that at the time no other dynamic models of rumen function (e.g. Baldwin *et al.*, 1987) had shown any greater capacity to predict either the total VFA concentration or the proportions of VFAs than that exhibited by the model of Dijkstra *et al.* (1992).

In an effort to include in the model more of the interactions between diet and rumen microbes and more of the interactions between the bacteria and protozoa, Dijkstra (1993) modified the model of Dijkstra *et al.* (1992) by separating the protozoa from the amylolytic bacteria. The new model is therefore a three-group representation of the total microbial population, with one of the groups representing the protozoa. We have reconstructed this model and repeated the calculations carried out to obtain the results in Fig. 3.1 (solid symbols). The new results show that the three-microbial-group model (Dikstra, 1993) produces no improvements – in fact, very little change at all – in the predictions of total VFA concentration, despite the fact that many aspects of the dynamics of protozoa are now simulated (Dijkstra and Tamminga, 1995). There is also virtually no change at all in the predictions of the proportions of VFAs.

A number of possible weaknesses in current efforts to predict VFA production have been suggested by Neal *et al.* (1992) and Dijkstra (1994a). These include an inadequate quantitative description of VFA absorption and a need to account for much greater shifts in fermentation pathways than is currently achieved using the stoichiometries of Murphy (1984) (see Table 3.1). The need to incorporate the effect of pH in both of these areas is also emphasized. In the following, we make no attempt to cover all of these issues. Instead, we focus only on the fermentation stoichiometries and consider a different approach, which incorporates more of the differences between microbial species.

Stoichiometries Characteristic of Microbial Groups

At first sight, it may seem surprising that there is minimal change in the predictions of VFA proportions (see Fig. 3.1) when such a substantial change is made in the representation of the microbial population, i.e. moving from a two-group to a three-group representation (Dijkstra, 1993). This, however, can be attributed very largely to the fact that the fermentation stoichiometries used in both models are associated with dietary components only (see Table 3.1). The dietary inputs to both models used to obtain the results in Fig. 3.1 are the same.

We now wish to consider the consequences of relating particular stoichiometries, not only to dietary component, but also to microbial group.

New stoichiometries were established for each of the three microbial groups (amylolytic bacteria, fibrolytic bacteria and protozoa). In each microbial group, stoichiometries were derived for the fermentation of the major carbohydrates in ruminant feeds: cellulose (β-hexose), hemicellulose (xylan; β-pentose), starch and soluble carbohydrate (both α-hexose). Individual stoichiometries for the relevant genera of bacteria or morphological type of ciliate protozoa and carbohydrate type were normalized to a carbon recovery of 100%. In deriving the stoichiometries, it was assumed that formate was converted to CO_2 and H_2 in those reactions where it was a product of fermentation.

Stoichiometries for protozoal fermentation of α-hexose and β-pentose were derived from the reactions reported for holotrichs and entodiniomorphids (Williams and Coleman, 1997, and papers cited therein). Stoichiometries for amylolytic bacteria fermenting α-hexose were derived from individual reactions of *Butyrivibrio*, *Eubacterium*, *Lachnospira*, *Prevotella*, *Ruminobacter*, *Selenomonas*, *Streptococcus*, *Succinimonas* and *Succinivibrio*. Amylolytic bacteria fermenting β-pentose were considered to be from the genera *Butyrivibrio*, *Prevotella*, *Selenomonas* and *Succinivibrio*. Fibrolytic bacteria fermenting β-hexose were *Butyrivibrio*, *Eubacterium*, *Fibrobacter* and *Ruminococcus*, and *Butyrivibrio* and *Ruminococcus* also fermented β-pentose. The number of original papers consulted was far too high for them to be cited here but most are cited by Krieg and Holt (1984), Sneath *et al.* (1986) and Stewart *et al.* (1997). Where details of fermentation reactions were either not available or not found, qualitative information on major and minor fermentation end-products were converted into stoichiometries with the aid of general metabolic information (Gottschalk, 1986).

Consensus stoichiometries were derived by combining the stoichiometries for individual bacterial genera or protozoal types in proportion with the contribution of the individuals to the function of the group. In doing this, consideration was given to detailed studies of bacterial and protozoal populations in the rumen (Latham *et al.*, 1974; Teather *et al.*, 1980, 1984; Van Gylswyk and Schwartz, 1984; Stewart, 1990; Briesacher *et al.*, 1992; Weimer *et al.*, 1999) and to the volume of individual cells in populations, which were calculated from available data on cell dimensions (Krieg and Holt, 1984; Teather *et al.*, 1984; Sneath *et al.*, 1986).

Equations describing the fermentation of lactate to propionate, acetate, CO_2 and H_2 were derived from a consensus of the individual reactions reported for *Megasphaera*, *Selenomonas* and *Anaerovibrio* (Krieg and Holt, 1984; Sneath *et al.*, 1986; Stewart *et al.*, 1997), whereas the conversion of succinate to propionate and CO_2 was considered to occur instantly. These latter reactions were included in the consensus reaction for each relevant feed carbohydrate and microbial group combination.

The protein (amino acid) fermentation stoichiometry was based on that given by Baldwin *et al.* (1977b: 363), by incorporating the stoichiometry for

pyruvate to branched-chain fatty acid into the stoichiometry for amino acid fermentation. This stoichiometry was used by all three microbial groups.

The new set of stoichiometries is summarized in Table 3.2. It is clear that there are major differences between the groups, so that predictions are expected to be sensitive to the relative proportions of the three microbial groups, even if these were to change independently of changes in the chemical composition of the diet.

Improvement in the Prediction of VFAs in the Rumen

The three-microbial-group model described by Dijsktra (1994b) has been modified to calculate the rate at which fermentation products are generated, using the new stoichiometries in Table 3.2. After incorporating these stoichiometries and repeating the calculations for the same diets noted in Fig. 3.1, we found an immediate improvement in the predictions of the proportions of VFAs. As expected, the predictions of VFA proportions are now much more sensitive to the relative proportions of the three microbial groups. As a consequence further improvements in predicting the proportions of VFAs, i.e. in addition to gains made by using the stoichiometries in Table 3.2, can be achieved by searching for a new set of parameters controlling the relative growth rates of the three microbial groups. The end results are shown in Fig. 3.2 (open symbols).

It is clear from Fig. 3.2 that there has been considerable improvement in the predictions of the proportion of acetate ($r^2 = 0.62$, open symbols in Fig. 3.2a, compared with $r^2 = 0.26$, filled symbols in Fig. 3.2a and in Fig. 3.1a) and the proportion of butyrate ($r^2 = 0.74$, open symbols in Fig. 3.2c, compared with $r^2 = 0.38$, filled symbols in Fig. 3.2c and in Fig. 3.1c). There has also been some improvement in the predicted proportions of propionate ($r^2 = 0.37$, open symbols in Fig. 3.2b, compared with $r^2 = 0.13$, filled symbols in Fig. 3.2b and in Fig.

Table 3.2. Stoichiometric coefficients* for rumen fermentation characteristic of microbial groups.

	Acetate			Propionate			Butyrate			Valerate		
Substrate	Ba	Bc	Po	Ba	Bc	Po	Ba	Bc	Po	Ba	Bc	Po
Soluble CHO and starch	0.90	0	0.99	0.85	0	0.02	0.10	0	0.49	0.024	0	0
Hemicellulose	1	1	1	0.36	0.34	0	0.23	0.25	0.50	0	0	0
Cellulose	0	1.3	0.99	0	0.53	0.22	0	0.085	0.49	0	0	0
Protein	0.50	0.50	0.50	0.15	0.15	0.15	0.13	0.13	0.13	0.24	0.24	0.24

*Moles of VFA produced per mole of substrate fermented.
Ba, amylolytic bacteria; Bc, cellulolytic bacteria; Po, protozoa.

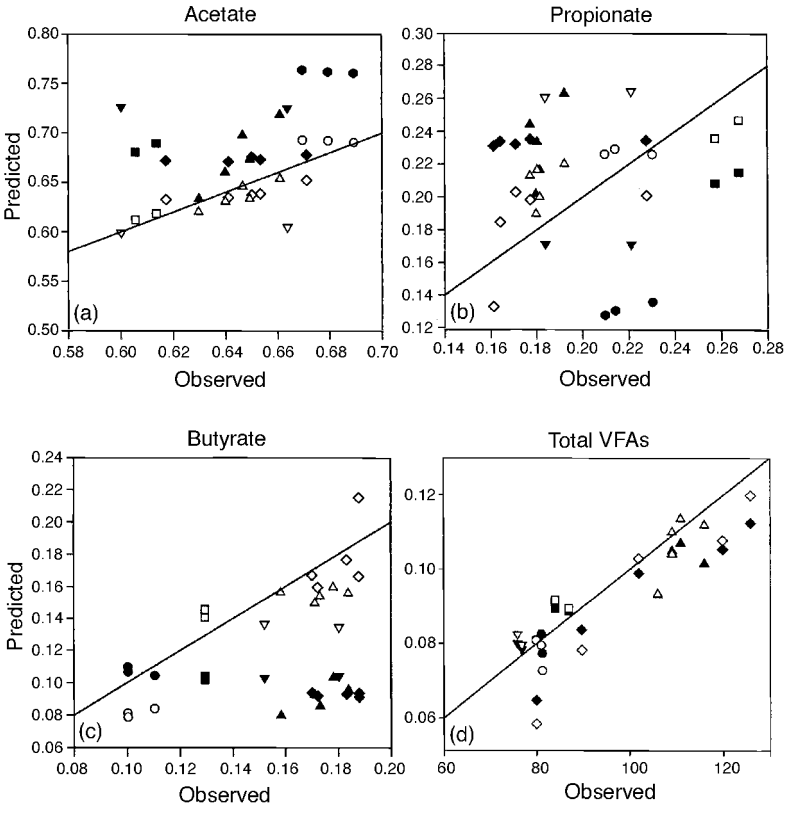

Fig. 3.2. The proportions of (a) acetate, (b) propionate, (c) butyrate and (d) total VFAs predicted by the rumen model of Dijkstra (1993) with the new fermentation submodel (open symbols) and the unchanged rumen model of Dijkstra (1993) (solid symbols) compared with experimental observations (horizontal axis). The symbols have the same meaning as those in Fig. 3.1.

3.1b), although in this case there remains significant scatter. The predictions of total VFAs (Fig. 3.2d) remain largely unchanged ($r^2 = 0.80$, open symbols in Fig. 3.2d, compared with $r^2 = 0.84$, filled symbols in Fig. 3.2d and in Fig. 3.1a). The predictions of other important quantities, such as the outflow of NDF, also remain largely unchanged. Substantial change was found in the predicted concentration/production of ammonia, where there was a significant reduction in the scatter ($r^2 = 0.13$, compared with $r^2 = 0.0$, not shown); however, the correct trend with diet was still not reproduced.

Conclusion

As the modelling of the total microbial population of the rumen has advanced to the point where three groups are now being represented, this has opened up the possibility of incorporating fermentation stoichiometries that are dependent not only on substrate but also on microbial group. Using information published in the literature, we have derived stoichiometries for the three microbial groups currently being represented, namely amylolytic bacteria, cellulolytic bacteria and protozoa. These stoichiometries show large differences between microbial groups (see Table 3.2). It has been possible, using these differences, to demonstrate a much greater capacity of rumen models to correctly predict the proportions of VFAs produced in rumen fermentation. It is concluded that, while there may be a number of reasons why rumen models have not yet been able to achieve accurate predictions of the proportions of different VFAs produced in the rumen, the need to use fermentation stoichiometries that reflect some of the major differences between microbial groups appears to be essential.

Acknowledgements

This research was supported in part by the Premium Australian Grains for Livestock Program, which is funded jointly by the Grains Research and Development Corporation, the Meat, Pig and Dairy Corporations and the Rural Industries Research and Development Corporation's Chicken Meat and Egg Programs. We would also like to thank Dr Jan Dijkstra for supplying the dietary information used to compare model predictions.

References

Baldwin, R.L. (1995) *Modelling Ruminant Digestion and Metabolism.* Chapman & Hall, London.

Baldwin, R.L. and Allison, M.J. (1983) Rumen metabolism. *Journal of Animal Science* 57 (Suppl. 2), 461–477.

Baldwin, R.L., Koong, L.J. and Ullyatt, M.J. (1977a) A dynamic model of ruminant digestion for evaluation of factors affecting nutritive value. *Agricultural Systems* 2, 255–288.

Baldwin, R.L., Koong, L.J. and Ulyatt, M.J. (1977b) The formation and utilization of fermentation end-products: mathematical models. In: Clarke, R.T.J. and Bauchop, T. (eds) *Microbial Ecology of the Gut.* Academic Press, London, pp. 347–391.

Baldwin, R.L., Thornley, J.H.M. and Beever, D.E. (1987) Metabolism of the lactating cow. II. Digestive elements of a mechanistic model. *Journal of Dairy Research* 54, 107–131.

Beever, D.E., Gill, M., Dawson, J.M. and Buttery, P.J. (1990) The effect of fishmeal on the digestion of grass silage by growing cattle. *British Journal of Nutrition* 63, 489–502.

Benchaar, C., Rivest, J., Pomar, C. and Chiquette, J. (1998) Prediction of methane from

dairy cows using existing mechanistic models and regression equations. *Journal of Animal Science* 76, 617–627.

Black, J.L., Beever, D.E., Faichney, G.J., Howarth, B.R. and Graham, N.McC. (1981) Simulation of the effects of rumen function on the flow of nutrients from the stomach of sheep: part 1 – description of a computer program. *Agricultural Systems* 6, 221–241.

Briesacher, S.L., May, T., Grigsby, K.N., Kerley, M.S., Anthony, R.V. and Paterson, J.A. (1992) Use of DNA probes to monitor nutritional effects on ruminal prokaryotes and *Fibrobacter succinogenes* S85. *Journal of Animal Science* 70, 289–295.

Dijkstra, J. (1993) Mathematical modelling and integration of rumen fermentation processes. PhD thesis, Agricultural University, Wageningen.

Dijkstra, J. (1994a) Production and absorption of volatile fatty acids in the rumen. *Livestock Production Science* 39, 61–69.

Dijkstra, J. (1994b) Simulation of the dynamics of protozoa in the rumen. *British Journal of Nutrition* 72, 679–699.

Dijkstra, J. and France, J. (1996) A comparative evaluation of models of whole rumen function. *Annals of Zootechnology* 45, 175–192.

Dijkstra, J. and Tamminga, S. (1995) Simulation of the effects of diet on the contribution of rumen protozoa to degradation of fibre in the rumen. *British Journal of Nutrition* 74, 617–634.

Dijkstra, J., Neal, H.D.StC., Beever, D.E. and France, J. (1992) Simulation of nutrient digestion, absorption and outflow in the rumen: model description. *Journal of Nutrition* 122, 2239–2256.

France, J., Thornley, J.H.M. and Beever, D.E. (1982) A mathematical model of the rumen. *Journal of Agricultural Science (Cambridge)* 99, 343–353.

Gottschalk, G. (1986) *Bacterial Metabolism*. Springer-Verlag, New York.

Horner, J.L., Coppock, C.E., Moya, J.R., Labore, J.M. and Lanham, J.K. (1988) Effects of niacin and whole cottonseed on ruminal fermentation, protein degradability and nutrient digestibility. *Journal of Dairy Science* 71, 1239–1247.

Hungate, R.E. (1966) *The Rumen and its Microbes.* Academic Press, New York.

Krieg, N.R. and Holt, J.G. (1984) *Bergey's Manual of Systematic Bacteriology*, Vol. 1, *Gram-Negatives.* Williams & Wilkins, Baltimore.

Latham, M.J., Sutton, J.D. and Sharpe, M.E. (1974) Fermentation and microorganisms in the rumen and the content of fat in the milk of cows given roughage rations. *Journal of Dairy Science* 57, 803–810.

Lescoat, P. and Sauvant, D. (1995) Development of a mechanistic model for rumen digestion validated using the duodenal flow of amino acids. *Reproduction, Nutrition and Development* 35, 45–70.

Murphy, M.R. (1984) Modelling production of volatile fatty acids in ruminants. In: Baldwin, R.L. and Bywater, A.C. (eds) *Modeling Ruminant Digestion and Metabolism, Proceedings of the 2nd International Workshop*. University of California, Davis, pp. 59–62.

Murphy, M.R., Baldwin, R.L. and Koong, L.J. (1982) Estimation of stoichiometric parameters for rumen fermentation of roughage and concentrate diets. *Journal of Animal Science* 55, 411–421.

Neal, H.D.StC., Dijkstra, J. and Gill, M. (1992) Simulation of nutrient digestion, absorption and outflow in the rumen: model evaluation. *Journal of Nutrition* 122, 2257–2272.

Reichl, J.R. and Baldwin, R.L. (1975) Rumen modelling: rumen input output-balance models. *Journal of Dairy Science* 58, 879–890.

Robinson, P.H. and Kennelly, J.J. (1990) Evaluation of a dudenal cannula for dairy cattle. *Journal of Dairy Science* 73, 3146–3157.

Robinson, P.H., Tamminga, S. and Van Vuuren, A.M. (1987) Influence of declining level of feed intake and varying the proportion of starch in the concentrate on rumen ingesta quantity, composition and kinetics of ingesta turnover in dairy cows. *Livestock Production Science* 17, 37–62.

Russell, J.B., O'Connor, J.D., Fox, D.G., Van Soest, P.J. and Sniffen, C.J. (1992) A net carbohydrate and protein system for evaluating cattle diets: I. Ruminal fermentation. *Journal of Animal Science* 70, 3551–3561.

Sneath, P.H.A., Mair, N.S., Sharpe, E.M. and Holt, J.G. (1986) *Bergey's Manual of Systematic Bacteriology*, Vol. 2, *Gram-Positives*. Williams & Wilkins, Baltimore.

Stewart, C.S. (1990) The rumen *Bacteroides*. In: van Gylswyk, N.O. and Lindgren, E. (eds) *Aspects of Rumen Microbiology and Metabolism.* Swedish University of Agricultural Sciences, Uppsala, pp. 56–67.

Stewart, C.S., Flint, H.J. and Bryant, M.P. (1997) The rumen bacteria. In: Hobson, P.N. and Stewart, C.S. (eds) *The Rumen Microbial Ecosystem*, 2nd edn. Elsevier Applied Science, London, pp. 10–72.

Sutton, J.D. (1985) Digestion and absorption of energy substrates in the lactating cow. *Journal of Dairy Science* 68, 3376–3393.

Teather, R.M., Erfle, J.D., Boila, R.J. and Sauer, F.D. (1980) Effect of dietary nitrogen on the rumen microbial population in lactating dairy cattle. *Journal of Applied Bacteriology* 49, 231–238.

Teather, R.M., Mahadevan, S., Erfle, J.D. and Sauer, F.D. (1984) Negative correlation between protozoal and bacterial levels in rumen samples and its relation to the determination of dietary effects on the rumen microbial population. *Applied Environmental Microbiology* 47, 566–570.

Thomas, P.C. and Martin, P.A. (1988) The influence of nutrient balance on milk yield and composition. In: Garnsworthy, P.C. (ed.) *Nutrition and Lactation in the Dairy Cow.* Butterworths, London, UK, pp. 97–118.

Van Gylswyk, N.O. and Schwartz, H.M. (1984) Microbial ecology of cellulose and hemicellulose metabolism in gastrointestinal ecosystems. In: Klug, M.J. and Reddy, C.A. (eds) *Current Perspectives in Microbial Ecology.* American Society of Microbiology, Washington, DC, pp. 588–599.

Weimer, P.J., Waghorn, G.C., Odt, C.L. and Mertens, D.R. (1999) Effect of diet on populations of three species of ruminal cellulolytic bacteria in lactating dairy cows. *Journal of Dairy Science* 82, 122–134.

Williams, A.G. and Coleman, G.S. (1997) The rumen protozoa. In: Hobson, P.N. and Stewart, C.S. (eds) *The Rumen Microbial Ecosystem,* 2nd edn. Elsevier Applied Science, London, pp. 73–139.

4

Simple Allometric Models to Predict Rumen Feed Passage Rate in Domestic Ruminants

Antonello Cannas[1] and Peter J. Van Soest[2]

[1]*Dipartimento di Scienze Zootecniche, University of Sassari, 07100 Sassari, Sardinia, Italy;* [2]*Department of Animal Science, Cornell University, Ithaca, NY 14853, USA*

Abstract

A database was developed from the literature (36 publications) to explore the mechanisms controlling rumen feed passage rate (K_p) and to predict it. The database included the results of 157 different dietary treatments and passage rate measurements with 45 treatments on dry sheep or wethers, 42 on lactating cows, 58 on dry cows, heifers or steers, four on buffaloes, and eight on goats. The treatments were selected by looking for the following requisites: diets with at least 20% forage; no dietary treatments in which the forage was chopped with screens smaller than 1 cm of nominal size; no lactating animals with fewer than 20 days in milk and no animals in the last third of the pregnancy; intake measured and not estimated; marked forage with identical characteristics and physical form of dietary forage; at least three animals per treatment; only chromium or rare earths as markers, given with a single pulse dose; K_p estimated with time-independent models. The choice of predictors was restricted to intake, body weight, dietary and forage CP, NDF and, when available, lignin. The best models found to predict rumen passage rate of the forages were:

$$Y = 1.82 \times \text{F-DMI}^{0.34}\, e^{0.036 \times \text{D-CP\%}} \qquad (R^2\text{: } 0.53\text{; CV of SEE: } 22.1\%)$$

$$Y = 1.82 \times \text{D-NDFI}^{0.40}\, e^{0.046 \times \text{D-CP\%}} \qquad (R^2\text{: } 0.53\text{; CV of SEE: } 22.2\%)$$

where Y = forage passage rate, in % h^{-1}; F-DMI = level of intake (% of BW) of forage DM; D-NDFI = level of intake (% of BW) of dietary NDF; D-CP% = dietary concentration of CP, in % of DM; CV of SEE = coefficient of variation of the standard error of the estimate over the mean response.

The level of intake scaled on metabolic size was a poorer predictor than the level of intake scaled on body weight. The model in which one of the predictors was the level of intake of NDF was preferred because it was biologically more appropriate. No

 Modelling Nutrient Utilization in Farm Animals (eds J.P. McNamara, J. France and D.E. Beever)

clear differences between chromium and rare-earth markers were found. The curvilinear pattern existing between forage NDF K_p and the level of intake of dietary NDF was explained by changes in the rumen pool size of NDF. When the models obtained from the whole database were applied to the small ruminants (sheep and goats) and the large ruminants (cattle and buffalo) subsets, the separate fits were not significantly better than those calculated on the whole database. Rumen passage rate of concentrates was linearly associated with that of forages (Concentrate K_p (% h^{-1}) = 1.572 × K_p forage (% h^{-1}) −0.925, r^2 = 65%, SEE =1.104, CV of SEE = 18.8%; n = 36). In conclusion, the passage rate of forages and concentrates can be predicted by using the same models and equations for domestic ruminants of different species and body size.

Abbreviations

F-DMI = forage dry matter (DM) intake (% of body weight (BW)); D-NDFI = dietary neutral detergent fibre (NDF) intake (% of BW); D-CPI = dietary crude protein (CP) intake (% of BW); D-CP% = dietary CP concentration (% of DM); D-NDF% = dietary NDF concentration (% of DM).

Introduction

Despite the existence of many experiments in which rumen passage rate (K_p) was measured or methods and models of marker excretion were compared, the prediction of rumen K_p of solids has been the objective of a limited number of publications.

Many of the relationships suggested were species-specific and intrinsically empirical (Evans, 1981; Owens and Goetsch, 1986; Lindberg, 1988; CSIRO, 1990; Lescoat and Sauvant, 1995). In contrast, the models of Mertens (1973), Aitchison *et al.* (1986), Illius and Gordon (1991) and Chilibroste *et al.* (1997) were not species-specific and made some effort to take a mechanistic approach or had some physiological justification. Most of these relationships were linear, with the independent variable scaled on body weight (BW). A different scaling factor was proposed only by Lescoat and Sauvant (1995) and Illius and Gordon (1991), while only Aitchison *et al.* (1986) and Illius and Gordon (1991) suggested curvilinear models.

It is still unclear if rumen K_p of solids should be predicted separately for forages and concentrates, if the relationship between K_p and predictors is linear or curvilinear and if K_p prediction should be species-specific. With the aim of answering these questions, the present work will attempt to develop simple mathematical models to predict rumen K_p of solids by using predictors measurable at farm level, with a clear biological importance and justification, and possibly valid for different ruminant species.

Model Development

Database construction

A database was created using the information found in 36 published scientific articles (cited by Cannas, 2000). The treatments were selected by looking for the following requisites: diets with at least 20% forage; no dietary treatments, in which the forage was chopped with screens smaller than 1 cm of nominal size; no lactating animals with fewer than 20 days in milk and no animals in the last third of the pregnancy; intake measured and not estimated; marked forage with identical characteristics and physical form of dietary forage; at least three animals per treatment; only chromium or rare earths as markers, given with a single-pulse dose; K_p estimated with time-independent models. Considering the differences in fermentative and physical characteristics between forages and concentrates, the prediction of K_p was done separately for each one of them.

Chromium and rare earths bind mostly to fibre (Van Soest, 1994). For this reason, the measurements of K_p obtained by marking forages should be considered as estimates of the K_p of their neutral detergent fibre (NDF) fraction. The treatments in which chromium was used as marker were considered separately from those in which rare earths were used, because of the differences existing between them in binding capacity and effects on the specific gravity of the particles (Van Soest, 1994). This also allowed the comparisons of the equations obtained with two different databases, to provide an internal validation process of the models.

Hypotheses on which the models were based

The equations that will be proposed to predict K_p were developed mainly by usual regressions techniques. However, they cannot be considered as 'fully empirical models', since they were developed on the basis of the following theoretical suggestions.

The passage rate can be mathematically related to independent variables that refer to the animal and to the diet. Among the potential predictors of K_p, importance must be given to the intake of indigestible particles and to animal BW. Since in ruminants gut contents and BW are linearly related (Demment and Van Soest, 1985), we can assume that ruminants of different body size, but with the same level of *ad libitum* feed intake of a certain diet, should have proportional amounts of feed in the rumen and, therefore, equal K_p. As a consequence, any explicit dependence of K_p on animal BW could be left out from prediction equations, provided that intakes are scaled on BW.

Statistical analysis

As a first step, data selected were fitted by using simple linear:

$$Y = a + bX \quad (1)$$

and simple curvilinear:

$$Y = aX^b \quad (2)$$

models, the last in the corresponding linear form, as obtained by natural logarithm transformation:

$$\ln Y = a + b \times \ln X \quad (3)$$

where Y = passage rate (K_p in % h^{-1}); X = level of intake of several variables considered as potential predictors (dry matter (DM), crude protein (CP), NDF of diet, forage or concentrate), scaled to BW or to metabolic weight (MW, equal to $BW^{0.75}$); a and b = parameters to be estimated.

Goodness of fit was evaluated with the usual statistics (coefficient of determination, R^2, standard error of estimate, SEE, and its coefficient of variation over the mean response, CV of SEE), and by the analysis of residuals, to highlight possible lack of fit. In the cases of significant lack of fit, more complex models were considered, both by adding a new independent variable and by checking the best form of its relation with K_p.

The following linear, or linearized, models were tested:

$$Y = a + bX + cZ \quad (4)$$

$$Y = aW^b \times Z^c \quad (5)$$

$$Y = aW^b \exp(cZ), \text{ linearized with natural logarithm to } \ln Y = \ln a + b \times \ln W + cZ \quad (6)$$

where: $Y = K_p$; W = level of intake of whole diet or forage DM, CP, NDF scaled to BW or to MW; Z = second predictor; a, b, c = parameters to be estimated. The choice of the second predictor was based on its capability to explain the trend of residuals.

Possible differences in K_p values, depending on the type of marker, on the type of forage (legumes or grasses) or on animal species (small ruminants, i.e. sheep and goats, versus large ruminants, i.e. cattle and buffalo), were tested by partitioning the whole database and performing separate analysis, or considering them as a third qualitative variable in the linearized regressions based on the whole database.

Once the best linearized model had been defined by multiple linear regression, the relationships between K_p and predictors were fitted to the data again, using non-linear regression techniques. Marquardt's compromise was adopted. Initial parameter values were obtained by back-transforming the estimates of the corresponding linearized equations. A final test to check if K_p predictions for

small ruminants were significantly different from those for large ruminants was performed by using the test of Ratkowsky (1983).

Prediction of the Rumen Passage Rate of Forages

Forages marked with chromium

The data analysed were taken from 17 published scientific articles, from which 27 dietary treatments and K_p measurements on small ruminants (23 on dry ewes, rams or wethers, four on wether goats) and 42 on large ruminants (18 on lactating cows, nine on dry cows, 11 on steers, heifers or oxen, four on adult buffaloes) were selected. The marked forage was made of grasses in 30 treatments, of legumes in 32 treatments and of mixed grasses + legumes in seven cases.

Both linear (equation 1) and linearized (equation 3) simple regression models showed the best fit with forage DM or dietary CP intake scaled to BW (F-DMI and D-CPI, respectively, as % of BW) as the independent variable, whereas MW resulted in a better scaling factor than BW when the level of intake of NDF was considered. However, except for D-CPI, the analysis of residuals highlighted a non-random distribution, with a concentration of most negative residuals in the range of low CP and high NDF dietary concentrations (D-CP% and D-NDF%, respectively) and of most positive residuals in the range of high D-CP% and low D-NDF%. Forage NDF K_p was generally higher in high-CP diets (Fig. 4.1).

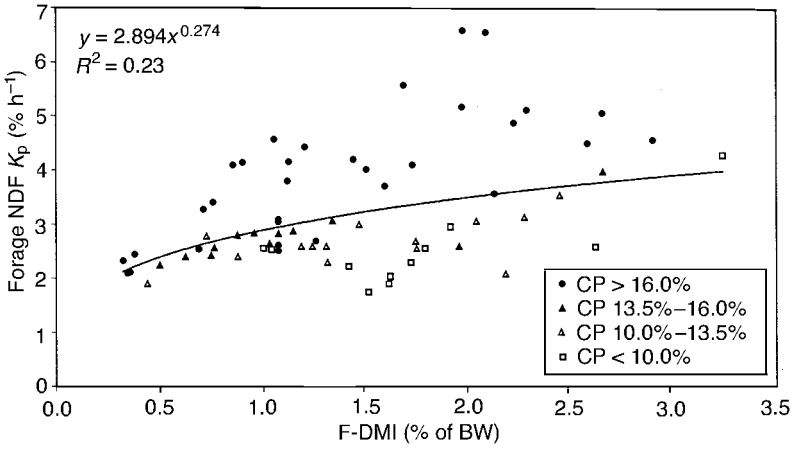

Fig. 4.1. Relationship between forage dry matter level of intake (F-DMI) and forage NDF K_p in the chromium-marked database. Treatment means were sorted based on their dietary CP concentration.

Among the multiple regression models tested to improve K_p prediction, the best results were achieved with the non-algebraic function (equation 6) in the linearized form obtained by logarithmic transformation. The best fit was obtained when D-CP% was used as the second predictor, Z, and the first variable was scaled to BW (Table 4.1).

Forages marked with rare earths

The data were taken from 21 published scientific articles, from which 26 dietary treatments and K_p measurements on small ruminants (22 on dry ewes, rams or wethers, four on lactating goats) and 62 on large ones (24 on lactating cows, one on dry cows, 37 on steers) were selected. The marked forage source was based on grasses in 37 treatments, on legumes in 47 treatments and on mixed grasses + legumes in four cases.

Similarly to the chromium database, the best independent variables to predict forage NDF K_p were D-CPI, F-DMI and the level of intake of NDF (D-NDFI, as % of BW) (see Table 4.1). The regressors based on MW were poorer predictors than those based on BW.

The best single regression used D-CPI as independent variable and had similar r^2 and CV of SEE to those of the best multiple regressions (see Table 4.1).

In contrast to the chromium-marked diets, the best second independent variable in multiple regressions was always D-NDF% instead of D-CP%. Forage NDF K_p tended to be higher in low-NDF diets (Fig. 4.2).

Pooled database

With the aim of studying markers, forage sources and animal species effects on K_p, the two databases previously analysed were compared and, when necessary, pooled.

When the type of marker was included in the regressions based on the whole data set as the qualitative independent variable, it had a significant effect in the regressions that had as predictors D-CPI and D-NDFI, while its effect was not significant in the regressions based on F-DMI. In any case, the effect of the type of marker was very small on both R^2 (increased between 0.01 and 0.03, depending on the variables considered) and CV of SEE (decreased between 0.3% and 0.8%). For this reason, this variable was discarded.

Most of the diets that had grasses as the forage source had lower K_p than those based on legumes, for similar levels of intake. The latter had much higher dietary CP content and much lower NDF content compared with the former. The statistical analysis showed that the regressor 'forage species' was significant ($P < 0.05$) only in the regressions in which ln(D-NDFI) was the first regressor and D-CP% the second. However, the addition of this third variable explained only a very small fraction of the variance, increasing the R^2 by only 0.01. Considering that forage NDF K_p was generally higher in high-CP diets (Fig. 4.3),

Table 4.1. Best linearized regressions for the chromium and the rare-earth databases (standard errors of the coefficients in parentheses).

Equations	R^{2*}	CV of SEE (%)	r
Chromium database ($n = 69$; mean $\ln(K_p) = 1.1246\%\ h^{-1}$)			
$\ln(K_p) = 1.581\ (0.059) + 0.349\ (0.041)\ \ln$(D-CPI)	0.52	18.3	
$\ln(K_p) = 1.063\ (0.036) + 0.274\ (0.061)\ \ln$(F-DMI)	0.23	23.3	
$\ln(K_p) = 0.369\ (0.077) + 0.329\ (0.041)\ \ln$(F-DMI) + 0.0485 (0.0051) D-CP%	0.66	15.2	NS
$\ln(K_p) = 1.490\ (0.035) + 0.266\ (0.078)\ \ln$(D-NDFI)	0.15	24.5	
$\ln(K_p) = 0.418\ (0.078) + 0.395\ (0.052)\ \ln$(D-NDFI) + 0.0529 (0.0054) D-CP%	0.64	15.7	−0.25
Rare-earth database ($n = 88$; mean $\ln(K_p) = 1.3147\%\ h^{-1}$)			
$\ln(K_p) = 1.697\ (0.048) + 0.330\ (0.036)\ \ln$(D-CPI)	0.49	17.4	
$\ln(K_p) = 1.044\ (0.050) + 0.467\ (0.072)\ \ln$(F-DMI)	0.33	20.1	
$\ln(K_p) = 1.509\ (0.097) + 0.406\ (0.063)\ \ln$(F-DMI) − 0.0084 (0.0016) D-NDF%	0.49	17.4	−0.18
$\ln(K_p) = 1.289\ (0.031) + 0.393\ (0.086)\ \ln$(D-NDFI)	0.20	22.0	
$\ln(K_p) = 1.859\ (0.082) + 0.443\ (0.068)\ \ln$(D-NDFI) − 0.0113 (0.0015) D-NDF%	0.49	17.3	NS

*Adjusted in the case of multiple regression.
CV of SEE, coefficient of variation of the standard error of estimate over the mean response; r, coefficient of correlation between the two independent variables; NS, not significant ($P > 0.1$); ln, natural logarithm.

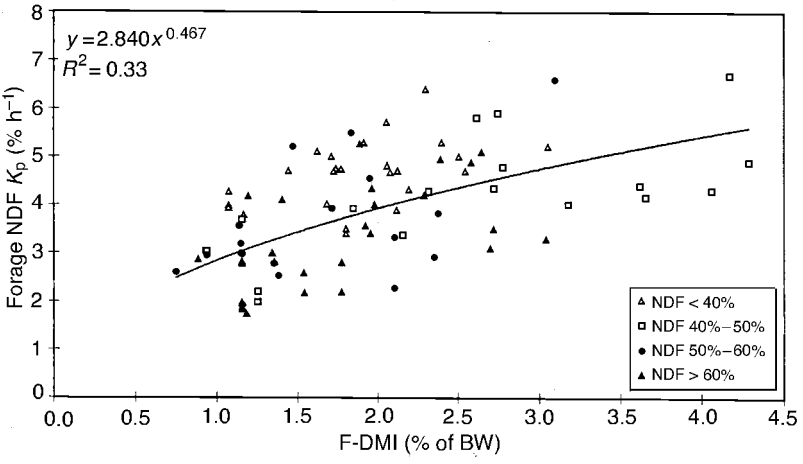

Fig. 4.2. Relationship between forage dry-matter level of intake (F-DMI) and forage NDF K_p in the rare-earth-marked database. Treatment means were sorted based on their dietary NDF concentration.

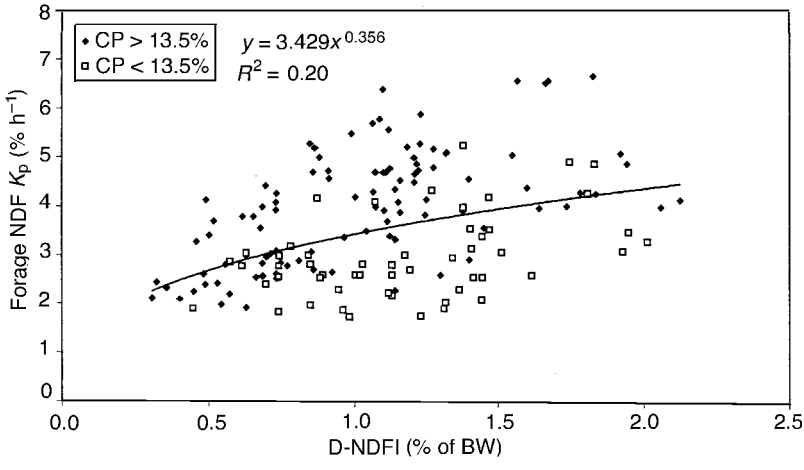

Fig. 4.3. Relationship between dietary neutral detergent fibre level of intake (D-NDFI) and forage NDF K_p in the pooled (chromium + rare earths) database. Treatment means were sorted based on their dietary CP concentration.

it seems that the forage source affected K_p, because it was correlated to dietary CP and NDF content and not for any other peculiar forage property.

In agreement with the visual comparison (Fig. 4.4), the results of the statistical analysis showed that the regressor 'animal species' was not significant ($P > 0.1$) when ln(D-NDFI) or ln(F-DMI) was the first regressor and D-CP%

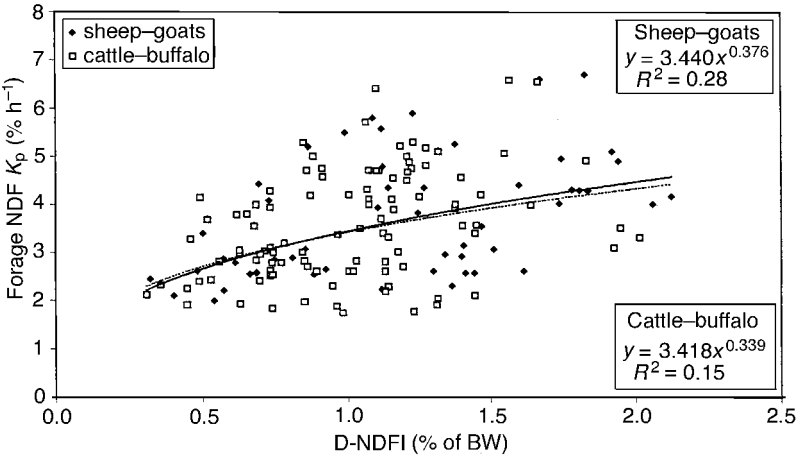

Fig. 4.4. Relationship between dietary neutral detergent fibre level of intake (D-NDFI) and forage NDF K_p in the pooled (chromium + rare earths) database. Treatment means were sorted by animal species.

the second. When the first regressor was ln(D-CPI), the predictor 'species' became significant but explained only a very small fraction of the variance, increasing the R^2 by only 0.07. Moreover, the Ratkowsky test showed that when D-NDFI and D-CP% were used as independent variables to predict forage NDF K_p, the fit to the pooled data was as appropriate as the separate fits to the small- and large-ruminant subsets. Therefore, it seems that the analysis of the database did not support any peculiar species effect in the prediction of forage K_p. Non-linear multiple regressions calculated for the two species subsets are reported in Table 4.2.

Since markers, forage sources and animal species seemed not to affect significantly the relationship between dietary parameters and K_p, chromium and rare-earths databases were pooled and non-linear regressions based on equation 6 were estimated (see Table 4.2).

Prediction of the Rumen Passage Rate of Concentrates

Part of the experiments included in the database measured both forage and concentrate K_p. A total of 36 measurements (26 on cattle, six on sheep and four on goats) were considered.

The variables dietary and concentrate level of intake, F-DMI, D-NDFI, D-CP% and D-NDF%, were poorly associated with concentrate K_p ($R^2 < 0.1$), while forage K_p was associated with concentrate K_p according to the following equation (standard errors of the coefficients in parentheses):

Table 4.2. Non-linear regressions to predict forage passage rate on the whole database ($n = 158$; mean $K_p = 3.612\%\ h^{-1}$), on the sheep–goat subset ($n = 53$; mean $K_p = 3.741\%\ h^{-1}$) and on the cattle–buffalo subset ($n = 105$; mean $K_p = 3.547\%\ h^{-1}$). The asymptotic standard errors of the coefficients are in parentheses.

Dataset	*W*	*Z*	*a*	*b*	*c*	R^2*	CV of SEE (%)	Bias
Whole	D-CPI		5.441 (0.182)	0.358 (0.030)		0.50	23.0	0.0015
Whole	F-DMI	D-CP%	1.820 (0.133)	0.338 (0.039)	0.0355 (0.0045)	0.53	22.1	−0.0025
Whole	D-NDFI	D-CP%	1.821 (0.136)	0.399 (0.046)	0.0455 (0.0045)	0.53	22.2	−0.0018
Sheep–goats	D-NDFI	D-CP%	2.126 (0.298)	0.423 (0.083)	0.0352 (0.0085)	0.42	24.8	−0.0041
Cattle–buffalo	D-NDFI	D-CP%	1.643 (0.142)	0.355 (0.058)	0.0520 (0.0052)	0.59	20.2	−0.0024

*Adjusted in the case of multiple regression based on equation 6.
CV of SEE, coefficient of variation of the standard error of estimate over the mean response.

$$\text{Concentrate } K_p\ (\%\ h^{-1}) = 1.572\ (0.198) \times K_p \text{ forage } (\%\ h^{-1}) - 0.925\ (0.876) \quad (7)$$

with $r^2 = 0.65$, SEE = 1.104, CV of SEE = 18.8%.

Discussion

The association found between forage NDF K_p and the predictors was lower when the level of intake was calculated on the $BW^{0.75}$ than on the BW^1. This was expected, considering that rumen contents increase linearly with body size (Demment and Van Soest, 1985). Despite this, some K_p prediction models (Sauvant and Archimede, 1989, cited by Lescoat and Sauvant, 1995; CSIRO, 1990) and most digestibility trials comparing different ruminant species use body size in terms of $BW^{0.75}$.

In our database, the best fit was obtained using non-linear models, in which one variable was based on the level of intake (F-DMI, D-NDFI, D-CPI) and the other one was associated with the quality of the diet (D-CP% or D-NDF%).

D-NDFI is the regressor whose biological importance is more easily explained, being the chemical component with the highest association with rumen fill (Van Soest, 1994). However, F-DMI showed similar or higher association with forage K_p than D-NDFI. Even though F-DMI and D-NDFI were highly associated ($r = 0.9$; $P < 0.001$), forages varied widely in chemical composition and physical characteristics. For this reason, F-DMI was expected to be less associated with rumen fill and forage NDF K_p than D-NDFI. A possible explanation is that, while forage intake in confined animals is usually measured with high accuracy and precision, NDF measurement precision is quite low, due to both the intrinsic variability associated with the method and, above all, the different methods used to measure NDF. These factors may have induced high variability in D-NDFI measurements, reducing its goodness as predictor. Despite this, considering the biological significance of this variable and the fact that part of the variation is methodological but does not truly affect K_p, D-NDFI should be preferred to F-DMI.

When simple models were considered, D-CPI was the regressor with the highest association with forage NDF K_p. D-CPI was associated with all the most important variables so far considered. This probably explains its importance but also precluded its use in models with more than one variable.

It is well known that ruminants can stretch their rumen to accommodate more feed, especially when they are fed low-quality diets and their requirements are not met (Mertens, 1973; Van Soest, 1994). Cannas (2000), modelling literature measurements of rumen contents, found that, as D-NDFI increased, rumen NDF contents (as % of BW) increased in a curvilinear and concave fashion. Therefore, it seems that the allometric pattern found between D-NDFI and forage NDF K_p was justified by increases of the content of NDF in the rumen as D-NDFI increased.

The same author also found that, at similar D-NDFI, most of the diets with at least 16% CP had lower rumen NDF contents than those with less than 16% CP. This would also explain why in our database, at the same level of intake, low-quality diets had lower forage NDF K_p than high-quality diets: the former diets probably stretched the rumen more and had higher rumen NDF contents and therefore lower K_p.

The importance of dietary CP for rumen dynamics and intake is well known (Van Soest, 1994). When there is shortage of nitrogen, bacterial cellulolytic activity is reduced, decreasing both the removal of feed by digestion and the intensity of particle breakdown. Both factors determine an increase in rumen fill and a reduction of intake and K_p. A positive effect of protein supplementation on intake and forage NDF K_p was observed in many experiments (e.g. McCollum and Galyean, 1985; Oosting and Waanders, 1993).

The role of NDF as the second variable could also be justified. Diets with high NDF concentrations often contain mature forages, which, because of their low degradation rates and extent of fibre digestion, tend to increase rumen fill (Van Soest, 1994) and decrease K_p.

Considering the similarity of the mechanisms proposed to explain the action of D-CP% and D-NDF% and their high correlation, it is difficult to establish which one has the larger effect on forage NDF K_p. In our models, D-CP% was preferred because it gave a better fit and for the importance of D-CPI as predictor.

Equations similar to that found with our database, linearly relating the K_p of concentrates with that of forages, were obtained by Colucci *et al.* (1990) and by Sauvant and Archimede (1989) (cited by Lescoat and Sauvant, 1995), whose equation is also used by the Cornell Net Carbohydrate and Protein System (CNCPS) (Sniffen *et al.*, 1992).

The biological significance of the relationship between forage NDF K_p and concentrate K_p is suggested by the limited or absent importance of the level of intake of concentrates on forage NDF K_p. It seems that, when animals eat a diet made of forages and concentrates, the 'push' for the passage of forage and concentrate particles is given only by forage particles, or, more precisely, by their NDF, while concentrate particles have a passive role, unless they have a considerable NDF content. The higher K_p of concentrates compared with forages is probably the result of the combined effect of their smaller particle size and higher specific gravity.

Conclusions

The study of the relationships among body size, dietary parameters and rumen passage rate of solids in domestic ruminants showed the following:

1. The scaling of the level of intake on BW allowed the comparison between ruminants of very different BW on the basis of a uniform criterion. No evidence was found to justify species differences.

2. The level of intake of NDF and the forage NDF K_p were associated by a curvilinear relationship, probably explained by the increase in rumen NDF contents as the level of intake of NDF increased.
3. The quality of the diets was an important factor affecting forage NDF K_p.
4. It appeared that the passage of both forage and concentrate particles is controlled by NDF intake, which is mostly of forage origin.
5. No clear differences in K_p estimates between chromium and rare-earth markers were found.

The models proposed suggest that if the appropriate predictors are used, small ruminants can be used in digestion or K_p experiments as models for large ruminants and vice versa.

Acknowledgements

This work was supported by a grant of the Italian Ministero Politiche Agricole e Forestali. The authors offer special thanks to Professor Aldo Cappio-Borlino for his valuable comments.

References

Aitchison, E., Gill, M., France, J. and Dhanoa, M.S. (1986) Comparison of methods to describe the kinetics of digestion and passage of fibre in sheep. *Journal of the Science of Food and Agriculture* 37, 1065–1072.

Cannas, A. (2000) Predicting energy and protein requirements and diet utilization by sheep based on the structure of the Cornell Net Carbohydrate and Protein System. PhD dissertation, Cornell University, Ithaca, New York.

Chilibroste, P., Aguilar, C. and Garcia, F. (1997) Nutritional evaluation of diets: simulation model of digestion and passage of nutrients through the rumen–reticulum. *Animal Feed Science and Technology* 68, 259–275.

Colucci, P.E., MacLeod, G.K., Grovum, W.L., McMillan, I. and Barney, D.J. (1990) Digesta kinetics in sheep and cattle fed diets with different forage to concentrate ratios at high and low intakes. *Journal of Dairy Science* 73, 2143–2156.

CSIRO, Standing Committee on Agriculture, Ruminants Subcommittee (1990) *Feeding Standards for Australian Livestock: Ruminants*. CSIRO Publications, East Melbourne, Australia.

Demment, M.W. and Van Soest, P.J. (1985) A nutritional explanation for body-size patterns of ruminant and nonruminant herbivores. *American Naturalist* 125, 641–672.

Evans, E. (1981) An evaluation of the relationships between dietary parameters and rumen solid turnover rate. *Canadian Journal of Animal Science* 61, 97–103.

Illius, A.W. and Gordon, I.J. (1991) Prediction of intake and digestion in ruminants by a model of rumen kinetics integrating animal size and plant characteristics. *Journal of Agricultural Science, Cambridge* 116, 145–157.

Lescoat, P. and Sauvant, D. (1995) Development of a mechanistic model for rumen

digestion validated using the duodenal flux of amino acids. *Reproduction, Nutrition, Development* 35, 45–70.

Lindberg, J.E. (1988) Retention times of small feed particles and of water in the gut of dairy goats fed at different levels of intake. *Journal of Animal Physiology and Animal Nutrition* 59, 173–181.

McCollum, F.T. and Galyean, M.L. (1985) Influence of cottonseed meal supplementation on voluntary intake, rumen fermentation and rate of passage of prairie hay in beef steers. *Journal of Animal Science* 60, 571–577.

Mertens, D.R. (1973) Application of theoretical mathematical models to cell wall digestion and forage intake in ruminants. PhD thesis, Cornell University, Ithaca, New York.

Oosting, S.J. and Waanders, A. (1993) The effect of rumen ammonia nitrogen concentration on intake and digestion of wheat straw by goats. *Animal Feed Science and Technology* 43, 31–40.

Owens, F.N. and Goetsch, A.L. (1986) Digesta passage and microbial protein synthesis. In: Milligan, L.P., Grovum, W.L. and Dobson, A. (eds) *Control of Digestion and Metabolism in Ruminants*. Prentice-Hall, Englewood Cliffs, New Jersey.

Ratkowsky, D.A. (1983) *Nonlinear Regression Modeling: a Unified Practical Approach*. Marcel Dekker, New York.

Sniffen, C.J., O'Connor, J.D., Van Soest, P.J., Fox, D.G. and Russell, J.B. (1992) A net carbohydrate and protein system for evaluating cattle diets: II. Carbohydrate and protein availability. *Journal of Animal Science* 70, 3562–3577.

Van Soest, P.J. (1994) *Nutritional Ecology of the Ruminant*, 2nd edn. Cornell University Press, Ithaca, New York.

5

Ruminal Metabolism of Buffer-soluble Proteins, Peptides and Amino Acids *In Vitro*

Peter Udén

Department of Animal Nutrition and Management, Swedish University of Agricultural Sciences, Box 7024, 750 07 Uppsala, Sweden

Abstract

A complex mechanistic model of soluble protein degradation was developed and fitted to literature data of *in vitro* rumen casein (CAS) and acid-hydrolysed casein (AHCAS) fermentation. Feed amino acid escape was estimated from this model and was compared with estimates made with a simple model of substrate degradation. The complex model could be reasonably fitted to the data set, assuming current understanding of ruminal protein degradation. It included five state variables and both mass action and Michaelis–Menten kinetics. Rates for bacterial extracellular degradation of CAS and subsequent uptake of peptides (PEP) were relatively similar; 1.46 and 0.88 h^{-1}, respectively. Ruminal escape was also estimated to be relatively similar for CAS and AHCAS, 26 and 23%, respectively.

Estimating ruminal protein degradation using a very aggregated model can be highly inaccurate, particularly when the observation time period is too short and protein-PEP degradation rate is low. It was believed that, if monitoring both protein and PEP, a model could be fitted which would be more likely to estimate escape, independent of observation period length.

Introduction

Experimental research has revealed part of the sequence of events leading to the degradation of proteins by ruminal microorganisms (Broderick *et al.*, 1991). The main features of this chain of events are thought to be as follows:

 Modelling Nutrient Utilization in Farm Animals (eds J.P. McNamara, J. France and D.E. Beever)

1. Soluble proteins adhere to the surface of the microbe. This was found to be a passive event, which takes place even at 0°C (Nugent and Mangan, 1981), probably as a result of high ion interaction between proteins and the microbial cell surface. Approximately 10 μg casein mg^{-1} bacterial protein may be bound in this process (Wallace, 1985). If the proteins are insoluble, the bacteria have to attach to the surface instead, before digestion can take place.
2. Extracellular digestion of the protein.
3. Active transport of oligopeptides and amino acids into the microbial cells. This transport is generally faster for the peptide than for the free amino acids (Prins *et al.*, 1979). For amino acids, it occurs at variable rates (Volden *et al.*, 1998).
4. Intracellular hydrolysis of peptides into amino acids and amino acids into ammonia.
5. Microbial synthesis of protein from amino acids, ammonia and possibly peptides.
6. Exchange of amino acids and ammonia with the medium.

For predicting dietary amino acid flow from the rumen, the disappearance of N *in sacco* (e.g. Mehrez and Ørskov, 1977) or the appearance of ammonia or amino acids *in vitro* (Broderick, 1987) have been used. In all cases, very simple kinetic models have been employed, ignoring all intermediate steps in the degradation process, focusing only on the disappearance of soluble protein or appearance of end-products. The underlying assumption has been that the rate-limiting step in the degradation process is the extracellular degradation of the intact protein. The theory of the *in sacco* method is further simplified by assuming that all N that is washed out of the bag is instantly degradable.

Objectives

The objectives were to develop a mechanistic model of soluble protein degradation with similar behaviour to an *in vitro* rumen system and to compare the estimated ruminal feed amino acid escape from this model, with estimates made using a simple model of substrate degradation.

The present objectives were formulated as a first step in the development of an applied model of protein degradation *in vivo*.

Materials and Methods

Data used in the present study were obtained from Broderick and Craig (1989). In this paper, *in vitro* incubations were performed with 0.5 g samples, 100 ml rumen inoculum and 200 ml buffer. Initial amino acid concentrations were approximately 15.2 mmol l^{-1} or 1700 μmol amino acids g^{-1} dry matter. Measurements were taken every 10 min for 120 min of the following:

1. Extracellular peptide-bound amino acids (AA) (PEP).
2. Intracellular free AA (ICAA).
3. Extracellular free AA (XCAA).
4. Total ammonia.

Several substrates were studied, including bovine serum albumin, casein (CAS), acid-hydrolysed casein (AHCAS) and enzymatically hydrolysed casein. Only the data for CAS and AHCAS were used for modelling purposes. CAS was chosen for being a relatively pure soluble protein, giving rise to detectable changes in all the aforementioned pools. AHCAS was believed to consist entirely of free AA and would serve as a test for parameter robustness with respect to AA uptake, exchange and deamination.

Both simple and complex degradation models were fitted to the data. Figure 5.1 shows the simple and complex degradation models used.

Consideration was given to the above-mentioned events when developing the complex model structure. In step 4, the intracellular (IC) PEP hydrolysis was assumed to be so rapid that it could be ignored. Mass action (MA) and Michaelis–Menten (M–M) kinetics were tested to describe pool fluxes in all possible combinations. The model was implemented in Powersim® and optimizations were done with Poweropt, a Simplex optimizer developed by Gustafsson (1998) and interfaced with Powersim. For the degradation of CAS, protein hydrolysis and PEP uptakes were first fitted and subsequently the other fluxes were parameterized, with a maximum of five parameters fitted simultaneously. Optimizations were terminated after 200 iterations.

Broderick (1987) used the simple model for an *in vitro* system where microbial protein synthesis, but not degradation, is inhibited and appearance of AA and ammonia (NH_3) is monitored over time. In the present study, no inhibitors were used, so uptake by microbes could occur. To compare the method of

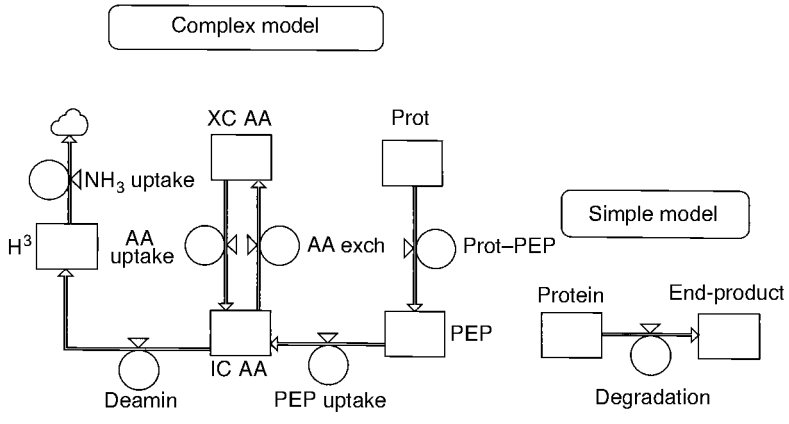

Fig. 5.1. Models for casein and acid-hydrolysed casein ruminal metabolism *in vitro*.

calculating CAS degradation from appearance of AA and NH_3 in an inhibited *in vitro* (IIV) system a new variable was derived:

$$CAS_{IIV} = 1727 - (NH_3 + XCAA + N \text{ uptake by microbes})$$

where 1727 equals CAS concentration at time zero.

In the study of Broderick and Craig (1989), uptake by the microbes was not recorded, but it could be estimated from the N balance. The CAS_{IIV} data set was fitted, assuming first-order kinetics, using the standard non-linear least-squares algorithm in Tablecurve™ (1996). Also the log-transformed data were fitted by linear regression. Estimations of a potential *in vivo* AA escape were done after fitting the models to the data.

Results and Discussion

Complex model

With both substrates, Michaelis–Menten kinetics gave a better fit for AA uptake and for deamination, but MA kinetics was adequate for the remaining fluxes. In CAS, the reasons for this may have been that the protein and PEP concentrations were never high enough to detect saturation behaviour. For AHCAS, an N-balance calculation revealed a shortage of 24% at time zero. Including a PEP pool with an equivalent starting value substantially improved model fit. It was also found that the microbial synthesis from both AA and ammonia was so low that it could be ignored. For CAS, however, only AA incorporation into microbial protein could be eliminated.

Results from model fitting to CAS data are shown in Fig. 5.2 and in Table 5.1. The behaviour of the PEP pool was quite reasonable and the uptake rate of peptides was even slower than protein hydrolysis rate ($0.88\ h^{-1}$), whereas protein hydrolysis was $1.46\ h^{-1}$. The observed ammonia evolution was almost linear from time zero and was difficult to simulate. Also, the early phases of the ICAA and XCAA pools showed very rapid changes, which were difficult to predict with the present model. The fitting of parameters was not weighted relative to expected measurement accuracy. Judging from the technique used, ICAA were probably the least trustworthy values and should perhaps have been given a lower weight than PEP, ammonia and XCAA.

For AHCAS (Fig. 5.3 and Table 5.1), the behaviour of the XCAA and ammonia pools was predicted better than for CAS, but the ICAA was again not well represented.

Comparable rate constants were not very similar between the two substrates and the affinity and V_{max} constants seemed to be particularly sensitive to the data noise. Personal experience of fitting M–M models to data has shown a great dependency on the data range for accurate fit. Reasonable fit was achieved only when flux ranges were sufficiently large – around $1/2V_{max}$.

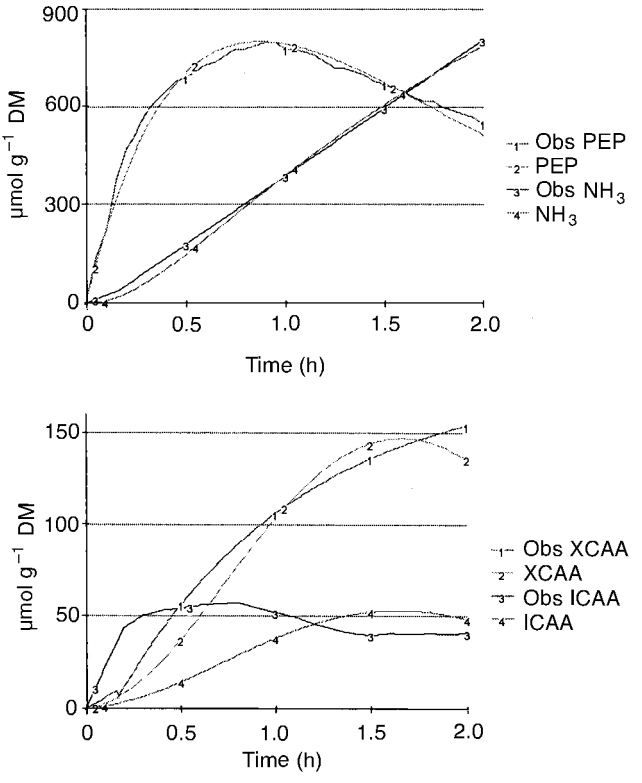

Fig. 5.2. Observed and simulated concentrations of peptides (PEP), NH_3, and extracellular (XCAA) and intracellular amino acids (ICAA) during *in vitro* ruminal fermentation of casein.

Simple model

Fitting the simple model to the CAS_{IIV} data resulted in vastly different estimates of degradation rates. The untransformed data showed an almost linear decline, resulting in a large negative asymptote and a very small rate of $0.008\ h^{-1}$, whereas the log-transformed data resulted in a high rate value of $0.50\ h^{-1}$. Regions of under- and overprediction were particularly evident, especially when fitting the log-transformed data.

Ruminal escape

Simulated estimates using the complex model were similar for both substrates – 26 and 23% for CAS and AHCAS, respectively. Escape values for the simple

Table 5.1. Parameter* estimates of the complex and simple models and estimated ruminal escape.

Substrate/model	Flux	k (h^{-1})	k_m (μmol g^{-1})	V_{max} (μmol g^{-1} h^{-1})	Escape of AA (%)†
Casein					
Complex model	Protein hydrolysis	1.46			
	PEP uptake	0.88			
	AA uptake		42	770	
	AA exchange	17			
	Deamination		14	720	
	NH_3 uptake	0.40			26
Simple model					
Direct fit		0.008			95
Log fit		0.50			25
Acid hydrolysed casein (AHCAS)					
Complex model	PEP uptake	0.62			
	AA uptake		0.01	390	
	AA exchange	3.9			
	Deamination		4.2	430	23

*k = Fractional rate constant in mass action reactions; k_m = affinity and V_{max} = maximum rate constants in Michealis–Menten reactions.
† Dilution rate: 0.1655 h^{-1} (Volden *et al.*, 1998).

model were very high (95%) when using the degradation rate obtained with the untransformed CAS_{IIV} data, but very similar (25%) when based on the log-transformed data. Fitting log-transformed data assumes errors to be proportional to the Y values, whereas fitting unweighted data assumes additive errors. The latter often seems a more valid hypothesis in substrate degradation studies when data ranges are within an order of magnitude or so. However, in the present study, the CAS_{IIV} decay curve was lacking any signs of an asymptote, which resulted in a totally unrealistic escape value using the untransformed data.

The simple model was the ultimate aggregation of a number of processes in the microbial degradation of casein and was not able to estimate escape when fitted to untransformed data. The effect of length of fermentation time seemed to play an important role and possibly the absence of a rate-limiting step. To investigate this, the complex model was used to simulate CAS_{IIV} output using fractional degradation rates of either 1.46 or 0.2 h^{-1} for the protein–PEP degradation step. The simple model was then refitted to the resulting untransformed data from the first 2 to 40 h time periods. Escape was calculated for both the complex and the simple model assuming a passage rate of 0.1 h^{-1}. The results in Table 5.2 clearly show the dependency on time-period lengths for estimating escape at a reasonable accuracy. Longer observation periods were required at the low protein–PEP degradation rate. On the other hand, if too much of the

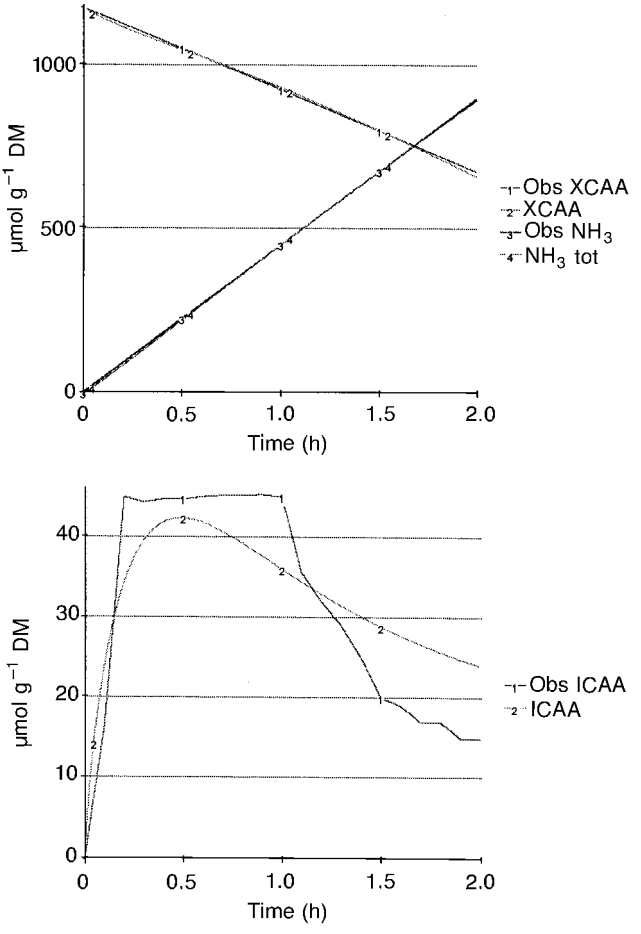

Fig. 5.3. Observed and simulated concentrations of NH_3 and extracellular (XCAA) and intracellular amino acids (ICAA) during *in vitro* ruminal fermentation of acid-hydrolysed casein.

asymptote was included, the escape values tended to be somewhat underestimated.

Conclusions

The complex model could be reasonably fitted to the data set, assuming current understanding of ruminal protein degradation. Rates for bacterial extracellular degradation of CAS and subsequent uptake of PEP appeared relatively similar. Ruminal escape was also estimated to be relatively similar for CAS and AHCAS.

Table 5.2. Estimates of protein degradation rates (k_d) and ruminal escape (ESC) as affected by length of observation period and the fractional degradation rate of protein to peptides (k_{PEP}). Estimates were made by fitting the simple model to data generated by the complex model.

Time period (h)	k_d (h^{-1})	ESC (%)	Actual (%)	k_d (h^{-1})	ESC (%)	Actual (%)
k_{PEP} = 1.46 h^{-1}				k_{PEP} = 0.2 h^{-1}		
0–2	0.013	88	17	0.004	96	38
0–4	0.31	24		0.004	96	
0–6	0.45	18		0.019	84	
0–8	0.51	16		0.076	57	
0–10	0.53	16		0.11	48	
0–20	0.55	15		0.16	38	
0–40	0.55	15		0.17	37	

The author believes that estimating ruminal protein degradation using the simple model in Fig. 5.1 can be highly inaccurate, particularly when the time period is short and the protein–PEP degradation rate is low. If both protein and PEP are monitored, a model could be fitted that should be more likely to estimate escape independent of observation period length.

References

Broderick, G.A. (1987) Determination of protein degradation rates using a ruminal *in vitro* system containing inhibitors of microbial nitrogen metabolism. *British Journal of Nutrition* 58, 463–475.

Broderick, G.A. and Craig, W.M. (1989) Metabolism of peptides and amino acids during *in vitro* protein degradation by mixed rumen organisms. *Journal of Dairy Science* 72, 2540–2548.

Broderick, G.A., Wallace, R.J. and Ørskov, E.R. (1991) Control of rate and extent of protein degradation. In: Tsuda, T., Sasaki, Y. and Kawashima, R. (eds) *Proceedings of Physiological Aspects of Digestion and Metabolism in Ruminants*. Academic Press, San Diego, pp. 541–592.

Gustafsson, L. (1998) PowerOpt. PowerOpt Test version 1.0. Free software from leif.gustafsson@lt.slu.se.

Mehrez, A.Z. and Ørskov, E.R. (1977) A study of the artificial fibre bag technique for determining the digestibility of feeds in the rumen. *Journal of Agriculture Science (Cambridge)* 88, 645–650.

Nugent, J.H.A. and Mangan, J.L. (1981) Characteristics of the rumen proteolysis of fraction I (18S) leaf protein from lucerne (*Medicago sativa* L). *British Journal of Nutrition* 46, 39–59.

Prins, R.A., Van Hal-Van Gestel, J.C. and Counotte, G.H.M. (1979) Degradation of amino acids and peptides by mixed rumen microorganisms. *Zeitschrift für Tiernahrung und Futtermitttelkunde* 42, 333–339.

Tablecurve™ (1996) Tablecurve 2D, version 4, SPCSS Inc.
Volden, H., Velle, W., Harstad, O.M., Aulie, A. and Sjaastad, V. (1998) Apparent ruminal degradation and rumen escape of lysine, methionine, threonine administered intraruminally in mixtures to high yielding cows. *Journal of Animal Science* 76, 1232–1240.
Wallace, R.J. (1985) Adsorption of soluble proteins to rumen bacteria and the role of adsorption in proteolysis. *British Journal of Nutrition* 53, 399–408.

6

Models to Interpret Degradation Profiles Obtained from *In Vitro* and *In Situ* Incubation of Ruminant Feeds

S. López,[1] J. France,[2] J. Dijkstra[3] and M.S. Dhanoa[4]

[1]*Departamento de Producción Animal, Universidad de León, E-24007 León, Spain;* [2]*Department of Agriculture, University of Reading, Earley Gate, Reading RG6 6AT, UK;* [3]*Animal Nutrition Group, Wageningen Institute of Animal Sciences (WIAS), Wageningen University, Marijkeweg 40, 6709 PG Wageningen, The Netherlands;* [4]*Institute of Grassland and Environmental Research, Plas Gogerddan, Aberystwyth SY23 3EB, UK*

Abstract

Degradation kinetic parameters are usually estimated from degradation profiles obtained using the polyester bag technique or the gas production technique. Models to describe either *in situ* disappearance curves or gas production profiles were derived from first principles by considering simple compartmental schemes, and by assuming first-order kinetics but allowing the fractional rate of substrate degradation to vary with time. Using this approach, the quantity of potentially degradable substrate remaining undegraded (S, g/g incubated) at any time (t, hours) during the incubation *in situ* or *in vitro* can be represented by the general expression, $S = S_0 \times [1 - \Phi(t)]$, where S_0 is the fraction which is potentially degraded over time and Φ is a positive monotonically increasing function with an asymptote at $\Phi = 1$. Several alternative functions can be candidates for Φ, depending upon the function chosen to represent the fractional degradation rate. From this, *in situ* disappearance (D, g/g incubated) can be expressed as $D = W + S_0 \times \Phi(t)$, where W is the intercept and represents the fraction which instantaneously disappears from the bag. Similarly, gas production profiles observed *in vitro* can be represented by $G = YS_0 \times \Phi(t)$, where G (ml) denotes total gas accumulation to time t and Y [ml gas (g degradable DM)$^{-1}$] is a constant

 Modelling Nutrient Utilization in Farm Animals (eds J.P. McNamara, J. France and D.E. Beever)

yield factor. In this chapter, a number of candidate models were fitted to several *in situ* and *in vitro* degradation profiles obtaining estimates of the degradation parameters. Extent of degradation was calculated for a given passage rate (k, h^{-1}), and a comparative study was carried out evaluating the estimated values for the extent of degradation obtained with the candidate models. Differences between values obtained from *in vitro* gas production profiles and from *in situ* disappearance curves are discussed.

Introduction

Mechanistic modelling can be used to derive kinetic parameters from data obtained *in vitro* or *in situ* for subsequent incorporation in holistic models to simulate whole-system behaviour. An appropriate model can be a useful tool to link the data obtained *in vitro* or *in situ* with the processes occurring in organs and tissues *in vivo*.

Ruminal degradation parameters are usually estimated from degradation profiles, obtained using either the polyester bag technique or the gas production method. In the first case, a time-course disappearance curve for each feed component is obtained *in situ* by measuring the amount of residue remaining in the bag at several time points. Disappearance curves are used to evaluate the kinetics of degradation of feeds in the rumen, by assuming that disappearance from the bag equals degradation of feed in the rumen. The gas production technique aims to measure the rate of production of fermentation gases that can be used to predict the rate of feed degradation, assuming that the amount of gas produced is directly proportional to the amount of substrate degraded. Both *in situ* disappearance curves and *in vitro* gas production profiles exhibit a range of shapes, from steep diminishing returns to pronounced sigmoidals. The biomathematical challenge is to derive meaningful equations capable of describing such a family of curves in order to estimate degradation parameters for the calculation of extent of degradation in the rumen.

Mathematical Derivation

To associate disappearance or gas production curves with digestion in the rumen, models have been developed based on compartmental schemes, which assume the feed comprises at least two fractions: a potentially degradable fraction, S, and an undegradable fraction, U. Fraction S will be degraded at a fractional rate, μ (h^{-1}), after a discrete lag time, L (h). The dynamic behaviour of the fractions is described by the differential equations:

$$dS/dt = 0, \qquad 0 \leqslant t < L \tag{1a}$$

$$= -\mu S, \qquad t \geqslant L \tag{1b}$$

$$dU/dt = 0, \qquad t \geqslant 0 \tag{2}$$

Therefore, the entities to be estimated or prescribed are the initial size of the fraction S, the size of U, the lag time (L) and the fractional degradation rate (μ). The fractional degradation rate can be considered an intrinsic characteristic of the feed, although once the feed is in the rumen, the degradation rate may also be affected by factors related to the animal.

An essential aspect of estimating the rate of degradation concerns the kinetics assumed for the process. The most commonly used model (Ørskov and McDonald, 1979) assumes first-order kinetics, implying that substrate degraded at any time is proportional to the amount of potentially degradable matter remaining at that time, with a constant fractional rate μ, and that only characteristics of the substrate limit degradation. This model has been extensively used, owing to its simplicity, but it is not capable of describing the large diversity of degradation profiles that have been observed (Dhanoa *et al.*, 1995) and cannot represent explicitly the reciprocal influences of substrate degradation and microbial growth. France *et al.* (2000) postulated that μ may vary with time according to different mathematical functions. From the various functions used to represent μ and on the basis of rate : state principles, different models can be derived to describe either *in situ* disappearance (López *et al.*, 1999) or *in vitro* gas production profiles (France *et al.*, 2000). Some of these functions are capable of describing both a range of shapes with no inflexion point and a range of sigmoidal shapes in which the inflexion point is variable. On substituting for the function proposed for μ and integrating, equation 1b yields an equation for the S fraction remaining during the incubation *in situ* or *in vitro* at any time t, which can be expressed in the general form:

$$S = S_0 \times [1 - \Phi(t)] \tag{3}$$

where S_0 is the zero-time quantity of the S fraction, $\Phi(t)$ is a positive monotonically increasing function with an asymptote at $\Phi(t) = 1$, and t is incubation time (h). *In situ* disappearance (D, g g^{-1} incubated) is given by:

$$D = W + S_0 - S = W + S_0 \times \Phi(t) \tag{4}$$

Similarly, gas production profiles observed *in vitro* can be represented by:

$$G = YS_0 \times \Phi(t) \tag{5}$$

where G (ml) denotes total gas accumulation to time t and Y (ml gas g^{-1} degradable DM) is a constant yield factor. Independent estimates of the parameters Y and S_0 cannot be obtained by non-linear regression because, on fitting equation 5, a single estimate for YS_0 (asymptotic gas production) is attained.

For each function, μ can be obtained from equations 1b and 3 as:

$$\mu = -\frac{1}{S}\frac{dS}{dt} = \frac{1}{(1-\Phi)}\frac{d\Phi}{dt} \tag{6}$$

This function constitutes the mechanistic interpretation of the degradation

processes. Rates of degradation and passage can be combined to calculate the extent of degradation of the substrate in the rumen (France *et al.*, 1990, 1993). In the rumen, if S is the amount of potentially degradable substrate remaining which is subjected to both passage and degradation, the rate of disappearance of S is given by:

$$\frac{dS}{dt} = -kS, \qquad t < L \tag{7a}$$

$$= -(k+\mu)S, \qquad t \geqslant L \tag{7b}$$

where k (h^{-1}) is the fractional rate of passage from the rumen, and is assumed constant. This constant can be obtained by using any available model for passage kinetics.

To obtain S, the solutions of these differential equations are:
by integration of (7a):

$$S = S_0\, e^{-kt}, \qquad t < L \tag{8a}$$

by integration of (7b):

$$\int_{S_L}^{S} dS/S = -\int_{L}^{t} \left\{ k + \frac{d\Phi/dt}{(1-\Phi)} \right\} dt = -\int_{L}^{t} k\,dt - \int_{\Phi_L}^{\Phi} \frac{d\Phi}{(1-\Phi)} \tag{8b}$$

i.e.:

$$S = S_0\, e^{-kt} \times (1 - \Phi), \qquad t \geqslant L \tag{9}$$

Using equations 6 and 9 and given a value for k, the extent of degradation in the rumen (E, g degraded g^{-1} ingested), estimated by using the parameters obtained from *in situ* disappearance curves, is given by the equation:

$$E = \frac{W + \int_{L}^{\infty} \mu S\,dt}{W + S_0 + U_0} = \frac{W + I}{W + S_0 + U_0} \tag{10}$$

where:

$$I = \int_{L}^{\infty} \mu S\,dt = S_0 \int_{L}^{\infty} \frac{d\Phi}{dt} e^{-kt}\,dt = S_0 \left[\left(\Phi e^{-kt} \right) \Big|_{t=L}^{\infty} + k \int_{L}^{\infty} \Phi e^{-kt}\,dt \right]$$
$$= kS_0 \int_{L}^{\infty} \Phi\, e^{-kt}\,dt \tag{11}$$

as $\Phi = 0$ when $t = L$ and $e^{-kt} = 0$ when $t = \infty$, and thus $(\Phi e^{-kt}) \big|_{t=L}^{\infty} = 0$. Therefore, for *in situ* disappearance profiles (López *et al.*, 1999):

$$E = \frac{W + kS_0 \int_L^{\infty} \Phi e^{-kt}\, dt}{W + S_0 + U_0} \quad (12)$$

where $\int_L^{\infty} \Phi e^{-kt}\, dt$ can be calculated by numerical integration if there is no analytical solution. Using a similar approach for *in vitro* gas production profiles, the expression to calculate extent of degradation would be (France *et al.*, 2000):

$$E = \frac{\int_L^{\infty} \mu S dt}{S_0 + U} = \frac{kS_0 \int_L^{\infty} \Phi e^{-kt}\, dt}{S_0 + U} \quad (13)$$

Equations 12 and 13 provide a general expression for calculating the extent of degradation, and are applicable to any model expressed in the form of equations 4 and 5.

Model Evaluation

The equations derived to calculate the extent of degradation of feeds in the rumen were tested with degradation profiles from eight hays. Five hays from sown grasslands and three hays harvested from permanent mountain (between 900 and 1300 m altitude) meadows were used in this study. The hays from established swards were: two from pure-stand legumes (alfalfa and red clover) and three mixtures (grass–clover mixture, mixed grass sward and vetch–cereal mixture). The hays from permanent mountain meadows were harvested either in June (two hays from the first cut) or from the September aftermath (one hay), so that they could be considered representative of those produced under practical conditions in north-west Spain. The hays were selected based on their variable botanical and chemical composition, in order to achieve a wide range in chemical composition (Table 6.1). Hays were grouped as leguminous or graminaceous, based on their botanical composition.

In situ disappearance profiles were obtained by the polyester bag technique (Ørskov and McDonald, 1979), using three adult ewes fitted with a permanent rumen cannula and fed on good-quality hay. Nylon bags (12.5×10.0 cm in size and made of filter cloth of pore size 50×27 μm), each containing approximately 5 g of sample (ground through a 2.5 mm sieve), were incubated in the rumen of each of the three sheep for periods of 3, 6, 9, 15, 24, 48 and 72 h. Once removed from the rumen, the bags were washed thoroughly under running cold water for 2 min and then washed in the cold-rinse cycle (20 min) of a washing-machine. Then, bags were oven-dried at 60°C for 48 h, incubation residues were determined and dry matter (DM) disappearance was calculated from the

Table 6.1. Chemical (g kg^{-1} dry matter (DM)) and botanical (legumes as proportion of the total DM) composition of the hays used in the study.

	Crude protein	Neutral detergent fibre	Acid detergent fibre	Permanganate lignin	Legumes (g g^{-1} DM)
Leguminous hays					
Alfalfa	207	428	313	80	1.00
Red clover	113	566	419	117	1.00
Vetch–cereal mixture	97	563	351	84	0.70
Grass–clover mixture	129	581	375	88	0.25
Graminaceous hays					
Permanent meadow hay 3, September aftermath	126	553	315	63	0.15
Permanent meadow hay 1, first cut	69	664	371	65	0.08
Permanent meadow hay 2, first cut	57	744	439	78	0.06
Grass hay	106	618	313	35	None

loss in weight. Zero-time wash values were measured by washing two bags per forage as described above, without previous incubation in the rumen.

Also, hays were incubated *in vitro* in buffered rumen fluid and gas production at different time intervals was measured, as described by Menke and Steingass (1988). The rumen liquor was obtained from the same sheep used in the *in situ* trial and receiving the same diet to ensure similar conditions for both techniques. The incubation medium with buffer and mineral solutions was prepared anaerobically, as described by Menke and Steingass (1988), and then rumen fluid was transferred to the buffered medium in the proportion 1 : 2 (vol vol^{-1}). After weighing 200 ± 4 mg of air-dried sample (ground through a 1 mm screen) of each hay into calibrated glass syringes (100 ml), 30 ml of rumen liquor : buffer mixture were anaerobically dispensed to each syringe (prewarmed at 39°C), and then all syringes were submerged in a water bath at 39°C. Readings (piston displacement) were recorded after incubation periods of 3, 6, 12, 24, 36, 48, 72 and 96 h. Duplicates of each sample were used.

The candidate models used to fit the *in situ* disappearance curves and gas production profiles were: simple Mitscherlich or exponential (EXP) (Ørskov and McDonald, 1979), generalized Mitscherlich (GM) (France *et al.*, 1993) and generalized Von Bertalanffy (VB) (López *et al.*, 1999) models. The expressions for Φ and μ for each model are shown in Table 6.2.

Each model was fitted to the data by non-linear regression, using the NLIN procedure of the Statistical Analysis Systems (SAS) package (1988). *E* was computed for each feed and model, using the corresponding estimates of the equa-

Table 6.2. Alternative functions for Φ in the general equations of the *in situ* disappearance curves $D = W + S_0 \times \Phi(t)$ and of the gas production profiles $G = YS_0 \times \Phi(t)$ (except for W, S_0 and L, the meanings of all the other parameters are specific to each model).

Model	$\Phi(t) =$		Fractional degradation rate (μ h^{-1})
Simple exponential	$1 - e^{-c(t-L)}$	(for $t > L$)	c
Generalized Mitscherlich	$1 - e^{-c(t-L) - d(\sqrt{t} - \sqrt{L})}$	(for $t > L$)	$c + \frac{d}{2\sqrt{t}}$
Generalized Von Bertalanffy	$\left(1 - e^{-ct}\right)^{1/v}$		$\frac{ce^{-ct}}{v} \frac{\Phi^{(1-v)}}{(1-\Phi)}$

tion parameters, and values for k of 0.033 h^{-1} (a mean value for sheep fed on forages at a level of intake close to maintenance) and 0.067 h^{-1}. For the model EXP, equation 12 resulted in the simple expression:

$$E = \frac{W(\mu + k) + \mu S_0 e^{-kL}}{(\mu + k)(W + S_0 + U_0)} \tag{14}$$

and equation 13 in:

$$E = \frac{\mu S_0 e^{-kL}}{(\mu + k)(S_0 + U_0)} \tag{15}$$

However, for models GM and VB, the integral of equations 12 and 13 had no simple analytical solution and had to be determined by numerical integration using the AREA function of GENSTAT (Genstat 5 Committee, 1987). The potential degradability ($W + S_0$) estimated for each hay from the polyester bag data was used as S_0 for the calculation of E, using gas production parameters, because values for this parameter were not determined *in vitro* and cannot be obtained by fitting equation 5.

For the comparisons between models and between *in situ* and gas production procedures in the estimation of the E values for hays, different statistical procedures were performed (Dhanoa *et al.*, 1999; López *et al.*, 1999).

Results

For these hays, the estimates of extent of ruminal degradation were similar for models EXP, GM and VB, using rate of passage values of 0.033 h^{-1} or 0.067 h^{-1} (Tables 6.3 and 6.4). Pairwise correlations within *in situ* and *in vitro* methods were close to unity. However, correlations only show the degree of association (i.e. closeness of pairwise data to the best-fit line), not the reproducibility. The latter is determined by the closeness of pairwise data to the line of equality, i.e. a line with slope of unity. To measure this coefficient of concordance or reproducibility (Lin, 1989), r_C values were calculated for three combinations of the selected models within the *in situ* and *in vitro* methods (Table 6.5). It can be seen from Table 6.5 that most of the values of r_C are close to the upper limit of unity, for both *in situ* and *in vitro* estimates of *E* values for the eight hays.

The *E* values obtained from the *in situ* polyester bag technique were on average 26% (ranging from 23 to 29%) greater than those from the *in vitro* gas production method (Table 6.6). Using model EXP, Dhanoa *et al.* (1999) proposed to correct the *E* values from the *in situ* procedure for particulate matter loss, assuming that passage losses for particulate matter escaping from the bag at zero time are according to the fractional passage rate, or assuming that there is no instantly degradable fraction. Yet these corrections failed to remove the discrepancy between *in situ* and *in vitro E* values (Table 6.6). However, hays were ranked in almost exactly the same order using the *E* values obtained with both techniques (Spearman rank correlation coefficient = 0.976), the values being closely related with a highly significant correlation coefficient ($r = 0.978$).

Discussion

Although ranking of and comparisons between hays according to their *in situ* or *in vitro E* values were similar, the estimates of *E* values obtained using the *in situ* polyester bag technique were numerically greater than those obtained using the *in vitro* gas production method. The first explanation for this bias could be the loss of particulate matter from the bag, as part of this material is lost without being degraded. However, the discrepancies persist when the *in situ* values are corrected for particle loss (Table 6.6) using the expressions derived by Dhanoa *et al.* (1999). The calculation for *E* using *in situ* parameters (equation 12) assumes that there is a soluble fraction (*W*) that is degraded completely and instantly in the rumen, whereas in the gas production technique the soluble and the insoluble but potentially degradable fractions are both degraded at the same rate (μ) and subject to passage, so neither substrate fraction can be completely degraded in the rumen. A comparison between values obtained with the two techniques was performed, assuming in both cases that the soluble fraction (*W*) is degraded at the same rate (μ) as the insoluble but degradable fraction (*E′* in Table 6.6). This calculation for the *in situ* data was proposed by Dhanoa *et al.* (1999), based on the assumption that the fraction remaining in the bag is rep-

Table 6.3. Extent of degradation of hays in the rumen (E, g g^{-1}) estimated from parameters obtained by fitting different models to the *in situ* disappearance curves, and for different passage rates (k, h^{-1}).

	Simple exponential model		Generalized Mitscherlich model		Generalized Von Bertalanffy model	
	$k = 0.033$	$k = 0.067$	$k = 0.033$	$k = 0.067$	$k = 0.033$	$k = 0.067$
Leguminous hays						
Alfalfa	0.688	0.636	0.688	0.635	0.688	0.636
Red clover	0.570	0.503	0.569	0.502	0.570	0.503
Vetch–cereal mixture	0.600	0.530	0.598	0.527	0.599	0.529
Grass–clover mixture	0.607	0.537	0.607	0.537	0.607	0.537
Graminaceous hays						
Permanent meadow hay 3, September aftermath	0.660	0.571	0.658	0.568	0.659	0.569
Permanent meadow hay 1, first cut	0.515	0.430	0.514	0.430	0.514	0.430
Permanent meadow hay 2, first cut	0.460	0.378	0.461	0.379	0.461	0.379
Grass hay	0.676	0.585	0.674	0.582	0.675	0.583

Table 6.4. Extent of degradation of hays in the rumen (E, g g^{-1}) estimated from parameters obtained by fitting different models to the gas production profiles, and for different passage rates (k, h^{-1}).

	Simple exponential model		Generalized Mitscherlich model		Generalized Von Bertalanffy model	
	$k = 0.033$	$k = 0.067$	$k = 0.033$	$k = 0.067$	$k = 0.033$	$k = 0.067$
Leguminous hays						
Alfalfa	0.508	0.372	0.516	0.382	0.517	0.383
Red clover	0.430	0.307	0.440	0.318	0.438	0.317
Vetch–cereal mixture	0.463	0.334	0.471	0.344	0.470	0.344
Grass–clover mixture	0.465	0.328	0.474	0.338	0.475	0.339
Graminaceous hays						
Permanent meadow hay 3, September aftermath	0.471	0.314	0.481	0.323	0.481	0.323
Permanent meadow hay 1, first cut	0.366	0.238	0.379	0.248	0.381	0.250
Permanent meadow hay 2, first cut	0.332	0.205	0.335	0.212	0.335	0.211
Grass hay	0.511	0.355	0.520	0.365	0.520	0.365

Table 6.5. Calculated values of the coefficient of reproducibility, r_C, for pairwise comparison of estimates of the extent of degradation (E, g g^{-1}) from the simple exponential (EXP), generalized Mitscherlich (GM) and generalized Von Bertalanffy (VB) models.

a. Concordance between models in the E estimates calculated with parameters obtained from *in situ* disappearance curves, and fractional passage rates of 0.033 h^{-1} (lower diagonal) or 0.067 h^{-1} (upper diagonal).

	EXP	GM	VB
EXP		0.9997	0.9999
GM	0.9998		0.9999
VB	0.9999	1.000	

b. Concordance between models in the E estimates calculated with parameters obtained from gas production profiles, and fractional passage rates of 0.033 h^{-1} (lower diagonal) or 0.067 h^{-1} (upper diagonal).

	EXP	GM	VB
EXP		0.9860	0.9851
GM	0.9900		0.9998
VB	0.9893	0.9998	

Table 6.6. Extent of degradation of hays in the rumen (E, g g^{-1}) for $k = 0.033$ h^{-1} estimated from parameters obtained by fitting the simple exponential model to the *in situ* disappearance curves or to the gas production profiles. *In situ* values have been corrected for particulate matter loss (E_c) or calculated assuming the soluble fraction is not instantly degraded (E'), following Dhanoa *et al.* (1999).

	E (*in situ*)	E (gas production)	E_c (corrected *in situ* E)	E'
Leguminous hays				
Alfalfa	0.688	0.508	0.669	0.624
Red clover	0.570	0.430	0.530	0.478
Vetch–cereal mixture	0.600	0.463	0.543	0.470
Grass–clover mixture	0.607	0.465	0.569	0.504
Graminaceous hays				
Permanent meadow hay 3, September aftermath	0.660	0.471	0.610	0.489
Permanent meadow hay 1, first cut	0.515	0.366	0.497	0.422
Permanent meadow hay 2, first cut	0.460	0.332	0.420	0.367
Grass hay	0.676	0.511	0.650	0.513

resentative of the substrate as a whole (there is no instantly soluble fraction), and reduced considerably the difference between *E* estimates obtained from *in situ* or *in vitro* data sets. However, *E* estimates seem to be significantly smaller than values reported in the literature for hays (MAFF, 1990), suggesting that the assumption may fail in describing the degradation kinetics of the soluble fraction. Even with this latter correction, some discrepancies between values estimated from both techniques were still noticeable for some of the forages used. These discrepancies can be attributed to fractional rates of substrate degradation (μ) in the *in situ* technique being higher than in the *in vitro* method, as demonstrated by López *et al.* (1998), despite the inclusion of the soluble fraction within the potentially degradable fraction with the latter method. The higher fractional rate of degradation of the soluble fraction is probably associated with higher propionate proportions of the total volatile fatty acids (VFA) produced. In a simulation study, Dijkstra *et al.* (1999) showed that such changes in the gas production yield during the course of incubation, created by changes in individual VFA production, resulted in an inaccurate extent of ruminal degradation values for the gas production method. The reasons for the discrepancies are therefore likely to be methodological differences between the two techniques. Possibly, rumen fluid is less active *in vitro* than *in situ*, and accumulation of end-products may affect long-term fermentation in batch cultures.

Another contributor to the discrepancies could be the assumption of a constant yield factor, *Y*, in the mathematical representation of the gas production profile (equation 5). Possible differences in gas yield per unit of substrate degraded are not directly important in the calculation of the extent of degradation *E*, as can be seen from the absence of *Y* in equation 13. However, if *Y* varies during the course of incubation, then the rate of gas production does not properly reflect the rate of substrate degradation. For example, a low yield at the start of the incubation period (coinciding with a high propionic acid production from rapidly degrading fractions, including the soluble fraction) and a high yield towards the end of the incubation period will underestimate the rate of substrate degradation and consequently *E*, as observed in a simulation study reported by Dijkstra *et al.* (1999). The value of *Y* might well vary during the course of incubation for a substrate with different chemical entities (e.g. fibre, starch, sugars), because starch and sugars generally have a higher fractional degradation rate than fibre and cause a lower pH in the rumen fluid.

A purpose of studies like this is to demonstrate and emphasize that other models, sensitive to biological features and diversity, are versatile alternatives to the commonly used simple exponential model for describing degradation profiles, which are insensitive to subtle departures from diminishing-returns behaviour. López *et al.* (1999) compared the performance of nine models for describing the *in situ* degradation profiles of 87 animal feeds. These profiles varied from having no inflexion point (i.e. diminishing-returns behaviour) to highly sigmoidal with a variable inflexion point. GM and VB performed well, producing similar estimates of *E* for a chosen rate of passage (the largest difference found was 1.5%), but EXP explained only a subset of the profiles, which

included hays. The choice of hays for this study created curve shapes favourable to any of the models used. Although goodness of fit achieved with GM and VB was slightly superior, the EXP model performed well too, although it is unable to describe sigmoidal profiles.

Models that smooth out important features contribute little to new knowledge. A good model should highlight departures from current understanding and challenge workers to seek plausible explanations. Now that expressions for ruminal extent of degradation for various models have been worked out (López *et al.*, 1999; France *et al.*, 2000), other workers are urged to try these more flexible models in their research, where appropriate, so as to generate a literature on diverse applications. This will enhance our understanding of degradation and fermentation kinetics, leading to better diet formulation and animal nutrition.

Acknowledgement

Financial support received from Comisión Interministerial de Ciencia y Technología (CICYT) Project no. AGF98–0188 is gratefully acknowledged.

References

Dhanoa, M.S., France, J., Siddons, R.C., López, S. and Buchanan-Smith, J.G. (1995) A non-linear compartmental model to describe forage degradation kinetics during incubation in polyester bags in the rumen. *British Journal of Nutrition* 73, 3–15.

Dhanoa, M.S., France, J., López, S., Dijkstra, J., Lister, S.J., Davies, D.R. and Bannink, A. (1999) Correcting the calculation of extent of degradation to account for particulate matter loss at zero time when applying the polyester bag method. *Journal of Animal Science* 77, 3385–3391.

Dijkstra, J., France, J., López, S. and Dhanoa, M.S. (1999) Impact of variation in yield of gas during incubation on simulated gas production and extent of ruminal degradation. In: *Proceedings of the British Society of Animal Science*. British Society of Animal Science, Edinburgh, p. 38.

France, J., Thornley, J.H.M., López, S., Siddons, R.C., Dhanoa, M.S., Van Soest, P.J. and Gill, M. (1990) On the two compartment model for estimating the rate and extent of feed degradation in the rumen. *Journal of Theoretical Biology* 146, 269–287.

France, J., Dhanoa, M.S., Theodorou, M.K., Lister, S.J., Davies, D. and Isac, D. (1993) A model to interpret gas accumulation profiles associated with *in vitro* degradation of ruminant feeds. *Journal of Theoretical Biology* 163, 99–111.

France, J., Dijkstra, J., Dhanoa, M.S., López, S. and Bannink, A. (2000) Estimating the extent of degradation of ruminant feeds from a description of their gas production profiles observed *in vitro*: derivation of models and other mathematical considerations. *British Journal of Nutrition* 83, 143–150.

Genstat 5 Committee (1987) *GENSTAT 5 Reference Manual*. Oxford University Press, Oxford, UK.

Lin, L.I.K. (1989) A concordance correlation coefficient to evaluate reproducibility. *Biometrics* 53, 255–268.

López, S., Carro, M.D., Gonzalez, J.S. and Ovejero, F.J. (1998) Comparison of different *in vitro* and *in situ* methods to estimate the extent and rate of degradation of hays in the rumen. *Animal Feed Science and Technology* 73, 99–113.

López, S., France, J., Dhanoa, M.S., Mould, F. and Dijkstra, J. (1999) Comparison of mathematical models to describe disappearance curves obtained using the polyester bag technique for incubating feeds in the rumen. *Journal of Animal Science* 77, 1875–1888.

MAFF (1990) *UK Tables of Nutritive Value and Chemical Composition of Feedingstuffs*. Rowett Research Services, Aberdeen, UK.

Menke, K.H. and Steingass, H. (1988) Estimation of the energetic feed value obtained from chemical analysis and *in vitro* gas production using rumen fluid. *Animal Research and Development* 28, 7–55.

Ørskov, E.R. and McDonald, I. (1979) The estimation of protein degradability in the rumen from incubation measurements weighted according to rate of passage. *Journal of Agricultural Science, Cambridge* 92, 499–503.

Statistical Analysis Systems (SAS) (1988) *SAS/STAT® User's Guide, Release 6.03*. SAS Institute Inc., Cary, North Carolina, USA.

7

Modelling Production and Portal Appearance of Volatile Fatty Acids in Dairy Cows

André Bannink,[1] Jan Kogut,[1] Jan Dijkstra,[2] James France,[3] Seerp Tamminga[2] and Ad M. van Vuuren[1]

[1]*Institute for Animal Science and Health (ID-Lelystad), ID TNO Animal Nutrition, PO Box 65, 8200 AB Lelystad, The Netherlands;* [2]*Animal Nutrition Group, Wageningen Institute of Animal Sciences (WIAS), Wageningen University, Marijkeweg 40, 6709 PG Wageningen, The Netherlands;* [3]*Department of Agriculture, University of Reading, Earley Gate, Reading RG6 6AT, UK*

Abstract

Values of stoichiometric coefficients were estimated to describe the production of volatile fatty acids (VFA) from fermented substrate in the rumen of lactating cows. Coefficient estimates were derived by regression of *in vivo* data of rumen digestion to a stoichiometric model with non-linear regression techniques. The model explained only part of the simulated range of VFA molar proportions. The theoretical potential of the statistical procedure was investigated by simulation studies. These studies revealed that, although the model explained only a small part of the simulated range of VFA molar proportions, coefficient estimates were fitted accurately when the ideal model is used. Simulation results closely corresponded to those obtained with regression of the *in vivo* data. An evaluation of the *in vivo* coefficient estimates with independent *in vivo* data showed again similar results and seemed to confirm the predictive potential of the coefficient estimates. Additionally, a model was developed which describes VFA metabolism by stomach epithelia. Inputs and outputs of the model are amounts of VFA produced in the rumen and VFA released to portal blood. The current model describes the absorption and the activation of VFA by CoA-synthetases as the first step in VFA metabolism. Activation of VFA was described by competitive inhibition between individual VFA. Parameters were derived from *in vitro* studies of CoA-synthetase activities in tissue samples of ovine or bovine rumen epithelium. The model is a first attempt to describe the interaction between

 Modelling Nutrient Utilization in Farm Animals (eds J.P. McNamara, J. France and D.E. Beever)

production, absorption and metabolism of VFA, and it assists in relating VFA molar proportions or production rates in the rumen to appearance rates or concentrations of VFA in portal blood.

Introduction

Development of nutrient-based models for dairy production demands accurate prediction of the type and amount of nutrient absorbed from the gastrointestinal tract. Volatile fatty acids (VFA) deserve attention because energy is mainly supplied as VFA and because VFA are important precursors for fatty acids in milk and for glucose.

The accuracy of predicting VFA absorption depends first on the accuracy of predictions of VFA production rates in the rumen. Stoichiometric coefficients of VFA production (Murphy *et al.*, 1982) used in extant rumen models result in large prediction errors of VFA molar proportions in rumen fluid (Bannink *et al.*, 1997). Another problem is that nutrient absorption cannot simply be estimated by the amount of nutrients disappearing from the lumen. Gastrointestinal tissues utilize a considerable portion of nutrients because of their intense metabolism and secretory functions. Moreover, gastrointestinal organs are dynamic in nature and their nutrient requirements change in response to the nutritional and physiological state of the cow. There is uncertainty about the extent of their metabolism in gastrointestinal tissues, and there is a lack of quantitative models of VFA metabolism by rumen epithelium in particular. This chapter describes attempts to obtain improvement on both issues.

Rumen VFA Production

With the aim of improving the prediction of the type of VFA produced during rumen fermentation, a new set of VFA coefficients was estimated with a simple stoichiometric model. The model describes the stoichiometry of conversion of five types of substrate (Sc, St, Hc, Ce, P = soluble carbohydrates, starch, hemicellulose, cellulose and protein) to four types of VFA (Ac, Pr, Bu, Bc = acetate, propionate, butyrate and other VFA) by the following set of eight equations (adapted from Murphy *et al.*, 1982). It was assumed that 1 mol of hexose or amino acid equivalent delivers 2.0 and 1.1 mol, respectively, of pyruvate, and that 1 mol of pyruvate allows formation of 1, 1, 0.5 and 0.5 mol of Ac, Pr, Bu and Bc, respectively.

$$P_{Ac} = [U_{Sc} \times c_{Sc,Ac} + U_{St} \times c_{St,Ac} + U_{Hc} \times c_{Hc,Ac} + U_{Ce} \times c_{Ce,Ac}] \times 2 + U_P \times c_{P,Ac} \times 1.1$$

$$P_{Pr} = [U_{Sc} \times c_{Sc,Pr} + U_{St} \times c_{St,Pr} + U_{Hc} \times c_{Hc,Pr} + U_{Ce} \times c_{Ce,Pr}] \times 2 + U_P \times c_{P,Pr} \times 1.1$$

$$P_{Bu} = U_{Sc} \times c_{Sc,Bu} + U_{St} \times c_{St,Bu} + U_{Hc} \times c_{Hc,Bu} + U_{Ce} \times c_{Ce,Bu} + U_{P} \times c_{P,Bu} \times 1.1/2$$

$$P_{Bc} = U_{Sc} \times c_{Sc,Bc} + U_{St} \times c_{St,Bc} + U_{Hc} \times c_{Hc,Bc} + U_{Ce} \times c_{Ce,Bc} + U_{P} \times c_{P,Bc} \times 1.1/2$$

$$MP_{Ac} = P_{Ac}/(P_{Ac} + P_{Pr} + P_{Bu} + P_{Bc})$$

$$MP_{Pr} = P_{Pr}/(P_{Ac} + P_{Pr} + P_{Bu} + P_{Bc})$$

$$MP_{Bu} = P_{Bu}/(P_{Ac} + P_{Pr} + P_{Bu} + P_{Bc})$$

$$MP_{Bc} = P_{Bc}/(P_{Ac} + P_{Pr} + P_{Bu} + P_{Bc})$$

where

P_i = production rate of VFA type *i* (mol day^{-1})

MP_i = molar proportion of VFA type *i* (mol mol^{-1})

U_j = utilization rate of substrate type *j* (mol day^{-1})

$c_{i,j}$ = fraction of substrate type *i* converted to VFA type *j* (mol mol^{-1})

The stoichiometric coefficients (c) in the model define the fraction of a specific type of substrate converted into a specific type of VFA. On the assumption that the partitioning between microbial growth and VFA production was identical for every type of substrate, estimation of the coefficient values becomes independent of the representation of microbial growth, which therefore was not represented in the present model. Using non-linear regression techniques, the calculated VFA molar proportions (MP) were regressed against observed values in rumen fluid with the observed rate of truly digested substrate in the rumen of lactating cows (U) as independent model inputs. Rumen digestion data were selected from a total of 86 concentrate diets (more than 50% concentrate) and 96 roughage diets (more than 50% roughage) tested in 48 rumen digestion trials with mostly Holstein-Friesians reported in literature.

Coefficient estimates

The values that were fitted for the stoichiometric coefficients differed significantly from previously published estimates (TD versus OR in Table 7.1), probably because the present data were obtained from rumen digestion trials on lactating cows only. As a consequence, the data were of a much less heterogeneous origin than those of Murphy *et al.* (1982), which were obtained from sheep and beef cattle or *in vitro*. Comparison of fitted and observed VFA molar proportions (Fig. 7.1a) demonstrated an accurate fit for the average VFA molar proportion, but a range of fitted values that was much smaller than the range of observed values. It was thought that this difference originated from the model not encompassing the full domain of the rumen fermentation stoichiometry.

Table 7.1. Comparison of reported (Murphy *et al.*, 1982) against newly estimated values of stoichiometric coefficients (*c*) of VFA production in the rumen of lactating cows consuming concentrate diets.

	Ac	Pr	Bu	Bc
$c_{Sc\text{-}OR}$*	0.45	0.21	0.30	0.04
$c_{Sc\text{-}TD}$	0.53	0.16	0.26	0.06
$c_{Sc\text{-}SF}$	0.54	0.13	0.27	0.06
$c_{St\text{-}OR}$	0.40	0.30	0.20	0.10
$c_{St\text{-}TD}$	0.49	0.32	0.15	0.05
$c_{St\text{-}SF}$	0.48	0.32	0.15	0.06
$c_{Hc\text{-}OR}$	0.56	0.26	0.11	0.07
$c_{Hc\text{-}TD}$	0.51	0.12	0.32	0.05
$c_{Hc\text{-}SF}$	0.50	0.13	0.31	0.07
$c_{Ce\text{-}OR}$	0.79	0.06	0.06	0.09
$c_{Ce\text{-}TD}$	0.68	0.12	0.20	0.00
$c_{Ce\text{-}SF}$	0.68	0.16	0.20	−0.03
$c_{P\text{-}OR}$	0.36†	0.37	0.20	0.07†
$c_{P\text{-}TD}$	0.44	0.18	0.17	0.21
$c_{P\text{-}SF}$	0.49	0.12	0.20	0.20

* For explanation of Ac, Pr, Bu, Bc, Sc, St, Hc, Ce and P see text; $c_{i\text{-}OR}$ = original coefficient estimates for substrate *i* published by Murphy *et al.* (1982), $c_{i\text{-}TD}$ = new coefficient estimates for substrate i based on rates of true digestion and on the assumption that partitioning of substrate use over microbial growth and VFA production was identical for every type of substrate, $c_{i\text{-}SF}$ = new coefficient estimates for substrate i based on estimated rates of substrate conversion into VFA.

† These specific $c_{P\text{-}OR}$ coefficients are not fully comparable because a different stoichiometric model was used in the present study.

One possible origin of error could have been the simplification in the stoichiometric model of equal partitioning of digested substrate between microbial growth and VFA production. The importance of this simplification was tested by repeating the above procedure of coefficient estimation, with estimates of the rate of substrate actually converted to VFA replacing rate of substrate truly digested as independent inputs. These estimates were obtained by running a much more detailed mechanistic model of rumen digestion, developed by Dijkstra *et al.* (1992). This model was forced to match the observed rates of rumen digestion by substitution of the sum of observed rate of truly digested substrate and calculated rate of substrate outflow for the original model equation of degradation rate of substrate (positive feedback of substrate not utilized by microorganisms). Other required model inputs, including rumen volume, rumen pH and fractional passage rates, were mostly available from the reports selected from literature. However, when model predictions of the amounts of

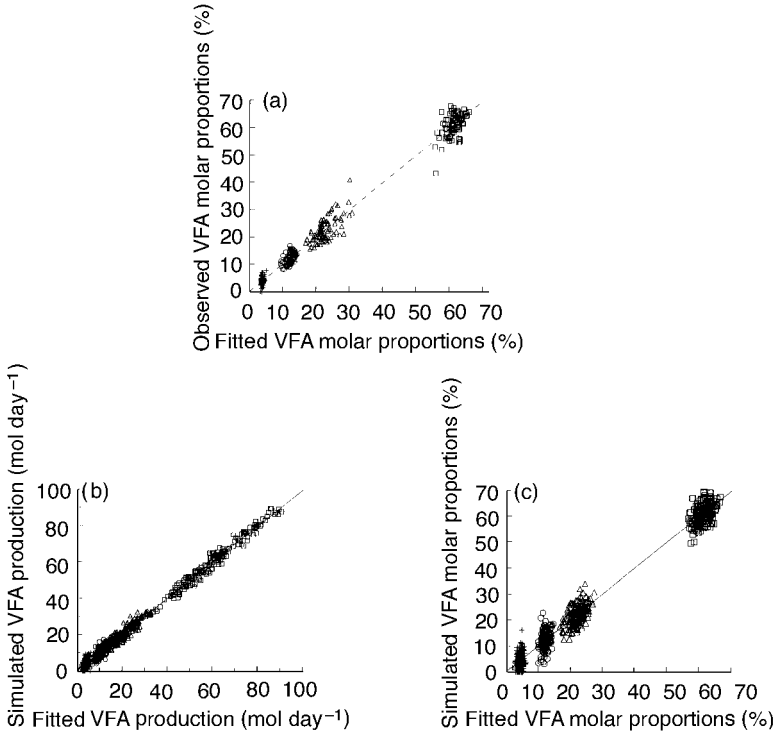

Fig. 7.1. Comparison of fitted values against: (a) observed VFA molar proportions on concentrate diets, (b) one of the ten sets of simulated VFA production rates, (c) one of the ten sets of simulated VFA molar proportions (□, Ac; △, Pr; ○, Bu; +, Bc).

substrate converted to VFA were used as input for the simple stoichiometric model described earlier, estimates of the stoichiometric coefficient changed only slightly (TD versus SF in Table 7.1). This finding indicates that the assumption of equal partitioning over microbial growth and VFA production only slightly affected coefficient estimates.

Simulation studies

In order to clarify the cause of the deviations in fitted VFA molar proportions, simulation studies were performed. With truly digested substrate as input to the stoichiometric model, with an arbitrarily chosen set of coefficient values and with the addition of a normal-distributed random error ($N(0,5^2)$) to the calculated VFA production rates, ten independent sets of simulated VFA molar proportions were obtained. Subsequent regression of the model against these ten

data sets gave accurate estimates of the stoichiometric coefficient values, which were not significantly different ($P < 0.05$, t-test) from the chosen set of coefficient values. Thus, the statistical method can distinguish between the contribution of every type of substrate to the production of a specific type of VFA if the ideal stoichiometric model is used. Predictions of VFA production rates corresponded with the simulated values (Fig. 7.1b). Nevertheless, deviations of fitted VFA molar proportions became apparent, which were similar to those obtained with regression of the *in vivo* data (Fig. 7.1c versus Fig. 7.1a). An increase in the size of random error added during simulation reduced the fraction of variation of simulated data that could be explained by the model. These results indicate that the deviations in fitted VFA molar proportions do not necessarily impair the accuracy of coefficient estimation and are a consequence of the statistical method followed. The effect seems to originate from regressing molar proportions of VFA which are not independent and which sum up to unity or 100% (see equations above).

Evaluation results

The results of the simulations made it interesting to test the prediction accuracy of the coefficient values newly obtained (TD, Table 7.1). Surprisingly, their evaluation with independent data from literature (Chan *et al.*, 1997; Joy *et al.*, 1997; Robinson *et al.*, 1997; Stensig and Robinson, 1997; Yang *et al.*, 1997; De Visser *et al.*, 1998) again showed a smaller range of predicted than of observed VFA molar proportions, similar to regression results discussed earlier (Fig. 7.2). Unfortunately, a corresponding evaluation of VFA production rates was not possible, because such data are not available from literature. A survey of some previous attempts to predict VFA molar proportions (Murphy *et al.*, 1982; Pitt *et al.*, 1996) demonstrates that the same phenomenon occurred in these studies. In deriving their set of stoichiometric coefficients, Murphy *et al.* (1982) also established systematic deviations between fitted and observed VFA molar proportions, whereas such systematic deviations seemed absent between predicted VFA production rates and the few values measured with isotope dilution techniques. Their findings thus correspond to the simulation results of the present study (Fig. 7.1b, c). Nevertheless, the evaluation results clearly showed that the new set of coefficient values gave a more accurate prediction of VFA molar proportions than the set derived by Murphy *et al.* (1982) for the independent data used in this study. The equations of Pitt *et al.* (1996) were not evaluated in this study because of uncertainty about the value of input parameters.

Other factors

In addition to the statistical effects observed in this study, other important factors not considered in the present model may have contributed to discrepancies

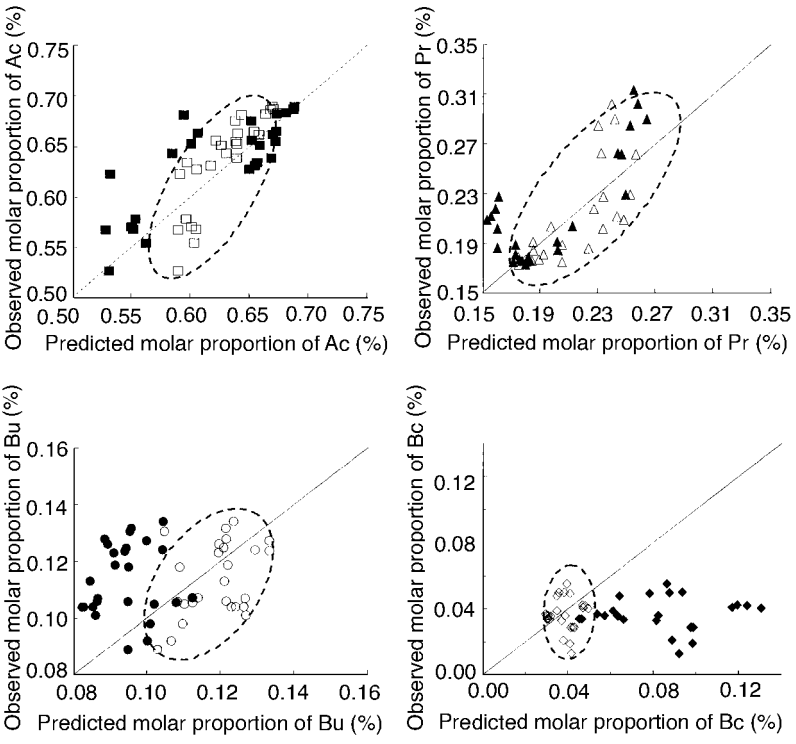

Fig. 7.2. Evaluation of stoichiometric coefficients of VFA production by independent observations (open symbols, new coefficient estimates (TD, Table 7.1); closed symbols, coefficient estimates derived by Murphy *et al.*, 1982). Independent coefficient estimates were used for roughage and concentrate diets. The root of mean squared prediction error for Ac (□), Pr (△), Bu (○) and Bc (◇) was 0.0241, 0.0210, 0.0120 and 0.0093, respectively, for the new coefficient values, and 0.0246, 0.0246, 0.0209 and 0.0469, respectively, for the coefficient values of Murphy *et al.* (1982). The dashed ellipses were drawn to indicate the similarity in the pattern of prediction errors with the new coefficient estimates and those obtained in the simulation studies (Fig. 7.1).

between observed and predicted VFA molar proportions. For example, fractional absorption rates were assumed to be identical for all VFA, but, particularly at low rumen pH, fractional rates of VFA absorption differ (Dijkstra *et al.*, 1993). Another important factor is a shift in fermentation stoichiometry with increased rates of substrate fermentation. The present model assumes a constant stoichiometry of VFA production from fermented substrate, which implies that, with an identical relative increase in fermentation rate for every type of substrate, exactly the same VFA molar proportions will be predicted. *In vivo*, however, increased rates of substrate fermentation favour a higher molar

proportion of Pr or Bu. The current model does not account for this effect, but an option to include it may be the expression of coefficient values $c_{i,j}$ as a function of pH (Baldwin, 1995), because rumen pH is a frequently published parameter and representative of fermentation rates in the rumen.

Implications

The results presented on modelling rumen fermentation stoichiometry indicate that: (i) errors of fitted VFA molar proportions do not automatically imply that rates of VFA production are predicted inaccurately or that estimates of the stoichiometric coefficients are irrelevant; (ii) predictions of VFA molar proportions by rumen models may demonstrate similar deviations, which is important to realize when the predictive potential of these models is evaluated; and (iii) to apply published coefficient estimates in rumen models it should be established that the concepts and assumptions of these models are in line with those the coefficients were derived from.

VFA Metabolism by Epithelium

The importance of VFA metabolism by rumen epithelium becomes clear when production or infusion rates of VFA in the rumen are compared with observed portal appearance rates of VFA. Activation of the three major VFA by coenzyme A (CoA) synthetases to acetyl-, propionyl- or butyryl-CoA is the first step in VFA metabolism to ketone bodies, lactate or carbon dioxide. Therefore, studying the kinetics of these enzymes is thought to be the key to understanding to what extent VFA are metabolized. Numerous assessments of the enzyme activity in tissue samples of rumen epithelium have been reported (reviewed by Bergman, 1990; Remond *et al.*, 1995). Although knowledge of the enzyme kinetics of VFA activation is crucial to understanding the extent of VFA metabolism, an integrated approach is needed, with the simultaneous representation of production, absorption and activation of VFA. For this reason, a simulation model was constructed as a first attempt to describe VFA metabolism by the epithelium of the ruminant stomachs. Basic model elements are rumen VFA production, VFA transport from rumen to portal blood and VFA activation by CoA synthetases present in epithelia (Fig. 7.3). The model consists of nine state variables for pools of Ac, Pr and Bu in rumen fluid and in the intracellular fluid of epithelial tissues of the reticulorumen and of epithelial tissues of the stomachs posterior to the reticulorumen. Concentrations of VFA are calculated by dividing pool sizes by volume of rumen fluid or intracellular fluid, or by dividing VFA flows by portal blood flow. Inputs and outputs to the model are rates of VFA production in the rumen and rates of VFA appearance in portal blood.

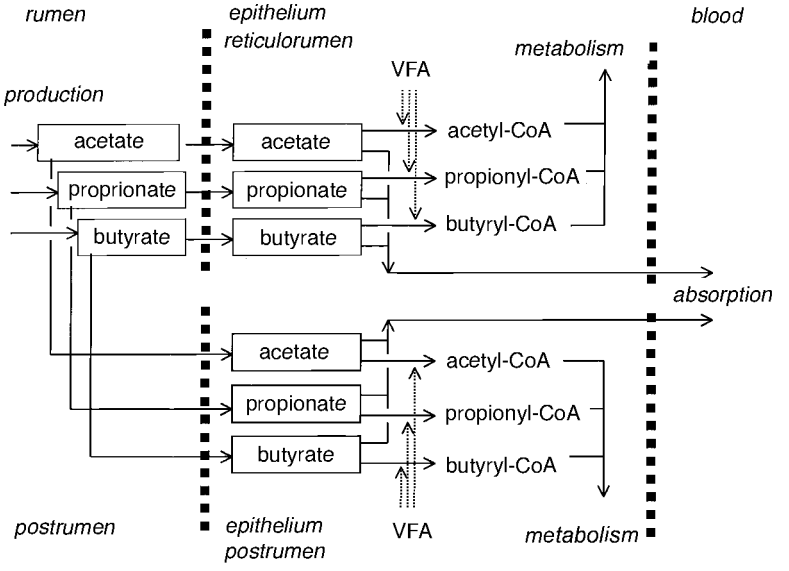

Fig. 7.3. A schematic representation of a simulation model for the production, absorption and metabolism of VFA, and the appearance of VFA in portal blood.

Transport of VFA

The kinetics of rumen VFA absorption were described according to Dijkstra *et al.* (1992), with a saturation of absorption rate at increasing VFA concentrations. Thus, according to their rumen concentration, fractional absorption rates will increase in the order of Ac, Pr and Bu. In addition, Dijkstra *et al.* (1992) described a non-linear increase in VFA absorption rate with a decrease in rumen pH, because, with pH values approaching p*K* values of VFA, more VFA will be in the undissociated form, which readily diffuses through cell membranes. At the prevailing pH in rumen fluid, most of the VFA will be in the anionic form, however, which does not readily diffuse through cell membranes (Bergman, 1990). Still, rates of VFA absorption are high, because it is facilitated by protonation of VFA anions at the membrane surface to undissociated VFA, which then diffuse through the membrane in the direction of the lowest concentrations. The continuous protonation of VFA and the simultaneous cotransport of ions bring a certain energy requirement for the epithelial cells and probably add to the saturability of the kinetics of VFA absorption. This principle of facilitated diffusion of VFA would apply to transport not only through the mucosal but also through the serosal membrane, because, compared with rumen fluid, an even higher proportion of VFA will be dissociated in intracellular fluid. For this reason, it was assumed that the kinetics used by Dijkstra *et al.* (1992) apply to VFA

transport through the membrane at both sides of the epithelium. However, initial simulations showed that the rate of VFA absorption from the rumen exceeded the sum of the rate of VFA transport from intracellular fluid to blood and the rate of VFA metabolism. This resulted in an unlimited accumulation of Ac (and, to a lesser extent, of Pr) in intracellular fluid, with concentrations exceeding 200 mmol l^{-1}. To avoid such unrealistic intracellular concentrations, rates of VFA transport from epithelium to blood were increased fivefold for all VFA.

Initially, VFA absorption was described by equations derived by Dijkstra *et al.* (1993) from *in vivo* measurements of VFA disappearance in the rumen. However, these equations described such a low absorption rate of Ac compared with that of Pr and Bu that the model always simulated a higher proportion of Ac in rumen fluid than in net appearance of VFA in portal blood. However, *in vivo* measurements invariably indicate the opposite result (Huntington, 1999) and hence, with the present conceptual approach, the equations of Dijkstra *et al.* (1993) did not lead to realistic results. Therefore, the equations from Dijkstra *et al.* (1992) were used.

Finally, VFA that leave the reticulorumen with fluid outflow were assumed to be absorbed completely posterior to the reticulorumen, because VFA concentrations drop to very low values in the abomasum, similar to those in the small intestine (Bergman, 1990).

Activation of VFA

The interaction between VFA in their rate of activation by CoA synthetase was described by enzyme kinetics of competitive inhibition. Although several studies on the activities of CoA synthetase in ovine and bovine rumen epithelium have been published, only a few studies systematically established interactions between individual VFA. In even fewer studies were multiple concentrations of VFA substrate tested, which would allow for the derivation of enzyme kinetics. Only Scaife and Tichivangana (1980) established enzyme activities for the whole range of VFA concentrations in ovine rumen epithelium and clearly demonstrated kinetics of competitive inhibition between VFA. However, the absolute level of enzyme activity was substantially lower (on average, about half) than that established in bovine rumen epithelium (Fig. 7.4) by Ash and Baird (1973) and Harmon *et al.* (1991). Qualitatively, the results of the three studies corresponded with an increasing activation rate in the order Ac, Pr and Bu, and an increasing (competitive) inhibition capacity in the same order. Only Harmon *et al.* (1991) tested all possible combinations of VFA and used distinct concentrations of Ac, Pr and Bu in the order of their relative production rates in the rumen. Therefore, parameter values of the enzyme kinetics of VFA activation were derived from this specific study by analysing the inhibition of VFA activation rate per concentration unit of inhibiting VFA. Such an analysis requires the maximum activation rate to be known. However, as Harmon *et al.* (1991)

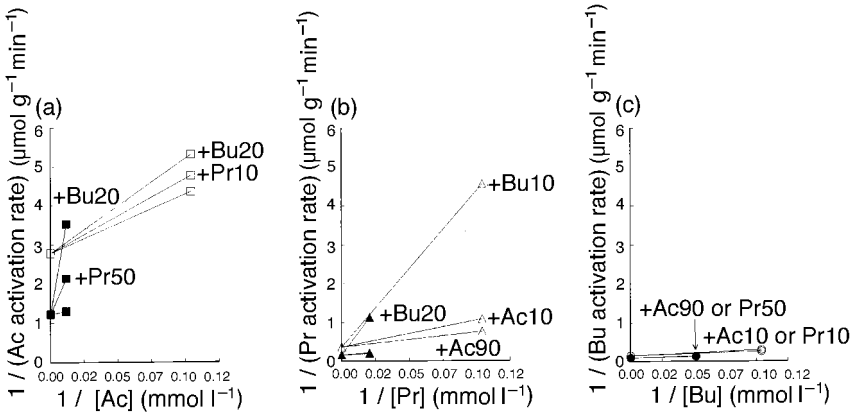

Fig. 7.4. Comparison of enzyme assays in bovine rumen epithelium by Harmon *et al.* (1991) and Ash and Baird (1973). The effect of the inhibiting VFA on the rate of VFA activation is demonstrated by a double reciprocal plot of activation rate (µmol g^{-1} tissue min^{-1}) and of the concentration of the activated VFA (mmol l^{-1}); (a) acetate, □ and Ac; (b) propionate, △ and Pr; (c) butyrate, ○ and Bu. The increase in the slope of drawn lines indicates the extent of inhibition by the inhibiting VFA. Intercepts with the *y* axis were not measured but estimated (see text of paragraph 'Activation of VFA' for explanation). Codes that guide the symbols indicate the type of inhibiting VFA and the added number indicates the concentration in mmol l^{-1} of the inhibiting VFA. A symbol not guided by a code indicates that no inhibiting VFA was used.

did not use saturating VFA concentrations, the maximum activation rates had to be estimated by assuming that the extent of saturation achieved at the VFA concentrations used by Harmon *et al.* (1991) was similar to that established by Scaife and Tichivangana (1980). Further, identical kinetics were assumed for VFA activation in the epithelial tissue of the reticulorumen, omasum and abomasum, because it was demonstrated that the latter two also have a high capacity for VFA metabolism (Pennington, 1952). Weight and water volume of epithelial tissues were calculated from the following assumptions: a tissue weight of 12 kg for reticulorumen and 10 kg for omasum and abomasum (Nagel and Piatkowski, 1972), containing 50% and 75% mucosa (Von Engelhardt and Hales, 1977), which consists of 20% epithelial cells and 20% dry matter (Weekes, 1974).

Simulation results

The behaviour of the model was studied by simulating the effect of three contrasting molar proportions and two production rates of VFA in the rumen on the molar proportions of VFA appearing in portal blood (Table 7.2). The results obtained were not straightforward and would have been difficult to understand

Table 7.2. Simulated effect of production rate and molar proportion of rumen VFA on extent of metabolism and molar proportion in portal blood.

Rumen production rate Ac : Pr : Bu (mol day^{-1})	Fermentation pattern Ac : Pr : Bu (%)	Extent of metabolism			VFA proportion in portal blood			VFA proportion in net appearance in portal blood‡		
		Ac	Pr (%)*	Bu	Ac	Pr (%)†	Bu	Ac	Pr (%)†	Bu
50§	70 : 15 : 15	16.9	42.3	85.0	90.1	7.8	2.1	84.2	12.5	3.3
50	50 : 35 : 15	17.3	38.9	84.9	79.9	17.9	2.2	63.6	32.9	3.5
50	50 : 15 : 35	16.7	32.3	83.1	84.9	9.8	5.3	72.2	17.6	10.3
100§	70 : 15 : 15	8.8	29.2	82.3	89.0	8.8	2.3	82.8	13.8	3.4
100	50 : 35 : 15	8.8	25.0	82.0	77.4	20.2	2.4	61.1	35.2	3.6
100	50 : 15 : 35	8.1	17.6	77.7	82.7	10.8	6.4	69.5	18.7	11.8
100‖	70 : 15 : 15	15.5	54.6	91.4	92.0	6.5	1.4	87.9	10.1	1.9
100	50 : 35 : 15	16.5	49.9	91.2	83.0	15.5	1.5	68.9	28.9	2.2
100	50 : 15 : 35	16.5	44.3	90.3	88.0	8.6	3.4	78.0	15.6	6.4

* Percentage of VFA produced in the rumen that does not appear in portal blood.
† Percentage of summed portal concentrations of Ac, Pr and Bu, or of portal–arterial concentration differences of Ac, Pr and Bu.
‡ Concentrations in portal blood corrected for arterial supply. Arterial concentrations assumed to change proportionally with rate of VFA production (reference values of 1.400, 0.040 and 0.013 mmol l^{-1} of Ac, Pr and Bu at a VFA production rate of 87 mol day^{-1} derived from Reynolds *et al.* (1988)).
§ 1200 g and 1500 g of epithelial cells in reticulorumen and in omasal and abomasal tissues; at VFA production rates of 50 and 100 mol day^{-1}, a rumen volume of 65 and 85 l, a volume of 15 and 20 l of stomachs posterior to the reticulorumen and fluid passage rates of 2.5 and 3.5 day^{-1} were assumed.
‖ It was assumed that, in response to the increase in VFA production rate from 50 to 100 mol day^{-1}, the increase in mass of epithelium of the ruminoreticulum is relatively larger than that of the omasum and abomasum. Hence, the mass of epithelial cells in reticulorumen and in the omasum and abomasum was arbitrarily increased to 2500 and 2000 g.

without a mathematical model. In all simulations the extent of metabolization increased in the order Ac, Pr and Bu. Changes in VFA molar proportion in the rumen had the largest effect on the extent of Pr metabolism. A doubling of VFA production without a change in epithelial weight decreased the extent of VFA metabolism by roughly 50, 35 and 5%. But high VFA production and absorption rates can lead to an increased weight of epithelial tissue, as will occur, for example, in early lactation with a rapid increase in feed intake. Increasing epithelial weight, in addition to a doubling of VFA production, made simulated extent of metabolism more comparable again to that simulated for low rates of VFA production (Table 7.2). Hence, studies of the extent of VFA metabolism should consider measuring not only the enzyme activity in samples of epithelial tissue but also the epithelial proliferation or the tissue mass involved. The simulation results demonstrated that the extent of metabolism of a specific VFA was determined not only by its molar proportion with rumen production but also by the molar proportions of the other VFA, by the rate of VFA production and by the weight of metabolizing epithelium. As a consequence, net absorption of a specific type of VFA in portal blood is not a constant fraction of the VFA molar proportion in rumen fluid.

Evaluation results

The present preliminary model of VFA metabolism was evaluated by comparing model predictions to observed portal net flows of VFA in lactating cows in early lactation (Lomax and Baird, 1983; Reynolds *et al.,* 1988; De Visser *et al.,* 1997). The model gave a reasonable explanation of the molar proportions of VFA appearing in portal blood (Table 7.3). However, results depend heavily on the assumptions made for the molar proportions and rates of VFA production in the rumen. Therefore, a more thorough evaluation and a further development of the model are clearly needed.

Implications

Although the VFA metabolism model gives some encouraging results, it needs to be developed further in several aspects. The model does not represent the energy requirement of epithelial cells as a possible driving force for VFA activation; it neglects uptake of nutrients from arterial blood (mainly acetate and glucose); it does not provide a mechanism for the regulation of ketogenesis, lactate production and complete oxidation of VFA, or for the transmembrane transport of VFA as affected by epithelial metabolism.

Table 7.3. Evaluation of VFA metabolism model.

	Observed dry matter intake (kg day^{-1})	Assumed pattern Ac:Pr:Bu (%)	Assumed production rate mol day^{-1}	Observed net VFA absorption			Predicted net VFA absorption		
				Ac	Pr (%)	Bu	Ac	Pr (%)	Bu
Reynolds *et al.* (1988) 60% maize silage 40% concentrate Holstein-Friesian cows	17.1	55:30:15*	100	67.7	28.7	3.6	68.9	28.6	2.5
Lomax and Baird (1983) 60% hay 40% concentrate Friesian × Ayrshire cows	8.3	55:25:20†	50	66.9	23.5	9.6	71.0	24.2	4.8
De Visser *et al.* (1997) Freshly cut ryegrass 10% concentrate Holstein-Friesian cows	15.7	60:20:20‡	100	72.7	21.9	5.4	74.5	20.4	5.1

* Concentrate and high starch content of maize silage assumed to result in high Pr proportions (Klusmeyer *et al.*, 1990; see also Table 7.1).
† Derived from Robinson *et al.* (1987), who observed Pr and Bu proportions near 20% on a diet of 65% hay and 35% concentrate.
‡ Derived from measured molar proportions of VFA in rumen fluid.

Conclusions

Changes in VFA concentrations in rumen fluid can only be succesfully related to those in portal blood when effects of VFA production in the rumen, VFA transport through epithelium and intracellular VFA metabolism are considered simultaneously. The present work is a first attempt to decribe these interactions, which can assist in understanding rumen and portal VFA data. Improvement in both the description of rumen fermentation stoichiometry and the extent of VFA metabolism by epithelial tissue is necessary to quantify the effect of nutrition and animal physiology on the delivery of VFA to portal blood as nutrients for the dairy cow.

References

Ash, R. and Baird, G.D. (1973) Activation of volatile fatty acids in bovine liver and rumen epithelium. *Biochemical Journal* 136, 311–319.

Baldwin, R.L. (1995) *Modelling Ruminant Digestion and Metabolism*. Chapman & Hall, London, UK.

Bannink, A., De Visser, H., Klop, A., Dijkstra, J. and France, J. (1997) Causes of inaccurate prediction of volatile fatty acids by simulation models of rumen function in lactating cows. *Journal of Theoretical Biology* 189, 353–366.

Bergman, E.N. (1990) Energy contributions of volatile fatty acids from the gastrointestinal tract in various species. *Physiological Reviews* 70, 567–590.

Chan, S.C., Huber, J.T., Theurer, C.B., Wu, Z., Chen, K.H. and Simas, J.M. (1997) Effects of supplemental fat and protein source on ruminal fermentation and nutrient flow to the duodenum in dairy cows. *Journal of Dairy Science* 80, 152–159.

De Visser, H., Valk, H., Klop, A., Van der Meulen, J., Bakker, J.G.M. and Huntington, G.B. (1997) Nutrient fluxes in splanchnic tissue of dairy cows: influence of grass quality. *Journal of Dairy Science* 80, 1666–1673.

De Visser, H., Klop, A., Van der Koelen, C.J. and Van Vuuren, A.M. (1998) Starch supplementation of grass harvested at two stages of maturity prior to ensiling: intake, digestion, and degradability by dairy cows. *Journal of Dairy Science* 81, 2221–2227.

Dijkstra, J., Neal, H.D.StC., Beever, D.E. and France, J. (1992) Simulation of nutrient digestion, absorption and outflow in the rumen: model description. *Journal of Nutrition* 122, 2239–2256.

Dijkstra, J., Boer, H., Van Bruchem, J., Bruining, M. and Tamminga, S. (1993) Absorption of volatile fatty acids from the rumen of lactating dairy cows as influenced by volatile fatty acid concentration, pH and rumen liquid volume. *British Journal of Nutrition* 69, 385–396.

Harmon, D.L., Gross, K.L., Krehbiel, C.R., Kreikemeier, K.K., Bauer, M.L. and Britton, R.A. (1991) Influence of dietary forage and energy intake on metabolism and acyl-CoA synthetase activity in bovine ruminal epithelial tissue. *Journal of Animal Science* 69, 4117–4127.

Huntington, G.B. (1999) Nutrient metabolism by gastrointestinal tissues of herbivores. In: Jung, H.-J.G. and Fahey, G.C. (eds) *Nutritional Ecology of Herbivores. Proceedings of the Vth International Symposium on the Nutrition of Herbivores*. American Society of Animal Science, Savoy, Illinois, USA, pp. 312–336.

Joy, M.T., DePeters, E.J., Fadel, J.G. and Zinn, R.A. (1997) Effects of corn processing on the site and extent of digestion in lactating cows. *Journal of Dairy Science* 80, 2087–2097.

Klusmeyer, T.H., McCarthy, R.D., Clark, J.H. and Nelson, D.R. (1990) Effects of source and amount of protein on ruminal fermentation and passage of nutrients to the small intestine of lactating cows. *Journal of Dairy Science* 73, 3526–3537.

Lomax, M.A. and Baird, G.D. (1983) Blood flow and nutrient exchange across the liver and gut of the dairy cow: effects of lactation and fasting. *British Journal of Nutrition* 49, 481–496.

Murphy, M.R., Baldwin, R.L. and Koong, L.J. (1982) Estimation of stoichiometric parameters for rumen fermentation of roughage and concentrate diets. *Journal of Animal Science* 55, 411–421.

Nagel, S. and Piatkowski, B. (1972) Untersuchungen des Pansenvolumens under der Pansenmasse von Milchkühen. *Archiv fur Tierernährung* 22, 449–456.

Pennington, R.J. (1952) The metabolism of short-chain fatty acids in the sheep. 1. Fatty acid utilization and ketone body production by rumen epithelium and other tissues. *Biochemical Journal* 51, 251–258.

Pitt, R.E., Van Kessel, J.S., Fox, D.G., Pell, A.N., Barry, M.C. and Van Soest, P.J. (1996) Prediction of ruminal volatile fatty acids and pH within the net carbohydrate and protein system. *Journal of Animal Science* 74, 226–244.

Remond, D., Ortigues, I. and Jouany, J.-P. (1995) Energy substrates for the rumen epithelium. *Proceedings of the Nutrition Society* 54, 95–105.

Reynolds, C.K., Huntington, G.B., Tyrrell, H.F. and Reynolds, P.J. (1988) Net metabolism of volatile fatty acids, D-β-hydroxybutyrate, nonesterified fatty acids, and blood gases by portal-drained viscera and liver of lactating Holstein cows. *Journal of Dairy Science* 71, 2395–2405.

Robinson, P.H., Tamminga, S. and Van Vuuren, A.M. (1987) Influence of declining level of feed intake and varying the proportion of starch in the concentrate on rumen ingesta quantity, composition and kinetics of ingesta turnover in dairy cows. *Livestock Production Science* 17, 37–62.

Robinson, P.H., Gill, M. and Kennelly, J.J. (1997) Influence of time of feeding a protein meal on ruminal fermentation and forestomach digestion in dairy cows. *Journal of Dairy Science* 80, 1366–1373.

Scaife, J.R. and Tichivangana, J.Z. (1980) Short chain acyl-CoA synthetases in ovine rumen epithelium. *Biochimica et Biophysica Acta* 619, 445–450.

Stensig, T. and Robinson, P.H. (1997) Digestion and passage of forage fiber in dairy cows as affected by fiber-free concentrate in the diet. *Journal of Dairy Science* 80, 1339–1352.

Von Engelhardt, W. and Hales, J.R.S. (1977) Partition of capillary blood flow in rumen, reticulum, and omasum of sheep. *American Journal of Physiology* 232, E53–E56.

Weekes, T.E.C. (1974) The *in vitro* metabolism of propionate and glucose by the rumen epithelium. *Comparative Biochemistry and Physiology* 49B, 393–406.

Yang, W.Z., Beauchemin, K.A., Koenig, K.M. and Roede, L.M. (1997) Comparison of hull-less barley, barley, or corn for lactating cows: effects on extent of digestion and milk production. *Journal of Dairy Science* 80, 2475–2486.

8

Modelling Energy Expenditure in Pigs

Jaap van Milgen and Jean Noblet

Station de Recherches Porcines, Institut National de la Recherche Agronomique, 35590 Saint-Gilles, France

Abstract

In pigs, more than 50% of the ingested energy is dissipated as heat. The heat production of animals can be measured using indirect calorimetry, which is based on the concept that heat is produced through oxidation of nutrients. A technique was developed that allows modelling the dynamics of heat production in large, open-circuit respiration chambers. The model assumes the existence of three major components of heat production: the fasting heat production (FHP), the thermic effect of feeding (TEF) and heat production due to physical activity ($HP_{activity}$). The TEF can be further divided into a short-term component (TEF_{ST}), which is due to processes such as ingestion and digestion, and a long-term component (TEF_{LT}), which is mainly due to the metabolism of nutrients. The FHP corresponds to the asymptotic heat production after at least 1 full day of fasting. Physical activity is measured through force sensors or through measurement of the duration of standing. Three data sets, with heat production measured in group-housed piglets (26 kg), individually housed growing pigs (69 kg) and gestating sows, were used to discuss the variation in heat production. The FHP was the main component of heat production (30 to 60% of metabolizable energy (ME) intake), whereas TEF_{ST} represented a relatively constant fraction of ME intake (approximately 8%). The TEF_{LT} was more variable, and ranged between 1 and 9% of ME intake. The $HP_{activity}$ represented between 8 (piglets and growing pigs) and 20% of ME intake (gestating sows).

Introduction

The cost of feed energy represents a major proportion of the total cost of pig production. It is therefore important to match the supply and requirement as

 Modelling Nutrient Utilization in Farm Animals (eds J.P. McNamara, J. France and D.E. Beever)

closely as possible. Traditionally, it is supposed that the energy requirement of animals can be divided into a maintenance component and a production component. Maintenance is defined as the level of feeding at which the requirement for nutrients are just met to ensure the continuity of vital processes so that there is no net gain or loss of nutrients in tissue and animal products (ARC, 1981). Although it is easily defined, the concept is more difficult to measure and apply. For example, growth can be considered a vital process for a growing animal. Therefore, maintenance does not represent a normal physiological state in a growing animal.

Ingested feed energy is excreted, deposited (primarily as protein and fat) or dissipated in the form of heat. The heat production of an animal represents more than 50% of the ingested energy, which underlines the necessity to quantify its components. Heat production can be measured through indirect calorimetry and is traditionally used to determine the daily energy balance of the animal. In the last few years, we have developed a modelling technique that allows determination of individual components of heat production (van Milgen *et al.*, 1997). The technique allows a better understanding and quantification of the mechanisms of energy metabolism. The goal of this chapter is to describe the hypotheses we made concerning the components of heat production and to illustrate these with results obtained from experiments using this modelling technique.

Calorimetry

Indirect calorimetry is based on the concept that heat can only be produced through oxidation of nutrients (carbohydrates, proteins and fat). The heat released after oxidation of each nutrient will be accompanied by a specific pattern of oxygen (O_2) consumption and carbon dioxide (CO_2) production. Consequently, the combination of O_2 consumption and CO_2 production (and urinary N and methane (CH_4) production) is used to calculate the heat production (Brouwer, 1965). To measure the O_2 consumption and CO_2 and CH_4 production, animals are placed in large, open-circuit respiration chambers. The change in gas concentrations, together with physical aspects of gas exchanges (i.e. changes in the air extraction rate, atmospheric pressure and temperature) and nitrogen balance, allows calculation of the daily heat production.

Because the respiration chambers are relatively large compared with the size of the animals, calculation of heat production by the animal can lead to noisy data when using short time intervals. We have therefore developed a data analysis model that allows the study of the short-term dynamics of gas exchanges in an open-circuit respiration chamber (van Milgen *et al.*, 1997). The model considers the respiration chamber as a compartment of fixed physical volume from which gases are extracted. An animal present in the respiration chamber will consume O_2 and produce CO_2. The goal of the model is to predict O_2 consumption and CO_2 production by the animal, so that predicted values of

$[O_2]$ and $[CO_2]$ at the gas analyser match the observed values as closely as possible. The model accounts for physical aspects of gas exchanges (e.g. small changes in temperature and atmospheric pressure) as well as for the O_2 consumption and CO_2 production by the animal. The physical aspects of gas exchange are driven by continuous measurements of atmospheric pressure, temperature in the respiration chamber and the gas extraction rate. Because the respiratory quotient does not necessarily equal unity, the entry rate of gas can be different from the extraction rate. Its calculation is based on the gas extraction rate and gas production or consumption by the animal (based on standard temperature and pressure).

Oxygen Consumption and Carbon Dioxide Production by the Animal

In order to explain the observed variation of $[O_2]$ and $[CO_2]$ at the gas analyser, a model was developed that accounts for the variation in O_2 consumption and CO_2 production by the animal. The four major components of the model are the fasting heat production (FHP), the long-term thermic effect of feeding (TEF_{LT}; or long-term heat increment), the short-term thermic effect of feeding (TEF_{ST}) and the physical activity. The model is based on the O_2 consumption and CO_2 production for each of the four components from which the heat production can be calculated (Brouwer, 1965) (without accounting for the contribution of nitrogen and methane to heat production). Figure 8.1 illustrates the components of heat production for a growing pig (60 kg) that is offered four meals per day (09.00, 13.00, 17.00 and 21.00). The heat production averages 15 MJ day^{-1} but there is considerable variation within a day. Also, heat production is higher during the diurnal period than during the nocturnal period, mainly because of the thermic effect of feeding and increased physical activity during the day.

It is obvious that the fasting heat production cannot be measured in fed animals. Therefore, following measurement of the energy balance in the fed state, food is withheld from the animals for at least 24 h. Although the fasting heat production may depend on the length of the fasting period, total heat production usually approaches a plateau at the end of the nocturnal period. It is assumed that this estimate of FHP reflects the heat production of an animal in a catabolic state, while maintaining a relationship with the anabolic (fed) state. In other words, this fasting heat production is not specific for the animal but may be affected by the prefasting state.

Similarly to the fasting state, normally fed animals also approach a constant level of heat production at the end of the nocturnal period (see Fig. 8.1). This basal heat production (BHP) is easier to observe when a limited number of meals is provided compared with *ad libitum* feeding (which may include nocturnal feed consumption). The difference between BHP and FHP is that the former reflects a postabsorptive, anabolic state, whereas the latter represents a

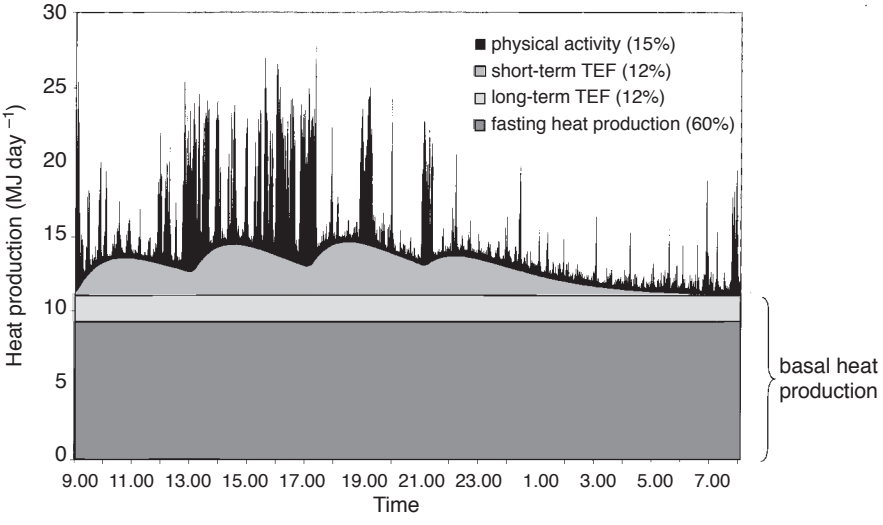

Fig. 8.1. Components of heat production in a growing pig (60 kg) fed at 2.4 MJ ME (kg BW)$^{-0.60}$ day^{-1} offered in four separate meals at 09.00, 13.00, 17.00 and 21.00. TEF, thermic effect of feeding.

catabolic state. Long-term metabolic processes, such as protein and lipid synthesis, are included in the BHP. The TEF_{LT} was defined as the difference between BHP and FHP and reflects the heat production due to long-term anabolic processes relative to the cost of catabolism. Although the BHP can be measured in fed animals, its decomposition in FHP and TEF_{LT} depends on the accuracy of the FHP measurement. If, for example, FHP were measured after a 48 h fasting period (rather than 24 h), its estimate would probably be lower, and a greater fraction of BHP would be attributed to TEF_{LT}. Modelling the transition from BHP (when fed) to FHP (when fasting) is, of course, arbitrary and is included as a first-order process, starting the morning when food is withheld.

Feed consumption (quantity and time of eating) is monitored continuously. The heat production associated with a meal largely exceeds the time of feed consumption and the delay is probably due to heat production during digestion and absorption of nutrients. The TEF_{ST} was modelled as a gamma distribution of time between feed intake and the corresponding heat production (Matis *et al.*, 1989). This module was parameterized to include the mean time between ingestion of a meal and the corresponding heat production. Heat production due to TEF_{ST} is cumulated over different meals (see Fig. 8.1) and declines, in this example, only during the nocturnal period, when no feed is distributed.

Physical activity of the animals is monitored through interruption of an infrared beam (standing or sitting) and, more recently, through force sensors, on which the metabolic cage is mounted. Any vertical force movement by the

animal results in an electric signal (Fig. 8.2), which is used as a model input and to which a component of O_2 consumption and CO_2 production is attributed. This method appears to be extremely sensitive, as it also detects movements when the animals are lying down. In a recent study, we detected increased physical activity of pigs at very high temperatures, only because the animals were respiring intensely.

Parameter Estimation

The model is described as a series of differential equations, which take into account the O_2 consumption and CO_2 production by the animal, as well as physical aspects of gas exchange in the respiration chamber. The model predicts the $[O_2]$ and $[CO_2]$ in the respiration chamber based on the measured inputs

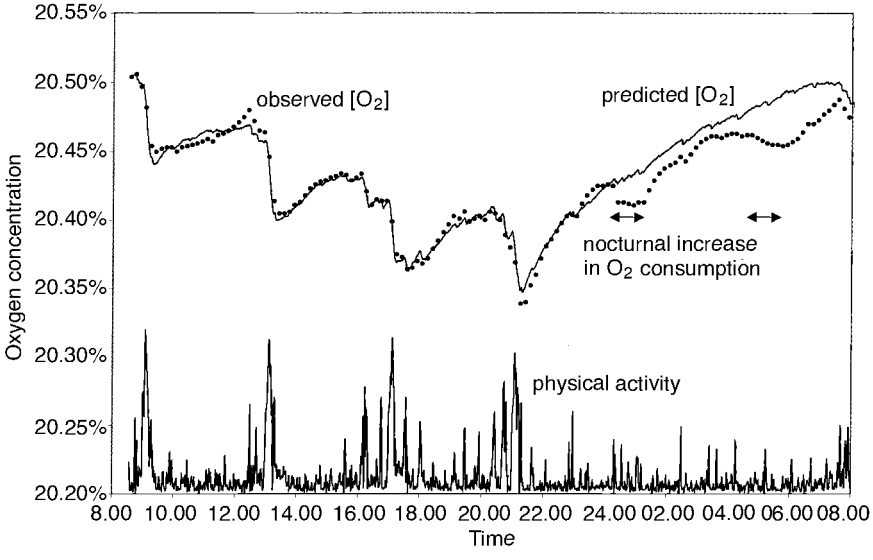

Fig. 8.2. Diurnal and nocturnal variation in oxygen concentration and physical activity measured in an open-circuit respiration chamber for a growing pig (60 kg). The animal was fed at 2.4 MJ ME (kg BW)$^{-0.60}$ day^{-1} and was offered four separate meals at 09.00, 13.00, 17.00 and 21.00. Apart from the increase in O_2 consumption (decrease in $[O_2]$) due to feed intake, there appear to be two additional, nocturnal increases in O_2 consumption starting at about midnight and 04.30. The (•) indicate the observed $[O_2]$, whereas the upper solid line indicates the estimated $[O_2]$ without correction for this nocturnal increase in O_2 consumption. The lower solid line is proportional to the signal of the force sensor on which the metabolism cage is mounted.

related to gas exchange (i.e. temperature, pressure, humidity and gas extraction rate) and inputs related to the animal (physical activity, the quantity and time of feed intake). These model inputs are based on 10 s averages of 500 measurements. Each data set is the result of 1 day of measurement and thus contains 8640 data lines. In order to reduce calculation time, every *n*th data line of $[O_2]$ and $[CO_2]$ is used, where *n* ranges from 1 to 6, depending on the experiment. Model parameters are obtained statistically by comparing the observed $[O_2]$ and $[CO_2]$ with the predicted $[O_2]$ and $[CO_2]$ (see Fig. 8.2). The model was initially developed with SimuSolv (Steiner *et al.*, 1990) and has since been transferred to Advanced Continuous Simulation Language (ACSL) Optimize (MGA Software, 1997).

The data analysis procedure described above has been routinely used for 4 years to analyse the components of heat production in pigs ranging from 20 kg body weight (BW) to gestating sows housed individually or in groups. Because the goal of the model is to explain the variation in heat production with a limited number of observed variables, data analysis becomes difficult when overlapping between independent variables occurs. For example, due to the large number of meals observed in an experiment with small (20–25 kg) group-housed pigs, we could not clearly distinguish the heat production due to physical activity from the TEF_{ST}. The remainder of the chapter will compile results from some of these studies.

The Data

The first study (A) concerns the effect of environmental temperature on young, growing pigs. Six groups of five pigs each were exposed to an environmental temperature of either 23 or 33°C. The pigs had free access to water and feed, and consumption was recorded for each animal individually. Measurements of heat production started at approximately 22 kg BW and lasted for 12 days, plus 1 day of fasting.

The effect of dietary protein content on the heat production in growing pigs was studied in the second study (B) (Le Bellego *et al.*, 1999, 2000). In the first part of the experiment (B1), five diets were prepared where protein was replaced by starch and/or fat, while supplementing with synthetic amino acids. The protein content of the diets varied between 18.9% and 12.3%. In the second part of the experiment (B2), three diets were formulated using traditional feed ingredients with different protein contents. The control diet was based on wheat, maize and soybean meal, resulting in a CP content of 17.4%. The other two diets were formulated by replacing soybean meal with wheat and maize either with or without addition of maize oil. The crude protein (CP) content of the latter two diets was approximately 14.5% and these diets were supplemented with synthetic amino acids. In experiments B1 and B2, approximately 2.630 MJ (kg $BW)^{-0.60}$ day^{-1} of metabolizable energy (ME) was provided in four separate meals. The effect of feeding frequency was studied in a third experiment (B3).

Two diets of experiment 2 were fed in either two or seven equal meals. A total of 69 energy balances were measured in this study.

The third study (C) focused on the effect of fibre level on the components of heat production in gestating sows (Ramonet *et al.*, 2000). An alternating diet of low fibre (14% neutral detergent fibre (NDF)) or high fibre (40% NDF) was fed at 37.2 MJ digestible energy (DE) day^{-1} as a single meal during four stages of gestation (40–110 days of gestation).

Fasting Heat Production

Table 8.1 lists the BW, ME intake, FHP and heat production due to physical activity ($HP_{activity}$) and the respective respiratory quotients for the three studies. Although the level of feed intake preceding the fasting period can have an important effect on the FHP, it is clear that BW is the main discriminating factor of FHP between the three studies. For mature animals, the FHP is often expressed as a function of BW raised to the power 0.75. However, for growing pigs, the exponent appears to be closer to 0.60 (van Milgen *et al.*, 1998). Non-linear regression of FHP on BW (i.e. $\ln(FHP) = \ln(a\ BW^b)$) indicated an even lower exponent ($b = 0.54$) with $a = 1005$ kJ $(kg\ BW)^{-0.54}\ day^{-1}$ (residual SD = 8.8% of FHP). There are strong indications that the level of feed intake influences the FHP, which seems to be due to the energy expenditure of visceral organs (Koong *et al.*, 1983; van Milgen *et al.*, 1998). To account for the effect of feeding level prior to fasting, the model $\ln(FHP) = \ln((a1 + a2\ ME/BW^{b2})\ BW^{b1})$ was used. It includes a component independent of feed intake ($a1$; kJ day^{-1}) and a scaled component-related feed intake ($a2$). The exponents $b1$ and $b2$ were not different from each other or from 0.60, so that the FHP can be expressed as $FHP = (645 + 0.056\ ME/(kg\ BW)^{0.60})\ (kg\ BW)^{0.60}$, with an RSD of 8.3%. In other words, growing pigs that consume 2500–3000 kJ $(kg\ BW)^{-0.60}\ day^{-1}$ will

Table 8.1. Components of heat production during fasting (mean ± SD).

Experiment	A	B	C
n	6	69	19
Housing	Groups of 5	Individually	Individually
BW after fasting (kg)	28.9 (2.3)	63.8 (4.0)	263.5 (24.4)
ME prior to fasting (MJ day^{-1})	22.70 (4.89)	31.02 (1.64)	34.64 (1.59)
FHP (MJ day^{-1})	6.17 (0.94)	9.54 (0.76)	20.45 (2.44)
$HP_{activity}$ (MJ day^{-1})	1.68 (0.51)	2.05 (0.46)	5.66 (1.88)
RQ_{FHP}	0.82 (0.03)	0.80 (0.05)	0.78 (0.07)
$RQ_{activity}$	0.72 (0.10)	0.78 (0.17)	0.82 (0.09)

BW, body weight; ME, metabolizable energy; FHP, fasting heat production; $HP_{activity}$, heat production due to physical activity; RQ_{FHP}, respiratory quotient during fasting; $RQ_{activity}$, respiratory quotient of activity.

have an FHP close to 800 kJ (kg BW)$^{-0.60}$ day^{-1}. Gestating sows are fed restrictively (1200 kJ (kg BW)$^{-0.60}$ day^{-1}), which results in a lower FHP (710 kJ (kg BW)$^{-0.60}$ day^{-1}). Recently, we reported that the FHP in growing pigs ranged between 900 and 1000 kJ (kg BW)$^{-0.60}$ day^{-1} (van Milgen *et al.*, 1998). In that study, FHP was corrected for standing activity only. Studies using both force sensors and infrared beams indicate that only 40–50% of activity is detected during standing, the remainder being detected when animals are lying down. Because the cost of physical activity is close to 200 kJ (kg BW)$^{-0.60}$ day^{-1}, it can explain a large part of the difference between these studies.

A more detailed analysis can be obtained by analysing the FHP separately for each experiment. Experiment A dealt with the effect of environmental temperature on the components of heat production in group-housed pigs. The FHP at 23°C was 16% higher than that at 33°C (890 vs. 750 kJ (kg BW)$^{-0.60}$ day^{-1}). However, a considerable part of this decrease can be attributed to decrease in voluntary feed intake (26% less at 33°C). Preliminary results of an experiment with 60-kg pigs indicate that a reduction of feed intake by one-third reduces FHP by approximately 10%. Neither feed composition (different levels of CP) nor feeding frequency affected FHP in growing pigs (experiment B). Also, there was no difference in the FHP between gestating sows fed a high- or low-fibre diet. Independently of the increase of BW, the stage of gestation significantly increased the FHP and probably reflects the increasing redistribution of energy from maternal to fetal tissues with advancement of gestation (Ramonet *et al.*, 2000).

For the three experiments, the respiratory quotient during fasting averaged 0.80. This indicates that, although glucose may contribute to the energy metabolism during fasting, oxidation of fatty acids and amino acids seems to be a priority. During fasting, it is possible that metabolically active tissues, such as the gastrointestinal tract, diminish in size. The constituents of these tissues (protein) will become available for oxidation.

Physical Activity

Pigs are lazy animals and have every reason to be so. Individually housed, growing pigs will stand 2 to 4 h day^{-1}, of which less than 1 h occurs during feed intake. While standing, the heat production is increased by approximately 60%. This increase appears to be several times larger in pigs compared with other domestic species (Noblet *et al.*, 1993). In our current experimental designs, $HP_{activity}$ consists of measuring the signal of the force sensors (mV) and estimation of the heat production per mV. The measured signal depends on the mounting of the metabolism cage on the force sensors. Consequently, comparison between experiments of the signal and the heat production per mV is not possible. However, the product of both measurements yields the daily $HP_{activity}$, which can be compared between experiments.

Although variation in body weight is probably the most important criterion affecting variation in $HP_{activity}$, social interactions between animals and space allowance may also be important. Analysis of $HP_{activity}$ (kJ day^{-1}) using only the data for individually housed animals (experiments B and C) indicated that $\ln(HP_{activity}) = \ln(130\ BW^{0.70})$. Nevertheless, considerable variation existed between individual animals (RSD = 31% of $HP_{activity}$). The animals in experiment A (group-housed pigs) produced much more heat during activity than the animals in the other experiments (on average 190 kJ $BW^{-0.70}$). Therefore, physical activity represents a major source of variation of heat production and failure to account for this may lead to erroneous estimates of the other components of heat production.

The results indicate that $HP_{activity}$ represents between 8 and 20% of the ME intake (Table 8.2). The higher levels are found for gestating sows, which are fed just above the maintenance energy requirement. For growing pigs, housed in groups or individually, between 8 and 13% of ME intake is used for physical activity. These lower values are partly due to the higher feeding level, because, when $HP_{activity}$ is expressed relative to FHP, the results become rather similar (34, 26 and 33% for experiments A, B and C, respectively). In other words, even though $HP_{activity}$ can be very variable between individual animals, it represents a relatively constant fraction of the maintenance energy requirement (or FHP).

Table 8.2. Effect of physiological stage and diet on the utilization of ME.

	Experiment					
	A (23°C)	A (33°C)	B (high protein)	B (low protein)	C (low fibre)	C (high fibre)
BW (kg)	33.2	28.2	69.8	69.4	266	264
ME intake (MJ day^{-1})	22.6	15.1	32.8	32.4	35.4	34.9
Energy utilization (% of ME intake)						
Retained energy	46.1	39.0	42.8	46.9	15.2	8.3
Heat production	53.9	61.0	57.2	53.1	84.8	91.7
FHP	31.0	35.8	30.9	30.8	56.9	59.8
Total TEF	12.9	12.3	18.3	14.6	7.6	12.0
TEF_{LT}			9.0	7.0	1.3	4.3
TEF_{ST}			9.3	7.6	6.3	7.7
$HP_{activity}$	10.0	12.9	7.9	7.7	18.6	20.2

BW, body weight; ME, metabolizable energy; FHP, fasting heat production; $HP_{activity}$, heat production due to physical activity; RQ_{FHP}, respiratory quotient during fasting; $RQ_{activity}$, respiratory quotient of activity.

Thermic Effect of Feeding

As indicated above, short-term and long-term components of TEF are proposed to distinguish a fraction with specific kinetics that can be related to ingestion of the feed from a fraction without distinguishable kinetics. The short-term component can be thought of as the heat production due to ingestion and digestion of the feed, whereas the long-term component is associated with metabolism of nutrients. This separation is, of course, arbitrary, as processes of nutrient uptake, absorption and metabolism occur simultaneously and a clear distinction of heat production associated with each process cannot be made.

In the experiments with growing pigs (B) and sows (C), both components of TEF were estimated (overlapping independent variables made this distinction difficult for experiment A). The TEF_{ST} represented approximately 8% of ME intake in both experiments, whereas TEF_{LT} represented a more variable fraction of ME (see Table 8.2). This suggests that the energetic cost of intake and digestion is relatively independent of the ultimate destiny of the nutrient and therefore represents a relatively constant fraction of ME. Once nutrients are absorbed, the efficiency of utilization depends to a large extent on the level of energy intake above maintenance and its ultimate utilization. Growing pigs will use a large part of the energy for protein and lipid deposition. Protein deposition is especially costly, which can explain the difference in TEF_{LT} between growing pigs and sows. A large part of the available nutrients in gestating sows is used for maintenance and only a small fraction is used for uterus and fetal growth.

The dietary origin of a nutrient can also affect its utilization. In experiment B, the dietary protein level was reduced while supplementing with synthetic amino acids. Excess amino acids are deaminated, after which the carbon chains can be used. The cost of deamination involves the loss of energy as urea and the cost of urea synthesis. As a result, excess dietary proteins are not used efficiently. This was confirmed by the finding that the total TEF was significantly lower for a low-protein diet (supplemented with amino acids) than for a high-protein diet. Relative to starch, reduction of excess dietary protein reduces heat production by 7 kJ (g protein)$^{-1}$ (Le Bellego *et al.*, 2000). An additional 3.5 kJ (g protein)$^{-1}$ is lost in the urine (primarily as urea).

A similar difference was found between a low- and high-fibre diet fed to gestating sows. The total TEF (as a fraction of ME intake) was higher for sows fed the high-fibre diet than for those fed the low-fibre diet (see Table 8.2). Although TEF_{LT} represents only a small fraction of ME intake, this fraction was (numerically) higher for sows fed a high-fibre diet compared with those fed a low-fibre diet. While TEF_{ST} is thought to represent most digestive processes, hindgut fermentation and synthesis of volatile fatty acids (VFAs) may lead to a more continuous heat production, accounted for through TEF_{LT} rather than TEF_{ST}. This hypothesis is supported by the fact that the appearance of TEF_{ST} after ingestion of a meal was later for the high-fibre diet than for the low-fibre diet. Sows fed the low-fibre diet required 6.4 h to dissipate 50% of TEF_{ST} after ingestion of a meal, whereas those fed the high-fibre diet required 7.5 h. From an energetic point of

view, it confirms the idea that the ME of fibre is used less efficiently than other energy sources (in this case, starch and protein).

Nocturnal Peak in Heat Production

The daily dynamics of heat production are caused by TEF_{ST} and $HP_{activity}$. These two phenomena explain a large part of the variation in heat production between the diurnal and nocturnal periods. As illustrated in Fig. 8.1, the nocturnal heat production in meal-fed animals is characterized by a decline in heat production, due to the diminishing effects of TEF_{ST} and reduced activity.

In many animals, we found that the gradual, nocturnal decline in heat production was interrupted by an additional peak of heat production (i.e. a decline in $[O_2]$ in Fig. 8.2). The peak usually appeared only once between 01.00 and 03.00. Ignoring its existence affected the model precision and estimation of parameters. We therefore manually included the occurrence of this 'ghost' phenomenon, to which a component of heat production was attributed. Although it typically represented 1–1.5% of the total daily heat production, it can represent up to 5% of the dynamic components of heat production (TEF_{ST} and $HP_{activity}$). The origin of this component heat production is not known. It may be related to the onset of rapid eye movement (REM) sleep, but it also appears to be influenced by nutritional status. Its occurrence in restrictively fed animals is much smaller and, so far, it has not been observed in fasting animals.

Conclusion

All ME that is not retained is lost as heat (or all ME that is not lost as heat can be retained). Studying the components of heat production can therefore help our understanding of energy requirements. The data analysis tool described here is based on the partitioning of heat production between fasting, thermic effect of feeding and physical activity and can be seen as a refinement of the classical notion of energy for maintenance and production. The model illustrates the fact that most of the dynamic components in heat production can be explained by the behaviour (eating and physical activity) of the animal. In the future, the tool will be used to quantify the contribution of the environment or different nutrients on the components of heat production (including thermoregulation). In a more general context, the approach described here may help to further develop models of growth prediction and evaluation of energy requirements of pigs in different circumstances.

Acknowledgements

Anne Collin, Laurent Le Bellego, Nathalie Quiniou, Yannick Ramonet and Serge Dubois are gratefully acknowledged for providing the data used in this analysis.

The Conseil Régional de Bretagne is acknowledged for providing financial support to attend the workshop.

References

ARC (1981) *The Nutrient Requirements of Pigs*. Commonwealth Agricultural Bureaux, Slough, England, 307 pp.

Brouwer, E. (1965) Report of sub-committee on constants and factors. In: Blaxter, K.L. (ed.) *Energy Metabolism. Proceedings of the 3rd Symposium*. Academic Press, London, pp. 441–443.

Koong, L.J., Nienaber, J.A. and Mersmann, H.J. (1983) Effect of plane of nutrition on organ size and fasting heat production in genetically obese and lean pigs. *Journal of Nutrition* 113, 1626–1631.

Le Bellego, L., van Milgen, J., Rademacher, M., Van Cauwenberghe, S. and Noblet, J. (1999) Effect of low protein diets on energy utilization in growing pigs. *Journal of Animal Science* 77 (Suppl. 1), 196.

Le Bellego, L., Noblet, J., van Milgen, J. and Dubois, S. (2000) Effets de la réduction du taux de protéines et de la fréquence de distribution des repas sur l'utilisation de l'énergie chez le porc en croissance. *Journées de la Recherche Porcine en France* 32, 217–225.

Matis, J.H., Wehrly, T.E. and Ellis, W.C. (1989) Some generalized stochastic compartment models for digesta flow. *Biometrics* 45, 703–720.

MGA Software (1997) *ACSL Optimize*. MGA Software, Concord, Massachusetts.

Noblet, J., Shi, X.S. and Dubois, S. (1993) Energy cost of standing activity in sows. *Livestock Production Science* 34, 127–136.

Ramonet, Y., van Milgen, J., Dourmad, J.Y., Dubois, S., Meunier-Salaün, M.C. and Noblet, J. (2000) The effect of dietary fibre on energy utilisation and partitioning of heat production over pregnancy in sows. *British Journal of Nutrition* 84, 85–94.

Steiner, E.C., Rey, T.D. and McCroskey, P.S. (1990) *SimuSolv – Modeling and Simulation Software*. Dow Chemical Company, Midland, Michigan.

van Milgen, J., Noblet, J., Dubois, S. and Bernier, J.F. (1997) Dynamic aspects of oxygen consumption and carbon dioxide production in swine. *British Journal of Nutrition* 78, 397–410.

van Milgen, J., Bernier, J.F., Lecozler, Y., Dubois, S. and Noblet, J. (1998) Major determinants of fasting heat production and energetic cost of activity in growing pigs of different body weight and breed/castration combination. *British Journal of Nutrition* 79, 509–517.

9

Aspects of Modelling Kidney Dynamics

Bruce Robson and Marijcke Vlieg

Applied Management and Computing Division, PO Box 84, Lincoln University, Canterbury, New Zealand

Abstract

The kinetics of mineral transport in the kidney has previously been described using Michaelis–Menten kinetics. Mathematical analysis of this phenomenon has indicated that a better fit to experimental data can be achieved by considering the joint effects of diffusion and active transport processes described using Michaelis–Menten kinetics. This has several benefits in that it allows a non-horizontal asymptote to describe the saturation effect, a biologically more realistic representation. This approach may be useful for describing the transport of any other material across membranes, such as the rumen wall. Application of this new technique will be illustrated for a model of magnesium metabolism in dairy cattle.

Introduction

Mechanistic models of animal metabolism saw their first introduction into the scientific literature two decades ago with the seminal work of Baldwin and Black (1979). France *et al.* (1982) with a rumen model and Gill *et al.* (1984) describing the absorption of energy-yielding nutrients in young sheep followed this, and a wide range of mechanistic models (Baldwin *et al.*, 1987; Danfær, 1990; Dijkstra *et al.*, 1992; Robson *et al.*, 1997) has been developed. All of these models are based on Michaelis–Menten kinetics to describe the uptake of nutrients or the transport of materials across biological membranes.

 Modelling Nutrient Utilization in Farm Animals (eds J.P. McNamara, J. France and D.E. Beever)

Background Theory

The mathematics of Michaelis–Menten kinetics is well described in France and Thornley (1984), Edelstein-Keshet (1988) and Thornley and Johnson (1990) and in general is given by:

$$u = \frac{v_m S}{K_m + S}$$

where u represents the flux of the material or nutrient, S the concentration of that material on the luminal or source side of the membrane, v_m the maximum flux at infinite concentration and K_m the concentration at which half the maximal flux occurs. This is just a rectangular hyperbola relationship and is shown in Fig. 9.1 with K_m and v_m both set to 1. It is important to note that the flux u asymptotically approaches v_m as S increases. This is, however, only one part of the hyperbola and there exists another, non-realistic but mathematically correct, branch of the hyperbola in the upper left quadrant. This is shown in Fig. 9.2.

Thornley and Johnson (1990: 51ff.) outline the mathematics necessary to cater for the situation where there is a diffusion process, describing the uptake of a metabolite into a cell, followed by an active transport process, using Michaelis–Menten kinetics, to describe the pumping of that metabolite out of the cell. The consequence of this from a mathematical viewpoint is that the normally vertical asymptote at $S = -K_m$ is now a sloping asymptote, given by:

$$u = \frac{K_m + S}{r} \tag{1}$$

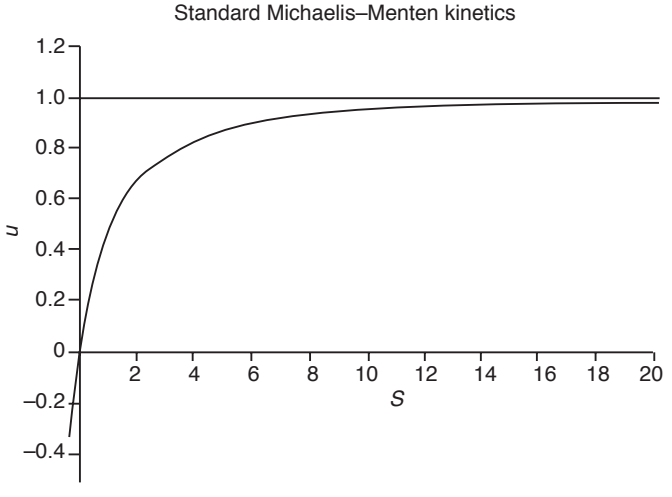

Fig. 9.1. Flux u as a function of concentration S, used to describe the active transport of material across a membrane.

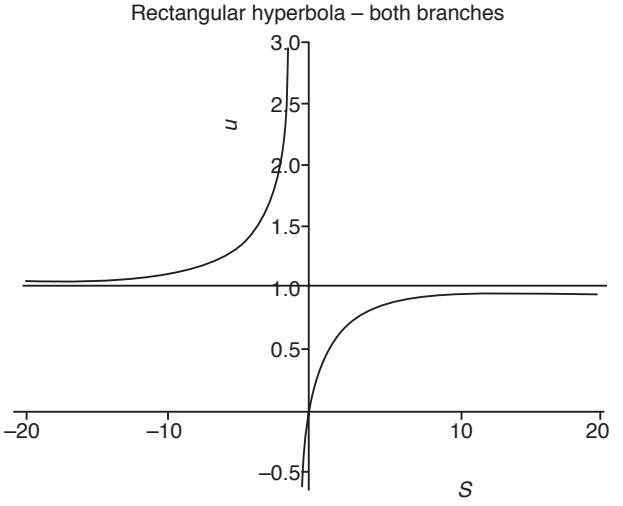

Fig. 9.2. Rectangular hyperbola used to describe Michaelis–Menten kinetics ($S > 0$) but also showing the non-realistic but mathematically important second branch for $S < -K_m$.

where r describes the resistance of the diffusive process. This description is thus one catering for a serial process, where the diffusion precedes the active transport.

If we now consider a situation where these diffusive and active transport processes occur in parallel, this is described by:

$$u = \frac{v_m S}{K_m + S} + c(S - S_0) \tag{2}$$

where c represents the diffusion coefficient and $S - S_0$ represents the concentration difference across the membrane. If we now collect terms in S in the numerator of the expanded right-hand side of equation 2, it can be written as:

$$u + cS_0 = \left(\frac{v_m S}{K_m + S}\right) \times \left(1 + \frac{cK_m}{v_m} + \frac{c}{v_m} S\right) \tag{3}$$

Equation 3 can be interpreted as follows. The flux u is reduced by a constant amount given by cS_0, as shown by shifting this term to the left-hand side of equation 3. The first term on the right-hand side represents the normal Michaelis–Menten kinetics. The second term on the right-hand side indicates that there is now a sloping asymptote for the hyperbola, with the slope given by c/v_m and the intercept on the $S = 0$ axis shifted from the normal unity (scaled by v_m) by an amount cK_m/v_m. This is illustrated in Fig. 9.3, where, without loss of generality, S_0 is set to zero.

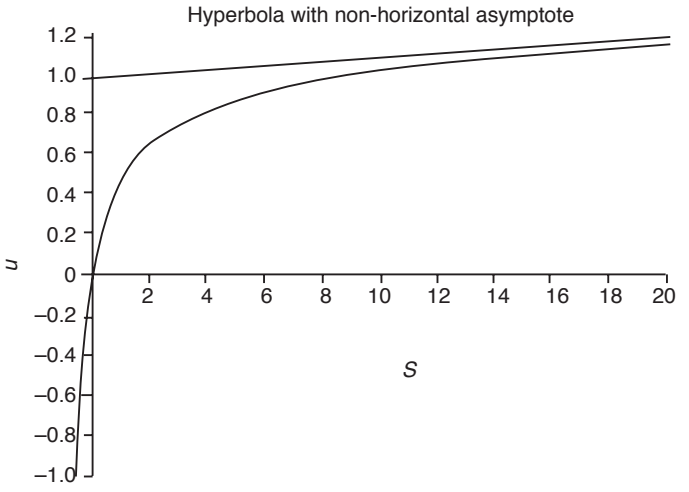

Fig. 9.3. Hyperbola with non-horizontal asymptote used to describe normal Michaelis–Menten kinetics in parallel with a diffusive process. Constants used are $v_m = 1$, $K_m = 1$, $c = 1/100$ (see text).

The real advantage of this view now arises when we take into account the other, non-realistic but mathematically correct, branch. This is shown in Fig. 9.4. Note that there is still the normal vertical asymptote at $S = -K_m$ (not shown). This formulation is different from the Thornley and Johnson (1990) model, in that their description gives a horizontal asymptote at $u = v_m$, with the previously vertical asymptote at $S = -K_m$ sloping as described by equation 1 above.

Kidney Magnesium Transport

Renal magnesium transport and its associated hormonal control mechanisms have been reviewed recently by De Rouffignac and Quamme (1994). Magnesium is reabsorbed at three sites within the kidney, with approximately 10–20% of the presented magnesium load being absorbed in the proximal tubule, ~60% absorbed in the cortical thick ascending limb of the loop of Henle (cTAL) and 5% absorbed in the distal tubule. In the cTAL, there are two possible pathways by which magnesium may be absorbed. These are the paracellular and the transcellular pathways. In the former, passive transport has been established as the transport mechanism (Shareghi and Agus, 1982), whereas, in the latter, di Stefano *et al.* (1993) have data suggesting that the magnesium absorption is associated with a voltage-dependent Na^+ gradient, which is maintained by an active transcellular process.

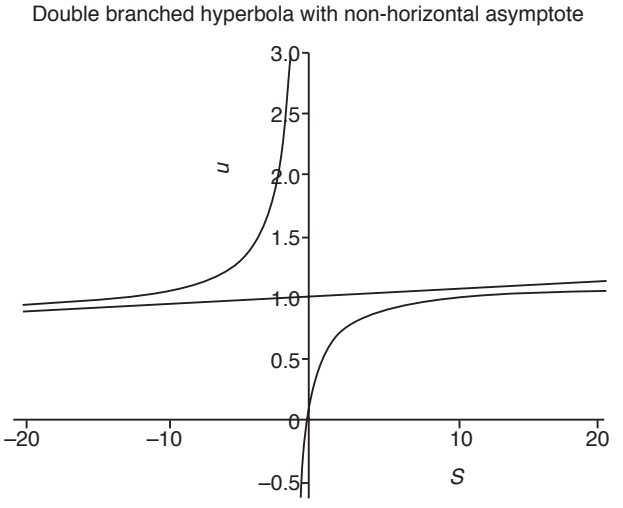

Fig. 9.4. Both branches of the hyperbola shown with non-horizontal asymptote. Constants used are as for Fig. 9.3.

These base mechanisms thus suggest that it is appropriate to model the homoeostasis of magnesium by the kidney using a combined active and passive transport process. Consequently, the relationship between the concentration of magnesium in plasma, y, and the flux of urinary magnesium excretion, x, is modelled by:

$$y = \frac{v_m x}{K_m + x} + cx \tag{4}$$

where the three parameters v_m, K_m and c are fitted from the plot of y versus x.

Application of Theory to Kidney Models

Most of the data available in the literature have plots in the form of plasma concentration on the y axis as a function of urinary excretion on the x axis (Kemp *et al.,* 1960). Consequently, it is necessary to invert the relationship above (equation 4) to obtain a plot of a flux (urinary output) on the y axis versus plasma concentration on the x axis. This gives two solutions from the quadratic in x which results from the rearranging of:

$$y = \frac{qx}{r + x} + tx \tag{5}$$

namely:

$$x_1, x_2 = \frac{1}{2t}\left(-(tr+q-y) \pm \sqrt{(tr+q-y)^2 + 4try}\right) \tag{6}$$

The terms under the square root in equation 6 are always positive, so to get a biologically meaningful solution we must choose the upper (positive) solution. Both solutions are plotted in Fig. 9.5 with $r = 1$, $q = 1$, $t = 0$ and in Fig. 9.6 with $r = 1$, $q = 1$, $t = 1/100$. This is just the inverse of the example relationship illustrated in Fig. 9.3 using the same parameters. Also shown in Fig. 9.6 is the sloping asymptote.

The real advantage of considering a sloping asymptote now becomes apparent. If the model behaviour were to give a resultant plasma concentration above the vertical asymptote at unity in Fig. 9.5 (not shown), the resultant urine output value would be negative. This is biologically unrealistic and can be seen to be the case by taking limits in Fig. 9.5 approaching the discontinuity from both the left and the right. However, as shown in Fig. 9.6, this problem no longer occurs.

Thus by being more biologically 'correct' in modelling kidney dynamics and introducing a diffusive term into the model description, we overcome a potentially tricky mathematical and numerical discontinuity. This is illustrated in Fig. 9.7, where, in dairy cattle, the plasma magnesium concentration and daily magnesium urinary output, corrected for creatinine excretion, are shown. A functional relationship of the form described by equation 5 above has been fit-

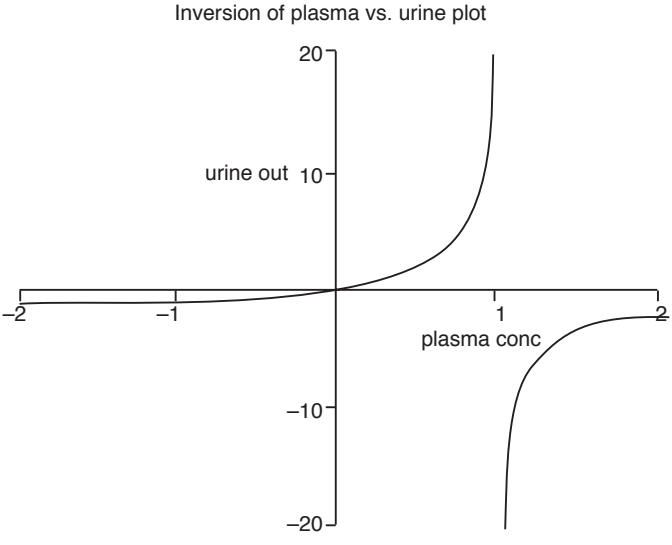

Fig. 9.5. Inversion of the plasma concentration versus urine output plot illustrating the discontinuity at unit plasma concentration.

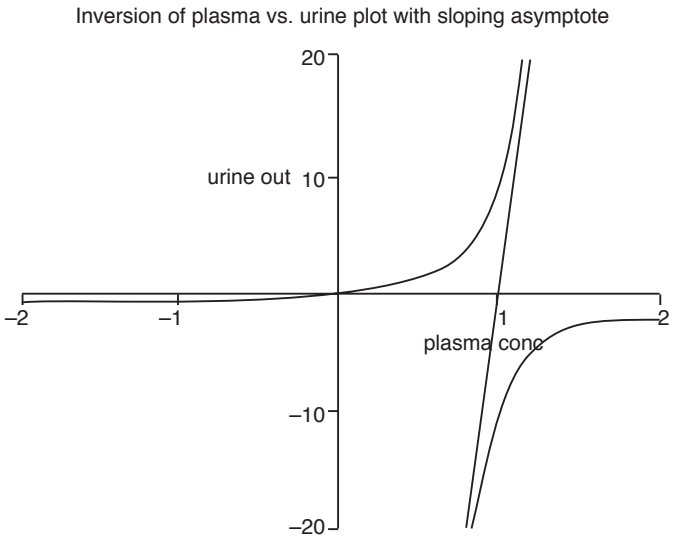

Fig. 9.6. Inversion of the plasma versus urine output plot illustrating the effect of a sloping asymptote.

ted to these data, using the Levenberg–Marquadt algorithm in SigmaPlot (Jandel Scientific, 1995). This relationship is shown, superimposed on these data, along with the parameter values.

Figure 9.8 displays the results of inverting the relationship given in Fig. 9.7. As a consequence of the sloping asymptote, the urine output will never be negative, which would be an obvious biological absurdity. This technique of including a sloping asymptote thus adds to the modelling techniques available by both improving biological reality and removing a mathematical discontinuity.

Discussion

Application of this new technique can be found in many areas and some examples follow.

Three new magnesium transport systems have been cloned from *Salmonella typhimurium* (Snavely *et al.*, 1989). These are coded by the loci *corA*, *mgtA* and *mgtB* and have been established to have different values of the Michaelis–Menten parameters, v_m and K_m. A potential application of the procedure outlined here can thus be seen when we apply the possibility of having two (or more) transport systems operating in parallel. If the K_m constants differ by a large amount – say, three orders of magnitude – we can approximate the combined flux as follows:

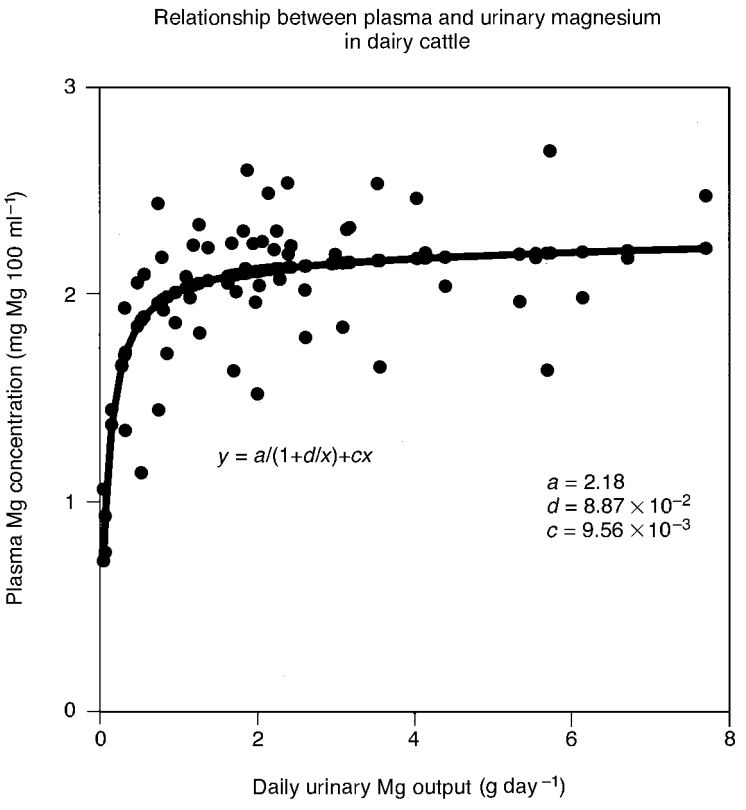

Fig. 9.7. Plasma magnesium concentration (mg Mg 100 ml^{-1}) versus daily urinary magnesium excretion (g day^{-1}). Data for dairy cattle sampled 24 September 1998 at Lincoln (from M. Thielen, A.B. Robson and A.R. Sykes, unpublished observations).

$$u = \frac{1}{1+\frac{1}{s}} + \frac{1}{1+\frac{1000}{s}} \tag{7}$$

This is shown in Fig. 9.9. Note the similarity between Figs 9.3 and 9.9.

It is also worth noting that Martens *et al.* (1991) have described a model for magnesium transport across the rumen wall that includes both the paracellular and the transcellular pathways. These are a combination of active and diffusive transport processes and as such could be a candidate for the mathematical model description described herein.

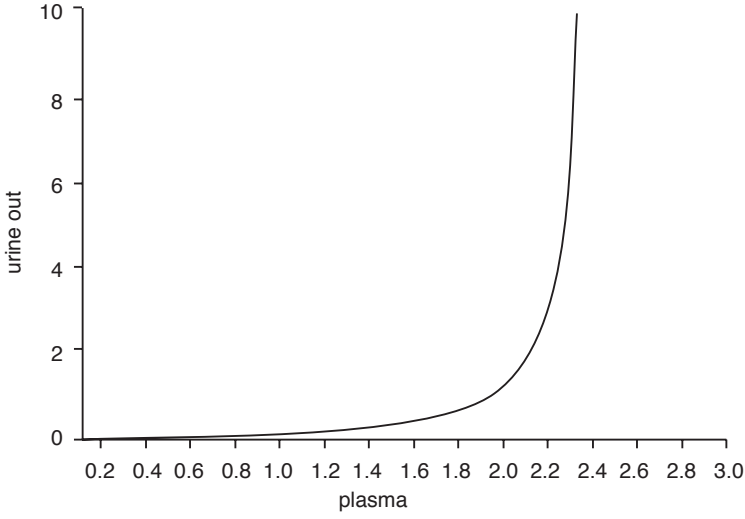

Fig. 9.8. Inversion of the superimposed relationship given in Fig. 9.7. The positive square root in equation 6 (see text) has been used with the values of $a = 2.18$, $d = 8.87 \times 10^{-2}$ and $c = 9.56 \times 10^{-3}$.

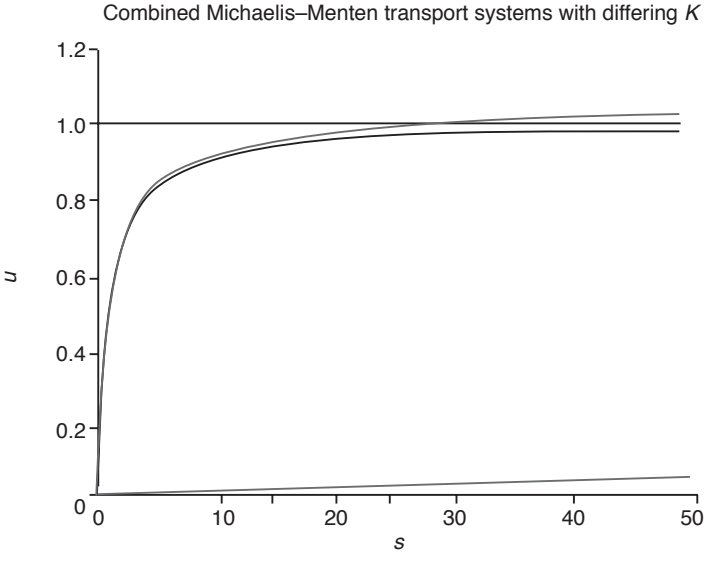

Fig. 9.9. Combined Michaelis–Menten transport systems operating in parallel. Values used are given in equation 7.

Summary

The work described in this chapter has extended the normal Michaelis–Menten description of the transport of flux across membranes by adding a diffusion term. This has been illustrated with some recently acquired data from dairy cows for the relationship between plasma magnesium concentration and daily urinary magnesium output. In contrast to the previous work of Thornley and Johnson (1990), who considered a diffusive process followed serially by a two-parameter Michaelis–Menten process, this work has described the Michaelis–Menten transport process combined in parallel with a diffusive process. It has also shown that the combined process could approximate two (or more) parallel Michaelis–Menten processes under certain conditions.

References

Baldwin, R.L. and Black, J.L. (1979) Simulation of the effects of nutritional and physiological status on the growth of mammalian tissues. *CSIRO Australian Animal Research Laboratories Technical Paper* 6, 1–35.

Baldwin, R.L., France, J. and Gill, M. (1987) Metabolism of the lactating cow I. Animal elements of a mechanistic model. *Journal of Dairy Research* 54, 77–105.

Danfær, A. (1990) *A Dynamic Model of Nutrient Digestion and Metabolism in Lactating Dairy Cows*. Report 671, the National Institute of Animal Science, Foulum, Tjele, Denmark.

De Rouffignac, C. and Quamme, G. (1994) Renal magnesium handling and its hormonal control. *Physiological Reviews* 74(2), 305.

Dijkstra, J., Neal, H.D.StC., Beever, D.E. and France, J. (1992) Simulation of nutrient digestion, absorption and outflow in the rumen: model description. *Journal of Nutrition* 122, 2239–2256.

di Stefano, A., Roinel, M., de Rouffignac, C. and Wittner, M. (1993) Transepithelial Ca^{2+} and Mg^{2+} transport in the cortical thick ascending limb of Henle's loop of the mouse is a voltage dependent process. *Renal Physiology and Biochemistry* 16, 157–166.

Edelstein-Keshet, L. (1988) *Mathematical Models in Biology*. Random House, New York, 586 pp.

France, J. and Thornley, J.H.M. (1984) *Mathematical Models in Agriculture: a Quantitative Approach to Problems in Agriculture and Related Sciences*. Butterworths, London, Boston, pp. 335.

France, J., Thornley, J.H.M. and Beever, D.E. (1982) A mathematical model of the rumen. *Journal of Agricultural Science, Cambridge* 99, 343–353.

Gill, M., Thornley, J.H.M., Black, J.L., Oldham, J.D. and Beever, D.E. (1984) Simulation of the metabolism of absorbed energy-yielding nutrients in young sheep. *British Journal of Nutrition* 52, 621–649.

Jandel Scientific (1995) *SigmaPlot for Windows*. Jandel Scientific, San Rafael, California.

Kemp, A., Deijs, W.B., Hemkes, O.J. and van Es, A.J.H. (1960) Basic source of magnesium metabolism III. Intake and utilization of magnesium from herbage by lactating cows. In: *Conference on Hypomagnesaemia*. British Veterinary Association, London, pp. 23–32.

Martens, H., Leonhard, S. and Gäbel, G. (1991) Minerals and digestion: exchanges in the digestive tract. In: Jouany, J.P. (ed.) *Rumen, Microbial Metabolism and Ruminant Digestion*. INRA Editions, Paris, France, pp. 199–216.

Robson, A.B., Field, A.C., Sykes, A.R. and McKinnon, A.E. (1997) A model of magnesium metabolism in young sheep: magnesium absorption and excretion. *British Journal of Nutrition* 78, 975–992.

Shareghi, G.R. and Agus, Z.S. (1982) Magnesium transport in the cortical thick ascending limb of Henle's loop of the rabbit. *Journal of Clinical Investigation* 69, 759–769.

Snavely, M.D., Florer, J.B., Miller, C.G. and Maguire, M.E. (1989) Magnesium transport in *Salmonella typhimurium*: Mg^{2+} transport by the CorA, MgtA, and MgtB Systems. *Journal of Bacteriology* 171, 4761–4766.

Thornley, J.H.M. and Johnson, I.R. (1990) *Plant and Crop Modelling: a Mathematical Approach to Plant and Crop Physiology*. Clarendon Press, Oxford, 669 pp.

10 Evaluation of a Representation of the Limiting Amino Acid Theory for Milk Protein Synthesis

M.D. Hanigan,[1] J. France,[2] L.A. Crompton[2] and B.J. Bequette[3]

[1]*Purina Mills, Inc., St Louis, MO 63144, USA;* [2]*Department of Agriculture, University of Reading, Earley Gate, Reading RG6 6AT, UK;* [3]*Rowett Research Institute, Bucksburn, Aberdeen AB21 9SB, UK*

Abstract

A model describing amino acid (AA) metabolism by the mammary glands of the lactating cow has been constructed (Hanigan *et al.*, 2000a). Milk protein production was predicted using a mathematical procedure to determine which among histidine (His), lysine (Lys), methionine (Met), threonine (Thr) and tyrosine plus phenylalanine (TP) was most limiting for milk protein synthesis. The minimum protein synthetic flux determined the overall rate of protein synthesis. The ability of the model to predict substrate removal and milk protein output was assessed, using the parameterization data (reference data) and an independent data set assembled from the literature (literature data). When the reference data were simulated, the model generally fitted the uptake data well. However, the model predicted milk protein yields poorly. Of the four experiments contained in the reference data set, only one experiment (C6) contained complete data for all driving AA. The model accounted for 53% of the observed variation in milk protein yields for C6, suggesting that inadequate data were the cause of inaccurate simulations for the remaining experiments in the reference data set. The model explained 43% of the observed variation in milk protein yields when the literature data set was simulated. Adoption of an alternative representation of milk protein synthesis, wherein all five driving AA affected milk protein synthesis simultaneously in a linear additive manner, resulted in a reduction in the accuracy of predictions of milk protein yields when C6 or the literature data set was simulated. Use of a Michaelis–Menten equation form to describe milk protein synthesis resulted in slight improvements in accuracy when the C6 data set was simulated and a reduction in accuracy when the literature data set was simulated. After

 Modelling Nutrient Utilization in Farm Animals (eds J.P. McNamara, J. France and D.E. Beever)

fitting sensitivity coefficients for a modified Michaelis–Menten equation to the literature data, the model described 60% of the observed variation in milk protein output. Attempts to derive sensitivity coefficients for the linear additive equation were unsuccessful, due to model instability caused by the equation. Based on the results herein, a modified version of the Michaelis–Menten equation appeared to represent the effects of essential AA effects on milk protein synthesis better than an equation considering a single limiting AA.

Introduction

A model of mammary amino acid (AA) metabolism has been developed and evaluated (Hanigan *et al.*, 2000a, b). Inputs to the model are arterial metabolite concentrations and mammary blood flow. Predicted outputs include mammary venous metabolite concentrations and milk protein yield. Histidine (His), lysine (Lys), methionine (Met), tyrosine plus phenylalanine (TP) and threonine (Thr) were represented as potentially limiting AA and thus primary driving variables of milk protein synthesis. These choices were based on apparent limitations proposed by various researchers (Fisher, 1972; Clark, 1975; Schwab *et al.*, 1976, 1992a, b; Clark *et al.*, 1978; Fraser *et al.*, 1991). Although AA removal was found to be adequately predicted by the model, milk protein synthesis was found to be poorly predicted (Hanigan *et al.*, 2000b). These results led to the proposal that concurrent consideration of multiple AA may offer a possible solution to the problem. A number of *in vivo* studies have been designed to examine AA limitations (Fisher, 1972; Schwab *et al.*, 1976, 1992a, b; Fraser *et al.*, 1991). Met and Lys were often found to be limiting, as determined from milk protein production responses. However, responses were generally associated with addition of one but not both AA. Clark *et al.* (1978) observed that three essential AA (EAA) elicited similar, yet independent, milk protein responses when added singly to a standard culture medium. These results contradict the representation of a single limiting AA and support the proposal of multiple limiting AA (Hanigan *et al.*, 2000b).

Attempts to elicit the mechanism of AA limitation with respect to protein synthesis have resulted in an extensive volume of literature. Early work examined the hypothesis that protein synthesis was limited by substrate supply, e.g. amino-acylated tRNA, at the step of elongation. However, Shenoy and Rogers (1977, 1978) concluded from their work that rates of protein synthesis were not limited by amino-acylated tRNA concentrations. Subsequent work examined the effects of AA limitations on initiation of protein synthesis. Although the mechanism of action has not been defined, it would appear that a number of AA independently affect rates of initiation of protein synthesis when concentrations of those AA are limiting (McGown *et al.*, 1973; Yokogoshi and Yoshida, 1980; Perez-Sala *et al.*, 1991). These results also support the concept of multiple limiting AA with independent effects and suggest that adoption of

such a representation of milk protein synthesis would result in more accurate predictions.

Although Clark *et al.* (1978) observed that milk protein secretion was significantly stimulated by three EAA, they also observed that it tended to be stimulated when concentrations of a number of other EAA were elevated. If EAA other than Met, Lys, His, TP and Thr limit milk protein synthesis under some circumstances, the choice of these EAA as driving variables may be the cause of poor predictions of milk protein synthesis (Hanigan *et al.*, 2000b).

The primary objective of this work was to test two alternative representations of milk protein synthesis: a linear additive equation and a Michaelis–Menten equation. A second objective was to evaluate the need for consideration of additional driving AA in the milk protein synthesis equation.

Methods

For this work, the model of Hanigan *et al.* (2000a) was used as the base model, with modifications as defined herein. The model was written in Advanced Continuous Simulation Language (ACSL®) and run using ACSL Tox software (Pharsight Corp., Mountain View, California, USA). All simulations were run on a Dell computer (Dell Computer Corp., Round Rock, Texas, USA) with an Intel Pentium 350 processor. The portion of the model dealing with milk protein synthesis is depicted in Fig. 10.1. The protein synthesis equations used in the base model were:

$$\hat{U}_{ni,Pm} = \frac{K_{ni,Pm} C_{ni}}{f_{i,Pm}} \tag{1}$$

$$U_{Aa,Pm} = \text{Minimum}\left(\hat{U}_{nHis,Pm}, \hat{U}_{nLys,Pm}, \hat{U}_{nMet,Pm}, \hat{U}_{nThr,Pm}, \hat{U}_{nTp,Pm}\right) \tag{2}$$

where $\hat{U}_{ni,Pm}$ (mol day^{-1}) denotes potential milk protein production from the *i*th AA (mol day^{-1}); $K_{ni,Pm}$ the rate constant for utilization of the *i*th AA; C_{ni} the transient intracellular concentration of the *i*th AA (mol l^{-1}); and $f_{i,Pm}$ the molar proportion of the *i*th AA in milk protein. From the potential production rates, the most limiting flux is chosen to represent the predicted rate of milk protein production ($U_{Aa,Pm}$).

Based on the observations of Hanigan *et al.* (2000b) and a review of the literature, two alternative representations of milk protein synthesis were evaluated. The first was:

$$U_{AA,Pm} = K_{EAA,Pm} \sum \left(\frac{C_{ni}}{iC_{ni}} \right)^{\text{Exp}_{ni,Pm}} \Big/ N \tag{3}$$

where $U_{AA,Pm}$ denoted the rate of synthesis of milk protein from AA (mol day^{-1}), $K_{EAA,Pm}$ denoted the rate parameter (mol day^{-1}) for conversion of AA to milk

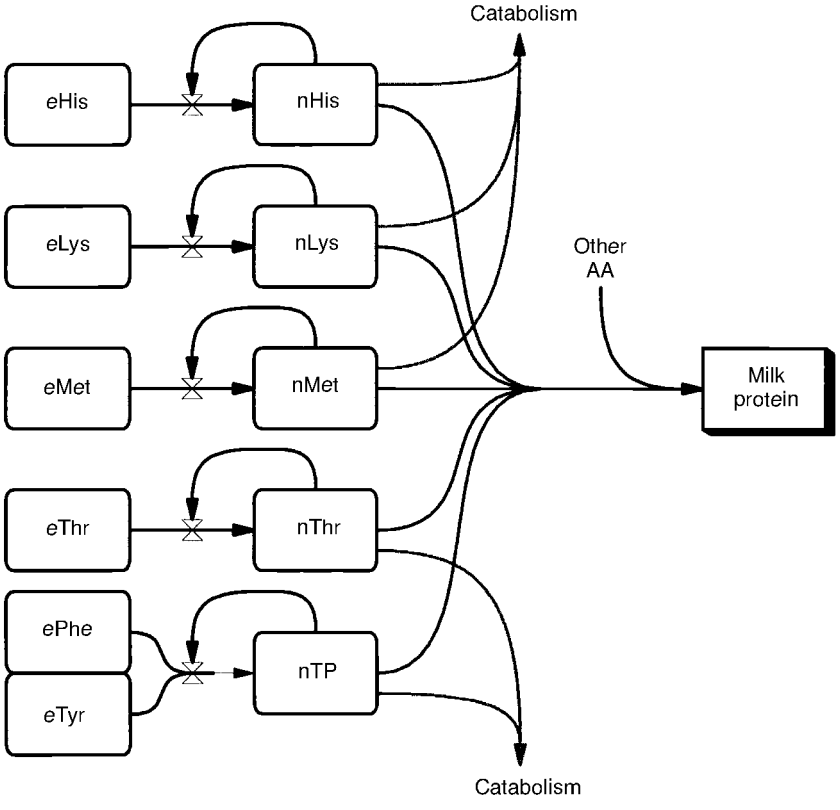

Fig. 10.1. Flow diagram depicting milk protein synthesis and essential amino acid metabolism in the udder of a lactating cow. Unshadowed boxes denote pools and arrows between pools denote fluxes. Arrows connected to the constrictor symbol denote feedback inhibition of the source pool on the flux associated with the constrictor symbol, i.e. nHis pool size acts as a feedback inhibitor of transfer of eHis to the nHis pool. The extracellular pools each have arterial inputs and venous outputs. These fluxes were not depicted on this diagram, in order to maintain simplicity. e, Extracellular; n, intracellular.

protein, iC_{ni} was a constant representing the reference concentration of the ith EAA, N represented the number of EAA considered, and $\text{Exp}_{ni,Pm}$ represented sensitivity exponents for each EAA. Initial values for $\text{Exp}_{ni,Pm}$ were set to 1.0, yielding an equation that was linear with respect to each EAA. With reference inputs, i.e. all inputs are equal to the reference values defined by Hanigan *et al.* (2000a), the ratio C_{ni}/iC_{ni} will equal 1 for each of the AA considered. If transient concentrations of an AA increase relative to the reference concentration, the ratio will become greater than 1 resulting in an increase in the rate of milk protein synthesis. Conversely, if transient concentrations of an AA fall relative to

the reference concentration, the ratio will become less than 1 and the rate of milk protein synthesis will decline. The responsiveness to these concentration changes can be adjusted using $\text{Exp}_{ni,Pm}$. The individual ratios are summed to represent the additive effects observed by Clark *et al.* (1978). The units for $K_{EAA,Pm}$ are mol day^{-1}. The value of $K_{EAA,Pm}$ was calculated from the reference data (Hanigan *et al.*, 2000a) and found to be 5.97 mol day^{-1}. EAA considered in equation 3 were His, Lys, Met, TP and Thr, following Hanigan *et al.* (2000a).

The second equation evaluated was of the Michaelis–Menten form:

$$U_{AA,Pm} = \frac{V_{AA,Pm}}{1 + \sum \left(\frac{k_{ni,Pm}}{C_{ni}} \right)^{\text{Exp}_{ni,Pm}}} \tag{4}$$

where $k_{ni,Pm}$ represented the apparent affinity constant (M) for each of the EAA considered. Again, $\text{Exp}_{ni,Pm}$ was included to allow adjustments in sensitivity, if needed, although initial values were set to 1. As the intracellular concentration data required to derive $k_{ni,Pm}$ are not currently available, the various $k_{ni,Pm}$ were assumed to be equal to iC_{ni}, yielding unit ratios. To allow adjustment of $k_{ni,Pm}$ in equation 4, while maintaining the observed flux rate of 5.97 mol day^{-1} for $U_{AA,Pm}$ with reference inputs, $V_{AA,Pm}$ was made a function of reference intracellular EAA concentrations, $k_{ni,Pm}$ and the exponents:

$$V_{AA,Pm} = 5.97 \left[1 + \sum \left(\frac{k_{ni,Pm}}{iC_{ni}} \right)^{\text{Exp}_{ni,Om}} \right] \tag{5}$$

Such a representation allowed $U_{AA,Pm}$ to remain equal to 5.97 mol day^{-1} at reference inputs regardless of the values adopted for the parameters. Additionally, this representation negated the need to derive $V_{AA,Pm}$ directly from data. This latter point is not trivial, as adequate data are not currently available for such a task.

A change to equations describing removal of the primary limiting EAA was required to support the above changes in the representation of milk protein synthesis. The change included consideration of intracellular EAA concentrations as a feedback inhibitor of removal. Such a consideration allowed for stimulation of removal of a given AA when intracellular concentrations of that AA declined, due to increased utilization for protein synthesis, as driven by increased removal of another AA. Such a representation reflects the observations of Bequette *et al.* (2000) and many others. Removal of the driving AA (U_{ei}, mol day^{-1}) considered in equation 3 and extracellular concentrations (C_{ei}, M) were defined as:

$$U_{ei} = K_i C_{ei} \frac{iC_{ni}}{C_{ni}} \tag{6}$$

$$C_{ei} = \frac{C_{ai}F_a}{K_i \frac{iC_{ni}}{C_{ni}} + F_a} \quad (7)$$

where K_i, C_{ai}, C_{ei} and F_a represented the rate parameter for removal of the ith EAA (l day^{-1}), arterial concentration of the ith EAA, extracellular concentration of the ith EAA (M) and arterial blood flow (l day^{-1}), respectively. See Hanigan *et al.* (1998b) for derivation of equations 6 and 7. The proposed change utilizes the ratio of the reference intracellular concentration over the transient intracellular concentration as an inhibitor. Use of this ratio allows retention of the original parameter estimate for K_i, as the ratio of concentrations will be 1 in the reference state. Increases in intracellular concentration relative to the reference concentration will inhibit removal and decreases will stimulate removal. Changes defined by equations 3 to 7 are depicted in Fig. 10.1.

Two data sets were used for this work. The first set comprised four experiments carried out by Metcalf and co-workers and was referred to collectively as the reference data set and individually by the experiment number assigned within the project that sponsored the work (C1, C3, C6 or C10). These experiments have been described previously (Metcalf *et al.*, 1994, 1996; Hanigan *et al.*, 2000a). The second set, referred to collectively as the literature data set, contained observations from 21 different experiments that have been published in the literature over the past 30 years (Fisher, 1972; Bickerstaffe and Annison, 1974; Derrig *et al.*, 1974; Spires *et al.*, 1975; Clark *et al.*, 1977; Peeters *et al.*, 1979; Rulquin, 1981; Drackley and Schingoethe, 1986; Yang *et al.*, 1986; Casper *et al.*, 1987; Illg *et al.*, 1987; Austin *et al.*, 1991; Miller *et al.*, 1991; Hanigan *et al.*, 1992; Cant *et al.*, 1993a, b; Choung and Chamberlain, 1993; Guinard *et al.*, 1994; Guinard and Rulquin, 1994a, b, 1995; Karunanandaa *et al.*, 1994; Baldwin and Hanigan, 1995; Griinari *et al.*, 1997a, b; Lykos and Varga, 1997; Lykos *et al.*, 1997).

Due to limitations associated with the single limiting AA approach when utilizing the base model, the variable Δ (proportionality constant for removal of non-free AA) was set to 0.57, as previously defined (Hanigan *et al.*, 2000b). Such a setting removed the observed mean bias in milk protein predictions. For all other simulations, Δ was set to 0.33, as originally defined (Hanigan *et al.*, 2000a). It was previously observed that the relationships among extracellular concentrations and removal for several substrates differed significantly for the literature data set as compared with the reference data set. As accurate estimates of substrate removal were critical to the objectives herein, the original uptake parameters were used for simulations of the reference data set and the following changes were adopted for simulations of the literature data set, based on the observations of Hanigan *et al.* (2000b): $K_{eLeu} = 7840$, $K_{eLys} = 16{,}960$, $K_{eMet} = 10{,}552$, $K_{ePhe} = 9650$, $K_{eIle} = 11{,}743$, $K_{eAc} = 27{,}360$, and $K_{eKb} = 13{,}243$ (l day^{-1} all).

Although ACSL Tox makes provision for fitting an error model to data, visual examination of the data indicated that variation did not scale with the magnitude of the variable. Therefore, an error model was not fitted. Variation explained was calculated using ACSL Tox. Regression analyses were performed using the REG procedure of SAS (SAS, 1994). Mean bias and residual variation were calculated as:

$$\text{Mean bias} = \frac{\sum(\text{observed} - \text{predicted})}{\text{number of observations}} \tag{8}$$

$$\text{Residual variation} = \sqrt{\text{RMSPE}^2 - \text{mean bias}^2} \tag{9}$$

where RMSPE represents the root mean square prediction error and was calculated as:

$$\text{RMSPE} = \sqrt{\frac{\sum(\text{observed} - \text{predicted})^2}{\text{number of observations}}} \tag{10}$$

Results

Results obtained from simulating the reference data set using the base model and with modifications defined by equations 3 and 4 are presented in Tables 10.1 and 10.2. Results for arginine and the branch-chain AA are presented for reference only and comments relating to EAA are exclusive of those four AA unless specified otherwise. With the exception of Lys, the variation in venous EAA concentrations explained by the model was reduced slightly by adoption of the alternative equations. Variation in milk protein yields explained by the model did not change significantly with adoption of equation 3 and increased slightly with equation 4.

Closer examination of the reference data set indicated that there were two deficiencies that may have a negative impact on predictions: (i) blood flow for C1 was predicted from milk yield (Hanigan *et al.*, 2000a), as the observed flows were found to be inconsistent with other experiments; and (ii) a number of EAA were missing from some or all of the observations for C1, C3 and C10, necessitating the use of mean values for the required arterial concentrations. Deviations from the predicted arterial concentration and blood flow values could explain a portion of the residual errors in milk protein predictions. Of the four experiments contained in the reference data, C6 was the only set with a complete description of all EAA and apparently valid measurements of blood flow. Therefore, simulations of C6 with the base and modified versions of the model were undertaken to evaluate model adequacy. Results from these simulations are also presented in Tables 10.1 and 10.2. For the base model, the

Table 10.1. Percentage of variation in mammary venous amino acid concentrations and milk protein yields explained by the model. Simulations were compared with the reference, C6 or literature data sets, as defined in the 'Methods' section. Milk protein yields were predicted from essential amino acids, using equation 2 (Base), equation 3 (Linear additive) or equation 4, with assumed (M-M standard) or derived (M-M fitted) values for $k_{ni,Pm}$ and $Exp_{ni,Pm}$. Amino acids examined were arginine (Arg), histidine (His), isoleucine (Ile), leucine (Leu), lysine (Lys), methionine (Met), phenylalanine (Phe), threonine (Thr), tyrosine (Tyr) and valine (Val).

	His	Lys	Met	Phe	Tyr	Thr	Arg	Ile	Leu	Val	Milk protein
Reference data											
Base model	93.55	89.69	75.59	77.05	81.84	57.93	78.2	79.37	84.16	91.24	0
Linear additive	91.21	92.85	65.91	71.79	79.57	51.35	78.2	79.37	84.16	91.24	0
M-M standard	91.11	92.69	69.41	72.5	79.72	52.35	78.2	79.37	84.16	91.24	12.24
C6 data											
Base model	97.5	0	77.82	70.33	68.25	57.93	75.16	80.91	83.79	94.37	53.29
Linear additive	98.62	8.31	73.05	68.87	65.53	51.35	75.16	80.91	83.79	94.37	49.75
M-M standard	98.63	4.66	74.06	65.22	62.7	52.35	75.16	80.91	83.79	94.37	55.02
M-M fitted*	98.76	8.92	67.54	67.66	65.21	49.75	75.16	80.91	83.79	94.37	29.52
M-M fitted†	98.66	0	59.16	52.35	50.02	52.52	75.16	80.91	83.79	94.37	5.08
Literature data											
Base model	33.71	33.71	66.43	40.89	12.95	60.29	46.02	66.87	63.81	88.51	43.78
Linear additive	35.15	0	75.7	30.91	0	55.46	46.02	66.87	63.81	88.51	34.26
M-M standard	35.7	0	74.14	26.81	0	55.82	46.02	66.87	63.81	88.51	34.42
M-M fitted*	33.87	0	77.01	35.43	0	55.96	46.02	66.87	63.81	88.51	46.54
M-M fitted†	32.91	4.64	79.71	44.65	0	57.41	46.02	66.87	63.81	88.51	60.16

* Affinity constants for equation 4 set to values listed in Table 10.3.
† Exponents for equation 4 set to values listed in Table 10.3.

Table 10.2. Mean bias and residual variation associated with predictions of mammary venous amino acid concentrations (μmol l^{-1}) and milk protein yields (kg day^{-1}). Simulations were compared with the reference, C6 or literature data sets, as defined in the 'Methods' section. Milk protein yields were predicted from essential amino acids using equation 2 (Base), equation 3 (Linear additive) or equation 4 with assumed (M-M standard) or derived (M-M fitted) values for $k_{ni,Pm}$ and $Exp_{ni,Pm}$. Amino acids examined were histidine (His), lysine (Lys), methionine (Met), phenylalanine (Phe), threonine (Thr) and tyrosine (Tyr).

	His	Lys	Met	Phe	Tyr	Thr	Milk protein
Mean bias							
C6 data							
Base model	−0.085	−12.00	−0.857	−2.56	−2.57	−0.114	−0.007
Linear additive	0.039	−9.97	−0.855	−2.71	−2.67	−0.158	−0.001
M-M standard	−0.067	−10.20	−0.957	−2.89	−2.85	−0.283	0.007
M-M fitted*	−0.034	−10.13	−0.921	−2.83	−2.80	−0.244	−0.238
M-M fitted†	−0.429	−10.94	−1.29	−3.54	−3.48	−0.696	−0.200
Literature data							
Base model	11.88	1.06	−1.61	0.14	−0.83	−7.42	0.075
Linear additive	12.42	−6.00	−2.64	−2.27	0.15	−9.07	0.026
M-M standard	12.03	−6.69	−2.98	−3.01	−0.33	−9.62	0.073
M-M fitted*	12.63	−5.60	−2.43	−1.82	0.41	−8.78	0.012
M-M fitted†	12.70	−5.35	−2.35	−1.66	0.55	−8.73	0.005
Residual variation							
C6 data							
Base model	2.23	4.49	1.32	1.50	1.65	7.49	0.060
Linear additive	1.65	5.48	1.51	1.39	1.74	8.05	0.063
M-M standard	1.65	5.54	1.41	1.40	1.69	7.97	0.059
M-M fitted*	1.57	5.11	1.67	1.26	1.55	8.18	0.073
M-M fitted†	1.58	4.72	1.71	1.29	1.61	7.93	0.076
Literature data							
Base model	20.94	10.63	4.84	6.12	12.62	5.36	0.153
Linear additive	20.32	11.82	3.44	6.22	13.39	5.30	0.182
M-M standard	20.44	11.91	3.34	6.11	13.33	5.18	0.169
M-M fitted*	20.46	11.97	3.45	6.13	13.31	5.24	0.169
M-M fitted†	20.63	11.64	3.20	5.69	13.08	4.88	0.143

* Exponents for equation 4 set to values listed in Table 10.3.
† Affinity constants for equation 4 set to values listed in Table 10.3.

percentage of milk protein yield variation explained by the model was much greater than when the entire reference data set was used. However, the benefits observed when the Michaelis–Menten equation was used to predict milk protein were less than the improvement observed for the entire reference data set.

Regression analyses (SAS, 1994) were undertaken to identify potential deficiencies in the models with respect to the C6 data. Residual errors associated with predictions of milk protein yields using equation 3 were positively correlated ($P < 0.1$) with observed uptakes of His, Lys, Met, phenylalanine (Phe) and tyrosine (Tyr). Visual appraisal of residual errors associated with predictions of milk protein synthesis indicated that errors of prediction were indeed linearly correlated with observed uptakes of the considered EAA, indicating that the responsiveness of the milk protein synthesis equation to these AA was improper. Analyses of C6 residuals when equation 4 was used yielded similar results.

Inclusion of $\text{Exp}_{ni,Pm}$ in equation 3 was the only provision made for sensitivity adjustments. However, either $\text{Exp}_{ni,Pm}$ or $k_{ni,Pm}$ can be adjusted to change sensitivity in equation 4. As the assumption that $k_{ni,Pm}$ was equivalent to iC_{ni} was made, it seemed prudent to determine whether a better set of parameter estimates for $k_{ni,Pm}$ could be derived before attempting derivation of the sensitivity exponents. Attempts to derive values for $k_{ni,Pm}$ from C6 data proved unsuccessful, despite the observed correlations in the regression analyses. The lack of success was probably due to additional variation introduced through the predictions of AA removal in the model as compared with use of observed removals in the regression analyses. An additional limitation to C6 with respect to defining coefficients for individual AA was the lack of independent variation in individual AA. Blood concentrations of AA were manipulated via alterations in the rate of feeding of a protected protein source, which resulted in high covariance among blood AA concentrations as compared with infusion of individual AA. Consequently, the data set was deemed inadequate for the task, and the literature data set, which contained a number of studies where individual EAA were either infused or fed, was used for further efforts. When $k_{ni,Pm}$ was fitted to the literature data set, significant improvements in overall model accuracy with respect to milk protein yield predictions were observed (see Table 10.1). However, there were a number of solutions that provided similar values for the log-likelihood function, indicating that the values in Table 10.3 are not unique. The improvement resulted from a reduction in mean bias as residual variation increased slightly (see Table 10.2). Parameter estimates for $k_{ni,Pm}$ are presented in Table 10.3. Although the values may not be unique, all solutions found had similar ratios for the individual parameters. The observation that the log-likelihood function increased as the values for $k_{ni,Pm}$ increased and that there were a number of solutions with essentially equivalent fits indicates that the relationship was linear with respect to AA concentrations and thus the data were inadequate to define both $V_{ni,Pm}$ and $k_{ni,Pm}$ (see equation 5).

An attempt to derive $\text{Exp}_{ni,Pm}$ was also undertaken for equations 3 and 4 by fitting the model to the literature data. As for the determination of $k_{ni,Pm}$, C6 data

Table 10.3. Derived parameters for equation 4 using the literature data set. $Exp_{ni,Pm}$ was set to 1 for the derivation of $k_{ni,Pm}$ and $k_{ni,Pm}$ was set to $2iC_{ni}$ for the derivation of $Exp_{ni,Pm}$.

Amino acid	$k_{ni,Pm}$	Standard deviation	$Exp_{ni,Pm}$	Standard deviation
Histidine	1.06	0.0002	2.58	0.735
Lysine	11.79	0.003	5.15	1.08
Methionine	0.803	9.6×10^{-5}	1.61	1.94
Threonine	1.77	0.0002	4.28	0.884
Tyrosine + phenylalanine	11.03	0.003	4.46	1.68

were found to be inadequate. During the fitting process, it was found that equation 3 destabilized the model at various combinations of exponent values, particularly when the exponent for Met was small and values for one or more other EAA were relatively large. This was due to inadequate responses to limiting supplies of Met (intracellular Met concentrations could not be maintained). This instability prevented successful derivation of parameter estimates and led to the conclusion that equation 3 was not amenable to use as a prediction equation for milk protein synthesis. Further attempts to refine the equation were abandoned. For fitting of $Exp_{ni,Pm}$ in equation 4, $k_{ni,Pm}$ was set equal to iC_{ni}. Although $Exp_{ni,Pm}$ was found to be definable, the standard deviations of the estimates were relatively large (data not shown). Examination of the equation and residual errors indicated that the sensitivity to changes in the exponents should have been symmetrical at concentrations less than and greater than iC_{ni} (a linear response). This was not the case when $k_{ni,Pm} = iC_{ni}$, where sensitivity to the exponents was much less at intracellular concentrations greater than iC_{ni} than at concentrations less than iC_{ni} (a curvilinear response). Utilizing the relationship $k_{ni,Pm} = 2iC_{ni}$ resulted in more symmetrical sensitivities and much better fits to the literature data (see Tables 10.1 and 10.2). Estimates for $Exp_{ni,Pm}$ with $k_{ni,Pm} = 2iC_{ni}$ are presented in Table 10.3. Utilizing these parameters, the model explained 60% of the observed variation in milk protein yields in the literature data set, despite poor predictions of Lys and Tyr removal (Fig. 10.2 and see Tables 10.1 and 10.2). Lysine residuals exhibited a linear bias and Tyr residuals exhibited a negative mean bias (see Fig. 10.2 and Table 10.2). Met and Phe removals were more accurately predicted, which may explain a portion of the improvement in predictions of milk protein (see Tables 10.1 and 10.2). Although simulations of C6 data using the above values for $Exp_{ni,Pm}$ appeared to result in much poorer predictions of Met and Phe removal and milk protein production, as measured by percentage of variation explained (see Table 10.1), residual variation did not increase significantly (see Table 10.2). As can be observed in Fig. 10.3, removal of the mean bias would result in excellent predictions of C6 milk protein yield observations.

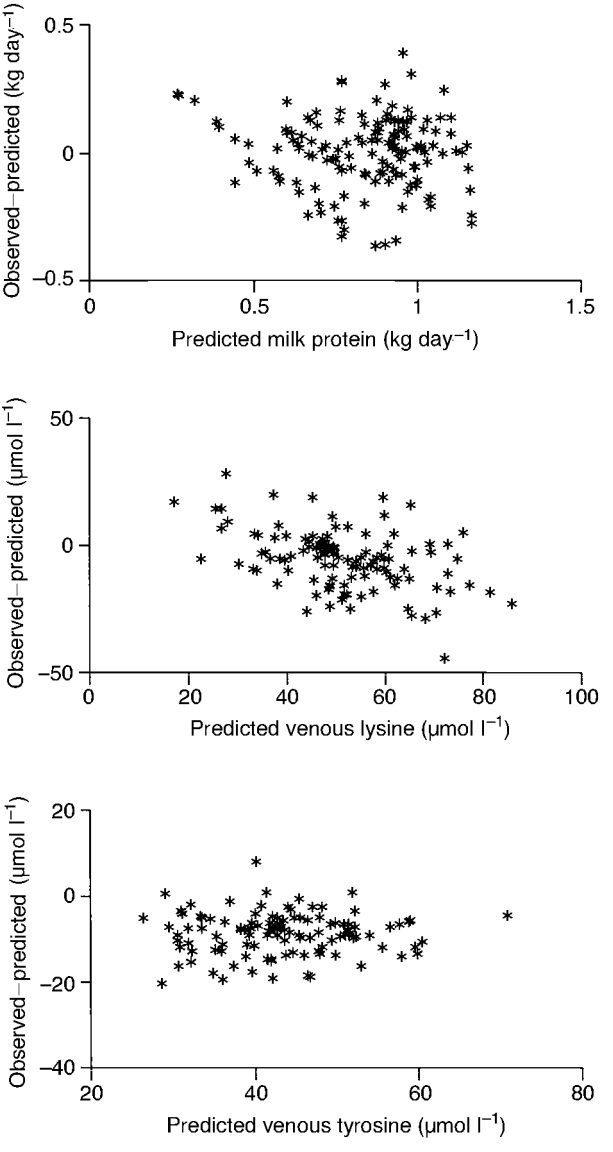

Fig. 10.2. Residual errors for milk protein yield and lysine and tyrosine venous concentrations versus predicted values. Simulations were of the literature data set, using equation 4, with $k_{ni} = 2iC_{ni}$ and $\text{Exp}_{ni,Pm}$ set to values listed in Table 10.3.

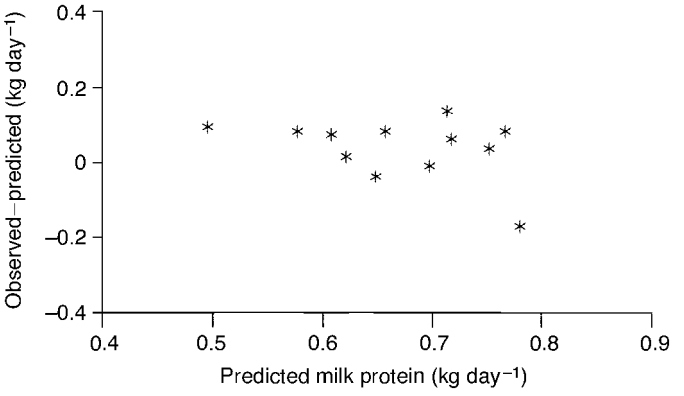

Fig. 10.3. Residual milk protein yield errors versus predicted values. Simulations were of C6, using equation 4, with $k_{ni} = 2iC_{ni}$ and $\text{Exp}_{ni,Pm}$ set to values listed in Table 10.3.

Regression analyses (SAS, 1994) were conducted using results from simulations of the literature data set when the derived values for $\text{Exp}_{ni,Pm}$ were used. Milk protein residuals were observed to be correlated with Lys, Met and Thr venous concentration residuals and observed uptakes of Lys, Thr, Met, acetate, leucine and glycerol (Table 10.4).

Table 10.4. Backward elimination regression analyses of residual errors for milk protein yield predictions. Simulations were of the literature data set using equation 4 with $k_{ni} = 2iC_{ni}$ and $\text{Exp}_{ni,Pm}$ set to values listed in Table 10.3. Residual errors for milk protein yields were regressed on observed uptakes of all essential amino acids, residual prediction errors for venous concentrations of essential amino acids and all major energy-yielding substrates. The overall regression was significant ($P < 0.0001$, $r^2 = 0.58$), with significant terms ($P < 0.1$) listed.

Variable	Parameter estimate	Standard error	F	$P > F$
Intercept	0.374	0.112	11.09	0.002
Lysine uptake	−0.00218	0.000422	26.62	0.0001
Residual lysine	−0.0326	0.00778	17.6	0.0001
Threonine uptake	0.00206	0.000623	10.9	0.002
Residual methionine	−0.0538	0.0193	7.78	0.008
Acetate uptake	0.00824	0.00297	7.68	0.008
Residual threonine	0.0286	0.0106	7.3	0.01
Leucine uptake	0.000206	9.92E-05	4.32	0.04
Glycerol uptake	−0.0001	5.01E-05	4.32	0.04
Methionine uptake	−0.00232	0.00120	3.72	0.06

F, statistic.

Discussion

Representation of protein synthesis as a function of a single limiting AA is commonly accepted as a valid representation by most animal scientists. Efforts reported herein are, to our knowledge, the first to examine alternative representations of the relationship between EAA supply to the udder and milk protein synthesis rates, including the limiting EAA representation.

Results from simulations of either a single well-defined study (C6) or a collection of studies available in the literature suggest that the single limiting EAA representation of milk protein synthesis explains 40–55% (see Table 10.1) of the observed variation in milk protein yields. However, a large positive mean bias (milk protein yields were consistently underpredicted) was observed when observed EAA supplies were not supplemented with additional EAA (Hanigan *et al.*, 2000b). Consideration of His, Lys, Met, Thr and TP simultaneously in either a Michaelis–Menten form or a linear form alleviates the need for additional supplementation of EAA inputs, although predictions of milk protein yields were initially slightly less accurate when each EAA was assumed to have an equal effect on milk protein synthetic rates (34–55% variation explained). Fitting individual sensitivity exponents to the literature data set resulted in an improvement in milk protein yield predictions, as measured by the log-likelihood function, percentage of variation explained, mean bias and residual variation. The relative values for the sensitivity exponents suggest that milk protein synthesis is most responsive to Lys, TP and Thr, with less sensitivity to His and Met. Similar ordering was observed when the affinity constants were fitted. The exponents were definable using the literature data set. However, values for the apparent affinity constants had to be assumed. Unique descriptions of both the affinity constants and the exponents would probably require observations of intracellular concentrations, arterial concentrations, venous concentrations and milk protein yields for each of the considered EAA. Additionally, these measurements would have to be made on animals where considerable independent variation in arterial concentrations has been introduced through infusion of a single EAA or some comparable method.

After the exponents for equation 4 were fitted to the literature data, the model appeared to explain less variation in the C6 data set, as defined by percentage of variation explained and residual variation. However, the cause of the low value for percentage of varation explained was due to a mean bias. As there was no evidence of a systematic error, representation of milk protein synthesis with a modified Michaelis–Menten equation appeared to have merit, although the rate parameters required to simulate C6 without bias would be different from those for the literature data set. The cause of this cannot be determined, although genetics and interlaboratory variation in methods are two of the potential reasons for this difference.

Correlations among venous concentration residual errors and milk protein residual errors (see Table 10.4) suggest that additional benefit could be realized if removal of Lys, Met and Thr were more accurately predicted. Correlations

among observed acetate and glycerol removal and milk protein residuals suggest that the energy status of the udder is important in determining the rate of milk protein synthesis. Such a relationship has been observed at the whole-animal level (Hanigan *et al.*, 1998a). Leucine was not considered one of the primary driving EAA. However, the observed correlation among leucine removal and milk protein residual errors suggests that it should be added to the model as a driver. The remaining correlations probably reflect the need to reparameterize the model after correction of the cited deficiencies. These changes could be expected to explain approximately half of the 40% variation unexplained by the model (see Table 10.4) and may result in a reduction in residual variation associated with C6 simulations. The remaining 20% is probably associated with genetic variation among cows, differences among laboratories, other animal-related factors, such as endocrine status, and measurement error. Although the changes undertaken herein and those proposed appear to have merit, a rigorous statistical evaluation of the changes adopted needs to be undertaken to determine whether the apparent improvement associated with the additions is indeed significant, relative to the expected improvement when random additional parameters are added.

In summary, utilization of a Michaelis–Menten equation form with exponents to adjust sensitivity to individual substrates appears to have merit relative to consideration of a single limiting AA. Sensitivity exponents were fitted to a data set and a unique solution was found when the apparent affinity constants were set to assumed values. Derivation of both the apparent affinity constants and the sensitivity coefficients will probably require more comprehensive data. Consideration of leucine as a driving EAA and acetate removal or possibly the energy status of the udder, ATP being a substrate for protein synthesis, would appear to explain a portion of the unresolved variation in milk protein yield predictions.

References

Austin, C.L., Schingoethe, D.J., Casper, D.P. and Cleale, R.M. (1991) Influence of bovine somatotropin and nutrition on production and composition of milk from dairy cows. *Journal of Dairy Science* 74, 3920–3932.

Baldwin, R.L. and Hanigan, M.D. (1995) Dynamic models of ruminant mammary metabolism. In: Baldwin, R.L. (ed.) *Modeling Ruminant Digestion and Metabolism*. Chapman & Hall, New York, pp. 370–412.

Bequette, B.J., Hanigan, M.D., Calder, A.G., Reynolds, C.K., Lobley, G.E. and MacRae, J.C. (2000) Kinetics of amino acid exchange by the mammary gland of lactating goats when histidine limits milk production. *Journal of Dairy Science* 83, 765–775.

Bickerstaffe, R. and Annison, E.F. (1974) The metabolism of glucose, acetate, lipids and amino acids in lactating dairy cows. *Journal of Agricultural Science* 82, 71–85.

Cant, J.P., DePeters, E.J. and Baldwin, R.L. (1993a) Mammary amino acid utilization in dairy cows fed fat and its relationship to milk protein depression. *Journal of Dairy Science* 76, 762–774.

Cant, J.P., DePeters, E.J. and Baldwin, R.L. (1993b) Mammary uptake of energy metabolites in dairy cows fed fat and its relationship to milk protein depression. *Journal of Dairy Science* 76, 2254–2265.

Casper, D.P., Schingoethe, D.J., Yang, C.M. and Mueller, C.R. (1987) Protected methionine supplementation with extruded blend of soybeans and soybean meal for dairy cows. *Journal of Dairy Science* 70, 321–330.

Choung, J.J. and Chamberlain, D.G. (1993) The effects of abomasal infusions of casein or soya-bean-protein isolate on the milk production of dairy cows in mid-lactation. *British Journal of Nutrition* 69, 103–115.

Clark, J.H. (1975) Lactational responses to postruminal administration of proteins and amino acids. *Journal of Dairy Science* 58, 1178–1197.

Clark, J.H., Spires, H.R., Derig, R.G. and Bennink, M.R. (1977) Milk production, nitrogen utilization and glucose synthesis in lactating cows infused postruminally with sodium caseinate and glucose. *Journal of Nutrition* 107, 631–644.

Clark, R.M., Chandler, P.T. and Park, C.S. (1978) Limiting amino acids for milk protein synthesis by bovine mammary cells in culture. *Journal of Dairy Science* 61, 408–413.

Derrig, R.G., Clark, J.H. and Davis, C.L. (1974) Effect of abomasal infusion of sodium caseinate on milk yield, nitrogen utilization and amino acid nutrition of the dairy cow. *Journal of Nutrition* 104, 151–159.

Drackley, J.K. and Schingoethe, D.J. (1986) Extruded blend of soybean meal and sunflower seeds for dairy cattle in early lactation. *Journal of Dairy Science* 69, 371–384.

Fisher, L.J. (1972) Response of lactating cows to the intravenous infusion of amino acids. *Canadian Journal of Animal Science* 52, 377–384.

Fraser, D.L., Orskov, E.R., Whitelaw, F.G. and Franklin, M.F. (1991) Limiting amino acids in dairy cows given casein as the sole source of protein. *Livestock Production Science* 28, 235–252.

Griinari, J.M., McGuire, M.A., Dwyer, D.A., Bauman, D.E. and Palmquist, D.L. (1997a) Role of insulin in the regulation of milk fat synthesis in dairy cows. *Journal of Dairy Science* 80, 1076–1084.

Griinari, J.M., Mcguire, M.A., Dwyer, D.A., Bauman, D.E., Barbano, D.M. and House, W.A. (1997b) The role of insulin in the regulation of milk protein synthesis in dairy cows. *Journal of Dairy Science* 80, 2361–2371.

Guinard, J. and Rulquin, H. (1994a) Effect of graded levels of duodenal infusions of casein on mammary uptake in lactating cows. 2. Individual amino acids. *Journal of Dairy Science* 77, 3304–3315.

Guinard, J. and Rulquin, H. (1994b) Effects of graded amounts of duodenal infusions of lysine on the mammary uptake of major milk precursors in dairy cows. *Journal of Dairy Science* 77, 3565–3576.

Guinard, J. and Rulquin, H. (1995) Effects of graded amounts of duodenal infusions of methionine on the mammary uptake of major milk precursors in dairy cows. *Journal of Dairy Science* 78, 2196–2207.

Guinard, J., Rulquin, H. and Verite, R. (1994) Effect of graded levels of duodenal infusions of casein on mammary uptake in lactating cows. 1. Major nutrients. *Journal of Dairy Science* 77, 2221–2231.

Hanigan, M.D., Calvert, C.C., DePeters, E.J., Reis, B.L. and Baldwin, R.L. (1992) Kinetics of amino acid extraction by lactating mammary glands in control and sometribove-treated Holstein cows. *Journal of Dairy Science* 75, 161–173.

Hanigan, M.D., Cant, J.P., Weakley, D.C. and Beckett, J.L. (1998a) An evaluation of postabsorptive protein and amino acid metabolism in the lactating dairy cow. *Journal of Dairy Science* 81, 3385–3401.

Hanigan, M.D., France, J., Wray-Cahen, D., Beever, D.E., Lobley, G.E., Reutzel, L. and Smith, N.E. (1998b) Alternative models for analyses of liver and mammary trans-organ metabolite extraction data. *British Journal of Nutrition* 79, 63–78.

Hanigan, M.D., Metcalf, J.A., Crompton, L.A. and France, J. (2000a) Modelling mammary amino acid metabolism in the lactating cow. 1. Model construction and parameterization. *Journal of Theoretical Biology* (submitted).

Hanigan, M.D., France, J., Crompton, L.A., Beever, D.E. and Bequette, B.J. (2000b) Modelling mammary amino acid metabolism in the lactating cow. 2. Pattern and sensitivity analyses and an independent challenge. *Journal of Theoretical Biology* (submitted).

Illg, D.J., Sommerfeldt, J.L. and Schingoethe, D.J. (1987) Lactational and systemic responses to the supplementation of protected methionine in soybean meal diets. *Journal of Dairy Science* 70, 620–629.

Karunanandaa, K., Goodling, L.E., Varga, G.A., Muller, L.D., McNeill, W.W., Cassidy, T.W. and Lykos, T. (1994) Supplemental dietary fat and ruminally protected amino acids for lactating Jersey cows. *Journal of Dairy Science* 77, 3417–3425.

Lykos, T. and Varga, G.A. (1997) Varying degradation rates of total nonstructural carbohydrates: effects on nutrient uptake and utilization by the mammary gland in high producing Holstein cows. *Journal of Dairy Science* 80, 3356–3367.

Lykos, T., Varga, G.A. and Casper, D. (1997) Varying degradation rates of total nonstructural carbohydrates: effects on ruminal fermentation, blood metabolites, and milk production and composition in high producing Holstein cows. *Journal of Dairy Science* 80, 3341–3355.

McGown, E., Richardson, A.G., Henderson, L.M. and Swan, P.B. (1973) Effect of amino acids on ribosome aggregation and protein synthesis in perfused rat liver. *Journal of Nutrition* 103, 109–116.

Metcalf, J.A., Beever, D.E., Sutton, J.D., Wray-Cahen, D., Evans, R.T., Humphries, D.J., Backwell, F.R.C., Bequette, B.J. and Macrae, J.C. (1994) The effect of supplementary protein on *in vivo* metabolism of the mammary gland in lactating dairy cows. *Journal of Dairy Science* 77, 1816–1827.

Metcalf, J.A., Wray-Cahen, D., Chettle, E.E., Sutton, J.D., Beever, D.E., Crompton, L.A., MacRae, J.C., Bequette, B.J. and Backwell, F.R.C. (1996) The effect of dietary crude protein as protected soybean meal on mammary metabolism in the lactating dairy cow. *Journal of Dairy Science* 79, 603–611.

Miller, P.S., Reis, B.L., Calvert, C.C., DePeters, E.J. and Baldwin, R.L. (1991) Relationship of early lactation and bovine somatotropin on nutrient uptake by cow mammary glands. *Journal of Dairy Science* 74, 3800–3806.

Peeters, G., Houvenaghel, A., Roets, E., Massart-Leën, A.M., Verbeke, R., Dhondt, G. and Verschooten, F. (1979) Electromagnetic blood flow recording and balance of nutrients in the udder of lactating cows. *Journal of Animal Science* 48, 1143–1153 .

Perez-Sala, D., Calleja, T.R., Parrilla, R. and Ayuso, M.S. (1991) Effect of alanine supply on hepatic protein synthesis in animals maintained on a protein free diet. *Molecular Cell Biochemistry* 108, 105–112.

Rulquin, H. (1981) Etude méthodologique sur la mesure des différences artério-veineuses mammaires chez la vache laitière. *Reproduction Nutrition Développement* 21, 31–46.

SAS (1994) *SAS/STAT® User's Guide, Version 6*, 4th edn. SAS Institute, Inc., Cary, North Carolina.

Schwab, C.G., Satter, L.D. and Clay, A.B. (1976) Response of lactating dairy cows to abomasal infusion of amino acids. *Journal of Dairy Science* 59, 1254–1270.

Schwab, C.G., Bozak, C.K. and Whitehouse, N.L. (1992a) Amino acid limitation and flow to duodenum at four stages of lactation. 1. Sequence of lysine and methionine limitation. *Journal of Dairy Science* 75, 3486–3502.

Schwab, C.G., Bozak, C.K., Whitehouse, N.L. and Olson, V.M. (1992b) Amino acid limitation and flow to the duodenum at four stages of lactation. 2. Extent of lysine limitation. *Journal of Dairy Science* 75, 3503–3508.

Shenoy, S. and Rogers, Q.R. (1977) Effect of starvation on the charging levels of transfer ribonucleic acid and total acceptor capacity in rat liver. *Biochimica et Biophysica Acta* 476, 218–227.

Shenoy, S. and Rogers, Q.R. (1978) Effect of dietary amino acids on transfer ribonucleic acid charging levels in rat liver. *Journal of Nutrition* 108, 1412–1421.

Spires, H.R., Clark, J.H., Derrig, R.G. and Davis, C.L. (1975) Milk production and nitrogen utilization in response to postruminal infusion of sodium caseinate in lactating cows. *Journal of Nutrition* 105, 1111–1121.

Yang, C.-M.J., Schingoethe, D.J. and Casper, D.P. (1986) Protected methionine and heat-treated soybean meal for high producting dairy cows. *Journal of Dairy Science* 69, 2348–2357.

Yokogoshi, H. and Yoshida, A. (1980) Effects of supplementation and depletion of a single essential amino acid on hepatic polyribosome profile in rats. *Journal of Nutrition* 110, 375–382.

11

Multiple-entry Urea Kinetic Model: Effects of Incomplete Data Collection

G. Zuur,[1] K. Russell[2] and G.E. Lobley[3]

[1]*Biomathematics and Statistics Scotland, Rowett Research Institute, Bucksburn, Aberdeen AB21 9SB, UK;* [2]*Waltham Centre for Pet Nutrition, Freeby Lane, Waltham on the Wolds, Melton Mowbray, Leicestershire LE14 4RT, UK;* [3]*Rowett Research Institute, Bucksburn, Aberdeen AB21 9SB, UK*

Abstract

The consequences of incomplete urine collection on whole-body urea kinetics have been investigated. Information on the fates of urea can be obtained from the addition of double-labelled urea to the body urea pool, either as a single dose or by continuous infusion. In both cases it is assumed that labelled urea can re-enter the gastrointestinal tract (GIT) on multiple occasions. Analyses of ^{15}N in urine and faeces allow the amount of urea-N utilized for anabolism (UUA) to be determined.

For such an approach to be valid, it is important that the collection period is sufficiently long (single-dose experiment) or that samples are taken at an isotopic steady state (continuous infusion). Otherwise, ^{15}N collected from urine and faeces will be incomplete, and hence the urea-N available for UUA will be overestimated. A similar problem occurs with incomplete recovery of urine or faeces. We investigated the effects of incomplete or inappropriate urine or faeces collection (or analytical errors which simulate collection errors) on the estimated fates of urea-N, using the following error types: (i) incomplete collection of urine; (ii) incomplete collection of faeces; and (iii) inappropriate collection period. Mathematical derivations show that such errors result in overestimation of UUA. To investigate the practical importance of such errors, these error types were applied to a single-dose urea kinetic experiment in humans and a continuous infusion study in sheep. The human (non-ruminant) study had low proportions of both urea production that entered the GIT and a low proportion of this entry that returned to the ornithine cycle, when compared with the sheep (ruminant) study (0.23 and 0.28 vs. 0.61 and 0.51, respectively). The application showed that errors on urine collection have a bigger impact on UUA than poor collection of faeces. Also, the effect of urine collection errors on UUA was larger

 Modelling Nutrient Utilization in Farm Animals (eds J.P. McNamara, J. France and D.E. Beever)

for the human compared with the sheep study. Return of ^{15}N into the body urea pool from protein turnover probably contributes an error of 2% or less.

Introduction

The ability to recycle urea to the digestive tract and use a proportion of this to support microbial amino acid synthesis that can be utilized by the host forms an important component of the N economy of animals. This has particular relevance to the ruminant (Sarraseca *et al.*, 1998), but may also play a beneficial role in non-ruminants, including humans (Jackson *et al.*, 1984, 1993; Jackson, 1998). Quantification of the anabolic use of urea-N is difficult but recent extensions of a simple stable-isotope approach have allowed this to be estimated indirectly. Urea with both N labelled ($^{15}N^{15}N$-urea) is added to the body urea pool and the appearance of $^{15}N^{15}N$-urea and $^{14}N^{15}N$-urea in urine allows the amount returned to the ornithine cycle to be calculated. By difference, the quantity used for anabolic purposes is estimated.

The $^{15}N^{15}N$-urea can be administered as a single dose or as a continuous infusion. With the single-dose technique, it is important to collect all ^{15}N appearing in urine and faeces. This means that the collection period should be sufficiently long and that no labelled material should be lost. When continuous infusion is used, it is important to collect ^{15}N in urine and faeces at an isotopic steady state. However, with a 'bad' sample, this can be discarded and replaced by an extra collection without penalty. For both experimental techniques, it is necessary to have good estimates of total urinary urea-N and faecal N production.

In this chapter, we examine the consequences of loss of labelled material due to improper collection. The following types of error are investigated: (i) a fixed proportion (< 100%) of urine is collected; (ii) a fixed proportion (< 100%) of faeces is collected; and (iii) the collection period is inappropriate.

First, a theoretical study was performed to investigate the effect of such errors on the estimated urea-N flows. Second, the practical importance of these error types was examined, using data from experiments on urea kinetics from humans and sheep. Both the theoretical study and the practical study are based on the urea kinetic model described in Lobley *et al.* (2000), which allows for multiple entries of labelled urea-N into the gut.

Model

Urea is mainly produced in the liver (urea-N entry rate (UER)). It is assumed that there are only two fates for the synthesized urea, namely a proportion u is excreted in urine (urinary urea-N elimination (UUE)) and the remainder enters the gastrointestinal tract (GIT) (GIT entry rate (GER)). Here the urea is hydro-

lysed to ammonia, which can undergo three fates: (i) a proportion r is returned to the ornithine cycle (ROC); (ii) a proportion f is excreted in faeces (urea-N to faecal excretion (UFE)); and (iii) the remaining proportion a ($= 1 - r - f$) is assumed to be used for anabolic purposes (urea-N utilized for anabolism (UUA)) through microbial protein synthesis (Fig. 11.1).

Model for urea-N

The urea-N pool is modelled as:

$$UER = UUE + GER$$

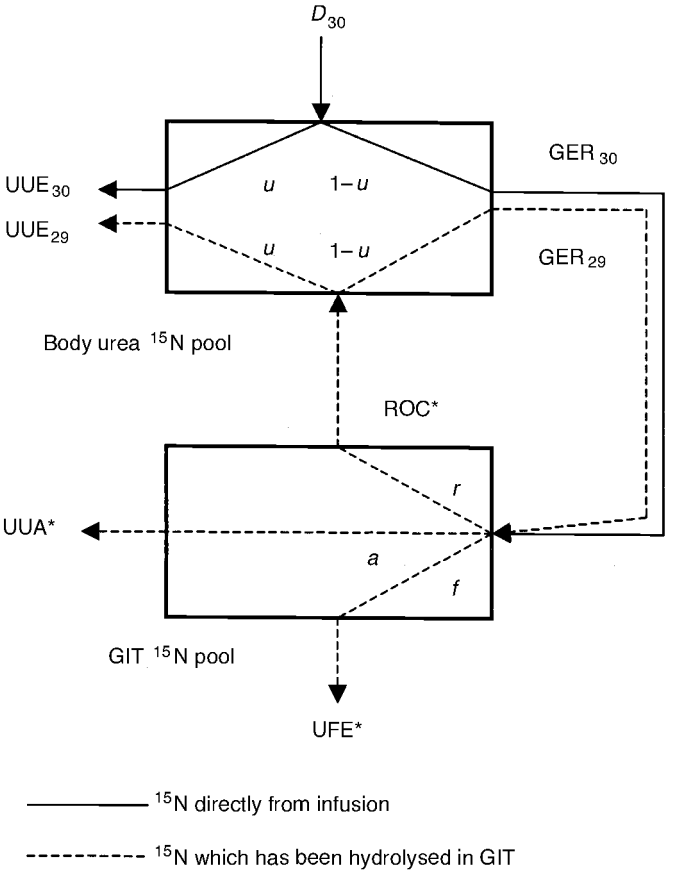

Fig. 11.1. Schematic layout of ^{15}N flows based on multiple-entry model. For explanation of terms, see description of model in text.

where:

$$\mathrm{UUE} = u\,\mathrm{UER} \tag{1}$$

$$\mathrm{GER} = (1 - u)\,\mathrm{UER} \tag{2}$$

For the GIT-N pool derived from urea-N, we have:

$$\mathrm{GER} = \mathrm{ROC} + \mathrm{UFE} + \mathrm{UUA}$$

$$\mathrm{ROC} = r\,\mathrm{GER}$$

$$\mathrm{UFE} = f\,\mathrm{GER} \tag{3}$$

$$\mathrm{UUA} = a\,\mathrm{GER}$$

$$r + f + a = 1$$

UER, UUE, GER, ROC, UFE and UUA are flows (mass/time), whereas the proportions u, r, f and a are dimensionless.

Model for ^{15}N

Administration of $^{15}N^{15}N$-urea to the urea pool, either as a single dose or as a continuous infusion, enables separation of the various fates of urea-N. The $^{15}N^{15}N$-urea entering the GIT is hydrolysed to labelled ammonia, part of which is returned (recycled) to the ornithine cycle. The probability of two ^{15}N atoms recombining to urea is regarded as negligible, so $^{14}N^{15}N$-urea is the product. Monitoring the appearances of $^{14}N^{15}N$- and $^{15}N^{15}N$-urea in blood or urine provides information on the amount of recycling occurring. Let D_{30} be the amount of ^{15}N, in the form of $^{15}N^{15}N$-urea, added to the urea pool. It is assumed that no $^{14}N^{15}N$-urea is added.

Assuming that isotopic inflows are equal to isotopic outflows, the ^{15}N flows to and from the body urea pool are given by:

$$D_{30} = \mathrm{UUE}_{30} + \mathrm{GER}_{30}$$

$$\mathrm{ROC}^{*} = \mathrm{UUE}_{29} + \mathrm{GER}_{29}$$

where the subscripts 29 and 30 refer to ^{15}N from $^{14}N^{15}N$- and $^{15}N^{15}N$-urea, respectively, and the asterisk * refers to ^{15}N. Assuming that labelled and unlabelled urea-N are treated identically in the body, we have (see also Fig. 11.1):

$$\mathrm{UUE}_{30} = u\,D_{30} \tag{4}$$

$$\mathrm{GER}_{30} = (1 - u)\,D_{30} \tag{5}$$

and:

$$\mathrm{UUE}_{29} = u\,\mathrm{ROC}^{*} \tag{6}$$

$$GER_{29} = (1 - u)\, ROC^{*} \tag{7}$$

Writing:

$$GER^{*} = GER_{29} + GER_{30} \tag{8}$$

the ^{15}N flows to and from the GIT are given by:

$$GER^{*} = ROC^{*} + UFE^{*} + UUA^{*}$$

Furthermore:

$$ROC^{*} = r\, GER^{*} \tag{9}$$

$$UFE^{*} = f\, GER^{*} \tag{10}$$

$$UUA^{*} = a\, GER^{*}$$

Note how equations 4–7 reflect that $^{14}N^{15}N$-urea appearing in the body urea pool from the ornithine cycle partitions similarly to the $^{15}N^{15}N$-urea from the dose. This means that for both newly produced $^{15}N^{15}N$- and recycled $^{14}N^{15}N$-urea a proportion $1 - u$ enters the GIT. This allows for multiple entries to, and returns from, the GIT, as the recycled $^{14}N^{15}N$-urea entering the GIT may again return to the urea pool via the ornithine cycle. This 'multiple-entry' model (Lobley *et al.*, 2000) differs from the single-entry model developed by Jackson *et al.* (1984, 1993), where all labelled urea returned to the body urea pool is assumed to be eliminated in urine and cannot re-enter the GIT. The single-entry model has equations 6 and 7 modified into $UUE_{29} = ROC^{*}$ and $GER_{29} = 0$, respectively.

Given measurements for D_{30}, UUE, UUE_{29}, UUE_{30} and UFE^{*}, all other quantities can be calculated.

Error types

Let UUE^{i} denote the amount of urinary urea-N from incomplete collection (indicated by superscript i). This is assumed to be a proportion p of the true amount, UUE:

$$p = UUE^{i}/UUE \tag{11}$$

By analogy, let:

$$p_{30} = UUE_{30^{i}}/UUE_{30} \tag{12}$$

$$p_{29} = UUE_{29^{i}}/UUE_{29} \tag{13}$$

$$p_{f} = UFE^{*i}/UFE^{*} \tag{14}$$

The error types for incomplete urine collection are formalized as follows.

Error A

A fixed proportion (< 100%) of urine is collected. It is assumed that this affects both labelled and unlabelled urea-N to the same extent:

$$p_{29} = p_{30} = p < 1$$

Furthermore, it is assumed that all faecal ^{15}N is collected:

$$p_f = 1$$

Error B

A fixed proportion (< 100%) of faecal ^{15}N is collected but with urine collection unaffected:

$$p_f < 1$$

$$p_{29} = p_{30} = p = 1$$

Error C

The collection period is inappropriate. Either the data collection period is too short (single-dose experiment) or data collection takes place before an isotopic steady state has been attained (continuous infusion). It is assumed that UUE is not affected, so that:

$$p = 1$$

As production of UUE_{29} involves the ornithine cycle, appearance will be delayed with respect to UUE_{30}. We assume, therefore, that the proportion collected is smaller for UUE_{29}:

$$p_{29} < p_{30} < 1$$

For this scenario, the collection of ^{15}N in faeces is probably also low; thus:

$$p_f \leqslant p_{29}$$

Comparison of the effects of errors A and B allows the relative importance of urine and faeces collection to be assessed, whereas error C highlights the effects of an inappropriate collection period.

Data

For the application, the error types chosen were as indicated in Table 11.1. For error A, four values for the proportion of total urine collected were considered, ranging from 80 to 99.9% (errors A1–A4). For error B, it is assumed that 0–99% of faecal ^{15}N is collected (errors B1–B4). This error type allows the importance of faecal ^{15}N collection to be assessed, even to the extent of not col-

Table 11.1. Proportions of urine and faeces collected for application. Proportions of UUE (p), UUE_{30} (p_{30}), UUE_{29} (p_{29}) and UFE^* (p_f) collected for errors A1–C4 are shown.

Error type	p	p_{30}	p_{29}	p_f
A1	0.8	0.8	0.8	1
A2	0.9	0.9	0.9	1
A3	0.95	0.95	0.95	1
A4	0.999	0.999	0.999	1
B1	1	1	1	0
B2	1	1	1	0.5
B3	1	1	1	0.75
B4	1	1	1	0.99
C1	1	0.9	0.7	0.5
C2	1	0.99	0.93	0.75
C3	1	0.999	0.98	0.89
C4	1	0.9999	0.999	0.99

lecting faeces. For error C, the daily proportions of $^{15}N^{15}N$- and $^{14}N^{15}N$-urea collected in urine and ^{15}N in faeces over a 5-day single-dose urea kinetic study on cats (Waltham Centre for Pet Nutrition, Melton Mowbray, UK) were used. The proportions collected over 1, 2, 3 and 4 days represent errors C1–C4, respectively.

Error types A1–C4 were applied to two data sets. The first is taken from Jackson *et al.* (1993), based on a single dose of labelled urea in six humans on a maintenance diet. Urinary urea-N was collected for 2 days. The second data set is from a continuous-infusion study in four sheep on a maintenance diet of grass pellets (Lobley *et al.*, 2000). Isotopic steady state was reached after 2 days, with urine and faeces collected and analysed over days 3 and 4. Two corrections were applied to the human data. First, UUE_{29} was corrected for $^{14}N^{15}N$ in the dose (Lobley *et al.*, 2000). Second, as no data on faecal ^{15}N were published for this study, a derived value for UFE^* was used, based on $f = 0.021$ (from a single human on a maintenance diet (P. Faber, personal communication)). The mean values of UUE, UUE_{30}, UUE_{29}, UFE^* and D_{30} for these two experiments are given in Table 11.2, together with the calculated flows and proportions.

Results

Mathematical derivations are first presented, followed by results from application to the human and sheep data.

Table 11.2. Measurements of UUE_{30}, UUE_{29}, UFE^*, UUE and D_{30} (in μmol N kg^{-1} day^{-1}). Human data based on Jackson *et al.* (1993), corrected for $^{14}N^{15}N$-urea in dose and to include faecal ^{15}N. Average values of six subjects. Sheep data taken from Lobley *et al.* (2000), average values of four sheep. The proportions and flows (μmol N kg^{-1} day^{-1}) are also shown for both data sets, based on the multiple-entry model.

Data set	UUE	D_{30}	UUE_{30}	UUE_{29}	UFE^*	u	r	f	a	UER	GER	ROC	UFE	UUA
Humans	11,380	22.1	17.1	1.15	0.112	0.77	0.28	0.02	0.70	14,707	3,327	925	70	2,333
Sheep	9,320	32.2	12.7	5.71	0.937	0.39	0.51	0.03	0.45	23,630	14,310	7,329	474	6,507

Mathematical derivations

Let u^i be based on data from incomplete collection of urine and faeces; $u^i = \mathrm{UUE}^i_{30}/D_{30}$. Then:

$$\frac{u^i}{u} = \frac{\mathrm{UUE}^i_{30}/D_{30}}{\mathrm{UUE}_{30}/D_{30}} = \frac{\mathrm{UUE}^i_{30}}{\mathrm{UUE}_{30}} = p_{30}$$

where the latter is obtained from equation 12. As $p_{30} < 1$ for error types A and C, $u^i/u < 1$. In other words, $u^i < u$ and the true proportion u is underestimated by a factor p_{30}. Error type B does not affect the calculation of u. From equations 11 and 12, we find the following for $\mathrm{UER}^i/\mathrm{UER}$:

$$\frac{\mathrm{UER}^i}{\mathrm{UER}} = \frac{\mathrm{UUE}^i \dfrac{D_{30}}{\mathrm{UUE}^i_{30}}}{\mathrm{UUE}\dfrac{D_{30}}{\mathrm{UUE}_{30}}} = \frac{\mathrm{UUE}^i}{\mathrm{UUE}}\frac{UUE_{30}}{\mathrm{UUE}^i_{30}} = \frac{p}{p_{30}}$$

For errors A and B, $p = p_{30}$, thus $\mathrm{UER}^i = \mathrm{UER}$, whereas for error C, $p > p_{30}$, hence $\mathrm{UER}^i/\mathrm{UER} > 1$, so UER^i gives an overestimate of UER.

Derivations for the remaining flows and proportions are given in the Appendix. The results are summarized in Table 11.3. As the three error scenarios lead to an underestimate of the amount of urea-N eliminated by the body, the urea-N retained for anabolism is overestimated. For error B, the proportion of urea-N gut entry that is eliminated in faeces (f) is underestimated and hence a is overestimated. As GER is not affected, UUA is also overestimated. Errors A and C result in underestimation of u, and hence overestimation of GER. Thus, both a and UUA are overestimated.

Results from application

Results for UUA from application of errors A1–C4 to the human and sheep data sets are shown in Fig. 11.2. For error A, the effects on UUA are more severe for the human data (e.g. 95% collection of urine leads to an overestimation of UUA

Table 11.3. Effect of data collection errors A–C on estimated flows and proportions, based on mathematical derivations (overestimation, ↑; underestimation, ↓; not affected, =; not clear, ?).

	u	r	f	a	UER	GER	ROC	UFE	UUA
Error A	↓	↓	↓	↑	=	↑	=	=	↑
Error B	=	=	↓	↑	=	=	=	↓	↑
Error C	↓	↓	↓	↑	↑	↑	?	↓	↑

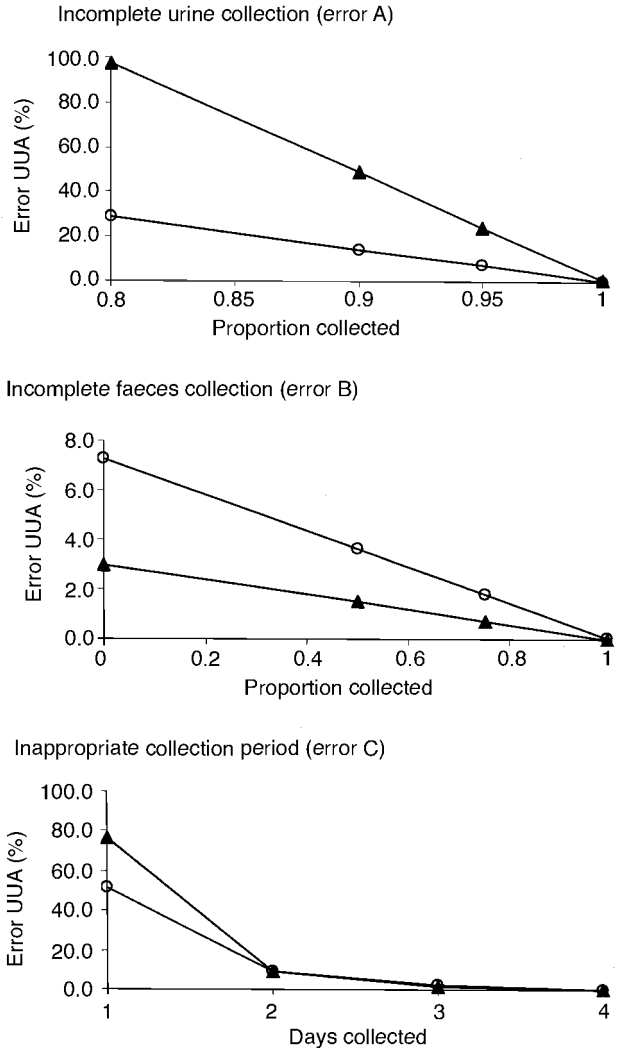

Fig.11.2. Effect of errors A1–C4 on UUA (humans, ▲–▲; sheep, ○–○).

of 7% and 24%, respectively, for the sheep and human data). Contrary to error A, the effects of error B on UUA are bigger for the sheep data, although even if no faeces are collected the error on UUA is still less than 8%. Furthermore, if collections are of insufficient length, e.g. days 1–3 or days 1–4 (C3, C4) rather than days 1–5, the error on UUA is small – less than 3%. Even if collection is only for days 1–2 (C2), the error only increases to 9%. For such errors, the effects on UUA are similar for the sheep and human data sets, whereas for C1 the effect becomes larger for the human data.

Table 11.4 shows the effects on all estimated flows. For error A and C, GER is overestimated, where the error is up to five times greater for the human data compared with the sheep data. For error C, underestimation of ROC is about twice as big for the human data.

Summary of results

Findings from mathematical derivations and practical studies can be summarized as follows.

- Incomplete collection of ^{15}N in urine or faeces results in overestimation of the amount of urea-N utilized for anabolic purposes (UUA).
- The effects of incomplete urine collection (error A) and inappropriate collection period (error C) on UUA are more severe for the human (non-ruminant) data than for the sheep (ruminant) data. In contrast, incomplete faeces collection (error B) has a bigger impact on the sheep data.
- The consequences of incomplete collection of ^{15}N in faeces (error B) are much smaller than for incomplete collection of ^{15}N in urine (error A).

Discussion

Why is the effect of incomplete collection of faeces on UUA much smaller than for urine? The amount of ^{15}N available for anabolic purposes is equal to the difference between ^{15}N in the dose and ^{15}N excreted in faeces and urine. For both the human and the sheep data, the proportion of total ^{15}N from the dose that is eliminated in urine is much greater than for faeces (82% vs. 0.5% for humans, 57% vs. 3% for sheep (see Table 11.2)). As a consequence, a 10% error on urine collection has a greater impact on the estimated amount of urea-N available for anabolism than a 10% error on faeces. It is therefore important that urine collection is complete and that the collection period is sufficiently long (single dose) or takes place at an isotopic steady state (continuous infusion). Use of collection markers (e.g. *p*-aminobenzoic acid) may allow for appropriate correction for incomplete urine recoveries.

Also, as relatively more of the dose is eliminated in faeces for sheep than for humans (3% vs. 0.5%), errors on faecal collection have a greater impact on estimation of UUA for sheep. These findings are mainly determined by the proportion $1-u$ of urea production entering the GIT; this is much higher for ruminants (0.23 and 0.61 for humans and sheep, respectively).

Although errors C1–C4 were based on incomplete collection of urine and faeces from a single-dose experiment, there is some resemblance with continuous infusion. For the sheep data, isotopic steady state was assumed for days 3 and 4, but, if data from only days 2 and 3 had been used, the collection error would have been similar to error C2. If data from days 1 and 2 had been used, the error would have been similar to C1.

Table 11.4. Percentage error on estimated flows, based on application of incomplete data collection (errors A1–C4) to human and sheep urea kinetics data (overestimation, +; underestimation, −; true zero, T).

	Humans					Sheep				
	UER	GER	ROC	UFE	UUA	UER	GER	ROC	UFE	UUA
A1	T	+68.4	T	T	+97.6	T	+13.0	T	T	+28.6
A2	T	+34.2	T	T	+48.8	T	+6.5	T	T	+14.3
A3	T	+17.1	T	T	+24.4	T	+3.3	T	T	+7.2
A4	T	+0.3	T	T	+0.5	T	+0.1	T	T	+0.1
B1	T	T	T	−100.0	+3.0	T	T	T	−100.0	+7.3
B2	T	T	T	−50.0	+1.5	T	T	T	−50.0	+3.6
B3	T	T	T	−25.0	+0.7	T	T	T	−25.0	+1.8
B4	T	T	T	−1.0	+0.0	T	T	T	−1.0	+0.1
C1	+11.1	+49.1	−12.4	−43.7	+76.3	+11.1	+18.3	−7.2	−40.3	+51.4
C2	+1.0	+4.5	−4.7	−24.0	+9.0	+1.0	+1.7	−3.3	−22.8	+9.0
C3	+0.1	+0.4	−1.7	−10.8	+1.6	+0.1	+0.2	−1.2	−10.4	+2.5
C4	+0.0	+0.0	−0.1	−1.0	+0.1	+0.0	+0.0	−0.1	−1.0	+0.2

The model presented in this chapter is based on the assumption that ^{15}N in the protein pool does not return to the body urea pool over the period of infusion. Any ^{15}N released from protein degradation that enters the body urea pool will be as $^{14}N^{15}N$-urea, and leads to an overestimation of urea-^{15}N as ROC. The magnitude of ^{15}N return from protein breakdown can be assessed based on the assumptions that the daily fractional rate of body protein breakdown varies from 0.02 to 0.1 and that 0.05–0.25 of this is oxidized. Assuming that all ^{15}N from amino acid oxidation is eliminated in urine as $^{14}N^{15}N$-urea, the errors on UUE_{29} caused by appearance of ^{15}N from protein breakdown vary from 0.25 to 5.7% (Fig. 11.3, based on sheep data from Table 11.2). For sheep, realistic values are probably a breakdown rate of 6% and oxidation rate of 15% (Harris *et al.*, 1992); these result in an error on UUE_{29} of 2.2%. These errors are of similar magnitude to technical or mechanical measurement errors on labelled urea-N in urine. Therefore, no significant information is lost by ignoring return of ^{15}N into the body urea pool from protein breakdown.

Acknowledgements

This research was funded by the Scottish Executive Rural Affairs Department. Thanks to P. Faber for access to human faecal data.

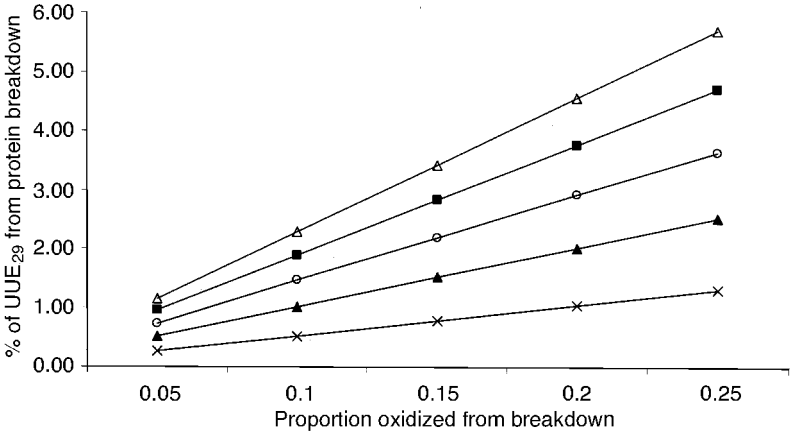

Fig.11.3. Percentage of UUE_{29} originating from protein breakdown, for various fractional protein breakdown rates (0.02, x–x; 0.04, ▲–▲; 0.06, ○–○; 0.08, ■–■; 0.10, △–△) and proportions oxidized.

Appendix

To investigate the effect of incomplete collection of urine and faeces, the unknown proportions (u, r, f and a) and flows (UER, GER, ROC, UFE and UUA) are expressed entirely in terms of the measured flows D_{30}, UUE_{30}, UUE_{29}, UFE^{*} and UUE. Simplified calculations of these unknown flows and proportions can be found in Lobley *et al.* (2000).
From equation 4:

$$u = \frac{\mathrm{UUE}_{30}}{D_{30}} \tag{A1}$$

From equation 1, UER = UUE/u, and substituting (A1) gives:

$$\mathrm{UER} = \mathrm{UUE}\frac{D_{30}}{\mathrm{UUE}_{30}} \tag{A2}$$

Rearranging equation 9, substituting equations 5, 7 and 8, and multiplying both numerator and denominator by u yields:

$$r = \frac{\mathrm{ROC}^{*}}{\mathrm{GER}^{*}} = \frac{\mathrm{ROC}^{*}}{(1-u)(\mathrm{ROC}^{*}+D_{30})} = \frac{u\,\mathrm{ROC}^{*}}{(1-u)(u\,\mathrm{ROC}^{*}+u\,D_{30})}$$

Substituting equations 4, 6 and A1 gives:

$$r = \frac{D_{30}}{D_{30}-\mathrm{UUE}_{30}}\frac{\mathrm{UUE}_{29}}{\mathrm{UUE}_{29}+\mathrm{UUE}_{30}} = \frac{D_{30}}{D_{30}-\mathrm{UUE}_{30}}\frac{1}{1+\dfrac{\mathrm{UUE}_{30}}{\mathrm{UUE}_{29}}} \tag{A3}$$

Then:

$$\frac{r^{i}}{r} = \frac{D_{30}-\mathrm{UUE}_{30}}{D_{30}-p_{30}\mathrm{UUE}_{30}}\frac{1+\dfrac{\mathrm{UUE}_{30}}{\mathrm{UUE}_{29}}}{1+\dfrac{p_{30}}{p_{29}}\dfrac{\mathrm{UUE}_{30}}{\mathrm{UUE}_{29}}} \tag{A4}$$

where p_{30} and p_{29} are defined in equations 12 and 13, respectively. Now $1 + p_{30}/p_{29}\,\mathrm{UUE}_{30}/\mathrm{UUE}_{29} > 1 + \mathrm{UUE}_{30}/\mathrm{UUE}_{29}$ (error C) and $D_{30} - p_{30}\,\mathrm{UUE}_{30} > D_{30} - \mathrm{UUE}_{30}$, so $r^{i}/r < 1$ for both A and C, whereas for B it is equal to unity.
Substituting equations A1 and A2 in equation 2 gives:

$$\mathrm{GER} = \frac{D_{30}-\mathrm{UUE}_{30}}{D_{30}}\frac{D_{30}}{\mathrm{UUE}_{30}}\mathrm{UUE} = \left(\frac{D_{30}}{\mathrm{UUE}_{30}}-1\right)\mathrm{UUE} \tag{A5}$$

Then:

$$\frac{\mathrm{GER}^i}{\mathrm{GER}} = p\frac{\dfrac{D_{30}}{p_{30}\mathrm{UUE}_{30}}}{\dfrac{D_{30}}{\mathrm{UUE}_{30}}-1} = \frac{\dfrac{p}{p_{30}}\dfrac{D_{30}}{\mathrm{UUE}_{30}}-p}{\dfrac{D_{30}}{\mathrm{UUE}_{30}}-1}$$

For A and C, the numerator exceeds the denominator. Hence $\mathrm{GER}^i/\mathrm{GER} > 1$ for A and C. For B, it equals unity.

Writing $\mathrm{ROC} = r\,\mathrm{GER}$ and substituting equations A3 and A5 gives:

$$\mathrm{ROC} = r\mathrm{GER} = \frac{D_{30}}{D_{30}-\mathrm{UUE}_{30}}\frac{1}{1+\dfrac{\mathrm{UUE}_{30}}{\mathrm{UUE}_{29}}}\frac{D_{30}-\mathrm{UUE}_{30}}{\mathrm{UUE}_{30}}\mathrm{UUE}$$

so that:

$$ROC = \frac{D_{30}}{\mathrm{UUE}_{30}}\frac{1}{1+\dfrac{\mathrm{UUE}_{30}}{\mathrm{UUE}_{29}}}\mathrm{UUE}$$

Then:

$$\frac{\mathrm{ROC}^i}{\mathrm{ROC}} = \frac{p}{p_{30}}\frac{1+\dfrac{\mathrm{UUE}_{30}}{\mathrm{UUE}_{29}}}{1+\dfrac{p_{30}}{p_{29}}\dfrac{\mathrm{UUE}_{30}}{\mathrm{UUE}_{29}}}$$

This equals unity for A and B. For C, the first ratio exceeds unity and the second ratio is less than unity, so the overall effect is not clear.

From equations 5, 7, 8 and 10 we have:

$$f = \frac{\mathrm{UFE}^*}{(1-u)(\mathrm{ROC}^*+D_{30})} = \frac{u}{1-u}\frac{\mathrm{UFE}^*}{\mathrm{UUE}_{29}+\mathrm{UUE}_{30}}$$

Substituting equation A1 and dividing numerator and denominator by UUE_{30} gives:

$$f = \frac{\mathrm{UFE}^*}{D_{30}-\mathrm{UUE}_{30}}\frac{1}{\dfrac{\mathrm{UUE}_{29}}{\mathrm{UUE}_{30}}+1} \tag{A6}$$

Then, using equation 14:

$$\frac{f^i}{f} = \frac{p_f \,\mathrm{UFE}^*}{D_{30} - p_{30}\mathrm{UUE}_{30}} \frac{1}{\dfrac{p_{29}}{p_{30}}\dfrac{\mathrm{UUE}_{29}}{\mathrm{UUE}_{30}} + 1} \frac{D_{30} - \mathrm{UUE}_{30}}{\mathrm{UFE}^*} \left(\frac{\mathrm{UUE}_{29}}{\mathrm{UUE}_{30}} + 1 \right)$$

which leads to:

$$\frac{f^i}{f} = \frac{D_{30} - \mathrm{UUE}_{30}}{D_{30} - p_{30}\mathrm{UUE}_{30}} \frac{\dfrac{\mathrm{UUE}_{29}}{\mathrm{UUE}_{30}} + 1}{\dfrac{p_{29}}{p_f\, p_{30}}\dfrac{\mathrm{UUE}_{29}}{\mathrm{UUE}_{30}} + \dfrac{1}{p_f}} \tag{A7}$$

This is less than unity for A and B. For C, $p_f \leqslant p_{29}$ so $p_{29}/p_f \geqslant 1$. Also, $1/p_{30} > 1$ and hence the denominators exceed the numerators so $f^i/f < 1$ for error C. Furthermore, equation A7 reduces to equation A4 for error structure A, so that for A the errors on r and f are the same.

From equations 3, A5 and A6:

$$\mathrm{UFE} = f\,\mathrm{GER} = \frac{\mathrm{UFE}^*}{D_{30} - \mathrm{UUE}_{30}} \frac{1}{\dfrac{\mathrm{UUE}_{29}}{\mathrm{UUE}_{30}} + 1} \frac{D_{30} - \mathrm{UUE}_{30}}{\mathrm{UUE}_{30}} \mathrm{UUE}$$

which leads to:

$$\mathrm{UFE} = \mathrm{UFE}^* \frac{\mathrm{UUE}}{\mathrm{UUE}_{29} + \mathrm{UUE}_{30}}$$

Then:

$$\frac{\mathrm{UFE}^i}{\mathrm{UFE}} = p_f \,\mathrm{UFE}^* \frac{p\mathrm{UUE}}{p_{29}\mathrm{UUE}_{29} + p_{30}\mathrm{UUE}_{30}} \frac{\mathrm{UUE}_{29} + \mathrm{UUE}_{30}}{\mathrm{UUE} \times \mathrm{UFE}^*}$$

which gives:

$$\frac{\mathrm{UFE}^i}{\mathrm{UFE}} = \frac{\mathrm{UUE}_{29} + \mathrm{UUE}_{30}}{\dfrac{p_{29}}{p_f\, p}\mathrm{UUE}_{29} + \dfrac{p_{30}}{p_f\, p}\mathrm{UUE}_{30}}$$

This equals unity for error A and is less than unity for error C ($p = 1$, $p_{29}/p_f \geqslant 1$ and $p_{30}/p_f > 1$, so the denominator exceeds the numerator). For B, $\mathrm{UFE}^i/\mathrm{UFE}$ reduces to p_f, so that $\mathrm{UFE}^i < \mathrm{UFE}$.

Also, $a = 1 - r - f$. Combined with $r^i \leqslant r$ and $f^i < f$, this gives $a^i/a > 1$. As $\mathrm{GER}^i \geqslant \mathrm{GER}$, $\mathrm{UUA}^i/\mathrm{UUA}$ also exceeds unity for all three errors.

References

Harris, P.M., Skene, P.A., Buchan, V., Milne, E., Calder, A.G., Anderson, S.E., Connell, A. and Lobley, G.E. (1992) Effect of food intake on hind-limb and whole-body protein metabolism in young growing sheep: chronic studies based on arterio-venous techniques. *British Journal of Nutrition* 68, 389–407.

Jackson, A.A. (1998) Salvage of urea-nitrogen in the large bowel: functional significance in metabolic control and adaptation. *Biochemical Society Transactions* 26, 231–236.

Jackson, A.A., Picou, D. and Landman, J.P. (1984) The non-invasive measurement of urea kinetics in normal man by a constant infusion of $^{15}N^{15}N$-urea. *Clinical Nutrition* 38C, 339–354.

Jackson, A.A., Danielsen, M.S. and Boyes, S. (1993) A non-invasive method for measuring urea kinetics with a single dose of $^{15}N^{15}N$-urea in free-living humans. *Journal of Nutrition* 123, 2129–2136.

Lobley, G.E., Bremner, D.M. and Zuur, G. (2000) Effects of diet quality on urea fates in sheep; assessed by refined, non-invasive [$^{15}N^{15}N$]urea kinetics. *British Journal of Nutrition* (in press).

Sarraseca, A., Milne, E., Metcalf, M.J. and Lobley, G.E. (1998) Urea recycling in sheep: effects of intake. *British Journal of Nutrition* 79, 79–88.

12

Evaluation of a Growth Model of Preruminant Calves and Modifications to Simulate Short-term Responses to Changes in Protein Intake

Walter J.J. Gerrits,[1] Peter L. van der Togt,[1] Jan Dijkstra[1] and James France[2]

[1]*Animal Nutrition Group, Wageningen Institute of Animal Sciences, PO Box 338, 6700 AH Wageningen, The Netherlands;* [2]*Department of Agriculture, University of Reading, Earley Gate, PO Box 236, Reading RG6 6AT, UK*

Abstract

Recently, a mechanistic simulation model was developed which integrates protein and energy metabolism of preruminant calves of 80 to 240 kg live-weight (LW). The model can be used to predict the rate of gain of weight, protein and fat from nutrient input. A serial slaughter experiment was conducted to obtain an independent data set for model evaluation purposes. The objective of the model evaluation exercise was to evaluate model predictions to different protein intakes in three LW ranges: 80–120 kg (three levels of protein intake), 120–160 kg (three levels of protein intake) and 160–240 kg LW (two levels of protein intake). In this experiment, 64 calves were used, of which 36 were slaughtered to determine chemical body composition. Four calves were slaughtered as a reference group at 80 kg LW and subsequently four per protein intake level at each of the pre-determined target weights. Model predictions were found satisfactory for live-weight gain and protein deposition, with root mean-square prediction errors (RMSPE) expressed as a percentage of the observed mean of below 7%. For fat deposition, the RMSPE was 18% (on average 26 g day^{-1}), of which 58% was due to a consistent underestimation. Closer examination of the experimental results from 80–120 kg LW revealed an adaptation of the calves to the sudden change in diets after the start of the experiment, still present at 120 kg LW and not predicted by the model. Modifications were made to the model, based on the hypotheses that (i) calves adapt their visceral protein mass quickly to a

 Modelling Nutrient Utilization in Farm Animals (eds J.P. McNamara, J. France and D.E. Beever)

new feeding level, and (ii) that the capacity of calves to make these corrections decreases with age or live-weight. The adapted model satisfactorily predicted short-term responses in live weight gain to sudden changes in protein intake but remains to be rigorously evaluated. The approach taken may also be valid for modelling short-term responses in intakes of other nutrients. It can, however, not be used when animals can adapt their rate of intake in an attempt to compensate for a nutrient deficiency (e.g. during qualitative feed restriction).

Introduction

Recently, a mechanistic simulation model was developed which integrates protein and energy metabolism of preruminant calves of 80 to 240 kg live-weight (LW) (Gerrits *et al.*, 1997a, b). The model can be used to predict the rate of gain of weight, protein and fat from nutrient input and was developed for designing feeding strategies for preruminant calves. In brief, this model simulates the partitioning of ingested nutrients through intermediary metabolism to growth. It contains ten state variables, comprising fatty acids, glucose, acetyl-coenzyme A (CoA) and amino acids as metabolite pools and fat, ash and protein in muscle, hide, bone and viscera as body constituent pools. Model parameters were estimated partly from literature and partly from experimental data (Gerrits *et al.*, 1996). The model simulates the growth of calves on a daily basis and is programmed in Advanced Continuous Simulation Language (ACSL) (Mitchell and Gauthier, 1981). At that time, comparison of model predictions with independent data was confined to limited published information. Therefore, an experiment was designed to generate independent data, and it was decided to specifically compare model predictions with: (i) the animal response to dietary protein intake at an average energy intake; and (ii) the changes in animal response to nutrients with body weight.

In this chapter, the comparison of model predictions with these experimental data will be discussed. Subsequently, adaptations to the model to improve model response to sudden changes in protein intake are presented and discussed.

An Experiment Designed to Evaluate Model Performance

Materials and methods

The objective of the model evaluation exercise was to evaluate model predictions to different protein intakes in three LW ranges: 80–120 kg (9, 12 or 15 g digestible protein kg $LW^{-0.75}$ day^{-1}), 120–160 kg (9, 12 or 15 g digestible protein kg $LW^{-0.75}$ day^{-1}) and 160–240 kg LW (7 or 12 g digestible protein kg $LW^{-0.75}$ day^{-1}). Throughout this chapter, treatments will be denoted by their

protein intake level, combined with their LW range. Calves on the 7 g protein treatment (160–240 kg LW) were fed the 12 g protein treatment until they reached 160 kg LW. In this experiment, 64 Holstein-Friesian × Dutch-Friesian crossbred male calves were used, of which 36 were slaughtered to determine chemical body composition (methods described by Gerrits *et al.*, 1996). For all calves, digestible energy intake from carbohydrate and fat (in a fixed proportion) was 0.7 MJ kg $LW^{-0.75}$ day^{-1}. Four calves were slaughtered as a reference group at 80 kg LW and subsequently four per protein intake level at each of the predetermined target weights (120, 160 and 240 kg LW) (van der Togt and Gerrits, 1998). Calves were weighed weekly. As an indicator for the error of predicted values relative to experimental values, the mean square prediction error (MSPE) was computed:

$$\text{MSPE} = \sum_{i=1}^{n} \left(O_i - P_i\right)^2 / n \qquad (1)$$

where O_i and P_i are the observed and predicted values, $i = 1, \ldots, n$; n = number of experimental observations (Bibby and Toutenburg, 1977). The root MSPE is a measure in the same units as the output and is expressed as a percentage of the observed mean. The MSPE was partitioned into overall bias, slope deviation and random (lack of linear correlation) variation components, according to the MSPE analysis proposed by Bibby and Toutenburg (1977).

Results

Comparison of experimental observations with model predictions

A comparison of the model predictions with the experimental observations is presented in Table 12.1. Model predictions were found satisfactory for LW gain and protein deposition, with a root MSPE of below 7%, the majority of which was unrelated to erroneous model predictions. For fat deposition, the root MSPE was 18%, of which 58% was due to a consistent underestimation of 26 g day^{-1}. In addition, the MSPE was 49% larger than the observed within-treatment variation. In contrast to the currently observed underpredictions, however, an earlier comparison of model predictions with the independent data of Meulenbroeks *et al.* (1986), obtained in respiration chambers, revealed an overprediction of 50 g fat day^{-1}, consistent at two feeding levels (see Gerrits *et al.*, 1997b). The difference then was attributed to a real difference between the respiration methodology (Meulenbroeks *et al.*, 1986) and the slaughter technique (Gerrits *et al.*, 1996), on which data the model was calibrated. It was not the technique *per se* that was blamed, but the possibility of increased maintenance requirements in the respiration units reducing the quantity of energy available for growth. The current underpredictions are probably the result of a similar error, i.e. an increased energy expenditure on non-growth processes in the

Table 12.1. Comparison between observed and predicted rates of gain of live-weight, empty body weight, nitrogen, fat, ash and water. Comparisons are made, pooling all observations over weight ranges (80–120, 80–160 and 160–240 kg) and treatments.

	Live-weight	Empty body weight	Nitrogen	Fat	Ash	Water
Number of animals	57	57	31	31	31	31
Predicted rate of gain, g day^{-1}	1219	1075	31.5	168	42.8	692
Observed rate of gain, g day^{-1}	1218	1101	31.8	194	47.2	651
Correlation coefficient, *r*	0.96	0.90	0.90	0.96	0.89	0.85
√MSPE,* %	2.9	6.1	6.0	17.6	13.0	32.1
Decomposition of √MSPE†						
Overall bias	0.00	0.15	0.03	0.58	0.52	0.45
Deviation slope from 1	0.03	0.16	0.21	0.18	0.39	0.02
Disturbance proportion	0.97	0.69	0.76	0.24	0.09	0.53
MSPE/MSE within treatments‡	0.23	0.72	0.54	1.49	0.72	1.32

*Mean square prediction error; see equation 1 in text.
† Decomposition of √MSPE into bias, deviation of the regression slope from 1 and the disturbance proportion (for explanation see text).
‡ MSPE, relative to the mean square error within treatments.

experiments of Gerrits *et al.* (1996), when compared with the current experiment. Gerrits *et al.* (1996) took extra measurements (i.e. quantitative collections of faeces and urine) from the animals. Unpublished calculations showed that harnessing calves for this purpose depresses growth rate during 14 days by an amount varying from 70 (at 120 kg LW) to 190 g day^{-1} (at 200 kg LW). The fat deposition rate is variable and fat is likely to be the first body component to be affected by environmental stress. Therefore, it is concluded that, while the underprediction of the fat deposition rate is slightly worrying, it does not necessarily result from erroneous assumptions in the model. Accurate predictions of fat deposition rates will therefore be difficult to accomplish.

Inadequate predictions of live-weight gain after sudden changes in feed intake

Closer examination of the experimental results revealed an adaptation of the calves to the sudden change in diets after the start of the experiment. During the pre-experimental period (up to 80 kg LW), the calves had been fed on a commercial feeding regime, slightly above the 12 g protein treatment. Both the measured and the predicted (i.e. simulated) response of LW gain to the dietary treatments in the course of time are given in Fig. 12.1. It shows the change in the rate of LW gain after a sudden decrease (the 9 and, to a lesser extent, the 12 g protein treatment) or increase (15 g protein treatment) in protein intake at

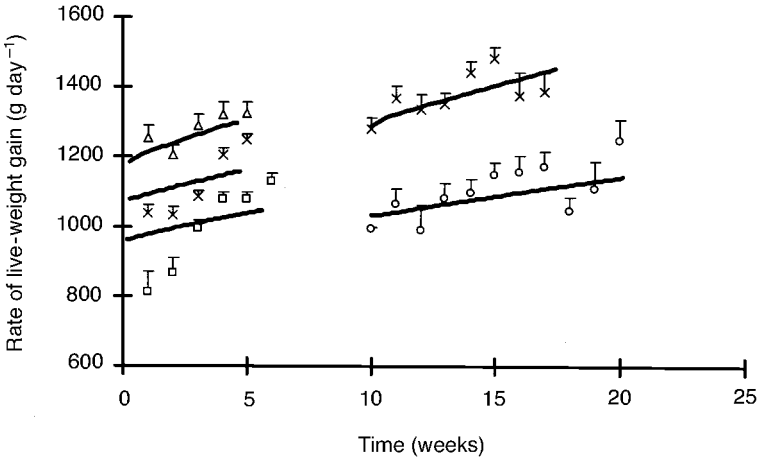

Fig. 12.1. Changes in the rate of live-weight (LW) gain with time for preruminant calves fed 7 (○), 9 (□), 12 (X) or 15 (△) g protein kg LW$^{-0.75}$ day^{-1}. Values are means ± SEM ($n = 4$). Solid lines represent the simulated responses, using the original model (Gerrits *et al.*, 1997a). At the start of the experiment ($t = 0$), calves were switched from a commercial feeding regime (13 g protein kg LW$^{-0.75}$ day^{-1}) to the experimental treatments. LW data are corrected for estimated changes in gut fill.

the start of the experiment. Model predictions of these short-term responses in LW gain were inadequate. For the 7 g protein treatment (starting at 160 kg), however, model predictions of the drop in LW gain after the change from the 12 to the 7 g protein intake and the subsequent increase in LW gain were adequate. For calves on all treatments, nutrient intakes increased linearly with LW$^{0.75}$, leading to an increase in the quantity of feed available for growth with time. This is the mechanism responsible for the steady increase in LW gain with time in the simulated response of all treatments but is not sufficient to predict the short-term adaptations in LW gain. These observations confirm earlier findings in the experiments of Gerrits *et al.* (1996). In line with the current data, the magnitude of the short-term responses seems positively related to the magnitude of change in nutrient intake but decreases with body weight.

The slaughter technique is, inherently, not very sensitive for detecting time-related changes in the priority of nutrient partitioning between various body tissues. By nature, serial slaughter trials are performed over a large LW range. In the present experiment, it was decided to obtain information about the response to nutrient intake over 40 kg LW intervals. Despite this complication, comparison of tissue deposition rates of the LW ranges 80–120 and 120–160 kg may give valuable information about the mechanisms involved in the adaptation to a sudden change in protein intake. Deviations from a normal increase in the rate of tissue deposition with time are indicative of an adaptive response.

When separating adaptive responses from normal time-related responses (caused by changes in feed intake with time) in this way, a sudden increase in protein intake seemed to increase whole-body fat, water and protein deposition rates. These changes were to a large extent caused by the organ fraction (including blood, the emptied gastrointestinal tract, liver, lungs, heart, kidneys, spleen and various small organs). In addition, organ protein deposition was increased. A sudden drop in protein intake led to decreased whole-body protein, fat and water deposition rates, changes which were only partly reflected in the organ fraction.

Although the data are not entirely conclusive, it seems reasonable to assume that calves adjust their organ machinery (i.e. organ protein mass) after a sudden change in protein intake to adapt to a new situation. Following a sudden increase in protein intake, net synthesis of organ protein increases quickly to accommodate the enhanced growth potential to be reached at the new feeding level. Conversely, a sudden decrease in protein intake should decrease the organ protein deposition rate. Any response of the organ protein mass is magnified at the whole-body level because of the large quantity of water associated with organ protein (the water : protein ratio of the organ fraction and of the whole body were found to be 5.1 and 3.3, respectively). Judging from the LW data, these adaptive responses may be completed within 4–5 weeks. Therefore, the 80–120 kg slaughter data may have been obtained over too wide an LW range to pick up these effects sensitively.

In addition, changes in gut fill are notorious for complicating interpretation of compensatory growth data. It is, however, an artefact of the LW measurement, rather than a biological phenomenon. Therefore, the LW data presented in this chapter (see Figs 12.1 and 12.5) are corrected for estimated changes in gut fill.

The mechanisms of responses of organ tissues to changes in feed intake have been shown to occur in pigs (Bikker *et al.*, 1996) and beef steers (Carstens *et al.*, 1991), but may be valid for describing the response to changes in the quantity of feed intake. Qualitative feed restriction and subsequent realimentation, however, particularly in functional ruminants, may have quite different effects on the total organ fraction, in particular on the size of the gastrointestinal tract (see, for example, Kamalzadeh, 1996).

Modifications to Simulate Short-term Adaptation to Changes in Protein Intake

Current representation of protein deposition in the model

The growth simulation model (Gerrits *et al.*, 1997a) distinguishes muscle, visceral, hide and bone protein as separate protein pools. The development of the muscle protein pool depends on substrate concentration (amino acids, acetyl CoA) and subsequently drives visceral, hide and bone protein development. For

that purpose, relationships between accretion rates of protein in muscle and protein in bone, hide and viscera were estimated from experiments of Gerrits *et al.* (1996). These relationships, represented by allometric equations, allow for bone and hide protein accretion to have some priority at low rates of muscle protein accretion. The allometric relationship between the accretion rates of muscle and organ protein is given by equation 2:

$$dQpv/dt = 0.065 \times (dQpm/dt)^{0.74} \quad (2)$$

Where *Qpv* denotes the quantity of visceral protein (kg of N) and *Qpm* the quantity of muscle protein (kg of N).

Adaptation of the model

The original relationship of equation 2 was extended by a multiplier, including: (i) a compensatory growth (CG) factor, adapting the preference of amino acid substrate for organ protein gain after a sudden change in protein intake; and (ii) an equation implementing the effect of LW on relationship (i). In part (i), sudden changes in protein intake are detected by changes in the muscle protein accretion rate relative to the ratio of organ to muscle protein mass present at that time (equation 3):

$$\text{CG factor} = -a + \frac{2a}{1 + \left(\frac{b}{\left[\frac{dQpm/dt}{Qpv/Qpm} \right]} \right)^{c}} \quad (3)$$

where *a*, *b* and *c* are positive constants. Equation 3 implies a sigmoidal response, with minimum and maximum values of $-a$ and *a*, respectively (Fig. 12.2). The constants *a*, *b* and *c* were calibrated, using the present experimental data, at 3, 0.47 and 8, respectively.

The effect of LW on compensatory growth is represented by equation 4:

$$\text{LW factor} = \frac{d \times e \times LW^{e-1}}{f^{e} + LW^{e}} \quad (4)$$

Where LW denotes live weight (kg) and *d*, *e* and *f* are positive constants, set to 4.5, 17.4 and 65.8, respectively, to accommodate the desired behaviour, illustrated by Fig. 12.3. With these parameter values, this function (S. Lopez, J. France, W.J.J. Gerrits, M.S. Dhanoa, D.J. Humphries and J. Dijkstra, 1999, unpublished) increases from 0 immediately after birth to reach a maximum of 1 around 70–90 kg LW, declining back to 0 at maturity.

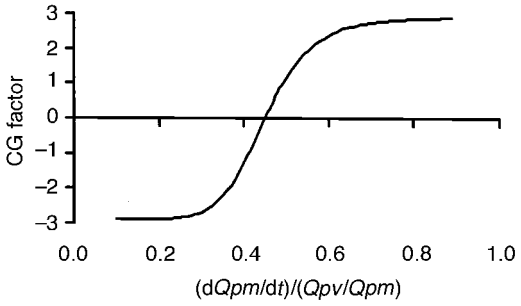

Fig. 12.2. The general behaviour of the compensatory growth correction factor (CG factor; equation 3 in text) with changing muscle protein deposition rate (d*Qpm*/d*t*), relative to visceral protein mass (*Qpv*) and muscle protein mass (*Qpm*). Parameter values for *a, b* and *c* are 3, 0.47 and 8, respectively.

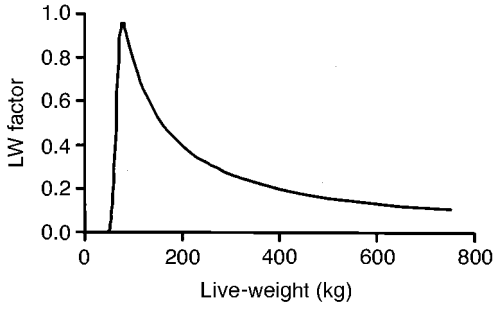

Fig. 12.3. The general behaviour of the live-weight correction factor (LW factor; equation 4 in text) with changing live-weight. Parameter values for *d, e* and *f* are 4.5, 17.4 and 65.8, respectively.

Subsequently, equation 2 was modified by the CG and LW factors, yielding equation 5:

$$\mathrm{d}Qpv/\mathrm{d}t = 0.065 \times \left(\mathrm{d}Qpm/\mathrm{d}t\right)^{0.74} \times \quad (\text{CG factor} \times \text{LW factor} + 1) \tag{5}$$

When the complete correction factor (CG factor × LW factor +1) equals 1, the normal organ protein deposition rate is realized. A correction factor below 0 implies net mobilization of organ protein (Fig. 12.4).

After modification of the model, simulation of the experimental treatments was repeated.

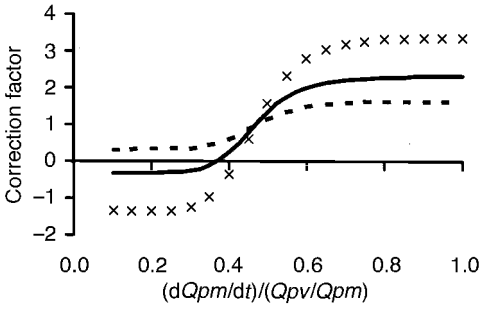

Fig. 12.4. The general behaviour of the complete correction factor (CG factor × LW factor + 1; see equation 5 in text), changing the protein deposition rate in viscera with changing muscle protein deposition rate (d*Qpm*/d*t*), relative to visceral protein mass (*Qpv*) and muscle protein mass (*Qpm*), for calves of 60 (–), 100 (x) or 180 (- - -) kg LW.

Preliminary results

The general behaviour of the correction factor (see equation 5) with changing muscle protein deposition rate, relative to organ and muscle machinery, is presented in Fig. 12.4 for calves of 60, 100 or 180 kg LW. A change in protein availability from the diet is sensitively reflected by changes in d*Qpm*/d*t*. The sigmoidal response is reduced at LW both below and above the presumed optimum (70–90 kg LW).

Results of reruns of the simulation of the experimental treatments using the modified model are shown in Fig. 12.5. Compared with the original model, the modified model responds to a sudden increase in protein intake (switching to the 15 g protein treatment at the start of the experiment) by increasing protein deposition in visceral organs by 34% maximum and 17% on average over the LW range. The energy costs were covered by a reduction of the fat deposition rate by 2.5 g day^{-1}. A sudden decrease in protein intake (switching to the 9 g protein treatment at the start of the experiment) causes an initial check in the rate of LW gain of 200 g day^{-1} (22 g day^{-1} average over the LW range) of the modified, compared with the original, model. Visceral protein reserves were mobilized during the first 6 days of this simulation (maximum 14 g day^{-1}) and, on average, visceral protein deposition rates were 17 and 11 g day^{-1} for the original and modified model, respectively. The average fat deposition rate was increased by 6.5 g day^{-1} using the modified model. Simulation of the 12 g protein treatment was unaltered, because protein intake was similar to that of the pre-experimental period.

Differences between the original and modified model were, as expected, less at higher LW. During simulation of the 7 g protein treatment (starting at 160 kg LW; about 10 weeks after the start of the experiment (see Fig. 12.5)), the

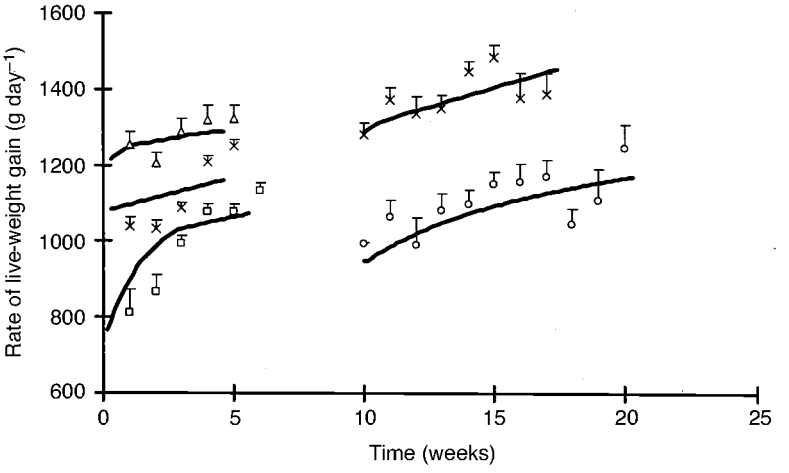

Fig. 12.5. Changes in the rate of live-weight (LW) gain with time for preruminant calves fed 7 (○), 9 (□), 12 (X) or 15 (△) g protein kg $LW^{-0.75}$ day^{-1}. Values are means ± SEM ($n = 4$). Solid lines represent the simulated response using the modified model (see text). At the start of the experiment ($t = 0$) calves were switched from a commercial feeding regime (13 g protein kg $LW^{-0.75}$ day^{-1}) to the experimental treatments. LW data are corrected for estimated changes in gut fill.

modified model predicted a lower rate of LW gain at the start of the simulation of about 85 g day^{-1}, compared with the original model. In addition, it took longer to correct the visceral protein mass back to normal, compared with the simulations at lower LW. Apart from a direct difference due to LW (see equation 4), this was also caused by the changes in visceral and muscle protein deposition being smaller relative to total mass (see equation 3).

Summarizing Statements

Comparison of model predictions with observations, acquired from an independent slaughter experiment, revealed that model predictions were satisfactory for LW gain and protein deposition, with a root MSPE of below 7%. For the rate of fat deposition, the root MSPE was 18% (on average 26 g day^{-1}), largely due to a consistent underestimation. It is concluded that this does not necessarily result from erroneous assumptions in the model. The model did not respond correctly to short-term changes in protein intake, which was indicated by inadequate prediction of changes in LW gain immediately after the dietary treatments were started (which differed widely from the nutrient intakes during the pre-experimental period). Modifications were made to the model, based

on the hypotheses that: (i) calves adapt their visceral protein mass quickly to a new feeding level; and (ii) that the capacity of calves to make these corrections decreases with age or LW. The modified model satisfactorily predicted short-term responses in LW gain to sudden changes in protein intake but remains to be rigorously evaluated. The approach taken may also be valid for modelling short term responses of animals to changes in intake of other nutrients. It cannot, however, be used in situations where, for example, animals can adapt their rate of intake in an attempt to compensate for a nutrient deficiency (e.g. during a qualitative feed restriction).

References

Bibby, J. and Toutenburg, H. (1977) *Prediction and Improved Estimation in Linear Models*. John Wiley & Sons, Chichester, UK.

Bikker, P., Verstegen, M.W.A., Kemp, B. and Bosch, M.W. (1996) Performance of fattening gilts (45–85) as affected by energy intake in earlier life. 2. Protein and lipid accretion in body components. *Journal of Animal Science* 74, 817–826.

Carstens, G.E., Johnson, D.E., Ellenberger, M.A. and Tatum, J.D. (1991) Physical and chemical components of the empty body during compensatory growth in beef steers. *Journal of Animal Science* 69, 3251–3264.

Gerrits, W.J.J., Tolman, G.H., Schrama, J.W., Tamminga, S., Bosch, M.W. and Verstegen, M.W.A. (1996) Effect of protein and protein-free energy intake on protein and fat deposition rates in preruminant calves of 80–240 kg liveweight. *Journal of Animal Science* 74, 2129–2139.

Gerrits, W.J.J., Dijkstra, J. and France, J. (1997a) Description of a model integrating protein and energy metabolism in preruminant calves. *Journal of Nutrition* 127, 1229–1242.

Gerrits, W.J.J., France, J., Dijkstra, J., Bosch, M.W., Tolman, G.H. and Tamminga, S. (1997b) Evaluation of a model integrating protein and energy metabolism in preruminant calves. *Journal of Nutrition* 127, 1243–1252.

Kamalzadeh, A. (1996) Prospects of compensatory growth for sheep production systems. PhD thesis, Wageningen Agricultural University, Wageningen, The Netherlands,

Meulenbroeks, J., Verstegen, M.W.A., Van der Hel, W., Korver, S. and Kleinhout, G. (1986) The effect of genotype and metabolizable energy intake on protein and fat gain in veal calves. *Animal Production* 43, 195–200.

Mitchell, E.L. and Gauthier, J. (1981) *Advanced Continuous Simulation Language. User Guide/Reference Manual*, 3rd edn. Mitchell and Gauthier Associates, Concord, Massachusetts.

van der Togt, P.L. and Gerrits, W.J.J. (1998) *Validation of a Growth Simulation Model of Preruminant Calves of 80–240 kg Live Weight* [in Dutch]. Internal report, Wageningen Agricultural University and TNO Nutrition and Food Research Institute (ILOB), Wageningen, The Netherlands.

13

Simulation of the Development of Adipose Tissue in Beef Cattle

R.D. Sainz and E. Hasting

Department of Animal Science, University of California, Davis, CA 95616, USA

Abstract

The goal of this modelling exercise was to evaluate genetic, nutritional and other factors affecting the distribution of fat in growing and finishing beef cattle. The model had the following objectives: (i) to predict the accretion of total body fat as a function of genotype, sex, implant status and nutrition; (ii) to predict the partition of fat in different depots throughout the animal's lifetime; and (iii) to examine the possible mechanisms for genetic and nutritional differences in fat distribution. This model appears to adequately describe normal growth and accretion fat in the whole body and in the four main depots. It represents a first step in the development of an analytical tool for the study of factors affecting fat deposition and distribution.

Introduction

Fat accretion in meat animals in general, and beef cattle in particular, is of great practical importance. Deposition of fat is less efficient than that of lean, and this is reflected in the very poor feed conversions of cattle nearing slaughter finish. In the US market, packers heavily discount beef carcasses containing less than about 28–30% fat, because this is the fat content that roughly corresponds to the Small marbling score (i.e. choice quality grade). On the other hand, excessive fat trim (i.e. internal, intermuscular and subcutaneous fat) is also penalized. Therefore, our market contains conflicting objectives for the production of fat, with intramuscular (marbling) fat commanding a price premium and other depots incurring penalties. In view of the importance of fat accretion and distribution for productive efficiency and market value, further study of the

 Modelling Nutrient Utilization in Farm Animals (eds J.P. McNamara, J. France and D.E. Beever)

genetic, nutritional and physiological factors affecting fat distribution seems warranted.

Fat (adipose) tissue is distinct from chemical fat, in that the former consists of many different cell types, dominated by adipocytes, which contain lipid, whereas the latter is the lipid that may be extracted by organic solvents (Allen *et al.*, 1976). Adipose tissue may be white or brown; the latter functions in specific situations as the site of thermogenesis and does not concern us here. White adipose tissue is characterized by the abundance of spherical adipocytes, containing a unilocular lipid droplet and a small volume of cytoplasmic material at the cell periphery. These adipocytes may vary between 15 and 250 μm in diameter, depending upon the size of the lipid droplet. The landmark studies of the Hammond group remain to this day the foundation upon which to build. That work showed that intramuscular fat is the last adipose depot to develop (Fig. 13.1; Hammond, 1955). As in all tissues, growth of adipose tissue must comprise both hyperplastic (i.e. increase in cell number) and hypertrophic (i.e. increase in cell size) growth. Hyperplasia includes the processes of proliferation and differentiation of fibroblast-like mesenchymal cells into adipocytes (Vernon, 1986). In the adipocyte, hypertrophy mainly involves accumulation of intracellular lipid. Changes in adipose cellularity during postnatal growth of cattle have been reported and reviewed by several authors (Moody and Cassens, 1968; Allen, 1976; Allen *et al.*, 1976; Robelin, 1981; Hood, 1982). Postnatal fat accretion occurs primarily through hypertrophy of existing adipocytes, with a smaller contribution of hyperplasia. For example, in Friesian bulls, the amount of total body fat increases 197-fold between birth and maturity, whereas the number of adipocytes only increases seven-fold and the mean adipocyte volume

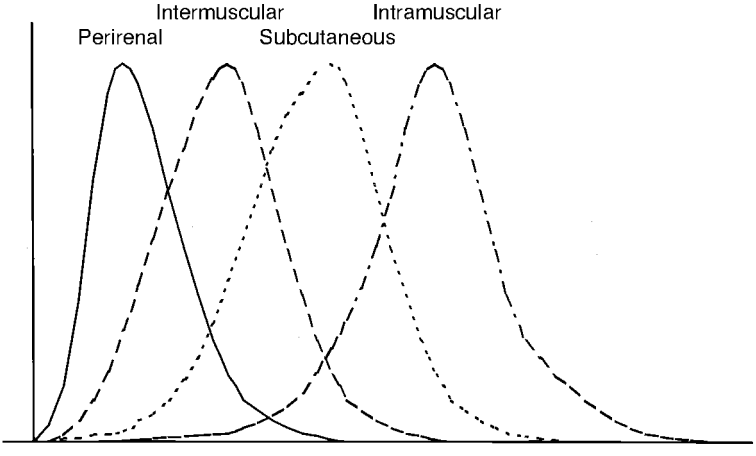

Fig. 13.1. Growth gradients among adipose depots (adapted from Hammond, 1955).

increases 29-fold during the same period (Robelin, 1986). This general observation, however, may obscure the fact that individual fat depots vary in their rates and timing of hyperplastic and hypertrophic growth. Cianzio *et al.* (1985) found that, from 11 to 19 months, subcutaneous, intermuscular, kidney and mesenteric fat depots in steers grew by hypertrophy, with little or no change in cell numbers. Intramuscular fat accretion, on the other hand, was due to the appearance of new adipocytes as well as increases in their lipid content. Therefore, we may conclude that, during the finishing phase, the earlier-developing depots (i.e. intermuscular, kidney and mesenteric fat) have completed their hyperplastic development and deposit fat by filling existing adipocytes, whereas the subcutaneous and intramuscular depots continue to recruit new adipocytes as well as filling existing cells with lipid.

Model Development

Objectives

The ultimate goal of this modelling exercise was to evaluate genetic, nutritional and other factors affecting the distribution of fat in growing and finishing beef cattle. To this end, a model describing the partition of fat into different depots was necessary. Therefore, this model had the following objectives:

1. To predict the accretion of total body fat as a function of genotype, sex, implant status and nutrition.
2. To predict the partition of fat in different depots throughout the animal's lifetime.
3. To examine the possible mechanisms for genetic and nutritional differences in fat distribution.

Methodology

In order to predict intake, growth and fat accumulation, the model developed by Oltjen *et al.* (1986) was adopted. This dynamic, mechanistic and deterministic model is based upon the concepts of hyperplasia (DNA accretion) and hypertrophy (protein accretion), validated by Baldwin and Black (1979). Accumulation of total body fat is described according to the net energy system (NRC, 1984), based upon the energy available after accounting for the requirements of maintenance and protein gain. This model is simple and robust and has been extensively tested and applied in the field. To this model were added equations representing the development and growth of adipose depots.

Four adipose depots are represented: visceral (Fv), intermuscular (Fi), subcutaneous (Fs) and intramuscular (Fm) fat. For each one, hyperplasia is represented as the accumulation of DNA (Dv, Di, Ds and Dm), according to the following equation:

$$d\,DNA_i/dt = kDNA_i \times DNA_i \times (DNA_{MAX_i} - DNA_i)$$

where *k*DNA is the growth coefficient for depot *i*, and DNA_{MAX} is the maximum or target amount of DNA in the depot. Deposition of triacylglycerol (FAT) into each depot is described by:

$$d\,FAT_i/dt = \Sigma\,(d\,FAT_i/dt)\,fDFAT_i$$

and

$$fDFAT_i = DNA_i\,[1 - (FAT_i/DNA_i)/(FAT_{MAX}/DNA_{MAX})]/\Sigma fDFAT_i$$

where $fDFAT_i$ is the fraction of total fat gain deposited in tissue *i*, and FAT_{MAX}/DNA_{MAX} is the maximum adipocyte size. Finally, in order to compare outputs with published data on subcutaneous (backfat) and intramuscular (marbling) fat, fat contents of these depots are converted to commonly used estimates according to:

$$\text{Backfat (mm)} = 1.457\,Fs^{0.643} \quad \text{(for small- and moderate-frame British breeds)}$$

$$\text{Backfat (mm)} = 0.284\,Fs^{1.017} \quad \text{(for large-frame Continental or dairy breeds)}$$

using relationships derived from the data reported by Charles and Johnson (1976). For intramuscular fat, total content (Fm) is divided into total muscle mass:

$$\text{IM fat (\%)} = 100\,Fm/(BW \times DP \times RPY)$$

where BW is body weight, DP is dressing % (default 0.63) and RPY is retail product yield (default 0.60). These are then converted to US Department of Agriculture (USDA) quality grades according to Table 13.1.

Table 13.1. Relationships among intramuscular fat content, marbling score and USDA quality grades (from Bailey, 1996).

Quality grade	Marbling score	% Intramuscular fat
Prime	Slightly abundant	10.13
Choice	Moderate	7.25
Choice	Modest	6.72
Choice	Small	5.04
Select	Slight	3.83
Standard	Traces	2.76

Parameter values

Equations for adipose depot hyperplasia and hypertrophy were parameterized using data on cell numbers and sizes from Robelin (1981) and Cianzio *et al.* (1985). Cell numbers were converted to kg DNA by assuming a constant DNA content of 6.2 pg nucleus^{-1}. Cell sizes (diameters) were converted to total lipid contents by assuming that adipocytes contain 85% triacylglycerol and are spherical. Values are shown in Table 13.2.

Model solution

The basic growth model and the adipose submodel are coded in Advanced Continuous Simulation Language (ACSL) (MGA Software, 1995). The model is solved using a fourth-order Range-Kutta fixed-step second-order algorithm, using a maximum 0.25-day integration interval.

Model Behaviour

The accretion of DNA in each of the adipose depots is shown in Figs 13.2 and 13.3. In the subcutaneous and intramuscular depots, no plateau is discernible in the data. In contrast, the visceral and intermuscular depots display clear maxima. However, there is some evidence of a second wave of hyperplasia,

Table 13.2. Parameter values. TG, triacylglycerols.

Parameter	Definition	Value
Dv_{max}	Maximum DNA in visceral adipose	0.000133 kg
Di_{max}	Maximum DNA in intermuscular adipose	0.000233 kg
Ds_{max}	Maximum DNA in subcutaneous adipose	0.000200 kg
Dm_{max}	Maximum DNA in intramuscular adipose	0.000100 kg
k_{Dv}	Growth coefficient for visceral adipose DNA	200 kg^{-1} day^{-1}
k_{Di}	Growth coefficient for intermuscular adipose DNA	100 kg^{-1} day^{-1}
k_{Ds}	Growth coefficient for subcutaneous adipose DNA	35 kg^{-1} day^{-1}
k_{Dm}	Growth coefficient for intramuscular adipose DNA	37 kg^{-1} day^{-1}
FAT_{MAX}/DNA_{MAX}	Maximum cell size in all adipose depots	4.5×10^5 kg TG kg DNA^{-1}

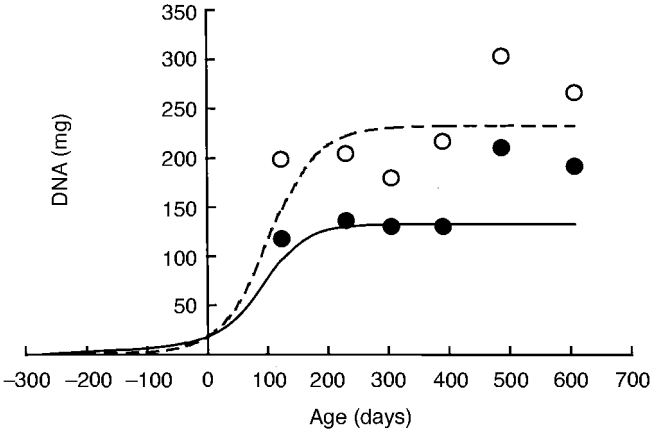

Fig. 13.2. Development of visceral (●) and intermuscular (○) adipose tissue cells, observed (symbols) and predicted (line) (data from Robelin, 1981).

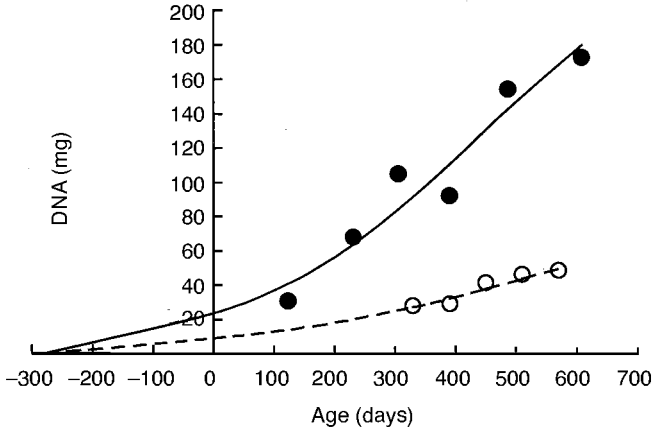

Fig. 13.3. Development of subcutaneous (●) and intramuscular (○) adipose tissue cells, observed (symbols) and predicted (line) (data from Robelin, 1981, and Cianzio *et al.*, 1985).

particularly in the visceral depot. This is in agreement with current concepts of adipose development – that is, hyperplasia within a depot proceeds and then ceases until some proportion of the adipocyte population reaches maximum size (*c.* 250 μm diameter), which then stimulates a second or third wave of cell recruitment, differentiation and hypertrophy (Allen *et al.*, 1976). For the purposes of this exercise, no provision for secondary hyperplasia has been incor-

porated, since most beef cattle would reach market finish prior to this occurrence. In the future, it may become necessary to include this phenomenon. Fig. 13.4 shows the accretion of triacylglycerol in each of the four depots. Even in the early-maturing tissues, hypertrophy continues, with little sign of a plateau, up to 600 days of age. As subcutaneous and intramuscular adipocytes proliferate, however, these tissues make up progressively larger proportions of the total body fat as the animal matures.

Future Directions

The submodel described here appears to adequately describe normal growth and accretion of fat in the whole body and in the four main depots. It represents a first step in the development of an analytical tool for the study of factors affecting fat deposition and distribution, and much remains to be done. As with all growth models, it is only as good as the estimates of nutrient inputs, so full testing of the model will require definition of feed intake and energy value throughout the life of the animal. Further model developments will include incorporation of nutritional elements into the equations for adipose hyperplasia, possible differences in lipogenesis and lipolysis among depots, examination of possible mechanisms for genetic differences and study of the effects of growth path or nutritional history.

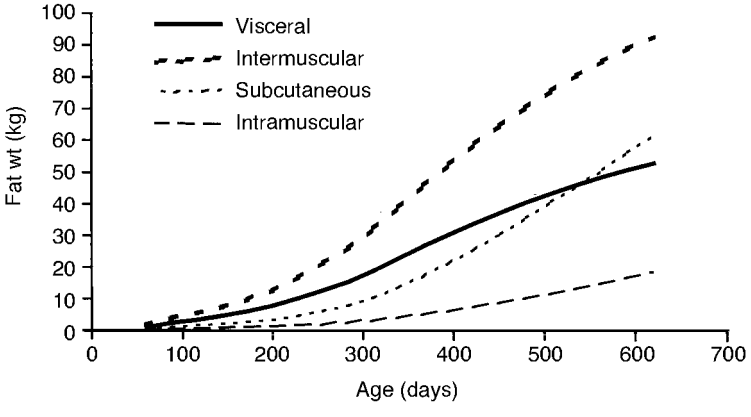

Fig. 13.4. Growth curves for visceral, intermuscular, subcutaneous and intramuscular fat.

References

Allen, C.E. (1976) Cellularity of adipose tissue in meat animals. *Federation Proceedings* 35, 2302–2307.

Allen, C.E., Beitz, D.C., Cramer, D.A. and Kauffman, R.G. (1976) *Biology of Fat in Meat Animals*. North Central Region Committee 91 Bulletin.

Bailey, C. (ed.) (1996) *Guidelines for the Uniform Beef Improvement Programs*. Beef Improvement Federation, Colby, Kansas.

Baldwin, R.L. and Black, J.L. (1979) *Simulation of the Effects of Nutritional and Physiological Status on the Growth of Mammalian Tissues: Description and Evaluation of a Computer Program*. Animal Research Laboratories Technical Paper, No. 6. Commonwealth Science and Industrial Research Organization, Melbourne, Australia.

Charles, D.D. and Johnson, E.R. (1976) Breed differences in amount and distribution of bovine carcass dissectible fat. *Journal of Animal Science* 42, 332–341.

Cianzio, D.S., Topel, D.G., Whitehurst, G.B., Beitz, D.C. and Self, H.L. (1985) Adipose tissue growth and cellularity: changes in bovine adipocyte size and number. *Journal of Animal Science* 60, 970–976.

Hammond, J. (1955) *Progress in the Physiology of Farm Animals*. Butterworths Scientific Publications, London.

Hood, R.L. (1982) Relationships among growth, adipose cell size, and lipid metabolism in ruminant adipose tissue. *Federation Proceedings* 41, 2555–2561.

MGA Software (1995) *ACSL Reference Manual*. MGA Software, Concord, Massachusetts.

Moody, W.G. and Cassens, R.G. (1968) A quantitative and morphological study of bovine longissimus fat cells. *Journal of Food Science* 33, 47–52.

National Research Council (NRC) (1984) *Nutrient Requirements of Beef Cattle*, 6th edn. National Academy Press, Washington, DC.

Oltjen, J.W., Bywater, A.C., Baldwin, R.L. and Garrett, W.N. (1986) Development of a dynamic model of beef cattle growth and composition. *Journal of Animal Science* 62, 86–97.

Robelin, J. (1981) Cellularity of bovine adipose tissues: developmental changes from 15 to 65 percent mature weight. *Journal of Lipid Research* 22, 452–457.

Robelin, J. (1986) Growth of adipose tissues in cattle: partitioning between depots, chemical composition and cellularity. *Livestock Production Science* 14, 349–364.

Vernon, R.G. (1986) The growth and metabolism of adipocytes. In: Buttery, P.J., Haynes, N.B. and Lindsay, D.B. (eds) *Control and Manipulation of Animal Growth*. Butterworths, London, pp. 67–84.

14

A Simple Nutrient-based Production Model for the Growing Pig

S. Boisen

Danish Institute of Agricultural Sciences, Research Centre Foulum, PO Box 50, DK-8830 Tjele, Denmark

Abstract

The basic principles for a simple nutrient partitioning model for the growing pig are outlined. The proposed model is meant for practical feed evaluation and is based on input data for the actual feed, the actual pig and the actual feeding situation. The system is composed of four steps, including: (i) characterization of the feed in relevant nutrient fractions (i.e. crude protein, crude fat, amino acids, fatty acids, starch and sugar) by chemical analyses; (ii) prediction of ileal digestibility of protein and dry matter and of total tract digestibility of organic matter, respectively, from *in vitro* digestibility analyses; (iii) calculation of potential energy generation and nutrient deposition by the use of standard equations; and (iv) prediction of actual energy generation and nutrient deposition and excretion, respectively, by the use of a simple animal model. The basal components of the model are feed intake and feed wastes, requirements for energy and protein maintenance, protein deposition capacity, and relationships between deposited protein and deposited water, ash and phosphorus, respectively. The output of the model is daily gain, feed utilization and composition of the gain.

Introduction

Feed evaluation based on pig models is becoming increasingly important in modern feed formulation (Moughan *et al.*, 1995). Animal models can be used for describing specific processes, e.g. nutrient digestion in the digestive tract (Bastianelli *et al.*, 1996), or they can be whole-animal models describing the growth of the animal. Growth models for pigs are generally nutrient-partitioning models, which attempt to trace the flow of energy and amino acids in the pig

 Modelling Nutrient Utilization in Farm Animals (eds J.P. McNamara, J. France and D.E. Beever)

body (e.g Black *et al.*, 1986; Moughan *et al.*, 1987). In another type of model, the metabolic model, the flow of specific nutrients and their metabolites is traced from reaction kinetics. Metabolic models have been used for describing specifically the metabolism in the lactating sow (Pettigrew *et al.*, 1992) and a model for the growing pig is under development (Danfær, Chapter 30, this volume). A computerized metabolic model has the potential for offering a detailed and sophisticated description of the complex intermediary metabolism and, consequently, for being an excellent tool for identifying goals for further research, as well as for practical feed evaluation. On the other hand, due to the complexity of the intermediary metabolism and the large number of factors influencing the individual steps in the biochemical processes, considerable effort is needed for a general documentation of a detailed metabolic growth model.

Generally, animal models rely completely on correct inputs of data on influencing factors for the actual production and, furthermore, on the system describing the value of digested feed in relation to production parameters, i.e. the feed evaluation system used. All animal simulation models have been developed according to the current energy evaluation systems, based either on digestible energy (DE), metabolizable energy (ME) or net energy (NE). In all systems, the energy value is basically calculated from digestible organic nutrient fractions, often used together with data for digestible amino acids.

However, the physiological utilization of DE and ME may be considerably influenced by the nutrient composition in the actual diet. On the other hand, NE is influenced by a number of specific factors relating to the actual feeding situation (Boisen and Verstegen, 1998a). The influence of these factors, e.g. feed intake and ingredient composition, genetic potentials and live-weight (LW) of the animals and environmental conditions, may lead to an actual NE value that is different from that determined under the experimental conditions. Consequently, data on energy value from current energy evaluation systems are generally not ideal for animal production models. Rather, data on the available (digestible) amounts of the relevant nutrient fractions in the diet should be used directly for characterizing the feed value (Boisen and Verstegen, 1998b).

Furthermore, data on amino acid digestibility used in most present protein evaluation systems refer to table values for the apparent ileal digestibility of amino acids. However, these values may be considerably influenced by the experimental conditions used for their determination, due to the influence of dietary protein level on the effect of endogenous protein losses (Boisen and Moughan, 1996a). Therefore, it is now generally accepted, that for a consistent protein evaluation, values of true or 'standardized' digestibility of amino acids should be used (Jondreville *et al.*, 1995; Boisen and Moughan, 1996b; Boisen, 1998; NRC, 1998; CVB, 1999; Rademacher *et al.*, 1999). Consequently, the ideal pattern of amino acid requirements (i.e. ideal protein) should be based on the composition of standardized digestible essential amino acids (Boisen, 1997).

Finally, even the use of a scientifically correct feed evaluation system and sophisticated computerized animal models may result in misleading outputs if the expected contents of digestible nutrients in the actual feed are not correct.

Because the concentration, as well as the digestibility, of nutrients may, in many feedstuffs, vary considerably (Black and Chapple, 1991), it is necessary to control for these variations by sufficient analyses of the actual feed samples. Recently, simple, quick and reliable *in vitro* enzyme digestibility analysis methods of different nutrient fractions have been developed (e.g. Boisen and Fernandez, 1995, 1997). Hence, adequate chemical analyses of the content of relevant nutrient fractions supplied with suitable analyses of their digestibility in the actual sample can now be included routinely in feed evaluation.

The aim of the present chapter is to describe the basic principles for a simple nutrient-partitioning model for the growing pig. The proposed model is meant for practical feed evaluation and is based on input data for the actual feed, characterized by those nutrient fractions which have been found to be relevant for describing the potential value of the feed.

Outline for the Model

The fundamental presupposition for a reliable simulation of animal performance is that the input data are correct. In models for use in feed evaluation, the input data on the feed obviously play a central and dominant role. Therefore, the feed needs to be characterized by those nutrient fractions which are relevant according to a scientifically correct feed evaluation system. Furthermore, the contents and digestibility of these fractions in the actual feed need to be carefully controlled.

Because the properties, e.g. the protein value, of single feedstuffs may not be additive, and because the value of complete diets may depend on their actual use, a correct feed evaluation needs to be performed according to the following levels of information:

1. Characterization of single feedstuffs and premixes in those nutrient fractions which are relevant for their optimal utilization in feed formulation and production.
2. Characterization of complete diets in those nutrient fractions/properties which are relevant for their optimal utilization in the different pig categories.
3. Calculation of the feed value in relation to the actual feeding conditions, including influencing factors from the animal and environment.

It follows that general feed evaluation that does not include animal simulation models (level 1 and 2) should only describe the feed according to its potential value, whereas feed evaluation with an integrated animal simulation model offers the opportunity for prediction of the actual value in the specific feeding situation (level 3).

A complete feed evaluation according to the presuppositions given above can be based on the following steps:

1. Chemical analyses for characterization of the feeds according to the composition of the relevant nutrient fractions. These include the three main organic

components: crude protein, crude fat and crude carbohydrates, which further need to be characterized by their contents of amino acids, fatty acids and starch + sugar, respectively.

2. *In vitro* enzyme digestibility analyses for predicting the amount of faecal digestible organic matter, ileal digestible protein and amino acids and postileal fermentable carbohydrates.

3. Calculations of the available amounts of the relevant nutrient fractions (ideal protein, residual N compounds, ileal digestible carbohydrates, fermentable carbohydrates, triacylglycerols and residual lipid compounds). From these fractions the potential feed value of the complete diet can be calculated. The potential feed value includes the protein value (ideal protein), the fat value (triacylglycerols) and the complemental energy value, i.e. physiologically available energy that is not included in the fractions describing the protein and fat value. Thus, the potential feed value describes the potential for energy generation and direct nutrient deposition and could be ideal for price-setting of the feed. However, for use in general recommendations for the different pig categories and for inputs to simulation models, information on all six nutrient fractions should be used.

4. Animal simulation model, e.g. growth model for the pig, for calculation of the actual feed value. Together with inputs on digestible nutrient fractions in the complete diet from step 3, data on daily feed intake and maximal protein deposition capacity play a dominant role in the actual feed utilization. From defined requirements for protein and energy, related to metabolic body weight, the actual feed utilization, daily weight gain and deposition of body components can be predicted. Furthermore, meat percentage of the carcass and excretion of surplus nutrients (N and P) can be predicted.

The evaluation of the feed according to the first two steps is common for single feedstuffs, premixtures and complete diets, whereas the evaluation of the feed according to the last two steps is only relevant for complete diets. A flow diagram including the key parameters in the four steps during the evaluation of complete diets is shown in Fig. 14.1.

The figure indicates that protein deposition capacity can be considered as a fundamental property in the growing pig because the deposition of water and ash is associated with protein deposition. Assuming that deposition of water and ash completely follow protein deposition, gain of weight will be about 4.4 times the weight of the deposited protein according to data on body composition from Jørgensen *et al.* (1985). Therefore, the securing of an adequate supply of all essential amino acids during growth is of the utmost importance for the production results, i.e. daily gain and feed utilization. It follows that the requirements, as well as the actual supply, of digestible amino acids, should be carefully controlled throughout the growing period.

Figure 14.1 also indicates that the direct deposition of carbohydrates is negligible. Generally, dietary carbohydrates have a much less direct effect on weight gain, primarily because digested and fermented carbohydrates are usually the

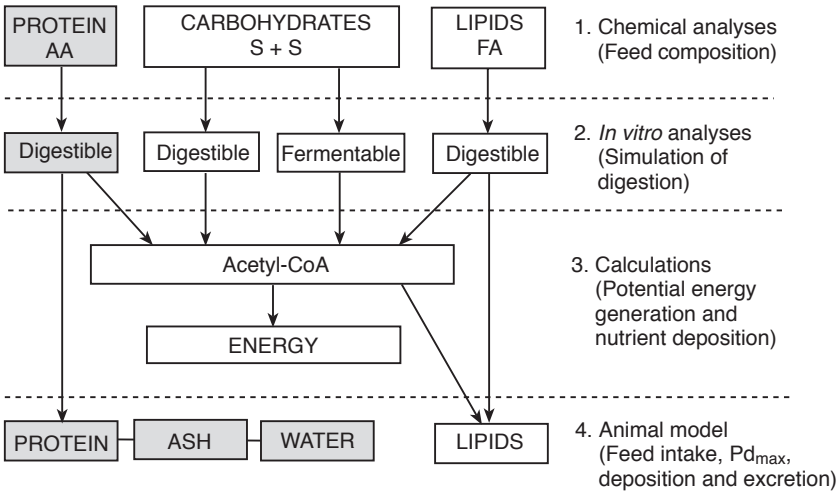

Fig. 14.1. A stepwise characterization of the feed value of complete diets. The first three steps lead to a characterization of the potential feed value for use in recommendations and price-setting. The last step predicts the actual feed value in relation to the specific feeding situation. AA, amino acids; S + S, sugar plus starch; FA, fatty acids; CoA, coenzyme A.

dominating energy source. On the other hand, if carbohydrates are not used for energy production, they will be available for fat synthesis. However, according to biochemical calculations, only 0.4 kg fat kg^{-1} digested carbohydrate and only 0.25 kg fat kg^{-1} fermented carbohydrate (via microbial production of short-chain fatty acids (SCFA)) can be produced.

Finally, Fig. 14.1 indicates that dietary lipids can be transferred almost unchanged to the tissues and deposited directly in the growing pig, either as structural lipids – in, for example, membranes and nerve tissue – or as depot fat in fat tissue. Suggesting the cost for the involved processes to be included in the maintenance requirements, the utilization of digested triacylglycerols can be assumed to be close to 1.0.

The integrated model of feed characterization and animal growth is illustrated in more detail in Fig. 14.2. The figure indicates the alternative routes for the nutrient flows for energy generation or deposition in the growing pig.

Furthermore, a model for the specific flow of N is illustrated in Fig. 14.3. The figure indicates the influence on the excretion pattern of N from the microbial activity in the hindgut. In fact, the amount of fermentable carbohydrates, which is the primary energy source for the bacteria, plays a central role in the calculation of N bound in the microbial biomass and thus in the prediction of the excretion route for surplus N.

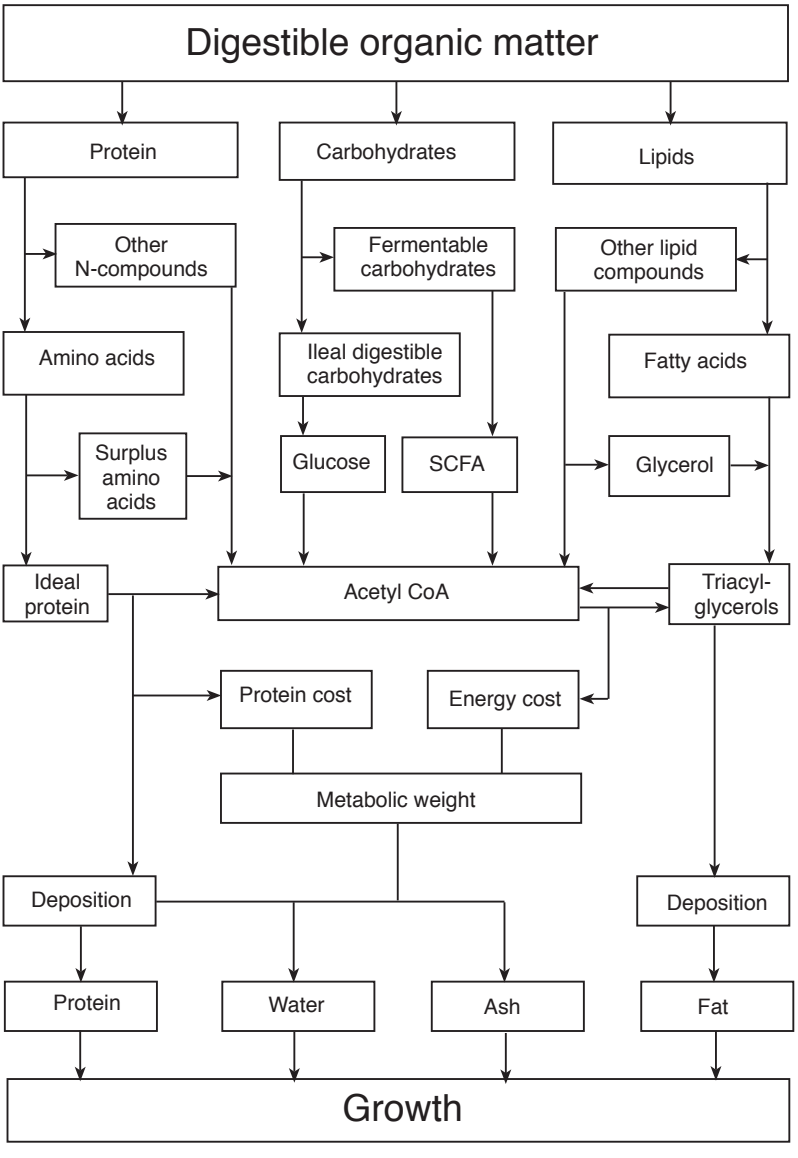

Fig. 14.2. Flow diagram of an integrated model for feed characterization and the transformations of feed components into physiological energy and body components. CoA, coenzyme A; SCFA, short-chained fatty acids.

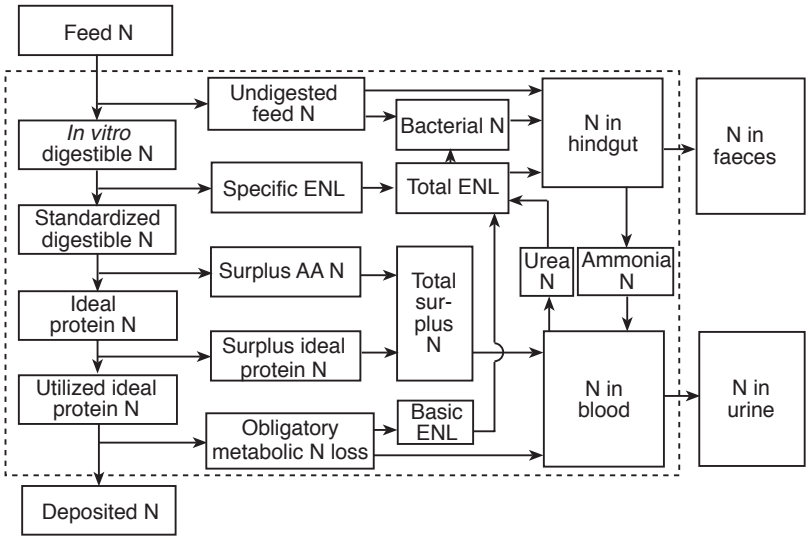

Fig. 14.3. Flow diagram for the main routes in nitrogen metabolism in the pig, including input (feed N), output (faeces N and urine N) and production value (deposited N). ENL, endogenous N loss; AAN, amino acid N.

Short Description of the Model

Input to the model

1. Actual feed composition (digestible nutrient fractions):
   (a) ideal protein (IP);
   (b) non-IP;
   (c) ileal digestible carbohydrates;
   (d) fermentable carbohydrates;
   (e) triacylglycerols (TG);
   (f) non-TG.
2. Actual feed intake (kg day^{-1}).
3. Actual feed wastes (percentage of diet).
4. Actual protein deposition capacity (Pd, g day^{-1})

Components of the model

1. Standard feed intake (Table 14.1).
2. Standard feed wastes.
3. Maximal protein deposition capacity, Pd_{max} (Table 14.2).
4. Relationship between deposited protein and water (Table 14.3).

Table 14.1. Changes in *ad libitum* feed intake of pigs during the live-weight period from 20 kg to 100 kg.

Live-weight (kg)	DE (MJ day^{-1})	Feed intake (kg day^{-1})			
20	(18)	1.32			
30	(22)	1.78			
40	(26)	2.24			
Energy density (MJ DE kg^{-1}):		12.0	13.0	14.0	15.0
50	30	2.50	2.31	2.14	2.00
60	34	2.83	2.62	2.43	2.27
70	38	3.17	2.92	2.71	2.53
80	41	3.42	3.15	2.93	2.73
90	44	3.67	3.38	3.14	2.93
100	47	3.92	3.62	3.36	3.13

Table 14.2. Maximal protein deposition (Pd_{max}) in pigs and estimated associated gain of other body components and total body-weight gain (g day^{-1}) at different live-weight (kg).

Live-weight	Pd_{max}	Water	Ash	Fat-free gain	Normal fat gain	Empty-body gain	Total gain
20	75	241	13	329	111	440	470
30	90	289	15	394	133	527	563
40	120	385	20	525	178	703	752
50	140	449	24	613	207	820	877
60	155	498	26	679	229	908	971
70	170	546	29	745	252	997	1066
80	175	562	30	767	259	1026	1097
90	180	578	31	789	266	1055	1128
100	180	578	31	789	266	1055	1128

5. Relationship between deposited protein and ash (Table 14.3).
6. Relationship between deposited protein and standard value for fat (Table 14.3).
7. Relationship between deposited protein and P (Table 14.3).
8. Energy requirements for maintenance.
9. Protein requirements for maintenance.
10. Standard gut fill.

Table 14.3. Composition of the total body of pigs at 20 and 90 kg live-weight (LW), respectively, and the relative average gain of the different body components (g kg^{-1} gain) during the period.

	Body composition (kg)				
	20 kg LW mean	90 kg LW		Gain (g kg^{-1} gain)	
		Gilts	Barrows	Gilts	Barrows
Protein	2.9	14.8	14.0	170	159
Water	11.7	50.2	47.4	550	510
Ash	0.6	2.6	2.5	29	27
Fat	1.9	15.2	18.4	190	236
Gut fill	2.9	7.2	7.7	61	69
Gain of body components relative to protein (or N)					
Water : Protein	4.03	3.39	3.39	3.24	3.21
Ash : Protein	0.21	0.18	1.18	0.17	0.17
Fat : Protein	0.66	1.03	1.31	1.12	1.48
P : N	0.208	0.204	0.204	0.196	0.196

Calculations by the model

1. Deposition of protein, water, ash and P.
2. Physiologically available energy from digested, non-deposited nutrients.
3. Surplus of metabolites (acetyl coenzyme A (CoA) equivalents) available for fat synthesis.
4. Deposition of fat from dietary fat and surplus metabolites.
5. Effect of fermentable fibre on the pattern of N excretion.

Output from the model

1. Daily gain (g day^{-1}).
2. Feed utilization (kg gain kg^{-1} feed).
3. Body composition of the growing pig until slaughter at 100 kg LW.
4. Meat percentage of the carcass.
5. Faecal and urinary excretion of N.
6. Faecal and urinary excretion of P.

Comments on the Model Components

As indicated above, several of the model components may be improved by the use of actual analyses (feed intake, feed wastes and Pd_{max}). Furthermore, the standard values given below are primarily used for illustration of the system and should be considered as only preliminary values.

Feed intake

Until 50 kg LW the capacity of the digestive tract limits feed intake and is described by the formula:

$$\text{Feed intake (kg day}^{-1}) = 0.046 \times \text{LW} + 0.40 \quad \text{(Moughan } \textit{et al.}\text{, 1995)}$$

After 50 kg LW, the feed intake is influenced by the energy density (Table 14.1).

The actual feed intake is influenced by a number of other factors relating to the feed (e.g. taste, physical properties), the animal (e.g. sex, health status) and the environment (e.g. temperature, stocking density).

Feed wastes

Data from Moughan *et al.* (1995) indicate increasing wastes from about 2% of feed intake at 30 kg LW to about 4% and 6% at 50 and 70 kg LW, respectively.

The actual wastes may be considerably influenced by the taste and physical nature of the diet (e.g. meal vs. pellets), as well as the feeding system and equipment.

Maximal protein deposition capacity (Pd_{max})

The protein deposition capacity is often characterized by an allometric function (Siebrits *et al.*, 1986). A maximum of 180 g day^{-1} at about 90 kg LW has been reported (Chwalibog *et al.*, 1996).

The actual function can vary considerably, depending on sex, genotype and several production factors, and the maximum of 180 g day^{-1} may be even higher for some modern lean genotypes.

Relation between deposited protein and water, ash and phosphorus

Water deposition and bone formation are closely related to protein deposition. Data from slaughter experiments of pigs at different LW (Jørgensen *et al.*, 1985) are used for calculation of the relationships (Table 14.3). The differences

between gilts and barrows given in Table 14.3 are probably smaller in modern lean genotypes.

The deposition of fat is considered to be independent of the protein deposition and can originate from dietary lipids, as well as from surplus carbohydrates and protein (Chwalibog *et al.*, 1992).

Energy requirements of maintenance

A number of different experiments have resulted in many different equations published in the literature. However, most equations lead to quite similar values in relation to LW. The energy requirements correspond to faecal digestible energy. The equation:

$$E_m\ (\text{MJ day}^{-1}) = 3.14 + 0.359 \times \text{LW}^{0.75}\ \text{(Thorbek } et\ al.\text{, 1984)}$$

expresses the daily maintenance requirement for metabolizable energy and is obtained from studies on Danish pigs. Therefore, this equation is used in the preliminary model. However, in the final model, the values should be transformed to requirements for the physiologically available energy.

Protein requirement for maintenance

A number of different experiments have resulted in many different equations published in the literature. However, in contrast to those on energy requirements, the equations result in quite different values. This may primarily be due to a difference in protein quality and probably also to actual values of amino acid digestibility other than those assumed. The equation:

$$\text{DNm (g day}^{-1}) = 2.69 + 0.160 \times \text{LW}^{0.75}\ \text{(Thorbek } et\ al.\text{, 1984)}$$

expresses the daily maintenance requirement for digestible N and is obtained from studies on Danish pigs. Therefore, this equation is used in the preliminary model. However, the protein requirements in the present Danish feed evaluation system correspond to faecal digestible crude protein. Therefore, in the final model, the values should be transformed to requirements for standardized digestible amino acids.

Gut fill

The data in Table 14.3 indicate that gut fill is about 6% of the total body weight. Therefore, the equation:

$$\text{Total body gain} = \text{Empty body gain}/0.94$$

is used in the model.

Example of Modelling

The relationship between the daily intake of all the nutrient fractions used for characterizing the feed and the composition of the daily gain in the pig is shown in Fig. 14.4. The calculated values are based on data obtained in a production experiment with a simple barley/soybean meal diet for growing pigs. The figure demonstrates a considerable surplus of ideal protein in the diet. Therefore, a maximal protein deposition, according to Table 14.2, is predicted. On the other hand, because dietary lipids are very low, a considerable portion of the deposited fat was synthesized from surplus metabolites (mainly from carbohydrates). Although a high protein deposition was obtained, the predicted results demonstrate a suboptimal composition of the nutrients. Hence, this very simple model strongly indicates that a more balanced diet with a higher fat value and a lower protein content would have improved the production results.

Further Developments

The described nutrition-based production model is a preliminary model and may still be improved by using more actual experimental data and a more detailed description of the influencing factors. Also, the influence of LW on digestibility of the nutrient fractions, in particular the fermentation of dietary

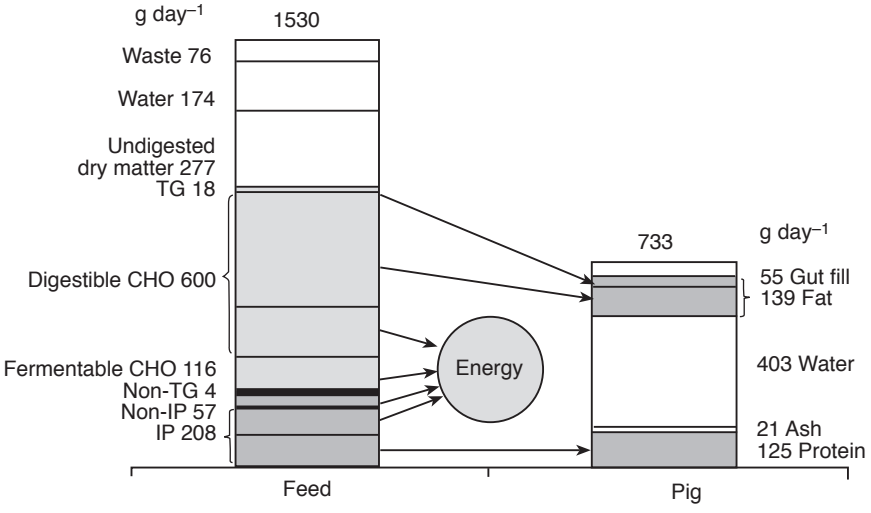

Fig. 14.4. Relationships between average daily intake of nutrients and average daily gain in pigs from 20 to 50 kg live-weight. The transformations of dietary nutrient fractions into body components and physiologically available energy are illustrated. CHO, carbohydrate; IP, ideal protein; TG, triglycerides.

fibre, can easily be incorporated in the model. Furthermore, the specific effects of dietary fibre on the digestibility of other nutrients, as well as on the physiological development of the digestive tract and gut fill, should be included in the second generation of this model.

During the further developments of the described simple nutrient-partitioning model, the outputs from the model will be currently compared with the outputs from a much more sophisticated dynamic metabolic model which is under development at our institute (Danfær, Chapter 30, this volume). In this model, the inputs on the feed are based on exactly the same characterization as that used in the present model and therefore the model provides a perfect basis for a direct comparison, as well as a guide for further improvements.

However, an important goal for further developments of the present model is that each step should be clearly described and documented, according to present knowledge, without losing its simplicity.

References

Bastianelli, D., Sauvant, D. and Rerat, A. (1996) Mathematical modeling of digestion and nutrient absorption. *Journal of Animal Science* 74, 1873–1887.

Black, J.L. and Chapple, R. (1991) Computer models would allow for more accurate formulation. *Feedstuffs*, June 24, 14–17.

Black, J.L., Campbell, R.G., Williams, I.H., James, K.J. and Davies, G.T. (1986) Simulation of energy and amino acid utilisation in the pig. *Research and Development in Agriculture* 3 (3), 121–145.

Boisen, S. (1997) Ideal protein – and its suitability to characterize protein quality in pig feeds: a review. *Acta Agriculturae Scandinavica, Sect. A. Animal Scence* 47, 31–38.

Boisen, S. (1998) A new protein evaluation system for pig feeds and its practical application. *Acta Agriculturae Scandinavica, Sect. A. Animal Science* 48, 1–11.

Boisen, S. and Fernandez, J.A. (1995) Prediction of the apparent ileal digestibility of protein and amino acids in feedstuffs and feed mixtures for pigs by *in vitro* analyses. *Animal Feed Science and Technology* 51, 29–43.

Boisen, S. and Fernandez, J.A. (1997) Prediction of the total tract digestibility of energy in feedstuffs and pig diets by *in vitro* analyses. *Animal Feed Science and Technology* 68, 277–286.

Boisen, S. and Moughan, P.J. (1996a) Dietary influences on endogenous ileal protein and amino acid loss in the pig – A review. *Acta Agriculturae Scandinavica, Sect. A. Animal Science* 46, 154–164.

Boisen, S. and Moughan, P.J. (1996b) Different expressions of dietary protein and amino acid digestibility in pig feeds and their application in protein evaluation: a theoretical approach. *Acta Agriculturae Scandinavica, Sect. A. Animal Science* 46, 165–172.

Boisen, S. and Verstegen, M.W.A. (1998a) Evaluation of pig feedstuffs and pig diets: energy or nutrient-based evaluation systems? 1. Limitations of present energy evaluation systems. *Acta Agriculturae Scandinavica, Sect. A. Animal Science* 48, 86–94.

Boisen, S. and Verstegen, M.W.A. (1998b) Evaluation of pig feedstuffs and pig diets: energy or nutrient-based evaluation systems? 2. Proposal for a new nutrient-based evaluation system. *Acta Agriculturae Scandinavica, Sect. A. Animal Science* 48, 95–102.

Chwalibog, A., Jakobsen, K., Henckel, S. and Thorbek, G. (1992) Estimation of quantitative oxidation and fat retention from carbohydrate, protein and fat in growing pigs. *Journal of Animal Physiology and Animal Nutrition* 68, 123–135.

Chwalibog, A., Jakobsen, K. and Thorbek, G. (1996) The pattern of protein retention in pigs from 2 to 120 kg live weight. *Archives of Animal Nutrition* 49, 181–186.

CVB (1999) *Veevodertabel*. Centraal Veevoederbureau, The Netherlands.

Jondreville, C., Van der Broeke, J., Gatel, F. and Van Cauwenberghe, S. (1995) *Ileal Digestibility of Amino Acids in Feedstuffs for Pigs*. Eurolysine/ITCF Publication, Paris, France, 52 pp.

Jørgensen, J.N., Fernandez, J.A., Jørgensen, H. and Just, A. (1985) Anatomical and chemical composition of female pigs and barrows of Danish Landrace related to nutrition. *Zeitschrift für Tierphysiologie, Tierernährung und Futtermittelkunde* 54, 253–263.

Moughan, P.J., Smith, W.C. and Pearson, G. (1987) Description and validation of a model simulating growth in the pig (20–90 kg liveweight). *New Zealand Journal of Agricultural Research* 30, 481–489.

Moughan, P.J., Verstegen, M.W.A. and Visser-Reyneveld, M.I. (1995) *Modelling Growth in the Pig*. EAAP Publication No. 78, Wageningen Pers, Wageningen, 238 pp.

NRC (1998) *Nutrient Requirements of Swine*, 10th revised edn. National Academic Press, Washington, DC, USA, 189 pp.

Pettigrew, J.E., Gill, M., France, J. and Close, W.H. (1992) A mathematical integration of energy and amino acid metabolism of lactating sows. *Journal of Animal Science* 70, 3742–3761.

Rademacher, M., Sauer, W.C. and Jansman, A.J.M. (1999) *Standardized Ileal Digestibility of Amino Acids in Pigs. The New System, 1999*. Degussa-Hüls, Hanau, Germany, 20 pp.

Siebrits, F.K., Kemm, E.H., Ras, M.N. and Barnes, P.M. (1986) Protein deposition in pigs as influenced by sex, type and livemass. 1. The pattern and composition of protein deposition. *South African Journal of Animal Science* 16, 23–27.

Thorbek, G., Chwalibog, A. and Henckel, S. (1984) *Nitrogen and Energy Metabolism in Pigs of Danish Landrace from 20 to 120 kg Live Weight: Norm for Protein and Energy Requirements for Maintenance and Growth*. Report no. 563, National Institute of Animal Science, Copenhagen, Denmark, 114 pp.

15

Second-generation Dynamic Cattle Growth and Composition Models

J.W. Oltjen,[1] A.B. Pleasants,[2] T.K. Soboleva[2] and V.H. Oddy[3]

[1]*Department of Animal Science, University of California, Davis, CA 95616, USA;* [2]*Ag Research, Ruakura Research Centre, Hamilton, New Zealand;* [3]*NSW Agriculture, Cattle and Beef Cooperative Research Center, University of New England, Armidale, New South Wales 2351, Australia*

Abstract

Establishing effective strategies for future improvement of beef production requires integration of knowledge of genetics, nutrition and economics to optimize quality and quantity of beef produced. Failure to achieve an effective strategy negatively impacts on sustainability of both land and market access. The challenge in optimizing is that each of the major system elements interacts dynamically in non-linear ways. Scientific tools to describe each component in static ways are available and under development, as are tools to incorporate non-linear dynamics. Modelling tools combining these into a framework for analysis of a production system allow for development of longer-term strategic planning than permitted with present methods. For the beef industry, the framework and methods used for analysis address the major issues of control of growth (meat yield) and composition. Our objective for the present model is to add the capacity to optimize genetic and resource base management for product yield and quality goals. Previously developed deterministic models of beef cattle growth and composition have been updated by including viscera pools and integrating protein metabolism with energy requirements. The model of DeMarco, based on our earlier work, serves as the basis whereby post-absorptive metabolism of protein is incorporated, using the concepts validated by Sainz for sheep. Genetic parameters have been integrated by converting current breeding value estimates into absolute physiological breeding values as described by Bourdon. Estimates are based on large data-set breed averages (Meat Animal Research Center, Clay Center, Nebraska). Additional concepts of Oddy, Ball and Pleasants for previous nutritional

 Modelling Nutrient Utilization in Farm Animals (eds J.P. McNamara, J. France and D.E. Beever)

effects on meat yield and as affected by age at which nutritional restriction occurs are included. In terms of impacts on producers, this model allows rational evaluation of diverse technical information. With regard to scientific knowledge, the impact is to integrate information about growth, nutrition, management and economics into testable models (hypothesis) of biological system behaviour, as well as identify gaps in technical information from different disciplines.

Introduction

Establishing effective strategies for future improvement of beef production requires the integration of knowledge of genetics, nutrition and economics to optimize the quality and quantity of beef produced. Failure to achieve an effective strategy has a negative impact on the sustainability of both land and market access. The challenge in optimizing strategy is that each of the major system elements interacts dynamically in non-linear ways. Scientific tools to describe each component in static ways are available and under development, as are tools to incorporate non-linear dynamics. Modelling tools combining these into a framework for the analysis of a production system allow for development of longer-term strategic planning than is permitted with present methods. For the beef industry, the framework and methods used for analysis address the major issues of control of growth (meat yield) and composition. Our long-term objective is to add the capacity to optimize genetic and resource-base management for product yield and quality goals. To do this well requires that composition be accurately predicted over a wide range of genetic and resource-input possibilities. In this chapter, methods to predict the composition of beef cattle are presented, starting from simple empirical relationships and adjustments and ending with our current work with dynamic models and new forms for partitioning energy among protein pools.

Whole-body Protein and Fat Prediction

Simpfendorfer (1974) developed a relationship between weight of empty-body fat (EBF, kg) and empty-body weight (EBW, kg) for British-breed beef steers:

$$EBF = 0.037\ EBW + 0.00054\ EBW^2 - 0.610$$

However, cattle on different planes of nutrition systematically vary from this line (NRC, 1996). Garrett (1987) found that the rate of empty-body fat gain (FG, kg day^{-1}) for similar British beef steers depends on EBW and rate of empty-body gain (EBG, kg day^{-1}):

$$FG = 0.007823\ EBW^{0.75}\ EBG^{1.097} - 0.1542\ EBG$$

Alternatively, Keele *et al.* (1992) predict body composition directly, based on rate and trajectory of gain, in a more comprehensive model. Thus, a simple way to

estimate body composition is to add the estimated fat gain over a period to an initial estimate of body fat, potentially taken from the equation of Simpfendorfer (1974), with or without adjustments. For example, TAURUS, a beef cattle ration formulation and performance prediction software package available from the University of California, adjusts for body condition score (CS, 1–9):

$$EBF_{pc} = (0.333 + 0.0833\ CS) \times (SBW - 54.6)/(8.26 + 0.01\ SBW)$$

where EBF_{pc} is percentage empty-body fat and SBW is shrunk body weight (kg). For cattle of different frame size or previous nutritional history, the National Research Council (NRC, 1996) suggests appropriate transformations, using an equivalent weight (EQW) in the equations, assuming cattle have similar body composition at the same degree of maturity (proportion of mature weight):

$$EQW = W\ (SRW/FW)$$

where W is weight, FW is the mature weight of an animal and SRW is the mature weight of the reference animal on which the equations in the system are based. Other systems (SCA, 1990; AFRC, 1993) also use an equivalent weight or maturity concept.

For animals fed similar rations over long periods, with well-defined end-points, the above methods have been quite successful in practice. Where they have been applied to predict composition of gain differences over short periods, such as occur for animals nearing a compositional end-point, or for animals with moderate to severe feed restriction early in growth, large errors have occurred. Fox *et al.* (1972) showed that, early in compensation after a period of feed restriction, increased protein gains occur, and later increased fat is gained compared with what is expected based on the methods above. Gains to 341 kg EBW contained 30% fat, while gains after that to 454 kg EBW contained 54% fat. Simpfendorfer (1974) would predict 35 and 47% fat in EBG, for the period to 341 and from 341 to 454 kg EBW, respectively. Interestingly, control cattle, not undergoing a period of feed restriction, gained 44% fat in both periods.

To precisely track changes in body composition during compensation or for cattle nearing a slaughter end-point, dynamic simulation models have been developed. Oltjen *et al.* (1986) proposed the use of a more general form, based on cell number and size mechanisms of growth, to predict net protein synthesis and integrated the model into the net energy to estimate gain of fat and lean tissue:

$$dDNA/dt\ (g\ day^{-1}) = 0.00429\ (DNAMX - DNA)\ NUT_1$$

$$dPROT/dt\ (kg\ day^{-1}) = 0.0461\ DNA^{0.73}\ NUT_2 - 0.143\ PROT^{0.73}$$

where NUT_1 and NUT_2 are nutritional modifiers, DNAMX is normal DNA content at maturity (assumed 385 g, based on relationships derived by Baldwin and Black (1979)), and PROT is empty-body protein. Parameters were estimated using non-linear least-squares fit of observed initial and final empty-body weights, compositions and metabolizable energy intakes (MEI) for over 1000

feedlot steers (Oltjen *et al.*, 1986). For animals of different mature size, rate constants are adjusted by the size-scaling factor, as proposed by Taylor (1980). Effects of energy intake on growth are added, using the NUT_1 and NUT_2 terms, by defining a ratio:

$$P = MEI/MEI_{NORM}$$

where MEI_{NORM} (MJ day^{-1}) is the pattern of MEI intake to achieve normal growth in the above equations (NUT_1 and NUT_2 equal 1):

$$MEI_{NORM} = (1.821 - 0.00145\ EBW)\ EBW^{0.73}$$

and rates of DNA accretion and PROT synthesis are respectively adjusted:

$$NUT_1 = -0.7 + 1.7\ P$$

$$NUT_2 = 0.83 + 0.2\ P/(0.15 + P)$$

Finally, daily empty-body fat gain is the net energy available after daily feed intake (FI, kg day^{-1}) is used for maintenance (MAINT) and protein gain:

$$MAINT\ (MJ\ day^{-1}) = 0.357\ EBW^{0.75}$$

$$dFAT/dt\ (kg\ day^{-1}) = ((FI\text{-}MAINT/NE_m)\ NE_g - 23.03\ dPROT/dt)/39.02$$

where NE_m and NE_g are net energy for maintenance and gain contents of the feed (MJ kg^{-1}), respectively. Empty-body weight is the sum of fat and fat-free body mass, where fat-free body mass is 22.01% protein (Garrett and Hinman, 1969):

$$EBW = FAT + PROT/0.2201$$

Since the model requires initial estimation of whole body DNA and protein or fat content, empirical relationships between these and animal weight, mature size and condition score are used for implementation (see EBFpc above).

The model was evaluated with respect to its ability to predict growth and composition of steers as affected by nutrition, initial condition, frame size and use of growth promotants. Using two independent data sets, the model predicted empty-body weight and fat content with standard deviations of 14 and 10 kg, respectively (Oltjen *et al.*, 1986). However, fat gain was underpredicted ($P < 0.01$) at high feed-energy concentrations. No adjustment for variable maintenance requirements could be identified in the data sets tested; however, Baldwin and Bywater (1984) have shown other factors normally accounted for within the definition of maintenance do affect energy expenditures. These are not accounted for in NRC (1996) or this model.

Although Oltjen *et al.* (1986) accounted for variations attributable to initial body composition and mature size, their model does not always yield acceptable estimates of fat gain. This is not unexpected, since fat accretion is computed after energy requirements for maintenance and protein gain are satisfied. Thus, any errors in estimates of maintenance or protein gain result in biased fat gain predictions. Further, feed energy available for fat accretion may not necessarily

be used at the same net efficiency as for energy gain of protein, as NRC (1996) assumes. This is why the Oltjen *et al.* (1986) model systematically errs with energy concentration of the diet.

Multiple Protein Pools

To more accurately predict growth on diets with extremes of energy concentration, more complex models which can account for variable maintenance requirements or differing efficiencies of absorbed energy use are needed. Di Marco *et al.* (1989) extended the growth equations used by Oltjen *et al.* (1986) to two pools of protein, body and viscera, two associated DNA pools and a body fat pool. DNA accretion is:

$$\mathrm{dDNA/d}t\ (\mathrm{g\ day^{-1}}) = \mathrm{K_{1i}\ PROT_i^{E_{1i}}\ (1 - DNA_i/DNAMX_i)\ NUT_{1i}}$$

for each protein pool, where K_{1i}, E_{1i} and $DNAMX_i$ (DNA_i content at maturity) are 1.5×10^{-7}, 1.19 and 112 g for body and 1.94×10^{-4}, 0.0967 and 95 g for viscera, respectively, of a reference steer for which DNA was measured (Di Marco *et al.*, 1987). Protein accretion is the difference between synthesis (SYN) and degradation (DEG):

$$\mathrm{SYN = VAaP_i\ PROT_i^{E_{2i}}(PROTMX_i/DNAMX_i - PROT_i/DNA_i)/(1 + KAaP/cAa)}$$

where $VAaP_i$, E_{2i} and $PROTMX_i$ (protein content at maturity) are 1.76×10^{-8}, 2.19 and 909 mol for body and 2.38×10^{-3}, 0.80 and 164 mol for viscera, respectively, KAaP is 0.002 M and cAa is total amino acid concentration in blood (typically 2 mmol l^{-1}).

$$\mathrm{DEG = KPAa_i\ PROT_i^{E_{3i}}\ Chor}$$

where $KPAa_i$ and E_{3i} are 0.027 and 0.87 for body and 0.466 and 0.60 for viscera, respectively, and Chor (catabolic hormones) is 1 for *ad libitum* feeding. Lipogenesis (LG, mol day^{-1}) is represented by the Michaelis–Menten equation:

$$\mathrm{LG = VTs/(1 + KTsF/c + K1Ts/(Ahor\ cGl))}$$

where

$$\mathrm{VTs = FxTs\ WtcytF^{EC}\ WtTs^{EF}}$$

When acetate or fatty acids are the source of fat synthesis, the constants FxTs, EC, EF, KTsF and K1Ts are 0.367, 1.375, 0, 0.0005 and 0.0015, or 0.03, 0.43, 1.03, 0.00015 and 0.0015, respectively. The weight of cytosol in adipose tissue (WtcytF) was set to 4% of total protein weight; triglyceride weight (WtTs) was calculated using reference steer relationships (Di Marco *et al.*, 1987). Other variables are anabolic hormones (Ahor), which was set to 1 for *ad libitum* conditions, plasma glucose (cGl, M), and plasma acetate or fatty acids (c, M). Lipolysis (LY, mol day^{-1}) may be represented:

$$LY = VTsFa/((1 + cFa/0.0001)\ Chor)$$

where cFa is plasma fatty acids and:

$$VTsFa = 0.1563\ WtcytF\ WtTs^{0.68}$$

Next, Di Marco and Baldwin (1989) added digestion and metabolism elements to the growth model. The integrated model, much too complicated to completely describe here, represents digestion as six nutrient fluxes, which are input to a metabolism component of nine state variables. Five of the state variables are from the growth model (body and viscera protein and DNA and fat); the other four are used in the growth model as inputs (plasma amino acids, acetate, lipids and glucose). Energy balance is achieved by ATP transactions, including oxidation, expenditure and nutrient turnover. The authors suggest that the model is useful for studies of complex interactions among diet, feed intake, age, physiological status, body composition, nutrient partitioning and energy costs associated with maintenance and growth. In particular, partial efficiencies of absorbed nutrients for different maintenance and production functions may be evaluated.

Separation of the protein pools by Di Marco *et al.* (1989) may account for variable maintenance requirements, demonstrated by Koong *et al.* (1982), wherein relatively smaller viscera were associated with decreased fasting heat production. Also, the metabolism submodel should correct the errors in prediction of fat gain, since the efficiency of each nutrient's use is explicitly represented. Nutrient prioritization, as in previous models (where fat is simply the energy left over after maintenance and protein gain), is not necessary, since equations representing affinity and use of metabolites allow direct competition for their use. Hence, when tested and accepted, this and similar models will also account for effects of the previous plane of nutrition and interactions between level of feeding and ration energy concentration. Further, the explicit representation of digestion products suggests that feeds must be represented by their chemical constituents in future systems. At present, their complexity and lack of identity (additional experimental data are needed to set parameter values with confidence) preclude general use.

At present we are left with the question, how can we incorporate the energetic effects of differential growth of viscera into today's growth and composition models? This is necessary so that efficiency and composition of gain can be accurately predicted for ruminant animals, which often go through periods of energy restriction. It may also yield an important side-benefit – a prediction of protein in non-visceral pools, which can be related to carcass yield. Although models like those of Di Marco *et al.* (1989) show promise, we are not yet able to accurately characterize feed chemical composition, which is a necessary input to the model. What is needed is an intermediate step, modifying the current feeding systems to partition energy between metabolically active and less active protein tissue.

In a collaborative effort between scientists in New Zealand, Australia and the USA, Soboleva *et al.* (1999) developed a dynamic model of the development

of the viscera (v), muscle (m) and fat (f) pools of a growing sheep. Muscle and viscera each have an upper bound (m^* and v^*, respectively). For muscle, m^* is fixed, although the possibility of reaching this level depends on both the current intake and the nutritional history of the animal. However, v^* is also affected by energy intake and depends on the previous nutrition. As in previous models (Oltjen *et al.*, 1986), net energy intake above maintenance (net energy for gain or retained energy, NEG) is used for viscera and muscle tissue gain before its use for fat accretion. Visceral tissues are more sensitive than muscle to changes of energy intake. Maintenance requirements and heat production are related to energy intake (MEI), but changes in maintenance requirements follow changes in intake with some time delay. This depends on both the magnitude and the duration of the change in energy intake. The model is expressed in terms of energy (kJ):

$$dm/dt = k_m\,(\mathrm{NEG} + c_m f_a)\,(1 - m/m^*)$$

$$dv/dt = k_v\,(\mathrm{NEG} + c_v f_a)\,(1 - v/v^*)^2$$

$$df/dt = \mathrm{NEG} - dm/dt - dv/dt$$

where:

$$v^* = cs_1\,\mathrm{MEI}/(1 + cs_2\,\mathrm{MEI})^2$$

and:

$$f_a = (1 - m/m^*)\,f/\,(f + f_0)$$

so that, if energy intake is near maintenance, body protein can be gained and fat lost in the immature animal. Constants are k_m, k_v, c_m, c_v, cs_1, cs_2 and f_0. Note that k_m and k_v separate the retained energy into m or v, and are not partial energetic efficiencies. The energy driving the growth of muscle and viscera is given by the term NEG:

$$\mathrm{NEG} = \mathrm{MEI} - \mathrm{HP}$$

where HP is total heat production, the sum of heat production for maintenance ($\mathrm{HP}_{\mathrm{maint}}$) and heat production for gain ($\mathrm{HP}_{\mathrm{gain}}$). Heat production for maintenance ($\mathrm{HP}_{\mathrm{maint}}$) is estimated:

$$\mathrm{HP}_{\mathrm{maint}} = \alpha_t\,\mathrm{EBW}^{0.75} + 0.09\,\mathrm{MEI}$$

which is the form of the Corbett *et al.* (1987) equation that partitions maintenance energy into that associated with metabolism and digestion of feed and:

$$\alpha_t = \alpha_0\,(1 + b(\mathrm{MEI}_t/\mathrm{MEI}_0 - 1)(1 - e^{-t/\tau}))$$

results in a lag in change of maintenance requirements after intake changes from MEI_0 to MEI_t. Here b and τ are constants; MEI_0 and α_0 are original values of intake and the maintenance coefficient. The heat production for gain is:

$$\mathrm{HP}_{\mathrm{gain}} = \mathrm{MEI} - \mathrm{HP}_{\mathrm{maint}} - \mathrm{NEG}$$

If one assumes a constant efficiency of feed energy use for gain (k_{gain}):

$$NEG = k_{gain} (MEI - HP_{maint})$$

or:

$$HP = MEI - k_{gain} (MEI - HP_{maint})$$

Otherwise any general form for HP can be used.

Data obtained by Ferrell *et al.* (1986), studying compensatory growth in intact male Suffolk × Rambouillet × Finnish Landrace lambs, were used to test the model. Lambs were assigned to gain 16 (H), 5 (M) or −6 (L) kg during period 1 (42 days), followed by assignments of 27 (S), 16 (H), 5 (M) or −6 (L) kg gain during period 2 in an incomplete 3 × 4 factorial design, with treatments HH, HM, HL, MH, MM, ML, LS, LH and LM (period 1 designated by the first letter and period 2 by the second). There were four lambs per treatment. Data for visceral protein alone were not available, so *v* has been defined as the sum of liver, heart, kidney, spleen and gastrointestinal tract protein, and *m* as the remaining empty-body protein for the example presented here. Measurements were made of the initial and final body weight, average daily energy intake and muscle, viscera and fat weight at slaughter. The dynamic system of three coupled non-linear differential equations was solved numerically, using initial conditions based on the body weight of the animals at the beginning of the trial. We assumed that initial *v* (protein content) was 8.15% of body weight and that *v* was 16.58% of the sum of liver, heart, kidney, spleen and gastrointestinal tract weight. To account for the effect of the level of energy intake on maintenance requirements, the value of α_0 was adjusted relative to the HH treatment, and initial intake (MEI_0) was set to 19,000 kJ day^{-1}. The results at day 84 from the simulation were compared with the measurements made on the animals at this time.

The problem of fitting the unknown parameters to the model is a simultaneous non-linear regression problem, given that the set of differential equations is solved numerically. The estimation involves simultaneous regression, since the same parameters occur in each of the three equations. This means that the estimation must take account of not only the different scales and variances that will occur between the three body components, but also the covariances that will exist between the residuals of these variables. For example, if fat had a greater variance than muscle or viscera, this would make the fat pool much more influential in determining the parameter values than muscle or viscera, unless this greater variance was taken into account in the estimation.

The corollary of least-squares parameter estimation for one equation is to minimize the determinant of the residuals for parameter estimation in simultaneous equations. This is also the maximum-likelihood estimate when the residuals are multivariate normal. The derivation is given in Bates and Watts (1988).

Initially, the parameter estimation was done by solving the set of differential equations numerically, using a Runge-Kutta method with adaptive step-size control (Press *et al.*, 1989) and a continuous-parameter genetic algorithm

(Haupt and Haupt, 1998) to minimize the determinant of the residual covariance matrix of muscle, viscera and fat. These estimates were used as the starting values for estimation, using Markov Chain Monte Carlo (Metropolis–Hastings algorithm, Tanner, 1996). This method also provided estimates of the parameter distributions.

Values for the coefficients in the model, which were chosen empirically to fit Ferrell *et al.* (1986), are given in Table 15.1. A comparison between the model predictions and the results measured by Ferrell *et al.* (1986) for empty-body weight, protein and fat are shown in Table 15.2. Given the uncertainties of the initial conditions, these results show that the model reproduces well the experimental results for the chosen parameters. Simple correlation coefficients of the relationship between parameters (Table 15.3) reveal strong relationships among c_m and f_0 ($r = 0.72$), cs_1 and m^* ($r = -0.71$), f_0 and m^* ($r = 0.67$) and cs_1 and f_0 ($r = -0.65$), suggesting that the equations allowing protein growth at near-zero energy retention are overparameterized and should be simplified. The value of k_m is highly correlated ($r = 0.86$) with fit of the model (DET), suggesting great sensitivity to the partition of NEG to muscle.

This model of animal growth is formulated at the macro level, and is designed to incorporate those features of the relationship between muscle and viscera observed by Jenkins and Ferrell (1983). This interaction was reviewed by Ball *et al.* (1997) in terms of the relationship to compensatory growth in animals – that is, viscera responds faster than muscle to changing energy intake by the animal, but this change has some time-lag. The model predicts that changes in the maintenance requirements of the animal follow changes in the viscera pool, resulting from changes in animal energy intake. This makes maintenance requirement a dynamic variable, depending on the nutritional history as well as the current energy intake. The results from the model are consistent

Table 15.1. Estimates of the parameters in the model of Soboleva *et al.* (1999) for sheep, based on the data of Ferrell *et al.* (1986).

Parameter	Value	Standard deviation	Units
k_m	0.36	0.01	
k_v	0.56	0.02	
c_m	221	10	kJ day^{-1}
c_v	−0.5	0.7	kJ day^{-1}
m^*	351,200	1,086	kJ
cs_1	1.33	0.02	day
cs_2	0.0000214	0.0000005	day kJ^{-1}
f_0	12.3	2.5	kJ
b	0.117	0.006	
τ	48	5	day
α_0	649	28	kJ day^{-1} kg$^{-0.75}$
k_{gain}	0.522	0.009	

Table 15.2. Comparison of model predictions and data of Ferrell *et al.* (1986) for empty-body weight, fat and visceral protein of sheep at 84 days.

	Empty-body weight (kg)		Empty-body fat (%)		Viscera* protein (kg)	
Treatment	Predicted	Observed	Predicted	Observed	Predicted	Observed
LM	21.32	22.76	16.35	17.59	0.283	0.257
LH	27.16	28.97	18.06	19.65	0.388	0.369
LS	33.81	33.98	19.73	18.65	0.485	0.481
ML	22.40	22.64	17.54	16.61	0.220	0.261
MM	30.34	32.55	18.99	21.45	0.406	0.329
MH	38.42	40.50	21.34	23.72	0.476	0.428
HL	32.27	33.12	19.92	18.25	0.374	0.329
HM	40.76	43.45	21.94	23.00	0.492	0.413
HH	47.80	48.11	23.84	24.22	0.534	0.498

* Liver, kidney, gastrointestinal tract, heart and spleen.

with the conjecture that the observed features of compensatory growth follow from the changes in the dynamics of body components in response to both the stage of maturity and feed intake.

The form of the maintenance function used is the traditional form adopted by nutritionists and may not be correct, especially in a dynamic situation. In particular, the estimate of α_0 is 649 kJ day^{-1} kg$^{-0.75}$ seems too high. One of the advantages of the way the model is formulated is that the performance of different functions describing heat production by the animal can be investigated – that is, the fit of the model to data with different functions for MAINT, using either traditional net energy concepts or more general functions for HP, which can be compared to choose the best functional description. Also, the function describing v^* can be refined, and careful analysis of Table 15.3 suggests that systematic biases in model structure, more than parameter value estimation, need further work.

Conclusions

Our hypothesis, expressed in the construction of the system of equations, is that variation in the growth of muscle, viscera and fat in sheep and cattle is moderated by the current size of the muscle and viscera pools relative to the mature weight of muscle and viscera. Mature weight of viscera is affected by energy intake level. Changes in energy intake change maintenance requirements smoothly, but with some delay. For producers, the model described herein allows rational evaluation of diverse technical information. With regard to scientific knowledge, the object is to integrate information about growth, nutrition, management and economics into testable models (hypotheses) of biological system

Table 15.3. Simple correlations between model parameters using Markov Chain Monte Carlo for the data of Ferrell *et al.* (1986).

	k_m	k_v	c_m	c_v	m^*	cs_1	cs_2	f_0	b	τ	α_0	k_{gain}	DET†
k_m	1.00												
k_v	−0.08	1.00											
c_m	0.22	0.34	1.00										
c_v	0.00	0.12	−0.13	1.00									
m^*	0.11	0.08	0.59	−0.34	1.00								
cs_1	−0.23	0.03	−0.56	0.27	−0.71	1.00							
cs_2	0.12	−0.26	−0.49	0.41	−0.56	0.37	1.00						
f_0	0.30	0.15	0.72	−0.14	0.67	−0.65	−0.44	1.00					
b	0.05	0.11	−0.13	0.28	−0.28	0.19	0.32	−0.13	1.00				
τ	−0.24	0.37	0.46	−0.09	0.50	−0.39	−0.52	0.39	−0.08	1.00			
α_0	−0.01	−0.16	−0.44	0.32	−0.38	0.26	0.60	−0.40	0.21	−0.28	1.00		
k_{gain}	0.17	−0.16	−0.27	0.08	−0.11	0.11	0.34	−0.17	−0.05	−0.45	0.36	1.00	
DET	0.86	−0.11	0.24	−0.05	0.20	−0.36	0.11	0.34	0.01	−0.18	−0.15	0.15	1.00

†Determinant of the residual covariance matrix of muscle (*m*), fat (*f*), and viscera (*v*).

behaviour, as well as identifying gaps in technical information from different disciplines.

References

AFRC (1993) *Energy and Protein Requirements of Ruminants*. CAB International, Wallingford, UK, 159 pp.

Baldwin, R.L. and Black, J.L. (1979) *Simulation of the Effects of Nutritional and Physiological Status on the Growth of Mammalian Tissues: Description and Evaluation of a Computer Program*. Animal Research Laboratories Technical Paper No. 6, Commonwealth Science and Industrial Research Organization, Melbourne, Australia, 35 pp.

Baldwin, R.L. and Bywater, A.C. (1984) Nutritional energetics of animals. *Annual Reviews of Nutrition* 4, 101–114.

Ball, A.J., Oddy, V.H. and Thompson, J.M. (1997) Nutritional manipulation of body composition and efficiency in ruminants. In: Corbett, J.L., Choct, M., Nolan, J.V. and Rowe, J.B. (eds) *Recent Advances in Animal Nutrition in Australia*. Department of Animal Science, University of New England, Armidale, New South Wales, Australia, pp. 192–208.

Bates, D.M. and Watts, D.G. (1988) *Nonlinear Regression Analysis*. John Wiley & Sons, New York, 365 pp.

Corbett, J.L., Freer, M. and Graham, N.McC. (1987) A generalised equation to predict the varying maintenance metabolism of sheep and cattle. In: Moe, P.W., Tyrell, H.F. and Reynolds, P.J. (eds) *Energy Metabolism.* Rowmam and Littlefield, Totowa, New Jersey, pp. 62–65.

Di Marco, O.N. and Baldwin, R.L. (1989) Implementation and evaluation of a steer growth model. *Agricultural Systems* 29, 247–265.

Di Marco, O.N., Baldwin, R.L. and Calvert, C.C. (1989) Simulaton of DNA, protein and fat accretion in growing steers. *Agricultural Systems* 29, 21–34.

Di Marco, O.N., Baldwin, R.L. and Calvert, C.C. (1987) Relative contributions of hyperplasia and hypertrophy to growth in steers. *Journal of Animal Science* 65, 150–157.

Ferrell, C.L., Koong, L.J. and Nienaber, J.A. (1986) Effect of previous nutrition on body composition and maintenance energy costs of growing lambs. *British Journal of Nutrition* 56, 595–605.

Fox, D.G., Johnson, R.R., Preston, R.L., Dockerty, T.R. and Klosterman, E.W. (1972) Protein and energy utilization during compensatory growth in beef cattle. *Journal of Animal Science* 34, 310–318.

Garrett, W.N. (1987) Relationship between energy metabolism and the amounts of protein and fat deposited in growing cattle. In: Moe, P.W., Tyrell, H.F. and Reynold, P.J. (eds) *Energy Metabolism of Farm Animals*. EAAP Publ. 32. Rowman and Littlefield, Totowa, New Jersey, pp. 98–101.

Garrett, W.N. and Hinman, N. (1969) Re-evaluation of the relationship between carcass density and body composition of beef steers. *Journal of Animal Science* 28, 1–5.

Haupt, R.L. and Haupt, S.E. (1998) *Practical Genetic Algorithms*. John Wiley & Sons, New York, 177 pp.

Jenkins, T.G. and Ferrell, C.L. (1983) Nutrient requirements to maintain weight of mature nonlactating, nonpregnant cows of four diverse breed types. *Journal of Animal Science* 56, 761–770.

Keele, J.W., Williams, C.B. and Bennett, G.L. (1992) A computer model to predict the effects of level of nutrition on composition of empty body gain in beef cattle: I. Theory and development. *Journal of Animal Science* 70, 841–857.

Koong, L.J., Ferrell, C.L. and Nienaber, J.A. (1982) Effects of plane of nutrition on organ size and fasting heat production in swine and sheep. In: Ekern, A. and Sundstøl, F. (eds) *Energy Metabolism of Farm Animals*. EAAP Publication 29, Agriculture University of Norway, Lillihammer, Norway, p. 245.

NRC (1996) *Nutrient Requirements of Beef Cattle*, 7th revised edn. National Academy Press, Washington, DC, 242 pp.

Oltjen, J.W., Bywater, A.C., Baldwin, R.L. and Garrett, W.N. (1986) Development of a dynamic model of beef cattle growth and composition. *Journal of Animal Science* 62, 86–97.

Press, W.H., Flannery, B.P., Teukolsky, S.A. and Vetterling, W.T. (1989) *Numerical Recipes in Pascal*. Cambridge University Press, Cambridge, 759 pp.

SCA (1990) *Feeding Standards for Australian Livestock: Ruminants*. CSIRO, Melbourne, Australia, 266 pp.

Simpfendorfer, S. (1974) Relationship of body type, size, sex, and energy intake to the body composition of cattle. PhD thesis, Cornell University, Ithaca, New York.

Soboleva, T.K., Oddy, V.H., Pleasants, A.B., Oltjen, J.W., Ball, A.J. and McCall, D.G. (1999) A dynamical model of body composition in sheep. *Proceedings of the New Zealand Society of Animal Production* 59, 275–278.

Tanner, M.A. (1996) *Tools for Statistical Inference*, 3rd edn. Springer, New York, 207 pp.

Taylor, StC.S. (1980) Genetic size-scaling rules in animal growth. *Animal Production* 30, 161–185.

16

Modelling Interactions Between Cow Milk Yield and Growth of its Suckling Calf

F. Blanc,[1] J. Agabriel[2] and P. Sabatier[3]

[1]*ENSAM-INRA, Productions Animales, 9 Place Viala, 34060 Montpellier Cedex 1, France;* [2]*INRA, URH, 63122 St Genès Champanelle, France;* [3]*ENV Lyon, 1 avenue Bourgelat, 69280 Marcy l'Etoile, France*

Abstract

A simple mechanistic model of the relationship between cow milk production and suckling calf growth is described. In this model, milk secretion of the mammary gland is regulated through the amount of milk currently present in the udder (short-term regulation) and through the amount of the cumulative residual milk (long-term regulation). At each suckling, the amount of milk drunk by the calf is used to satisfy its energy requirements for maintenance and growth. The relationship between cow milk production and the calf 's growth is studied through the amounts of milk taken off at each suckling and through the suckling frequency.

Simulations reveal the impact of the milk secretion level, calf birth weight and suckling frequency on calf 's growth. It appears that the calf 's growth is higher when the suckling frequency increases and that the effect of calf birth weight on its post-partum growth is highly dependent on the mother's milk secretion level. The response of the dam to the amounts of the milk taken off by the calf depends highly on the sensitivity of the mammary gland to the negative action of the residual milk.

Introduction

The production of suckler herds relies mainly on two major factors – the number of weaned offspring per cow per year and the calf weight at weaning. In French beef cattle systems, the calf is reared by its dam for 6–9 months. During the suckling period, when the calf follows its mother, it suckles seven to eight

 Modelling Nutrient Utilization in Farm Animals (eds J.P. McNamara, J. France and D.E. Beever)

times a day for about 10 min at each time (Albright and Arave, 1997). In France, in some traditional situations, cow and calf are reared separately and are brought together twice a day for a 15 min suckling period. From birth to weaning, calf live-weight gain is closely linked to the amounts of available milk, which depend both on the calf milk intake capacity and on the level of cow milk production. Cow milk production mainly depends on its genetic potential but is further modulated by nutritional factors and other environmental factors, including calf behavioural effects, acting through the intensity and the frequency of milk removal from the udder. Numerous studies showed the influence of the calf on the dam's milk output and on the shape of the lactation curve. In the Salers breed (a French hardy breed), it has been clearly demonstrated that the cow's milk production is increased by the number of suckled calves (Petit *et al.*, 1978), thus illustrating the adaptive capacity of the cow's mammary gland to this stimulation. It has also been shown that the daily frequency of suckling may alter milk secretion. Available data are, however, lacking to fully describe the milk secretion response of the suckling cow according to varying suckling patterns. Furthermore, the literature has described the existence of reciprocal cow–calf interactions, which may influence calf growth through changes in the milk production of its dam. The functional mammary gland is the limiting element of the cow–calf system, as its response is the result of numerous regulatory processes, which are explored in the present model. Our objective was to predict the time courses of the milk output of the suckler cow and the growth of the calf by means of a simple mechanistic model, which integrates an interaction between the dam and its offspring through the suckling patterns. This model is derived from the concept of a previous model depicted by Neal and Thornley (1983), and is associated with an empirical model (INRA, 1978) depicting the conversion of the milk energy intake into growth.

Description of the Model

Hypotheses

The dam–offspring system operates only during the rearing period, when the calf 's diet is exclusively made of milk (until 40 days after parturition). The suckler cow is characterized by its milk production potential and its udder milk-stocking capacity. The calf is characterized by its growth potential, which is assumed to depend only on birth weight. In order to simplify the analysis of this system, the environment (breeding conditions, cow feeding, animal health, etc.) is assumed not to interfere with the system. Under these hypotheses, the cow and its calf can fully express their respective potential of milk production and growth.

Identification of state variables and flux

The overall scheme is shown in Fig. 16.1. This model includes three state variables: the number of the mammary secretory cells, the amount of milk in the udder and the live-weight of the calf. The variables and parameters of the model are listed in Table 16.1.

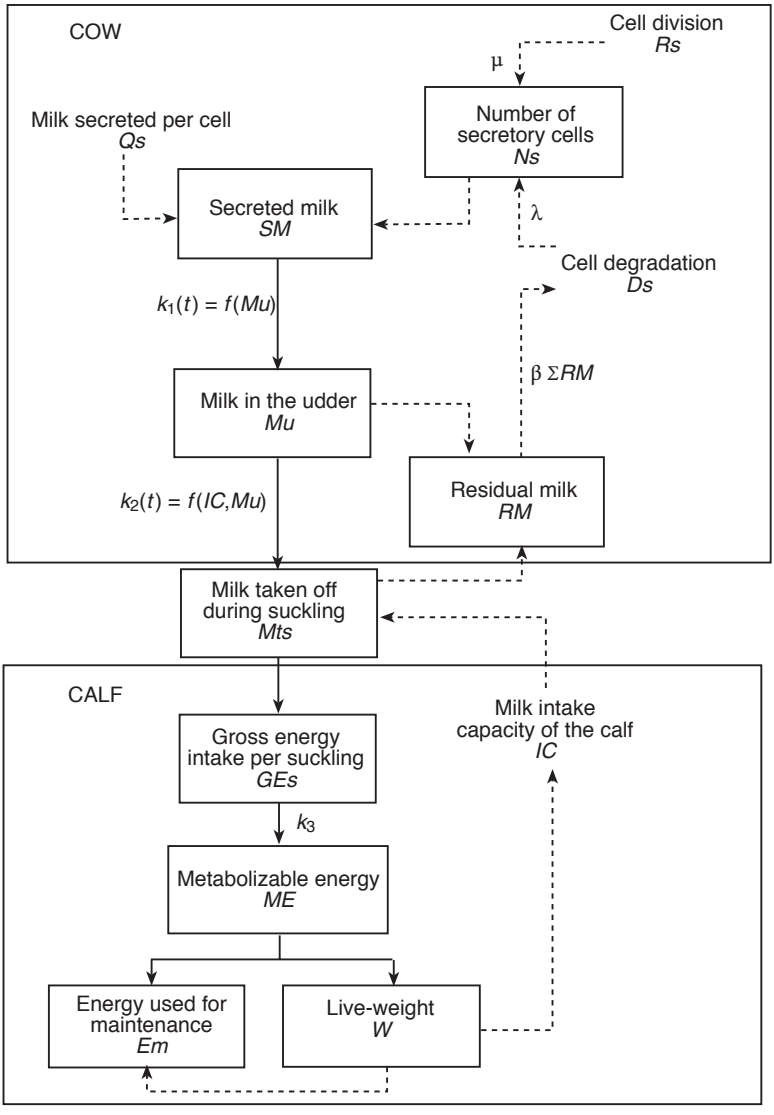

Fig. 16.1. Model of the suckling cow–calf system. Solid lines denote processes of transformation or transport; broken lines denote the influence of one variable on another one.

Table 16.1. Principal variables and parameters of the model.

	Description	Symbol	Unit	Reference value	Sensitivity*
Independent variable	Time	t	h	–	
State variables	Number of secretory cells	Ns	–	–	
	Milk in the udder	Mu	kg	–	
	Live-weight of the calf	W	kg	–	
Other variables and quantities	Secreted milk	SM	kg	–	
	Cumulative residual milk	RM	kg	–	
	Milk taken off during the suckling	Mts	kg	–	
	Gross energy intake per suckling	GEs	kJ	–	
	Metabolizable energy	ME	kJ	–	
	Energy for maintenance	Em	kJ	–	
	Energy for growth	Eg	kJ	–	
	Milk intake capacity of the calf	IC	kg	–	
Parameters	Cell milk secretion rate	Qs	kg h^{-1}	2.1×10^{-4}	++
	Cell division rate	μ	h^{-1}	8.4×10^{-4}	++
	Basal cell degradation rate	λ	h^{-1}	9×10^{-4}	+
	Sensitivity to the residual milk	β	$kg^{-1}\,h^{-1}$	5×10^{-5}	–
	Filling rate	δ	–	0.75	++
	Parameter of the growth function	k_{em}	kJ	418	+
	Parameter of the growth function	k_w	kJ h kg^{-2}	0.9	++
	Parameter of the growth function	$p1$	–	0.355	++
	Parameter of the growth function	$p2$	–	0.833	++
	Parameter of IC	α	–	0.2	+
	Allometry coefficient for IC	θ	–	0.75	+++
	Maximal milk capacity of the udder	Mu_{max}	kg	15	–
	Maximum number of secretory cells	Ns_{max}	–	8000	++
	Calf birth weight	W_{ini}	kg	40	++
	Initial number of secretory cells	Ns_{ini}	–	800	–

* The indicator of sensitivity is $S = \left| \frac{(W_{p+10} - W_{p-10})}{W_{p_{ref}}} \right|$, with W_{p+10} = simulated value of W for a parameter value set to $p = p_{ref} + 10\% \times p_{ref}$ and W_{p-10} = simulated value of W for a parameter value set to $p = p_{ref} - 10\% \times p_{ref}$.
–, $S \leqslant 1\%$; +, $1\% < S \leqslant 5\%$; ++, $5\% < S \leqslant 10\%$; +++, $S > 10\%$.

Secretory cells

Similarly to Neal and Thornley (1983), time variations of the milk production level were assumed to depend only on the time course of the number of secretory cells (Ns). The quantity of milk secreted per cell (Qs) is assumed to be constant during lactation. Thus, Qs is a parameter that may alter the milk potential. The number of secretory cells (Ns) was assumed to be the net result of cell divi-

sions (*Rs*) and cell degradations (*Ds*). The cell division rate, μ, is assumed to be constant, while cell degradation is assumed to have two components:

- the natural death rate, λ, which is constant;
- the degradation induced by the cumulative residual milk (*RM*), which represents a long-term regulation of the milk secretion modulated by the intensity of the removals made by the calf. This degradation is inflected by the parameter β, which represents the sensitivity of the cow to the residual milk.

These assumptions lead to the following differential equation:

$$\frac{\mathrm{d}Ns}{\mathrm{d}t} = \begin{array}{l}\text{cell division} - \text{cell natural death} - \text{cell degradation induced} \\ \text{by the residual milk}\end{array}$$

$$\frac{\mathrm{d}Ns}{\mathrm{d}t} = Rs - Ds = \mu \times (Ns_{\max} - Ns) - \left[\lambda \times Ns + (\beta \times RM) \times Ns\right] \quad (1)$$

where *RM* is the cumulative residual milk since the first suckling.

Milk content of the mammary gland

Milk that is stored in the udder (*Mu*) and available for the calf is assumed to result from two opposite fluxes, the filling flux and the removal flux.

FILLING FLUX. The filling flux depends on the milk secretion potential, i.e. maximal (*SM*), and on a time-dependent filling function $k_1(t,Mu)$. *SM* is the result of both the actual number of secretory cells and the amount of milk secreted per cell:

$$SM(t) = Ns(t) \times Qs$$

$k_1(t,Mu)$ is a growth function, which integrates the described (Wilde and Peaker, 1990) short-term regulation of milk secretion, related to the amount of milk currently present in the udder (*Mu*). $k_1(t,Mu)$ describes the decrease of the milk filling flux parallel to the increase of the udder filling level:

$$k_1(t,Mu) = \delta\left(1 - \frac{Mu(t)}{Mu_{\max}}\right)$$

where $Mu_{\max}$ is the maximal milk capacity of the udder.

REMOVAL FLUX. The removal function (milk drunk or taken off per suckling: *Mts*) has a time component ($k_2(t)$), which determines the suckling frequency, and a quantitative component, which characterizes the importance of the milk removed by the calf. $k_2(t)$ is a pulse function, whose value is 1 during the suckling bout and 0 at other times. Each suckling is assumed to last 10 min

and to start at definite times. The amount of milk removed during the suckling is assumed to depend on the milk intake capacity of the calf (*IC*) and on the amount of milk present in the udder just before suckling (*Mu*):

Amount of milk taken off per suckling (*Mts*)
- If $IC \geqslant Mu_{\text{present just before suckling}}$ then $Mts = Mu_{\text{present just before suckling}}$
- If $IC < Mu_{\text{present just before suckling}}$ then $Mts = IC$

IC is assumed to depend only on the live-weight (*W*) of the calf by the following allometric relationship: $IC = \alpha\, W^{\theta}$, where α and θ are constants.

The time course of *Mu* is then described by the following differential equation:

$$\frac{\mathrm{d}Mu}{\mathrm{d}t} = \text{secreted milk} - \text{milk taken off during suckling}$$

$$\frac{\mathrm{d}Mu}{\mathrm{d}t} = k_1(t, Mu) \times SM - Mts = k_1(t, Mu) \times Qs \times Ns - k_2(t) \times Mts \qquad (2)$$

Calf live-weight

The live-weight of the calf (*W*) varies according to the level of energy intake, because, during the first weeks of the calf 's life, milk is its only source of energy. The gross energy intake at each suckling (*GEs*) depends on *Mts* and on milk composition (Sjaunja *et al.*, 1991):

$$\text{Milk gross energy (kJ kg}^{-1}) = 38.25 \times \text{F} + 24.16 \times \text{P} + 16.51 \times \text{L} + 20.69$$

with concentrations of fat (F), protein (P) and lactose (L) in g kg^{-1}. In the present situation, milk composition is assumed to be constant (i.e. F = 45; P = 35 and L = 48 (g kg^{-1})), so that the gross energy content is 3380 kJ kg^{-1} milk. Only the metabolizable energy, ME, is used for maintenance and growth requirements. The conversion coefficient from gross to metabolizable energy available for the calf equals $k_3 = 0.868$ (INRA, 1978), i.e. the milk drunk provides 2918 kJ ME kg^{-1}. Maintenance energy requirements of the calf (Em) depend on its body weight, according to the following relationship:

$$\text{Em(kJ)} = k_{\text{em}} W^{0.75}$$

where $k_{\text{em}} = 418$ kJ of ME (INRA, 1978).

The time course of the calf 's weight is a function of the amount of the metabolizable energy remaining above maintenance energy requirements (ME − Em) and follows this differential equation:

$$\frac{\mathrm{d}W}{\mathrm{d}t} = f(\text{ME} - \text{Em})$$

Two situations may occur:

- The available metabolizable energy is greater than maintenance energy requirements, so that:

$$\frac{dW}{dt} = \left(\frac{ME - Em}{kw \times W^{p1}} \right)^{p2} \quad (3)$$

  where $Em = k_{em} \times W^{0.75}$ (INRA, 1978).
- The available metabolizable energy is lower than maintenance energy requirements. In such a case, the calf mobilizes body fat reserves and growth is affected. The efficiency of conversion of body fat into energy for maintenance is assumed to be 0.8, so that 1 g of mobilized body lipid will provide 31.3 kJ of ME (Agabriel and Petit, 1987). The variation of the weight is assumed to be equal to the variation of the amount of body lipids mobilized to satisfy the maintenance energy requirements:

$$\frac{dW}{dt} = \left(\frac{ME - Em}{31.3} \right) \quad (4)$$

Experimental data set

Milk measurements were obtained on 20 Salers and 20 Limousin cow–calf pairs. Controls started from the day following calving until 40 days post-partum and were made twice a week. In this trial, dams and offspring were reared separately. Calves had access to their mother twice a day, at 7 a.m. and 4 p.m. for 10 min. Milk controls consisted in weighings just before and after suckling (Le Neindre, 1973). Thus two types of data were available: the weight of the calves and the amounts of milk suckled.

Numerical assumptions

Few data are available in the literature to determine the values of the different parameters of the model. The same values as those of Neal and Thornley (1983) were chosen for *Qs* and initial *Ns* (Ns_{ini}). Furthermore, Mu_{max} was assumed to be lower in a suckled than in a dairy cow, so Mu_{max} was set at 15 kg. Furthermore, θ was set to 0.75, so that the milk intake capacity of the calf (*IC*) was proportional to its metabolic weight. The parameters of equation 3 were set to the adjusted values obtained from Holstein calves (INRA, 1978). Values of the other parameters were graphically fitted on Salers experimental data.

Results and Discussion

Behaviour of the system

Simulations were undertaken in contrasting situations, such as when the cow's milk production could be limiting ($Mu < IC$), or not ($Mu \geqslant IC$, the calf being unable to take off the whole available udder milk at suckling) (Fig. 16.2), or when residual milk (RM) left at each suckling exerted its negative effect on the number of secretory cells.

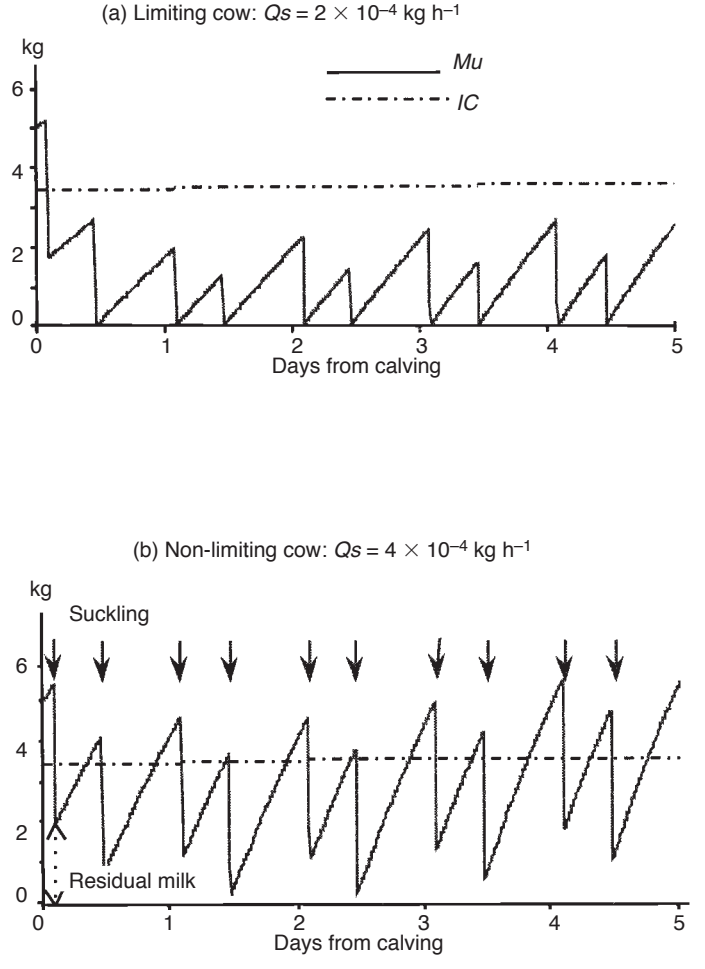

Fig. 16.2. Simulated time courses of the milk in the udder (*Mu*) and the milk intake capacity of the calf (*IC*) illustrating situations when the dam milk secretion level is limiting (a) and when it is not (b). Common parameter values are indicated in Table 16.1 except when specified in figures.

Time courses of predicted calf weight and calf milk intake capacity both fit well with average observed values in Limousin animals (Fig. 16.3). From previous *in vivo* studies, it can be considered that the main differences between these two breeds is the milk potential (D'hour *et al.*, 1995) and the calf birth weight (the mean W_{ini} of Limousin calves is 5 kg lower than that of Salers). Besides, this breed difference is well described by the model simply changing the *Qs* and W_{ini} parameters.

Sensitivity analysis

We considered the weight of the calf at 40 days of age as the response of the model. The sensitivity of the model to a ±10% variation of the different parameters is reported in Table 16.1. The calf live-weight is highly sensitive to parameters that determine the milk secretion level of the dam (*Qs*, μ, Ns_{max}) and also to parameters that play a part in the conversion of the energy intake into live-weight gain (parameters of equation 3). Concerning the initial values of the variables, the model appears mainly sensitive to the calf birth weight (W_{ini}).

Simulated effect of the dynamics of milk removal

The system's trajectory varies with suckling frequency (Table 16.2). The main gap is observed between a single daily suckling and a twice-a-day suckling. In the first case, the cumulative residual milk increases greatly between days 10 and 30, which induces a decrease of the number of secretory cells. Thus, calf growth is very limited (260 g day^{-1} vs. 905 g day^{-1}). In the case of the single suckling situation, simulation shows that the milk intake capacity of the calf (*IC*) is the first limiting factor, while, in the other situations ($\geqslant$ two sucklings a day), the level of milk secretion becomes limiting. The amount of milk taken off at each suckling is inversely related to suckling frequency (*Mu* just before suckling is lower than *IC*). When the number of daily sucklings is greater than two, the amount of residual milk remains low and there is little negative effect on the milk yield of the cow.

However, when the suckling frequency is high, the model seems to overestimate the calf live-weight gain (1190 g day^{-1} with eight sucklings per day). The present model does not take into account a possible satiety effect, which may operate along with the suckling process. This satiety effect may also operate in the case of two successive sucklings occurring at a short time interval and would reduce the amount of milk removed from the udder. Such a satiety coefficient (for example, ranging from 1 to 0 in a defined time range) could be inserted in the mathematical expression of *IC*.

(a) Time course of calf live-weight (*W*) in the case of a system with two sucklings a day (07.00 and 16.00).

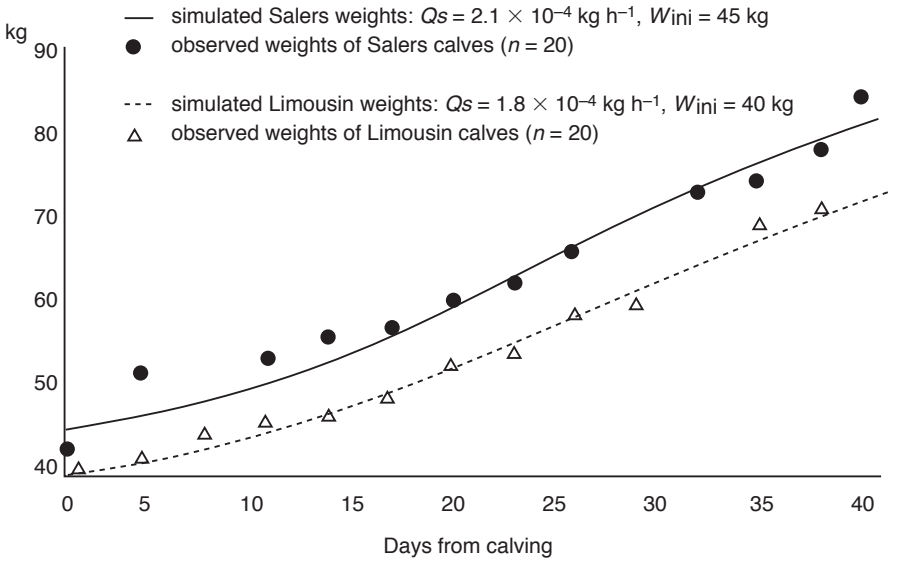

(b) Time course of calf milk intake capacity (*IC*) in the case of a system with two sucklings a day (07.00 and 16.00).

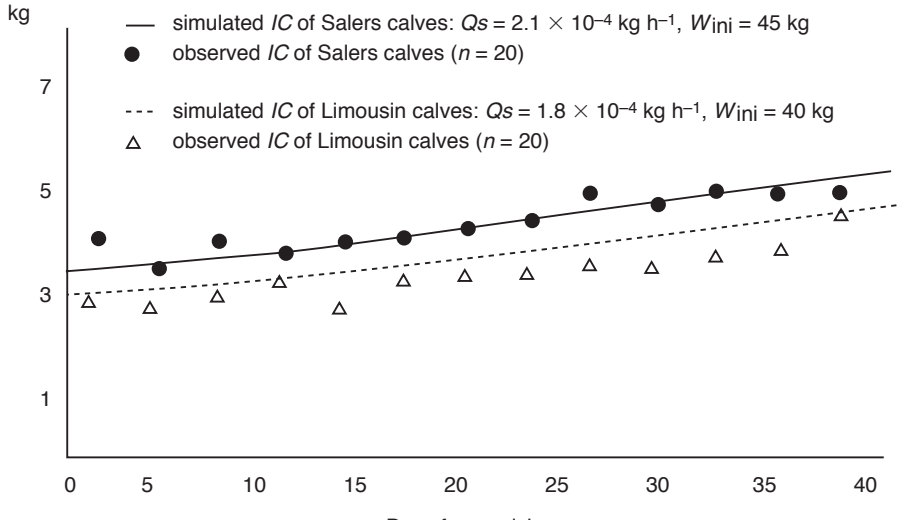

Fig. 16.3. Comparison between observed and simulated time courses of calf live-weight (a) and calf milk intake capacity (b), changing the cell milk secretion rate (*Qs*) and the calf birth weight (W_{ini}) to take into account different among cattle breeds: Salers (S) and Limousin (L). Common parameter values are indicated in Table 16.1 except when specified in figures.

Table 16.2. Simulated effects of suckling frequency on the number of secretory cells after 40 days, the cumulative residual milk during a 40-day period and the calf weight at the age of 40 days.

Suckling frequency	Once a day	Twice a day	Eight times a day
Number of secretory cells*	1040	3064	2713
Cumulative residual milk (kg)	101.3	4.9	15.4
Calf live-weight (kg) (birth live-weight = 45 kg)	55.4	81.2	92.6

* Arbitrary unit.

Simulated effect of the milk secretion potential of the cow on the growth of its calf

Qs partly determines the cow's milk potential. For increasing *Qs* values, ranging from 1×10^{-4} to 3×10^{-4} kg cell^{-1} h^{-1}, calf live-weight gains simulated in the 40-day period following calving increase (Table 16.3). When *Qs* is above the upper range, i.e. $> 3 \times 10^{-4}$ kg cell^{-1} h^{-1}, cow's milk production at the start of the lactation is greater than calf milk intake capacity: the residual milk increases at each suckling and induces its negative retroaction on the secretory cells and a decrease of the milk production. Hence the cow milk production becomes limiting around the 30th day of lactation (when $Qs = 4 \times 10^{-4}$ and $W_{ini} = 45$ kg) and the time course of the calf weight bends. Such a retroaction cannot be analysed through simple *in vivo* experimentation.

Simulated effect of the milk intake capacity of the calf

As expressed in this model, the milk intake capacity of the offspring depends on its live-weight, which, in turn, depends strongly on its birth weight (W_{ini}). The effect of the calf birth weight on its subsequent growth differs according to the milk production level of the cow (Fig. 16.4). When the cow milk production is limiting, the growth of the lightest calves at birth is higher than that of the heaviest calves. However, when the milk production of the cow is not limiting,

Table 16.3. Simulated effect of the milk secretory potential of the mammary cells (*Qs*) on the calf live-weight gain.

Qs (kg cell^{-1} h^{-1})	1×10^{-4}	2×10^{-4}	3×10^{-4}	4×10^{-4}
Calf live-weight at 40 days (kg) (birth live-weight = 45 kg)	58.8	80.3	91.6	91.3
Live-weight gain between 0 and 40 days (g day^{-1})	345	882	1165	1150

(a) Cow milk production limiting: $Qs = 2.1 \times 10^{-4}$, $\beta = 5 \times 10^{-5}$, $Mu_{max} = 15$, $Ns_{ini} = 800$

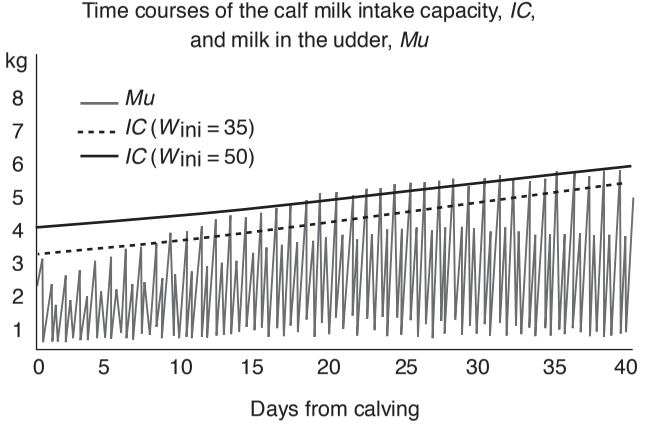

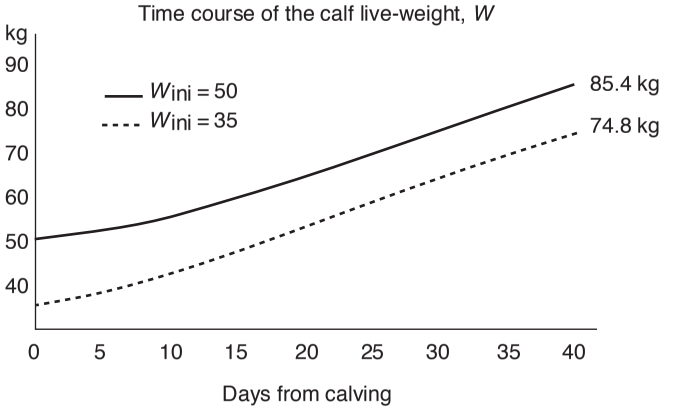

(b) Cow milk production non-limiting: $Qs = 3.5 \times 10^{-4}$, $\beta = 5 \times 10^{-6}$, $Ns_{ini} = 1000$

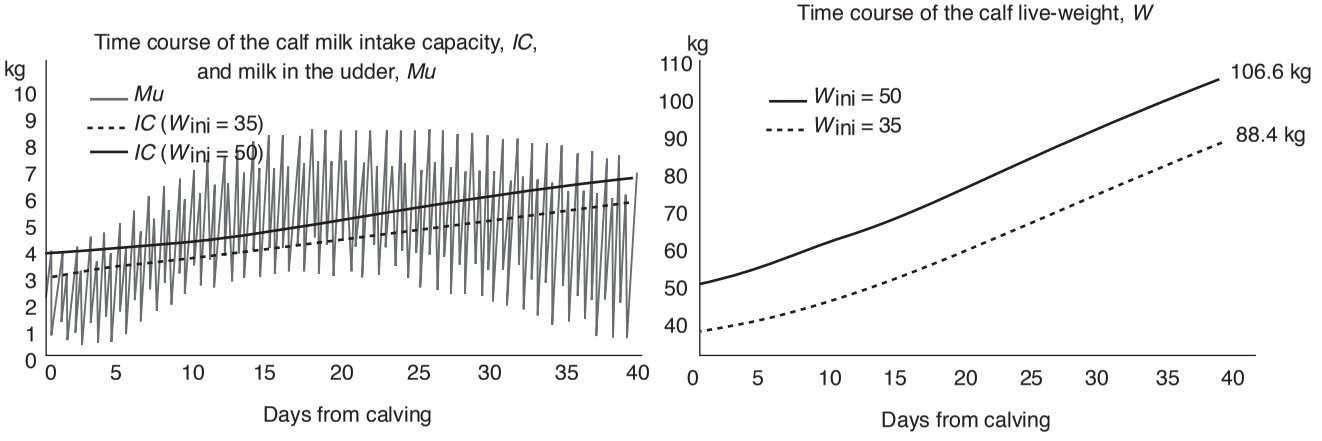

Fig. 16.4. Simulated effect of calf birth weight (W_{ini}) on the time courses of milk in the udder (*Mu*), calf milk intake capacity (*IC*) and calf live-weight (*W*), changing parameters of the cow milk production level (Qs, β, N_{sini}) to depict situations where the cow milk production is limiting (a) or not (b). Common parameters values are indicated in Table 16.1 except when specified in figures.

the calves that were the heaviest at birth achieve the best growth: a difference of 10 kg at birth is translated into differences in daily weight gains of from 40 to 65 g day^{-1}.

Simulated effects of the interaction between the sensitivity of the cow to the residual milk and the calf birth weight on the growth

The time course of the number of secretory cells is highly sensitive to changes in the value of the β parameter, which characterizes the sensitivity of the mammary gland to the residual milk. In the case when the milk production of the cow is not limiting at the beginning of lactation (Ns_{ini} =1000, $Qs = 3.5 \times 10^{-4}$), an increase of the β parameter induces a global decrease of the number of secretory cells. Moreover, the maximum of milk secretion is reached earlier, the persistence decreases, the milk production of the cow becomes rapidly limiting and the daily live-weight gain of the calf declines.

For a given birth weight, the model predicts that the weight gains of the calf will be higher if its dam is relatively insensitive to the effect of residual milk (Table 16.4). Furthermore, at a given level of sensitivity to the residual milk, the calf weight gains increase with birth weight. The model reveals an interaction between these two factors (Table 16.4): there is a combination of the β parameter and W_{ini} where the trajectory of the system goes through an optimum regarding calf growth performance (weight gain maximum in regard to the birth weight). Thus, when β successively equals 5×10^{-6}, 5×10^{-5} and 5×10^{-4}, a difference of 10 kg at birth (45 kg − 35 kg) is respectively expressed by a difference of 12.7, 15.6 and 15.8 kg at 40 days.

Conclusions and Prospects

This model makes it possible to separate the respective influences of the dam and its offspring on the elaboration of the calf growth performance, because its originality relies on the dynamic link between these two subsystems. The interest of

Table 16.4. Simulated body weight (kg) of the calf at 40 days according to the sensitivity of the cow to the residual milk (β) and to the calf birth weight (W_{ini}). Growth (g day^{-1}) during the 40 days post-partum period is indicated in parentheses.

	β		
W_{ini}	5×10^{-6}	5×10^{-5}	5×10^{-4}
35	88.4 (1335)	75.5 (1012)	60.4 (635)
40	95.1 (1377)	83.8 (1095)	69.9 (747)
45	101.1 (1402)	91.1 (1152)	76.2 (780)
50	106.6 (1415)	98.0 (1200)	82.2 (805)

this model lies in the fact that it reports situations where the dam and the offspring are limiting. Concerning the dam, two levels of regulation of the milk production were studied. The first one concerns the effect of potential milk secretion of the mammary gland which, for an individual, is the number of secretory cells and, among individuals, the milk secretion level per cell. The second regulation process links the number of secretory cells to the intensity and frequency of milk removals performed by the calf.

The mammary gland submodel could be improved in two ways. Firstly, *Qs* should vary with lactation (Knight and Peaker, 1984) and according to the nutritional level of the cow (D'hour *et al*., 1995). It would also be of interest to modulate in time the negative influence of the residual milk on the number of secretory cells, so that the lactation curve could exhibit various maxima. An alternative could be to consider the cumulative effect of residual milk on a shorter period, which may be of greater physiological significance.

The reciprocal effect of the calf on the milk production of its dam has been mainly approached through its milk intake capacity, which is assumed to vary according to birth weight. The simulations revealed that the effect of birth weight on the growth closely depends on the milk secretion level of the mother. The calf submodel can be improved by using a mechanistic model of growth, such as that described by Gerrits *et al.* (1997).

Lastly, this model will have to be validated and thereafter extended to the whole rearing period when the calf diet is composed of milk and solid food, in order to be able to predict the time course of the live-weight from parturition to weaning. Furthermore, this model could be adapted to other mammalian species in which suckling is important for offspring performances and/or survival.

References

Agabriel, J. and Petit, M. (1987) Recommandations alimentaires pour les vaches allaitantes. *INRA, Bulletin Technique* 70, 153–166.

Albright, J.L. and Arave, C.W. (1997) *The Behaviour of Cattle*. CAB International, Wallingford, UK, 306 pp.

D'hour, P., Petit, M., Pradel, P. and Garel, J.P. (1995) Evolution du poids et de la production laitière au pâturage de vaches allaitantes Salers et Limousines dans deux milieux. *Rencontres Recherche Ruminants* 2, 105–108.

Gerrits, W.J.J., Dijkstra, J. and France, J. (1997) Description of a model integrating protein and energy metabolism in preruminant calves. *Journal of Nutrition* 127, 1229–1242.

INRA (1978) *Alimentation des ruminants*. INRA Editions, Versailles, 471 pp.

Knight, C.H. and Peaker, M. (1984) Mammary development and regression during lactation in goats in relation to milk secretion. *Quarterly Journal of Experimental Physiology* 69, 331–338.

Le Neindre, P. (1973) Observations sur l'estimation de la production laitière des vaches allaitantes par la pesée du veau avant et après la tétée. *Annales de Zootechnie* 22, 413–422.

Neal, H.D.S.C. and Thornley, J.H.M. (1983) The lactation curve in cattle: a mathematical model of the mammary gland. *Journal of Agricultural Science, Cambridge* 101, 389–400.

Petit, M., Garel, J.P. and Le Neindre, P. (1978) Allaitement de deux veaux par des vaches de race Salers. I. Productions comparées de vaches allaitant 1 ou 2 veaux. *Annales de Zootechnie* 27, 533–551.

Sjaunja, L.O., Baevre, L., Junkkarinen, L., Pedersen, J. and Setala, J. (1991) A Nordic proposal for an energy corrected milk (ECM) formula. In: *Proceedings of the 27th Biennial Session of the International Committee for Animal Recording (ICAR), Paris, France, 2–6 July 1990*. EAAP Publication, No. 50, pp. 156–157.

Wilde, C.J. and Peaker, M. (1990) Autocrine control in milk secretion. *Journal of Agricultural Science, Cambridge* 114, 235–238.

17

A Mechanistic Dynamic Model of Beef Cattle Growth

Thierry Hoch and Jacques Agabriel

Unité de Recherche sur les Herbivores, Institut National de la Recherche Agronomique (INRA), Centre de Clermont-Theix, 63122 Saint Genès Champanelle, France

Abstract

This chapter presents a mechanistic dynamic model that aims to predict variations of protein and lipid contents of beef cattle carcass. Proteins and lipids in carcass and non-carcass tissues have been distinguished to account for the different energy metabolism of these two components of the body. Evolution of each compartment is determined by the instantaneous balance between synthesis, which depends on metabolizable energy supply, and degradation. Allometric equations are used to relate fat-free mass to protein content and full body weight to empty one.

Comparison between simulation and measurements concerning continuously growing animals, for which data on body composition are available, underlines the relevance of the major hypotheses governing the model. Calibration and validation on body-weight data of respectively discontinuously and continuously growing steers corroborate this idea. The model has been proven to be sensitive to parameters related to proteins, and particularly protein contents at maturity, which may be deduced from our knowledge. It is concluded that such a model may be useful in the future to predict evolution of body composition. Nevertheless, it has to be tested and validated with various data sets, and particularly those concerning the evolution of body components of compensatory growing beef cattle.

Introduction

The French INRA system for evaluating energy requirements of growing beef cattle is based on an empirical model developed by Robelin (1986), who fitted a Gompertz curve on body-weight data for different Continental breeds and used allometric equations to assess the development of tissues. Similarly, energy

 Modelling Nutrient Utilization in Farm Animals (eds J.P. McNamara, J. France and D.E. Beever)

requirements for growing cattle established by the National Research Council (NRC, 1996) were derived from static relationships. The advantages of such models lie in their simplicity, since they often consider only variations of body weight, whose equation is obtained by a statistical adjustment. This simplicity allows these models to predict growth fairly well with a limited number of parameters, when animals are managed in a continuous manner.

Nevertheless, growing animals often undergo successive phases of nutritional restriction and realimentation, as a consequence of variable nutritional supplies. As a matter of fact, static empirical models are not adapted for representing these alternating phases, particularly when compensatory growth allows animals to grow faster after a period of restriction than continuously well-fed animals.

Moreover, as noted by Oltjen (1993), predictive models of nutrition and growth have evolved to more mechanistic models. A mechanistic approach is better suited for variable growth and also allows the incorporation of recent advances in our knowledge of metabolic processes, which have arisen from experimental investigations. Thus, there is now a growing need for application models that take into account physiological mechanisms of growth and that may be adapted to various nutritional situations.

The present chapter describes a first modelling approach, which aims at predicting growth of beef cattle in a dynamic and mechanistic way. Indeed, we have developed a mechanistic model that links the body composition of growing and finishing cattle, in terms of proteins and lipids, to energy intake and its variations. The conceptual scheme and equations will be described first, after which we shall detail the comparison of the model with measurements and the biological interpretations allowed by this type of modelling.

Conceptual Scheme of the Model and Related Equations

Compartments

Body composition can be characterized by its protein and lipid content, since fat-free mass is allometrically related to protein content (Robelin and Daenicke, 1980; Geay *et al.*, 1987). Consequently, this model is basically constructed on variations of body protein and lipid contents, like the models developed by Oltjen *et al.* (1986) and later Di Marco *et al.* (1989). However, these models considered that variations of the protein compartment were influenced mainly by the body DNA content, which has not been included in our work, because of lack of data. Inspired by Di Marco *et al.* (1989), we have distinguished proteins in body and viscera. The distinction between carcass tissues and non-carcass ones, which comprise viscera, hide and head, is justified by the major role played by splanchnic tissues in the energy metabolism of ruminants (Ortigues and Doreau, 1995). Variations of the four compartments (proteins and lipids in carcass and non-carcass tissues) are described by the same processes – synthesis and degra-

dation (France *et al.*, 1987) – and are assumed to be determined by metabolizable energy intake. The influence of protein supply on cattle growth is not taken into account, but the model should make it possible to include this dependence later. Moreover, because of a similar need for simplicity, suckling and weaning periods have not been considered in our approach.

Mathematical formulation

These considerations thus lead to the following formulation for each of the four compartments :

$$\frac{dX}{dt} = \text{Synthesis} - \text{Degradation} \tag{1}$$

where X represents one of the compartments.

For proteins, we have considered that synthesis and degradation rates could be expressed as the sum of a basic rate, corresponding to protein turnover, and another term which determines accretion or mobilization. Lipid turnover, which is of much smaller importance, has not been taken into account.

Protein turnover

Millward *et al.* (1981) related protein turnover rate in rats to body weight (BW) and calculated turnover rates in muscle and non-muscle tissues: $3.53\ BW^{0.69}$ g protein day^{-1} in muscle and $11.3\ BW^{0.5}$ g protein day^{-1} in non-muscle. Lobley *et al.* (1980) estimated for a mature cow a rate of protein synthesis in muscle of between 400 and 450 g day^{-1}. We linked turnover rates to metabolic weight (MW, where MW = empty-body weight $(EBW)^{0.75}$) and, according to these experimental results, used values of 0.35 g day^{-1} $(MW/100)^{-1}$ for basic synthesis and degradation rates for carcass and 1 g day^{-1} $(MW/100)^{-1}$ for non-carcass tissues. In any case, protein turnover does not influence variations of protein compartments, since the same term has been employed for synthesis and degradation.

Synthesis

Synthesis rate is linked to metabolizable energy (ME) supply. Like France *et al.* (1987) and Danfær (1991), we have described anabolic reactions by a Michaelis–Menten equation, multiplying a maximal synthesis velocity by an energy-dependent function, bounded by 0 and 1:

$$\text{Synthesis} = \text{SynMax}\frac{\text{ME}}{k_E + \text{ME}} \tag{2}$$

where ME is metabolizable energy, k_E is the half-saturation constant and SynMax is the maximal synthesis rate.

When energy supply is not limiting, whole-animal growth follows a Gompertz curve (Robelin, 1986). In our model, maximal synthesis rate has thus been expressed through a Gompertz-type equation and therefore decreases as the animal approaches maturity. The result is:

$$\text{SynMax} = \alpha X \ln\left(\frac{X_{\max}}{X}\right) \tag{3}$$

where α is a constant (day^{-1}) and $X_{\max}$ is maximal X content.

Maximal protein and lipid contents are not considered in the same way. For carcass and non-carcass tissues, maximal protein contents correspond to contents at maturity and are time-constant. On the other hand, maximal lipid quantities in carcass and non-carcass depend on the development of the animal. They therefore increase in a linear manner with physiological age, estimated by the ratio actual protein content vs. protein content at maturity in each compartment. Maximal lipid contents, $\text{Lip}_{\max}$, are thus related to the weight of each compartment in the following way, for example, in the carcass:

$$\text{Lip}_{\text{Carc max}} = \left(\text{Lip}_0 + \text{Lip}_c\left(\frac{\text{Prot}_{\text{Carc}}}{\text{Prot}_{\text{Carc max}}}\right)\right)\text{W}_{\text{carc}} \tag{4}$$

where Lip_0 and Lip_c are coefficients of the linear relationship between the maximal lipid proportion in each compartment and physiological age.

Degradation

The degradation process has been formalized differently for proteins and for lipids.

PROTEINS. As in protein synthesis, it was assumed that total degradation rate was the sum of a basic term, equivalent for synthesis and degradation, and a rate related to the compartment. The latter rate could be responsible for mobilization. We considered that, for each compartment, the degradation rate decreased with the physiological age of the animals, in the same way as the maximal synthesis rate:

$$\text{Deg(Prot)} = \gamma\ \text{Prot} \ln\left(\frac{\text{Prot}_{\max}}{\text{Prot}}\right) \tag{5}$$

LIPIDS. The daily degradation rate was considered as being proportional to the state of the compartment (Danfær, 1991). Nevertheless, for carcass as well as

for non-carcass lipids, the model takes into account a minimal threshold (Lip_{min}), corresponding to structural lipids:

$$Deg(Lip) = \delta(Lip - Lip_{min}) \quad (6)$$

This threshold has been estimated at 5% of carcass or non-carcass weight.

Empty- and full-body weight

Allometric relationships are used to deduce empty-body weight from protein or lipid contents. Similar equations have been used to relate carcass and non-carcass weights to the proteins and lipids of these two compartments. From Geay *et al.* (1987), fat-free mass (FFM) is fairly well related to protein content, in an allometric fashion:

$$FFM = b_0(Prot)^{b_1} \quad (7)$$

To calculate empty-body, carcass and non-carcass weights, the FFM of these components is then added to each lipid content. Parameters b_0 and b_1 differ between equations. These parameters have been estimated using data from Jenkins and Ferrell (1997), who analysed the body composition of cattle of different breeds under various feed availabilities and who differentiated carcass from hide and offal. Their measurements enable us to distinguish between carcass and non-carcass tissues in the equations.

Similarly, an allometric equation has been used to relate full-body weight (FBW) to empty-body weight (EBW):

$$FBW = c_0(EBW)^{c_1} \quad (8)$$

As described by Robelin and Daenicke (1980), parameters c_0 and c_1 differ from one breed to another, with c_1 varying from 1.023 to 1.046. However, this formula does not adequately predict variations of gut fill at the beginning of a realimentation period, after underfeeding with a rough forage. The gut fill may decrease when the animal is fed a more digestible diet. This decrease is expressed by the fraction p of the full response estimated by equation 9:

$$p = 1 - \exp\left(-\frac{t}{\tau}\right) \quad (9)$$

where t is actual time after realimentation and τ is a constant delay. Considering a delay of 15 days, animals recover 87% of the maximal gut fill after 1 month, which seems to be realistic.

Ordinary differential equations have been integrated over time through a Runge-Kutta method. Accretion or mobilization for each compartment is determined by the instantaneous balance between synthesis and degradation.

Results

We shall first focus on the calibration and validation of the model at the global level of the animal, before interpreting model results from a physiological and metabolic point of view.

Calibration and validation

Calibration and validation of our model require data on metabolizable energy intake as well as on body composition or body weight for the whole growing phase of beef cattle. These conditions greatly restrict the number of experiments and data available to calibrate or validate our model, especially as many parameters differ from each other between different breeds.

At present, we have been using data from Robelin (1986), who described variations of body composition for continuously growing Charolais bulls, and from Saubidet and Verde (1976). The latter measured the energy intake and FBW of Angus steers, growing either discontinuously (data used for calibration) or continuously (data used for validation). For both data sets, animals had already been weaned and were approximately 8 months of age. Charolais bulls were measured individually, whereas data from 24 Angus steers were put together by Saubidet and Verde (1976). These data sets enabled us to adjust two sets of parameters of the same model.

Figure 17.1 shows that the model fits relatively well with the data of body composition (i.e. proteins and lipids) of continuously growing bulls. The development over time of Charolais EBW shows classic features of continuous growth. Simulated EBW increases almost constantly for 500 days before growth rate decreases when approaching mature physiological age. As for calibration on FBW data of discontinuously growing steers (Fig. 17.2), it can be noticed that: (i) the model simulates quite well the partial compensation for animals first restricted and then well fed thereafter; and (ii) the influence of gut fill decrease on FBW cannot be neglected at the beginning of the realimentation period. Validation on continuously growing Angus steers roughly corroborates basic model hypotheses, although the model fails in representing a slower growth of the animals at the end of the simulation period, particularly around day 200. Nevertheless, for the whole simulation period, the difference in average daily gain between model and validation data hardly exceeds 100 g day^{-1}.

Carcass yield

Data from Robelin (1986) also concerned variations of carcass yield of continuously growing bulls. As demonstrated by Fig. 17.3, carcass yield estimated by the model, calculated by the ratio carcass weight vs. EBW, roughly follows tendencies arising from data. From the model, as well as from data, it appears that

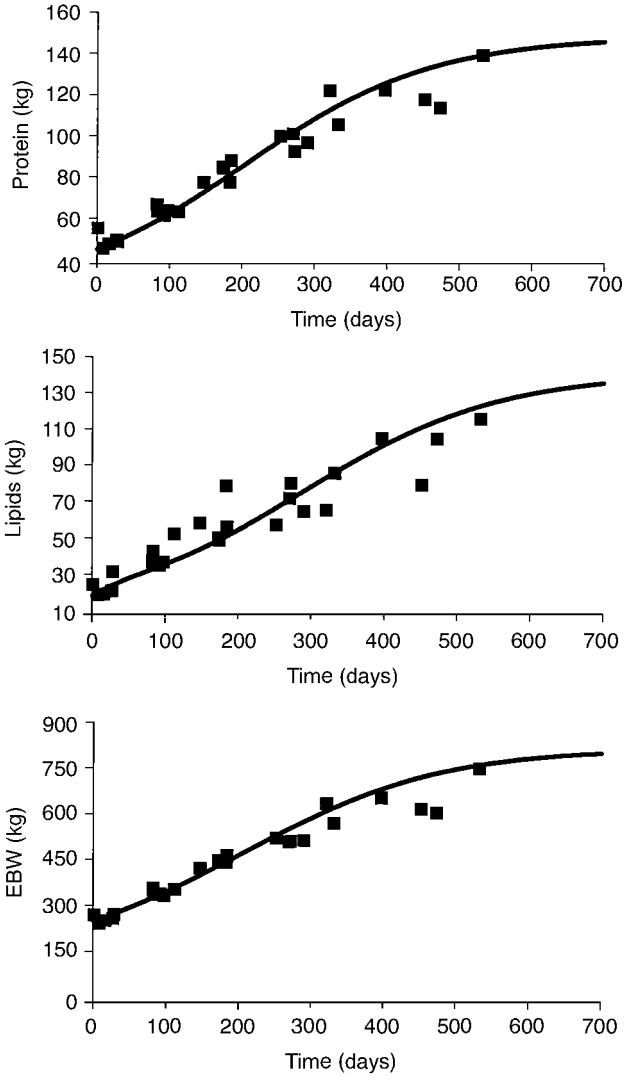

Fig. 17.1. Comparison between model and measurements (■) for Charolais bull proteins, lipids and empty-body weight. Individual data from Robelin (1986).

viscera grow more rapidly than the carcass at the beginning of the period, since offal tissue development is a prerequisite for maximal growth achievement. Once this development is achieved, carcass weight increases in turn and carcass yield tends to stabilize. However, variations of simulated carcass yield are too weak and occur too late, especially compared with the low carcass yield values measured after weaning.

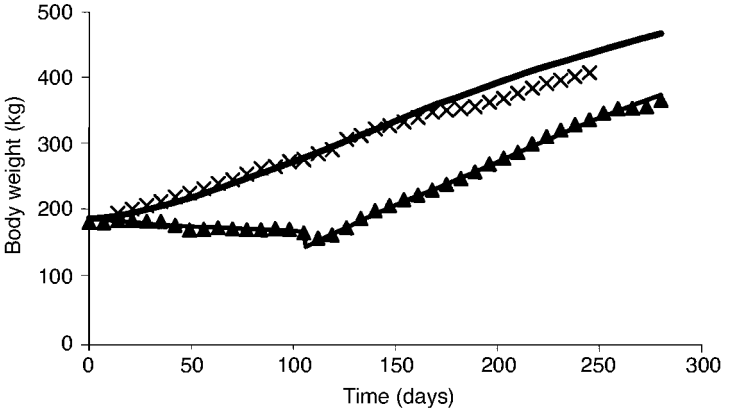

Fig. 17.2. Comparison between model and measurements for Angus steer body weight: calibration (▲) and validation (X). Data from Saubidet and Verde (1976), representing groups of 24 animals.

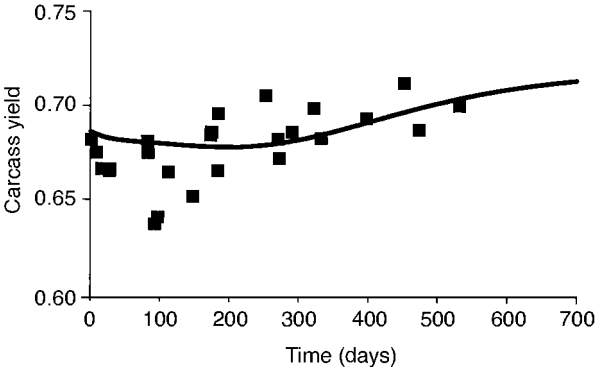

Fig. 17.3. Variations of Charolais bull carcass yield simulated and observed (■). Individual data from Robelin (1986).

Synthesis and degradation rates

Rates of synthesis and degradation for proteins and lipids in carcass and non-carcass have been plotted on Fig. 17.4, for the model applied to Charolais bulls. Protein synthesis or degradation rates always remain stronger than those concerning lipids. Patterns of protein synthesis and degradation differ, whether they concern carcass or non-carcass tissues. For the carcass, protein synthesis and degradation reach a maximum (900 g day^{-1} for synthesis and 700 g day^{-1} for degradation), which occurs simultaneously with the maximal protein accre-

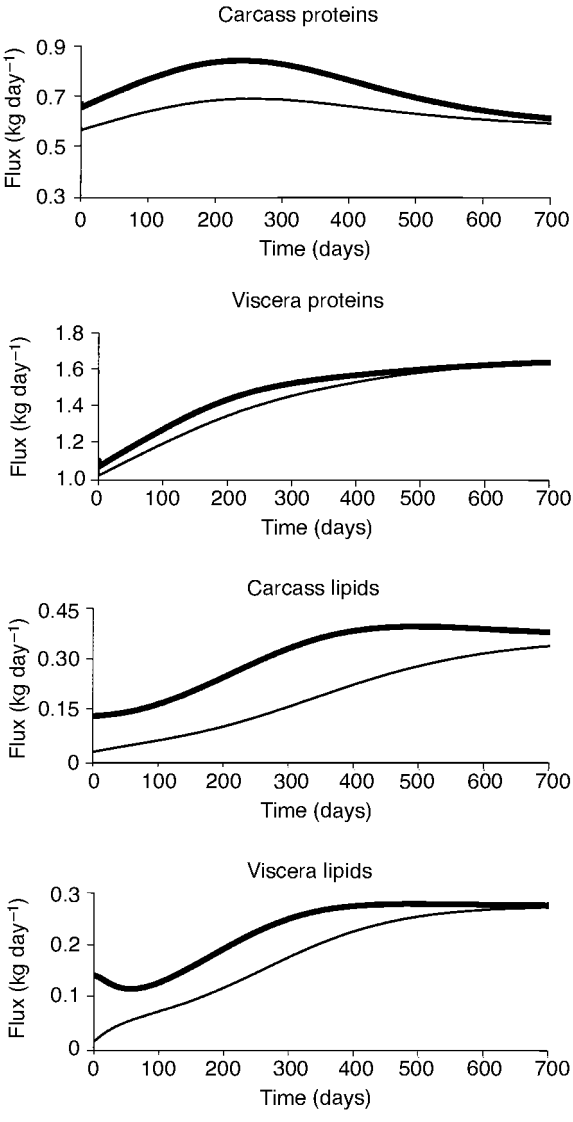

Fig. 17.4. Simulated temporal evolution of synthesis (thick line) and degradation (thin line) fluxes for proteins and lipids in carcass and non-carcass tissues.

tion, 200 days after weaning. This coincides approximately with the puberty period for Charolais bulls. Rates then decline slowly. After 700 days, synthesis and degradation are almost merged, therefore resulting in a weak protein accretion in muscle.

Protein synthesis and degradation in non-carcass tissues are always stronger than in the carcass, because of a higher protein turnover in the viscera. Rates increase continuously during the growth of the animals, from above 1 kg day^{-1} at the beginning of the simulation to more than 1.6 kg day^{-1} at the end. Protein accretion, represented by the difference between synthesis and degradation, declines faster in non-carcass tissues than in the carcass. It also appears that protein accretion reaches its maximum sooner in non-carcass than in carcass tissues, which is in concordance with a prior development of viscera during the growth period. Maximal rates of lipid synthesis and degradation in the carcass are not observed at the same time as maximal lipid accretion, occurring at between 300 and 400 days of simulation. Maximal synthesis rate reaches a threshold of 400 g day^{-1} at 500 days, whereas degradation still increases. In the same way as for proteins, lipid synthesis and degradation in non-carcass reach a plateau (around 300 g day^{-1}) sooner than in the carcass, and maximal lipid accretion in these organs also occurs earlier than in the carcass.

Variations over time of body protein and lipid contents for discontinuous growth

Figure 17.5 describes the variations over time of proteins and lipids in carcass and non-carcass for Angus steers fed discontinuously, which were used to calibrate the model. During the restriction phase, carcass proteins slightly increased, which denotes the possibility of muscle growth simultaneously with body-weight loss. On the other hand, the non-carcass protein compartment was more sensitive to nutritional restriction and showed a constant decrease. Lipids were also mobilized throughout the restriction period. At the beginning of the realimentation phase, proteins increased first, followed by lipid compartments.

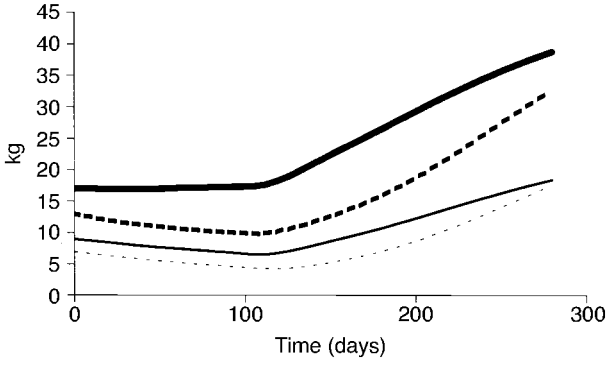

Fig. 17.5. Temporal evolution of the four compartments in Angus steers growing discontinuously: proteins (solid line) and lipids (dashed or dotted line) in carcass (thick line) and non-carcass (thin line).

Sensitivity analysis

Sensitivity analyses were performed on parameters and initial conditions of the model applied to Charolais bulls. Table 17.1 synthesizes parameters concerned with an associated sensitivity coefficient (SC). We first simulated EBW either by adding to or by subtracting from parameters 10% of their value. The sensitivity coefficient we used is obtained by the absolute difference between the two final weights (after 700 days of simulation), divided by the reference (no parameter variation) EBW, i.e. 808.59 kg in this case – in other words:

$$SC = \frac{\left|EBW_{+10} - EBW_{-10}\right|}{EBW_{ref}} \tag{10}$$

The model is mostly sensitive to parameters related to protein compartments, particularly carcass proteins. Indeed, carcass protein content at maturity plays a major role in the simulation of EBW. Slightly less important are non-carcass proteins at maturity and the synthesis rate of carcass proteins. On the other hand, lipid synthesis and degradation rates, as well as minimal lipid content, have a very weak influence on EBW. The only parameters relative to lipids to which simulated EBW appears to be slightly sensitive concern the linear increase of maximal lipid content with physiological age. Moreover, the model is quite insensitive to initial values of the four compartments.

Discussion

This modelling approach has proved the ability of a mechanistic model to reproduce variations over time of compartments governing animal growth. Distinguishing protein and lipid contents in carcass and non-carcass tissues allowed us to simulate the different synthesis and degradation rates, which are time-varying and depend on metabolizable energy intake. Compared with previously developed empirical models (Robelin, 1986), such a mechanistic approach is able not only to simulate explicitly the main compartments of the body, but also to deduce from simulation interesting practical results, such as carcass yield.

Moreover, a mechanistic model allows results to be interpreted from a physiological point of view. For instance, studying degradation and synthesis fluxes underlines the relevance of the major hypotheses building the model. Simulated fluxes for carcass protein are in accordance with data from McCarthy *et al.* (1983) and, more recently, Van Eenaeme *et al.* (1998), who measured synthesis fluxes of between 0.8 and 1 kg day^{-1} in the muscles of large-frame steers and bulls. McCarthy *et al.* (1983) also measured a decrease of protein synthesis and degradation rates with age. Furthermore, as demonstrated by simulated fluxes, those associated with protein synthesis or degradation appear higher than those concerning lipid compartments. This is in accordance with the idea that

Table 17.1. Sensitivity coefficient (SC) for parameters and initial conditions of the model.

Name of the parameter	Signification	Unit	Nominal value	Sensitivity coefficient
$Protc_{max}$	Carcass proteins at maturity	kg	100	+++
$Protv_{max}$	Non-carcass proteins at maturity	kg	65	++
α_c	Synthesis rate for carcass proteins	day^{-1}	0.03	++
α_v	Synthesis rate for non-carcass proteins	day^{-1}	5.25×10^{-2}	+
β_c	Synthesis rate for carcass lipids	day^{-1}	0.05	−
β_v	Synthesis rate for non-carcass lipids	day^{-1}	0.1	−
k_E	Half-saturation constant for metabolizable energy	MJ	125	+
γ_c	Degradation rate for carcass proteins	day^{-1}	9×10^{-3}	+
γ_v	Degradation rate for non-carcass proteins	day^{-1}	1.75×10^{-2}	+
δ_c	Degradation rate for carcass lipids	day^{-1}	5×10^{-3}	−
δ_v	Degradation rate for non-carcass lipids	day^{-1}	0.01	−
Lip_0	Maximal lipid proportion at theoretical physiological age 0	No unit	0.1	+
Lip_c	Augmentation coefficient of the maximal lipid proportion	No unit	0.1	+
L_{min}	Minimal proportion of lipids in the body	%	5	−
Initial conditions				
$Protc_0$	Initial carcass proteins	kg	28	−
$Protv_0$	Initial non-carcass proteins	kg	17	−
$Lipc_0$	Initial carcass lipids	kg	13	−−
$Lipv_0$	Initial non-carcass lipids	kg	5	−−

−−, $SC < 10^{-3}$; −, $10^{-3} < SC < 10^{-2}$; +, $10^{-2} < SC < 5 \times 10^{-2}$; ++, $5 \times 10^{-2} < SC < 10^{-1}$; +++, $SC > 10^{-1}$.

maintenance energy requirement is mainly due to protein turnover (Russel and Wright, 1983). Studying the evolution of body compartments for discontinuous growth is also informative. The Angus steers model simulated a decrease mainly in non-carcass tissues during the restriction period, as observed by Ryan *et al.* (1993).

Ideally, the model has to be validated using a data set different from the one used for its calibration. These two steps have been carried out for Angus steers data and the results show the possibility of using our model later as a predictive tool. Nevertheless, such a study also underlines the need for a large quantity of data concerning energy intake over time and corresponding body composition, for both continuous and discontinuous growth. Because of the scarcity of such data, extending this model to a wide range of breeds will inevitably require an adjustment of parameters on partial data sets, including, for instance, body weight, carcass yield or even adipose tissue weight. As far as parameter values are concerned, sensitivity analysis provides a useful tool, since some parameters to which the model has been proved to be sensitive can be deduced from knowledge and expertise (e.g. protein contents at maturity, maximal lipid proportions). This reduces, but does not eliminate, uncertainty on parameters, which represents one of the main drawbacks of such a model.

The four-compartment conceptual scheme appears to be suited to our purpose, which consists of predicting animal growth in any case of nutritional supply. Consequently, it seems that this model structure will be kept for future studies. Nevertheless, the formulation of processes may be improved, as a result of increasing knowledge about growth mechanisms.

Acknowledgements

The authors are particularly grateful to Yves Geay, D. Micol, M. Vermorel and M. Petit for their helpful comments and discussions on this work.

References

Danfær, A. (1991) Mathematical modelling of metabolic regulation and growth. *Livestock Production Science*, 27, 1–18.

Di Marco, O.N., Baldwin, R.L. and Calvert, C.C. (1989) Simulation of DNA, protein and fat accretion in growing steers. *Agricultural Systems*, 29, 21–34.

France, J., Gill, M., Thornley, J.H.M. and England, P. (1987) A model of nutrient utilization and body composition in beef cattle. *Animal Production* 44, 371–385.

Geay, Y., Micol, D., Robelin, J., Berge, P. and Malterre, C. (1987) Recommandations alimentaires pour les bovins en croissance et à l'engrais. *Bulletin Technique CRZV Theix, INRA* 70, 173–183.

Jenkins, T.G. and Ferrell, C.L. (1997) Changes in proportions of empty body depots and constituents for nine breeds of cattle under various feed availabilities. *Journal of Animal Science* 75, 95–104.

Lobley, G.E., Milne, V., Lovie, J.M., Reeds, P.J. and Pennie, K. (1980) Whole body and tissue protein synthesis in cattle. *British Journal of Nutrition* 43, 491–502.

McCarthy, F.D., Bergen, W.G. and Hawkins, D.R. (1983) Muscle protein turnover in cattle of different genetic backgrounds as measured by urinary N^{τ}-methyl histidine excretion. *Journal of Nutrition* 113, 2455–2463.

Millward, D.J., Bates, P.C. and Rosochacki, S. (1981) The extent and nature of protein degradation in the tissues during development. *Reproduction Nutrition Développement* 21, 265–277.

NRC (National Research Council) (1996) *Nutrient Requirements of Beef Cattle.* National Academy Press, Washington, USA, 242 pp.

Oltjen, J.W. (1993) Integration of energy concepts by modeling techniques. *Journal of Dairy Science* 76, 1812–1816.

Oltjen, J.W., Bywater, A.C. and Baldwin, R.L. (1986) Development of a dynamic model of beef cattle growth and composition. *Journal of Animal Science* 62, 86–97.

Ortigues, I. and Doreau, M. (1995) Responses of splanchnic tissues of ruminants to changes in intake: absorption of digestion end products, tissue mass, metabolic activity and implications to whole animal energy metabolism. *Annales de Zootechnie* 44, 321–346.

Robelin, J. (1986) Composition corporelle des bovins: évolution au cours du développement et différences entre races. Thèse de Doctorat d'Etat ès Sciences Naturelles, Université de Clermont-Ferrand II, 391 pp.

Robelin, J. and Daenicke, R. (1980) Variations of net requirements for cattle growth with liveweight, liveweight gain, breed, and sex. *Annales de Zootechnie* 29, 99–118.

Russel, A.J.F. and Wright, I.A. (1983) Factors affecting maintenance requirements of beef cows. *Animal Production* 37, 329–334.

Ryan, W.J., Williams, I.H. and Moir, R.J. (1993) Compensatory growth in sheep and cattle. II. Changes in body composition and tissue weights. *Australian Journal of Agricultural Research* 44, 1623–1633.

Saubidet, C.L. and Verde, L.S. (1976) Relationship between live weight, age and dry-matter intake for beef cattle after different levels of food restriction. *Animal Production* 22, 61–69.

Van Eenaeme, C., Evrard, M., Hornick, J.L., Baldwin, P., Diez, M. and Istasse, L. (1998) Nitrogen balance and myofibrillar protein turnover in double muscled Belgian Blue bulls in relation to compensatory growth after different periods of restricted feeding. *Canadian Journal of Animal Science* 78, 549–559.

18

Modelling Nutrient Utilization in Growing Cattle Subjected to Short or Long Periods of Moderate to Severe Undernutrition

G.Q. Witten and F.D. Richardson

Department of Mathematics and Applied Mathematics, University of Cape Town, Rondebosch 7701, South Africa

Abstract

In the semiarid tropics rainfall is seasonal and varies widely between years. Consequently, grazing animals are subjected to short or long periods of moderate to severe undernutrition. Undernutrition in young ruminants affects their chances for survival and the time required to reach the weight and body composition at which they are suitable for slaughter or able to work as draught animals or, if female, to conceive and rear offspring. Animals can adapt to undernutrition by differential mobilization of tissues. Initially the weights of the liver and small intestine decrease rapidly which leads to a reduction of the animal's energy expenditure. Fat and protein are catabolized to meet the requirements for maintenance. When the nutritional restriction is removed, animals may respond in different ways. Partial or complete compensation may occur if previously restricted animals increase their growth rate relative to that of their unrestricted contemporaries. However, there may be no compensation. The ability to predict the probable short- and long-term consequences of undernutrition will support the planning and evaluation of measures to ameliorate undernutrition in a specific environment.

A model (RUMET) has been developed that simulates rumen function and nutrient utilization during continuous growth, undernutrition and realimentation for growing cattle. The model simulates changes in the weights of ash (bone), muscle, adipose tissue, liver and small intestine and the relative effects of these changes on the maintenance expenditure. The model may be used to predict energy expenditure, liveweight changes and the probability of survival during periods of undernutrition. Voluntary intake, liveweight gains and changes in body composition may be predicted for animals given diets of different composition during realimentation following a period of undernutrition.

 Modelling Nutrient Utilization in Farm Animals (eds J.P. McNamara, J. France and D.E. Beever)

Introduction

On the semiarid and arid rangeland, rainfall is seasonal and varies from year to year. Animals therefore experience periods of varying food availability, which affect their ability to express their genetic potential for growth. In both the short and long term, during undernutrition, when the growth of an animal falls below its genetic potential, many workers have shown in many experiments (Foot and Tulloh, 1977; review article by O'Donovan, 1984) that, when food subsequently become abundant, growth rates accelerate and exceed the growth rates of continuously well-fed animals. However, the response of an animal to a period of undernutrition is variable, due partly to the complex processes of digestion and metabolism. The response depends on the severity and length of restriction, the age of the animal when the restriction was imposed and the quality of the food during undernutrition. Partial compensation is possible when restricted animals increase their growth rate but do not attain the same weight for age as those animals not restricted. In some cases, there is no increase in growth rate of a restricted animal once the restriction is removed, and hence there is no compensation. For example, Allden (1970) found that the restriction of lambs less than 15 kg live-weight resulted in significantly lower live-weights at 3 years of age, as the growth curve was displaced in time.

Animals are able to adapt to undernutrition because the food needed to maintain a constant body weight is not a function of weight but decreases with time in response to low feed intake (Ledger and Sayers, 1977). One of the factors that contribute to compensatory growth is a reduced maintenance requirement of animals during undernutrition at the early stages of realimentation. This reduction in maintenance increases the energy available for growth and the extent of this contribution depends on the persistence of the reduced maintenance requirement during realimentation; the longer the reduction in maintenance persists, the greater the contribution to compensatory growth. When food intake is restricted, the metabolically active tissues, such as the digestive tract and the liver, are likely to be reduced in size and activity (Taylor and Murray, 1991).

Over the past decade, there has been considerable progress in modelling of both rumen and intermediary metabolism processes, due to the increased availability of data and computer power and, more importantly, the new concepts that have been formulated, due to the increase in knowledge. However, two problems still occur:

1. Most mathematical models are developed to simulate continuous growth and do not adequately predict animal responses to limited (submaintenance) feeding.
2. Although it was suggested by France *et al.* (1987) that the modelling focus should also be on the integration of components to increase adequate predictions, the integration of models of whole digestive processes and metabolism has been slow.

The aim of this chapter is to describe the development of a mathematical model (RUMET) that simulates the effects of undernutrition and to account for some of the factors that influence maintenance energy requirements over time. The model simulates both digestion and tissue metabolism.

General Model Structure

Two mechanistic models, a rumen model, developed by Dijkstra *et al.* (1996), and an intermediary metabolism model, developed by France *et al.* (1987), were modified and integrated. The framework of the model is shown in Fig. 18.1 and the scheme of the model is shown in Fig. 18.2. The rumen model comprises 15 state variables and the intermediary metabolism model nine state variables. Four zero pools are defined for the postruminal gastrointestinal tract, which represent nutrients available for absorption. Output from the rumen is stoichiometrically converted to their C6 and C2 equivalents and used as input to the intermediary metabolism submodel. Because the time-scale of the rumen model is in hours and that of the intermediary metabolism model is in days, all the rate constants of the rumen model were multiplied by 24 so that both models can be integrated simultaneously.

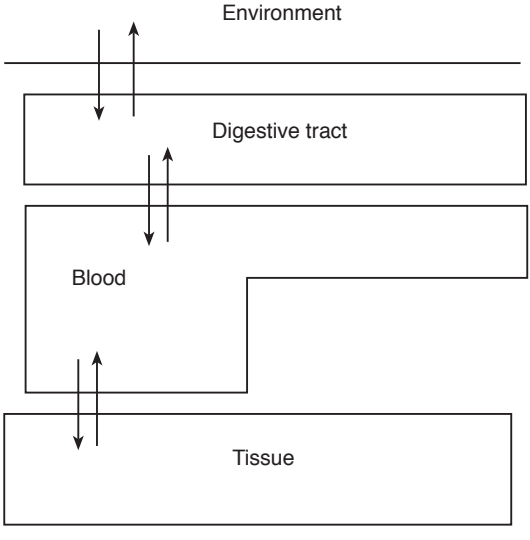

Fig. 18.1. General framework for the RUMET model.

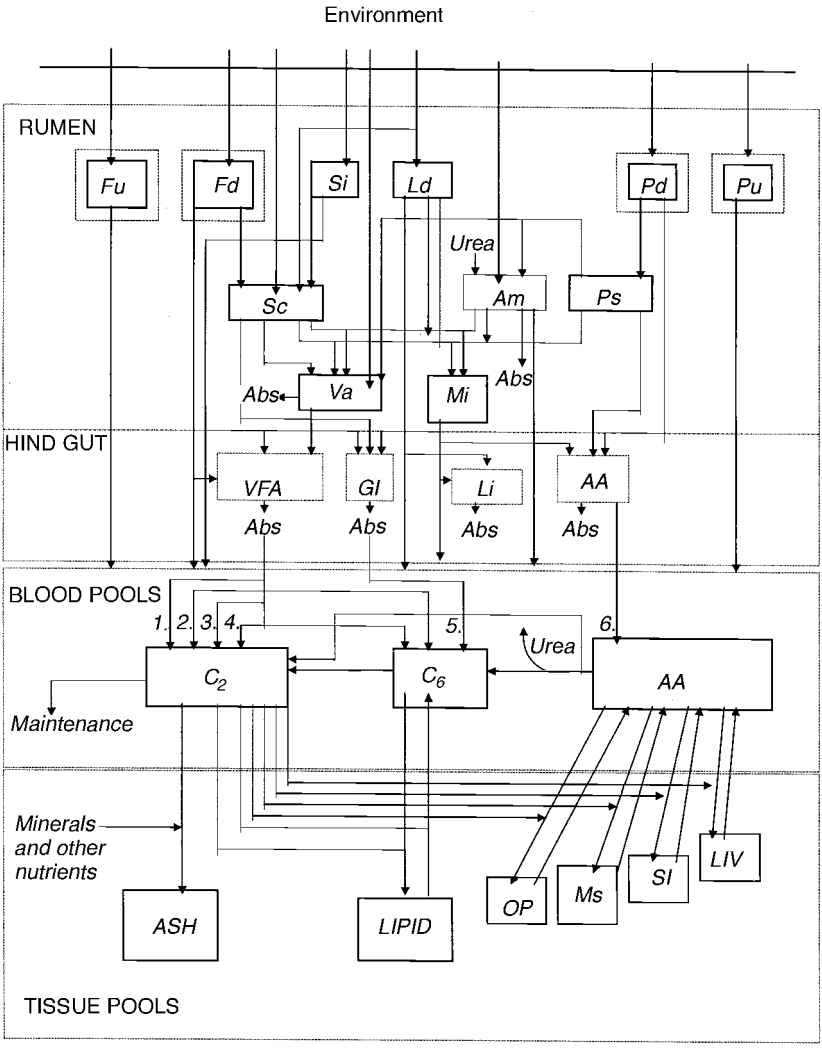

Fig. 18.2. An integrated rumen and intermediary metabolism model. The absorption of 1. acetate, 2. stearate, 3. butyrate, 4. propionate, 5. glucose and 6. amino acids is shown.

Model Input

The total dry-matter intake, *DMITOT* (kg day^{-1}), is estimated from the rumen volume *Rvol* (l), maximum concentration of dry matter in the rumen, *cDMRV* (g l^{-1}) and the fractional rate of disappearance of dry matter from the rumen, *kRuEx*:

$$DMITOT = kRuEx \times cDMRv \times Rvol \quad (1)$$

The fractional rate of disappearance of dry matter from the rumen (*kRuEx*) is calculated as the total loss of dry matter from the rumen by absorption, by passage and as gas, *UDMRu*, and the total weight of dry matter in the rumen, *RumenDM*; *kRUEx* = *UDMRu*/*RumenDM*. The concentration of the dry matter in the rumen (*cDMRu*) was estimated from the value of the concentration of dry matter in the rumen from Czerkawski (1986). The rumen volume is related to live-weight by the equation of Butterfield (1988):

$$Rvol = Rvolmat\ (3.0\ Xwt + (1 - 3.0)\ Xwt^2) \quad (2)$$

where *Xwt* = *Weight*/*Wmax*, *Rvol* is the volume of the rumen (l), *Rvolmat* is the volume of the rumen at maturity (assumed to be 75 l for a 650 kg mature steer), *Weight* is the weight of the animal (kg) and *Wmax* is the mature weight of the animal (assumed to be 650 kg). A routine was added to ensure that the rumen volume does not decrease if an animal of less than 75% mature size loses weight.

The Rumen Model

The mechanistic model of rumen function developed by Dijkstra *et al.* (1996) has been modified to predict the voluntary food intake, digestion and absorption of nutrients by cattle grazing tropical rangeland. When animals eat tropical forages, the food entering the rumen consists of a high proportion of coarse fibrous particles and these affect the pattern of digestion in the rumen and the passage of matter to the duodenum. When fibrous particles enter the rumen, microbes must become attached to them before fermentation can begin. In addition, the size or specific gravity of digesta particles must reach a critical value before they can pass from the rumen. The undegradable protein (*Pu*), insoluble undegradable protein (*Pd*), undegradable fibre (*Fu*) and degradable fibre (*Fd*) components of forage are associated with these coarse particles. For these reasons, 12 additional pools have been added to the model of Dijkstra *et al.* (1996) to simulate these components in the rumen. For each of the forage components (*Fd*, *Fu*, *Pu*, *Pd*), there are three rumen pools, so that the lag at the start of fermentation and selective passage of forage particles may be simulated. The representation of the disappearance of both forage protein and forage fibre is based on model III of Allen and Mertens (1988) (Fig. 18.3), but the action of rumen microorganisms is represented explicitly.

The model of forage fibre in the rumen is set out below, and the equations for the submodel of forage protein are of exactly the same form.

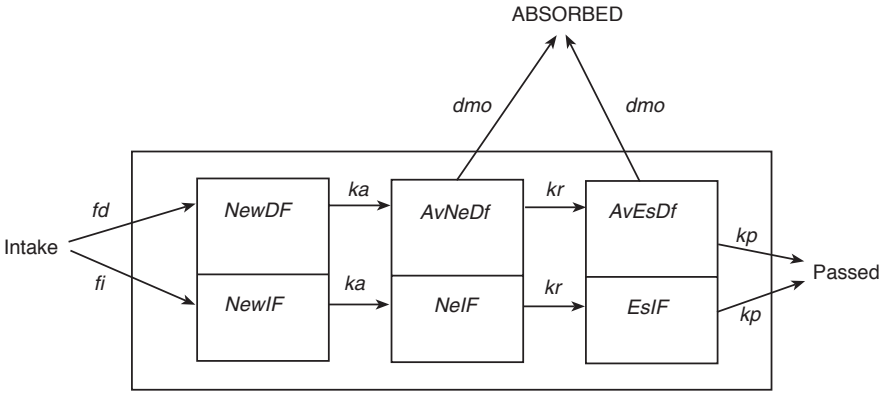

Fig. 18.3. Dynamic model of fibre digestion and intake. *fd, fi,* fractions of potentially digestible and indigestible fibre in diet; *DF, IF,* potentially digestible and indigestible fibre; *New, Ne, Es, Av,* newly eaten, non-escapable particles, escapable particles and particles available for microbial degradation; *ka, kr, kp,* fractional rates of microbial colonization, reduction in size and passage; *dmo,* fractional rate of degradation by microorganisms.

Forage undegradable fibre

Forage unavailable non-escapable undegradable fibre, *QUNFu*

$$InUFu = DFu1 \tag{3a}$$

$$UUFuUA = kUaFu \times QANFu \tag{3b}$$

$$\mathrm{d}QUnFu/\mathrm{d}t = InUFu - UUFuUA \tag{3c}$$

Forage available unescapable undegradable fibre, QANFu

$$PAFuUA = UUFuUA \tag{4a}$$

$$UAFuAE = kAEFu \times QAEFu \tag{4b}$$

$$\mathrm{d}QANFu/\mathrm{d}t = PAFuUA - UAFuAE \tag{4c}$$

Forage available escapable undegradable fibre, QAEFu

$$PEFuAE = UAFuAE \tag{5a}$$

$$UEFuEeX = kforEx \times QAEFu \tag{5b}$$

$$\mathrm{d}QAEFu/\mathrm{d}t = PEFuAE - UEFuEeX \tag{5c}$$

Forage degradable fibre

Forage unavailable non-escapable degradable fibre, QUNFd

$$InUFd = DFd1 \tag{6a}$$

$$UUFdUA = kUAFd \times QUNFd \tag{6b}$$

$$\mathrm{d}QUNFd/\mathrm{d}t = InUFd - UUFdUA \tag{6c}$$

Forage available unescapable degradable fibre, QANFd

$$PAFdUA = UUFdUA \tag{7a}$$

$$UAFdASc = kFdSc1(Cmi/CrefMi)\ QANFd \tag{7b}$$

$$UAFdAE = kAEFd \times QANFd \tag{7c}$$

$$\mathrm{d}QANFd/\mathrm{d}t = PAFdUA - UAFdASc - UAFdAE \tag{7d}$$

Forage available escapable degradable fibre, QAEFd

$$PEFdAE = UAFdAE \tag{8a}$$

$$UAFdASc = kFdSc1\ (Cmi/CrefMi)\ QAEFd \tag{8b}$$

$$UEFdEeX = kforEx \times QAEFd \tag{8c}$$

$$\mathrm{d}QAEFd/\mathrm{d}t = PEFdAE - UAFdASc - UEFdEeX \tag{8d}$$

The fibre and protein components are transferred from the unavailable pool to the available pool and from the available unescapable to the available escapable pool at the same fractional rate as the digesta particles. Consequently, the values of *kUAPu*, *kUAPd*, *kUAFu* and *kUAFd* are the same and *kAEPu*, *kAEPd*, *kAEFd* and *kAEFu* are the same. Another modification to the rumen model was the addition of a routine to calculate the molar proportions of volatile fatty acids (VFA) from the data of Reed *et al.* (1968).

Intermediary Metabolism Model

The output of the rumen model and subsequent absorption from the digestive tract serve as input to the intermediary metabolism model.

Three changes were made to the intermediary metabolism model of France *et al.* (1987). Metabolizable energy expenditure for maintenance (MEM) was shown to be closely correlated ($r = 0.96$) with the weights of visceral organs in growing cattle (Ferrel and Jenkins, 1985) and sheep (Ferrel *et al.*, 1986; Burrin *et al.*, 1990). This is a result of the high energy expenditure of the visceral organs, especially the liver and small intestine (Koong *et al.*, 1982). To account for the contribution of the visceral organs to basal metabolism, the aggregated

protein pool was divided into four: liver protein (*LIV*) pool, small-intestine protein (*SI*) pool, muscle protein (*MUS*) pool and other protein (*OP*) pool. Consequently, total basal metabolism (*TBM*) was divided as follows:

$$TBM = a\,(LIV)^{0.67} + b\,(SI)^{0.67} + c\,(LB)^{0.67} + d\,(LIPID)^{0.67} \quad (9)$$

where *TBM* is total basal metabolism (MJ), *a*, *b*, *c* and *d* are parameters, MJ $kg^{-0.67}$ day^{-1} ($a = 3.74$, $b = 1.1434$, $c = 0.560342$, $d = 0.246711$) and *LB* and *LIPID* are lean body weight (kg) and fat (kg), respectively. The parameters *a* and *b* were calculated by assuming that 25%, 12% and 63% of the total basal metabolism is accounted for by the liver protein, small intestine protein and viscera-free tissue (kg), respectively. The parameters *c* and *d* were calculated based on their ratio in Baldwin *et al.* (1987).

Taylor *et al.* (1981) indicated that animals attained various equilibrium states at different feeding levels. Taylor and Murray (1991) postulated that the liver is affected by feeding level and that the adaptation of the liver to undernutrition is complete before the adaptation by the body weight – that is, the liver attains its equilibrium weight before body weight changes significantly. For this reason an equation relating equilibrium body weight (*EQBW*) and food intake (kg day^{-1}) was derived from the data of Taylor *et al.* (1981). The maximum liver protein weight (*LIVM*) and maximum small-intestine protein weight (*SIM*) was expressed as a function of the proportion of the equilibrium body weight:

$$EQBW = 66.75\,(WEIGHT)^{0.96} \quad (10)$$

$$LIVM = m_1\,(EQBW) \quad (11)$$

$$SIM = m_2\,(EQBW) \quad (12)$$

where *EQBW* is the equilibrium body weight (kg), *LIVM* is the equilibrium liver weight (kg), *SIM* is the equilibrium small-intestine weight (kg) and m_1 and m_2 are parameters ($m_1 = 0.022189$, $m_2 = 0.025145$).

In addition to the digestive and metabolic effects, circulating metabolite concentrations affect nutrient partitioning by means of the production and the metabolism of a number of hormones. Two general hormones having anabolic (H_A) or catabolic (H_C) functions were defined on the assumption that, in many cases, the hormonal state is reflected in the concentration of circulating glucose (Baldwin *et al.*, 1987):

$$(H_A) = (C_{GL}/C_{GL_{\text{ref}}})^2 \quad (13)$$

$$(H_C) = (C_{GL_{\text{ref}}}/C_{GL})^2 \quad (14)$$

where C_{GL} and $C_{GL\text{ref}}$ are the current and reference glucose concentrations (0.036 kg carbon m^{-3} blood), respectively. Catabolic hormones affect the rate of lipolysis and gluconeogenesis and the anabolic hormones affect the rate of protein synthesis.

Application of the Model

The model was run using DRIVER (Hahn and Furniss, 1988) to simulate the pattern of weight changes in the experiment reported by Foot and Tulloh (1977). In that experiment, there were two groups of steers: a group whose diet was such as to maintain a constant body weight (CW group) and another group (WL/WG group) that lost 15% of its initial body weight (body weight at the beginning of the experiment) and was then fed to regain its initial weight. At the beginning of the weight-loss phase (phase 1), the ME intake was reduced, so that the WL/WG group lost an average of 0.5 kg of body weight per day (for 100 days). The ME intake was then increased for about 42 days, so that their initial body weight was regained. Body composition changed during and after the restricted period. Model predictions of body composition were compared with the results of Foot and Tulloh (1977) in Table 18.1 (experimental values are enclosed in parentheses). The model also shows how maintenance expenditure varies as the weights of the liver and small intestine change over time.

Table 18.1. Initial body composition and predicted empty-body weight (EBW) and body composition of cattle fed to lose and regain body weight (WL/WG group) or to maintain weight for 47 days (CW group) (experimental values are enclosed in parentheses).

	WL/WG group			
	Initial body composition	Restricted phase	Recovery phase	CW group
Days	0	100	43	143
Empty-body weight (kg)	238.60 (253.5)	191.43 (215.48)	237.06	237.32 (257.2)
Liver protein (kg)	4.91 (4.4)	3.62 (3.5)	5.56	3.56 (3.2)
Muscle protein (kg)	32.95	30.85	30.30	30.43
Ash (kg)	11.128 (11.6)	12.17 (12.1)	12.71	13.19 (12.5)
Lipid (kg)	28.92 (24.2)	14.07 (20.7)	22.86	23.97 (31.0)
Water (kg)	147.74 (164.6)	124.93 (164.6)	150.90	150.30 (161.9)
ME intake (MJ day^{-1})	77.62	23.36	68.90	64.79
Food intake (kg day^{-1})	6.55	2.20	5.94	5.60

Model Results

During phase 1, the model showed that, when the ME intake is decreased by an average of 0.54 MJ day^{-1}, the animal lost 0.5 kg day^{-1} of live-weight. Consequently, the liver responded quickly (within 2 days) and lost 26% of its weight. The liver was also shown to attain its final equilibrium weight before body weight had changed significantly (Taylor and Murray, 1991). There was a lag in the response of the lipid and muscle pools, the lipid responding after 7 days and the muscle after about 14 days. The weight of ash, a surrogate for the skeleton, increased by 9.4% in phase 1, but its rate of gain decreased in phase 2, which was also shown by Foot and Tulloh (1977).

Figure 18.4 shows how the maintenance energy for the constant-weight steer and the weight-loss steer changes over the 100-day period.

Conclusions

In ruminants, the profile of nutrients available for absorption generally differs largely from that present in the ingested feed. The type and amount of feed nutrients absorbed can significantly affect the amount and composition of products. Thus, there is an obvious need to understand the mechanisms responsible for the transformation of ingested to absorbed nutrients (Gill and Oldham, 1993). Whilst research on various aspects of this transformation has yielded valuable information, the concentration of research on individual components, rather than on the integration of knowledge, has resulted in insufficient information on many important mechanisms that link the individual components, and thereby hampers adequate predictions of the supply of nutrients to carcass components. France *et al.* (1987) concluded that their intermediary metabo-

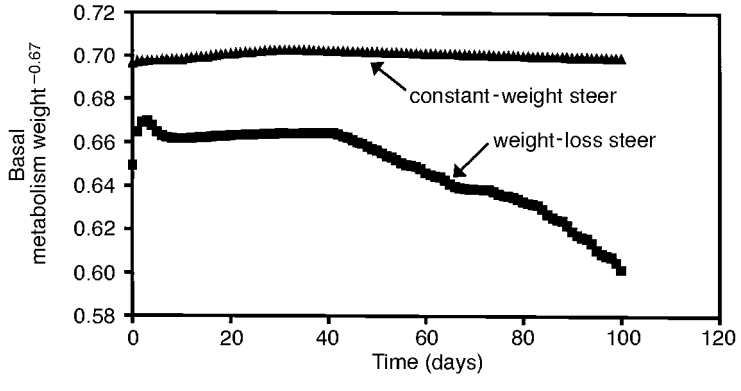

Fig. 18.4. Changes in basal metabolism per unit metabolic size.

lism model did not predict body composition in all situations and suggested that the model be linked with a model of rumen digestion to improve the estimation of nutrient inputs.

The RUMET model has contributed to our understanding and improved predictions of body weight and composition during and following a period of undernutrition. During nutritional restriction, the RUMET model shows that tissues are differentially mobilized and that the greatest losses occur in the liver and small intestine. Losses in these tissues can be expected for two reasons: first, the amount of nutrients processed by these tissues is decreased during nutritional restriction and, secondly, these tissues are extremely active metabolically and have a high maintenance requirement. The visceral organs exhibit quick responses to undernutrition, whereas the peripheral tissues (for example, the muscle) show a lag in their response to undernutrition. During nutritional restriction, the rumen volume does not decrease. At the end of the restricted period, the animal has a large rumen relative to its body size. At this point, the visceral tissues are small and therefore the maintenance requirement is low. As a consequence, when more dry-matter intake is available, the feed intake relative to body size increases dramatically. Also, the enhanced food intake in relation to size and the reduced maintenance requirements imply that proportionately more nutrients will be available for growth purposes.

In practice, however, this may not be the case; food intake will slowly increase and not as suddenly as the model predicts. This sudden increase in the rate of growth may also have an effect on the body composition at the end of the realimentation. The model thus increases our understanding of the mechanisms involved in compensatory growth. An important need for further investigation is whether the model can simulate the body composition after different degrees of nutritional restriction and also to examine the effects of different rates of weight loss and weight gain.

References

Allen, M.S. and Mertens, D.R. (1988) Evaluating constraints on fiber digestion by rumen microbes. *Journal of Nutrition* 118, 261–270.

Allden, W.G. (1970) The effects of nutritional deprivation on the subsequent productivity of sheep and cattle. *Nutrition Abstracts and Reviews* 40, 1167.

Baldwin, R.L., France, J., Beever, D.E., Gill, M. and Thornley, H.M. (1987) Metabolism of the lactating cow III. Properties of mechanistic models suitable for evaluation of energetic relationships and factors involved in the partition of nutrients. *Journal of Dairy Research* 54, 133.

Burrin, D.G., Ferrell, C.L., Britton, R.A. and Bauer, R.M. (1990) Level of nutrition and visceral organ size and metabolic activity in sheep. *British Journal of Nutrition* 64, 439–448.

Butterfield, R.M. (1988) *New Concepts in Sheep Growth*. Sydney University Press, Sydney.

Czerkawski, J.W. (1986) *An Introduction to Rumen Studies*. Pergamon Press, Oxford, UK.

Dijkstra, J., France, J., Neal, H.D.StC., Assis, A.G., Aroeira, L.J.M. and Campos, O.F. (1996)

Simulation of digestion in cattle fed sugarcane: model development. *Journal of Agricultural Science, Cambridge* 127, 231–246.

Ferrel, C.L. and Jenkins, T.G. (1985) Energy utilization by Hereford and Simmental males and females. *Animal Production* 41, 53–61.

Ferrel, C.L., Koong, L.J. and Nienaber, J.A. (1986) Effect of previous nutrition on body composition and maintenance energy costs of growing lambs. *British Journal of Nutrition* 56, 595–605.

Foot, J.Z. and Tulloh, N.M. (1977) Effects of two paths of liveweight change on the efficiency of feed use and on body composition of Angus steers. *Journal of Agricultural Science, Cambridge* 88, 135–142.

France, J., Gill, M., Thornley, J.H.M. and England, P. (1987) A model of nutrient utilization and body composition in beef cattle. *Animal Production* 44, 371–385.

Gill, M. and Oldham, J.D. (1993) Growth. In: Forbes, J.M. and France, J. (eds) *Quantitative Aspects of Ruminant Digestion and Metabolism*. CAB International, Wallingford, UK, pp. 383–403.

Hahn, B.D. and Furniss, P.R. (1988) A description of DRIVER: an interactive modelling tool. *South African Journal of Science* 84, 749–753.

Koong, L.J., Ferrel, C.L. and Nienaber, J.A. (1982) Effects of plane of nutrition on organ size and fasting heat production in swine and sheep. In: Eker, A. and Sundstol, F. (eds) *Energy Metabolism of Farm Animals*. EAAP Publication 29, Agriculture University of Norway, Institute of Animal Nutrition, Ås, pp. 245–248.

Ledger, H.P. and Sayers, A.R. (1977) The utilization of dietary energy by steers during periods of restricted food intake and subsequent realimentation 1. The effect of time on the maintenance requirements of steers held at constant live weights. *Journal of Agricultural Science, Cambridge* 88, 11–26.

O'Donovan, P.B. (1984) Compensatory gain on cattle and sheep. *Nutrition Abstracts and Review (Series B)* 54, 389–410.

Reed, W.D.C., Elliot, R.C. and Topps, J.H. (1968) Effect of level of intake and roughage content of cattle diets on digestibility, urinary and mineral losses, and certain aspects of rumen function. *The Rhodesian Journal of Agricultural Research* 6(2), 81–91.

Taylor, StC.S. and Murray, J.I. (1991) Effect of feeding level, breed and milking potential on body tissues and organs of mature, non-lactating cows. *Animal Production* 53, 27–38.

Taylor, StC.S., Turner, H.G. and Young, G.B. (1981) Genetic control of equilibrium maintenance efficiency in cattle. *Animal Production* 33, 179–194.

19

An Integrated Cattle and Crop Production Model to Develop Whole-farm Nutrient Management Plans

T.P. Tylutki and D.G. Fox

Department of Animal Science, Cornell University, Ithaca, NY 14853, USA

Abstract

An integrated modelling approach is needed to efficiently utilize nutrients within the farm boundary to control the risk of non-point-source pollution while maintaining farm profitability. The Cornell University Nutrient Management Planning System (CuNMPS) is being developed for that purpose. The CuNMPS consists of three computer programs designed to: (i) optimize herd nutrition (Cornell Net Carbohydrate and Protein System (CNCPS) version 4.0); (ii) optimize crop, soil and manure nutrient management; and (iii) optimize crop rotations.

The CuNMPS software was evaluated on a case-study farm, a 500-cow dairy near Homer, New York. The CNCPS version 4.0 was used to predict site-specific nutrient requirements, nutrient balances, feed budgets, manure production and N, P and K excretion for each group of cattle on the farm with the current programme. This result was then used by the crop rotation spreadsheet to evaluate the match of the current feeding programme with current crop rotations and yields by field and in total. Then alternatives to improve nutrient use in the herd were developed with the CNCPS, and then were evaluated with the crop rotation software. The Nutrient Management Planning for Crop Production was used to predict mass nutrient balances, distribution of manure and supplemental fertilizer recommendations for the current programme and each alternative considered.

A new feeding and cropping programme was designed to minimize purchased feeds to minimize nutrient imports and reduce costs. Intensively managed grass was substituted for maize on the wet, erodible hillsides in the crop rotation programme. In the new plan, only the flat valley land is rotated with maize and lucerne, and hectares seeded each year are reduced 22% by this change. The grasses provide a sink for the excess N from manure, improving the nutrient management. However,

 Modelling Nutrient Utilization in Farm Animals (eds J.P. McNamara, J. France and D.E. Beever)

an additional silo must be constructed to add this extra source of forage, and equipment changes must be made to permit rapid, early harvest of the grass forage. Milk production remains constant but costs $40,000 less to produce. The percentage of the ration that is home-raised is increased to 78%, reducing purchased N, P and K 55, 48 and 82%, respectively. This new plan has the environmental benefit of reducing erosion, which also reduces the potential for phosphorus pollution of water bodies.

Introduction

Livestock operations in North America and Europe are being challenged with preventing contamination of water associated with manure and fertilizer nutrients while at the same time keeping their farms competitive and profitable. Less than one-third of the nitrogen (N), phosphorus (P) and potassium (K) imported on to New York dairy farms each year leave the farm as saleable product (Klausner, 1995). The remaining nutrients either accumulate in the soils or are lost to the environment.

Samples from a stream draining cropland on a case-study dairy farm in New York averaged 14.4 p.p.m. nitrate-N and 0.41 p.p.m. of total P during the growing season, which exceed the US Environmental Protection Agency standards (maximum of 10 p.p.m. and 0.1 ppm for nitrate-N and total P, respectively) (Houser *et al.*, 1996). Over a 15-year period, well-water nitrate concentrations in the intensively cropped area on another case-study farm in New York increased from 3.3 to 7 mg kg^{-1} % versus no change in nitrate concentration in wells in the unfarmed hillside (Wang *et al.*, 1999). Soil test P increased from 6 to 24 kg ha^{-1} % in the intensively cropped valley floor, due to P imports exceeding exports by an average of 70% during the 15 years of this study. In all of these studies, the feeding programme, herd productivity and proportion of feed nutrients grown on the farm influenced nutrient accumulation and the potential for nutrients to enter the environment.

To address this problem, the Cornell University Nutrient Management Planning System (CuNMPS) is being developed and evaluated. The goal of this software is to determine soil fertility and crop nutrient requirements, herd nutrient and feed requirements, manure nutrient management and feed availability with alternative crop rotations. The software consists of four components: (i) calculating a mass nutrient balance; (ii) evaluating and improving the animal feeding programme; (iii) evaluating and modifying crop rotations; and (iv) developing a crop and manure nutrient management plan. The CuNMPS provides computer tools for use by consultants for use in developing nutrient management plans that: (i) maximize the yields of crops suited for the particular soil types, while utilizing manure as a fertilizer source; (ii) maintain or improve herd production through improved ration formulation; (iii) maintain or improve farm profitability; and (iv) decrease the potential for ground- or surface-water pollution.

This chapter describes the application of the CuNMPS, using a case-study farm.

Materials and Methods

The case-study farm is a 500-cow commercial dairy located in Homer, New York, USA. The farm is located over the Homer–Cortland aquifer, which provides all the drinking-water for approximately 50,000 people. The evaluation was conducted using the data from 1 July 1996 to 30 June 1997. At this time, the farm had 500 cows and 430 ha. Soils present on the farm are a mix of level, well-drained soils and moderately well-drained sloping soils. The well-drained level soils are in a maize (for silage) and lucerne rotation. The sloping fields are composed of heavier textured soils, which have a low water-leaching potential, but a high runoff potential.

Herd feeding programme evaluation

The Cornell Net Carbohydrate and Protein System version 4.0 (CNCPS 4.0), as described by Tylutki and Fox (1997) and Fox *et al.* (1999), was used to evaluate the herd feeding programme, and to develop alternatives. Table 19.1 (a and b) describe the herd and rations that were used in the analysis. Two assumptions are made in the initial phases of developing a nutrient management plan with CNCPS 4.0: (i) the herd is in a steady-state condition (neither expanding nor reducing herd numbers); and (ii) the rations being fed are representative of the whole year. This analysis did not include the hutch calves and younger transition heifers, since they are fed a complete calf feed until approximately 100 kg. In the analysis, the older heifers in the transition group were included with the open heifer group, and hospital cows were included with the fresh cow group, since they receive the same ration. Refusals (from the lactating cows, which are fed to the open heifers) were assumed to have the same composition as maize silage.

Evaluation of crop rotations

The crop rotations computer program was used to predict supply of farm-produced feeds with the current and alternative crop rotations to produce feed that matches both the available land resources and the feed needs of the herd for optimum production. The program and its application are described by Kilcer (1997).

Table 19.1a. Case-study herd description.

Group	Number of head	Age (months)	Days preg.	Days in milk	Lact. number	Milk (kg day^{-1})	Fat (%)	Protein (%)	Weight (kg)	Body condition score
Hutch calves	44	1							55	
Transition heifers	64	4							100	
Open heifers	160	11							363	
Bred heifers	106	22	172						454	
Dry cows	100	45	253		2.1				636	
Fresh cows/hospital pen	96	50	70	62	2.6	34.3	4.7	3.0	587	2.55
1st-calf heifers	93	36	150	182	1.2	31.8	3.7	3.1	572	2.92
High cows	216	60	123	183	3.0	36.5	3.7	3.0	677	2.83
Low cows	43	60	157	332	2.5	19.1	4.2	3.4	726	3.59
Average/totals	922	37	173	197	2.4	32.7	3.9	3.1	654*	2.95*

*Averages are representative of lactating cows only.

Table 19.1b. Rations fed at the case-study farm as of 12 June 1997.

Ingredient	Open heifers*	Bred heifers	Dry cows	Fresh/ hospital	1st-calf heifers	High cows	Low cows
Corn silage		0.36	2.95	9.03	9.08	9.25	6.21
MML haylage						1.36	
Grass hay 14%				0.91		0.91	
Grass hay 11%	1.99	6.24	4.72		2.03		4.68
Maize meal			0.23	2.72	3.48	2.92	1.60
Gluten feed	1.77	2.66		2.98	4.00	5.27	3.68
Cottonseed				0.32	1.11	1.42	
Protein mix†			0.59	3.77	3.26	4.10	1.83
Canola meal		0.03	1.36	2.36	0.80		
Minerals	0.12	0.14	0.13		0.10		0.16
Refusals	3.86						

* Units are kg dry matter day^{-1}. Includes older transition heifers. Younger transition heifers and hutch calves are not included because they are fed a complete purchased ration.
† The protein mix is a custom mix that includes minerals.
MML, mixed, mostly legume.

Evaluation of the crop and manure nutrient management plan

The crop nutrient management plan component was used to develop manure spreading and fertilizer recommendations for each field, based upon manure and soil test results and yield potential of the crop/soil. The goal is to maximize recycling of manure nutrients while minimizing leakage into the environment. The details of this program and its application have been described by Bannon and Klausner (1997) and Klausner *et al.* (1998).

Mass nutrient balance

Information computed by the CNCPS and crops, soils and manure nutrient management programs were used to compute the farm mass balance, as described by Bannon and Klausner (1997). A mass nutrient balance is an analysis of the nutrient flows across the farm boundary. It provides an index of nutrients remaining within the farm boundary that must be managed. Depending upon how the results are expressed, the index can be used to compare results with those of other farms or to analyse the rate of nutrient accumulation within the farm boundary.

Results and Discussion

Initial evaluation

The mass nutrient balance values (77.3% for N, 67.5% for P and 64.7% for K) agree with those reported by Klausner (1993) for herds of all sizes. This herd imports 9.1%, 12.7%, and 0% of their N, P and K, respectively, from fertilizer, compared with the average of 33% in the study of Klausner (1993). These differences were due to the crop nutrient management plan followed by the case-study farm.

Table 19.2 summarizes the evaluation of the base feeding programme. The CNCPS predicted total milk production for the year (5,597,538 kg) agreed with actual production. The rations were 54% purchased feed, which is typical for many dairy farms. This results in a large percentage of nutrients imported (74% for N, 77% for P and 50% for K). Manure production was predicted by the CNCPS to be 39,078 kg day^{-1}, agreeing with the manure production computed in the crop nutrient management planning program (Bannon and Klausner, 1997), when wash water from the milking system and bedding are added.

The crop rotation evaluation by Kilcer (1997) indicates that this farm must import feeds to meet the energy, protein and forage needs required by the cattle. As more feed is imported by a farm to meet energy and protein requirements, phosphorus and potassium are usually imported in quantities much higher than are required by the cows and crops (Tamminga, 1992). Analysis of

Table 19.2. CNCPS 4.0 evaluation of nutrients excreted with the current feeding programme.

Herd analysis			
Total milk production	5,597,538 kg year^{-1}		
Av. milk production of lactating cattle	34.2 kg cow^{-1} day^{-1}		
Av. gain of growing cattle	0.36 kg day^{-1}		
Av. wt of all cattle	526 kg		
Rations			
Av. percentage raised	46%		
Av. percentage purchased	54%		
Av. ration cost cwt^{-1} milk	$4.74		
Av. ration cost kg^{-1} gain	$19.12		
Total ration cost of herd	$1,900.46 day^{-1} $694,142 year^{-1}		
Nutrients	N	P	K
Av. percentage purchased	74%	77%	50%
Excreted (kg year^{-1})	91,662	19,764	51,862
Urinary (kg year^{-1})	41,783	375	33,331
Faecal (kg year^{-1})	49,878	19,388	18,531
Product (kg year^{-1})	32,596	6,004	11,299
Efficiency of nutrient use	36%	30%	22%
Manure	kg day^{-1}		
Predicted total manure	39,078		
Predicted faecal	22,913		
Predicted urine	16,164		

1 cwt = 45.4 kg.

forage required versus forage grown revealed a large discrepancy. The analysis suggested a large surplus of maize silage (365 Mt) and a large deficit of hay silage (−279 Mt). This led to a concern regarding the ratios of what was grown (73.6% maize : 26.4% hay silage) vs. what was fed (64.8% maize : 35.2% hay silage). Further analysis indicated that the farm had high maize silage storage losses. Crop rotations and yields on some of the hill soils and crop storage practices were identified as potential limiting factors.

An analysis of the farm's current crop and manure nutrient management plan was also completed (Bannon and Klausner, 1997). Since ammonia is not conserved on this farm, there is not enough manure nitrogen to meet the crops' requirements, resulting in overapplication of P and K compared with the annual crop nutrient requirement (Table 19.3).

Table 19.3. Crop and manure nutrient balances.

	Total collected (kg)	Total crop requirement (kg)	Surplus/ Deficit (kg)
Total N	90,755	36,502	54,253
Available N			
with NH_3 conservation	67,555		31,054
without NH_3 conservation	25,152		−11,350
P_2O_5	35,140	8,490	25,742
K_2O	57,159	7,219	49,940

Proposed modifications in the herd and crop management programmes

The goal in revising the herd feeding and cropping plans was to minimize purchased feeds to minimize nutrient imports. It was concluded that this farm has the potential to improve management of the hay crops to increase yield and quality. Field rotations were changed to plant highly erodible, acidic hill soils to intensively managed grasses and to intensify production of maize and lucerne on the better-quality soils, mostly in the more level valleys. Grass also serves as a nutrient sink for manure.

The feeding programme was then revised to utilize the feeds that would be produced. The major change was the substitution of grass silage for part of the lucerne and maize silage. This change has dramatic implications (Table 10.4). The amount of maize meal required for the new feeding programme is 32% higher than the base; however, maize meal is a low-N, P and K feed. Ration cost was decreased by $40,150 annually. Milk production remained constant; however, the percentage of the ration that is home-raised increased to 78%. The average percentage of purchased N was decreased by 55%, P was decreased by 48% and K was decreased by 82%. Manure production was increased by 10%, due to the higher forage intake of the herd, resulting in higher indigestible feed dry matter. The resulting crop rotation required to support this indicates a shortage of hay silage (−156 Mt) and a surplus of maize silage (146 Mt) during the seeding year of the grass. As the rotation is implemented, yields will increase.

Full implementation of the proposed feeding and cropping programme would lower the nutrients remaining from 77.3% to 52% for N, 65.5% to 50% for P and 64.7% to −58% for K. Phosphorus soil test levels would continue to rise, but at a slower rate, and the farm would begin reducing potassium levels in the soil.

Conclusions and Implications

This case-study analysis was our first attempt at developing an integrated nutrient management plan with the CuNMPS. Through integration of the herd feed-

Table 19.4. CNCPS 4.0 prediction of manure nutrients produced with the revised feeding programme.

Herd analysis			
Total milk production	5,597,538 kg year^{-1}		
Av. milk production of lactating cattle	34.2 kg cow^{-1} day^{-1}		
Av. gain of growing cattle	0.39 kg day^{-1}		
Av. wt of all cattle	526 kg		
Rations			
Av. percentage raised	78%		
Av. percentage purchased	22%		
Av. ration cost cwt^{-1} milk	$4.33		
Av. ration cost kg^{-1} gain	$17.15		
Total ration cost of herd	$1,790.22 day^{-1} $653,877 year^{-1}		
Nutrients	N	P	K
Av. percentage purchased	33%	40%	9%
Excreted (kg year^{-1})	94,249	15,507	74,026
Urinary (kg year^{-1})	37,037	352	51,059
Faecal (kg year^{-1})	57,212	15,155	22,967
Product (kg year^{-1})	32,791	6,068	11,314
Efficiency of nutrient use	35%	39%	15%
Manure	kg day^{-1}		
Predicted total manure	42,999		
Predicted faecal	25,650		
Predicted urine	17,349		

ing and farm cropping programmes, it was predicted that feed purchases could be decreased considerably, while maintaining herd performance. This was accomplished by accurately balancing rations around the crop rotation that makes best use of the farm's soil resources. Decreasing purchased feeds also decreased the loading of N, P and K on this farm, which should lower the risk of nutrients leaking into the air and water when the recommended manure management plan is followed.

In conducting and evaluating this case-study, it became apparent that the herd feeding and crop production plans need to be integrated with each other and with the farm business records to develop the most feasible and profitable whole-farm plan. For example, further economic analysis is required to account for the effects of the new cropping system on feed production costs, storage requirements and capital and labour costs. Although each component appeared feasible, the integrated plan may not be economically feasible. Consequently, we are developing a structure for integrating the CuNMPS components, including

a linkage with the farm's business record-keeping system. Much of the integrated CuNMPS will be implemented on the farm's computer for daily entry of data and for use in making daily management decisions. The farm's consultants (herd feeding, crop production and business records) will need to work together to develop the whole-farm plan and to provide support during implementation.

Currently, data are being collected on the case-study farm that will be used to refine our approach to developing the system, and to evaluate the CuNMPS components and integrated system as they are developed. When completed, the evaluation of the CuNMPS will be expanded to include other farms.

References

Bannon, C.D. and Klausner, S.D. (1997) Application of the Cornell Nutrient Management Planning System: predicting crop requirements and optimum manure management. In: *1997 Proceedings of the Cornell Nutrition Conference for Feed Manufacturers*. Cornell University, Ithaca, New York, USA, pp. 36–44.

Fox, D.G., Tylutki, T.P., Pell, A.N., Van Amburgh, M.E., Chase, L.E., Pitt, R.E. and Rasmussen, C.N. (1999) The *Cornell Net Carbohydrate and Protein System Version 4.0 for Evaluating Herd Nutrition and Nutrient Excretion. Model Documentation Revised for CNCPS Version 4.0.* Cornell Animal Science Department, Cornell University, Ithaca, New York, USA.

Houser, J.B., Pitt, R.E., Hutson, J.L. and Wright, P.E. (1996) Integrating knowledge to improve dairy farm sustainability VI: Measuring nutrient loads from a drainage basin within the farm boundaries. In: *Dairy Farm Sustainability Final Report.* Cornell University Animal Science Mimeograph Series 188, ABEN Staff Report No. 96–1, ARME Research Bulletin 96–07, and SCAS Research Series 96–4, Ithaca, New York, USA, pp. 105–117.

Kilcer, T. (1997) Application of the Cornell Nutrient Management Planning System: optimizing crop rotations. In: *1997 Proceedings of the Cornell Nutrition Conference for Feed Manufacturers.* Cornell University, Ithaca, New York, USA, pp. 45–53.

Klausner, S.D. (1993) Mass nutrient balances on dairy farms. In: *1993 Proceedings of the Cornell Nutrition Conference for Feed Manufacturers.* Cornell University, Ithaca, New York, USA, pp. 126–129.

Klausner, S.D. (1995) *Nutrient Management: Crop Production and Water Quality.* NRAES-101, Northeast Regional Agricultural Engineering Service, Ithaca, New York, USA.

Klausner, S.D., Fox, D.G., Rasmussen, C.N., Pitt, R.E., Tylutki, T.P., Wright, P.E., Chase, L.E. and Stone, W.C. (1998) Improving dairy farm sustainability I: An approach to animal and crop nutrient management planning. *Journal of Production Agriculture* 11, 225–233.

Tamminga, S. (1992) Nutrition management of dairy cows as a contribution to pollution control. *Journal of Dairy Science* 75, 345–357.

Tylutki, T.P. and Fox, D.G. (1997) Application of the Cornell Nutrient Management Planning System: optimizing herd nutrition. In: *1997 Proceedings of the Cornell Nutrition Conference for Feed Manufacturers.* Cornell University, Ithaca, New York, USA, pp. 54–65.

Wang, S.J., Fox, D.G., Cherney, D.J.R., Klausner, S.D. and Bouldin, D. (1999) Impact of dairy farming on well water nitrate level and soil content of phosphorus and potassium. *Journal of Dairy Science* 82, 2164–2169.

20

Modelling Nutrient Utilization by Livestock Grazing Semiarid Rangeland

F.D. Richardson,[1] B.D. Hahn[1] and S.J. Schoeman[2]

[1]*Department of Mathematics and Applied Mathematics, University of Cape Town, Rondebosch 7701, South Africa;* [2]*Department of Animal Science, University of Stellenbosch, Stellenbosch 7600, South Africa*

Abstract

Planning and management of rangeland production systems are difficult as rainfall, forage production and composition and animal productivity all vary widely between years, between regions and within landscapes. Furthermore, behaviour of the system in a specific year may be influenced by conditions in previous years. An objective of modelling is to increase understanding of the mechanisms within the system that influence the effects of rainfall, stocking rates and management strategies on the productivity of both vegetation and livestock in the short and long term. Nutrient utilization by domestic livestock is the link between the animal and plant components of the system. Modelling such complex systems presents some particular and interrelated problems. Firstly, the time scales which characterize the individual processes of the system vary from hours for rumen fermentation to years for changes in populations of different plant species. Long-term changes in rangelands depend on the cumulative effects of short-term processes. Secondly, simulation of at least 100 years is necessary for patterns of vegetation changes in relation to management strategies to emerge and because stochastic features such as rainfall, frost and fire drive the system, runs must be replicated. Consequently detailed mechanistic models of the whole system are unsuitable for simulating rangeland productivity in the long term. Thirdly, if simple models are used the necessary detail of representation of specific processes changes with changes in vegetation and in management strategies. Instead of building a complex model of the whole system, a hierachy of dynamic computer models is being developed. A mechanistic model simulates the availablity of forage and the performance of individual breeding and growing animals on a daily basis. This model has deterministic submodels of diet selection, intake, digestion and

 Modelling Nutrient Utilization in Farm Animals (eds J.P. McNamara, J. France and D.E. Beever)

partition of nutients between milk, conceptus, body protein and fat. Model output shows that the total amount of rainfall, its distribution during the season and stocking rate all affect the performance of the system. The output of extensive runs of the mechanistic model are encapsulated in a few simple formulae for each vegetation state to represent plant and animal dynamics in a long-term model of a rangeland supporting cattle and goats. This model may be used to show how various management strategies influence long-term responses of the system in terms of vegetation state and livestock production.

Introduction

Arid and semiarid regions account for 55% of the land area of sub-Saharan Africa and for 57% of its domestic ruminants (Sandford, 1995). Livestock products from these regions constitute between 14 and 19% of the total value of agricultural production in the subcontinent (Scoones, 1995). Multipurpose herds and flocks on extensive rangeland support large numbers of pastoral livelihoods and contribute substantially to many national economies. Semiarid rangeland systems are non-equilibrium, as rainfall varies widely between years (coefficient of variation (CV) > 0.4); consequently there are substantial temporal variations in forage production and animal performance (Behnke and Scoones, 1993). Rangelands are also heterogeneous in space and even within landscapes, due to differences in soils. The most serious problem, as far as pastoralists are concerned, is that there are irregular critical shortages of fodder, which lead to livestock losses and threaten livelihoods and, in extreme cases, human lives. Such crises can be planned for, not only to provide a safety net against human destitution and death, but also to provide a means for rapid recovery after a crisis (Swift, 1995). In addition, grazing and management can lead to long-term changes in vegetation, with consequent reductions in plant and animal productivity (Dye and Spear, 1982; Archer, 1996). Carry-over effects are important; for example, forage availability in one year may influence milk yields and calf growth in the following year, especially if rainfall during the second year is below average.

Effective planning and management require that the behaviour of the system is understood. Modelling the behaviour of rangeland is considered to be preferable to an approach based solely on monitoring for the prediction of the long-term response to a wide range of management strategies (Biot, 1993). Simulation models, when calibrated for specific rangelands, allow for the response of both plants and animals to different management strategies to be studied for 100 years or more. One objective is to increase understanding of the mechanisms within the system that influence the effects of rainfall and of the numbers and kinds of animals on changes in vegetation and on the output of animal products.

Simple models of productivity may be used in economic and decision-

support models. For example, Gillard and Monypenny (1990) as part of an economic model used ranch records to show that the components of animal productivity (live-weight changes, calving and mortality rates) are related to a single variable (pasture proxy = mm ha beast^{-1}), which combines area per animal and annual rainfall to represent forage availability. However, these models do not fit the data closely ($R^2 = 0.61$), probably because they do not allow for soil differences, the timing of rainfall and differences in the condition of vegetation and animals at the start of the year. Dye and Spear (1982) found that the relation between herbage yield and annual rainfall varied substantially with soil type. Simple models, such as those of Jones and Sandland (1974) and Gillard and Monypenny (1990), usually ignore long-term changes in vegetation, which can have a large impact on animal production (Dean and Macdonald, 1994; Archer, 1996). A major problem is that species changes may not become apparent even after 20 years, which is often the limit of field observations (Wiegand *et al.*, 1998).

Computer models of rangeland vegetation dynamics, such as those reviewed by Wiegand *et al.* (1998), simulate the influence of grazing management on plant communities over very long periods of time; however, they do not predict animal productivity. There is a need to link models of vegetation, including species dynamics, with livestock models, so that the long-term interrelations between rainfall, management strategies and rangeland productivity may be examined.

Complex mechanistic models of rangeland production systems have been developed (Richardson *et al.*, 1991; Illius *et al.*, 1998). If milk production is simulated mechanistically, the integration interval should not exceed 0.01 days. This means that extremely long runs of the model are required to simulate 100 years. Because variation in rainfall, both between and within years, and the probabilities of fire and frost are stochastic and changes in vegetation state depend on coincidences between many factors, runs need to be replicated before the probability of such changes may be predicted with confidence.

Recently, frame-based models have been developed to simulate the long-term consequences of different management strategies on both vegetation and livestock productivity (Hahn *et al.*, 1999). Key factors or processes that influence the productivity of the system and the relations between vegetation, climate and animals are represented in frame-based models by phenomenological submodels, consisting of a few equations and tables or rules, which may change with changes in the state of vegetation. Here phenomenology is used in the same way as by Parks (1982) – 'the scientific description of actual phenomena with the avoidance of all interpretation, explanation and evaluation' – although simulated rather than real phenomena are involved. This is justified if the mechanistic models accurately simulate the behaviour of actual systems.

The equations and tables required for the frame-based models may be derived from survey data and the results of experiments. However, these empirical data are usually only available for a limited number of sites and data for a specific area may only be suitable for the present state of the vegetation; different

data will be required if the species composition changes. This is supported by Walker and Langridge (1996), who pointed out that a lack of suitable site data is an obstacle to the building and calibration of suitable rangeland models. In this chapter, the feasibility is examined of using mechanistic models based on sound biological principles to generate the information required for long-term models of rangeland under conditions where no suitable empirical data are available. The output from several runs of a mechanistic model for years of different rainfall and different animal numbers is encapsulated in the simple phenomenological models required. These models predict:

1. The quantity and botanical composition of available forage.
2. The amounts of the different parts of each species that are eaten. These quantities determine the intakes of nutrients and the influence of livestock on the vegetation.
3. Growth rates, milk yields and fibre production of grazing animals.
4. Reproductive and mortality rates for each class of livestock.

Mechanistic Models

The mechanistic models comprise three submodels: plant submodel, diet selection, intake and digestion submodel and animal production submodel. In this chapter, the mechanistic model for a semiarid savannah, where rainfall occurs in the warmest part of the year and temperature does not limit herbage growth, is described. A similar model is being developed for the arid shrublands of the succulent Karoo. Because the model is large, comprising some 44 differential equations, a general description of the submodels is given, because a list of all the equations and parameters is not provided in this chapter.

Plant submodel

The herbage growth submodel for savannah regions is essentially that developed by Dye (1984) for areas where grass growth is limited by soil moisture and temperatures during the rainy season do not limit plant growth. The model has been reformulated as a system of differential equations. It has been modified to allow for differences in soil water storage capacity and effects of the magnitude of stored carbohydrate on grass growth early in the following season. Daily rainfall is partitioned between runoff, storage in the soil profile and loss by deep drainage. Soil moisture decreases as a result of evaporation and of transpiration, which is estimated as a function of the weight of green leaf and soil moisture. The net dry-matter growth rate depends on the transpiration rate and is allocated to different parts of the plant in relation to time since the start of growth and the availability of soil water. The death rate of green leaves increases with time and with a decrease in soil moisture. Standing herbage decreases as a

result of grazing and the decay of dead material; the rate of decay increases during the rainy season. For areas where bush makes a significant contribution to animal diets, a woody plant submodel, based on that of Teague (1987), is used.

Diet selection, intake and digestion submodel

An important component in the interactions between plants and animals is the amount and kinds of material eaten by grazing animals. Two methods are used to simulate the composition and digestibility of the diet selected by grazing animals. The proportion of each component in the diet of animals grazing savannah ranges is modelled as a function of the fraction of each component in the available herbage and the relative preference of animals for that fraction (Orsini, 1990). When arid shrublands with several species are simulated, a selection submodel based on the MIAMH model of Genin and Quiroz (1993) is used. The principal symbols used in the intake submodel are listed in Table 20.1.

The model combines three mechanisms of food intake regulation, using the approach of Poppi *et al.* (1994). First, the rate at which the animal is able to eat herbage also limits intake; this depends on size of the mouth, herbage density and the maximum number of bites per day. The maximum number of bites per day, B_{max} increases from zero at birth to 38,000 day^{-1} at 16 weeks. Maximum bite size is a function of arcade breadth, *Arc*, which is related to the peak weight already attained by an animal (equation m1) (Taylor *et al.*, 1987). Peak weight is used, as arcade breadth does not decrease if an animal loses weight.

Table 20.1. Principal symbols used in the food intake submodel.

Symbol	Description	Units
Arc	Dental arcade breadth	mm
B_{max}	Maximum number of bites per day	
E	Total energy in body	MJ
Ecg	Energy content of the gain	MJ kg^{-1}
Fdm	Faecal dry matter output	kg day^{-1}
G	Grass density	kg DM ha^{-1}
J	Adjustment factor	Dimensionless
K_h	Parameter of adjustment equation	kg grass DM ha^{-1}
K_b	Maximum weight of grass per bite	kg DM mm Arc^{-1}
Md	Present milk yield	kg day^{-1}
n	Rate constant of gain	Dimensionless
Qf	Maturity coefficient of intake	Dimensionless
W	Live-weight	kg
W_p	Peak live-weight	kg
W_{max}	Live-weight at maturity	kg
Xcow	Live-weight as fraction of mature weight	Fraction

$$Arc = 8.25\ W_p^{0.29}\ W_{max}^{0.07} \quad \text{(m1)}$$

In the savannah model, the intake, I, is adjusted for grass density, G, assuming a sigmoidal response, to calculate an adjustment factor, J (Johnson and Parsons, 1985; Thornley, 1998):

$$J = (G/Kh)^q/(1 + (G/Kh)^q) \quad \text{(m2)}$$

$$I = J\ K_b\ B_{max}\ Arc \quad \text{(m3)}$$

Secondly, intake may be limited by the capacity of the digestive system. This is modelled as a function of the rate of output of faecal dry matter (DM) and the digestibility of the diet selected. Where the rumen degradation characteristics of the diet are available, they may be used to predict intake instead of digestibility. Both faecal output (*Fdm*) and rumen volume are related to body weight and are maximal when the animal's weight as a fraction of mature weight, *Xcow*, is 0.75 (Butterfield, 1988). The value of *Qf* is assumed to be 3.0. In animals weighing less than 0.75 of their mature weight, potential faecal output and rumen volume are assumed not to decrease with a decrease in live-weight. This is because *ad libitum* intakes of animals that have lost weight are greater than in animals of the same weight that have grown continuously (Saudibet and Verde, 1976). Faecal output and rumen volume both increase with milk yield in lactating animals.

$$Xcow = W\ W_{max}^{-1} \quad \text{(m4)}$$

$$Fdm = Fmat\ (Qf\ Xcow + (1 - Qf)\ Xcow^2) + 0.075Md \quad \text{(m5)}$$

Dry-matter intake increases with the digestibility of the selected diet. As the nutritional values of forage are expressed in terms of metabolizable energy (ME), I is a function of *Fdm* and ME concentration in the selected diet (*MED*) (equation m6):

$$I = Fdm/(1 - (MED/18.4)/0.82) \quad \text{(m6)}$$

The term *MED*/18.4 is the metabolizability of the diet, as the gross energy of forage is assumed to be 18.4 MJ kg^{-1}; ME is assumed to be 0.82 of digestible energy (Khan and Spedding, 1984).

Thirdly, in sucking calves the maximum ME intake is determined by their growth potential. Consequently, the calf only eats sufficient forage to make good the difference between ME supplied by milk and its requirements. Potential energy retention is estimated from present body weight, weight at maturity and the energy value of gain, equation m7 (Bruce *et al.*, 1984). The energy value of gain may be estimated from the equations of the Agricultural Research Council (ARC, 1980):

$$dE/dt = Ecg\ (n\ W \log(W/W_{max})) \quad \text{(m7)}$$

The rate constant in equation m7 is a function of W_{max} (equation m8):

$$n = (36.4\ W_{max}^{0.27})^{-1} \quad \text{(m8)}$$

The simulated intake is the smallest of those predicted by the three mechanisms.

Animal production submodel

Dietary energy and body reserves are partitioned between competing processes within the animal, using the method of Finlayson *et al.* (1995). Potential rates of fat and protein accretion, conceptus growth and milk production are predicted and adjusted according to the animal's nutritional status. The current model specifically simulates the effects of nutrition during late pregnancy on growth of the conceptus and udder development, both of which affect the growth and survival of the young.

The model also accommodates the influence of nutrition and the daily rate of milk removal during early lactation on subsequent potential milk yield. Potential milk yields are simulated mechanistically by the model of Neal and Thornley (1983), which has been extended to include the effect of nutrition on the production and loss of secretory cells. Thus the model may be used to assess the effects of partial milking of suckling cows on calf growth and survival and on reconception rates.

Conception rates are modelled as a sigmoid function of the ratio of present body weight to mature body weight. Daily mortality rates of cattle older than 6 months depend on current body weight as a proportion of the peak weight previously attained by that specific animal (Moore *et al.*, 1995). Preweaning daily mortality is related to the present weight of calves as a fraction of the weight predicted by the standard growth curve for calves of that age and genotype (Moore *et al.*, 1995).

Implementation of mechanistic model

The model is run using the interactive program DRIVER (Hahn and Furniss, 1988). This package is designed to accommodate models that incorporate submodels of different mathematical types and to simulate episodic events, such as rainfall. The model can use recorded daily rainfall data, if available, or daily rainfall may be simulated for a site of specific latitude and longitude, using RAINGEN (Zucchini *et al.*, 1992). The savannah model comprises 44 differential equations, which are integrated using a second-order Runge-Kutta method, with an integration step of 0.1 days for models of growing animals and 0.01 days if lactating females are simulated.

An effective soil depth of 900 mm and field capacity of 29 mm water 100^{-1} mm of soil are assumed (Dye, 1984), unless site data are available. Time of mating may be specified by the user; the default date (15 November) ensures that calves are born just before the average date of onset of the main rains. At

the start of a run, which may simulate 1 or more years, the default initial values for cow live-weight and the weights of protein and fat are 336.9, 62.1 and 71.5 kg, respectively.

Comparison between simulated and experimental values

Model output was compared with a factorial experiment in south-western Zimbabwe in which Afrikaner cows grazed range at two stocking rates, 0.123 and 0.270 cows ha^{-1} and were given three different amounts of protein-rich concentrates as a supplement during the dry season (Richardson and Khaka, 1981, 1983, 1984). Cows were subjected to the same treatment for at least 4 years, and each year the oldest 20% of cows in each group were replaced by maiden heifers. Cows subjected to a specific stocking rate grazed the same set of paddocks in a rotational system for the duration of the experiment, so that the cumulative effects of stocking rate on both range and animals could be studied. In view of the numbers of animals involved, an adequate area of uniform range, similar to that simulated by Dye (1984), was not available. The sets of paddocks used for each stocking rate contained similar proportions of each rangeland type. Only about half of the land had soils similar to those used by Dye (1984) and a large proportion had shallow soils and sparse vegetation. This illustrates the difficulty of finding suitable data for the validation of rangeland models and the need to develop models that incorporate spatial variability.

The mechanistic model may be used to show how timing of rainfall influences the pattern of grass growth. The maximum rate of grass growth in 1982 occurred later in the season than in 1981 and this is a reflection of lower cumulative rainfall throughout the season (Fig. 20.1).

Results are presented for animals that were given no concentrates. The model closely simulates the effects of stocking rate on cow and calf live-weights and on reconception rate (see Table 20.2). The predicted variation in animal

Table 20.2. Comparison between model prediction and experimental values for the productivity of cattle grazing semiarid range over 3 successive years (experimental values are enclosed by parentheses).

Stocking rate (cow ha^{-1})	Year	Rainfall (mm)	Cow live-weight (kg)	Reconception rate	Calf weight at 210 days (kg)
0.123	1979/80	508	366 (358)	0.484 (0.57)	167.1 (166.7)
0.123	1980/81	759	349 (343)	0.635 (0.71)	161.6 (168.4)
0.123	1981/82	367	350 (365)	0.686 (0.47)	172.4 (177.3)
0.270	1979/80	508	329 (318)	0.207 (0.06)	140.0 (122.4)
0.270	1980/81	759	297 (312)	0.188 (0.19)	141.9 (134.1)
0.270	1981/82	367	303 (332)	0.224 (0.24)	145.6 (131.4)

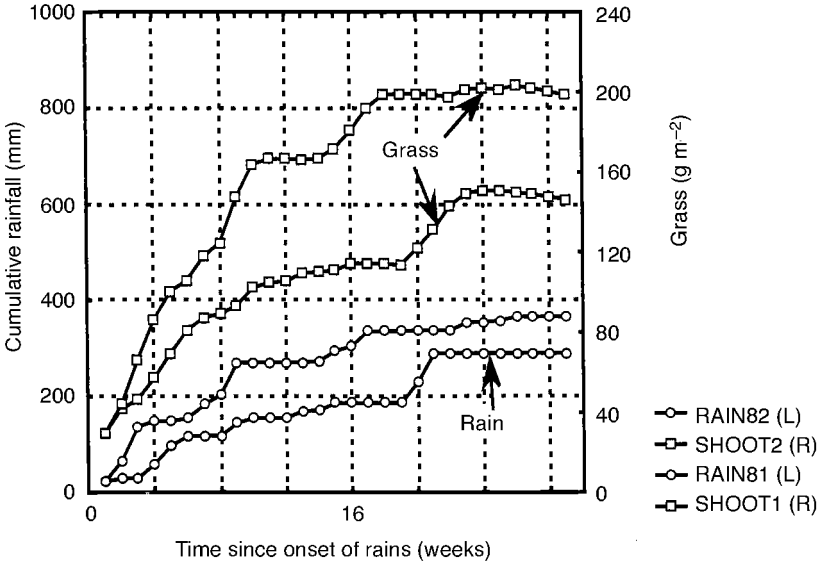

Fig. 20.1. Effect of timing of rainfall on grass growth.

performance between years is small, which agrees with the results of the experiment, and the trend of variation between years is reasonable, because there were no years of severe drought (annual rainfall < 250 mm) during the period of the experiment. The adverse effects of the relatively low rainfall in 1981/82 were probably masked by the early onset of the rains in that year (Fig. 20.1, discussed below in the section on dry-matter intake). The experiment was terminated before the late-rainfall year of 1982/83.

Phenomenological Models

The phenomenological models are derived by using STATISTICA (1998) to fit regression equations to the output of several runs of the mechanistic model to produce relatively simple formulae, just as would be done with the data from field experiments. These simple models form part of the frame-based ecosystem model, such as that of Hahn *et al.* (1999), or of economic models. In addition, they aid understanding of the factors that influence the processes concerned. These models may be used either as the actual regression equations or may be summarized in the form of rules. They provide quantitative descriptions of feed intake and the amounts of each component eaten, weight changes of different classes of animals, milk yields and reproductive and survival rates. Rainfall records used to drive the mechanistic model vary stochastically. Consequently, model predictions may be scattered around the fitted line, as the rainfall pattern

influences both plant and animal performance. One advantage of this approach is that many more treatments and years may be simulated than is possible with conventional experimentation. Furthermore, phenomenological models may be formulated for appropriate time steps. Yearly or 6-monthly intervals are suitable for both ecological and economic models. The combined use of mechanistic and phenomenological models can lead to greater understanding of how different factors influence the behaviour of the system. All the examples of phenomenological models shown below are for savannah rangeland grazed by cattle; the principal symbols are shown in Table 20.3. In these models, grass growth and stocking rate are combined to form one variable – forage availability:

$$F_i = G_i\, Ah^{-1} \qquad \text{(p1)}$$

Grass density for the wet season is yield of grass (kg ha^{-1}) when there are no animals. At the start of the dry season, grass density is grass yield less the amount removed by grazing animals during the wet season.

Dry-matter intake

As food intake is the major variable driving animal productivity, mechanistic model predictions of dry-matter intake (DMI) for the wet (I_w) and dry seasons (I_d) have been analysed in relation to forage availabilty. The wet season is assumed to last for 165 days, starting on 15 November, followed by a dry season of 200 days, although the actual onset and end of the rains may vary between years. The relations between DMI and F_w or F_d are represented by asymptotic functions (Snedecor and Cochran, 1967), although they could be equally well described by two intersecting straight lines (Fig. 20.2). DMI increases at a decreasing rate, with an increase in F_i, reaching a maximum when intake is limited by the capacity of the digestive system. The time of the onset of sufficient rain to initiate substantial growth of grass affects the total amount of grass eaten during the rainy season (see Fig. 20.2). If the onset of the main rains is late, animals have to eat dead mature grass of low digestibilty for a substantial part of the assumed wet season and their intakes will be reduced accordingly. Separate models are fitted for years of early and late rains – equations p2 and p3:

Early rains:

$$I_w = 1573.1 - 1396.6 \exp(-0.000316\, F_w)\; r^2 = 0.953 \qquad \text{(p2)}$$

Late rains:

$$I_w = 1382.4 - 884.7 \exp(-0.000193\, F_w)\; r^2 = 0.991 \qquad \text{(p3)}$$

Intake during the dry season does not appear to be influenced by the timing of the rains and only one equation, p4, is fitted:

$$I_d = 1669.1 - 1935.1 \exp(-0.000250\, F_d)\; r^2 = 0.870 \qquad \text{(p4)}$$

The consumption of forage by sucking calves may be substantial and affect the amount of standing herbage at the end of the year. No simple model can be

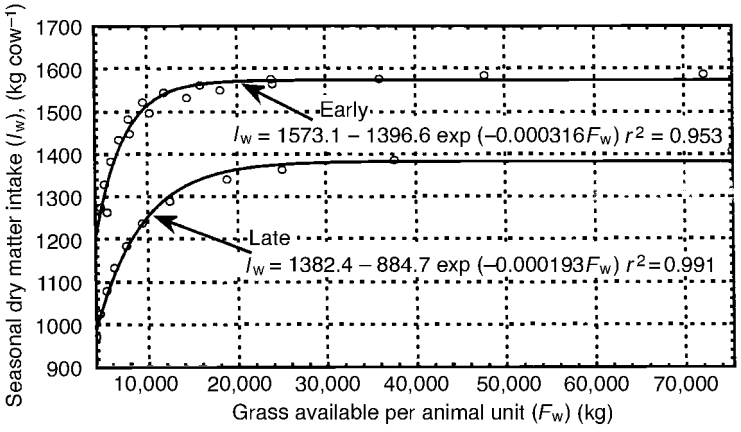

Fig. 20.2. Dry-matter intakes of lactating cows during the wet season in years of early and late rains.

derived to accurately predict forage consumption of calves from forage availability and milk consumption, because three different mechanisms are involved. If an estimate is required for an ecological model, it may be calculated from calf live-weight at the end of the period and milk consumption:

$$I_c = 0.237 + 3.961\ W_c - 0.306\,\mathrm{Mc}\quad R^2 = 0.985 \tag{p5}$$

Table 20.3. Principal symbols used in the phenomenological model.

Symbol	Description	Units
Ah	Stocking rate	Cow ha^{-1}
Cr	Conception rate of cows	Fraction
F_w	Forage availability, wet season	kg DM LSU^{-1}
F_d	Forage availability, dry season	kg DM LSU^{-1}
G_w	Potential grass density (wet season)	kg DM ha^{-1}
G_d	Grass density (dry season)	kg DM ha^{-1}
I_c	Calf forage intake to one year	kg
I_w	Total dry matter intake (wet season)	kg DM cow^{-1}
I_d	Totaly dry matter intake (dry season)	kg DM cow^{-1}
Mc	Calf milk consumption	kg year^{-1}
My	Total milk yield, 210-day lactation	kg cow^{-1}
Md	Daily milk yield	kg cow^{-1} day^{-1}
Sc	Cow survival rate	Fraction year^{-1}
Sk	Calf survival rate to one year old	Fraction
W_c	Weight of calf at end of wet season	kg
W_y	Weight of weaned calf at one year	kg

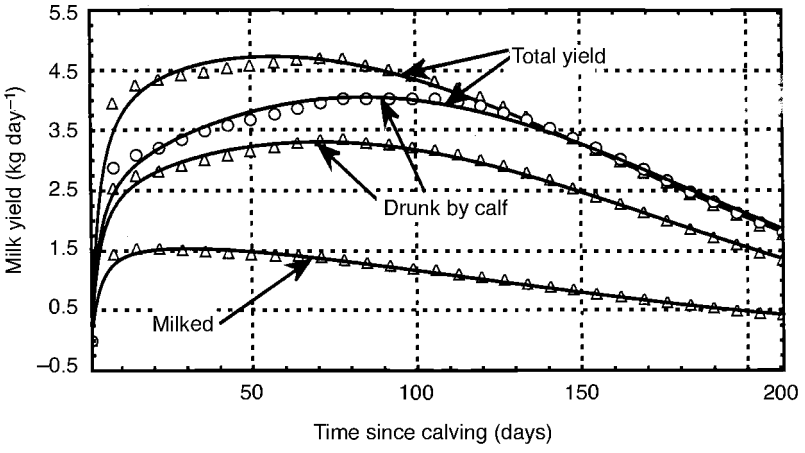

Fig. 20.3. Predicted total milk yields of suckling cows that were either milked or not milked and the amounts removed by the calf or by milking. △, Cow milked; ○, cow not milked.

Milk production

The amount of milk consumed by sucking calves is a major factor determining their growth and survival. In addition, milking suckling cows provides an important source of protein for pastoral communities. The mechanistic model shows that total daily milk yields increase when cows are milked (Fig. 20.3). The model of Williams (1993) was fitted to the model output. The higher yields of cows that are milked are due to increased production during the first half of lactation. During this period, the rate of milk secretion of non-milked cows is limited by the rate at which their calves remove milk. Although milking leads to an increase in milk yield, the increase is less than the amount removed by milking, so milk consumption by the calf is reduced (see Fig. 20.3).

Total lactation yield is closely related to herbage availability and this relation is influenced by the time of the onset of the rains. Cows produce more milk in a year when the rains start early rather than late (Table 20.4). Within the same year, suckling cows that are milked produce more milk in a lactation than those that only suckle their calves. When the model is run for a year of low rainfall and a stocking rate of 0.2 livestock units (LSU) ha^{-1}, it predicts that the cows weigh only 353.64 kg and contain 54.80 kg protein and 52.54 kg fat. At parturition, their udder secretory tissue is 0.65 of that in cows weighing 406.2 kg. When these values are used as the initial values at the start of the season, predicted milk yields are substantially lower than those of heavier cows for similar values of herbage availability (see equation p10 and Table 20.4).

Table 20.4. Effects of milking, timing of rainfall and previous nutrition on parameters of the phenomenological model of total milk yield of cows in relation to herbage availability during the wet season, $My = A_m - b_m \exp(-c_m F_w)$.

Equation no.	Cow hand-milked	Post-partum live-weight	Time of onset of rains	A_m	b_m	c_m
p6	Yes	406.2	Late	750.2	146.8	0.00112
p7	Yes	406.2	Early	800.1	137.7	0.00178
p8	No	406.2	Late	673.3	180.8	0.00085
p9	No	406.2	Early	713.1	155.2	0.00145
p10	No	353.6	Early	543.4	224.9	0.00212

Calf growth and survival

The fitted models show how the time of the onset of the rains, milking and forage availability affect the growth of calves until they are 1 year old (Table 20.5). One year has been chosen, as it represents the cumulative effects of rainfall and stocking rate over both the wet and dry seasons. Milking the dam leads to a substantial reduction in live-weight at 1 year and so does a delay in the onset of rains, especially at low grass availability, which is a reflection of a high stocking rate. Calf survival to 1 year is also reduced by milking, low forage availability and late rains (Table 20.6).

Conception rate

Conception rates of lactating cows are related to grass availability (F_w). The live-weight of the cow just before calving at the start of the rainy season has a major effect on the subsequent conception rate (Cr), shown by different constant terms for cows of different live-weight at this stage (equations p18 and p19). Very light stocking rates, which lead to high grass availability, do not ameliorate the effects of cows being in a very poor condition at the start of the rains:

Cow live-weight 406 kg:
$$Cr = 0.5938 - 0.5438 \exp(-0.000199 F_w) \quad \text{(p18)}$$

Cow live-weight 354 kg:
$$Cr = 0.4635 - 0.3682 \exp(-0.000114 F_w) \quad \text{(p19)}$$

Frame-based Model

The savannah frame model simulates animal production and vegetation changes in relation to rainfall patterns and management strategies over periods of 200 years (Hahn *et al.*, 1999). Cattle graze a rangeland area of 1000 ha, with

Table 20.5. Effects of milking and timing of rainfall on parameters of a phenomenological model ($W_y = A_w - b_w \exp(-c_w F_w)$) of weight ($W_y$) at one year of weaned calves of cows weighing 406 kg post-partum in relation to herbage availability (F_w).

Equation no.	Cow hand-milked	Time of onset of rains	A_m	b_m	c_w
p11	Yes	Late	147.55	249.40	0.000204
p12	Yes	Early	168.55	867.52	0.000375
p13	No	Late	212.91	349.79	0.000186
p14	No	Early	230.88	710.01	0.000294

Table 20.6. Effects of milking and timing of rainfall on parameters of a phenomenological model $Sk = A_s - b_s \exp(-c_s F_w)$ of survival rate (Sk) to 1 year of calves of cows weighing 406 kg in relation to herbage availability (F_w).

Equation no.	Cow hand-milked	Time of onset of rains	A_s	b_s	c_s
p15	Yes	Late	0.8264	1.7777	0.00009
p16	Yes	Early	0.9998	9.7728×10^2	0.00115
p17	No	Late	0.9900	4.2072×10^7	0.00327

an upper stratum of bush or low trees and undergrowth dominated by grass. Each year consists of a wet and a dry season. At the start of a run, the herd is assumed to consist of 75 mature cows, 25 2-year-old cattle, 25 yearlings and 50 calves. The 200-year runs are replicated to estimate average cattle sales and milk production and the probabilities of cattle mortality rate exceeding 0.75 or of the range becoming degraded to thicket.

This model may be used to examine and compare different management strategies for communal rangeland. In the first option, A, 'boom and bust', no special measures are taken to prevent severe mortality during drought years, cows are milked and only 3-year-old steers are sold. In strategy B, cows are milked and measures are taken to prevent mortality exceeding 0.78 in drought years by selling animals before forage becomes very scarce, by supplementary feeding or by moving them to areas where forage is still available. In addition, 0.1 of mature cows are sold each year when cattle numbers exceed 100. Option C represents a commercial system, where cattle numbers are not allowed to exceed 0.2 LSU ha^{-1}, by selling additional animals whenever the stocking rate increases above this.

Annual cattle sales are lowest for the 'boom and bust' strategy and highest for the commercial strategy (Table 20.7). Taking steps to limit mortality to 0.78 does not reduce the probability of mortality exceeding 0.75, but limiting the stocking rate leads to a substantial reduction in the probability of severe losses.

Table 20.7. Predictions of long-term performance of cattle subjected to three management strategies.

Strategy	A Mortality not controlled	B Mortality controlled	C Commercial
Handmilking	Yes	Yes	No
Annual cattle sales	15.8	34.3	54.6
Probability of mortality exceeding 0.75	0.046	0.056	0.012

Mortality in the communal herd in Gazankulu was approximately 0.75 in 1983/84 and in 1991/92 (Dikeni *et al.*, 1996), which seems to indicate that pastoralists adopt strategy B (Fig. 20.4a,b).

Discussion and Conclusion

The present study supports the concept of Gillard and Monypenny (1990) that the components of animal productivity are functions of some index of herbage availability. The underlying relation between dry-matter intake and forage availability was found to be asymptotic (see Fig. 20.2). Consequently, the finding that all the other components of production are asymptotic functions of herbage availability is not surprising. Because diet composition, digestibility and nutrient utilization are represented explicitly in the mechanistic model, the output depends on all these factors and so their effects are encapsulated in the phenomenological models.

This investigation has shown that simple phenomenological models of the components of rangeland production systems for specific sites and management options may be derived from the output of generalized mechanistic models. The work has also shown how the parameters of these models vary with changes in rainfall pattern, milking policy and present condition of the animals. Rules may be formulated for choice of appropriate values for parameters, as in the frame-based model of Hahn *et al.* (1999). Alternatively, functions may be developed to estimate suitable parameter values for specific circumstances, using a method analagous to that of Williams (1993).

Frame-based ecosystem models that use phenomenological models similar to those described above have been used to study the long-term responses of rangeland systems, in terms of animal production and vegetation state, to various management strategies (Hahn *et al.*, 1999).

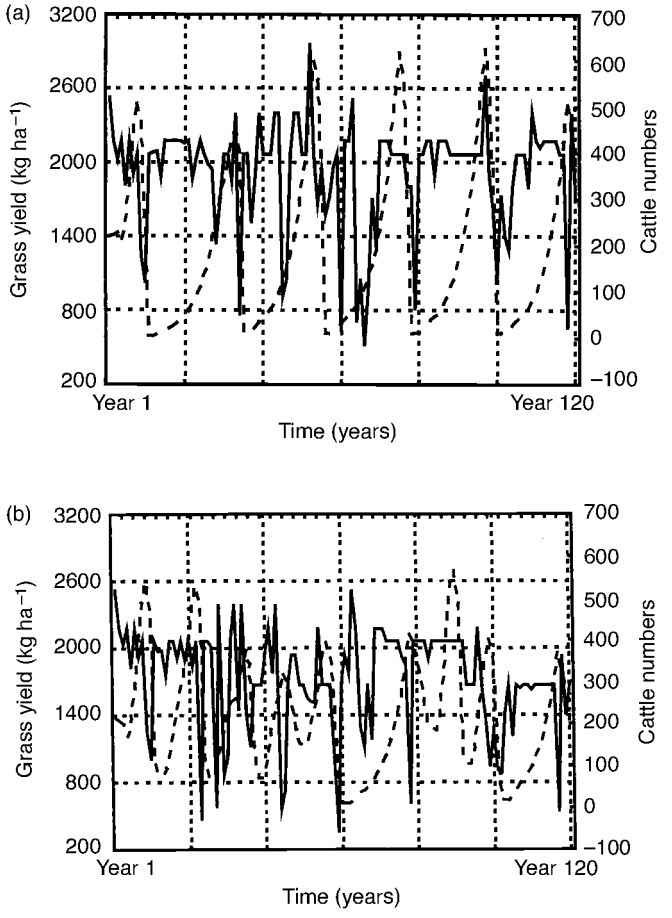

Fig. 20.4. Grass yields and cattle numbers in relation to time. (a) No measures taken to reduce mortality, cows milked. (b) Steps taken to reduce mortality, cows milked. ——, Grass yield; ---, cattle numbers.

References

Agricultural Research Council (ARC) (1980) *The Nutrient Requirements of Ruminant Livestock*. Commonwealth Agricultural Bureaux, Slough, 351 pp.

Archer, S. (1996) Assessing and interpreting grass–woody plant dynamics. In: Hodgson, J. and Illius, A.W. (eds) *The Ecology and Management of Grazing Systems*. CAB International, Wallingford, UK, pp. 101–134.

Behnke, R.H. and Scoones, I. (1993) Rethinking range ecology: implications for rangeland management in Africa. In: Behnke, R.H., Scoones, I. and Kerven, C. (eds) *Range Ecology at Disequilibrium*. Overseas Development Institute, London, pp. 1–30.

Biot, Y. (1993) How long can high stocking densities be sustained. In: Behnke, R.H.,

Scoones, I. and Kerven, C. (eds) *Range Ecology at Disequilibrium*. Overseas Development Institute, London, pp. 153–172.

Bruce, J.M., Broadbent, P.J. and Topps, J.H. (1984) A model of the energy system of lactating and pregnant cows. *Animal Production* 38, 351–362.

Butterfield, R.M. (1988) *New Concepts of Sheep Growth*. Department of Veterinary Anatomy, University of Sydney, Sydney, 168 pp.

Dean, W.R.J. and Macdonald, I.A.W. (1994) Historical changes in stocking rates of domestic livestock as a measure of semi-arid and arid rangeland degradation in the Cape Province, South Africa. *Journal of Arid Environments* 26, 281–298.

Dikeni, L., Moorhead, R. and Scoones, I. (1996) *Land Use and Environment Policy in the Rangelands of South Africa*. Land and Agriculture Policy Centre, Johannesburg, South Africa.

Dye, P.J. (1984) Prediction of variation in grass growth in a semi arid induced grassland. PhD thesis, University of the Witwatersrand, Johannesburg.

Dye, P.J. and Spear, P.T. (1982) The effects of bush clearing and rainfall variability on grass yield and composition in South West Zimbabwe. *Zimbabwe Journal of Agricultural Research* 20, 103–118.

Finlayson, J.D., Cacho, O.J. and Bywater, A.C. (1995) A simulation model of grazing sheep: 1. Animal growth and intake. *Agricultural Systems* 48, 1–25.

Genin, D. and Quiroz, R. (1993) MIAMH, a predictive model of range ruminant diets in patchy environments. *Agricultural Systems* 43, 381–395.

Gillard, R. and Monypenny, R. (1990) A decision support model to evaluate the effects of drought and stocking rate on beef cattle properties in Northern Australia. *Agricultural Systems* 34, 37–52.

Hahn, B.D. and Furniss, P.R. (1988) A description of DRIVER: an interactive modelling tool. *South African Journal of Science* 84, 749–753.

Hahn, B.D., Richardson, F.D. and Starfield, A.M. (1999) Frame-based modelling as a method of simulating rangeland production systems in the long term. *Agricultural Systems* 62, 29–99.

Illius, A.W., Derry, J.F. and Gordon, I.J. (1998) Evaluation of strategies for tracking climatic variation in semi-arid grazing systems. *Agricultural Systems* 57, 381–398.

Johnson, I.R. and Parsons, A.J. (1985) A theoretical analysis of grass growth under grazing. *Journal of Theoretical Biology* 12, 345–367.

Jones, R.J. and Sandland, R.L. (1974) The relation between animal gain and stocking rate: derivation of the relation from the results of grazing trials. *Journal of Agricultural Science, Cambridge* 83, 335–341.

Kahn, H.E. and Spedding, C.R.W. (1984) A dynamic model of herd production systems: 2. An investigation of various factors influencing the voluntary intake of dry matter and the use of the model in their validation. *Agricultural Systems* 13, 63–82.

Moore, A.D., Mayer, D.G., Pepper, P.M. and Freer, M. (1995) *Modelling Research Data on Reproduction and Mortality of Cattle and Sheep*. Drought Plan Working Paper No. 5, CSIRO, Alice Springs, Australia, 32 pp.

Neal, H.D.StC. and Thornley, J.H.M. (1983) The lactation curve: a mathematical model of the mammary gland. *Journal of Agricultural Science, Cambridge* 101, 389–400.

Orsini, J.P.G. (1990) 'SummerPack', a user friendly simulation software for the management of sheep grazing dry summer pastures or stubbles. *Agricultural Systems* 33, 361–376.

Parks, J.R. (1982) *A Theory of Feeding and Growth of Animals*. Springer-Verlag, Berlin, 320 pp.

Poppi, D.P., Gill, M. and France, J. (1994) Integration of theories of intake regulation in growing ruminants. *Journal of Theoretical Biology* 167, 129–145.

Richardson, F.D. and Khaka, R.V. (1981) Stocking rate and the provision of different amounts of protein-rich concentrates to cattle grazing on veld. In: *Annual Report 1979/80, Division of Livestock and Pastures*. Department of Research and Specialist Services, Salisbury, Zimbabwe, pp. 49–57.

Richardson, F.D. and Khaka, R.V. (1983) Stocking rate and the provision of different amounts of protein-rich concentrates to cattle grazing on veld. In: *Annual Report 1980/1, Division of Livestock and Pastures*. Department of Research and Specialist Services, Harare, Zimbabwe, pp. 31–37.

Richardson, F.D. and Khaka, R.V. (1984) Stocking rate and the provision of different amounts of protein-rich concentrates to cattle grazing on veld. In: *Annual Report 1981/2, Division of Livestock and Pastures*. Department of Research and Specialist Services, Harare, Zimbabwe, pp. 48–58.

Richardson, F.D., Hahn, B.D. and Wilke, P.I. (1991) A model for the evaluation of different production strategies for animal production in developing areas: an overview. *Journal of the Grassland Society of Southern Africa* 8, 153–159.

Sandford, S. (1995) Improving the efficiency of opportunism: new directions for pastoral development. In: Scoones, I. (ed.) *Living with Uncertainty*. Intermediate Technology Publications, London, pp. 174–182.

Saudibet, C.L. and Verde, L.S. (1976) Relationship between live weight, age and dry-matter intake for beef cattle after different levels of food restriction. *Animal Production* 22, 61–69.

Scoones, I. (1995) New directions in pastoral development in Africa. In: Scoones, I. (ed.) *Living with Uncertainty*. Intermediate Technology Publications, London, pp. 1–36.

Snedecor, G.W. and Cochran, W.G. (1967) *Statistical Methods*. Iowa State University Press, Ames, Iowa, USA.

STATISTICA for Windows (1998) StatSoft Inc., Tulsa, Oklahoma.

Swift, J. (1995) Dynamic ecological sytems and the administration of pastoral development. In: Scoones, I. (ed.) *Living with Uncertainty*. Intermediate Technology Publications, London, pp. 153–173.

Taylor, StC.S., Murray, J.I. and Illius, A.W. (1987) Relative growth of incisor arcade breadth and eating rate in cattle and sheep. *Animal Production* 45, 453–458.

Teague, W.R. (1987) Defoliation and browse production of Acacia karroo (Hayne) in the Eastern Cape, South Africa. PhD thesis, University of the Witwatersrand, Johannesburg.

Thornley, J.H.M. (1998) *Grassland Dynamics: An Ecosystem Simulation Model*. CAB International, Wallingford, UK, 241 pp.

Walker, B.H. and Langridge, J.L. (1996) Modelling plant and soil water dynamics in semi-arid ecosystems with limited site data. *Ecological Modelling* 87, 153–167.

Wiegand, T., Jeltsch, F,. Bauer, S. and Kellner, K. (1998) Simulation models for semi-arid rangelands of Southern Africa. *African Journal of Range and Forage Science* 15, 48–60.

Williams, J.C. (1993) Influence of farm, parity, season and litter size on the lacatation curve parameters of white British dairy goats. *Animal Production* 57, 99–104.

Zucchini, W., Adamson, P. and McNeil, L. (1992) A model of Southern African rainfall. *South African Journal of Science* 88, 103–109.

21

Using the Cornell Net Carbohydrate and Protein System Model to Evaluate the Effects of Variation in Maize Silage Quality on a Dairy Farm

T.P. Tylutki,[1] D.G. Fox,[1] M. McMahon[2] and P. McMahon[2]

[1]*Department of Animal Science, Cornell University, 330 Morrison Hall, Ithaca, NY 14853, USA;* [2]*McMahon's EZ Acres, Homer, NY 13077, USA*

Abstract

Forage analysis information is used for developing rations, crop rotations and manure nutrient management plans in the Cornell University Nutrient Management Planning System (CuNMPS). The CuNMPS and other similar models use as inputs steady-state conditions on the farm (milk production, herd size, group dynamics, diets, feed composition, farm size and crop production). This steady-state assumption may result in nutrient management plans with large errors, which may introduce risks in income and production variability. One source of error in assuming steady-state conditions is variation in feed composition. The CuNMPS and other nutrient management planning models used to develop nutrient management plans typically rely on either historical forage analysis or infrequently measured compositional values. Methods for incorporating variance have been proposed; however, none have been implemented. The objectives of this study were to determine the amount of variation in a home-raised forage, how this variation affects predicted performance and nutrient excretion by lactating cows and whether this variation can be accounted for in a field-level model, such as the Cornell Net Carbohydrate and Protein System (CNCPS).

Each load of maize (*Zea mays*) harvested for silage was sampled at harvest and analysed for neutral detergent fibre (NDF) and dry matter (DM) on a commercial 500-cow dairy farm. Averages (49.4 and 26.1% for NDF and DM, respectively) and standard deviations (4.52 and 3.59 units for NDF and DM, respectively) along with

 Modelling Nutrient Utilization in Farm Animals (eds J.P. McNamara, J. France and D.E. Beever)

feeding error (±3% of formulated as fed amounts) were evaluated with the CNCPS (version 4.0). Results indicate that this range in NDF, DM and feeding error caused predicted variation in income over feed costs ($40,000 year^{-1}), feed requirement (73 Mt DM maize silage year^{-1}) and N and P excretion (110 and 37 kg year^{-1}of N and P, respectively) per 100 cows annually. Accounting for this variation in current and future nutrient management models is required to optimize returns over feed costs, while decreasing nutrient excretion.

Introduction

The primary objective of the Cornell Net Carbohydrate and Protein System (CNCPS) model is to provide a structure for consultants, producers and agri-service personnel to apply research findings to develop more efficient feeding programmes (Fox *et al.*, 1998). In order to accomplish this, the CNCPS relies on inputs that can be obtained on a farm. One input that is critical to account for is variation in feed composition. Typically, diets are formulated with some level of safety factor to account for on-farm variation. As safety factors are decreased in order to decrease nutrient excretion and ration cost, there is an increased risk of variation in performance and profitability due to on-farm variation in feed composition. Tylutki and Fox (1997) demonstrated that nutrient excretion could be decreased and profitability increased by decreasing the use of safety factors; however, steady-state conditions were assumed.

Industrial manufacturing has incorporated variance, and acceptable levels for variance, as components of quality control protocols for many years (Black, 1991). There have also been methods suggested for improving quality control through the use of control charts in commercial feed manufacturing (St-Pierre and Kauffman, 1998). However, little has been done to utilize these methods in production agriculture. As suggested by St-Pierre (1998), uncertainty in inputs and parameter estimates may result in loss of farm income and a decrease in food production nationally in an effort to decrease nutrient excretion.

These issues will become more important as animal feeding operations are required to decrease inputs to satisfy environmental regulations. Howie (1999) reported that more than 50% of the N and 76% of the P entering the average Dutch farm is in the form of purchased feed. In order to decrease these inputs, greater emphasis will be placed on modelling. Models must be able to accurately predict performance and excretion under a wide range of conditions and feedstuff variation to meet this challenge.

The objectives of this study were to determine: (i) the amount of variation in a home-raised forage; (ii) how this variation affects predicted performance and nutrient excretion by lactating cows; and (iii) whether variation can be accounted for in a field-level model, such as the CNCPS.

Materials and Methods

This study was conducted on a 500-cow commercial dairy operation located north-west of Homer, New York, USA (42.38N, 076.10W). Average daily milk production was 31.8 kg cow^{-1} at the time of this analysis. The farm has 460 tillable hectares. In 1998, 130 ha was harvested as maize (*Zea mays*) for silage. Fields vary in elevation (250 to 650 m) and soil type (well-drained, gravelly loams, found on the valley floor, to shallow, acidic clays, at the higher elevations). The valley floor is situated over an aquifer (10 to 15 m to aquifer), and a stream flows through most of the valley fields. The farm has been following a crop/manure nutrient management plan for 4 years, and rations have been formulated with the CNCPS version 4.0 (v4.0) since April 1999.

Sample collection and chemical analysis

Maize (*Z. mays*) harvested for silage was chosen to develop the methodology, given that it is harvested in a short time period for an entire year. Maize was harvested (based on whole-plant dry matter) beginning 1 September 1998 and was completed on 26 September 1998. The maize was harvested with a John Deere 6710 self-propelled harvester with a kernel processor. At the bunk silo, truck drivers sampled each load after unloading (average load size 6.3 Mt) by taking several small grab samples and placing them in a sample bag (approximately 150 to 200 g total wet weight). Drivers logged sample identification, field identification and day of harvest for each sample. Samples were collected from all trucks daily and either frozen (−15°C) or taken directly to a commercial laboratory (DairyOne Forage Analysis Laboratory, Ithaca, New York, USA). Samples were then analysed for dry matter (DM, %) and neutral detergent fibre (NDF, %DM). Additional data included date of planting, hybrid, soil test results (pH and soil phosphorus level) and field elevation. Means and standard deviations (SD) were calculated for both NDF and DM using Release 8.0.2 of SPSS for Windows (SPSS Inc., Chicago, Illinois, USA).

Diet evaluation using the CNCPS

A lactating-cow ration, formulated in early July by the farm's consultant with the CNCPS v4.0, was used for a sensitivity analysis. This version of the CNCPS includes mineral requirements, mineral excretion, nitrogen excretion, manure production (faecal, urinary and total), whole-herd excretion and feed requirements (Tylutki and Fox, 1997). It was used to evaluate predicted performance and total nitrogen and phosphorus excretion of one group of lactating cows in the herd. The ration contained 7.72 kg dry matter of maize silage (31.94% of diet DM) and was formulated to provide the nutrients to support 43.58 kg milk

day^{-1}. In all iterations, total dry-matter intake was held constant at the group average as of early July 1999 (24.2 kg cow^{-1}).

For the base analysis, the NDF of the maize silage was set to equal the average of the 974 samples collected at harvest. Dry matter of the maize silage was then varied from 24 to 32% in steps of 2 units. The next set of evaluations was completed with the mean NDF minus 1 SD (same range in DM) to predict results if the forage is consistently higher in quality. The third set of iterations was completed with the mean NDF plus 1 SD (same range in DM) to predict results if the forage is consistently lower in quality. The fourth set of iterations reduced the as-fed amount 3% (average NDF, DM varied 24 to 32% in steps of 2 units) to predict results if there is underfeeding due to feeder error. The final set of iterations increased the as-fed amount 3% (average NDF, DM varied 24 to 32% in steps of 2 units) to predict the effect of overfeeding due to feeder error. The first three sets of iterations address forage quality variation, whereas the last two sets address feeding error. Both of these areas are vital parts of a quality control protocol for the feeding system.

Values computed by the CNCPS that were used in other analyses included: % maize silage in the diet, income over feed costs at the milk production allowed by the first limiting nutrient ($ per 100 cows year^{-1}), maize silage inventory required (Mt DM per 100 cows year^{-1}), and total nitrogen and phosphorus excreted (kg per 100 cows year^{-1}). The most limiting nutrient milk production is based upon CNCPS predictions of metabolizable energy, metabolizable protein or amino acid allowable milk production for a given ration. In all cases of this analysis, amino acids were the first limiting nutrients (either isoleucine or leucine was predicted as the first limiting amino acid).

Results and Discussion

The resulting data set included 974 data points. Neutral detergent fibre in the dry matter averaged 49.4%, with a standard deviation of 4.52 units, a minimum of 37.0% and a maximum of 70.0%. Dry matter at harvest averaged 26.1%, with a standard deviation of 3.59 units, a minimum of 18.0% and a maximum of 45.0%.

Model predictions of economics, inventory and total nitrogen and phosphorus excretion

Table 21.1 summarizes the impact of the variation in NDF and DM and feeding error on predicted income over feed costs and feed requirements. Variation due to either NDF or harvest DM has the potential to have a large effect on income over feed costs (range of $21,792 per 100 cows annually) on this farm. As shown in Table 21.1, the variation in income over feed costs is highest when the quality (NDF + 1 SD) of the maize silage is reduced. The addition of feeding error

Table 21.1. Changes in predicted income over feed costs and feed requirements with variation in maize silage NDF and DM and feeding error.

Variable	Change in % maize silage DM in diet	Change in income over feed costs*	Change in maize silage required†
Harvest DM (24% to 32% DM)			
At NDF −1 SD	6.2%	$6,482	61
At av. NDF	6.2%	$11,720	61
At NDF + 1 SD	6.2%	$12,370	61
Harvest NDF (DM held at 28%)			
Av. NDF to NDF − 1 SD	0.0%	−$6,652	0
Av. NDF to NDF + 1 SD	0.0%	$6,953	0
NDF + 1 SD to NDF − 1 SD	0.0%	−$13,604	0
Combined (both NDF and DM vary)			
Range	6.2%	$21,792	61
CV	7.1%	2.1%	7.2%
Feeding error (97% of as-fed formulated fed vs. formulated)			
24% maize silage DM	−3.9%	$8,094	−38
26% maize silage DM	−2.2%	$5,486	−22
28% maize silage DM	−0.7%	$2,125	−6
30% maize silage DM	0.9%	−$550	8
32% maize silage DM	2.3%	$33,061	22
Feeding error (103% of as-fed formulated fed vs. formulated)			
24% maize silage DM	−2.6%	$4,572	−26
26% maize silage DM	−1.0%	$1,244	−9
28% maize silage DM	0.7%	−$1,762	6
30% maize silage DM	2.2%	−$5,525	21
32% maize silage DM	3.7%	−$7,880	36
Combined (both feeding error and DM vary)			
Range	7.5%	$40,940	73
CV	7.2%	3.4%	7.2%

* $14 cwt^{-1} milk per 100 cows annually.
† Mt dry matter per 100 cows annually.
1 cwt = 45.4 kg.

to quality variation further magnifies the problem ($40,940 range in income over feed costs per 100 cows annually). From a quality control standpoint, this is very logical and follows manufacturing trends. As raw product variation increases and quality decreases, variation in production, inventory and income increases (Black, 1991).

The variation in forage quality and feeding error had a substantial effect on nitrogen and phosphorus excretion (Table 21.2). The coefficients of variation (CVs) are considerably lower (ranges of 110 and 37 kg per 100 cows annually for nitrogen and phosphorus, respectively), but are large enough to be of concern, given environmental regulations. The impact of variation in feedstuff composition on this farm is even greater than that shown in this analysis, since we have information indicating that the other forages grown on the farm vary in a similar manner.

Table 21.2. Changes in total nitrogen and phosphorus excretion with variation in maize silage DM and NDF and feeding error.

Variable	Change in total N excretion*	Change in total P excretion*
Harvest DM (24% to 32% DM)		
At NDF −1 SD	110	−29
At Av. NDF	68	−29
At NDF + 1 SD	75	−29
Harvest NDF (DM held at 28%)		
Av. NDF to NDF − 1 SD	4	0
Av. NDF to NDF + 1 SD	−7	0
NDF + 1 SD to NDF − 1 SD	11	0
Combined (both NDF and DM vary)		
Range	110	29
CV	0.4%	0.9%
Feeding error (97% of formulated amount is fed)		
At 24% maize silage DM	−42	20
At 26% maize silage DM	−16	13
At 28% maize silage DM	−4	4
At 30% maize silage DM	13	−4
At 32% maize silage DM	35	−9
Feeding error (103% of formulated amount is actually fed)		
24% maize silage DM	−22	15
26% maize silage DM	−4	5
28% maize silage DM	16	−2
30% maize silage DM	18	−11
32% maize silage DM	42	−16
Combined (both feeding error and DM vary)		
Range	84	37
CV	0.3%	1.0%

* kg 100 cows^{-1} per year.

These results show that feedstuff variation and feeding accuracy have a substantial effect on farm profitability and nutrient excretion. Inclusion of variance in feedstuff composition in models is needed to formulate rations that minimize excretion, while maintaining performance and profitability. Having the capability to project ranges in nutrient excretion and loading is valuable in developing crop rotation selection and manure nutrient management plans. This capability could also be used to stimulate research and educational programmes that reduce variation in feed composition.

Information needed in order to be able to account for variance in models includes: (i) number of samples required from each feed to accurately describe the variance; (ii) feed components that need to be analysed; and (iii) the economic value of this level of sampling. Each farm must develop its own feed database to ensure accuracy. This may be a limiting factor in gaining producer acceptance, as the cost of developing the database could be quite high. Initially, reference variances could be used (for example, from a commercial laboratory). However, the use of standard variance values may introduce additional risk, as the amount of variance appears to be farm (management)-dependent. This intensive sampling is a component of the whole-farm quality control programme and is continuous, as it appears that variance changes with cropping season and crop. We do not have a simple way to determine the profitable level of investment in a quality control programme on a particular farm.

As margins continue to decrease and competition increases, higher levels of quality control will be required. Sources of variation will need to be identified as either controllable, partially controllable or uncontrollable. The NDF at harvest may be classified as partly uncontrollable, whereas feeding error is controllable. Acceptable levels of variation then need to be assigned to the source of the variation. The acceptable level is dependent upon the source of variation and the goals of management. It is possible in production agriculture for coefficients of variation for the controllable and partially controllable sources to not exceed 5%. This level of acceptable variation should allow the farm to maintain the highest level of profitability and competitiveness. Achieving these levels will require models to be used on the farm.

Impact on future model development

This was our first attempt at evaluating the effect of quality variation with the CNCPS. These results indicate that forage composition variation needs to be accounted for in our model. As a first step to account for variation within the structure of the CNCPS, we have included the ability to iteratively process a ration by altering the amounts of an ingredient at a step-size set by the user in CNCPS version 4.0. Currently, the limiting factor in these calculations is the time requirement to complete the calculations. As more variables are added to the iteration, time increases dramatically. For example, iterating feed amounts with a large step size (1 kg) of one feed may take as little as 5 s, whereas stepping

through two ingredients with a small step size (0.1 kg) may take 50 min and three feeds with a 0.1 kg step size may take 10 days (typical time duration predicted by CNCPS v4.0, which is computer-dependent).

As model development continues, variation in feed amounts, as well as key chemical components (NDF, crude protein, soluble protein, dry matter), needs to be included to improve accuracy in formulating and evaluating a ration. Applications include: (i) formulation of a ration that may be slightly more expensive but is less sensitive to variation; (ii) ration formulation that minimizes potential nutrient excretion by optimizing performance, taking into account acceptable variability; (iii) predicted ranges in performance, excretion and income due to variation in feedstuffs; and (iv) ability for nutritionists to explain better why performance varies.

Another approach that is being pursued is including variance in a linear optimization. In this approach, rations are optimized on a least-cost basis, with a maximum ration variance (initially for crude protein) included as a constraint. While early in development, initial evaluations of this approach suggest it may be the most practical method. More planning, research and development need to occur in order to determine which key variance components need to be included and at what sensitivity, so that the process is field-usable.

References

Black, J.T. (1991) *The Design of the Factory with a Future.* McGraw-Hill, New York, USA, 233 pp.

Fox, D.G., Chase, L.E, Pell, A.N., Pitt, R.E. and Van Amburgh, M.E. (1998) The Cornell Net Carbohydrate and Protein System: a model to predict cattle nutrient requirements under widely varying conditions. In: *Proceedings of the Comparative Nutrition Society*. Comparative Nutrition Society, Silver Springs, Maryland, Alberta, Canada, pp. 53–58.

Howie, M. (1999) Regulations force Dutch farmers to modify manure handling. In: Muirhead, S. (ed.) *Feedstuffs.* Feedstuffs, Minnetonka, Minnesota, USA, p. 9.

St-Pierre, N.R. (1998) Animal grouping strategies, sources of variation and economic factors affecting nutrient balance on dairy farms. *Journal of Dairy Science* 81 (Suppl. 1), 287.

St-Pierre, N. and Kauffman, A. (1998) Economic design of control charts for monitoring feed production processes. *Journal of Dairy Science* 81 (Suppl. 1), 255.

Tylutki, T.P. and Fox, D.G. (1997) Application of the Cornell Nutrient Management Planning System: optimizing herd nutrition. In: *1997 Proceedings of the Cornell Nutrition Conference for Feed Manufacturers.* Cornell University, Ithaca, New York, USA, pp. 54–65.

22

Challenge and Improvement of a Model of Post-absorptive Metabolism in Dairy Cattle*

J.P. McNamara and G.J. Phillips

Department of Animal Sciences and the Nutrition Program, Washington State University, Pullman, WA 99164–6351, USA

Abstract

We have been conducting research to improve quantitative descriptions of metabolism in lactating dairy cows depicted in an existing mechanistic, computer-assisted model. The objective was to challenge this model with data collected in *in vivo* and *in vitro* experiments on high-producing dairy cattle fed a range of energy. Cows that varied in genetic propensity for milk production and dietary fat intake were used. Dietary inputs, milk component outputs, body fat, nutrient concentrations in blood and maximal velocity and substrate sensitivity of adipose-tissue metabolic reactions were observed. The model simulated yields of milk components within 5% of observed means. Simulated lipid metabolism and accumulation of body fat were adequate in many situations; however, the model response to changes in energy intake was too sensitive. This inadequacy was especially noticeable in later lactation, when body fat accumulation was simulated to be too high. Lack of precision in long-term dynamic changes indicates inadequacy in parameters describing energy-utilizing reactions. This severe challenge of the model supports its functionality. The model can be used to test hypotheses concerning the relation of body fat and protein use to milk production. Current knowledge as depicted in the model would suggest that a wide range of body fat at calving does not change milk production or body protein loss for cows fed adequately. In simulations, decreasing body protein at calving decreases milk production, while increasing body protein results in a greater loss of body protein without altering milk production. Unknown variation in use of amino acids by muscles hinders our ability to predict milk protein responses to changes in

* College of Agriculture and Home Economics Research Center, Washington State University, Pullman. Project Numbers 0107, 0249 and 0862. Supported in part by grants from the National Institutes of Health (RD24529) and Washington Dairy Products Commission (8063). Research conducted in conjunction with Cooperative States Research Service Regional Research Project NC-185, Metabolic Relationships in Supply of Nutrients for Lactating Cows.

 Modelling Nutrient Utilization in Farm Animals (eds J.P. McNamara, J. France and D.E. Beever)

nutrient intakes. Further experiments must be designed to determine utilization of nutrients in viscera, muscle and adipose tissue, and must encompass sufficient range in genetic ability, nutrient input and time to adequately describe the dynamic and integrated nature of metabolic reactions.

Introduction

We have been involved in an effort to challenge and improve an existing model of the metabolic transactions in the lactating cow (Baldwin *et al.*, 1987a,b; McNamara *et al.*, 1991a,b; Baldwin, 1995; McNamara and Baldwin, 2000). The model is biochemically based, deterministic and dynamic. Ruminal breakdown and fermentation of feedstuffs, absorption and chemical interactions in the body are explicitly described. The model describes biological reactions in mathematical forms, so that new concepts, hypotheses and experimental data can be judged consistently against this integrated, quantitative description. A limitation in knowledge of dairy cattle nutrition has been the lack of direct observations of metabolic interactions in tissues of cows of varying merit or consuming a variety of diets. To have a quantitative understanding, such as is available in many areas of physics and chemistry, direct determination of parameters in subcellular or organ systems is necessary. These observations are then used to determine how the overall behaviour of the model can be improved.

Use of dietary fat to optimize dairy performance is an example of when a quantitative, integrated approach is needed. Dietary fat is beneficial for the productive efficiency of cows, which reduces the environmental impact of milk production (Palmquist, 1994; Wu and Huber, 1994). Recently, the most attention has been paid to improved capture of nitrogen by dairy cattle, in response to increased concerns about the impact of nitrogenous compounds on the environment. It still remains a challenge to feed the proper amount and balance of nutrients, which maximize output and reduce nitrogenous losses, because we do not have an adequate mechanistic description of these processes. Therefore, the null hypotheses were: (i) quantitative descriptions in a mechanistic, dynamic model of metabolism in the dairy cow (Baldwin, 1995) are adequate to describe effects of fat and starch intake on milk component output; and (ii) the model is adequate to describe the effects of dietary fat intake on adipose tissue metabolism of high-yielding cows. High-producing dairy cattle were fed diets that varied in amounts of fat. It must be stated explicitly that this work was not undertaken to prove how good the model may be or to 'make the model fit the data', but rather to define, in a systematic manner, areas in the model which are inadequate and need further work. Another objective was to run a series of simulations to test hypotheses on the effect of various amounts of body fat and protein at calving on milk production of cows fed adequately post-partum.

Methods

Detailed descriptions of the animals and rations and results of observations, as well as some preliminary model challenges, have been published previously (Harrison *et al.*, 1995; McNamara *et al.*, 1995; McNamara and Baldwin, 2000). Brief synopses of designs are presented here, with details on modelling simulations. The model used is mechanistic; thus it uses characteristics of cellular and subcellular processes to describe the metabolism of the whole animal. It is dynamic, in that it integrates chemical reactions over time. Equations and parameters in the model were derived from direct experimental observations or from extrapolation from non-lactating cattle or other species where data from cows were not available (Baldwin, 1995). The integration interval is usually set at 1/100th of a day and data are output daily or weekly, as needed. The model describes the use of pools such as rumen volatile fatty acids (VFA), protein and microbes, body triglyceride (Ts) and body protein (Pb). After absorption, the metabolism of glucose, fatty acids, acetate and total amino acids is described. Mammary reactions include the synthesis of milk lactose, fat and protein. Equations describing synthesis and degradation are usually aggregated at the pathway level.

The initial conditions of the animal are described in terms of body weight (BW), percentage body fat and protein, if known, and mammary capacity. The latter is usually obtained from records (production in previous lactation or earlier in present lactation). Feed intakes are input, and simulation is conducted over a period of time from 1 to 305 days, depending on the objective of the evaluation. Major outputs are milk, milk lactose, fat and protein, empty-body weight (EBW), Ts and Pb. Several other variables are calculated and may be output, depending on the objective of the modelling simulations. The model is written in Advanced Continuous Simulation Language (see Baldwin, 1995).

Three groups of 12 multiparous Holsteins were fed a diet of grass silage, lucerne hay and concentrate for 1 month pre-partum and allowed free access to this diet for the first 16 days of lactation. Previous-lactation milk yields of cows on each treatment were: 10,003, 9846 and 9573 (standard deviation (SD) 1490) kg 305 days^{-1}. Starting at 17 days in milk (DIM), animals were fed *ad libitum* one of three totally mixed diets, which supplied 1.47, 1.49 and 1.53 Mcal of net energy – lactation (NE_l) kg^{-1} and 2.5, 4.4 and 6.3% total fat (Table 22.1). The fat and energy of the control ration (CONT) was varied by replacing 12% of the concentrate with whole cottonseeds (WCS) and by replacing an additional 2.7% of the concentrate with calcium salts of long chain fatty acids (WCSFA). Diets met or exceeded all nutritional requirements for animals of this productive merit, and contained 19% crude protein (CP) and approximately 38% rumen-undigested protein (RUP), calculated from published values (NRC, 1989).

Adipose-tissue biopsies were obtained at −15, 15, 60, 120 and 240 days from parturition and *in vitro* incubations were conducted to estimate the parameters describing lipogenesis and esterification. The fat-cell size of

Table 22.1. Dietary compositions and model nutrient inputs.

	Control	WCS	WCSFA
Feed item (% of DM)			
Lucerne hay, prebloom	23.0	23.0	23.0
Concentrate mix	54.0	42.0	39.3
Grass silage	23.0	23.0	23.0
Whole cottonseeds		12.0	12.0
Long-chain fatty acids			2.7
Dietary analyses			
DM (%)	75.7	76.3	74
CP (% of DM)	19.0	19.0	19.0
Fat (% of DM)	2.5	4.4	6.0
NDF (% of DM)	36.8	37.4	36.4
ADF (% of DM)	16.8	19.4	19.4
Lignin (% of DM)	6.7	6.9	7.3
Ash (% of DM)	9.2	9.6	9.2
Model nutrient inputs (kg kg^{-1} of DM)			
Organic acids	0.010	0.010	0.010
Lactate	0.010	0.010	0.010
Pectin	0.020	0.020	0.020
Feed lipid	0.025	0.044	0.044
Feed fat	0.000	0.000	0.019
Starch	0.285	0.266	0.248
Hemicellulose	0.200	0.170	0.170
Cellulose	0.101	0.125	0.125
Lignin	0.067	0.069	0.073
Insoluble protein	0.075	0.073	0.073
Soluble protein	0.115	0.117	0.117
Insoluble ash	0.046	0.048	0.046
Soluble ash	0.046	0.048	0.046

DM, dry matter; NDF, neutral detergent fibre; ADF, acid detergent fibre.

subcutaneous adipocytes and BW were used to determine total body lipid content from equations validated in our laboratory and others (Waltner *et al.*, 1994). The *in vitro* rates and the total body lipid mass were used to estimate the whole-body fluxes of acetate to body fat (AcTs), fatty acids to body fat (FaTs) and lipolysis of body fat (TsFa). Output of milk was recorded daily, and components were recorded from monthly samples.

Modelling simulations

Equation forms, parameter values and pertinent data used to set parameters in the model have been published (Baldwin, 1995; McNamara and Baldwin,

2000). Inputs to the model were the intakes of dietary nutrients, taken from analyses of feeds and observed feed intakes (see Table 22.1). The simulation used the average observed dry-matter intake (DMI) for period 1 (weeks 3 to 17) and then shifted to the mean DMI for 2-week periods until 245 DIM. Initial conditions for observed BW, Ts and UCELLS (mammary capacity; 1000 = 30 kg of milk approximately) (Table 22.2) were set to match the mean of the groups being simulated for the beginning of lactation.

Results and Discussion

This trial was designed to test the effects of inclusion of both plant fat (from WCS) and ruminally protected fat (WCSFA) on milk production and metabolism of lipid in adipose tissue. This trial extended for an entire lactation, so that we could test the dynamic effects of relatively small errors in parameter values. In this simulation, the initial runs were adjusted to reflect lactose (milk) production of the CONT group for the first 6 weeks of lactation by altering UCELLS (see Table 22.2). Initial EBW and Ts were set to observed values. The maximal

Table 22.2. Parameter values in present simulations and default model parameters.*

	CONT	WCS	WCSFA	Default
Milk (lactose) synthesis capacity				
UCELLS	1450	1450	1450	1000
Milk fat synthesis capacity				
VAcTm (mol day^{-1})	0.00527	0.00527	0.00527	0.007
VFaTm (mol day^{-1})	0.000729	0.000729	0.000729	0.001
Milk protein synthesis capacity				
VAaPm (mol day^{-1})	0.00238	0.00238	0.00238	0.0025
Degradation of milk production curve				
K_{lhor} (% day^{-1})	0.009	0.009	0.009	0.0102
Initial body weight				
iBW (kg)	622	634	624	650
Initial body fat				
iTsf (% iBW)	15.6	18.3	16.1	15.8

* See Baldwin (1995) and McNamara and Baldwin (2000) for full descriptions of terms and definitions.

velocity parameters for milk fat and milk protein synthesis were set to match those of the control cows as described above (see Table 22.2). The lactation curve of control animals was compared with initial simulations, and the parameter that sets the rate of decay of the lactation curve (K_{lhor}) was decreased 10% to match the more persistent lactation curves noted in our herd (see Table 22.2).

The model simulated control milk production rates and responses to dietary fat adequately (Tables 22.3 and 22.4). For milk and fat corrected milk (FCM), simulated values were within 5% of observed means, with the exception of milk production on WCFSA treatment in late lactation. For milk and milk components, in no case did the model output differ from the observed treatment mean by more than 11% and most were within 7%. All these measures were within the SD of this variable. Milk protein yield and percentage tended to be oversimulated in early lactation and undersimulated in late lactation. Milk fat yield tended to be undersimulated in late lactation. However, total milk component output for the 305 days fell within 3% of observed in almost all cases and was less than 5% for all means.

For the response to WCS, the model predicted the response within 5 percentage points of observed. For example, in early lactation, observed milk fat percentage increased 7.43% and the model predicted a 2.67% increase (Table 22.3). For the lactation as a whole, with the exception of response of milk fat yield and milk protein percentage on the WCSFA treatment, the observed and simulated percentage responses were within 4% and usually 3% units. The observed increase in milk fat yield of cows fed WCSFA compared with CONT was 7.62%, while simulated was 2.58%. The observed change in milk protein percentage of cows consuming WCSFA from 21 to 245 DIM was −4.28%, while the simulated response was 1.50% higher than CONT.

Addition of both sources of fat (WCSFA) resulted in a transient decrease in feed intake (mean 1.7 kg day^{-1} for 14 weeks). This resulted in a daily deficit of 290 g CP day^{-1} for cows fed WCSFA relative to control for these 14 weeks, after which time the intake was equal to or greater than the control-group cows. With this lower protein intake, milk yield was 5% lower and milk protein yield was 8% lower in early lactation, consistent with many previous studies (Palmquist, 1994; Wu and Huber, 1994). The model predicted the depression in milk lactose yield caused by the lower intake in early lactation; however, it failed to adequately predict the increase in milk and milk protein yield in later lactation. Although the model responds in the appropriate direction to changes in nutrient input, and predicts milk component yield within a few percentage points of observed, it cannot as yet predict subtle, but real, shifts in milk composition due to shifts in diet composition over long periods of time.

In the analysis of the accumulation of body fat (see Table 22.4) and the specific reactions of lipid metabolism (Table 22.5), we discovered potential inadequacies in understanding explicitly represented in the model. Observed body fat (see Table 22.4) is calculated from actual body weight and fat-cell size, using equations generated on a data set in our lab (Waltner *et al.*, 1994). We should

Table 22.3. Observed and simulated production of dairy cattle fed rations varying in fat content.

	CONT		WCS		WCSFA		
Variable	Obs	Sim	Obs	Sim	Obs	Sim	SD
21 to 119 DIM							
DM intake (kg day^{-1})	23.0	23.0	23.9	23.9	21.3	21.3	1.1
Milk production (kg day^{-1})	43.3	43.9	43.1	44.1	41.1	41.6	2.1
4% FCM (kg day^{-1})	38.2	39.8	38.8	40.5	39.4	38.7	2.0
Milk fat (kg day^{-1})	1.39	1.48	1.44	1.53	1.53	1.48	0.10
Milk fat (%)	3.23	3.37	3.47	3.46	3.68	3.55	0.21
Milk protein (kg day^{-1})	1.32	1.37	1.29	1.39	1.21	1.33	0.05
Milk protein (%)	3.03	3.12	3.14	3.15	2.91	3.21	0.07
120 to 245 DIM							
DM intake (kg day^{-1})	21.6	21.6	22.8	22.8	22.7	22.7	0.80
Milk production (kg day^{-1})	33.4	33.6	33.8	33.5	35.4	32.8	2.4
4% FCM (kg day^{-1})	29.1	29.8	28.8	30.3	28.9	30.4	2.0
Milk fat (kg day^{-1})	1.16	1.09	1.17	1.12	1.22	1.15	0.08
Milk fat (%)	3.47	3.23	3.45	3.36	3.45	3.51	0.15
Milk protein (kg day^{-1})	1.11	1.04	1.14	1.04	1.12	1.01	0.05
Milk protein (%)	3.32	3.08	3.39	3.09	3.17	3.09	0.07

CONT, control fed cows; WCS, whole cottonseed ration fed cows; WCSFA, whole cottonseeds and long-chain fatty acid ration fed cows; Obs, observed values; Sim, simulated values; SD, standard deviation of observed values; DM, dry matter.

Table 22.4. Observed and simulated data on body fat in dairy cattle.*

	Control		WCS		WCSFA	
Variable	Obs	Sim	Obs	Sim	Obs	Sim
Body lipids (kg)						
Week 2	101	69	109	84	98	71
Week 9	90	55	104	85	81	64
Week 17	98	65	105	110	100	93
Week 35	125	101	134	186	135	205

* From McNamara and Baldwin (2000). Dairy cattle were fed lucerne hay (23% of dry matter (DM)), grass silage (23% of DM) and 54% concentrate diets (Control), same diet with 12.7% of whole cottonseeds in the concentrate, replacing maize (WCS); and WCS plus an additional 1.89% of ruminally protected long-chain fatty acids (WCSFA) from 17 to 305 DIM. Simulations were run on the mechanistic model of Baldwin (1995) from 1 to 245 DIM. Intakes of nutrients were simulated explicitly. Initial body weight and fat and pretreatment milk yields were used to set initial parameter values.

continue to look for more precise techniques if we are to become truly quantitative in this area; nevertheless, the model simulation of body fat agreed with observations for control cows throughout lactation and for all groups for the first several weeks of the trial.

In later lactation, errors in model prediction of body fat accumulation are noted. For cows fed WCS or WCSFA, overaccumulation of body fat was significant by 119 DIM. In the WCSFA simulations, the change in body fat was almost 100 kg more than observed. Inclusion of dietary fat in WCS and WCSFA had a marked depressive effect on lipogenesis *in vitro* (see Table 22.5), but not in total body fat esterification. Inclusion of dietary fat depressed feed intake in the early portion of the trial, and the model did simulate the effects of less intake on metabolism. However, prolonged inclusion of fat had a continued depressive effect on lipogenesis from acetate (observed), even though the energy balance returned to a positive state and energy intake and glucose availability were higher in these cows than in controls. The model failed to simulate the continued depression of lipogenesis due to increased fat intake. This is not surprising, as there are no equations in the model describing such a reaction. There were no data on cow adipose tissue available at the time the model was being constructed to suggest such a phenomenon. The net incorporation of fatty acids into body fat (the result of AcTs + FaTs − TsFa) was also higher in simulated than in observed states for cows fed WCS and WCSFA rations; however, the simulation error was not as great as for lipogenesis, suggesting that the model simulated esterification and lipolysis in such a way as to 'correct' for the error in lipogenesis (see Table 22.5).

In a quantitative modelling research programme, one must carefully analyse potential errors in the experiments and models in order to identify experiments that will further reduce model error. The several paragraphs below

Table 22.5. Observed and simulated rates of lipid metabolism in adipose tissues of cows fed rations varying in fat content.

	CONT		WCS		WCFSA	
Variable	Intake*	Abs†	Intake	Abs	Intake	Abs
Period 21 to 119 DIM						
Triglyceride (g day^{-1})	568		1012		1389	
Fatty acid (g day^{-1})	492	384	878	742	1283	1009
Period 120 to 245 DIM						
Triglyceride (g day^{-1})	525		972		1389	
Fatty acid (g day^{-1})	456	346	844	691	1283	998
	Obs	Sim	Obs	Sim	Obs	Sim
Digestibility (Fa/Tg) (%)‡						
21 to 119 DIM		67.7		73.4		72.6
120 to 245 DIM		65.8		71.1		71.9
Digestibility (Fa/Fa) (%)‡						
21 to 119 DIM		78.3		84.5		78.6
120 to 245 DIM		75.9		81.9		77.8
Acetate conversion to body fat (AcTs) (g fatty acid day^{-1})						
63 DIM	1.6	618	2.4	624	0.3	406
119 DIM	50.0	698	10.0	704	14.0	595
245 DIM	78.0	765	29.0	797	46.8	685
Net incorporation of fatty acids (AcTs + FaTs − TsFa) (g day^{-1})						
63 DIM	129	3	117	317	105	227
119 DIM	259	160	153	498	367	646
245 DIM	315	406	191	746	690	890

* This column indicates observed grams triglycerides intake per day.
† This column indicates simulated grams fatty acid absorbed per day.
‡ All digestibility figures are simulated values based on observed intakes and simulated absorptions. The notation Fa/Tg indicates the calculation of fatty acid absorbed (simulated) divided by triglcyeride intake (actual), whereas Fa/Fa indicates fatty acid absorbed (simulated) divided by fatty acid intake (actual, where the glycerol content of the observed triglyceride intake was subtracted to give the actual fatty acid intake). This is simply to demonstrate that, with this simulation, we are tracking the nutrients absorbed to assess total balance; we are not calculating digestibility from the more practical approach of (intake − faeces)/(intake).
CONT, control fed cows; WCS, whole cottonseed ration fed cows; WCSFA, whole cottonseeds and long-chain fatty acid ration fed cows; Obs, observed values; Sim, simulated values.

provide one such analysis. One experiment alone is not usually cause to negate the accumulated knowledge of many previous experiments as embodied in a quantitative model. Also, the process is explicitly not to 'force a fit' of the model to the reality of one experiment. The analytical process can only identify potential points of error, which must be corroborated in further studies. Only a complex experiment such as this one involving *in vivo* and *in vitro* measurements allows such a severe test of the model and helps identify specific model limitations.

The first possibility is that our measures of feed intake could be in error. Within 1 SD, we could account for approximately 1 kg day^{-1} of DMI either above or below the mean. Sensitivity analyses that either added or subtracted 0.5 kg of starch or fibrous carbohydrate (cellulose and hemicellulose) would account for about 19 to 38 kg of body fat over 119 days. Thus, errors in feed analysis and thus model nutrient inputs could account for a percentage of the accumulated errors. The large dynamic (time) effect of small changes in feed intake and analytical error points to the need for continued precision in feed analysis techniques and continued improvement in the feed databases available to researchers.

The error in body fat accumulation was 77 kg and 97 kg on WCS and WCSFA treatments, respectively, compared with the observed body fat. The high rates of body fat accumulation were probably not due to an overprediction of absorption (AbsFa), as predicted absorption rates of fatty acids were quite close to observed rates in other experiments (see Table 22.5). Digestibility of ruminally protected fat was increased in the WCSFA simulations, as would be expected from past experience (Palmquist, 1994). However, true digestibility as a percentage of fat may decrease with increasing fat (Palmquist, 1994). The amount of potential error in body fat due to a 10% error in digestion could be calculated. If actual digestion of fatty acids were 10% less than estimated from observed intakes, the model would have absorbed 10% too much. That amount of fat, from 14 to 245 DIM, would account for 8 kg body fat on WCS and 13 kg on WCSFA, or 10 and 13%, respectively, of the accumulated error in body fat.

We have already noted that milk production was predicted within a few percentage points of observations, and total milk fat was simulated very close to actual rates until the last few weeks of the simulation. If we use the mean value of milk fat synthesis simulated between 120 and 245 DIM, this results in a shortfall of 13 and 18 kg of milk fat compared with observed. If we assume that this fat would have gone to body fat instead, this accounts for 17 and 19% of the oversimulation of body fat accumulation for WCS and WCSFA.

The model did increase the oxidation of fatty acids 10 to 20% for the WCS simulation compared with controls, and another 20 to 30% on the WCSFA simulation (McNamara and Baldwin, 2000). It is unlikely, but not impossible, that the cows could oxidize another full kg lipid day^{-1}. More importantly, in the model, as in the cow, oxidation of nutrients is based on demand functions, which are thermodynamically and stoichiometrically related to work by the tissues. There is no justification for the higher amounts of fat consumed to

increase metabolic demand. Neither is their any justification at this point for suggesting some uncoupling phenomenon. Thus the error probably does not arise solely from too low a rate of fatty acid oxidation. It is interesting that the model, based on thermodynamic relationships among chemical interactions, predicted such an increase in FaCd, when such data did not exist during model development. Even today, only a limited understanding of fatty acid oxidation exists for dairy cattle fed added fat (Palmquist, 1994). This points to the utility of models, well-validated in many but not all aspects, to point out potential mechanisms in areas where data are lacking, thus identifying potential useful experiments.

The difference between model behaviour and observations may be related to experimental error. First, we may have underestimated actual body fat accumulation and, secondly, the animals actually did oxidize fatty acids at higher rates than predicted from energy-requiring reactions. We must dismiss the latter until experimental evidence is available. The first hypothesis can be discussed in relation to errors in the observed measurements. If our estimate of body fat was 1 SD lower than actual amounts, that would account for 23 kg out of the 77 kg error on WCS and 97 kg error on WCSFA. Combined with the 27 and 32% potential errors in digestion and milk fat synthesis, these three sources would account for only 57% of the error in the WCS simulation and 56% for WCSFA. Also, as discussed earlier for the error in measuring feed intake, we have no more reason to believe that the actual body fat was lower, rather than higher, than the observed means.

Thus, potential model errors in digestion of fat and milk fat synthesis may have accounted for 27% of the body fat accumulation error on WCS and 32% on WCSFA. Several errors may exist related to this fat accumulation. This anabolic reaction is altered by acetate availability, glucose availability (for glycerol synthesis) and 'anabolic hormone' (Ahor). In the model, Ahor is a function of glucose concentration compared with the reference of 3 mmol l^{-1} at energy balance = 0. All anabolic reactions are thus a direct function of glucose availability in the postabsorptive section of the model (see Ahor, Table 22.1). Blood glucose in the simulations was usually greater than observed for cows fed CONT and WCS rations. In cows fed WCSFA, simulated blood glucose was lower until late lactation, primarily because of the depression in intake and therefore in glucose precursors (McNamara and Baldwin, 2000). It could be hypothesized that the increase in blood glucose increased the anabolic hormone concentration in the model (which it did) and that this led to the increase in lipogenesis and body fat accumulation. However, this would not explain the correct simulation of body fat on CONT treatments when simulated blood glucose was high, or the oversimulation of body fat on WCSFA treatments when simulated blood glucose was generally low. Most importantly, it does not explain why the model describes a higher amount of glucose available (that is, where is the glucose in the simulations arising?).

Another potential error is that, in reality, excess fatty acids may have a direct depressive effect on lipogenesis. The model has no provision for such an

effect, as no such data existed when the model was constructed. We suggest that such a reaction, including a direct inhibition of lipogenesis by fatty acids, would result in improved performance of the model. Additional experiments will be necessary to test this hypothesis.

We think the most likely interpretation for the majority of the lack of precision is that errors in adipose tissue accumulation are a function of errors arising elsewhere in the metabolic reactions occurring in the cow. Stated another way, in terms of nutrient flux, a cow is a closed system obeying thermodynamic laws. If we simply reduced the parameter values describing lipid synthesis in the adipose tissue, the model would still accumulate energy. The model (as the cow) cannot simply expend excess energy without explicit demand from energy-requiring reactions.

Thus there are several possibilities for sources of error pertaining to energy use in the cow. Let us assume that observed means were indeed an accurate measure of the cows on this trial, and that errors in glucose use exist. This analysis indicates that the errors at the adipose tissue have their causes in reactions describing energy use and thus glucose or fatty acid oxidation in visceral and body tissues, and not solely from errors in the adipose tissue parameters. In the model, as in the cow, the major driving force for glucose oxidation is demand for ATP for biosynthetic or maintenance reactions (Baldwin *et al.*, 1987a,b; McNamara *et al.*, 1991a,b; Baldwin, 1995). Two quantitatively important reactions are visceral and muscle protein turnover. We know that errors in estimation of these reactions are significant; present values, as embodied in the model, are probably underestimations of the costs of these turnovers, especially in high-producing dairy cattle and in later lactation (McNamara and Hillers, 1989; McNamara *et al.*, 1995). We previously discovered that during lactation, even when cows are in positive energy balance, triglyceride turnover is maintained at rates two to four times that found in non-lactating cows (McNamara and Hillers, 1989; McNamara *et al.*, 1995). This is likely because the high rates of milk fat secretion are associated with a faster turnover of noradrenaline in adipose tissue (which increases lipolysis), simultaneously with increased secretion of insulin in late lactation (which stimulates lipogenesis and esterification) (McNamara, 1994). If the same neuroendocrine signals are acting on muscle, a similar phenomenon of increased turnover and associated energy costs will occur.

The total integration of the analyses of potential errors in metabolic reactions leads to the hypothesis that our knowledge of dairy cattle metabolism as integrated in this mechanistic model contains subtle but real inadequacies in describing the metabolism of energy-yielding nutrients, primarily glucose. These errors include potential errors in digestion, in adipose tissue and in mammary use of acetate and long-chain fatty acids, and underestimates of the rates and energy costs of protein turnover reactions. These errors are greater during late lactation than earlier. To put model error in perspective to energy terms, the 97 kg error in body fat over the period of 14 to 245 DIM on cows fed WCSFA is 0.42 kg day^{-1}. Using the National Research Council (NRC, 1989) figure for

fat at 7.3 Mcal metabolizable energy (ME) kg^{-1}, that is, 3.1 Mcal day^{-1}. An average cow on this trial was consuming approximately 22 kg of dry matter (DM) day^{-1}, or 60 Mcal ME day^{-1}. Thus the greatest cumulative model error, in the worst case, was approximately 5% of the mean daily ME intake of the cows, which is approximately equal to the coefficient of variation in intake.

References

Baldwin, R.L. (1995) Lactation. In: *Modelling Ruminant Digestion and Metabolism*. Chapman & Hall, New York, USA, pp. 469–518.

Baldwin, R.L., France, J. and Gill, M. (1987a) Metabolism of the lactating cow. I. Animal elements of a mechanistic model. *Journal of Dairy Research* 54, 77–105.

Baldwin, R.L., France, J., Beever, D.E., Gill, M. and Thornley, J.H.M. (1987b) Metabolism of the lactating cow. III. Properties of mechanistic models suitable for evaluation of energetic relationships and factors involved in the partition of nutrients. *Journal of Dairy Research* 54, 133–145.

Harrison, J.H., McNamara, J.P., Kincaid, R.L., Waltner, S.S., Loney, K.A., Riley, R.E. and Cronrath, J.D. (1995) Effect of whole cottonseeds and calcium salts of long-chain fatty acids on performance of lactating dairy cows. *Journal of Dairy Science* 78, 181–183.

McNamara, J.P. (1994) Lipid metabolism in adipose tissue during lactation: a model of a metabolic control system. *Journal of Nutrition* 124, 1383S–1391S.

McNamara, J.P. and Baldwin, R.L. (2000) Estimation of parameters describing lipid metabolism in lactation: challenge of existing knowledge described in a model of metabolism. *Journal of Dairy Science* 83, 128–143.

McNamara, J.P. and Hillers, J.K. (1989) Regulation of bovine adipose tissue metabolism during lactation 5. Relationship of lipid synthesis and lipolysis with energy intake and utilization. *Journal of Dairy Science* 72, 407–418.

McNamara, J.P., Kincaid, R.L., Harrison, J.H., Waltner, S.S. and Becker-Khaleel, B. (1991a) Challenging and improving models of energy metabolism: parameters of lipid metabolism during pregnancy and lactation in dairy cattle. In: Wenk, C. and Boessinger, B. (eds) *Energy Metabolism in Farm Animals*. EAAP Publication No. 58, ETH-Zentrum, Zurich, Switzerland, pp. 32–35.

McNamara, J.P., Pettigrew, J.E., Baldwin, R.L., Close, W.H., Walker, J. and Oltjen, J.L. (1991b) Information needed for mathematical modeling of energy metabolism. In: Wenk, C. and Boessinger, M. (eds) *Energy Metabolism in Farm Animals*. EAAP Publication No. 58, ETH-Zentrum, Zurich, Switzerland, pp. 468–472.

McNamara, J.P., Harrison, J.H. and Kincaid, R.L. (1995) Lipid metabolism in adipose tissue of cows fed high fat rations high in lactation. *Journal of Dairy Science* 78, 2782–2796.

National Research Council (NRC) (1989) *Nutrient Requirements of Dairy Cattle*. 6th revised edn, Update 1989. National Academy Press, Washington, DC.

Palmquist, D.L. (1994) Metabolism of fats and their role in animal efficiency. *Journal of Nutrition* 124, 1392S–1401S.

Waltner, S.S., McNamara, J.P., Hillers, J.K. and Brown, D.L. (1994) Validation of indirect measures of body fat in lactating dairy cattle. *Journal of Dairy Science* 77, 2570–2579.

Wu, Z. and Huber, J.T. (1994) Relationship between dietary fat supplementation and milk protein concentration in lactating cows: a review. *Livestock Production Science* 39, 141–150.

23

A Rodent Model of Protein Turnover to Determine Protein Synthesis, Amino Acid Channelling and Recycling Rates in Tissues

H.A. Johnson, R.L. Baldwin and C.C. Calvert

Department of Animal Science, University of California, Davis, CA 95616, USA

Abstract

Amino acids for protein synthesis can arise from extracellular (Ec), plasma (Pls) or intracellular (Ic) sources or protein degradation through recycling. Experimentally, the amino acid sources sampled may not represent these specific pools and therefore not represent true sources of amino acids used for aminoacyl tRNA (Tr) formation. As a result, estimates of protein fractional synthesis rates (FSR) may not reflect true protein synthesis rates. Three models of brain, liver and muscle were created to represent different sampling methods used for partitioning free amino acid precursor pools. The Ec + Pls model separates the intracellular and aminoacyl tRNA pools of free leu from a combined sample of plasma and extracellular pools. The Ec + Ic + Tr model separates plasma amino acids from a combined extracellular, intracellular and aminoacyl tRNA pool. The Ec + Ic model separates plasma and aminoacyl tRNA from a combined extracellular and intracellular free amino acid pool. Data from a pulse dose of ^{14}C-U-leu was used to estimate FSR and determine the source of amino acids for aminoacyl tRNA (protein synthesis). The pulse dose-specific radioactivity data were fitted to dynamic, theoretical models representing protein turnover in brain, liver and muscle for a non-growing 20 g mouse. Estimates of recycling were higher with the Ec + Pls than the Ec + Ic model, with liver at 90.4% and 76.2%, muscle at 91.1% and 86.1% and brain at 95.2 and 68.3%, respectively. Protein synthesis rates estimated using the Ec + Ic and Ec + Pls models were 81.9 and 117% day^{-1} in liver, 14.8 and 16.2% day^{-1} in brain and 14.7 and 14.0% day^{-1} in muscle, respectively. The Ec + Ic + Tr model underestimated protein synthesis in all tissues, because the specific radioactivity of the combined precursor pool (Ec + Ic + Tr) was very high relative to the specific radioactivity of the protein pool. At high rates of recycling, intracellular and extracellular specific radioactivities no longer approximate

 Modelling Nutrient Utilization in Farm Animals (eds J.P. McNamara, J. France and D.E. Beever)

the true precursor specific radioactivity (aminoacyl tRNA). Therefore current methods of estimating FSR in tissues incorporate error associated with incorrectly estimating precursor pool specific radioactivity.

Introduction

Estimates of protein fractional synthesis rates (FSR) of tissues using radiotracers are based on measurements of specific radioactivities of protein and precursor pools. The true precursor pool for protein synthesis is aminoacyl tRNA. However, since separation and quantification of aminoacyl tRNA is difficult, other pools are sampled to approximate aminoacyl tRNA specific radioactivity. Precursor pools sampled include plasma free amino acids (Pls), extracellular free amino acids (Ec), intracellular free amino acids (Ic), aminoacyl tRNA (Tr) or combinations of these pools. Choice of source pool specific radioactivity is defined by the experimental method used to separate or partition free amino acids. For instance, Bernier and Calvert (1987) homogenized carcasses in HCl to separate free amino acids and protein. The supernatant, including Pls, Ec, Tr and Ic amino acids, was used to estimate leu specific radioactivities. Obled *et al.* (1991) used a similar method to separate free and bound amino acids but also measured Pls specific radioactivity from tissue-free (Ec, Tr and Ic) amino acid specific radioactivity. Smith *et al.* (1988) measured Tr, Pls and Ec plus Ic specific radioactivities to estimate amino acid recycling and FSR. In some tissues, extracellular space has been estimated and then intracellular and extracellular concentrations and specific radioactivities are estimated from plasma and tissue concentrations of free amino acids (Hider *et al.*, 1971). The consequences of partitioning free amino acids into combinations of Pls, Ec, Ic and Tr for estimates of FSR in tissues have not been examined quantitatively. In this study, rodent models of protein turnover described previously (Johnson *et al.*, 1999a,b) and data from Lajtha (1959) in brain, liver and muscle were used to estimate specific radioactivities in Ec + Pls, Ec + Ic + Tr and Ec + Ic. The results were used to evaluate the impact of sampling methods of precursor specific radioactivities on protein FSR.

Models

Three models for each tissue were created. All equations are based on mass-action kinetics between pools and were published previously in Johnson *et al.* (1999a). The first model (Ec + Pls) partitions free amino acids into Tr, Ic and combined Pls and Ec pools (Fig. 23.1). Leu intake (μmol leu min^{-1}) and leu dose (μCi ^{14}C leu μmol leu^{-1}) enter the Ec + Pls pool and leu is oxidized from the Ic pool. Leu fluxes to aminoacyl tRNA from the Ec + Pls and Ic pools are unidirectional, based on the assumption that it would be energetically inefficient and

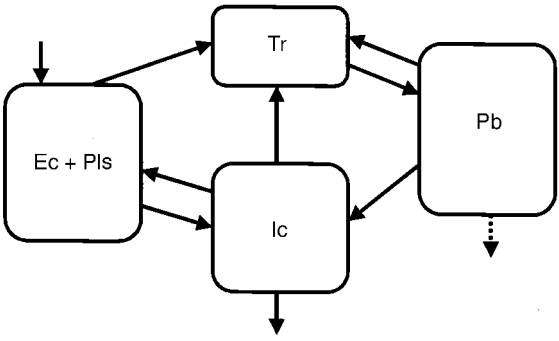

Fig. 23.1. The Ec + Pls model of the rodent tissue protein turnover. The dashed arrow represents leu in protein exported from the tissue and was only present in the liver tissue model.

therefore unlikely that leucyl tRNA is deacylated once it is formed (Johnson *et al.*, 1999a). Protein synthesis is represented by the flux from Tr to leu in protein (Pb) and protein degradation by the flux from Pb to Ic. Recycling is the flux from Pb to Tr. The units for all pool sizes are μmol leu and all fluxes are μmol leu min^{-1}. Pls and Ec are assumed to equilibrate rapidly. Therefore their specific radioactivities are assumed to be similar and the pools are combined. Experimentally, the specific radioactivity of Ic is determined by estimating extracellular space and correcting free amino acid (supernatant) specific radioactivity for μCi ^{14}C leu in Ec. Extracellular space can be estimated using inulin or sorbitol as extracellular markers (Hider *et al.*, 1971).

The second model (Ec + Ic + Tr) partitions free amino acids into Pls and combined Ec, Ic and Tr pools (Fig. 23.2). Leu in the protein pool exchanges with the combined Ec, Ic and Tr pool, representing protein synthesis and protein degradation. There is no representation of recycling or of different pools as sources of leu for protein synthesis, since all free leu associated with the cell is represented as one pool. The Ec + Ic + Tr model represents most experiments in which the specific radioactivity of leucyl tRNA is not determined.

The third model (Ec + Ic) partitions free amino acids into Pls, Tr and combined Ec and Ic pools (Fig. 23.3). Protein synthesis, protein degradation and recycling are represented by the same fluxes as in Ec + Pls (see Fig. 23.1). However, Ec and Ic are assumed to exchange leu rapidly and therefore the specific radioactivities of Ec and Ic are assumed to be similar and are combined.

Data

Specific radioactivity changes over time; initial pool sizes and the ^{14}C leu dose were obtained from data in Lajtha (1959). The data were based on a whole-body

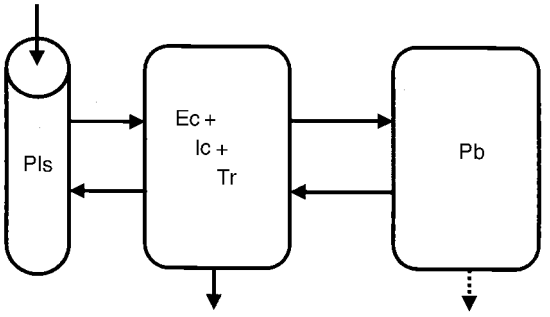

Fig. 23.2. The Ec + Ic + Tr model of the rodent tissue protein turnover. The dashed arrow represents leu in protein exported from the tissue and was only present in the liver tissue model.

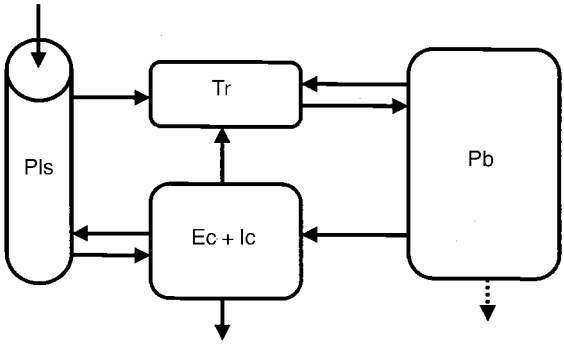

Fig. 23.3. The Ec + Ic model of the rodent tissue protein turnover. The dashed arrow represents leu in protein exported from the tissue and was only present in the liver tissue model.

dose of 0.2 μCi ^{14}C-U-leu and 0.025 μmol leu given to 20 g (100-day) mice. Six mice were pooled for each time point. Specific radioactivities were measured at 3, 5, 10, 20, 30, 45, 60 and 120 min in plasma, brain, liver and muscle. Organs were frozen and homogenized with 5% trichloroacetic acid. The extract was designated as the portion containing free leu (Ec + Ic + Tr) and the precipitate was the protein portion.

Specific radioactivity data were already separated into Pls, free leu and leu in protein by Lajtha (1959); so the specific radioactivity of the free leu from the data was assumed to equal the specific radioactivity of the Ec + Ic + Tr pool and the Ec + Ic pool for the Ec + Ic + Tr and Ec + Ic models, respectively. To create the Ec + Pls specific radioactivity data, plasma free amino acid specific radioactivity was assumed to equal the specific radioactivity of extracellular free amino acid.

Then free amino acid specific radioactivities were corrected for leu associated with aminoacyl tRNA and extracellular free amino acid pool sizes to determine the specific radioactivities of the intracellular pools.

Methods

Data were fitted using a generalized reduced gradient within Advanced Continuous Simulation Language (ACSL) Optimize (MGA, 1999). ACSL Optimize uses the method of maximum likelihood to estimate parameters based on data input into a model. Model parameters are chosen to maximize the likelihood of fitting the experimental data. Errors are assumed to be normally distributed and statistically independent. For all models, leu intake, ^{14}C leu dose to the tissue and model predicted FSR (PFSR) were estimated based on fitted specific radioactivities. For the Ec + Pls and Ec + Ic models, the fluxes of leu to Tr indicating the source of leu (Pls, Ec, Ic, Ec + Ic and Pb) for aminoacyl tRNA were also adjusted to fit the data. For the Ec + Ic + Tr models, the exchange of leu between the Pls and Ec + Ic + Tr pools were fitted to the data. The models also predicted μmol leu incorporated into protein min^{-1} (protein synthesis rate (PSR)).

Results and Discussion

The best fits of the data were obtained with the Ec + Pls models (Figs 23.4, 23.7 and 23.10). The only brain model that was able to maintain specific radioactivity differences between Pls (or Ec + Pls) and Ic, Ec + Ic + Tr or Ec + Ic was

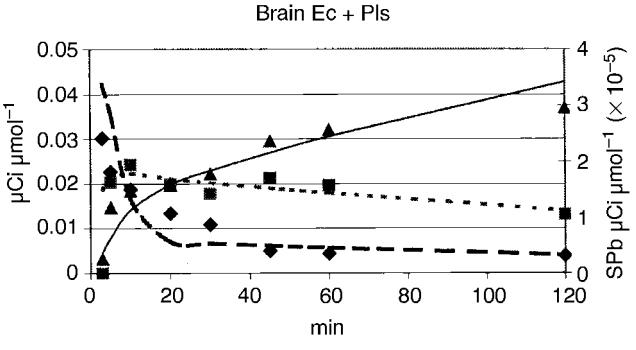

Fig. 23.4. Observed and predicted specific radioactivities by the brain model with free leu partitioned into Ic, Tr and Ec + Pls pools. S prefix represents specific radioactivity. Observed SPb = ▲, predicted SPb = —, observed SIc = ■, predicted SIc = ···, observed SEc + SPls = ◆, predicted SEc+SPls = – – –.

Ec + Pls (Figs 23.5 and 23.6). None of the liver models were able to replicate the specific radioactivity of the protein pool (Figs 23.7, 23.8 and 23.9). The protein specific radioactivities predicted by the Ec + Ic + Tr and Ec + Ic models were too low, except for specific radioactivities at 120 min. None of the liver models could duplicate the decrease in protein specific radioactivities at 120 min, even with high recycling. The brain models also overpredicted protein specific radioactivities at 120 min, but were able to fit the other time points well (less than 20% errors of prediction). The muscle models (Figs 23.10, 23.11 and 23.12) simulated the experimental data best. For muscle models, all source pool specific radioactivities equilibrated by 120 min and there was no decrease in specific radioactivity of the protein pool.

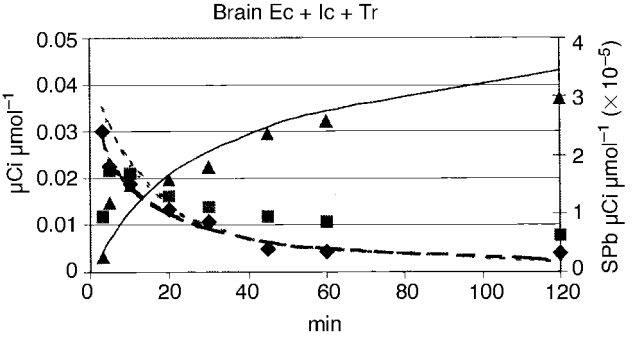

Fig. 23.5. Observed and predicted specific radioactivities by the brain model with free leu partitioned into Pls and Ec + Ic + Tr pools. S prefix represents specific radioactivity. Observed SPb = ▲, predicted SPb = —, observed SEc + SIc + STr = ■, predicted SEc + SIc + STr = ⋯, observed SPls = ◆, predicted SPls = – – –.

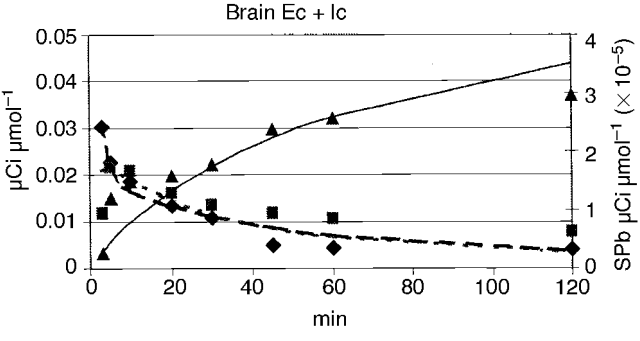

Fig. 23.6. Observed and predicted specific radioactivities by the brain model with free leu partitioned into Pls, Tr and Ec + Ic pools. S prefix represents specific radioactivity. Observed SPb = ▲, predicted SPb = —, observed SEc + SIc = ■, predicted SEc + SIc = ⋯, observed SPls = ◆, predicted SPls = – – –.

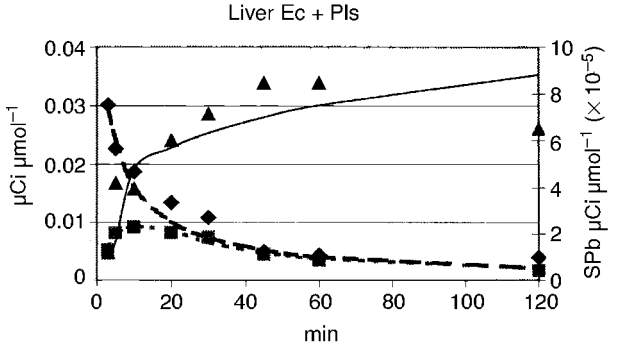

Fig. 23.7. Observed and predicted specific radioactivities by the liver model with free leu partitioned into Ic, Tr and Ec + Pls pools. S prefix represents specific radioactivity. Observed SPb = ▲, predicted SPb = —, observed SIc = ■, predicted SIc = ⋯, observed SEc + SPls = ◆, predicted SEc + SPls = – – –.

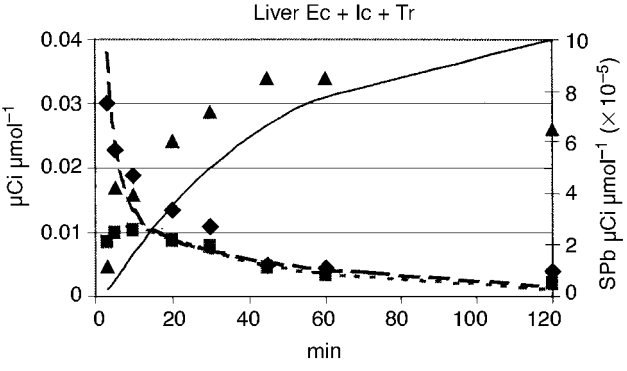

Fig. 23.8. Observed and predicted specific radioactivities by the liver model with free leu partitioned into Pls and Ec + Ic + Tr pools. S prefix represents specific radioactivity. Observed SPb = ▲, predicted SPb = —, observed SEc + SIc + STr = ■, predicted SEc + SIc + STr = ⋯, observed SPls = ◆, predicted SPls = – – –.

More data points at the beginning and end of the experiment would have ensured that the peak specific radioactivities in each pool were measured and would have given more information about the plateau or drop in protein specific radioactivities in liver and brain at the end of the experiment. In addition, food intake and composition of the experimental animals can affect specific radioactivity data (Johnson *et al.*, 1999b). Although initial pools sizes were given in Lajtha's paper (Lajtha, 1959), no intake information was available. Therefore

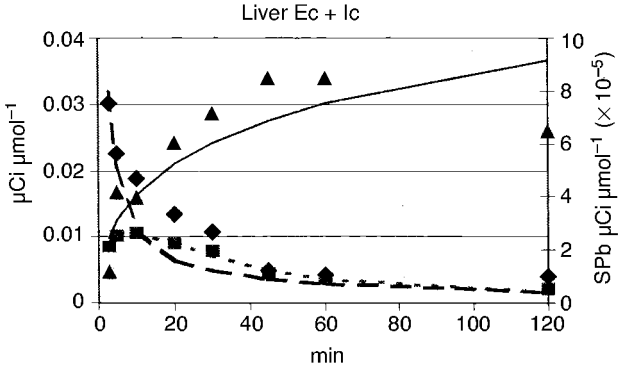

Fig. 23.9. Observed and predicted specific radioactivities by the liver model with free leu partitioned into Pls, Tr and Ec + Ic pools. S prefix represents specific radioactivity. Observed SPb = ▲, predicted SPb = —, observed SEc + SIc = ■, predicted SEc + SIc = ⋯, observed SPls = ◆, predicted SPls = – – –.

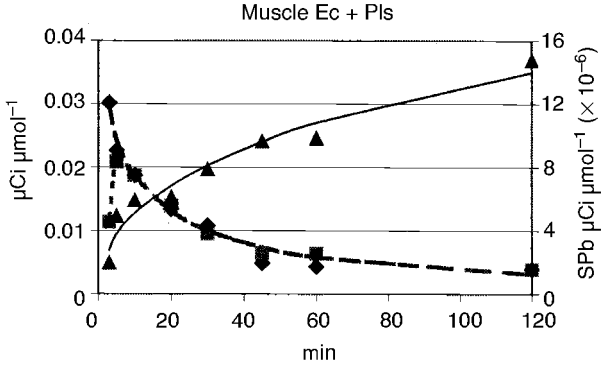

Fig. 23.10. Observed and predicted specific radioactivities by the muscle model with free leu partitioned into Ic, Tr and Ec + Pls pools. S prefix represents specific radioactivity. Observed SPb = ▲, predicted SPb = —, observed SIc = ■, predicted SIc = ⋯, observed SEc + SPls = ◆, predicted SEc + SPls = – – –.

the models may not be the best representation of the data and/or there may be another set of model parameters that fit the data better. However, the solutions were stable when parameters were varied, and most predictions of individual specific radioactivity data points were within 20% (experimental error) of observed values.

The Ec + Ic + Tr models simulated specific radioactivities that implied very

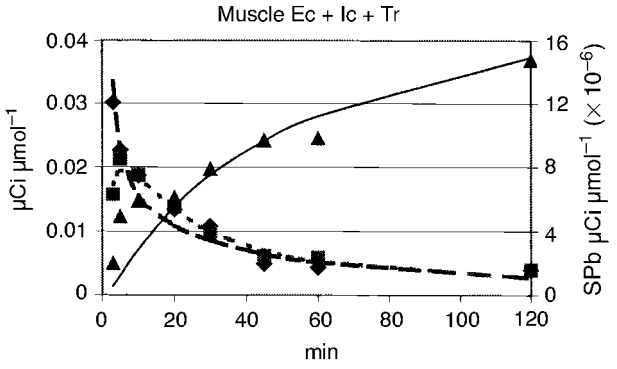

Fig. 23.11. Observed and predicted specific radioactivities by the muscle model with free leu partitioned into Pls and Ec + Ic + Tr pools. S prefix represents specific radioactivity. Observed SPb = ▲, predicted SPb = —, observed SEc + SIc + STr = ■, predicted SEc + SIc + STr = ⋯, observed SPls = ◆, predicted SPls = – – –.

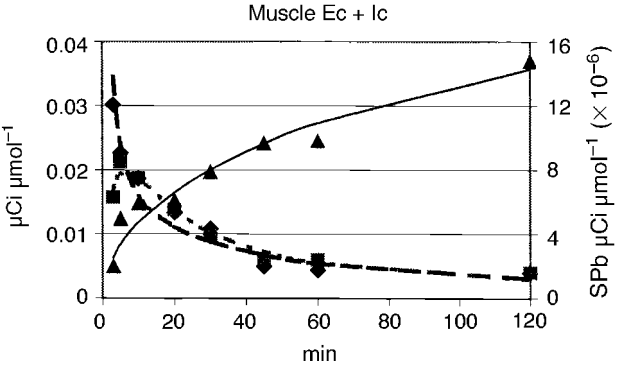

Fig. 23.12. Observed and predicted specific radioactivities by the muscle model with free leu partitioned into Pls, Tr and Ec + Ic pools. S prefix represents specific radioactivity. Observed SPb = ▲, predicted SPb = —, observed SEc + SIc = ■, predicted SEc + SIc = ⋯, observed SPls = ◆, predicted SPls = – – –.

low estimates of protein synthesis. In Table 23.1, PFSR and PSR estimates are much lower for the Ec + Ic + Tr models. The combined specific radioactivities of the Ec, Ic and Tr pools were relatively high and dilution of the protein specific radioactivity from any other source was not possible. The rate of protein synthesis had to be low to match observed data. Therefore the Ec + Ic + Tr models, which represent measurements of Pls, supernatant and protein specific radioactivites, may result in low estimates of protein synthesis and contribute to the

Table 23.1. Comparison of predicted FSR (PFSR in % day^{-1}) by the models, using different free leu pools to approximate aminoacyl tRNA specific radioactivity, with protein synthesis rates (PSR in μmol min^{-1}) and with other estimated rates summarized from Lajtha (1959) and Johnson *et al.* (1999a). Standard deviations are in parentheses following the values. FSR summarized by Johnson were from flooding dose (FFSR) and continuous infusion (CIFSR) experiments. Values from Lajtha were from a pulse-dose experiment.

	FFSR (Johnson)	CIFSR (Johnson)	FSR (Lajtha)	PFSR	PSR
Brain	15.9	12.4 (8.7)	13.2		
Ec + Pls				16.2 (1.6)	0.00140
Ec + Ic + Tr				5.00 (0.49)	0.000434
Ec + Ic				14.8 (1.3)	0.00129
Liver	91.7 (34)	64.2 (39)	125		
Ec + Pls				117 (6.1)	0.0335
Ec + Ic + Tr				27.0 (0.00045)	0.00825
Ec + Ic				81.9 (7.62)	0.0250
Muscle	13.7 (5.5)	9.30 (5.6)	9.80		
Ec + Pls				14.0 (0.78)	0.0421
Ec + Ic + Tr				2.45 (0.21)	0.00744
Ec + Ic				14.7 (0.00030)	0.04467

wide variation in estimates of FSR. Addition of a Tr pool to the model (Ec + Pls and Ec + Ic models) increased PFSR and indicated the importance of including the specific radioactivity of aminoacyl tRNA in experimental measurements.

Standard deviations of estimates of FSR in rodents from literature are high (see Table 23.1). FFSR and CIFSR represent estimated FSR summarized from literature based on the flooding-dose and continuous-infusion methods, respectively. Consequently, although all of the predicted FSR were different, they were within a standard deviation unit of literature values. Variations in FSR estimates could be due to differences between animals, because different animals are used at each time point and estimates of FSR change with the length of the experiment (Lajtha, 1959; Johnson *et al.*, 1999b), or due to differences in partitioning free amino acids in experimental methods.

PFSR that were predicted by the model were also close to FFSR and CIFSR for the Ec + Pls and Ec + Ic models. Ec + Pls models represent experimental methods where Pls and supernatant free amino acids were separated and then, by using an estimate of extracellular space, intracellular specific radioactivity was estimated. The key assumption was that the specific radioactivities of plasma and extracellular free amino acids were equivalent. This assumption appears to be valid, since PFSR with this model was similar to literature values. However, the Ec + Ic model also yields similar estimates of PFSR. Since both

include a Tr pool, it may be more important to include aminoacyl tRNA as a separate pool than to partition Ec from Pls or Ic. This implies that the net contributions of Ec to Pls or Ic pools were low. All of these estimates were based on pulse-dose data. These conclusions may not be true for flooding-dose data, since the flooding-dose method involves large, non-physiological doses of unlabelled amino acid.

Predictions of the source of free amino acids for protein synthesis from fitting the specific radioactivity data to the models are shown in Table 23.2. No single pool was the source of free amino acids. Amino acids from recycling were consistently higher than predicted by other methods (Smith and Sun, 1995). Since the only experimental measurement that reflects recycling is the specific radioactivity of aminoacyl tRNA, it is extremely important that it is measured and included as a pool in the models.

With all models, the specific radioactivities of the source pools appeared to be high relative to the protein specific radioactivity. As a result, recycling was high in order to keep the protein specific radioactivity low in the Ec + Pls and Ec + Ic models. Recycling was not explicitly represented in the Ec + Ic + Tr model. Therefore protein synthesis was predicted to be much lower. So these solutions may be specific to this data set. More data are needed to challenge these conclusions.

Conclusions

Aminoacyl tRNA needs to be included as a pool in the model and should be measured experimentally with other pool specific radioactivities. Addition of a

Table 23.2. Percentage of free leu for aminoacyl tRNA from different sources (plasma (Pls), extracellular (Ec), intracellular (Ic), extracellular plus intracellular (Ec + Ic) and protein (Pb)) relative to amount of protein synthesized as predicted by the models. Standard deviations are in parentheses following the values.

	% Pls	% (Ec + Pls)	% Ic	% Ec + Ic	% Pb
Brain					42*
Ec + Pls		4.77 (3.3)	0		95.2 (14.5)
Ec + Ic	7.50			24.2 (12.7)	68.3 (5.9)
Liver					53*
Ec + Pls		7.63 (0.38)	1.96 (0.16)		90.4
Ec + Ic	22.5 (9.5)			1.36	76.2 (6.51)
Muscle					55*
Ec + Pls		7.25 (1.6)	1.62		91.1 (29)
Ec + Ic	13.9 (0.0021)			0	86.1 (0.0007)

*Percentage recycling as predicted by Smith and Sun (1995).

small, rapid turnover pool to the models, such as aminoacyl tRNA, is needed to estimate recycling and can account for higher FSR when the specific radioactivity of the source pools (Ec + Pls, Ec + Ic + Tr, Ec + Ic) is high relative to the specific radioactivity of the protein pool.

Estimates of FSR vary widely. The variation is due to differences in methods for partitioning the free amino acid pools to estimate aminoacyl tRNA. No single pool is the exclusive free amino acid source for aminoacyl tRNA (protein synthesis) and none of the methods for partitioning free amino acid includes measuring the specific radioactivity of aminoacyl tRNA. Therefore recycling, which according to these data is high, is not included in estimates of FSR. In addition, estimates of FSR decrease over time. Therefore the time at which the specific radioactivity of the source pool and protein pool are measured experimentally is critical in estimating FSR.

The model structures and fits of the specific radioactivity data may not accurately represent all that occurs in protein synthesis. As with any solutions to non-linear systems, there may be alternative solutions that better represent the data. For instance, none of the model structures or parameters fitted could reproduce the decrease in specific radioactivity of the liver and brain protein pools at 120 min. Data which include more time points to catch the peaks in specific radioactivity of all the pools and the decrease in specific radioactivity of the protein pool (more than one experimental time point) would provide a better challenge to the models. A description of experimental conditions, including time, amount and leu amino acid content of feedings and specific radioactivity levels in the rest of the body, would provide a better accounting to estimate amino acid tissue intake and tissue dose of radiolabelled amino acid.

References

Bernier, J.F. and Calvert, C.C. (1987) Effect of a major gene for growth on protein synthesis in mice. *Journal of Animal Science* 65, 982–995.

Hider, R.C., Fern, E.B. and London, D.R. (1971) Identification in skeletal muscle of a distinct extracellular pool of amino acids, and its role in protein synthesis. *Biochemical Journal* 121, 817–827.

Johnson, H.A., Baldwin, R.L., France, J. and Calvert, C.C. (1999a) Development and evaluation of a model of whole body protein turnover based on leucine kinetics in rodents. *Journal of Nutrition* 129, 728–739.

Johnson, H.A., Baldwin, R.L., France, J. and Calvert, C.C. (1999b) Recycling, channeling and heterogeneous protein turnover based on leucine kinetics in rodents. *Journal of Nutrition* 129, 740–750.

Lajtha, A. (1959) Amino acid and protein metabolism of the brain – V. Turnover of leucine in mouse tissues. *Journal of Neurochemistry* 3, 358–365.

Mitchell and Gauthier Assoc. (MGA) Inc. (1999) *Optimize, ACSL: Advanced Continuous Simulation Language*. MGA Inc., Concord, Massachusetts.

Obled, C., Barre, F. and Arnal, M. (1991) Flooding-dose of various amino acids for measurement of whole-body protein synthesis in the rat. *Amino Acids* 1, 17–27.

Smith, C.B. and Sun, Y. (1995) Influence of valine flooding on channeling of valine into tissue pools and on protein synthesis. *American Journal of Physiology* 268, E735–E744.

Smith, C.B., Deibler, G.E., Schmidt, K. and Sokoloff, L. (1988) Measurement of local cerebral protein synthesis *in vivo*: influence of recycling of amino acids derived from protein degradation. *Proceedings of the National Academy of Sciences, USA* 85, 9341–9345.

24

Modelling Relationships Between Homoeorhetic and Homoeostatic Control of Metabolism: Application to Growing Pigs

D. Sauvant[1] and P.A. Lovatto[1,2]

[1] *Laboratoire INRA–INAPG de Nutrition et Alimentation, INAPG, 16 rue Claude Bernard, 75231 Paris Cedex 05, France;* [2] *Universidade Federal de Santa Maria/CNPq, DZ/CCR 97119–900, Santa Maria-RS, Brazil*

Abstract

Diet formulation has to consider the multiple responses of animals to the diet. Their responses are assessed and expressed in terms of feed efficiency, quality of the food product, environmental impact and animal behaviour, welfare and health. To achieve this new purpose the first step is to apply a systemic approach to the organism acknowledging the major driving forces of nutrient fluxes and the second step is to model these forces. This chapter deals with these aspects in the case of the growing animal. Although the model presented only includes the minimum of information necessary to simulate growth and influences of diet, it was capable of realistic simulations of the metabolic flow during growth and during a shortage of amino acids.

Introduction

Animal production is now facing various challenges and constraints that must be taken into consideration. The previous era of animal feeding was that of maximization of feed efficiency. The new era also considers controls of some productions (quotas) and the impact of feeding on the composition and the quality of animal products, on the environment and on animal health and well-being. To contribute to the practical integration of these new challenges, scientific targets and practical concepts of animal nutrition have to evolve (Sauvant, 1992).

 Modelling Nutrient Utilization in Farm Animals (eds J.P. McNamara, J. France and D.E. Beever)

Thus the traditional concept of formulating diets to cover the nutritional requirements determined by the genetic potential has to shift to a new situation, in which diet formulation is performed considering the multiple responses of the animal to diets. These responses are assessed and expressed in terms of feed efficiency, quality of the product, environmental impact and animal behaviour, welfare and health.

This new paradigm in animal nutrition and feeding raises new issues for research, which has so far mainly been focused on building feed unit systems to achieve the traditional target. The major task has now become to build models that are capable of understanding and predicting the animal response to diet. To achieve this new purpose, the first step is to apply a systemic approach to the organism (Sauvant, 1994), acknowledging the major driving forces of nutrient fluxes (Fig. 24.1). In a second step, the issue is to model these forces. This chapter deals with these aspects in the case of the growing animal. To illustrate the concepts developed in this chapter, a model was developed in the case of the growing pig through a model that was recently presented (Lovatto and Sauvant, 1999).

Systemic Approach to the Organism and its Regulation

A better understanding and prediction of animal responses to diet require, first of all, consideration of the animal as a complex system that is closely controlled by endogenous regulation driving the flow of nutrients. In this regard, it is believed that each live being includes in its genome its teleonomic project, as described by Monod (1970). This project comprises two subprojects, that of the

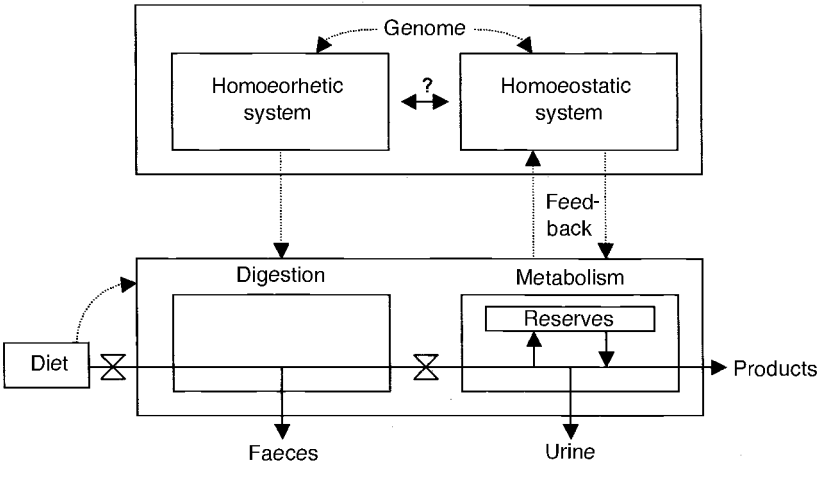

Fig. 24.1. Systemic approach to the organism.

perenniality (strategic purposes) of the species and that of the survival of the individual (tactical purposes). To achieve these aims, live organisms possess two major systems of regulation. The regulating system of teleophoresis (Chilliard, personal communication, 1986) is targeted by the species perenniality and the regulating system of homoeostasis by the survival. These two systems control the metabolic flows of nutrients and they frequently interact.

Teleophoretic regulation (TR), also called homoeorhetic (HR) (Bauman and Currie, 1980), controls the functions of reproduction – pregnancy, lactation, egg production, etc. – but also growth, which can be regarded as a delay of maturation before achieving the ability to participate in the reproductive processes. A debate remains as to whether teleophoresis and homoeorhesis are actually synonymous. This does not seem to be strictly the case, because, for instance, maintenance and physical activities are considered to be of a homoeorhetic nature (Bauman, 1999), but not teleophoretic (Chilliard and D. Sauvant, unpublished, 1999). TR or HR is 'encoded' in the genome and exerts a close control, without feedback, on multiple sites and functions (i.e. a pleiotropic effect). The dynamic properties of HR regulation are almost systematically of a long-term nature (weeks or months). Considered from the viewpoint of modelling, HR regulation suffers from a lack of basic and mechanistic knowledge. Therefore, it is necessary to model it through theoretical and relevant principles and models (Sauvant and Phocas, 1992; Sauvant, 1994; Bastianelli and Sauvant, 1997). HR regulation is not directly involved in the marginal responses of the animal to diet (see below).

Homoeostatic regulation (HS) acts through feedback loops to adapt the organism to the environmental perturbations with which it may be faced. The initial event of HS regulation is a signal registered by a specific system (sudden shift in temperature, wave of entry of nutrients into the organism, shortage in energy, sudden arrival of a dominant congener, etc.). If necessary, this initial event triggers a cascade of physical and/or metabolic adaptations. Due to this type of situation, most HS regulation is of a very short-term nature. The pathways and modalities of HS regulation are highly diverse. Moreover, the degree of sophistication of HS regulation largely varies according to the level of vital significance of the particular nutrient. For strategic elements, such as glucose or Ca, complicated regulation, including hormonal systems, has been developed through evolution. For most of the metabolites, there is only passive and local regulation through structures (biomembranes, etc.) which leads to control of the flows of metabolites according to mass-action laws. Considered from the viewpoint of modelling, these last aspects are fairly easy to represent. For more sophisticated systems, including hormones, a minimum model can generally be built by taking into consideration the short-term variations of circulating concentrations of nutrients (glucose, Ca, P, etc.) and hormones (insulin, glucagon, calcitonine, etc.), which are generally fairly sound. The HS system is largely involved in marginal responses to diet (see below).

From the perspective of modelling animal responses to diet, it is necessary to consider the third major driving force – the flow of nutrients. The outcome of

diet intake and subsequent absorption of nutrients is a global mass-action law effect, which greatly alters some flows of metabolites. The major origin of animal responses to diet is the outcome of HS regulation, which acts as a dynamic buffer between the inflows of nutrients issuing from the diet and the chronic demand for them, driven by HR control.

A satisfactory mechanistic model of responses to diet cannot be built without taking into consideration the three above-mentioned driving forces of metabolic flows. As far as we are aware, no published model has until now attempted to clearly represent these aspects.

Model Construction

Structure of the model (Fig. 24.2)

The system comprises circulating blood and two major tissue compartments: the body proteins (BP) and body lipids (BL). At a lower level of organization, it integrates seven metabolic subcompartments. Six correspond to individual (lysine, threonine and tryptophan) and pooled amino acids (AA) (methionine + cystine, other essential AA, and non-essential AA). These amino acids were considered in a free form in the plasma and included in the body proteins. The other metabolic compartment corresponds to the pooled molecules of carbon chains, mainly glucose. This compartment is further separated into fatty acids and glucose.

Plasma metabolites are related to their corresponding tissue compartments and they also receive flows from the absorption of nutrients. Free plasma amino acids can be deaminated as well. They are also involved in protein losses, both endogenous and from the integument. The metabolic inflows from diet intake and digestion were calculated from values of ileal digestibility of amino acids and the other carbon molecules (Noblet *et al.*, 1989).

System of regulation of the metabolic flows

General concept

All published mechanistic models of growth contain a basic assumption to drive metabolic flows. The more aggregated models included a classical – Gompertz or logistic – equation of growth, to induce growth (for example, Siebrits *et al.*, 1986; Whittemore *et al.*, 1988; Ferguson and Gous, 1993). The less aggregated models consider that the DNA compartment grows according to a logistic process (for example, Baldwin and Black, 1979; Oltjen *et al.*, 1986) and induces growth of protein or the empty body. These approaches were based on a 'multiplicative' concept of modelling the growth rate (dQ/dt), which corresponds to the product of a function of acceleration by a breaking function ($B(Q)$):

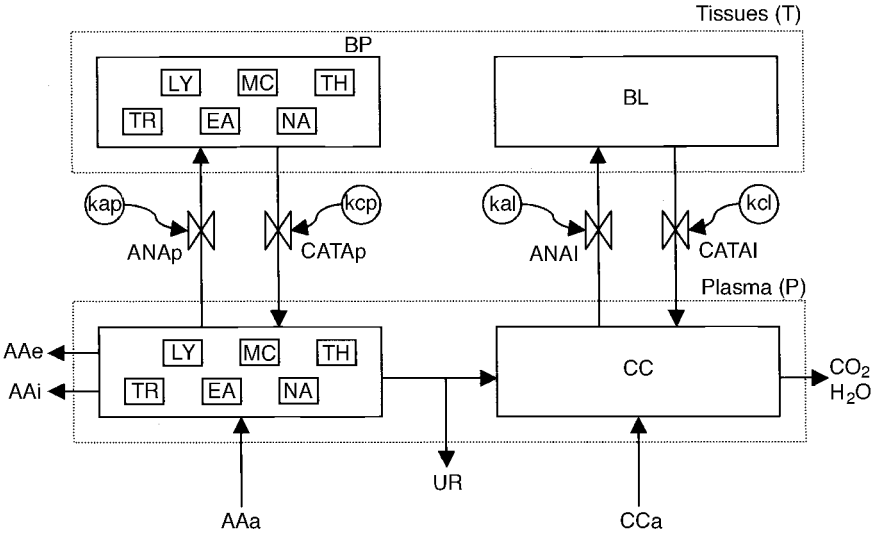

Fig. 24.2. Diagram of model. Two body compartments: tissues, T (proteins, BP; lipids, BL), and plasma, P. Biochemical subcompartments: lysine (LY); methionine + cystine (MC), threonine (TH), tryptophan (TR), other essential amino acids (EA), non-essential amino acids (NA), carbon chains (CC). Inflows: amino acids (AAa), carbon chains (CCa). Outflows: endogenous digestive losses (AAe), integument losses (AAi), urea (UR), respiratory chain (CO_2, H_2O). Metabolic flows: anabolism (ANAp, ANAI), and catabolism (CATAp, CATAI). Auxiliary variables: fractional rates of anabolism (kap, kal) and catabolism (kcp, kcl).

$$dQ/dt = \text{constant} \times Q \times B(Q)$$

It seems to us more mechanistic to adopt an 'additive' concept of the growth rate, which corresponds to the algebraic sum of the anabolic (*ANA*) and catabolic (*CATA*) flows:

$$dQ/dt = ANA - CATA$$

ANA and *CATA* are generally functions of *Q*. This type of approach was proposed by von Berthalanffy (1973).

Integration of teleophoretic regulation

The adopted representation of HR regulation considers that the fractional rates of anabolism (*ka*) and catabolism (*kc*) of tissue compartments follow exponential decay over time. For example, for the anabolism the expression is:

$$ka = kaa + kai \times e^{-ca \times t}$$

The initial fractional rate (*kaa* + *kai*) decreases according to a first-order process with a relative rate of decay, *ca*, until the rate of the adult status (*kaa*). The values

of *ka* are larger than those of *kc*; *ka* and *kc* converge asymptotically toward the *kaa* value. For example, the basic equations of fractional rates of growth of protein tissue in pig were:

$$ka = 0.03 + 0.074e^{-0.022t}$$

$$kc = 0.03 + 0.056e^{-0.035t}$$

The kinetics of *ka* and *kc* correspond to trends which had already been observed *in vivo* in several species (Simon, 1988; Pomar *et al.*, 1991; Knap and Schrama, 1996). Moreover, this principle has already been integrated in the model of growth presented by Danfær (1991). The fractional rates were integrated within dynamic differential equations where flows of anabolism and catabolism followed the first-order process of the size of the compartment *Q* (BP or BL):

$$dQ/dt = ka \times Q - kc \times Q$$

The numerical integration of this type of equation led to the calculation of the flows of anabolism and of catabolism, the growth rate and the corresponding growth curve $Q = f(\text{time})$, which exhibited a point of inflexion.

Integration of homoeostatic regulation

Homoeostatic regulation was first applied to the flux of circulating metabolites. The target was to maintain their concentration within the range of values observed in the literature. Therefore the driving variable was calculated, for a given nutrient *NU*, as the difference between the actual value, *NUt*, and the set value, *NUs*, which was the mean of published values at normal physiological status. To achieve this homoeostatic target, we applied the simple principle of the 'ball placed in a groove'. Concretely, for a given metabolite, anabolic flows, $y = ANAt$, have been considered as a positive exponential function of *x*, where $x = NUt - NUs$ (Fig. 24.3). The intercept value of *y* corresponding to $x = 0$ is the value of the anabolic flow determined by homoeorhetic regulation (see above). For the catabolic flow, *CATAt*, a symmetric approach was adopted to achieve the above-mentioned 'groove principle'. Thus *y* is a negative exponential function of the already defined variable *x*. For $x = 0$ the intercept value of *CATAt* was that determined by homoeorhetic regulation (see Fig. 24.3). In this way, the concentrations of the blood metabolites were maintained within their normal observed range.

After several runs and validation phases, this principle was considered as valid only for short-term shortage of nutrients in relation to labile reserves. For long-term shortage and reserves of low lability, it was necessary to establish a second principle of HS regulation aimed at correlating the tissue turnover with the nutritive status of the organism. Figure 24.4 summarizes this principle, where *ANAt* and *CATAt* were positively related with the driven variable *x*.

A third principle of homoeostatic regulation has been applied for the con-

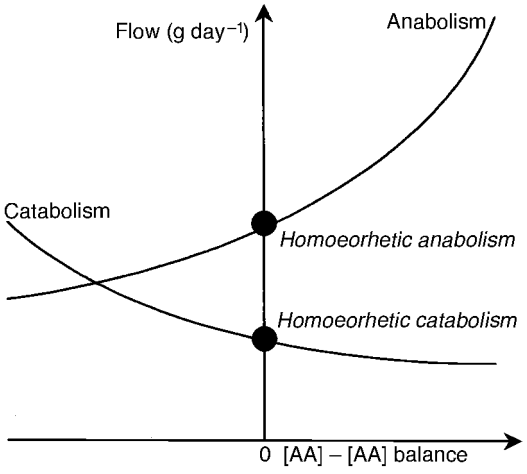

Fig. 24.3. The homoeostatic regulation principle applied to the circulating metabolites (visceral proteins).

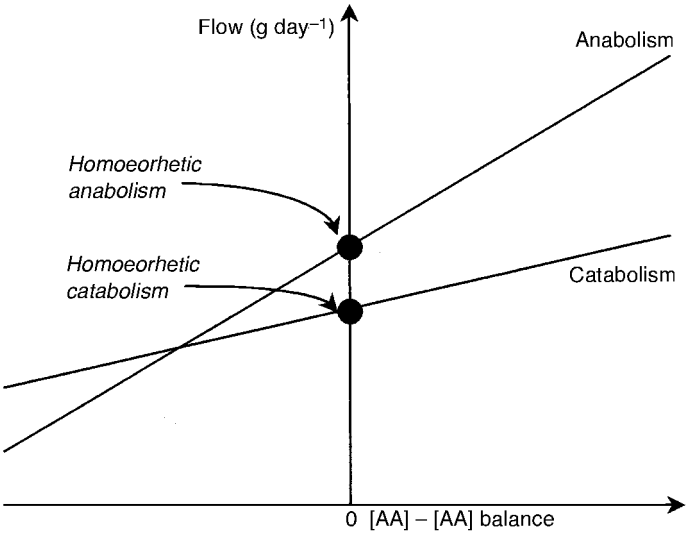

Fig. 24.4. The homoeostasis regulation principle applied to the circulating metabolites (carcass proteins).

trol of the flow of oxidation of free amino acids. It has been supposed that this flow depends, according to the mass-action law, on the concentration of the whole free amino acids pool in the blood. The principle of such a relation has already been observed experimentally, in particular in growing pigs (Sève and

Ballèvre, 1991). It has been assumed that this oxidative process was addressed to the various amino acids on the basis of their relative circulating proportions. In practice, this principle of randomization has not been confirmed. Nitrogen moieties liberated by this process are transformed into urea and excreted in urine. A similar principle of the mass-action law was applied to the oxidation of circulating carbon chains as well.

The relationship between the major 'driving forces' of the metabolic flows

It has been considered that in a growing organism there is potential competition between two major systems of control: those corresponding to homoeorhetic regulation and those generated by the entry of nutrients from the diet and subsequent homoeostatic adaptation. In order to study these two aspects and their interrelations, two models were built:

- The 'homoeorhetic submodel', in which the pilot was constituted by homoeorhetic regulation. This regulation, which expresses the potential growth of the animal, allowed the calculation of the nutritional requirements and the feed supplies to meet them.
- The 'nutrient-driven submodel', where the intake of nutrients was controlled by the farmer. This model allowed the simulation of the alterations of the values of the parameters around the values calculated with the previous model.

Simulations

Simulations were conducted with a time step of 0.001 day, in order to take into account homoeostatic regulation. The period of simulation corresponded to the growing and finishing phases of a pig of 25 kg initial live-weight and during 130 days of measured weights. The integration was performed on the Professional Dynamo Plus software (Pugh-Roberts, 1986), according to Euler's method.

Validation

Two examples of validation are presented. Figures 24.5 and 24.6 indicate the simulated values of body gains of protein and lipid. The model provided the kinetics of tissue growth, which was fairly consistent with the global evolution of these tissues as given from the literature. The large differences which separated the various references are mainly due to the genotypes of the experimental animals.

The model was submitted to variations of the diet lysine contents (0.55 to 2%) during the simulation period. Effects of these variations in lysine supplies

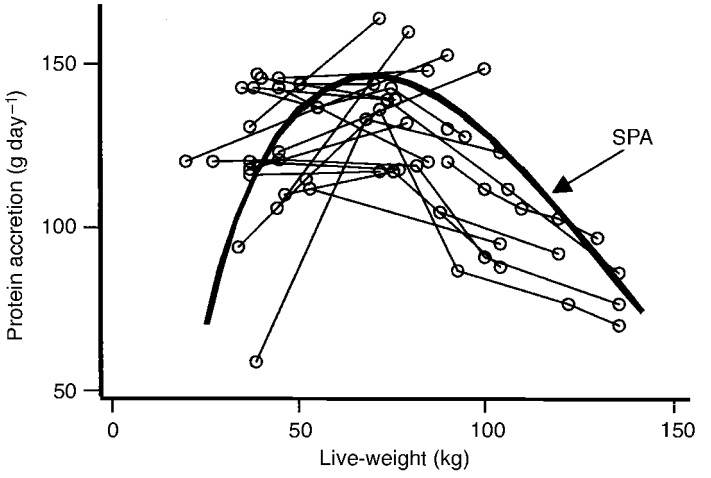

Fig. 24.5. Simulated protein accretion (SPA) on homoeorhesis and observed in literature.

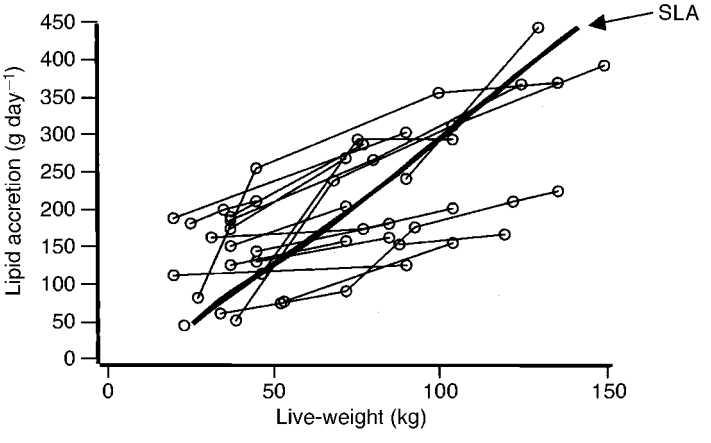

Fig. 24.6. Simulated lipid accretion (SLA) on homoeorhesis and observed in literature.

on protein and lipid accretions have been simulated at 35 and 70 kg of live-weight (LW). The model responses are globally coherent with published values of protein (Fig. 24.7) and lipid deposition (Fig. 24.8). It is interesting to stress the capacity of the model to channel to the lipid tissue the excess of carbon chains coming from the deamination of the relative surplus of amino acids due to the shortage in lysine.

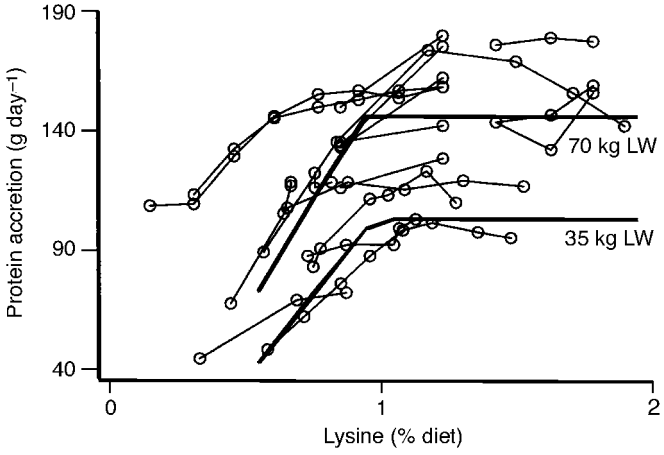

Fig. 24.7. Simulated protein accretion on lysine shortage and observed in literature.

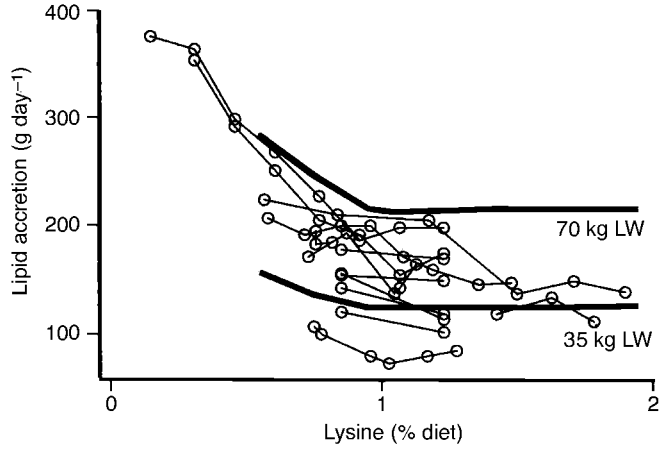

Fig. 24.8. Simulated lipid accretion on lysine shortage and observed in literature.

Discussion and Conclusion

The model presented constitutes a 'minimal model', which only includes the minimum of information necessary to simulate growth and some well-known influences of diet. Despite its simple structure, the model was capable of realistic simulations of the metabolic flows during growth and in a situation of shortage of amino acids. The model should undergo other validations; also it has significant limitations, among which must be stressed:

- its inability to integrate the different existing genotypes by the lack of specific values of parameters of the homoeorhesis system (see above);
- its inability to integrate the energy as a limiting factor in protein deposition;
- its inability to express as such the phenomena of compensatory growth.

References

Baldwin, R.L. and Black, J.L. (1979) *Simulation of the Effects of Nutritional and Physiological Status on the Growth of Mammalian Tissues: Description and Evaluation of a Computer Program*. CSIRO Aust. Anim. Res. Lab. Tech. Paper No. 6, p. 1.

Bastianelli, D. and Sauvant, D. (1997) Modelling the mechanisms of pig growth. *Livestock Production Science* 51, 97–107.

Bauman, D.E. (1999) Endocrine regulation of nutrient partitioning during lactation: homeostasis and homeorhesis revisited. In: *IXth ISRP Symposium, Pretoria* (in press).

Bauman, D.E. and Currie, W.B. (1980) Partitioning of nutrients during pregnancy and lactation: a review of mechanisms involving homeostasis and homeorhesis. *Journal of Dairy Science* 63, 1514–1529.

Danfær, A. (1991) Mathematical modelling of metabolic regulation and growth. *Livestock Production Science* 27, 1–18.

Ferguson, N.S. and Gous, R.M. (1993) Evaluation of pigs genotypes. 1. Theoretical aspects of measuring genetic parameters. *Animal Production* 56, 233–243.

Knap, P.W. and Schrama, J.W. (1996) Simulation of growth in pigs: approximation of protein turnover parameters. *Animal Science* 63, 533–547.

Lovatto, P.A. and Sauvant, D. (1999) Régulation du métabolisme des acides aminés chez le porc en croissance. *Journées de la Recherche Porcine en France* 31, 355–359.

Monod, F. (1970) Le hasard et la necessité, Ed. Le Seuil, Paris.

Noblet, J., Fortune, H., Dubois, S. and Henry, Y. (1989) *Nouvelles bases d'estimation des teneurs en energie digestible, métabolisable et nette des aliments pour le porc*. INRA, L'Hermitage, 106 pp.

Oltjen, J.W., Bywater, A.C., Baldwin, R.L. and Garret, W.N. (1986) Development of a dynamic model of beef cattle growth and composition. *Journal of Animal Science* 62, 86–97.

Pomar, C., Harris, D.L. and Minvielle, F. (1991) Computer simulation model of swine production systems: II. Modeling body composition and weight of female pigs, fetal development, milk production, and growth of suckling pigs. *Journal of Animal Science* 69, 1489.

Pugh-Roberts (1986) *Professional Dynamo Plus. Reference Manual*. Pugh-Roberts Associates, Cambridge, Massachusetts.

Sauvant, D. (1992) La modélisation systémique en nutrition. *Reproduction Nutrition Développement* 32, 217–230.

Sauvant, D. (1994) Modelling homeostatic and homeorhetic regulations in lactating animals. *Livestock Production Science* 39, 105–113.

Sauvant, D. and Phocas, F. (1992) A mechanistic model to simulate the long term regulation of the dairy cow nutrition, *Journal of Dairy Science* 7, 168 (Abstr.).

Sève, B. and Ballèvre, O. (1991) Approches métaboliques du besoin en acides aminés chez le porc en croissance, *Journées de la Recherche Porcine en France* 23, 91–110.

Siebrits, F.K., Kemm, E.H., Ras, M.N. and Barnes, P.M. (1986) Protein deposition in pigs as influenced by sex, type and live mass. 1. The pattern and composition of protein deposition. *South African Journal of Animal Science* 16, 29–37.

Simon, O. (1988) Metabolism of proteins and amino acids. In: Bock, H.D., Eggum, B.O., Low, A.G., Simon, O. and Zebrowska, T. (eds) *Protein Metabolism in Farm Animals*. Oxford University Press, Oxford, UK, 452 pp.

von Berthalanffy, L. (1973) *General System Theory*. New York.

Whittemore, C.T., Tullis, J.B. and Emmans, G.C. (1988) Protein growth in pigs. *Animal Production* 46, 437–445.

25

Model for the Interpretation of Energy Metabolism in Farm Animals

A. Chudy

Forschungsinstitut für die Biologie Landwirtschaftlicher Nutztiere, Dummerstorf, Forschungsbereich Ernährungspysiologie 'OSKAR KELLNER', Justus-von-Liebig-Weg 2, D-18059 Rostock, Germany

Abstract

The chapter presents a new model for nutrient-dependent utilization of feed energy and energy metabolism based on the balance of ATP-bound energy (ATP concept). The ATP potential of absorbed feed nutrients is gradually used at different levels of the metabolism, up to the surplus of ATP potential, which can be stored as body fat or protein and/or transferred in secretory products (milk, eggs). Except chemical heat regulation, all metabolic processes consume or produce ATP-bound energy. From this point of view, ATP synthesis is the only one real energy utilization and only the efficiency of ATP synthesis from partially utilized substrates controls energy metabolism (heat production). The balance of ATP-bound energy is the only additive net energy balance, because we can express the feed energy, maintenance requirements and body nutrients (gain, secretions) in an uniform additive scale, the ATP-related energy, which is derived from experimentally estimated or calculated relationships of nutrient utilization by ATP synthesis.

The described principles agree with experimental results, and open up new possibilities for conceptual thinking, for carrying out experiments based on new information and for creation of a new universal system for energetic feed evaluation.

Introduction

In research on energy metabolism, the ongoing approach is the assumption of two separate parts of the metabolism, for maintenance and for production (synthesis). This has introduced such terms as 'utilization for gain' (k_g) or for protein

 Modelling Nutrient Utilization in Farm Animals (eds J.P. McNamara, J. France and D.E. Beever)

(k_p) and fat retention (k_f) above energy equilibrium and 'utilization for maintenance' (k_m) in the range of malnutrition (Fig. 25.1). One of the most used models is expressed in the following equation:

$$\text{Metabolizable energy (ME) [kJ]} = k_p\,[\text{kJ kJ}^{-1}] \times \text{protein retention [kJ]} + k_f\,[\text{kJ kJ}^{-1}] \times \text{fat retention [kJ]} + a_m\,[\text{kJ (kg}^x)^{-1}] \times \text{LW (kg)}^x$$

This model is no longer adequate, because the preconditions, such as additivity of all variables, do not allow for interactions between nutrients. Also, this cannot take into account the wide range of rates of metabolism, and it assumes thermoneutrality. In addition, a satisfactory range of variation of fat and protein retention cannot be realized experimentally. Although the intention of this system was to estimate absolute values of utilization of metabolizable energy or net energy, what were in reality measured were a small number of events out of the wide spectrum of interactions between catabolic processes from feed or body nutrients, anabolic processes using substrates directly from feed or from body components and thermodynamic compensation between amount of feed nutrients and tissue priorities for substrate use. This lack of consideration of these interactions especially affects results of difference trails or statistical evaluations of metabolic principles.

Therefore it is necessary to create a new theoretical concept for the interpretation of energy metabolism in animals, so that we are better able to explain any results and to conceive modern and successful designs for effective experiments and research activities. The aim of this chapter is to present a new model

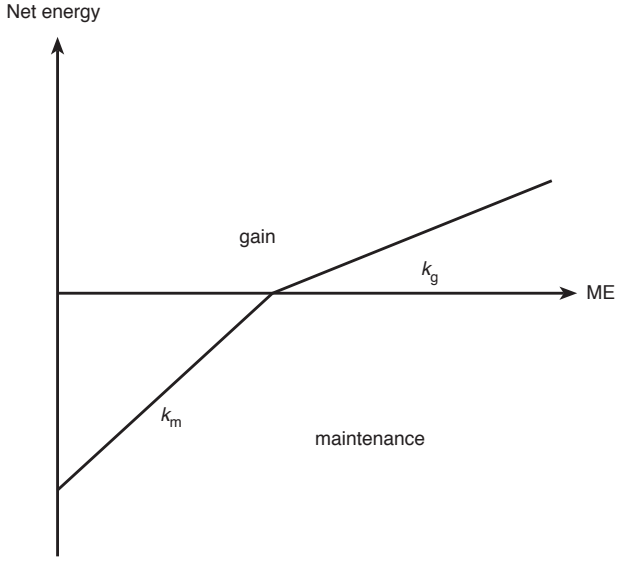

Fig. 25.1. Model of energy utilization.

of nutrient (substrate) utilization of feed energy on the basis of the ATP balance (the ATP concept).

Fundamentals

The ATP concept

The utilization of the realizable energy in feeds and in body nutrients is determined by pathways including turnover of compounds and therefore it depends on the nutrients themselves. The cardinal question is how the model reflects the agreement between feed utilization depending on the nutrient composition of the feed and the animal requirements according to their physiological state. Nutrient and energy metabolism is characterized by energy transfer from feed nutrients to body nutrients. The animal has the ATP potential of the absorbed nutrients for disposition. The use of ATP energy for the different metabolic functions, however, mainly depends on animal factors, especially on the physiological state.

The ATP potential of the feed nutrients is gradually used at different levels of metabolism up to the surplus (excess) of ATP potential, and then the excess is stored as body fat or protein or transferred in secretory products (milk, eggs). All these processes of substrate and energy utilization are therefore linked to ATP synthesis.

The ATP concept can be characterized as follows:

1. All metabolic processes consume or produce ATP-bound energy. The only exception is the regulation of heat related to environmental temperature, which determines the heat requirement (HR).
2. The nutrients synthesized in the body (retained as gain and/or secretion products) are simply the result of a transfer of the ATP potentials of feed nutrients or – by turnover – partly from body nutrients. They represent transfer of energy potentials from one state to another, not energy actually utilized, and therefore these processes are not involved in the real energy metabolism.
3. From this it follows that in the organism only one real energy utilization takes place – the ATP synthesis out of substrates from feed nutrients and body nutrients, subdivided into two parts: breakdown to acetyl-coenzyme A (CoA) first and then the citric acid cycle. Therefore, finally only the efficiency of the ATP synthesis from partially utilized substrates controls energy metabolism, especially heat production, quantitatively and qualitatively.
4. ATP-bound energy is not able to be stored. Therefore the ATP pool is permanently in equilibrium. The actual substrate origin of the ATP pool cannot be determined at the level of the ATP pool.
5. If there is a surplus of ATP-bound energy, the organism is able to store this through transfer of the ATP potentials in body fat or protein retention, as well as secretion of animal products (milk, eggs), or to do physical work.

6. The balance of ATP-bound energy is the only one additive net energy balance in the organism, because we can express the feed energy, requirements and body nutrients in an additive scale, the ATP-related energy, derived from experimental estimated or calculated relations of utilizations of nutrients by ATP synthesis :

> ATP energy (potential) of feed = ATP energy consumption for maintenance function (non-thermal energy requirement) + ATP energy consumption for synthesis of body nutrients − ATP energy synthesis from catabolism of body nutrients (including turnover) + ATP energy consumption for muscular work + ATP energy (potential) retained in gain and/or secretion products (fat and protein)

Consideration of interactions

The model must consider many interactions and priorities, which have an influence on the energy and substrate metabolism of the animals.

Heat requirement

The heat requirement is characterized by the equilibrium of the exchange of heat with the environment for maintaining the body temperature. It is defined by the heat production at a given level of feeding. In cases where feed intake is increased, this initiates a compulsory expenditure of heat from the processes of synthesis for energy retention (production). The heat requirement is an important parameter to characterize animals, and not enough attention as been paid to this in research on energy metabolism. The energy (heat) requirement for the maintenance of homoeothermy has the highest priority. If the heat production from maintenance and synthesis processes is not sufficient to cover the heat requirement, the organism catabolizes nutrients only for this aim. This thermoregulatory heat production depends on age and/or environmental temperature (Chudy, 1997). Below this feed level, the effects of compensation occur between the heat from chemical regulation and heat from the processes of synthesis. This influences the partial energy utilization for productive performance up to 100% measured above maintenance (Zhang and Coon, 1997). In this range of energy metabolism, additivity on the basis of net energy cannot be expected between maintenance and production.

The experimentally determined heat requirement (HR) can be expressed by equations with body weight (metabolic size (kg LW^x)), environmental temperature and other parameters as dependent variables. Such an example is the following relationship for pigs, kept at 18°C environmental temperature, derived from our respiration experiments (Jentsch *et al.*, 1983):

$$HR\ [MJ\ day^{-1}] = 0.00003\ x^3 + 0.0071\ x^2 - 0.4004\ x + 16.908$$
$$R^2 = 0.9786;\ x = LW\ [kg]\ (range > 30\ to \leqslant 125\ kg)$$

This relationship characterizes the minimum of heat production. Therefore, in this model it is first necessary to prove whether this essential condition is fulfilled. If not, the heat production must be increased up to heat requirement, regardless of whether the released energy from ATP is to be useful.

For energy metabolism investigations, the range above the 'heat requirement', the thermoneutral zone, is of more interest. Below thermoneutral conditions, the energy metabolism can be subdivided into the reactions for covering the non-thermal maintenance requirement, for synthesis and 'turnover' of body nutrients and secretions and for muscular work. But, in reality, a separate energy metabolism for maintenance is non-existent. The gain or secretion of body nutrients is the overall positive difference between synthesis and breakdown processes. All these metabolic processes need ATP-bound energy and are equivalent to the ATP potential of the feed and/or metabolized body nutrients. The heat production is quite a lot higher than necessary for maintaining the body temperature and the heat surplus must be totally dissipated into the environment. The energy metabolism is mainly determined through the ATP-bound energy requirement. Consequently, for modelling energy metabolism, only the energy metabolism in the state of thermoneutrality is of interest.

Priorities in the intermediate metabolism

We know two ways of synthesis: the direct incorporation of fatty acids (FA) and amino acids (AA) by fat and protein synthesis, respectively, and the fat synthesis substantially via the C_2 step, acetyl-CoA, from all nutrients, as well as the synthesis of non-essential amino acids.

We could verify in experiments:

- that by overnutrition (feed level > 1) carbohydrates (glucose) will be catabolized with priority to ATP synthesis, which means supplying energy for maintenance and synthesis processes, and feed fat will be mainly incorporated into body fat directly (Chudy, 1967; Chudy and Schiemann, 1969a, b);
- that in growing animals protein synthesis (direct incorporation of amino acids) has a higher priority than breakdown of protein for energy supply in energy deficiency. In order to maintain protein synthesis, the body fat is broken down to supply energy (Hoffmann *et al.*, 1991; Hoffmann and Klein, 1993);
- that in the range of overnutrition essential and non-essential amino acids will be incorporated directly into body protein, but fatty acids will not be resynthesized via acetyl-CoA and mainly incorporated into body fat directly and through turnover, causing ATP consumption.

The efficiency of energy utilization (ATP consumption) depends on the synthesis of body substance by direct incorporation of fatty and amino acids in body fat and body protein, as well as from the amount of 'turnover reactions'. Measurements of the utilization of energy are, to a large extent, influenced by feed fat, as well as by the supply of substrates for protein synthesis, depending on the quantity and quality of protein (amino acids).

Model of Energy Metabolism

In the mathematical formulation of energy metabolism on the basis of the ATP concept, the main problem is to quantify the ATP-bound energy, which cannot be measured absolutely. Accordingly, we can only work with relative sizes, derived from the differences in efficiency of the substrates by ATP synthesis.

The following sizes are relevant in the model.

Measurable absolute parameters

Absorbed energy (AE) = a_1[MJ g^{-1}] S_i [g]

i.e. gross energy of the absorbed substrates (S_i) in the metabolic pool.

Energy retention (ER) = a_1[MJ g^{-1}] S_i [g]

where S_i = body protein (amino acids) and body fat (fatty acids and glycerine).

Fat retention (FER) = a_{1i}[MJ g^{-1}] S_i [g]

where S_i = body fat (fatty acids (FA_i) and glycerine (GL)).

Protein retention (PER) = a_{1i}[MJ g^{-1}] S_i [g]

where S_i = body protein (amino acids (AA_i)).

Urine energy (UE) = a_1[MJ g^{-1}] S_i [g]

i.e. energy contents of the urine (S_i).

Urine N (UN) = N [g day^{-1}]

i.e. N excretion in urine.

Heat production (HP) = AE − ER − UE

Energy metabolism

INCORPORATION

Amino acids = a_{1i}[MJ g^{-1}] × AA_i [g] × k_3 {mol ATP AA_i [MJ AE]$^{-1}$}

Fatty acids = a_{1i}[MJ g^{-1}] × FA_i [g] × k_3 {mol ATP FA_i [MJ AE]$^{-1}$}

Glycerine = a_{1i}[MJ g^{-1}] × GL_i [g] × k_3 {mol ATP GL [MJ AE]$^{-1}$}

FAT SYNTHESIS OUT OF ACETYL-CoA

Fatty acids = S_i [mol_3 ATP MJ AE^{-1}] + k_4 {mol ATP FA_i [MJ AE]$^{-1}$}

Glycerine = S_i [mol_3 ATP MJ AE^{-1}] + k_5 {mol ATP GL [MJ AE]$^{-1}$}

AMINO ACID SYNTHESIS

$$\text{Non-essential AA} = S_i\,[\text{mol}_4\ \text{ATP MJ AE}^{-1}] + k_6\ \{\text{mol ATP AA}_i\,[\text{MJ AE}]^{-1}\}$$

For application in research and practice, because the ATP yield cannot be measured directly, the only possibility is to quantify the efficiency of energy utilization between the nutrients and individual substrates for ATP synthesis. Such experimental estimations must be carried out below maintenance under thermoneutral conditions and by elimination of gluconeogenesis.

Relative (indirectly measurable) parameters

Relation of utilization, related to glucose, by:

$$\text{ATP synthesis } (k_i) = k_i = S_i\,[\text{mol ATP MJ AE}^{-1}] \times (S_{\text{Glucose}}[\text{mol ATP MJ AE}^{-1}])^{-1}\ (= 13.5)$$

$$\text{to acetyl-CoA } (k_{1i}) = k_{1i} = S_i\,[\text{mol}_1\ \text{ATP MJ AE}^{-1}] \times (S_{\text{Glucose}}[\text{mol ATP MJ AE}^{-1}])^{-1}\ (= 13.5)$$

$$\text{from acetyl-CoA } (k_{2i}) = k_{2i} = S_i\,[\text{mol}_2\ \text{ATP MJ AE}^{-1}] \times (S_{\text{Glucose}}[\text{mol ATP MJ AE}^{-1}])^{-1}\ (= 13.5)$$

where $k_i = k_{1i} + k_{2i}$. See Table 25.1, relative per MJ, last column.

As a premise, a coupling yield of 3 mol ATP $NADH^{-1}$ is assumed generally in order to eliminate double representations and calculations in this model. Since only the relations between the nutrients (substrates) are of interest, it is unimportant whether we use a yield of 2 or 3 mol ATP $NADH^{-1}$. That applies so long as any one nutrient- and/or substrate-specific differentiation is not accepted.

The model of energy metabolism (see Fig. 25.2) generalizes and quantifies the following knowledge in bioenergetics. The starting-point is the currently available metabolism pool of free substrates (*Si*) (nutrients). This pool is supplied from:

- the absorption of feed nutrients, the digestion splitting products of the food components, in particular amino acids, fatty acids, glycerine and carbohydrates (monosaccharides) and volatile fatty acids;
- the 'turnover' (amino acids, fatty acids, glycerine);
- mobilized body nutrients (amino acids, fatty acids, glycerine) if energy and specific substrate are in deficit.

In this connection mobilized body protein (AA) and fat (FA and glycerine) – compared to feed nutrients – are measured as digestible (protein) or metabolizable energy (fat), respectively. The real energy is the gross energy of substrates at the beginning of utilization processes. Whereas in the metabolism at cell level, the origin of the substrates cannot be differentiated, as explained earlier, the substrates are intended for individual purposes and therefore equally predestined for the specific metabolic pathways.

Table 25.1. ATP potentials of the elemental nutrients by oxidative breakdown (according to Bergner, 1996).

	Content			ATP to C_2 step		ATP total			Relative		
Nutrient	g mol^{-1}	kJ mol^{-1}	kJ g^{-1}	mol	%	mol	mol g^{-1}	mol MJ^{-1}	mol^{-1}	g^{-1}	MJ^{-1}
Glucose	180	2,820	15.7	14	36.8	38.0	0.21	13.5	100	100	100
Volatile fatty acids											
Acetate	60	876	14.6	−2	−20.0	10.0	0.17	11.4	26.3	79	85
Propionate	74	1,537	20.8	6	33.3	18.0	0.24	11.7	47.4	115	87
Butyrate	88	2,197	25.0	4	14.3	28.0	0.32	12.7	73.7	151	95
Isobutyrate	102	2,195	21.5	15	55.6	27.0	0.26	12.3	71.1	125	91
Valerate	102	2,838	27.8	11	31.4	35.0	0.34	12.3	92.1	163	92
Isovalerate	102	2,838	27.8	−1	−2.9	35.0	0.34	12.3	92.1	163	92
Lactate	74	1,373	18.6	6	33.3	18.0	0.24	13.1	47.4	115	97
Alcohol	46	1,367	29.7	4	25.0	16.0	0.35	11.7	42.1	165	87
Formiate	46		0.0	0	0.0	0.0	0.00		0.0	0	
Fat											
Glycerine	92	1,662	18.1	10	45.5	22.0	0.24	13.2	57.9	113	98
Fatty acids (FS), even number											
Caproate	116	3,497	30.1	8	18.2	44.0	0.38	12.6	115.8	180	93
Caprylate	144		0.0	13	21.3	61.0	0.42		160.5	201	0
Caprinate	172	6,091	35.4	18	23.1	78.0	0.45	12.8	205.3	215	95
Laurate	200	7,392	37.0	23	24.2	95.0	0.48	12.9	250.0	225	95
Myristate	228	8,694	38.1	28	25.0	112.0	0.49	12.9	294.7	233	96
Palmitate	256	9,970	38.9	33	25.6	129.0	0.50	12.9	339.5	239	96
Stearate	284	11,300	39.8	38	26.0	146.0	0.51	12.9	384.2	244	96
Arachidate	312	12,657	40.6	43	26.4	163.0	0.52	12.9	428.9	247	96

Fatty acids (FS), odd number											
Propionate	74	1,537	20.8	6	33.3	18.0	0.24	11.7	47.4	115	87
Valerate	102	2,838	−27.8	11	31.4	35.0	0.34	12.3	92.1	163	−92
Fatty acids, unsaturated											
Linolic acid	280		0.0	34	23.9	142.0	0.51		373.7	240	0
Protein (AA)											
Glycine	75	983	13.1	−1.5	−33.3	4.5	0.06	4.6	11.8	28	34
Alanine	89	1,625	18.3	1.5	11.1	13.5	0.15	8.3	35.5	72	62
Serine	104	1,437	13.8	−1.5	−14.3	10.5	0.10	7.3	27.6	48	54
Cystine	89	2,227	25.0	4.5	27.3	16.5	0.19	7.4	43.4	88	55
Proline	115	2,727	23.7	16.5	57.9	28.5	0.25	10.5	75.0	117	78
Hydroxyproline	131	1,979	15.1	4.5	21.4	21.0	0.16	10.6	55.3	76	79
Glutamic acid	117	2,261	19.3	13.5	52.9	25.5	0.22	11.3	67.1	103	84
Glutamine	132	2,924	22.2	13.5	52.9	25.5	0.19	8.7	67.1	92	65
Aspartic acid	132	1,619	12.3	0	0.0	12.0	0.09	7.4	31.6	43	55
Threonine	119	2,100	17.6	5.5	31.4	17.5	0.15	8.3	46.1	70	62
Threonine (aminoacetone)	119	2,100	17.6	7.5	38.5	19.5	0.16	9.3	51.3	78	69
Methionine	117	3,558	30.4	7.5	38.5	19.5	0.17	5.5	51.3	79	41
Valine	117	2,930	25.0	18.5	60.7	30.5	0.26	10.4	80.3	123	77
Leucine	131	3,580	27.3	1.5	4.0	37.5	0.29	10.5	98.7	136	78
Isoleucine	131	3,580	27.3	14.5	37.7	38.5	0.29	10.8	101.3	139	80
Lysine	146	3,682	25.2	7	22.6	31.0	0.21	8.4	81.6	101	62
Arginine	174	3,790	21.8	15	55.6	27.0	0.16	7.1	71.1	74	53
Histine	155	3,317	21.4	10.5	46.7	22.5	0.15	6.8	59.2	69	50
Tryptophan	204	5,565	27.3	6.5	15.3	42.5	0.21	7.6	111.8	99	57
Phenylalanine	165	4,646	28.2	0.5	1.4	36.5	0.22	7.9	96.1	105	58
Tyrosine	180	4,478	24.9	3.5	8.9	39.5	0.2	8.8	103.9	104	65

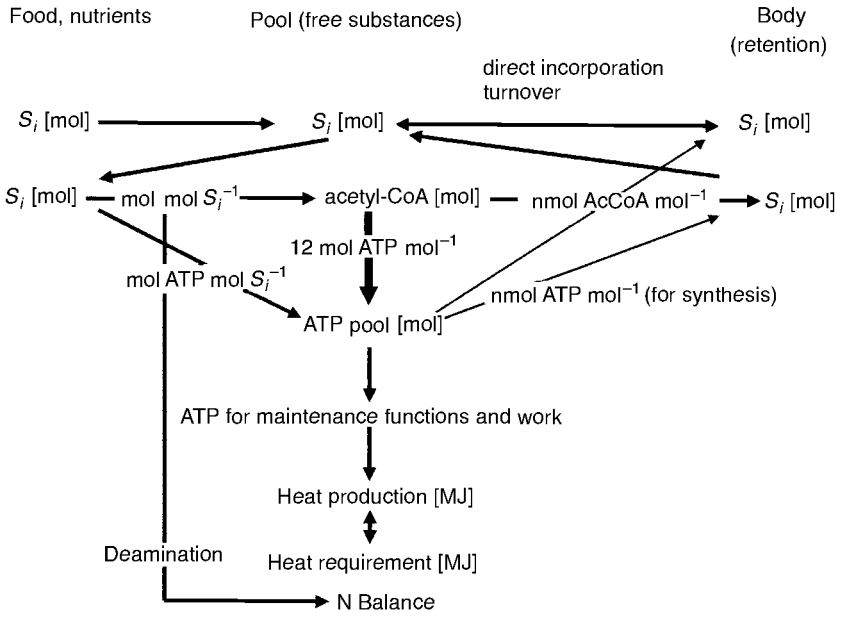

Fig. 25.2. Model of energy metabolism. ACoA, acetyl-CoA.

In the energy metabolism, the nutrients are oxidized to acetyl-CoA. This is the greatest unification of the nutrients in the metabolism after digestion. Acetyl-CoA is the elemental substance for fat synthesis and/or energy production via ATP synthesis in the citric acid cycle. Acetyl-CoA is the key substance and the most important fork in energy metabolism – to release ATP energy or to store ATP potentials. ATP synthesis and fat synthesis are connected to all nutrients through acetyl-CoA. But fat synthesis can take place only when surplus acetyl-CoA is available in the metabolic pool. It can be presupposed that there is a permanently available pool of free acetyl-CoA, regenerated from oxidative processes. Therefore it is necessary in the model to divide the utilization into two types of processes: the processes leading to acetyl-CoA and the processes leading from acetyl-CoA for ATP or fat synthesis. The yield of ATP is shown in Table 25.1 (as the basic data for the model calculations) for oxidation of nutrients to acetyl-CoA and for ATP synthesis in the citric acid cycle.

The ATP output in the first step to acetyl-CoA is higher than assumed and varied among the substrates. This amounts to 36.8% by glucose, varied by volatile fatty acids from −20% (acetate) to 55.6% (isobutyrate), varied for fatty acids up to ~25% and varied by amino acids between −33% (glycine) and 60.7% (valine) of total oxidation ATP output. The special feature is that this ATP output, as well as ATP synthesis and fat synthesis, is cumulative and cannot be differentiated in the ATP pool. This mixing of ATP yield from breakdown of the nutrients for energy delivery and synthesis reactions is effective for the

organism, but complicates the differentiation of the metabolism processes and increases the variation of energy metabolism measurements, depending on endogenous and exogenous factors. The consequence is that one cannot ascertain the variation in energy utilization for nutrient breakdown and fat synthesis from the ATP pool alone. Even including the substrate-specific interactions and different extent of turnover of amino and fatty acids, obtaining an objective measurement of energy utilization may be doubtful. This problem will be eliminated by a well-founded concept for experimental design and a purposeful definition of the experimental conditions, in order to receive effective results in energy metabolism measurements.

The output of the second step (the citric acid cycle) is that every mole of acetyl-CoA represents a potential of 12 mol ATP in the case of coupling of 3 mol ATP $NADH^{-1}$ and/or 9 mol ATP at 2 mol ATP $NADH^{-1}$.

The major differences in energetic efficiency between the individual substrates are presented by the glucose-related ATP potential in the last two columns of Table 25.1. The relations of utilization (per MJ) varied in the case of volatile and long-chain fatty acids between 85% (acetate) and 97% (lactate) and in the case of amino acids between 34% (glycine) and 84% (glutamic acid) in relation to the ATP potential of glucose.

ATP-bound energy cannot be stored; therefore, the synthesis and consumption of ATP must always be held in balance. From the ATP pool is fed first the ATP equivalents for requirements of energy for maintaining the life functions, the potentials and the transport, as well as the requirement for work and other metabolic demands. This ATP requirement is not quantifiably bound to definitive material reactions (synthesis).

The first step for energy gain is direct incorporation of nutrients. Direct incorporation is the preferred metabolic pathway for amino acids for protein synthesis (growth and secretion – milk, egg mass) and for ⩾70% of fatty acids by fat synthesis. These processes occur in both turnover and substance accumulation (retention and/or secretion). In the case of incorporation, the ATP potential, accumulated in the relevant substrate, passes in total directly into the animal product synthesized from it (gain and/or secretion).

Both the incorporation of substrates (AA and FA) used for turnover and the extended synthesis of body protein and fat and the condensation of acetyl-CoA to fatty acids and glycerine, i.e. fat synthesis, require ATP-bound energy from the ATP pool. The incorporation requirement, according to Bergner (1996), by protein synthesis is about 8 mol ATP mol^{-1} peptide bond. The calculated ATP requirement for fat synthesis (according to Bergner, 1996) is performed in Table 25.2 for palmitate and laurate, as well as glycerine, synthesized out of different basic substrates. It resulted on average in 0.45 mol ATP mol^{-1} ATP of the fatty acid and/or valued with 0.2 mol ATP mol^{-1} ATP of glycerine and/or may be assumed with ~0.4 mol ATP mol^{-1} ATP of body fat. However, this ATP consumption may also be viewed as a kind of energy storage, since a major part can be regenerated during the breakdown of the body fat. This requirement of ATP-bound energy for synthesis must be covered by the breakdown of other

Table 25.2. ATP requirement for fat synthesis (according to Bergner, 1996).

Nutrient substrate	Fat synthesis: Product	Fat synthesis: mol substrate	Fat synthesis: mol acetyl-CoA	Fat synthesis: up to acetyl-CoA	ATP consumption (3 mol $NADH^{-1}$): mol ATP mol^{-1} FA	ATP consumption (3 mol $NADH^{-1}$): mol ATP mol^{-1} ATP FA	ATP consumption (3 mol $NADH^{-1}$): mol ATP g^{-1} FA	ATP consumption (3 mol $NADH^{-1}$): mol ATP MJ^{-1} FA	ATP: Accumulation mol ATP mol^{-1} (3 mol $NADH^{-1}$)	ATP: Consumption (total) mol ATP (3 mol $NADH^{-1}$)
Carbohydrates										
Glucose	Palmitate	5	10	70	61	0.47	0.24	6.12	129	181
Glucose	Laurate	4	6	56	43	0.45	0.22	5.82	95	139
Glucose	Glycerine	1		0	8	0.18	0.04	2.41	44	46
Volatile fatty acids										
Acetate	Palmitate	16	16	−32	55	0.43	0.21	5.52	129	247
Acetate	Laurate	12	6	−24	39	0.41	0.20	5.28	95	158
Butyrate	Palmitate	6	12	18	59	0.46	0.23	5.92	129	209
Lactate	Palmitate	8	8	48	56	0.43	0.22	5.62	129	152
Alcohol	Palmitate	8	8	32	56	0.43	0.22	7.58	129	152
Propionate	Glycerine	2	3	12	10	0.23	0.05	3.01	44	54

substrates (e.g. carbohydrates, glucose). Because all synthesis and all vital processes – with the exception of chemical heat regulation – require ATP-bound energy, all energetic conversions only run by means of ATP synthesis.

Accordingly, the energy of substrates is only utilized via ATP synthesis, so that finally only the efficiency of the utilized substrates for ATP synthesis provides the animal organism quantitatively and qualitatively with its energy metabolism, especially heat production. This is determined through the kind and the volume of the individual substrates utilized by ATP synthesis.

Since, in addition, energy retention in body substance and/or for secretions finally represents a transformation and accumulation of ATP potentials, we can express the body nutrients (gain and secretions) in the same ATP energy units as feed nutrients (substrates). Therefore the balance of ATP-bound energy (ATP potentials) is the only real net energy balance, additive over all performances, in the animal organism. The net energy is the substrate's inherent free enthalpy. By accumulation of ATP potentials in body substance (secretions), the proportional part of free enthalpy passes over into the animal body.

Energy metabolism can be simulated as follows, on the basis of the described model ideas.

Basic data are:

- Substrate supply (intake) (carbohydrates, amino acids, fatty acids and glycerine).
- Protein and fat retention (composition of amino and fatty acids), measured or calculated.
- N balance (urine N excretion).
- Heat production (under thermoneutral conditions) or digestible/metabolizable energy intake.

An example is demonstrated in Table 25.3 for the comparison of energy metabolism calculated according to the model or by experimental measured energy metabolism of piglets at 23 kg LW below thermoneutral conditions (32°C).

From the absorbed substrate supply, it is possible to compute, according to Table 25.1, the breakdown to acetyl-CoA and the corresponding ATP yield, as well as the acetyl-CoA pool from before the breakdown. The assumptions are thereby a direct incorporation of amino acids, as far as the requirement of amino acids is covered for protein retention from amino acid intake, an incorporation of approximately 70% of the feed fatty acids and a breakdown of amino acids to acetyl-CoA in accordance with the urine N excretion. Also considered are the priorities in energy metabolism – such as that carbohydrates are the major supplier of ATP synthesis. The expenditure of energy (ATP) for the synthesis of fat and the equal retention of ATP results from calculations, according to Tables 25.1 and 25.2, equivalent to the measured or predicted fat retention.

Since the requirement of ATP-bound energy for maintaining life functions and potentials cannot be registered quantitatively, it may be estimated using the previously mentioned operations. ATP synthesis for these functions increases until the potential amount in the total utilizable substrates reaches the same

Table 25.3. Model of energy utilization (piglet, 23 kg LW).

	Substrate Intake						Body						
Substrate	Contents (g kg^{-1})	substrate (mol kg^{-1})	ATP total (mol)	Enthalpy total (kJ)	Enthalpy* free (kJ)	N (g)	Body-protein (g 16 g N^{-1})	N (g)	Difference: feed-retention	Enthalpy (kJ)	ATP (mol)	Enthalpy* free (kJ)	ATP total (mol)
Casein	**125 g**						**Protein 67 g**						
Glycine	18.4	0.32	0.180	39.320	5.8	0.565	5.8	0.725	-0.028	67.0	0.307	9.879	0.852
Alanine	30.3	0.43	0.726	87.344	23.4	0.747	6.6	0.696	-0.009	101.2	0.841	27.074	1.339
Serine	46.7	0.54	0.709	96.998	22.8	0.939	4.2	0.375	0.035	46.5	0.340	10.936	0.598
Cystine	4.4	0.04	0.083	11.135	2.7	0.075	1.2	0.093	-0.003	17.4	0.129	4.147	0.191
Proline	96.9	1.00	3.563	340.875	114.7	1.748	4.6	0.375	0.093	86.6	0.906	29.158	1.160
Asparagine	70.5	0.61	0.915	123.449	29.5	2.146	10.6	1.495	0.014	100.0	0.741	23.863	1.235
Glutamic acid	214.2	1.66	5.291	469.158	170.4	2.906	15.5	0.989	0.127	182.0	2.053	66.102	2.697
Tyrosine	49.6	0.30	1.481	167.925	47.7	0.533	4.0	0.207	0.021	73.6	0.649	20.912	0.781
Threonine	38.5	0.38	0.926	99.750	29.8	0.667	4.6	0.363	0.017	64.1	0.595	19.160	0.839
Valine	55.7	0.56	2.135	205.100	68.7	0.985	5.5	0.441	0.033	109.1	1.135	36.556	1.433
Leucine	95.6	0.85	3.984	380.375	128.3	1.481	8.8	0.630	0.054	186.8	1.957	63.004	2.374
Isoleucine	49.8	0.44	2.118	196.900	68.2	0.771	5.0	0.358	0.025	106.1	1.141	36.752	1.379
Lysine	74.6	0.58	2.248	266.945	72.4	2.040	8.8	1.131	0.026	169.6	1.428	45.980	1.796
Methionine	26.7	0.20	0.488	88.950	15.7	0.357	2.6	0.164	0.012	47.3	0.259	8.350	0.366
Histine	28.6	0.21	0.591	87.071	19.0	1.096	4.7	0.853	0.003	76.2	0.517	16.653	0.701
Phenylalanine	52.4	0.36	1.643	209.070	52.9	0.624	4.3	0.244	0.025	91.1	0.715	23.034	0.872
Arginine	36.2	0.23	0.776	212.463	25.0	1.624	6.8	1.466	0.000	215.8	0.789	25.391	1.022
Tryptophan	10.7	0.06	0.319	41.738	10.3	0.201	0.9	0.083	0.004	18.0	0.138	4.437	0.164
Protein	999.8		28.173	3124.564	907.175	19.504	104.5	10.689	0.451	1758.5	14.639	471.4	19.800

Fat 30 g						**Fat 21g** (from feed fat)					
Palmitate	890	3.72	14.404	1113.275	463.8		0.033	779.3	10.083	324.677	10.708
Glycerine	110	1.24	0.819	61.861	26.4		0.011	43.3	0.573	18.457	0.677
			15.223	1175.136	490.191		0.045	822.6	10.656	343.134	11.386
Carbohydrates 391 g						**Fat 68 g** (synthesized from acetyl-CoA)					
Glucose	1000	5.56	82.544	6125.667	2657.9	Palmitate	2523.4	32.650	1051.33	48.089	
			82.544	6125.667	2657.931	Glycerine	140.2	1.856	59.766	2.531	
								2663.6	34.506	1111.1	50.620
						Fat 89 g (total)		3486.2	45.163	1454.23	62.006
Total	546		125.94	10425.37	4055.297	19.504	10.689	5244.7	59.802	1925.62	81.806

Balance	Feed	Retention	Maintenance	Related to $kg^{0.75}$
Acetyl-CoA (mol)	6.871	4.221	2.651	0.252
ATP (mol)	125.94	59.80	66.14	6.297
N (g)	19.504	10.689	8.815	0.839
Free enthalpy[1] (kJ)	4,055	1,926	2,130	203
Enthalpy (kJ)	10,425	5,245	5,181	493
Experiment (kJ)	10,428	5,241		494

*32.2 kJ mol^{-1} ATP.

amount of heat production under thermoneutral conditions. The ATP equivalent freed from this metabolism, expressed in mol ATP, corresponds with the 'ATP maintenance requirement', including additional (previously unaccounted for) expenditure of ATP-bound energy for the turnover. This 'ATP requirement' would have to be an approximately constant size under defined conditions, while the appropriate heat production represents a variable size, depending on the efficiency of ATP synthesis of utilized substrates. We can register a good agreement between the experimental measurements (at 32°C of ambient temperature) and the model computation.

Application of Modelling Results

Consequently, the basis for application of this model is the balance of the ATP potentials as the real net energy balance in energy metabolism under thermoneutral conditions. The way to derive the necessary parameters is as follows.

The basic data are measurable in adult animals under conditions of malnutrition and thermoneutrality:

- relations of utilization of ME (ER ME^{-1}) for catabolic processes between the major nutrients, related to carbohydrates (= 100), as:

$$\text{protein} : \text{fat} : \text{fibre} : \text{sugar} : \text{starch} = k_1 : k_2 : k_3 : k_4\ (=100) : k_5\ (=100)$$

and

- the contents of metabolizable energy (ME) of the adequate digestible nutrients [kJ ME g^{-1}],

$$\text{ME [MJ]} = me_1 dcp + me_2 dcf + me_3 dst + me_4 dsu + me_5 dfi$$

The nominal value for the ATP potential can be calculated if one multiplies the relation factor as relative energy efficiency with the ME contents of the digestible nutrients:

$$\text{Nominal ATP potential (nATP-p): } a_i = k_i \times me_i\ 100^{-1}$$

$$\text{Nominal ATP potential of feed} = a_1 dcp + a_2 dcf + a_3 dst + a_4 dsu + a_5 dfi$$

$$\text{Nominal ATP potential of body nutrients (retention)} = (a_1 bp + a_2 bf)$$

$$\text{Nominal ATP potential of feed} = \text{nATP-p maintenance} + \text{nATP-p for work} + \text{nATP-p-synthesis} + \text{nATP-p retention}$$

or in total:

$$\text{Nominal ATP potential for metabolic processes} = \text{nATP-p feed} - \text{nATP-p retention}$$

where *d* = digestible, *cp* = crude protein, *cf* = crude fat, *st* = starch, *su* = sugar, *fi* = fibre (rest), *b* = body.

The gross energy of the substrates, which is used for ATP synthesis to cover

energy expenditure for maintenance, work and the synthesis of body nutrients, minus the energy of the accumulated body nutrients (retention) and energy of urine excretion leaves the heat production (HP), according to the usual formula:

HP[MJ ME] = absorbed energy of feed nutrients (substrate) (AE) − energy retention and/or secretion (body nutrients) (ER) − urine energy (UE)

On the basis of the 'nominal ATP potential' as the universal scale for the energy value, it is possible to create a new system of uniform energetic feed evaluation for all kinds of animals and directions of production (Chudy, 1998).

Conclusions

Modelling by means of the above model of energy metabolism opens new possibilities for the development of concepts and for carrying out experiments with new knowledge and with simultaneous clarification of energy research. The ATP concept serves as a basis for conceptual thinking and can give a new upswing to energy research. The energetic processes are quantified in total quite well on the basis of the ATP concept, in accordance with current biochemical knowledge, and the dynamics of nutrient and energy metabolism of monogastric animals can be modelled explicitly. The fundamentals described open up new possibilities to create a new universal system of energetic feed evaluation.

References

Bergner, H. (1996) In: Bergner, H. and Hoffmann, L. (eds) *Bioenergetik und Stoffproduktion landwirtschaftlicher Nutztiere*, Vols 1–3. Harwood Academic Publishers, Amsterdam, pp. 1–318.

Chudy, A. (1967) Zur energetischen Verwertung der Nähr- und Futterstoffe für Erhaltung und Fettbildung. Modellversuche an Ratten. Dissertation, Akademie Landwirtschaftswissenschaften Berlin. 166 pp.

Chudy, A. (1997) Dependence of heat production on feed level and ambient temperature in heifers in the range of malnutrition. In: McCracken, K.J., Unsworth, E.F. and Wylie, A.R.G. (eds) *Energy Metabolism of Farm Animals. Proceedings of the 14th Symposium on Energy Metabolism*. CAB International, Wallingford, pp. 307–310.

Chudy, A. (1998) Energy metabolism and energetic feed evaluation in pigs. In: *Proceeding of International Conference on Pig Production*. International Academic Publishers, Beijing, China, pp. 360–364.

Chudy, A. and Schiemann, R. (1969a) Zur energetischen Verwertung der Nähr- und Futterstoffe für Erhaltung und Fettbildung. *Archiv für Tierernährung. Bd.* 19(4), 231–247.

Chudy, A. and Schiemann, R. (1969b) *Utilization of Dietary Fat for Maintenance and Fat Deposition in Model Studies with Rats*. EAAP Publication No. 12, Oriel Press, Newcastle, pp. 161–168.

Hoffmann, L. and Klein, M. (1993) Energieumsatz von Küken bei niedriger Umgebungstemperatur. *Archiv für Tierernährung, Berlin* 43, 113–146.

Hoffmann, L., Schiemann, R. and Klein, M. (1991) Energieumsatz wachsender Broiler in Abhängigkeit von der Umgebungstemperatur. *Archiv für Tierernährung, Berlin* 41, 167–181.

Jentsch, W., Schiemann, R. and Hoffman, L. (1983) Gemeinschaftsuntersuchungen zur Präzisierung des Energie- und Proteinsbedarfs bei Mastschweinen. 2. Mitteilung: Energie- und Nährstoffumsatz bei Masthybriden im Mastabschnitt von 30–110 kg. *Archiv für Tierernährung, Berlin* 33(7/8), 552–570.

Zhang, B. and Coon, C.N. (1997) Modelling metabolizable energy utilisation in laying hens. In: McCracken, K.J., Unsworth, E.F. and Wylie, A.R.G. (eds) *Energy Metabolism of Farm Animals. Proceedings of the 14th Symposium on Energy Metabolism*. CAB International, Wallingford, pp. 89–92.

26

Linear Models of Nitrogen Utilization in Dairy Cows

E. Kebreab,[1] R. Allison,[2] R. Mansbridge,[2] D.E. Beever[1] and J. France[1]

[1]*Centre for Dairy Research, Department of Agriculture, University of Reading, Earley Gate, PO Box 236, Reading RG6 6AT, UK;* [2]*ADAS Bridgets, Martyr Worthy, Winchester SO21 1AP, UK*

Abstract

Linear models describing relationships between nitrogen (N) intake and N output were constructed based on N-balance data from experiments conducted at the Centre for Dairy Research (CEDAR). The models were then applied to a second set of data derived from a series of N-balance experiments conducted at the Agricultural Development and Advisory Service (ADAS) Bridgets. The CEDAR models described the data from ADAS Bridgets as well as independently fitted models, despite the fact that different diets were given to the cows at the two centres. The variance explained in the ADAS Bridgets data was lower, possibly due to variations in the source and level of energy intake. The variations indicate the possibility of mitigating N losses from dairy cows by diet manipulation. Models currently used in practice underestimate N output for the two data sets and the models described herein may be useful as a basis for better estimation of N excretion. Excretion of N in faeces is preferable, due to its potentially less harmful effect on N pollution to the environment, particularly with regard to volatilization of ammonia and leaching to groundwater reserves, and future models will need to estimate faecal output and the proportion of faecal : urinary N excreted by dairy cows more accurately.

Introduction

There has been an increased use of protein supplements in the UK in order to improve milk production, particularly milk protein content. Increased use of protein supplements is also due to their being a cheaper source of energy than

 Modelling Nutrient Utilization in Farm Animals (eds J.P. McNamara, J. France and D.E. Beever)

traditional energy sources. Although the conversion rate of nitrogen (N) to animal product is often as low as 30–35% (Kirchgessner *et al.*, 1994), marginal milk N responses are still achieved with increase in dietary N above 450 g N day^{-1} (Kebreab *et al.*, 2000). This may be because amino acids are also being used via gluconeogenesis as a source of glucose for the synthesis of extra milk fat and lactose.

Excess N is excreted in faeces and urine, thus contributing to atmospheric and hydrosphere pollution (Kirchgessner *et al.*, 1994). Average annual N excreta are estimated to be about 100 kg cow^{-1} (Smith and Frost, 2000), which, with about 2.5 million dairy cows in the UK (MAFF, 1999), significantly contributes to environmental pollution. Mathematical modelling has been used to predict the amount of N in milk and potential N losses from dairy farms and their contribution to environmental pollution. Estimates of ammonia emissions to the atmosphere are based on linear equations that predict N excretion from average milk yield and crude protein content of the diet (ECETOC, 1994). The objective of this chapter is to evaluate alternative linear models developed at the University of Reading's Centre for Dairy Research (CEDAR), using independent N-balance experiments conducted at the Agricultural Development and Advisory Service (ADAS) Bridgets. These alternative models could ultimately be used to predict N losses from dairy farms in the UK.

Materials and Methods

Five N-balance experiments using Holstein-Friesian dairy cows in early or mid-lactation were conducted at CEDAR from 1995 to 1997. The cows were fed 30 different diet types, consisting of ten grass silages and six concentrates. The silages were made from either directly cut or partially wilted perennial ryegrass (*Lolium perenne*), which received either 75 or 150 kg N ha^{-1}. The concentrates used were formulated to give higher proportions of either degradable fibre, soluble sugars, high (barley) and low (maize) degradable starch and different protein degradabilities. The data from these experiments were collated and linear models developed, using the General Linear Modelling Procedure of Genstat (Genstat 5 Committee, 1994).

At ADAS Bridgets, a series of four N-balance experiments were carried out, using early and mid-lactation Holstein-Friesian dairy cows as part of the Minimum Impact Dairy Systems (MIDaS) study (Peel *et al.*, 1997). Each experiment was based on a Latin square design, with each experimental period being 3 weeks in duration. The first 2 weeks of each period were for diet adaptation and a total collection of faeces and urine was made during the third week. Diets were formulated using various strategies to improve the capture of dietary N in milk in order to reduce N losses to the environment. These included reducing N supply, changing the type of rumen-N supplied, investigating the amount and balance of rumen-degradable protein and fermentable energy and formulating

rations using the Cornell Net Carbohydrate and Protein System (CNCPS) (Fox *et al.*, 1992).

Results

Over the range of 280–640 g N intake day^{-1}, there was a strong linear relationship between N intake (NI) and N in excreta ($N_{excreta}$) for the experiments conducted at CEDAR:

$$N_{excreta} = 30 + 0.62\ NI \quad (R^2 = 0.78) \tag{1}$$

A similar but weaker linear relationship was established for data collected at ADAS Bridgets. By setting the value of N excretion at zero intake, as in the above equation, to aid comparison (which did not significantly affect the residual sum of squares compared with the 'best-fit' equation), the following equation was obtained for ADAS Bridgets data:

$$N_{excreta} = 30 + 0.63\ NI \quad (R^2 = 0.42) \tag{2}$$

Thus equation 1 predicts N in excreta for the ADAS experiments as well as equation 2 (Fig. 26.1).

Similarly, the effect of N intake on milk output was analysed and linear models from the two sets of data were compared (Fig. 26.2). Based on the CEDAR data, N in milk (N_{milk}) was linearly related to N intake (equation 3). Data

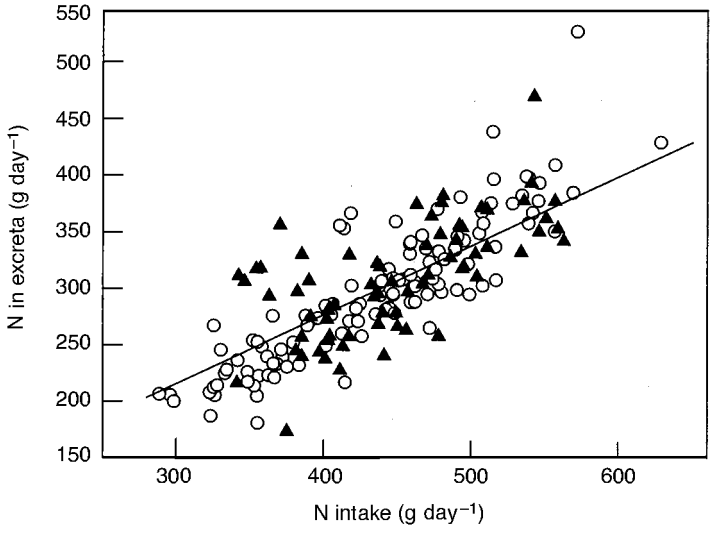

Fig. 26.1. Effect of N intake on the N excreted in faeces and urine for cows from CEDAR (○) and ADAS Bridgets (▲). The fitted line is given by equation 1.

from ADAS Bridgets gave a similar linear relationship between milk N and N intake (equation 4).

$$N_{milk} = 38.2 + 0.19\ NI \quad (R^2 = 0.3) \tag{3}$$

$$N_{milk} = 38.2 + 0.20\ NI \quad (R^2 = 0.3) \tag{4}$$

Discussion

It is surprising that empirical equations derived from CEDAR data are so applicable to ADAS Bridgets data. However, this work is consistent with observed trends in N excretion and N utilization for milk production in intensive dairy farming systems in the UK. From equations 1 and 2, about 62–63% (plus 30 g) of N fed to dairy cows in UK is excreted in faeces or urine, thus contributing directly to N pollution of the environment. This study predicts that only 19–20% of N in the diet is incorporated as milk N. The small gains from increasing N intake beyond 450 g day^{-1} in terms of milk production are offset by more than threefold waste of N in faeces and urine. Furthermore, Lockyer and Whitehead (1990) estimated ammonia volatilization from urinary N to be at least five to six times higher than from faecal N and, at intakes of 570 g N day^{-1}, 90% of intake would be excreted in a urine : faeces ratio of 4 : 1 (Scholefield *et al.*, 1991). Management practices and selecting appropriate types of protein and

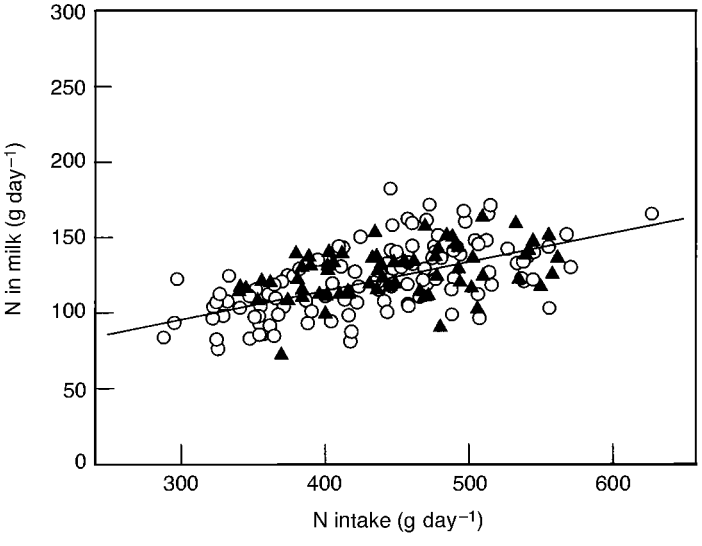

Fig. 26.2. Effect of N intake on milk N for cows from CEDAR (○) and ADAS Bridgets (▲). The fitted line is given by equation 3.

energy sources might improve N retention and utilization. The variability in the data, especially from ADAS Bridgets, suggests that N utilization under different treatments might have been affected by feed sources as well as N intake levels.

The currently used method of estimation of N loss from dairy farms is based on the crude protein content of the diet and average milk yield (ECETOC, 1994). However, comparison of the estimates with the extrapolation of N output from the above experiments shows that the method underestimates the annual N loss from dairy farms, at least in the UK. Although the linear equations reported here cannot be used directly for estimating annual N excretion, they highlight the extent of the problem and new models are required to predict N excretion and ammonia emission more accurately.

Acknowledgement

MAFF Environmental Protection Division is thanked for funding this work.

References

European Centre for Ecotoxicology & Toxicology of Chemicals (ECETOC) (1994) *Ammonia Emissions to Air in Western Europe*. Technical Report No. 62, ECETOC, Brussels, 196 pp.

Fox, D.G., Sniffen, C.J., O'Connor, J.D., Russell, J.B. and Van Soest, P.J. (1992) A net carbohydrate and protein system for evaluating cattle diets: III Cattle requirements and diet adequacy. *Journal of Animal Science* 70, 3578–3596.

Genstat 5 Committee (1994) *Genstat 5 Release 3 Reference Manual*. Clarendon Press, Oxford.

Jentsch, W., Schiemann, R. and Hoffman, L. (1983) Gemeinschaftsuntersuchungen zur Präzisierung des Energie- und Proteinsbedarfs bei Mastschweinen. 2. Mitteilung: Energie- und Nahrstoffumsatz bei Masthybriden im Mastabschnitt von 30–110 kg. *Archiv für Tierernährung, Berlin* 33(7/8), 552–570.

Kebreab, E., Castillo, A.R., Beever, D.E., Humphries, D. and France, J. (2000) The effects of management practices prior to and during ensiling and concentrate type on nitrogen utilisation and pollution in lactating dairy cows. *Journal of Dairy Science* 83, 1274–1285.

Kirchgessner, M., Windisch, W. and Roth, F.X. (1994) The efficiency of nitrogen conversion in animal nutrition. *Nova Acta Leopoldina* 70, 393–412.

Lockyer, D.R. and Whitehead, D.C. (1990) Volatilization of ammonia from cattle urine applied to grassland. *Soil Biology and Biochemistry* 22, 1137–1142.

MAFF (1999) *Agricultural and Horticultural Census: 1 June 1988*. Government Statistical Service, York, UK.

Peel, S., Chambers, B.J., Harrison, R. and Jarvis, S.C. (1997) Reducing nitrogen emissions from complete dairy farm systems. In: Jarvis, S.C and Pain, B.F. (eds) *Gaseous Nitrogen Emissions from Grasslands*. CAB International, Wallingford, pp. 383–390.

Scholefield, D., Lockyer, D.R., Whitehead, D.C. and Tyson, K.C. (1991) A model to predicted transformations and losses of nitrogen in UK pastures grazed by beef cattle. *Plant and Soil* 132, 165–177.

Smith, K.A. and Frost, J.P. (2000) Nitrogen excretion by farm livestock with respect to land spreading requirements and controlling nitrogen losses to ground and surface waters. Part I: cattle and sheep. *Bioresource Technology* 71, 173–181.

27

Isotope Dilution Models for Partitioning Amino Acid Uptake by the Liver, Mammary Gland and Hindlimb Tissues of Ruminants

L.A. Crompton,[1] J. France,[1] B.J. Bequette,[2] J.A. Maas,[1] M.D. Hanigan,[3] M.A. Lomax[4] and J. Dijkstra[5]

[1]*Department of Agriculture, University of Reading, Earley Gate, PO Box 236, Reading RG6 6AT, UK;* [2]*Rowett Research Institute, Greenburn Road, Bucksburn, Aberdeen AB21 9SB, UK;* [3]*Purina Mills Inc., St Louis, MO 63144, USA;* [4]*Department of Agriculture, University of Aberdeen, 581 King Street, Aberdeen AB24 5UA, UK;* [5]*Animal Nutrition Group, Wageningen Institute of Animal Science (WIAS), Wageningen University, Marijkeweg 40, 6709 PG Wageningen, The Netherlands*

Abstract

Isotope dilution models for partitioning leucine uptake by the liver and mammary gland, and tyrosine uptake by the hindlimb of ruminants have been constructed and solved in the steady state. The models require the measurement of plasma flow rate through the tissue beds in combination with leucine/tyrosine, α-ketoisocaproate and carbon dioxide concentrations and plateau isotope enrichments/specific radioactivity (SRA) in the arterial and venous pools from each tissue and plateau leucine/tyrosine enrichment/SRA in the tissue intracellular free pool or its assumed proxy during a constant infusion of tracer leucine/tyrosine. If assumptions are made, model solutions permit the calculation of steady state flux rates for leucine/tyrosine influx, efflux, oxidation and transamination, and leucine/tyrosine fluxes representing the synthesis and degradation of constitutive and export proteins. Using model solutions and appropriate literature values for organ protein mass and leucine/tyrosine content of the tissue, total (constitutive and export) protein fractional synthetic rates can be estimated for all three tissues. The models can be applied to other amino acids with similar metabolic fates within the tissues. Linking the models consecutively will

 Modelling Nutrient Utilization in Farm Animals (eds J.P. McNamara, J. France and D.E. Beever)

allow quantitative description of interorgan amino acid metabolism and may indicate aspects of regulation that could be manipulated to direct more amino acid towards the productive tissue.

Introduction

The ability to predict accurately dietary nitrogen utilization for production in the ruminant depends on a clear understanding of amino acid metabolism from the gut to productive tissues such as the mammary gland and muscle. Present on-farm support systems are not satisfactory, because they comprise a blackbox approach to interorgan amino acid metabolism and so have no basis for response-type predictions. We have been developing steady-state kinetic models of amino acid metabolism across the liver, mammary gland and hindlimb, which we hope will improve the prediction of nutrient supply to and utilization by ruminants for growth and lactation.

Steady-state isotope dilution kinetics has been used to construct and solve mathematical models for partitioning leucine (LEU) uptake by the liver (France *et al.*, 1999) and mammary gland (France *et al.*, 1995) and tyrosine (TYR) uptake by the hindlimb (Crompton *et al.*, 1999). These models allow the estimation of LEU/TYR influxes and effluxes from the organs/tissues and also enable the simultaneous estimation of tissue protein synthesis and degradation. The models have been used to resolve *in vivo* isotopic data and to estimate fractional synthesis rates (FSRs) for total protein (constitutive and export) in all three tissues. In addition, for hindlimb tissues, the FSR estimates are assumed to represent muscle, but have always included an unquantified contribution from non-muscular tissues. We also report the application of the hindlimb model to assess the contribution of non-muscle tissues to hindlimb tissue protein metabolism.

The Models

Three isotope dilution models, describing the partition of LEU uptake by the liver and mammary gland of dairy cows and TYR uptake by the hindlimb of sheep, have been constructed and solved in the steady state. The schemes adopted for each tissue are shown in Fig. 27.1. For all the schemes, the boxes represent extracellular and intracellular pools, while the fluxes between pools and into and out of the system are shown by arrowed lines. The liver model (Fig. 27.1a) contains three intracellular and six extracellular pools. The intracellular pools represent α-ketoisocaproate (KIC), free LEU and LEU in export protein (pools 5, 6 and 7, respectively) while the extracellular ones represent portal vein, hepatic artery and hepatic vein KIC and LEU (pools 1–4, 8 and 9). The mammary model (Fig. 27.1b) contains two intracellular pools representing free LEU and

LEU in milk protein (pools 2 and 3, respectively) and two extracellular pools representing arterial and venous LEU (pools 1 and 4). The hindlimb model (Fig. 27.1c) contains one intracellular pool representing free TYR (pool 2) and two extracellular pools representing the arterial and venous TYR pools supplying and draining the tissue bed (pools 1 and 3, respectively). All three schemes assume that the only entry of label into the systems is via the input fluxes to the extracellular pools and that, for the duration of the infusion, the enrichment of constitutive protein can be regarded as negligible. Within each scheme, conservation-of-mass principles were applied to each pool to generate two sets of ordinary differential equations (one set for total LEU/TYR and one set for labelled LEU/TYR), which describe the dynamic behaviour of the system. Algebraic manipulation of the equations enables the models to be solved for the unknown steady-state fluxes.

The inputs required for model solution are blood flow rate across the tissue, LEU/TYR, KIC and carbon dioxide concentrations and plateau isotope enrichments/specific radioactivity (SRA) in the arterial and venous pools from each tissue and plateau LEU/TYR enrichment/SRA in the tissue intracellular free pool or its assumed proxy. Using these data and a limited number of assumptions, the models can be solved to calculate the steady-state flux rates for LEU/TYR influx, efflux, oxidation and transamination, and LEU/TYR fluxes representing the synthesis and degradation of constitutive and export proteins. Using the model solutions and appropriate literature values for organ protein mass and LEU/TYR content of the tissue, total (constitutive and export) protein FSRs can be estimated for all three tissues.

Application

Application of the models is illustrated using data from experiments conducted in our laboratories. The *in vivo* liver and mammary gland studies were conducted in multicatheterized Holstein-Friesian dairy cows (six liver, three mammary gland) during weeks 20–30 of lactation. Average cow data were: body weight 620 kg; dry-matter intake (DMI) 16 kg day^{-1} (60:40 concentrate:grass silage, 135 g crude protein kg^{-1} dry matter (DM)); milk yield 23 kg day^{-1}. On sample days, the animals were given a constant jugular vein infusion of [1-^{13}C]LEU (700 mg h^{-1}) for 8 h. Blood samples were taken simultaneously from the catheters in the dorsal aorta and the portal and hepatic veins for liver studies and from catheters in the intercostal artery and subcutaneous abdominal vein for mammary gland studies. All simultaneous samples were taken hourly during the last 4 h of the isotope infusion for the measurement of blood flow rate (by dye dilution, *p*-aminohippuric acid) and LEU metabolism by the portal-drained viscera and liver and the mammary gland.

The hindlimb model was used to resolve *in vivo* radioisotope data obtained from experiments with multicatheterized lambs during a constant jugular vein infusion of [2,3-^{3}H]TYR (74 kBq min^{-1}) tracer for 6 h. Blood samples were

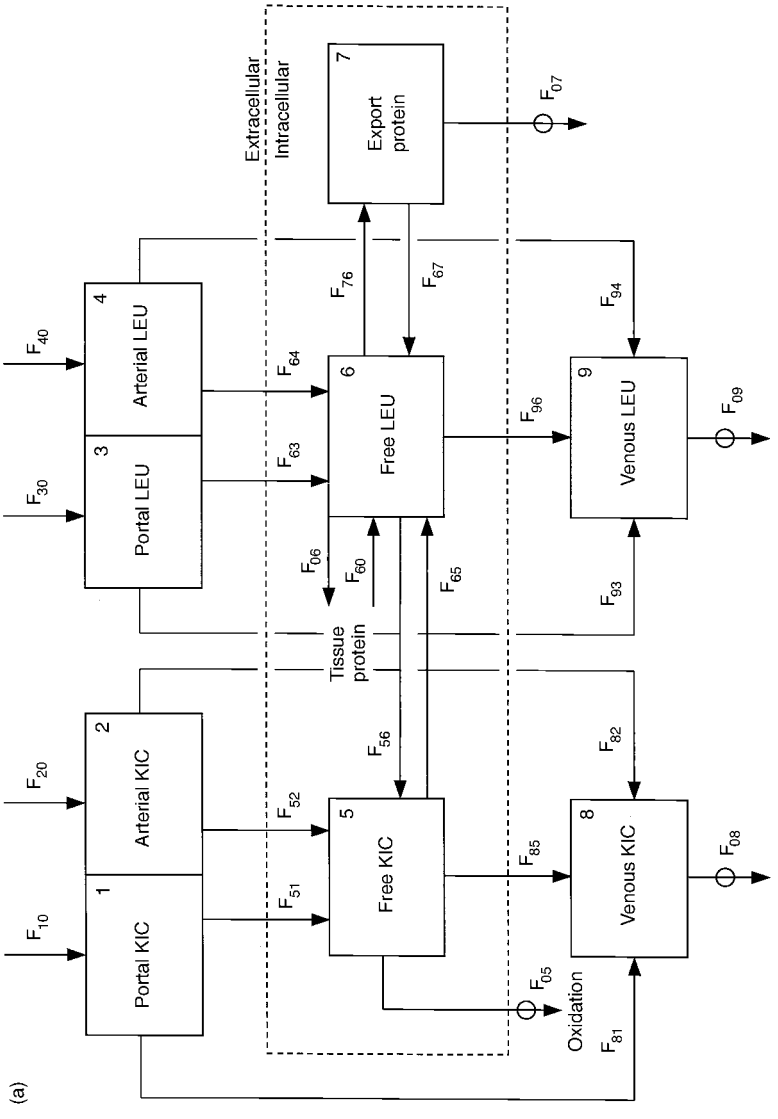
(a)
Extracellular
Intracellular
1
Portal KIC
2
Arterial KIC
3
Portal LEU
4
Arterial LEU
5
Free KIC
6
Free LEU
7
Export protein
8
Venous KIC
9
Venous LEU
Tissue protein
Oxidation
F10
F20
F30
F40
F51
F52
F63
F64
F56
F65
F76
F67
F07
F85
F82
F08
F05
F81
F60
F06
F96
F94
F09
F93

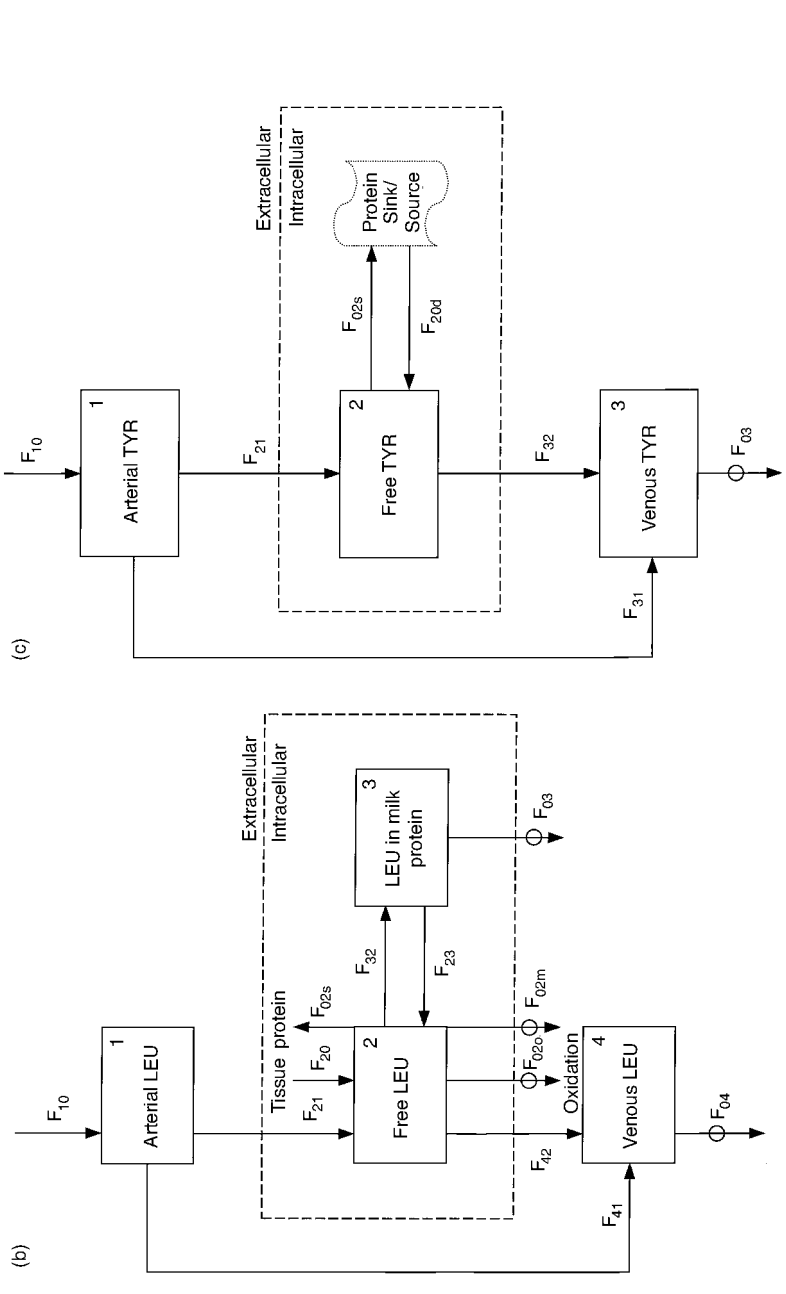

Fig. 27.1. Schemes for the uptake and partition of amino acids across ruminant tissues. The small circles indicate fluxes that need to be measured experimentally. (a) Liver – leucine. (b) Mammary gland – leucine. (c) Hindlimb – tyrosine.

taken simultaneously from catheters in the carotid artery and deep femoral vein (inserted via the recurrent tarsal vein) every 30 min during the last 2 h of the isotope infusion for the measurement of TYR metabolism across the hindlimb tissues. Blood flow rate across the hindlimb was measured using the diffusion equilibrium technique (see Crompton and Lomax, 1993). TYR kinetics was measured across the hindlimb of nine lambs (30 kg) fed a range of DMI, from 118–1555 g day^{-1}, as described previously (Crompton and Lomax, 1993).

The estimates of tissue protein synthesis in the liver, mammary gland and hindlimb calculated from model solutions for these experiments are shown in Table 27.1.

For the liver, the constitutive protein synthesis rate is always much larger than the export protein synthesis rate, the contribution of the latter ranging between 9 and 21% of the total rate of protein synthesis (see Table 22.1). FSR for the liver protein was, on average, 43.4% day^{-1}, but varied widely (23–55% day^{-1}). This is consistent with liver protein FSRs reported for other ruminants. However, in contrast to the liver, export protein synthesis from the mammary gland, namely milk protein, accounted for between 60 and 88% of total protein synthesis (see Table 27.1). Total protein FSRs for the mammary gland averaged 44.5% day^{-1} for the three animals, but had a reduced spread compared with that for the liver, only varying between 39 and 53% day^{-1}, again consistent with previous reports in ruminant tissue. The solutions from the hindlimb model demonstrated that the flux of TYR into constitutive protein accounted for, on average, only 0.724 of the TYR influx into the hindlimb, mean (SEM) values were 1.40 (0.15) and 2.02 (0.27) nmol min^{-1} g^{-1}, respectively. The average calculated FSR for hindlimb tissue was 6.1% day^{-1}, which is higher than previous reports for muscle protein synthesis in lambs.

As anticipated, the calculated rates of constitutive protein synthesis, and consequently the FSR of tissue protein for all three tissues studied, were sensitive to changes in the intracellular free LEU/TYR enrichment/SRA, the assumed precursor pool.

Table 27.1. Constitutive and export protein synthesis rates and FSRs for tissue protein in the liver, mammary gland and hindlimb of ruminants (mean values with the number of observations in parentheses).

	Liver (4)	Mammary gland (3)	Hindlimb (9)
Protein synthesis (g day^{-1})			
Constitutive	807	296	
Export	116	856	
Export (% of total)	12.6	74.3	
Protein FSR (% day^{-1})	43.4	44.5	6.1

Discussion

The present models have refined the calculation of liver and mammary gland protein synthesis into constitutive tissue and export protein, but, as with any continuous-infusion approach to measuring protein synthesis, the models all require an accurate estimate of the enrichment/SRA of the tracer amino acid in the precursor pool. All three models have assumed a single homogeneous pool from which all proteins are synthesized. For the liver and mammary gland, this is probably an oversimplification, which has consequences for the estimation of protein synthesis. There is limited evidence to suggest that proteins destined for export are probably synthesized on the rough endoplasmic reticulum (ER) and preferentially utilize amino acids as they enter the cell (Fern and Garlick, 1976; Connell *et al.*, 1997). As the ER is associated with extracellular components of the cell, the isotopic activity of free amino acids in this part of the cell will be closer to that of blood. In contrast, constitutive proteins are synthesized on polysomes within the cell cytosol, and the precursor pool would include intracellular free amino acids or perhaps preferential use of amino acids released from protein degradation (e.g. Smith and Sun, 1995). The concept of cellular compartmentalization may need to be incorporated into compartmental models of protein turnover in the future.

The reason for the high FSRs of hindlimb tissue relative to previous reports for muscle tissue is the heterogeneity of hindlimb tissues: that is, although muscle is the predominant tissue present in the hindlimb, the preparation also contains skin and bone, which have a much higher rate of protein turnover relative to that in muscle and thus contribute a disproportionately large amount towards the FSRs for hindlimb tissue. Comparison of hindlimb FSRs with FSRs measured simultaneously directly in muscle showed that the contribution of protein synthetic rates in non-muscular tissues to hindlimb tissue synthetic rates was 0.445 (0.053). FSRs for hindlimb and muscle were both significantly correlated with DMI. There was no significant difference between the slopes of these lines ($P = 0.779$), but there was a significant difference between the intercepts of 2.59% day^{-1} ($P = 0.022$). These results indicate that the 44% contribution from non-muscular tissues accounts for a significant proportion of hindlimb tissue protein synthesis, but that this proportion appears constant over a range of feed intakes.

Despite some limitations, the models described are useful tools for partitioning the uptake of amino acids by the ruminant liver, mammary gland and hindlimb. The level of representation adopted means that all three models could be applied to other amino acids with similar metabolic fates within the liver, mammary gland and hindlimb. Linking the models consecutively will allow quantitative description of interorgan amino acid metabolism and may indicate aspects of regulation that could be manipulated to direct more amino acid towards the productive tissue. If the models are to be rigorously applied, future *in vivo* studies must measure directly the intracellular free amino acid

enrichment/SRA, in conjunction with the measurements of blood enrichments and flow rates.

Acknowledgement

This work was funded by a consortium of the Ministry of Agriculture, Fisheries and Food (MAFF), Biotechnology and Biological Sciences Research Council (BBSRC), Milk Development Council, Purina Mills Inc. and Nutreco.

References

Connell, A., Calder, A.G., Anderson, S.E. and Lobley, G.E. (1997) Hepatic protein synthesis in the sheep: effect of intake as monitored by use of stable-isotope-labelled glycine, leucine and phenylalanine. *British Journal of Nutrition* 77, 255–271.

Crompton, L.A. and Lomax, M.A. (1993) Hindlimb protein turnover and muscle protein synthesis in lambs: a comparison of techniques. *British Journal of Nutrition* 69, 345–358.

Crompton, L.A., France, J. and Lomax, M.A. (1999) An isotope dilution model for partitioning tyrosine uptake by the hindlimb tissues of lambs. In: Lobley, G.E., White, A. and MacRae, J.C. (eds) *Protein Metabolism and Nutrition: Book of abstracts of the VIIIth International Symposium on Protein Metabolism and Nutrition*. Wageningen Pers, Wageningen, The Netherlands, p. 5.

Fern, G.D. and Garlick, P.J. (1976) Compartmentation of albumin and ferritin synthesis in rat liver *in vivo*. *Biochemical Journal* 156, 189–192.

France, J., Bequette, B.J., Lobley, G.E., Metcalf, J.A., Wray-Cahen, D., Dhanoa, M.S., Backwell, F.R.C., Hanigan, M.D., MacRae, J.C. and Beever, D.E. (1995) An isotope dilution model for partitioning leucine uptake by the bovine mammary gland. *Journal of Theoretical Biology* 172, 369–377.

France, J., Hanigan, M.D., Reynolds, C.K., Dijkstra, J., Crompton, L.A., Maas, J.A., Bequette, B.J., Metcalf, J.A., Lobley, G.E., MacRae, J.C. and Beever, D.E. (1999) An isotope dilution model for partitioning leucine uptake by the liver of the lactating dairy cow. *Journal of Theoretical Biology* 198, 121–133.

Smith, C.B. and Sun, Y. (1995) Influence of valine flooding on channelling of valine into tissue pools and on protein synthesis. *American Journal of Physiology* 268, E735–E744.

28

The Conversion of a Scientific Model Describing Dairy Cow Nutrition and Production to an Industry Tool: the CPM Dairy Project

R.C. Boston,[1] D.G. Fox,[2] C. Sniffen,[3] E. Janczewski,[1] R. Munson[1] and W. Chalupa[1]

[1]*Department of Clinical Studies, NBC, School of Veterinary Medicine, University of Pennsylvania, PA 19348, USA;* [2]*Department of Animal Science, Cornell University, Ithaca, NY 14853, USA;* [3]*W.H. Miner Agricultural Research Institute, Chazy, NY 12921, USA*

Abstract

This chapter describes our efforts to convert a large dairy cow nutrition model suite into a commercial product. The scientific model chosen as the basis for the product was the Cornell Net Carbohydrate and Protein System (CNCPS) and the product deriving from this effort was the Cornell Pennsylvania Miner Dairy (CPM-Dairy) Program.

Introduction

At the fourth meeting of the International Workshop for Modeling Nutrient Use in Farm Animals, we (Boston *et al.*, 1994) presented a paper on model testing and evaluation and there we exposed aspects of the effort needed to commercialize scientific models. Specifically, it was pointed out that the same systematic approach to the development, verification and validation of computer software should be applied to computer-based mathematical models, as they seek broad-based field application.

 Modelling Nutrient Utilization in Farm Animals (eds J.P. McNamara, J. France and D.E. Beever)

There was considerable debate at this meeting regarding the appropriateness of this use of scientific models. One perspective taken was that models serve to test hypotheses and that once the testing is complete the models have 'served their purpose'. Indeed, using them beyond this point was viewed as inappropriate. Another perspective was that models which are, by scientific measures, successful add knowledge to their application domain and that it is quite inappropriate to deny their incorporation into a predictive or evaluative setting associated with their base domain.

We believe that scientific models do have a place in the commercial environment and in this chapter we should like to describe aspects of our efforts to convert a large scientific model suite into a commercial product. The scientific model we chose as the basis for our product was the Cornell Net Carbohydrate and Protein System (CNCPS), and the product deriving from this effort was the Cornell Pennsylvania Miner Dairy (CPM-Dairy) program.

Methods

A model basis for CPM-Dairy (the evaluator)

The objectives in developing the CPM-Dairy software included the provision of a stable, efficient and economic software system for the accurate formulation of dairy cow rations. This imposed the condition that the product should be available for a fairly basic computer hardware configuration, and should require no additional software or operating system features. Furthermore, it meant that the software should be based on a current, industry-accepted and peer-reviewed ration analysis model and that its operation should be efficient in regard to field-based decision needs. Finally, it implied that its operational integrity should not be susceptible to user intervention, i.e. the integrity of the model should be protected within the CPM-Dairy environment.

Operationally it was envisaged that the user would specify: (i) the production unit (the animal); (ii) the environment (e.g. temperature, humidity, wind speed, hair depth, mud presence and night cooling); (iii) the production goals; (iv) the list of feeds and mixes from which a ration could be comprised; and finally (v) the feed ingredient levels (the ration), and then the software would provide the user with an array of 'indices' concerning the adequacy of the ration. The 'indices' would include accounts concerning the nutritional needs of the animal being met in regard to its welfare and the production goals.

Over and above the obvious needs of dry matter, energy, protein, etc., we were also anxious to explore the incorporation of amino acid balance and amino acid ratios, as these have been shown to have an impact on milk production and composition (Schwab *et al.*, 1992; Rulquin *et al.*, 1993).

Only one model in use at the time of the CPM-Dairy conception seemed to meet all our criteria and that was the CNCPS, developed by Sniffen, Fox, Van Soest and Russell (Fox *et al.*, 1992; Russell *et al.*, 1992; Sniffen *et al.*, 1992;

VandeHar *et al.*, 1992). This was a spreadsheet model, which used the following:

1. A dairy cattle feed characterization scheme, described by Van Soest *et al.* (1991), and Sniffen *et al.* (1992).
2. A model of rumen fermentation and bacterial growth in the dairy cow, described by Russell *et al.* (1992).
3. An account of nutritional yields from dairy cattle feeds, described by Sniffen *et al.* (1992).
4. A set of equations describing the nutritional requirement of dairy cattle under various conditions, assembled by Fox *et al.* (1992).

Figure 28.1 illustrates the functional basis for the CNCPS model. We see that this delivers the operational and functional needs of the CPM-Dairy software.

Since the strengths and weaknesses of CNCPS are also conferred on CPM-Dairy, it is appropriate to recall the abiding principles underpinning the development of (successive versions of) the CNCPS evaluator:

- Accepted scientific foundations provide the basis for each subsystem incorporated.
- All nutrients and nutrient flows are balanced.
- Processes are portrayed to the resolution of 24 h, i.e. rate processes are daily average effects.
- Response submodels based on field research are incorporated into CNCPS to describe processes such as growth and dry-matter intake.

The target setting for CPM-Dairy

We mentioned above that key non-functional criteria (Pressman, 1987) for CPM-Dairy were as follows:

- It would be efficient from the field deployment perspective.
- Its operational integrity could be assured (i.e. not susceptible to corruption by the user).
- It would require no additional software or operating systems tools for its operation.
- It would execute on a fairly basic computer configuration.
- Its operation would be self-explanatory.

With these concepts at the heart of our implementation plan, the natural setting for the product at the time of its inception was the '16-bit' Microsoft C Programming Environment. To see why this was the case we review the requirements.

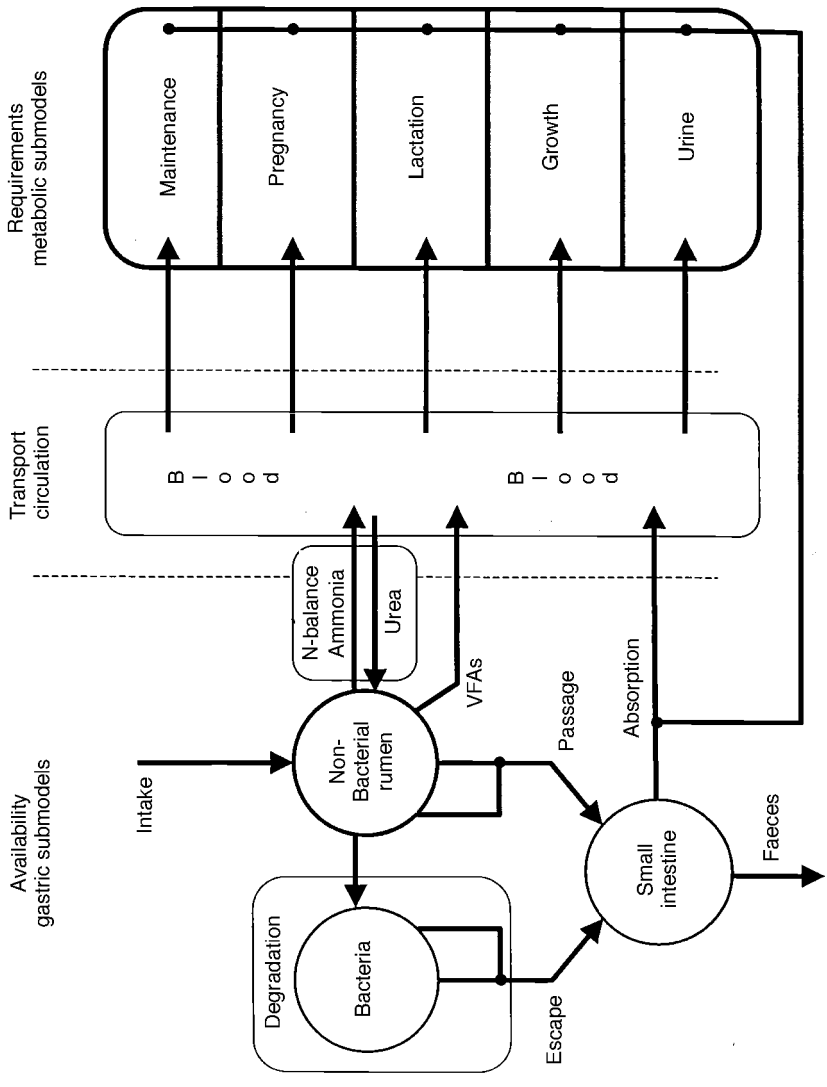

Fig. 28.1. A functional overview of the CNCPS evaluator. Lines with arrows indicate feed or nutrient flows. Lines terminating with 'bullets' indicate pool-regulated nutrient flows. VFAs, volatile fatty acids.

Field-efficient

Here we mean that any processing by CPM-Dairy relating to ration analysis should take no longer than an expert dairy nutritionist him/herself would take, and hopefully considerably less time. Although somewhat nebulous in this sense, we agreed that this would imply that seconds, as opposed to minutes, were allowed in CPM-Dairy's processing steps. Accordingly, to expedite processing, all coding was implemented, as efficiently as possible, in the C programming language. The 16-bit compiler was used, as that was the only robust C compiler at the time. Furthermore, the Microsoft C compiler incorporated the essential graphical interface generation facilities (window management and dialogue box control, for example) that our design required.

Operational integrity and software independence

Early versions of CNCPS, including one developed by the group from the University of Pennsylvania, were coded as spreadsheet systems, using either Lotus 123 or Quattro Pro. The reasons for this were obvious; it required no programming skill to code the system, and it was very easy to change the code if needed. Unfortunately, this led to an array of serious problems for the product. Its execution was slow, its code was susceptible to non-structured and unverifiable developments (by anyone who wanted to recode aspects of the system) and its functionality could not be extended using third-party modules. Furthermore, to some degree, the product was not independent of its environment.

It is clear that offering an unmaintainable product, such as a spreadsheet system, would have presented us with a formidable user support burden.

Minimal hardware needs

Recognizing that our target community (see below) for the CPM-Dairy software would vary greatly in regard to their sophistication with digital technologies and their uptake of these, we decided that our first release of CPM-Dairy should run on the most basic of computer hardware. This meant that videographics array (VGA) screens, 16-bit processing environments and possibly out-of-date dynamic linking libraries (dlls) would be amongst the mix of computing environments we would need to negotiate. Accordingly, our programming environment needed to be set as 'low' as possible, so as not to presume more advanced features than we could anticipate, and this again pointed to the 16-bit Microsoft C compiler.

Self-explanatory operation

It was our belief that the most successful of the new graphical user interface (GUI)-driven software evolving under Windows (predominantly Windows 95 at this point) was that which required little, or no, documentation to get started

and to maintain operation flow. Indeed, 'intuitive' software such as this rarely used more than electronic, context-sensitive help to assist the user in the situation where guidance was needed. Accordingly, we designed our system such that all windows were clearly set out, were descriptively titled, incorporated 'tip' bars prompting the user in regard to data entry items, and data entry units, and supported context-sensitive and general help in a consistent fashion.

Software design

Our design plan for CPM-Dairy included provision for the following:

- A feed dictionary.
- An automatic balancing system.
- A production unit specification facility.
- A feed management facility.
- A report generator.
- A ration evaluator.
- A file management facility.
- An integrated help system.

Architecturally, these facilities were envisioned as shown in Fig. 28.2.

The feed dictionary

Sniffen *et al.* (1992) have described how nutritional data relating to feeds can be measured, and they have even given comprehensive accounts of how that information could be stored on a computer (for feed evaluation) and how the feed nutrients could be mathematically manipulated to enable the assessment of feeds for various functions critical to the nutrition of the dairy cow. Indeed, the CNCPS was largely based on the ideas presented by Sniffen *et al.* (1992). CPM-Dairy was designed to follow essentially the same pattern. In this regard, feeds are characterized in the feed dictionary in terms of the following properties: dry matter, energy properties (neutral detergent fibre (NDF), effective NDF, starch, fat, lignin and soluble fibre net energy), protein properties (crude protein (CP), soluble protein, non-protein nitrogen, acid detergent fibre insoluble protein, neutral detergent fibre insoluble protein and undegradable protein), ash, amino acids, minerals, vitamins and fractional digestion rates. Net energy and undegraded protein are only used in the modified National Research Council (MNRC) optimizer of CPM-Dairy.

To ease the use of the feed dictionary, as well as to streamline the execution of CPM-Dairy, the dictionary of feeds was in fact broken down into seven subdictionaries, namely, forage, protein, energy, minerals/vitamins, commercial and two reference (forage and grain) subdictionaries. The organization of the information in each of the subdictionaries followed a similar format.

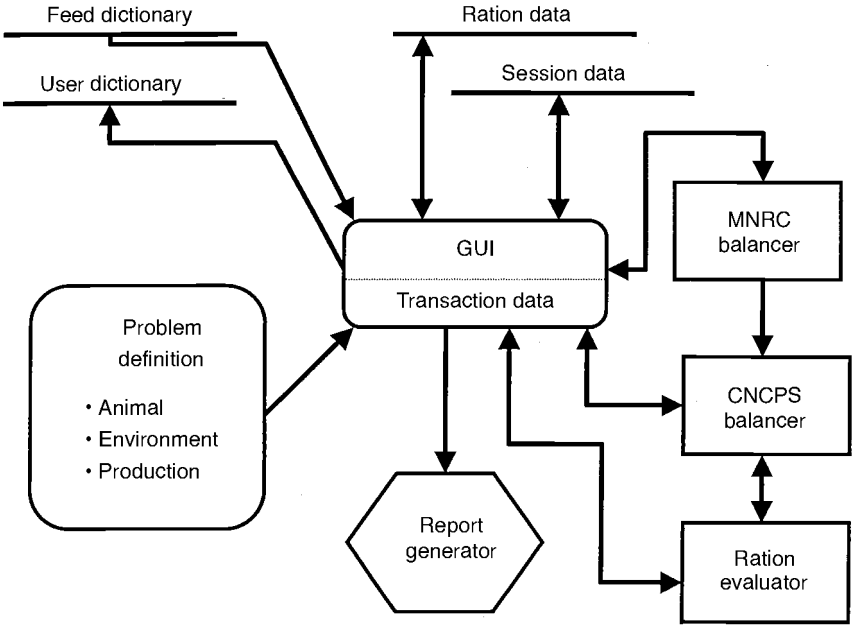

Fig. 28.2. An architectural overview of CPM-Dairy. Regular boxes represent processing modules, rounded boxes represent data display and data collection modules and the hexagon represents a data output module. Horizontal lines represent data stores, and the arrow lines represent data exchange. MNRC, modified National Research Council.

The feed evaluator

At the heart of the CPM-Dairy is the CNCPS (Fox *et al.*, 1992; Russell *et al.*, 1992; Sniffen *et al.*, 1992; VandeHar *et al.*, 1992). Called our evaluator, each time any aspect of a feed or any aspect of the animal or production goals are changed, the evaluator can be enlisted to assess the nutritional consequences of the change.

Our plan for CPM-Dairy was to always be employing the most recently field-tested and validated version of the CNCPS as the CPM-Dairy evaluator. The Cornell group (under Fox's leadership) would prototypically implement new scientific information with an impact on dairy cow production into CNCPS and, when the new adjustments had been validated in the field, the new code would be sent to the Pennsylvania group for implementation in CPM-Dairy. By this means, CPM-Dairy's evaluator is kept current and scientifically sound.

We designed the screen displays for results from the evaluator run to expose either National Research Council (NRC)-like information or more comprehensive ration analysis results. The NRC-like display (called the MNRC display, for modified NRC, uses slightly different approaches from that of NRC) includes dry

matter, energy and protein balance information, whereas the more detailed display (CNCPS) included metabolizable energy (ME) and metabolizable protein (MP) balances, as well as detailed information on peptides, ammonia and three essential amino acids (methionine, lysine and isoleucine).

Automatic balancing

The popularity of the Spartan system demonstrated the degree to which users appreciated the inclusion of autobalancing facilities within ration management software. Autobalancing here means the least-cost assemblage of a feed mix which as near as possible meets the nutritional needs of the dairy cow. For rations based on NRC (1989), such a task falls under the class of linear programming problems, since the objective is linear, the requirements are static and the nutritional yield of the feeds is linear. Indeed, we can express this problem as follows:

Find x_j, the amount of feed item j, such that:

$$\sum_j c_j x_j$$

is a minimum and:

$$r_{li} < \sum_j w_{ij}\, x_j < r_{mi} \qquad i = 1 \text{ to number of constraints}$$

where c_j is the unit cost of feed j, w_{ij} is the unit yield of feed j to meet nutritional constraint i, r_{li} is a lower limit of requirement of nutrient i and r_{mi} is an upper limit or requirement of nutrient i. MNRC constraints included dry matter, net energy of lactation, absorbed protein, soluble protein, non-structural carbohydrate (NSC), NDF and fat.

We planned the implementation of the MNRC optimizer (O'Connor *et al.*, 1993) in CPM-Dairy for two reasons: (i) to enable CPM-Dairy users familiar with NRC to have some point of reference in regard to rations that were produced from CPM-Dairy using the more sophisticated evaluator; and (ii) to facilitate the first step for a non-linear optimizer.

The CNCPS evaluator is inherently non-linear in regard to the way digesta flow affects nutrient yield from the feed fractions. This is because the feeds have an impact on their own passage and hence their degradative yield. Non-linearity is not a problem regarding requirements, since the feed amounts do not have a direct impact on requirements. Indeed, the requirements are only evaluated once per 'production analysis' and this determination sets values like r_{li} and r_{mi} above. The objective of a CNCPS ration optimizer would still be least cost, and hence this adds no further complexity to the problem.

The optimization scheme we used was developed by the Systems Programming Group at the University of Maryland (Zhou and Tits, 1997) and employed a forward sequential quadratic programming approach.

Unfortunately, some of the yield equations used in CNCPS depend on discontinuous functions. The science within CNCPS emanated from different research centres where non-overlapping experimental boundaries meant that gaps existed in the knowledge. To deal with this problem, we developed two approaches: replacing the piecewise segments of two models with smooth nonlinear functions (where adjoining models had sensible intersections), and building transition functions to smoothly fill gaps between published models (Fig. 28.3).

Animal input and production goals specification

Animal requirements are in part determined by the animal demographics, namely, age, weight, breed, parity and stage of lactation. The other part to this 'equation' relates to the animal's environment and the target product (milk volume, milk protein and milk fat). To ease entry of this 'problem definition' information, we proposed assembling the salient pop-out dialogue boxes under a common-definition menu item in the menu bar. Of particular note is that we have incorporated a modified (Van Amburgh *et al.*, 1998) version of the NRC (1996) beef cattle requirements growth model to facilitate more accurate calculation of the nutritional burden of growth in the dairy cow.

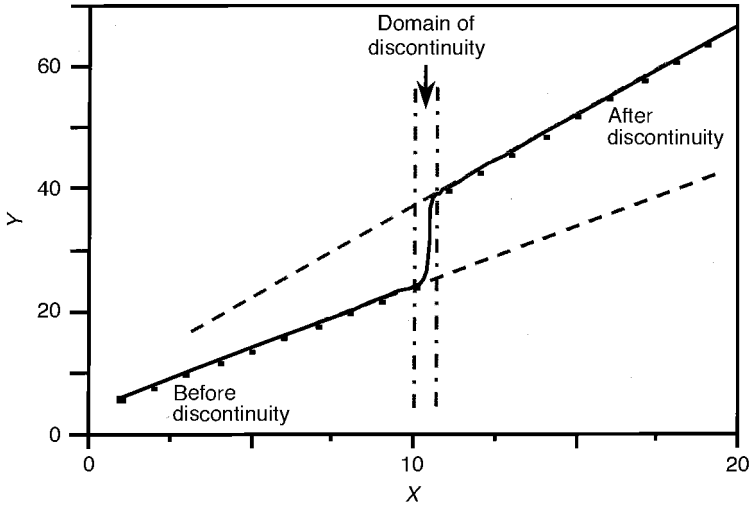

Fig. 28.3. Demonstration of the application of transition functions to bridge two discontinuous models. Here the model prior to the discontinuity has the form $2x + 4$ (where x denotes a feed activity level, and '$2x + 4$' is a model of the nutrient yield from that feed, for example) and the model after the discontinuity has the form $3x + 7$. The discontinuity exists in the activity range $10 < x < 11$. The transition function bridging the two models has the logistic form.

File management facility

To integrate activities in an episode of use of CPM-Dairy, we conceived of the notion of a session. Specifically, a session embodied all the information elicited from the user and contributed from CPM-Dairy to ensure that the user could return to the session at a later time without any loss of integrity. Components of a session included animal, environment, farm unit, production goals, optimization information and feed data. It was planned that, at any time during an episode of CPM-Dairy use, the user would be able to save this session data securely in a file for subsequent retrieval.

As well as session files, CPM-Dairy supported feedbank files and ration files.

Report generator

We have mentioned that critical information derived in conjunction with an activation of CPM-Dairy's evaluator is visible in the evaluator's dialogue box. This dialogue box is also referred to as the 'ration dialogue box' and it contains the salient guides to the user regarding nutrient surpluses and deficits deriving from the ration.

Beyond this, almost all the ration analyses from the evaluator are accessible to the user in an array of carefully assembled reports. Here, under the 'display' menu command, 11 topical reports are available to provide a comprehensive account of ration-related information.

Feed management facilities

In a fashion similar to the Quattro Pro version of CNCPS and similar also to Spartan, CPM-Dairy has an extended array of feed management tools as follows:

- Feed items explicitly specified and saved.
- Feed dictionaries compiled by the user and saved.
- Rations created and saved.
- Mixes created from ration ingredients, and from other feeds, on a proportional basis and then manipulated as a single entity in regard to ration allocation.

Testing and evaluating CPM-Dairy

In conjunction with routine white box and alpha testing, respectively undertaken by the programming team and the expert users at the development centre, we also utilized black box and beta testing to further validate the product. Skilled dairy cow nutritionists from industry and education were sent prerelease (beta) copies of CPM-Dairy and asked to fill in a survey regarding their reactions to various features of the product.

Additionally, and in conjunction with black box testing, we have compiled both rations and production information for around 500 dairy cow studies published over the last 30 years, and we propose examining the predictive power of CPM-Dairy against the reported values.

Results

The CPM-Dairy system

The release version of CPM-Dairy (CPM-Dairy 1.0) is a menu-driven, partially moded system (i.e. one that has some commitment to strictly sequenced processing) which encapsulates data collection and displays results in a set of efficiently organized dialogue boxes.

A menu bar provides access to the services and, when any of these services are activated, a dialogue box is displayed, from which the user can peruse results or make changes, as needed. An important dialogue box is the evaluator (or ration) dialogue box. This is activated when an existing session is retrieved or by selecting the service 'Ration' from the 'Define' menu command.

In Fig. 28.4, we see a (typical) screen shot of the evaluator dialogue box. The left panel exposes the ration and the (lower) right panel presents the CPM-Dairy evaluation of the ration. The buttons in the upper right provide access to special services associated with more detailed aspects of ration manipulation. The two radio button pairs toggle the display between 'dry matter' and 'as-fed' feed accounting and between MNRC and CNCPS display information, as needed.

Once a feed item is selected (clicked) from within the ration, the evaluator dialogue box 'Edit' button becomes active and this enables us to edit aspects of the selected feed. Alternatively, the 'ShowAll' button within the evaluator dialogue box is always active and this permits us to display details of feed items, either within the ration or within one of the feed dictionaries. If we need access to protein information for a feed item within a ration, for example, we would 'open' the ration feed list and toggle 'on' the protein radio button within the (ShowFeeds) dialogue box. To find an alternative feed with higher CP, we might open the 'Protein' feed dictionary and explore feed items there.

Finally, to edit the constraints for the optimizers (MNRC or CNCPS), we click either of these buttons from the evaluator dialogue box services. If we select CNCPS optimization, we see the CNCPS optimizer dialogue box . Here constraints can be set by nutrient and by ingredient amount. There are 12 constraints which can be selected to assist in balancing the ration. Whereas execution of the MNRC optimizer is almost instantaneous, the CNCPS optimizer, with its need to negotiate non-linear equations, routinely takes between 10 s and about 1 min to achieve a least-cost ration.

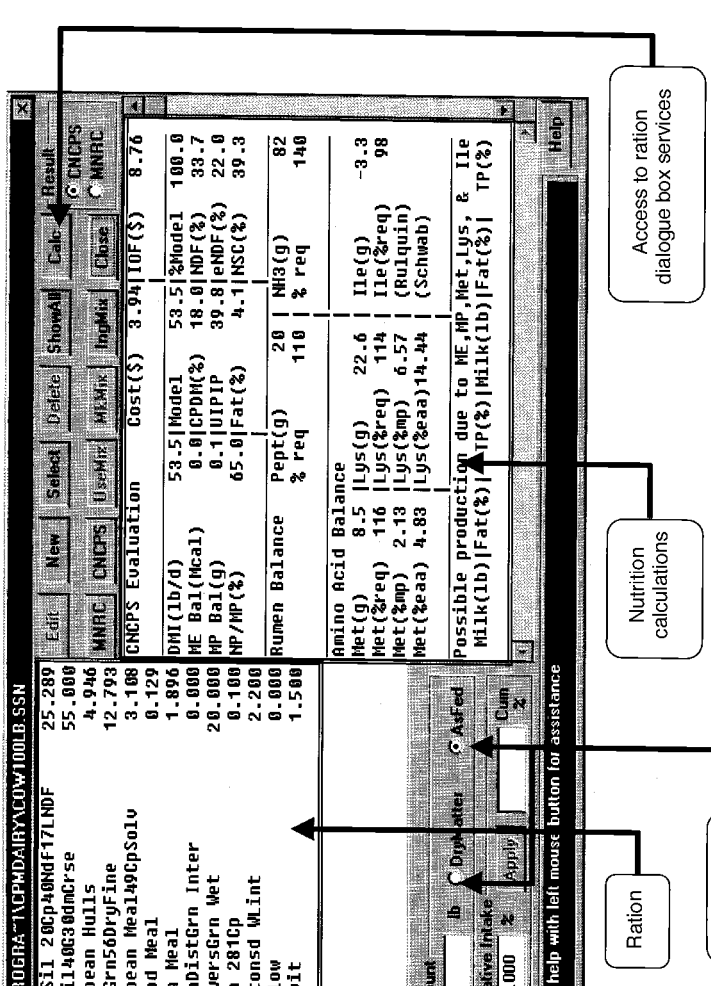

Fig. 28.4. The evaluator dialogue box in CPM-Dairy. Specifically shown are the 'ration' panel, the 'nutrient calculations' panel, the buttons providing access to the evaluator (or ration) dialogue box services and the display radio buttons.

An application of CPM-Dairy

CPM-Dairy is used by veterinarians, nutrition consultants and the feed industry to evaluate and formulate rations for dairy cattle.

At New Bolton Center, our Field Investigation Unit was presented with a case where milk production in a 200-cow dairy was only 30 kg day^{-1}, although cows were milked three times daily and were treated with bovine somatotrophin. Early-lactation cows frequently went 'off feed' and had diarrhoea. Faeces contained undigested maize, believed to be high-moisture maize.

There were two high-production groups (heifers and high-production cows) and a low-production group. The heifers and high-production cows were housed in a new free-stall barn with excellent ventilation and cow comfort. Cows were fed three times daily with frequent 'push-up' of feed. Feed bunk space was 0.52 m per cow with no headlocks, and cows had good water access. The remaining milking cows were housed in a renovated free-stall barn. They were fed twice daily with frequent 'push-up' of feed. Feed bunk space and ventilation were good. Non-lactating cows were housed on a bedded pack.

CPM-Dairy was used to evaluate the existing rations and to formulate new rations. In Table 28.1 are details of pre-CPM-Dairy and CPM-Dairy rations for the high producing animals (heifers and high-producing cows).

The pre-CPM-Dairy ration was formulated for a target of 39 kg milk day^{-1} with 3.6% fat and 3.1% crude protein. According to CPM-Dairy, this ration was low in metabolizable protein and would only support 34.4 kg milk day^{-1}. Poor amino acid ratios (Met/MP = 1.89; Lys/MP = 6.24) could reduce milk production by 1.6 kg day^{-1}, so that expected milk on the basis of metabolizable protein and balance of amino acids was only 32.8 kg day^{-1}. The ration was marginal in eNDF (21% vs. the guideline of 23% of ration dry matter (DM)) and contained 41.5% NSC. High-moisture maize, which has an initial high rate of fermentation in the rumen, contributed a substantial amount of NSC (4 kg NSC day^{-1}; 17.8% of ration DM and 42% of NSC). The carbohydrate profile of the ration could have contributed to the 'off-feed' and diarrhoea problems.

Objectives in formulating the new ration were to: (i) provide less NSC without compromising total carbohydrate fermentability; (ii) increase eNDF; (iii) correct the deficiency of metabolizable protein; and (iv) improve amino acid balance.

Reducing amounts of high-moisture maize (19 vs. 24% DM) and lucerne silage (15 vs. 27% DM), increasing the amount of maize silage (37 vs. 23% DM) and including soybean hulls (7 vs. 0% DM) reduced NSC (39.0 vs. 41.5%), but did not affect total-ration carbohydrate (72.3 vs. 71.9% DM). Although NSC was lower, total fermentable carbohydrates were higher (45 vs. 43% ration DM), because of the high ruminal fermentation of NDF in soybean hulls and maize silage. Increasing ration forage (52 vs. 50% DM) and including soybean hulls increased NDF (33.3 vs. 30.4%) and eNDF (22.9 vs. 21.0%).

Replacing a portion of the soybean meal and all of the maize distillers' grains and dry brewers' grains with animal and marine proteins increased the

Table 28.1. Rations for a 612 kg cow producing 39 kg milk day^{-1} with 3.6% fat and 3.1% crude protein.

	Ration	
	Pre-CPM-Dairy	CPM-Dairy
Ingredients (% DM)		
Lucerne silage	27.14	15.21
Maize silage	22.79	37.16
High-moisture maize	24.23	18.95
Soybean hulls		6.92
Soybean meal	5.63	3.91
Maize distillers' grains	5.51	
Dry brewers' grains	3.34	
Whole cottonseed	9.29	10.00
Fish meal		1.38
Blood meal		0.55
Animal–marine protein blend		3.38
Megalac	0.59	
Megalac Plus		0.49
Salt	0.40	0.22
Sodium bicarbonate	0.50	0.80
Mineral and vitamin mix	0.58	1.03
Total dry matter (kg day^{-1})	22.46	22.46
Cost ($ day^{-1})	3.65	3.82
Carbohydrates		
Non-structural* (% DM)	41.5	39.0
Non-structural (kg day^{-1})	9.33 (78%)†	8.78 (79%)
Neutral detergent fibre (% DM)	30.4	33.3
Effective neutral detergent fibre (% DM)	21.0	22.9
Neutral detergent fibre (kg day^{-1})	6.84 (35%)	7.49 (41%)
Available	5.44 (56%)	4.17 (47%)
Unavailable	1.40 (0%)	2.33 (0%)
Total (% DM)	71.9	72.3
Total (kg day^{-1})	15.67	15.77 (45)
Total fermentable (kg day^{-1})	9.76	10.05
Total fermentable (% DM)	43.1	44.7
Protein		
Crude (% DM)	18.6	17.8
Undegraded (% CP)	33.7	37.2
Metabolizable (kg day^{-1})	2.28 [100%]‡	2.49 [100%]
Bacterial	1.25 [55%]	1.34 [54%]
Undegraded	1.03 [45%]	1.15 [46%]
Metabolizable amino acids		
Methionine (g day^{-1})	43	55
Met/MP	1.89	2.19
Lysine (g day^{-1})	142	173
Lys/MP	6.24	6.94
Nutrient-limited milk (kg day^{-1})		
Metabolizable energy	44.0	43.8
Metabolizable protein	34.4	39.1
Rulquin ratio§	32.8	39.0

* Includes sugars, starch, pectin, β-glucans and acids produced during silage fermentation. Silage acids are not fermented further in the rumen and do not provide energy for bacterial growth.
† Values in parentheses are ruminal fermentability of carbohydrate fractions.
‡ Values in brackets are percentages of metabolizable protein.
§ Responses to amino acid ratios calculated according to equations in Rulquin *et al.* (1993) and added to metabolizable protein-limited milk.

supply of metabolizable protein from rumen-undegraded protein by 0.12 kg (1.15 vs. 1.03 kg day^{-1}). Metabolizable protein from bacteria was increased (1.34 vs. 1.25 kg day^{-1}) for two reasons. First, bacterial growth is driven mainly by energy derived from fermentation of carbohydrates. As noted above, the CPM-Dairy ration contained more rumen-fermentable carbohydrates (45 vs. 43% DM, 10.05 vs. 9.76 kg day^{-1}) than the pre-CPM-Dairy ration. Secondly, bacterial growth is decreased when rumen pH decreases. The CPM-Dairy ration contained more eNDF than the pre-CPM-Dairy ration. This stimulates cud chewing, increases salivary flow and improves ruminal buffering. More metabolizable protein from rumen escape protein and from bacterial protein alleviated the deficiency of metabolizable protein, so that milk yield based on metabolizable protein provided by the CPM-Dairy ration was 39.1 kg day^{-1} compared with 34.4 kg day^{-1} for the pre-CPM-Dairy ration.

Animal and marine proteins and ruminal bacteria are excellent sources of lysine. Thus, the combination of ruminal escape and bacterial protein improved Lys/MP (6.94 vs. 6.24). Fish meal, but not blood meal or rumen bacteria, is a good source of methionine. Met/MP (2.19 vs. 1.89) was improved by using Megalac Plus (Alimet in calcium salts of long-chain fatty acids (LCFA)) to supplement methionine in rumen escape and bacterial protein. The amino acid balance of the CPM-Dairy ration would only reduce milk 0.1 kg day^{-1} compared with 1.6 kg day^{-1} with the pre-CPM-Dairy rations. Thus, on the basis of metabolizable protein supply and amino acid balance, expected milk was 39 kg day^{-1}, or 6.2 kg day^{-1} more than on the pre-CPM-Dairy ration.

After 1 week on the new high-production rations and a similarly formulated low-production ration, total herd milk production was 4 kg day^{-1} higher. Cud chewing increased and manure consistency improved. Off-feed problems were dramatically reduced.

Two weeks after the ration change, manure still contained excessive undigested high-moisture maize. Grinding the high-moisture maize through a 0.635 cm screen reduced maize in faeces and milk production increased another 2 kg day^{-1}. Herd milk production now averaged 36 kg day^{-1}. For the next 12 months, average milk production for the total herd was 36 to 38 kg day^{-1}.

Interest in the first year of CPM-Dairy

In the year following its release (in October 1998), about 1000 copies of CPM-Dairy have been distributed to individuals and organizations within the USA and overseas. Internationally, groups from Canada, Mexico, South America, Japan, Australia, Italy, England, Ireland and Germany have acquired and used copies of CPM-Dairy 1.0.

Although we have not specified the target consumer of our product, our emphases – high utility, simple use, availability across a broad range of computer platforms – have meant that the software appears to have had appeal

across a wide spectrum of the dairy-related community. We produce a full version of CPM-Dairy, called CPM-Teach, usable for about 6 months, which we provide free to educational institutions across the USA.

At the University of Pennsylvania, four of our graduate courses use CPM-Dairy to varying degrees, ranging from very heavily in our dairy cattle nutrition course to moderately in our general nutrition course. At Cornell University, CPM-Dairy is used in the undergraduate animal nutrition labs.

We have presented about 40 workshops to industry personnel in ten countries, showing how CPM-Dairy functions are accessed and explaining how the biological and production information gleaned from it can be used to sharpen nutritional practices.

Discussion

This chapter has been about the issue of converting a scientific model or model suite into a commercial product. Many of the decisions and difficulties we ran into with this project related to the state of computing at the time we started to gain project momentum. Developing the program in 16-bit C meant that memory space was always an issue and it also meant that the interface had to be programmatically assembled. If the project were just starting (i.e. 3–4 years after our actual start), we would have used 3GL tools to build the interface, and we would have used the Access-style (Jet Engine-driven) database capabilities to maintain the data and also to accommodate user-configured reports. However, at the time we commenced, the 16-bit C environment was the best amongst viable contenders.

In our initial explorations with non-linear optimization, we equivocated concerning starting values for the optimizer's activities. The starting-point must be feasible, and the sticking-point for us here was whether or not to impose an MNRC optimization to initialize starting values for the CNCPS optimization. The gains in using the MNRC first were twofold: (i) we could always reproduce CNCPS final solutions; and (ii) we always seemed to get to sensible solutions to CNCPS activities following this procedure. The downside here is that imposing an MNRC run for non-linear optimization initialization meant that user selection of a starting-point was denied and hence a possibly lower-cost ration could never be found. At this point, and to stabilize the optimizer for field use, we have elected to impose the MNRC run first.

Acknowledgements

The authors take pleasure in thanking Dr Rick Kohn and Mr Peter Moate for their help with aspects of the CPM-Dairy project and with the preparation of this manuscript.

References

Boston, R.C., Ferguson, J.D., Kohn, R.A. and Black, J.L. (1994) Model testing and evaluation. In: Ministry of Agriculture (eds) *IV International Workshop on Modeling Nutrient Utilization in Farm Animals, 3–5 October 1994, Denmark*. National Institute of Animal Science, Tjele, Denmark, pp. 25–34.

Fox, D.G., Sniffen, C.J., O'Connor, J.D., Russell, J.B. and Van Soest, P.J. (1992) A net carbohydrate and protein system for evaluating cattle rations: III Cattle requirements and diet adequacy. *Journal of Animal Science* 70, 3578.

Hanna, O.T. and Sandall, O.C. (1995) *Computational Methods in Chemical Engineering. Revised Simplex Algorithm*. Prentice Hall, New York.

NRC (1996) *Nutrient Requirements of Beef Cattle*, 7th revised edn. Nutrient Requirements of Domestic Animals. NRC, Washington, DC.

NRC (1989) *Nutrient Requirements of Dairy Cattle*, 6th revised edn. Nutrient Requirements of Domestic Animals. NRC, Washington, DC.

O'Connor, J.D., Sniffen, C.J., Fox, D.G. and Chalupa, W. (1993) A net carbohydrate and protein system for evaluating cattle rations: IV Predicting amino acid adequacy. *Journal of Animal Science* 71, 1.

Pressman, R.S. (1987) *Software Engineering: a Practitioner's Approach*, 2nd edn. McGraw-Hill, New York.

Rulquin, H., Pisulewski, P.M., Verite, R. and Guinard, J. (1993) Milk production and composition as a function of postruminal lysine and methionine supply: a nutrient response approach. *Livestock Production Science* 37, 69–90.

Russell, J.B., O'Connor, J.D., Fox, D.G., Van Soest, P.J. and Sniffen, C.J. (1992) A net carbohydrate and protein system for evaluating cattle rations: I Ruminal fermentation. *Journal of Animal Science* 70, 3551.

Schwab, C.G., Bozak, C.K., Whitehouse, N.L. and Mesbah, M.M.A. (1992) Amino acid limitation and flow to the duodenum at four stages of lactation. 1. Sequence of lysine and methionine limitation. *Journal of Dairy Science* 75, 3503–3518.

Sniffen, C.J., O'Connor, J.D., Van Soest, P.J., Fox, D.G. and Russell, J.B. (1992) A net carbohydrate and protein system for evaluating cattle rations: II Carbohydrate and protein availability. *Journal of Animal Science* 70, 3562.

Van Amburgh, M.E., Galton, D.M., Bauman, D.E., Everett, R.W., Fox, D.G., Chase, L.E. and Erb, H.N. (1998) Effect of three prepubertal body growth rates on performance of Holstein heifers during first lactation. *Journal of Dairy Science* 81, 527–538.

VandeHar, M., Buckholz, H., Beverly, R., Emery, R., Allen, M., Sniffen, C. and Black, R. (1992) *Spartan Ration Evaluator/Balancer for Dairy Cattle*. Michigan State University, East Lancing.

Van Soest, P.J., Robertson, J.B. and Lewis, B.A. (1991) Methods for dietary fibre, neutral detergent fiber, and non starch polysaccharides determination in relation to animal nutrition. *Journal of Dairy Science* 74, 3583–3595.

Zhou, J.L. and Tits, A.L. (1997) *User's Guide for FFSQP Version 3.5*. Electrical Engineering Department and Institute for Systems Research, University of Maryland, College Park.

29

The Utilization of Prediction Models to Optimize Farm Animal Production Systems: the Case of a Growing Pig Model

P. Jean dit Bailleul,[1,2,3] J.F. Bernier,[2] J. van Milgen,[4] D. Sauvant[3] and C. Pomar[1]

[1]Agriculture and AgriFood Canada, CP 90, 2000 Road 108 East, Lennoxville, Quebec J1M 1Z3, Canada; [2]Université Laval, Département des Sciences Animales, Pavillon Paul-Comtois, Ste Foy, Quebec G1K 7P4, Canada; [3]Laboratoire de Nutrition et Alimentation (INRA–INAPG), 16 rue Claude Bernard, 75231 Paris Cedex 05, France; [4]Station de Recherche Porcines, Institut National de la Recherche Agronomique, 35590 Saint Gilles, France

Abstract

In the last 25 years, mathematical models for growing animals have been developed to predict growth from knowledge on animal biology. The increasing precision of these models allows them to be used to evaluate economic return and/or environmental impact of the simulated production system. It is also possible to incorporate these models into optimization routines to determine feeding programmes or slaughter management policies. To evaluate the usefulness of this aproach, a simplified growing pig model was developed to determine the feeding management system that maximizes net return in commercial growing/finishing production systems. The model is mechanistic, deterministic, dynamic and aggregated at the whole-animal level. The overall model has four different submodels. The first estimates the growing pig's maximal energy and protein requirements for the entire growing period. The second submodel determines the least-cost diet meeting those requirements. The third submodel simulates the animal's growth in terms of protein and fat deposition. The last submodel calculates the net economic return from the simulated production system. Finally, a non-linear optimization algorithm finds the feeding programme that maximizes net return.

 Modelling Nutrient Utilization in Farm Animals (eds J.P. McNamara, J. France and D.E. Beever)

Model results indicate that maximal net returns are obtained by restricting protein intake by 6 to 30% of the maximal requirements. Model results also show that the payment grid used in several countries is the most important factor to be taken into account to maximize revenue. Also, our results indicate that carcass reference and feedstuff prices have only a limited impact on the feeding programme that achieves maximal net return. This study shows that growth models may help to determine optimal production strategies from an economic and an environmental point of view.

Introduction

Pig production is a highly competitive industry, characterized by small margins between costs and revenues. In this context, maximizing economic efficiency is crucial. Because feed is the single largest production cost factor, representing more than 60% of the overall production cost, the determination of the most profitable feeding programme in relation to the pig's characteristics becomes an essential component of production efficiency. Moreover, various studies (De Lange and Schreurs, 1995; Moughan *et al.*, 1995) have shown that maximizing technical criteria does not always yield the highest net return.

Mathematical models representing the growth of pigs are developed to evaluate the animal response to changes in production strategies, to improve profitability, to improve concepts about biological systems and to define research priorities (Black, 1995). The most recent pig growth models represent the animal metabolism from a mechanistic perspective, predicting growth from the knowledge of genotype and diet composition (Whittemore, 1983, 1986, 1998; Moughan, 1984; Black *et al.*, 1986; Pomar *et al.*, 1991; Ferguson *et al.*, 1994). Improving profitability with such models requires the user to manually determine the combination of the most significant production factors, such as genotype, feeding programme or diet composition, that achieves the highest net return. In addition, feedstuff and carcass prices are changing continuously and optimal production strategies may therefore change over time. Furthermore, feed prices and production costs are specific to each production system. In the past, empirical models have been proposed that optimize economic return from technical production variables (Sonka *et al.*, 1976; Crabtree, 1977; Boggess *et al.*, 1984). However, these models are of limited use in practice, because of the lack of representation of animal response to changing production circumstances. Black *et al.* (1989) developed the first optimization software where the animal response was predicted by a mechanistic pig growth model. This optimization system is used by the pork industry today. The economically optimal solution is obtained by a linear algorithm, which assumes that system responses to alternative production factors are linear (J. Black, 1998, personal communication).

The present study was undertaken to develop a decision support system to help managers in evaluating production alternatives and to find optimal man-

agement strategies. To evaluate the usefulness of this tool, a simplified pig growth model was included in an integrated non-linear optimization system to study optimal dietary protein concentration in a two-phase feeding growing–finishing production system. The complete optimization system is described by Jean dit Bailleul (1998). This system is a prototype of a larger model currently under development and described by Benchakroun *et al.* (1995).

Description

The integrated optimization system is composed of: (i) a simplified growth model; (ii) a diet formulation algorithm; and (iii) a non-linear optimization routine. The growth model describes growth as a dynamic process, following the principles proposed by Whittemore (1983). The model is deterministic, dynamic and aggregated at the whole-animal level, with two primary body components (total body protein and total lipid mass). Ash and water are estimated from body protein accretion, as suggested by Kotarbinska (1971). Gut content is estimated as 5% of the empty weight, as proposed by Whittemore (1983). Body weight is defined as the algebraic sum of the body chemical components (i.e. protein, lipids, ash, water and gut content). Meat yield in carcass is predicted from body chemical composition (Jean dit Bailleul, 1998). Feed intake is predicted as proposed by the Agricultural Research Council (ARC, 1981) from the animal body weight and from the digestible energy content of the diet. Energy requirements for maintenance are estimated as a function of body weight, while protein requirements for maintenance are determined by body protein mass. The animal potential for protein retention is assumed to be a non-linear function of age and is represented by a Gompertz function (Pomar *et al.*, 1993). Protein retention is assumed to be limited either by the amount of lysine available for growth or by the animal potential. Energy available for lipid retention is then calculated as the difference between digestible energy intake and the energy expenditures for maintenance, energy used for protein retention and energy losses due to protein deamination and urea synthesis. Simulated animals are characterized by their potential for protein accretion and by their energetic appetite. The growth model has been tested for accuracy by comparing simulated results with those published in the literature. Validation results confirmed that the model accurately predicts the animal's response to changes in amino acids, feed or energy intake (Jean dit Bailleul, 1998).

Assuming that protein deamination is minimal and that pigs are fed *ad libitum*, digestible energy intake represents the energy requirements, while the minimal amount of balanced amino acids needed to reach the animal's protein deposition potential represents its amino acid requirements. The ratio between total daily protein requirements and appetite determines the minimal protein concentration in diets. Amino acid requirements are established in agreement with the amino acid composition of an ideal protein.

Minimal amino acid requirements, expressed in terms of g MJ^{-1} of digestible energy (DE), are used to formulate a least-cost diet. Dietary energy concentration was fixed at 14 MJ of DE kg^{-1} of diet. These amino acids and energy concentrations are used as inputs by a linear programming algorithm (Dantzig, 1990) to obtain the least-cost formula. Seventeen feedstuffs were used in this study and were those available from a feed company in Quebec, Canada, during 1995. Nine of these were ingredients rich in protein, including synthetic lysine. Ingredients were defined by their price and nutritional composition, the latter being taken from the literature (INRA, 1989). Ingredient composition included DE and digestible amino acid concentrations. Ingredient prices were average values recorded by the feed manufacturer during the first week of each month during 1995. The digestible fraction of lysine and the pool of other amino acids of each ingredient were estimated by multiplying the crude amino acid content by the corresponding digestibility coefficient. Digestibility coefficients used in this evaluation did not account for endogenous losses and were taken from the literature (RPNA, 1993). For simplicity, the metabolic availability of all the absorbed amino acids was assumed to be equal to 100%. The balanced amino acid fraction of the dietary protein was estimated by comparing the amino acid profile of the digestible protein to the profile of an ideal protein (ARC, 1981).

An optimization routine based on the gradient method (Kuester and Mixe, 1973) was adapted to the overall optimization system. This routine finds the length of the first feeding phase and the level of satisfaction of the protein requirements (ρ) that maximizes or minimizes an objective function (e.g. maximization of net return). This routine proceeds as follows:

1. A starting-point for the length of the feeding phase and ρ is chosen (X_0,Y_0) and the objective function is evaluated.
2. For each independent variable, the objective function is evaluated at a small distance (±δ) from the starting-point ($X = X_0 \pm \delta$; $Y = Y_0 \pm \delta$).
3. For each independent variable, the point giving the highest increment (or decrement) of the objective function is retained and becomes the new starting-point. Steps 1–3 are repeated until no further gains (or losses) are obtained for the objective function.
4. While approaching the maximum (or minimum), the incremented distance δ is halved and steps 1 to 4 are repeated until the distance δ becomes lower than a fixed relative value (1E-6) .

Each evaluation of the objective function starts by evaluating the maximum balanced protein-to-energy requirements ratio of both feeding phases. Maximum amino acid requirements are weighted by 'ρ' and the feed formulation algorithm determines a least-cost diet that satisfies the weighted protein requirements for each feeding period. Finally, the pig growth model simulates the animal response to the weighted protein diets and feeding intervals. The objective function is then evaluated. When costs and revenues are needed to evaluate the objective function, total costs are calculated, including fixed, vari-

able, feeding and mixing costs. Revenues are calculated according to a reference market price, the grade and the carcass weight. Net return is calculated by subtracting costs from revenues. A reference table is used to calculate the carcass grade (also referred to as the index) from a combination of lean yield estimation and the carcass weight. In Quebec, the steps between the table's grids usually correspond to 2% lean yield and can represent important changes in carcass value. A sensitivity analysis of the main model parameters describing the animal (appetite and protein deposition potential) and protein intake (ρ) was performed by changing parameter values between 0.8 and 1.2 times the default values. The rest of the parameters were kept constant to the default values. Results obtained for parameters describing the animal were obtained by maximizing net return in terms of \$ pig place^{-1} year^{-1}, while those obtained from changes of ρ are simulation results without optimization. Only the most important results from the sensitivity analysis are shown in this study. Other results are presented in Jean dit Bailleul (1998). To simplify the interpretation, the sensitivity analysis was done with the assumption that the index was always 110%, which is close to the average value obtained by farmers.

Results and Discussion

Production objectives

The modelled effect of production objectives on optimized parameter values, growth performance and production net returns are presented in Table 29.1. Results obtained by meeting the maximal requirements during both the growing and the finishing periods may represent those obtained in commercial farms when diets are formulated based on factorial methods of determination of protein requirements. In these cases, it is assumed that protein deposition is not limited by protein supply throughout the growing period.

When the unique objective is to maximize carcass lean yield, simulation results suggest that producers should use diets with high protein content (see Table 29.1). Diets rich in protein are required to maximize protein retention while decreasing lipid retention. In fact, it is assumed in the model that pigs fed *ad libitum* eat to satisfy their energy requirements in terms of digestible energy. Increasing dietary protein concentration without modifying energy density reduces the availability of energy for lipid deposition as a result of the losses in protein deamination and in synthesis and excretion of urea (Noblet *et al.*, 1989). However, this maximal carcass lean yield objective also causes a degradation of ADG (-120 g day^{-1}), reduces feed efficiency (-0.05 kg kg^{-1}) and, especially, increases nitrogen excretion (+20 kg pig place^{-1} year^{-1}). Nevertheless, the underlying model hypotheses may not always be valid. In fact, excess levels of protein may become a metabolic burden for pigs (Stahly *et al.*, 1979), and this is not accounted for in the model. These results may be overly simplistic, but they show the model response to increases in protein concentration of diets. In

Table 29.1. Effect of the production objective on optimized parameters, growth performance and net returns.

Item	Production objective							
	Satisfy maximal protein requirements	Maximize carcass muscle content (%)	Maximize ADG (g day^{-1})	Maximize feed efficiency (kg kg^{-1})	Minimize total growing–finishing time (days)	Maximize net return		
						($ pig^{-1})	($ day^{-1})	($ place^{-1} year^{-1})
Level of satisfaction of maximal protein requirements (ρ)* (g g^{-1})	1.000	1.824	0.987	1.009	0.989	0.919	0.925	0.922
Duration of the first growing period (days)	45	96	18	18	18	38	35	35
Total growing–finishing time (days)	100.1	114.8	99.3	99.3	**99.3**	100.1	100.0	100.0
Average daily gain (g day^{-1})	883	770	**890**	890	890	883	884	884
Average body protein retention (g day^{-1})	124.2	113.3	124.4	124.4	124.4	123.1	122.6	122.6
Carcass lean yield (%)	59.76	**60.73**	59.68	59.69	59.68	59.61	59.62	59.62
Feed efficiency (kg kg^{-1})	0.342	0.297	0.345	**0.345**	0.345	0.342	0.343	0.343
Feeding cost ($ pig^{-1})	70.97	96.29	71.31	71.52	71.31	70.26	70.27	70.27
Net return ($ pig^{-1})	9.46	−18.30	9.25	9.04	9.25	**10.17**	10.17	10.17
($ day^{-1})	0.095	−0.159	0.093	0.091	0.093	0.102	**0.102**	0.102
($ place^{-1} year^{-1})	31.36	−53.52	30.87	30.16	30.87	33.71	33.75	**33.76**
Nitrogen excretion (kg pig^{-1})	4.80	12.33	4.39	4.41	4.39	4.52	4.52	4.50
(kg place^{-1} year^{-1})	15.93	36.05	14.65	14.72	14.65	14.99	14.98	14.94

* Pigs are fed to maximal requirements when ρ = 1.
Bold indicates optimized value.

all cases, feeding high-protein diets to reduce carcass fat is not necessarily the best strategy to increase revenues (see Table 29.1).

When the production objective is to maximize ADG or feed efficiency or to minimize the growing–finishing length, pigs are fed to achieve maximal weight gain and therefore they should be almost unrestricted in protein or fat deposition (ρ close to 1). However, the net return is about \$3 pig place^{-1} year^{-1} lower when compared with economically optimal production strategies. Moreover, these production objectives seem to be economically worse than the satisfaction of protein requirements (−\$0.50 pig place^{-1} year^{-1}), but better than the former when compared in terms of nitrogen excretion (−400 g pig^{-1}). These results are partly explained by the reduction of the growing–finishing time (−0.8 day).

Feeding programmes designed to maximize net returns are fundamentally different from those developed to maximize technical criteria (e.g. ADG, feed efficiency). The main difference occurs in the satisfaction of the maximal protein requirements and in the length of the two feeding phases. Using the Quebec situation of 1995, feeding 92.5% of the maximal protein requirements of the pigs and using the first diet for 36 days would improve revenue by 7.6% compared with feeding according to nutritional requirements. Given the fact that pigs increase their feed intake with body weight, the first feeding period becomes longer in order to obtain a cheaper second diet with a lower protein content. Moreover, the combination of a single diet per period and the changing requirements implies excessive feeding of protein if maximum protein accretion is the objective. Using diets that do not fully fulfil the maximal requirements means that protein retention will be reduced for a few days while being in excess for the rest of the period. However, nitrogen excretion is hardly affected, because the overall growing–finishing period is somewhat longer. There are no important differences between the three economic objectives analysed in this study.

Effect of the level of satisfaction of protein requirements (ρ) on animal response and economic returns

The effect of modifying the level of satisfaction of protein requirements on simulated animal response and net production returns is shown in Table 29.2. These results show that, when pigs are fed under maximal requirements, ADG and average protein retention increase as protein intake increases. This is in agreement with Tuitoek *et al.* (1997). Maximal ADG, protein retention and feed efficiency are reached when dietary protein is close to requirements ($\rho = 1$). The consequences of overfeeding pigs with protein ($\rho > 1$) appear to be smaller than underfeeding ($\rho < 1$). In any case, maximal net returns are obtained for levels of satisfaction of protein requirement lower than 1: that is, to maximize the net return from growing–finishing systems, farmers should feed the average pig below the maximal requirements as estimated by factorial methods. These results are in agreement with experimental results obtained by De Lange and

Table 29.2. Effect of the level of satisfaction of protein requirements (ρ) on simulated growth performance and net return.

	Level of satisfaction of maximal protein requirements (ρ) (g g^{-1})*								
	0.70	0.75	0.80	0.85	0.90	0.95	1.00	1.05	1.10
Duration of the first growing period (days)	35	35	35	35	35	35	35	35	35
Total growing–finishing time (days)	108.1	104.9	102.7	101.2	100.3	99.8	99.7	99.9	100.2
Average daily gain (g day^{-1})	818	843	861	874	882	886	887	885	883
Average body protein retention (g day^{-1})	100.8	109.5	116.3	120.1	122.4	123.4	123.9	123.7	124.0
Feed efficiency (kg kg^{-1})	0.320	0.329	0.335	0.339	0.342	0.343	0.343	0.343	0.342
Feeding cost ($ pig^{-1})	73.22	71.71	70.82	70.36	70.24	70.39	70.77	71.31	71.88
Net return ($ $place^{-1}$ $year^{-1}$) without payment grid	18.15	25.16	29.69	32.44	33.65	33.55	32.31	30.36	28.29
Net return ($ $place^{-1}$ $year^{-1}$) with payment grid	10.44	17.24	21.61	24.25	25.00	33.55	32.31	30.36	28.29
Nitrogen excretion (kg $place^{-1}$ $year^{-1}$)	14.49	14.33	14.41	14.56	14.79	15.08	15.39	15.72	16.02

*Pigs are fed to requirements when ρ = 1.

Schreurs (1995) and Moughan *et al.* (1995) and with simulated growing–finishing systems with the AUSPIG model (cited by Moughan *et al.*, 1995).

Results from this study also show that, for the average pig, the net return difference between classification classes is \$2.50 pig^{-1}, which represents \$7.50 pig $place^{-1}$ $year^{-1}$. Of course, this absolute value is affected by the reference carcass price. The steps of the grid of reference used to calculate the grades in Quebec induce step-like response to changes in model parameter values. When optimizing net return, feeding programmes tend to reach the higher index classes by maximizing lean yield in carcasses. As stated before, lean yield can be increased by decreasing energy efficiency with high-protein diets or by having longer first feeding periods. A simulation model representing variation between pigs would have smoother responses to protein intakes and, probably, lower protein levels in the optimal feeding programmes. Therefore, optimal protein intakes obtained by this model may be overestimated.

Effect of the appetite of pigs on animal response and economic returns

The effect of the energetic appetite of pigs on optimized parameters, growth performance and net return when optimizing net return is shown in Table 29.3. Net return increases with the increase in feed intake (+\$55 pig $place^{-1}$ $year^{-1}$). This is explained by the increase of average daily weight gain (+380 g day^{-1}) and the reduction of the number of days to reach slaughter weight, which reduces the charges proportional to the number of days and the total feed intake. The increase of ADG with increases of feed intake results mainly from protein retention (+10 g day^{-1} between 0.80 and 0.85 of the energetic appetite). However, as feed intake increases, protein retention represents a lower percentage of weight gain (from 14.7% to 12.6%). These changes in the relative contribution of protein deposition to the total weight gain explain why feed efficiency increases rapidly (from 0.314 to 0.342) until the maximum is reached at the standard appetite value, after which it decreases (from 0.343 to 0.341). These results also indicate that the optimal level of satisfaction of protein intake (ρ) increases with increasing appetite of the pigs (from 0.742 to 0.922 and from 0.812 to 0.886). This is explained by the fact that the marginal cost of protein in the diet increases more rapidly than protein concentration. In general, either feeding diets close to requirements (ρ close to 1) with a short first period (about 35 days) or feeding diets under requirements (ρ close to 0.85) with a long first period (about 60 days) is a good combination for net return. However, feeding diets close to requirements (ρ close to 1) with long first periods (about 60 days) or feeding diets under requirements (ρ close to 0.85) with a short first period (about 35 days) give lower net returns. These combinations result in two local optima, from which a global optimum should be determined. The important variation occuring between 1.05 and 1.10 times the energetic appetite corresponds to a change from one local optimum to the other.

Table 29.3. Effect of the energetic appetite of pigs on optimized parameters, growth performance and net return.*

	Energetic appetite (default value = 1)								
Variable	0.80	0.85	0.90	0.95	1.00	1.05	1.10	1.15	1.20
Level of satisfaction of maximal protein requirements (ρ)† (g g^{-1})	0.742	0.804	0.862	0.909	0.922	0.922	0.812	0.849	0.886
Duration of the first growing period (days)	53	45	39	36	35	35	53	49	45
Total growing–finishing time (days)	134.1	121.3	112.0	105.1	100.0	95.6	92.2	88.3	84.9
Average daily gain (g day^{-1})	659	729	789	841	884	925	959	1002	1042
Average body protein retention (g day^{-1})	97.0	107.0	114.3	120.1	122.6	125.2	126.1	129.0	130.7
Feed efficiency (kg kg^{-1})	0.314	0.329	0.337	0.342	0.343	0.343	0.341	0.341	0.341
Feeding cost ($ pig^{-1})	76.14	73.20	71.55	70.73	70.27	69.93	69.53	69.41	69.42
Net return per pig place per year ($ $place^{-1}$ $year^{-1}$)	−3.45	10.31	20.65	28.09	33.76	38.84	43.61	48.20	52.06
Nitrogen excretion per pig place per year (kg $place^{-1}$ $year^{-1}$)	12.71	13.15	13.71	14.33	14.94	15.46	15.31	16.04	16.81

*Potential protein retention parameters were kept constant.
†Pigs are fed to maximal protein requirements when ρ = 1.

Effect of the potential for protein deposition on animal response and economic returns

The effect of changes in the potential for protein deposition on the optimized parameters, growth performance and net returns is presented in Table 29.4. These results show that, when the potential for protein retention increases, net return increases accordingly (+\$72 pig place^{-1} year^{-1}). This increase is the result of the reduction of feeding cost and of the proportional charges associated with the increase of ADG (+222 g day^{-1}). For pigs with a high potential for protein deposition, a diminution of ρ makes it possible to limit the increase of the feeding cost. The increase of ρ is counterbalanced by the reduction of the length of the first period between 0.8 and 1.05 times potential for protein deposition.

Conclusion

The results of the model prototype presented here indicate that optimal production alternatives are highly specific to the animal potential and to the payment system used in different countries. These results also confirm the hypothesis that it is not economically beneficial to feed pigs to meet their maximal requirements or to maximize performance parameters. The ultimate objective of a production system should be the determination of the optimal feeding programmes. The profitability of the growing–finishing production systems should increase with animals with a large appetite and a high potential for protein deposition.

Acknowledgements

This study was partly financed by the Fédération des Producteurs des Porcs du Quebec. We thank F. Dubeau of Sherbrooke University for the useful discussion about the mathematical optimization systems. We also thank Génétiporc Inc. for providing some data used in this study.

References

ARC (1981) *The Nutrient Requirements of Pigs*. Commonwealth Agricultural Bureaux, Farnham Royal, 307 pp.

Benchakroun, H., Dubeau, F., Dussault, J.P., Jean dit Bailleul, P. and Pomar, C. (1995) *Revision of the Traditional Diet Formulation Model*. Rapport du DMI No. 84, Sherbrooke University, Quebec, Canada.

Black, J.L. (1995) The evolution of animal growth models. In: Moughan, P.J., Verstegen, M.W.A. and Visser-Reyneveld, M.I. (eds) *Modelling the Growth in the Pigs*. EAAP Publication No. 78, Wageningen Pers, Wageningen.

Table 29.4. Effect of changes of the potential for protein deposition on optimized parameters, growth performance and net return.*

	Potential for protein deposition (default values = 1)								
Item	0.80	0.85	0.90	0.95	1.00	1.05	1.10	1.15	1.20
Level of satisfaction of maximal protein requirements (ρ)† (g g^{-1})	0.905	0.914	0.916	0.920	0.922	0.921	0.905	0.878	0.856
Duration of the first growing period (days)	51	49	44	39	35	33	31	29	28
Total growing–finishing time (days)	114.9	111.4	107.2	103.5	100.0	96.8	93.9	91.4	89.1
Average daily gain (g day^{-1})	770	794	825	854	884	914	942	968	992
Average body protein retention (g day^{-1})	91.9	98.4	107.1	114.9	122.6	130.7	138.2	145.4	152.2
Feed efficiency (kg kg^{-1})	0.299	0.308	0.320	0.331	0.343	0.354	0.365	0.375	0.385
Feeding cost ($ pig^{-1})	78.83	76.61	74.36	72.27	70.27	68.36	66.53	64.84	63.32
Net return per pig place per year ($ $place^{-1}$ $year^{-1}$)	−2.51	6.12	15.21	24.44	33.76	43.15	52.50	61.35	69.68
Nitrogen excretion per pig place per year (kg $place^{-1}$ $year^{-1}$)	15.51	15.14	15.36	15.16	14.94	14.69	14.36	13.92	13.58

*The appetite for digestible energy was kept constant.
†Pigs are fed to maximal protein requirements when ρ = 1.

Black, J.L., Campbell, R.G., Williams, I.H., James, K.J. and Davies, G.T. (1986) Simulation of energy and amino acid utilisation in the pig. *Research and Development in Agriculture* 3(3), 121–145.

Black, J.L., Fleming, J.F. and Davies, G.T. (1989) A computer modelling package for the nutritional management of pigs. *Australian Poultry and Feed Convention* 7, 273–278.

Boggess, W.G., Olson, K.D. and Heady, E.O. (1984) Gain isoquants and production functions for swine. In: Heady, E.O. and Bhide, S. (eds) *Livestock Response Functions*. Iowa State University Press, Ames, pp. 267–301.

Crabtree, J.R. (1977) Feeding strategy economics in bacon pig production. *Journal of Agricultural Economy* 28(1), 39–52.

Dantzig, G.B. (1990) The diet problem. *Interfaces* 20(4), 43–47.

De Lange, C.F.M. and Schreurs, H.W.E. (1995) Principle of model application. In: Moughan, P.J., Verstegen, M.W.A. and Visser-Reyneveld, M.I. (eds) *Modelling the Growth of Pigs*. EAAP Publication No. 78, Wageningen Pers, Wageningen, pp. 187–208.

Ferguson, N.S., Gous, R.M. and Emmans, G.C. (1994) Preferred components for the construction of a new simulation model of growth, feed intake and nutrient requirements of growing pigs. *South African Journal of Animal Science* 24(1), 10–17.

INRA (1989) *L'Alimentation de monogastriques : porc, lapin, volailles*. INRA, Paris, 282 pp.

Jean dit Bailleul, P. (1998) Modélisation et optimisation du revenu net de l'engraissement de porcin. MSc thesis, Laval University, Quebec, 125 pp.

Kotarbinska, M. (1971) The chemical composition of the body in growing pigs. *Roczniki nauk Rolniczych Seria B – Zootechniczna* 93(1), 129–135.

Kuester, J.L. and Mixe, J.H. (1973) *Optimization Techniques with Fortran*. McGraw-Hill, 500 pp.

Moughan, P.J. (1984) Prediction of dietary protein quality based on a model of the digestion and metabolism of nitrogen in the growing pig. *New Zealand Journal of Agricultural Research* 27, 501–507.

Moughan, P.J., Kerr, R.T. and Smith, W.C. (1995) The role of simulation models in the development of economically-optimal feeding regimens for the growing pigs. In: Moughan, P.J., Verstegen, M.W.A. and Visser-Teyneveld, M.I. (eds) *Modelling the Growth of Pigs*. EAAP Publications No. 78, Wageningen Pers, Wageningen, pp. 209–222.

Noblet, J., Fortune, H., Dubois, S. and Henry, Y. (1989) *Nouvelles bases d'estimation des teneurs en énergie digestible, métabolisable et nette des aliments pour le porc*. INRA, Paris, 105 pp.

Pomar, C., Harris, D.L. and Minvielle, F. (1991) Computer simulation model of swine production systems I: modeling the growth of young pigs. *Journal of Animal Science* 69, 1468–1488.

Pomar, C., Pommier, S., Gariepy, C. and Peticlerc, D. (1993) The effect of genotype, castration, growth hormone-releasing factor and feed restriction on body composition of pigs from 20 to 95 kg liveweight. *Journal of Animal Science* 71 (Suppl. 1), 143.

RPNA (Rhône Poulenc Nutrition Animale) (1993) *Rhodimet Nutrition Guide*. 39 pp.

Sonka, S.T., Heady, E.O. and Dahm, P.F. (1976) Estimation of gain isoquants and a decision model application for swine production. *American Journal of Agricultural Economy* 58(1), 466–474.

Stahly, T.S., Cromwell, G.L. and Aviotti, M.P. (1979) The effect of environmental temperature and dietary lysine source and level on the performance and carcass characteristics of growing swine. *Journal of Animal Science* 49, 1242.

Tuitoek, K., Young, L.G., de Lange, C.F.M. and Kerr, B.J. (1997) The effect of reducing excess dietary amino acids on growing–finishing pig performance: an evaluation of the ideal protein concept. *Journal of Animal Science* 75, 1575–1583.

Whittemore, C.T. (1983) Development of recommended energy and protein allowances for growing pigs. *Agricultural Systems* 11, 159–186.

Whittemore, C.T. (1986) An approach to pig modelling. *Journal of Animal Science* 63, 615–621.

Whittemore C.T. (1998) *The Science and Practice of Pig Production*, 2nd edn. Blackwell Science, Oxford, UK.

A Pig Model for Feed Evaluation

30

Allan Danfær

Danish Institute of Agricultural Sciences, Research Centre Foulum, PO Box 50, 8830 Tjele, Denmark

Abstract

This chapter describes a dynamic, semi-mechanistic model of growing pigs. The purpose of the model is to predict growth rate and growth composition from given feed inputs and thereby serve as a basis for a new, nutrient-based feed evaluation system for slaughter pigs.

The model consists of two submodels, one describing nutrient digestion and absorption, and one describing the metabolism of absorbed nutrients and their retention in the body pools of protein, lipid and ash. Required inputs to the model are: (i) characteristics of the food, such as dry matter content, chemical composition of dry matter, digestibilities and fermentabilities of individual chemical fractions; (ii) characteristics of the pig, such as age at the beginning of simulation, sex, and genetic capacities for protein and lipid retention; and (iii) environmental characteristics such as the ambient temperature. Model outputs are the simulated numeric values of all state and rate variables. From these numbers, the model calculates the predicted pig performance: food intake, retention of protein, lipid, ash and water, production of heat and methane, as well as faecal and urinary excretion of energy and matter.

Some examples of simulated data obtained with the model are given in the chapter. The results of simulation were found to be realistic and biologically meaningful. In one test, the model was used to simulate the net energy value of 15 different diets. For each diet, the feed value simulated by the model was closer to the 'true' value determined experimentally than to the value estimated by the present Danish net energy system.

It is concluded that a new feed evaluation system for growing pigs is needed. The possibilities and perspectives in the development of such a system based on a dynamic, whole animal simulation model like the one described are discussed.

 Modelling Nutrient Utilization in Farm Animals (eds J.P. McNamara, J. France and D.E. Beever)

Introduction

In terms of feed evaluation, it is useful to distinguish between the potential value and the production value of feeds. The potential value is necessary for a commercial price setting of foodstuffs and should express the quantity of nutrients and energy available to the animal. The production value of a feed mixture is an expression of the animal performance obtained with this feed. This means that the production value is also dependent on the actual utilization of the available nutrients. A given foodstuff or a given diet has just one potential value (as estimated from nutrient composition and nutrient digestibility) whereas the production value of a given feed can be different at various conditions of production (level of food intake, age and physiological stage of the animals).

As a tool to optimize the composition of pig diets, a feed evaluation system should be able to determine the potential value of foodstuffs and also to predict production values of diets at given feeding conditions. In fact, the production value of a given diet in a given situation cannot be determined until the food has been eaten and the animal performance has been recorded. However, the purpose of a feed evaluation system is to estimate the value of the food in advance, i.e. before it is given to the animals. Therefore, it is necessary to have a method to predict what the food does to the pigs. The most suitable tool to solve this problem is probably a mathematical simulation model, in which the most important processes of nutrient digestion, metabolism and utilization are described in such a way that the animal performance and thereby the food's production value can be predicted. This value can then be expressed in a number of ways, depending on desired goals in pig production, e.g. as MJ net energy (NE) kg^{-1} food, as kg (or MJ) lean and fat tissue kg^{-1} (or MJ^{-1}) food or as g nitrogen and phosphorus excretion kg^{-1} food.

The purpose of this chapter is to present a dynamic simulation model of growing pigs, designed as a basis for a new system for the evaluation of pig diets. Some shortcomings of present feed evaluation systems are briefly discussed.

Present Net Energy Systems

These are, to a large extent, empirical and are rather poor imitations of the digestive and metabolic processes that govern animal performance. The energy and the protein value of feeds are determined separately by two independent systems. In Denmark, the net energy value, feed unit for pigs (FU_p) kg^{-1} dry matter (DM), is calculated from the chemical composition of the feed, the *in vitro* digestibility of organic matter, an empirical relationship between dietary N and urinary energy and, finally, an empirical relationship between metabolizable energy (ME) and NE (Boisen and Fernández, 1992). The protein value of a feed is expressed as g digestible amino acid(s) FU_p^{-1} and is calculated from the amino acid content and tabulated apparent faecal digestibility of crude protein in individual foodstuffs (Andersen and Just, 1983).

One assumption with the Danish net energy system is that the utilization of metabolizable energy (k = NE ME^{-1}) depends only on the energy concentration (MJ ME kg^{-1} DM) (Just, 1982), whereas factors like feeding level and animal physiological stage are not taken into account. The utilization of ME is higher below than above maintenance (Graham, 1969; see also Emmans, 1994) and hence the NE value (MJ kg^{-1} DM) of a given diet decreases exponentially with increasing food intake above the maintenance level. Data presented by Thorbek (1975) show that the net energy value, as determined in balance and respiration trials with growing pigs, increases in a curvilinear fashion with increasing live-weight from 20 to 90 kg (Fig. 30.1). This variation in feed value is not reflected by the NE value calculated from the chemical composition of the feed according to the Rostock system (Nehring *et al.*, 1970). These data illustrate clearly why it is important to distinguish between the potential value (NE calculated) and the production value (net energy) of feeds.

The reason for the increasing NE value during the growth period is that: (i) the ratio of lipid to protein retention increases with age and live-weight; and (ii) the utilization of ME (k) is higher in lipid than in protein retention (Thorbek, 1975; Tullis, 1982). The ratio of lipid to protein retention increases linearly with the live-weight (Thorbek, 1975), but the increase in the feed's production value diminishes (see Fig. 30.1). This could be explained by the energy cost of

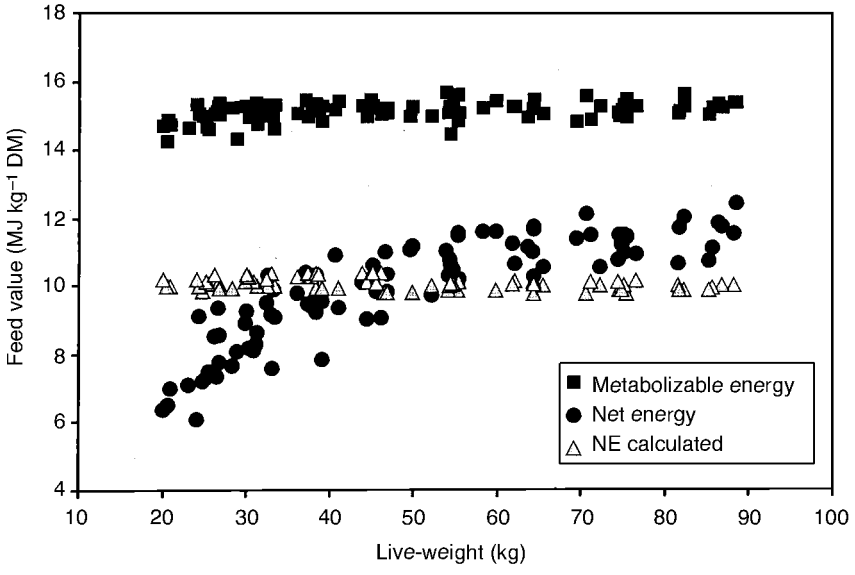

Fig. 30.1. Feed values (MJ kg^{-1} DM) of a pig diet fed at different live-weights. ME (squares) and NE (circles) determined experimentally (= production values) and NE (triangles) calculated from the chemical composition of the diet (= potential value). (From Thorbek, 1975.)

protein turnover, which can be calculated at different live-weights, using data from Mulvaney *et al.* (1985), Sève *et al.* (1986, 1993), Bergen *et al.* (1989) and Simon (1989), and assuming that the energy need for protein synthesis and for protein degradation is 5 and 0.5 mol ATP mol^{-1} amino acid, respectively. Calculated in this way, the energy cost of protein turnover per unit of protein retained increases exponentially with the live-weight and hence the utilization of ME for protein retention ($k_P = NE_P ME_P^{-1}$) decreases with increasing live-weight.

In summary, the utilization of ME in a given diet is dependent on the level of feed intake and on the physiological age of the animals. This is not considered explicitly in present feed evaluation systems and these are therefore imprecise in predicting the production value of pig diets. Furthermore, there is no biological reason to have two independent evaluation systems, one for energy and one for protein.

A Model of Growing Pigs

Model type and input and output data

The presented model is dynamic and semi-mechanistic. It consists of two submodels, one describing nutrient digestion and absorption, and one describing the metabolism of absorbed nutrients, as well as their retention in the body pools of protein, lipid and ash. A flow diagram of the major digestive and metabolic processes included in the model is shown in Fig. 30.2. The digestion submodel is empirical, as the rates of nutrient absorption are calculated simply as dietary intake and endogenous secretion minus excretion with faeces and with fermentation gases. The rates of faecal excretion are calculated by use of apparent faecal digestibility coefficients. The submodel of body tissue metabolism is mainly mechanistic, i.e. the behaviour of the model is determined by its component parts (nutrients and metabolites) and their interactions (flows of matter).

Inputs to the model are: (i) characteristics of the food, such as dry matter content, chemical composition of dry matter (crude protein, crude fibre, NFE and crude fat) and digestibilities of the individual chemical fractions; (ii) characteristics of the pig, such as age at the beginning of the simulation period, sex and genetic capacities for protein and lipid retention; and (iii) characteristics of the environment, such as temperature in the pig house.

Model outputs are the simulated numerical values of all state and rate variables at any time point during the simulation. From these numbers, the model calculates the predicted animal performance: food intake, retention of protein, lipid, ash and water, heat and methane production, as well as excretion of energy and matter in faeces and urine.

Powersim® is used as the simulation software, but the feed input data are calculated in an Excel spreadsheet, which contains a feed table with informa-

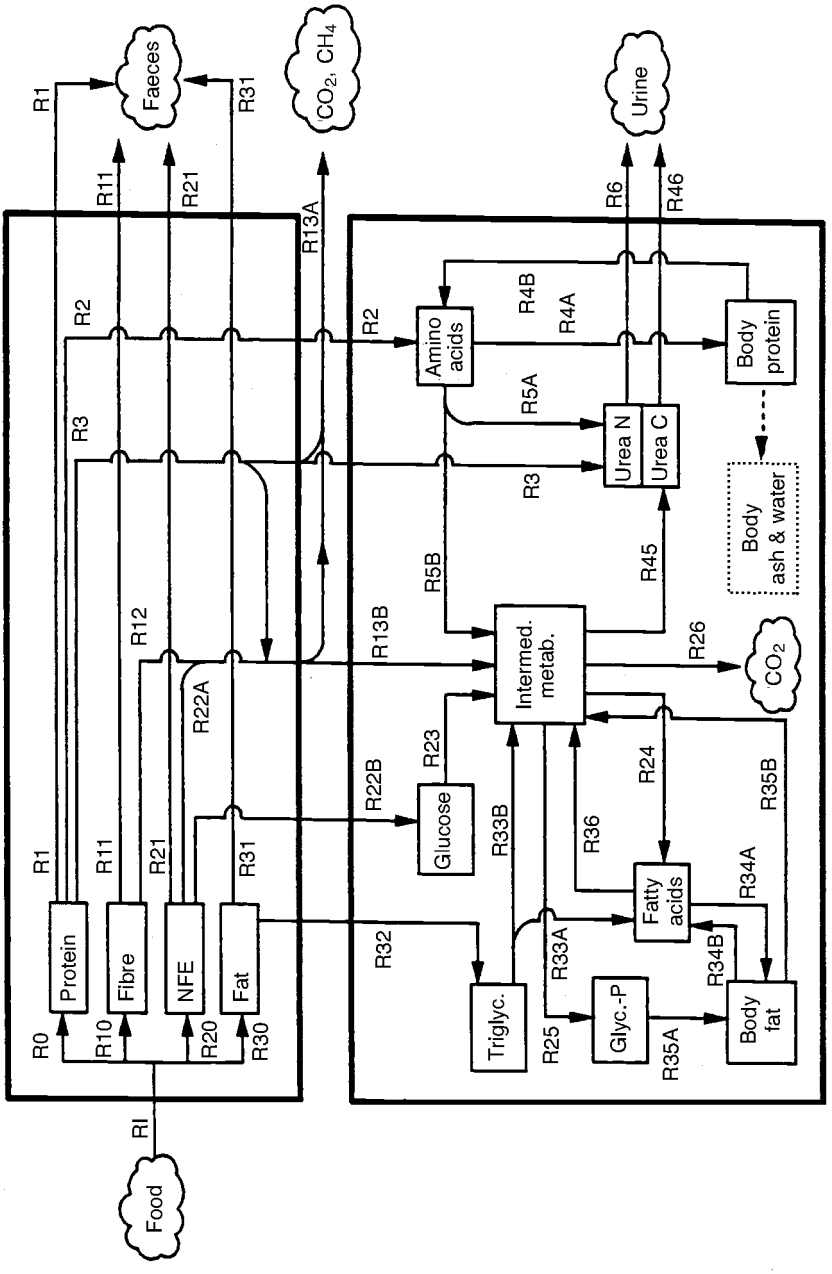

Fig. 30.2. Flow diagram of a dynamic simulation model of growing pigs.

tion on chemical composition, digestibility coefficients, etc. of individual feedstuffs. The relevant input parameters from any diet composed of the tabulated ingredients are calculated in the spreadsheet and transferred to the model during simulations.

A model outline

In the following, the individual state variables (shown as small boxes in Fig. 30.2) and rate variables (shown as numbered arrows) are explained. Unless otherwise stated, the dimension of the state variables is mol N for nitrogenous compounds and mol C for carbohydrate and lipid compounds. The dimension of the rate variables is mol N day^{-1} or mol C day^{-1}.

RI is the rate of food intake (kg day^{-1}). The rates of nutrient absorption, such as R2 (amino acids), R3 (ammonium), R13B (short-chain fatty acids (SCFA)), R22B (glucose) and R32 (chylomicron triglycerides), are calculated on the basis of nutrient intake, such as R0 (crude protein), R10 (crude fibre), R20 (NFE) and R30 (crude fat), and the digestibilities and fermentabilities of these nutrients. The rate variables R1, R11, R21, R31 and R13A describe faecal excretion of protein, fibre, NFE and fat and production of fermentation gases, respectively.

Absorbed amino acids are synthesized into body protein (R4A) or catabolized (R5A). R4B is the rate of body protein degradation and R4 = R4A − R4B is the rate of protein retention. Nitrogen from catabolized amino acids and from absorbed ammonium is synthesized into urea and excreted with the urine (R6). R46 is the rate of urinary carbon excretion. Triglycerides absorbed in chylomicrons are hydrolysed into fatty acids (R33A) and glycerol (R33B). Body fat is synthesized by esterification of fatty acids with glycerol-P (R34A and R35A), and the rates of lipolysis into fatty acids and glycerol are denoted as R34B and R35B, respectively. R34 + R35 = R34A + R35A − (R34B + R35B) is the rate of body fat retention. Keto acids from amino acid deamination (R5B), SCFA (R13B), glucose (R23), glycerol (R33B + R35B) and long-chain fatty acids (R36) enter a common pool of intermediary metabolites. This pool supplies substrates for the synthesis of fatty acids (R24) and glycerol-P (R25), carbon for urea and other compounds in the urine (R45), as well as fuel for oxidative pathways (R26).

Mathematical Descriptions

Most of the rate variables in the metabolism submodel are defined according to saturation (Michaelis–Menten) kinetics. The mathematical form of a rate variable with this type of kinetics is $R = Rm/(1 + K/[S])$, where Rm is the maximum rate, K is the affinity factor and $[S]$ is the substrate concentration. In some of the rate variables, the K parameter is not a constant, but is regulated by the mass

of the substrate or the product pool, as described by Danfær (1990). Other rate variables are defined with the assumption of first-order mass-action kinetics: $R = kS$, where k is the fraction of the substrate pool (S) metabolized or transferred per time unit. In the following, the mathematical formulations of some key areas in the model (digestion and absorption, protein retention and turnover, ash and water retention, lipid retention and turnover, energy metabolism and food intake) are presented in more detail.

Digestion and absorption

The rate of faecal N excretion is:

$$R1(t) = R1A(t) + R1B(t)$$

where $R1A(t)$ = undigested dietary protein = $R0(t)$ (1 − AFDP/CP) − $R1B(t)$ (mol N day^{-1}), $R1B(t)$ = endogenous protein loss = R0(t) EPL/CP (mol N day^{-1}), $R0(t)$ = rate of crude protein intake (mol N day^{-1}), AFDP = apparent faecal digestible protein (g kg^{-1} DM), CP = dietary crude protein (g kg^{-1} DM) and EPL = faecal loss of endogenous protein (g kg^{-1} DM).

The absorption rate of dietary amino acids is:

$$R2(t) = R0(t)\ RIDP/CP$$

where RIDP = real ileal digestible protein (g kg^{-1} DM).

AFDP is calculated from tabulated values of apparent faecal digestibility coefficients, and RIDP is calculated from *in vitro* ileal digestibility coefficients for individual foodstuffs. Although these parameters are used as constants in the model, they are related through EPL and fermented dietary protein, $R3(t)$ when expressed as g kg^{-1} DM:

$$RIDP = AFDP + EPL - R3(t)$$

The rate of dietary protein fermentation in the hindgut equals the rate of ammonia/ammonium absorption:

$$R3(t) = R0(t) - R2(t) - R1A(t) \text{ (mol N day}^{-1}\text{)}$$

The rate of faecal crude fibre excretion is:

$$R11(t) = R10(t)\ (1 - DCFi/CFi)$$

where $R10(t)$ = rate of crude fibre intake (mol C day^{-1}), DCFi = apparent digestible crude fibre (g kg^{-1} DM) and CFi = dietary crude fibre (g kg^{-1} DM).

The rate of crude fibre fermentation in the hindgut is:

$$R12(t) = R10(t)\ DCFi/CFi \text{ (mol C day}^{-1}\text{)}$$

The rate of faecal NFE excretion is:

$$R21(t) = R20(t)\ (1 - DNFE/NFE)$$

where R20(t) = rate of NFE intake (mol C day^{-1}), DNFE = apparent digestible NFE (g kg^{-1} DM) and NFE = dietary NFE (g kg^{-1} DM).

The rate of NFE fermentation in the hindgut is:

$$R22A(t) = R20(t)\ DNFE/NFE \times K22$$

where K22 = fermentable fraction of digestible NFE, and the rate of glucose absorption is:

$$R22B(t) = R20(t)\ DNFE/NFE\ (1 - K22)$$

The rate of hindgut fermentation of protein, fibre and NFE is:

$$Ferm(t) = R3(t)\ 3.8 + R12(t) + R22A(t)\ (\text{mol C day}^{-1})$$

and the rates of fermentation gas production and SCFA absorption are:

$$R13A(t) = Ferm(t)\ 9/33$$

$$R13B(t) = Ferm(t)\ 24/33$$

The rate of faecal crude fat excretion is:

$$R31(t) = R30(t)\ (1 - DCF/CF)$$

where R30(t) = rate of crude fat intake (mol C day^{-1}), DCF = apparent digestible crude fat (g kg^{-1} DM) and CF = dietary crude fat (g kg^{-1} DM).

Finally, the rate of lipid absorption is defined as:

$$R32(t) = R30(t)\ DCF/CF\ (\text{mol C day}^{-1})$$

Rates and composition of growth

The fractional rate of body protein synthesis (% of the pool per day) can be described as an exponential function of the body protein pool (P):

$$\alpha(t) = X_1 + Y_1 \exp(-Z_1 P(t))$$

where X_1 = fractional rate at $P(t) \sim \infty$ (% day^{-1}), $X_1 + Y_1$ = fractional rate at $P(t) = 0$ (% day^{-1}), Z_1 = rate constant (kg^{-1}) and $P(t)$ = mass of protein pool at time t (kg).

The parameter values ($X_1 = 6.723$, $Y_1 = 19.751$, $Z_1 = 0.799$) are derived from published data on protein turnover in growing pigs (Mulvaney *et al.*, 1985; Sève *et al.*, 1986, 1993; Bergen *et al.*, 1989; Simon, 1989). The absolute rate of body protein synthesis is then derived as:

$$R4A(t) = \alpha(t)P(t)10 \times 0.16/14.01\ (\text{mol N day}^{-1})$$

The rate of body protein retention is defined as:

$$R4(t) = R4m(t)/(1 + K4/AA(t))$$

where R4m(t) = maximum rate of protein retention (mol N day^{-1}), $K4$ = affin-

ity factor for protein retention (mol N) and AA(t) = mass of amino acid pool (mol N).

The maximum rate of protein retention is the derivative (d$P(t)$/dt) of a protein growth curve obtained with pigs fed ad lib with diets of optimum composition for rapid growth. A Gompertz equation can be used to describe such a curve (France and Thornley, 1984):

$$P(t) = P_b \exp(X_2(1 - Y_2))$$

where $X_2 = \ln(P_m/P_b)$, $Y_2 = \exp(-Z_2 t)$, Z_2 = rate constant (day^{-1}), P_m = mass of protein pool at maturity (kg), P_b = mass of protein pool at birth (kg) and t = age of the pig (days). Differentiation of this growth equation gives:

$$\mathrm{R4}m(t) = \mathrm{d}P(t)/\mathrm{d}t = Z_2 P(t) \ln(P_m/P(t))1000 \times 0.16/14.01 \text{ (mol N day}^{-1})$$

The parameter values are estimated from data of Tullis (1982): $Z_2 = 0.0115$ and $P_m = 35.9$, and from Nielsen (1973): $P_b = 0.22$. It follows from this mathematical description that the simulated rate of body protein retention is dependent on both the genetic capacity for protein growth (expressed by the parameters P_m and Z_2) and the nutritional status (expressed by the parameter AA(t)). Protein retention has a high priority in the body and, therefore, the affinity factor for this process is assumed to be low: $K4 = 0.001$ mol N.

The rates of protein synthesis, R4A(t), and protein degradation, R4B(t), are used in the model for calculation of the heat production related to protein turnover (see later) and also to control the mass of the free amino acid pool, AA(t). The rate of body protein degradation is defined as:

$$\mathrm{R4B}(t) = \mathrm{R4A}(t) - \mathrm{R4}(t) \text{ (mol N day}^{-1})$$

The body pools of ash and water are assumed to be allometrically related to the body protein pool. This is defined as follows (France and Thornley, 1984):

$$\mathrm{Ash}(t) = \exp(X_3 \ln(\mathrm{P}(t) + Y_3) \text{ (kg)}$$

$$\mathrm{Water}(t) = \exp(X_4 \ln(P(t) + Y_4) \text{ (kg)}$$

Data from the work of Tullis (1982) are used to parameterize these equations ($X_3 = 0.9566$, $Y_3 = -1.4451$, $X_4 = 0.8950$, $Y_4 = 1.3968$).

The rate of fatty acid retention (mol C day^{-1}) in body fat is defined as:

$$\mathrm{R34}(t) = \mathrm{R34}m(t)/(1 + K34/\mathrm{FA}(t))$$

where R34$m(t)$ = maximum rate of fatty acid retention (mol C day^{-1}), $K34$ = affinity factor for fatty acid retention (mol C) and FA(t) = mass of fatty acid pool (mol C).

The maximum rate is the derivative of a Gompertz equation describing a fat growth curve obtained with pigs fed ad lib:

$$\mathrm{R34}m(t) = \mathrm{d}F(t)/\mathrm{d}t = Z_5 \times F(t) \ln(F_m/F(t))1000 \times 3 \times 17.37/861.1$$

where $F(t)$ = mass of body fat pool (kg), F_m = maximum mass of body fat pool (kg) and Z_5 = rate constant (day^{-1}).

Parameter values of F_m (= 73) and Z_5 (= 0.0118) are derived from the experiment of Tullis (1982), the numbers 17.37 (mol C mol^{-1} fatty acid) and 861.1 (molecular weight of triglyceride) are calculated from data of Dunshea *et al.* (1992b). The rate of lipid retention accounted for as glycerol is calculated simply as:

$$R35(t) = R34(t)/17.37 \text{ (mol C day}^{-1})$$

To the knowledge of the author, very few data on *in vivo* lipid turnover rates in growing pigs have been published. Fractional rates of lipogenesis, lipolysis and lipid accretion in pigs of 80 kg live-weight have been estimated in one study as 2.3, 0.8 and 1.5% of the body lipid pool per day, respectively (Dunshea *et al.*, 1992a, b). It is assumed in the model that the ratio of lipid retention rate to lipid synthesis rate decreases linearly from conception to the stage of maximum body lipid mass, i.e. when the rate of retention is zero:

$$R34(t)/R34A(t) = \beta(t) = Z_6(1 - F(t)/F_m)$$

where $Z_6 = \beta(t)$ at conception ($F(t) = 0$).

At $F(t) = 16.4$ kg, $\beta(t) = 1.5/2.3 = 0.65$ (Dunshea *et al.*, 1992b) and at $F(t) = F_m = 73$ kg (Tullis, 1982), $\beta(t) = 0$. Hence, Z_6 can be estimated as $0.65(1 + 1/(73/16.4 - 1)) = 0.84$. The rates of lipogenesis from fatty acids and glycerol are then:

$$R34A(t) = R34(t)/(Z_6(1 - F(t)/F_m)) \text{ (mol C day}^{-1})$$

$$R35A(t) = R34A(t)/17.37 \text{ (mol C day}^{-1})$$

and the corresponding rates of lipolysis:

$$R34B(t) = R34A(t) - R34(t) \text{ (mol C day}^{-1})$$

$$R35B(t) = R35A(t) - R35(t) \text{ (mol C day}^{-1})$$

Energy metabolism

The rate of energy input to the pool of intermediary metabolites, $EI(t)$, is the product sum of the individual nutrients (keto acids, $R5B(t)$; acetate, propionate and butyrate, $R13B(t)$; glucose, $R23(t)$; glycerol, $R33B(t) + R35B(t)$; fatty acids, $R36(t)$, and their combustion values (MJ mol^{-1} C): 0.546, 0.438, 0.509, 0.546, 0.467, 0.552 and 0.624, respectively) (from Blaxter, 1989). The simulated rate of heat production by aerobic oxidations, $H26(t)$, includes the following components (modified from Emmans, 1994): fasting heat production (related to the mass of body protein, $P(t)$), heat of digestion (related to the excretion of faecal organic matter), heat of urea synthesis (related to the excretion of urinary nitrogen, $R6(t)$), heat of protein turnover (related to the rates of protein synthesis, $R4A(t)$, and degradation, $R4B(t)$), and heat of lipid turnover (related to the rates of fatty acid synthesis, $R24(t)$, activation of fatty acids with co-

enzyme A, R34A(t), and phosphorylation of glycerol, R25(t)). The rate of change of the energy level in the pool of intermediary metabolites is calculated in the model as:

$$\mathrm{dEim}(t)/\mathrm{d}t = \mathrm{EI}(t) - \mathrm{H26}(t) - \mathrm{R24}(t)10.832/17.37 - \mathrm{R25}(t)1.655/3 - \mathrm{R45}(t)0.546 \ (\mathrm{MJ\ day^{-1}})$$

The number 0.546 is the energy concentration (MJ $\mathrm{mol^{-1}}$ C) in urine (Thorbek, 1975; Blaxter, 1989). Integration of the parameter dEim(t)/dt gives the energy level of the intermediary metabolite pool, Eim(t), which is used for the simulation of food intake.

Regulation of food intake

The rate of food intake in the model is composed of a basal part and an additional part, which is dependent on Eim(t):

$$\mathrm{RI}(t) = \mathrm{RIbas}(t) + \mathrm{dRI}(t) \ (\mathrm{kg\ food\ day^{-1}})$$

The basal rate, RIbas(t), is described by a set of equations in which the intake is related to live-weight, sex, digestible energy concentration and environmental temperature (NRC, 1987). The second part of the intake equation is defined as:

$$\mathrm{dRI}(t) = 10(\mathrm{EimI} - \mathrm{Eim}(t))^3$$

where EimI = initial energy level in the intermediary metabolite pool (MJ).

With this formulation, the simulated rate of food intake is increasing hyperbolically with the live-weight, but is also regulated by the energy status of the model pig. In this way, the model tends to maintain a steady state by adjusting the energy intake to the energy requirements for syntheses and oxidations.

Animal performance and feed value

The predicted animal performance is calculated from simulated values of specific state and rate variables in the model. The live-weight (LW) (kg) is the sum of the body pools of protein, lipid, ash and water, plus the mass of gut contents, which is assumed to be a constant fraction of LW (Tullis, 1982). The daily gain (kg $\mathrm{day^{-1}}$) is the differential form of the LW versus time curve. In the same way, the rates of body protein and body lipid accretion are calculated as d$P(t)$/dt and d$F(t)$/dt, respectively. The rate of total heat loss (MJ $\mathrm{day^{-1}}$) is the sum of aerobic heat production, H26(t), and fermentation heat, which is calculated from the rates of protein (R3(t)), fibre (R12(t)) and NFE (R22A(t)) fermentation in the hindgut. The rates of change in the energy content of all state variables (pools) in the model are summed to give the energy balance (MJ $\mathrm{day^{-1}}$). The total NE obtained is the energy balance plus the net energy requirement for

maintenance, the latter calculated as 0.351 $LW^{0.75}$ (MJ day^{-1}) (Just *et al.*, 1983). As the production value of a feed is an expression of predicted animal performance, the feed value can be given as NE (MJ kg^{-1}) or as FU_P kg^{-1}, where one FU_P is equivalent to 7.72 MJ NE (Just, 1982).

Simulation Results

In this section, a few examples of simulated data obtained with the model described above are presented.

As previously stated, the simulated rate of protein retention in this model is dependent on both the genetic capacity for protein growth and the nutritional status of the pig. This is illustrated in Fig. 30.3, which shows a simulated interaction between genetic potential and diet composition. Diets with increasing concentration of digestible protein (79–151 g kg^{-1} feed) are 'fed' ad lib from 75 to 140 days of age to pigs having a low potential (P_m = 35.9 kg, Z_2 = 0.0115 day^{-1}) or a high potential for protein growth (P_m = 40.0 kg, Z_2 = 0.0140 day^{-1}). In the 'low-potential' pigs, the simulated rate of protein retention is increased with the digestible protein content up to the level of 110 g kg^{-1} while the response of the 'high potential' pigs is extended to the level of 130 g kg^{-1}.

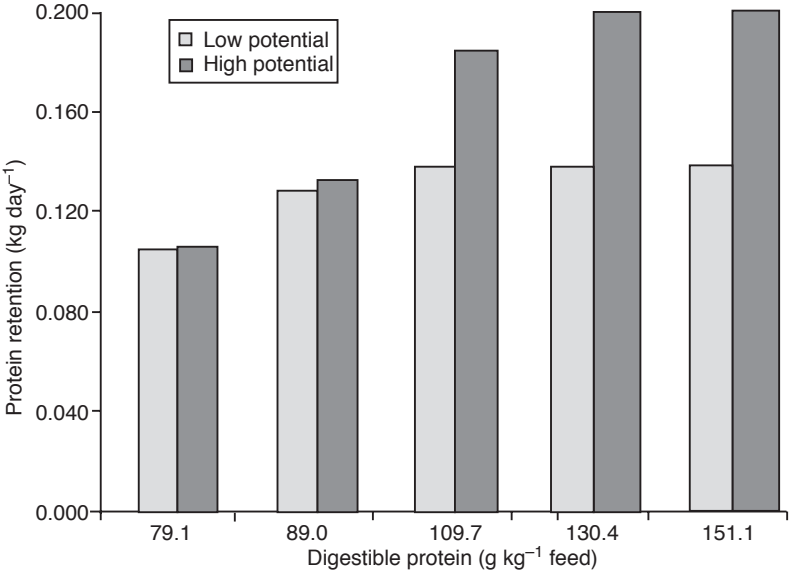

Fig. 30.3. Simulated responses of digestible protein (g kg^{-1} feed) on body protein retention (kg day^{-1}) in ad lib fed pigs with a low and a high genetic potential for protein gain. The observed growth period is from 75 to 140 days of age.

Simulated feed values of a given diet at increasing live-weights are shown in Fig. 30.4. The predicted production value of this diet is expressed both as metabolizable energy (MJ kg^{-1} DM) and as net energy (MJ kg^{-1} DM), and neither of these values is constant throughout the simulated growth period (20–90 kg LW). The ME value decreases slightly with increasing live-weight because of an increasing surplus of dietary protein (and hence an increasing loss of urinary energy), while the NE value increases in a curvilinear mode. The potential value of the diet (NE calculated) is derived from its chemical composition according to the Danish FU_P system (Just, 1982) and is therefore constant. These simulated results are in agreement with the experimental findings on utilization of ME for growth (Thorbek, 1975), as discussed earlier (see Fig. 30.1).

The last example is a comparison of feed values determined in 15 different diets by: (i) balance and respiration trials with 45 kg boars (Noblet *et al.*, 1993); (ii) calculations according to the Danish FU_P system (Just, 1982); and (iii) simulations with the present model, using the same conditions with regard to sex, food intake, live-weight and protein gain as in the experiment of Noblet *et al.* (1993). The results are presented in Fig. 30.5 as MJ NE kg^{-1} DM. For all 15 diets, the feed value simulated by the model is closer to the 'true' one determined experimentally than the one estimated by the Danish system. With this system, the NE values (MJ kg^{-1} DM) of the individual diets were calculated from the ME values determined experimentally by Noblet *et al.* (1993) according to the

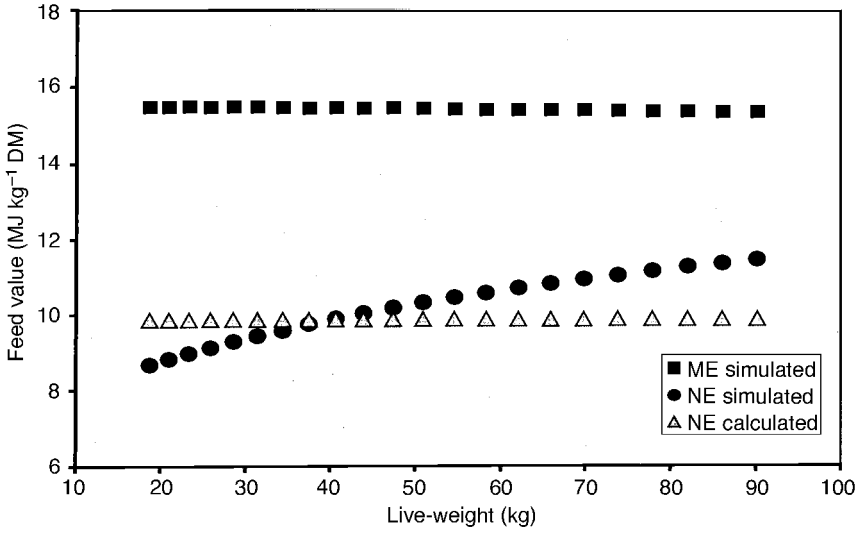

Fig. 30.4. Simulated feed values (MJ kg^{-1} DM) of a pig diet at different live-weights. ME (squares) and NE (circles) represent production values, and NE (triangles), calculated from the chemical composition of the diet, represents the potential value.

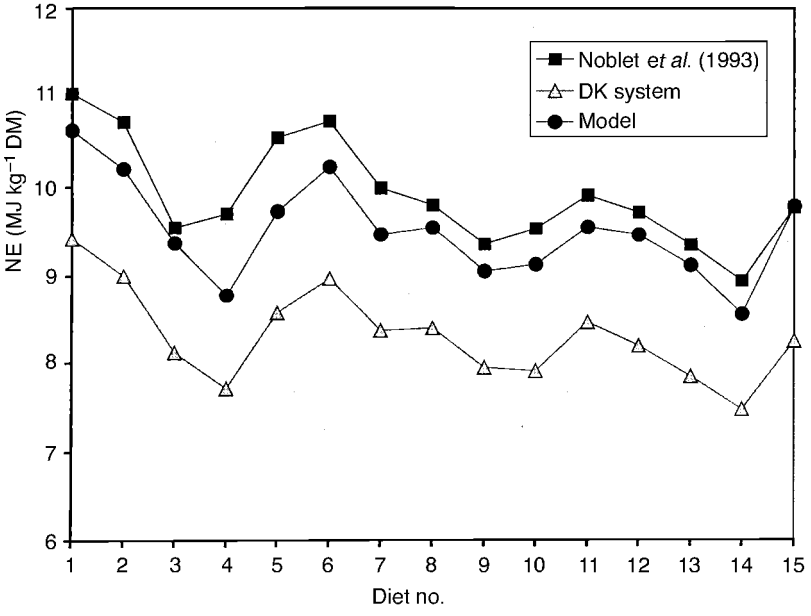

Fig. 30.5. Net energy values (MJ kg^{-1} DM) of different pig diets estimated experimentally (squares), according to the present Danish FU_P system (triangles) and by model simulations (circles).

equation: 0.75 ME (MJ kg^{-1} DM) − 1.88. The experimental findings on chemical composition (crude protein, crude fat, crude fibre, NFE) and digestibility of the individual fractions (Noblet *et al.*, 1993) were used as input to the simulation model. From the simulated animal performance, the NE value of each diet was calculated as energy balance + net energy for maintenance.

Summary and Perspectives

In this chapter, it has been argued that, in terms of feed evaluation, it is important to distinguish between the potential value and the production value of feeds. The production value is defined to be an expression of animal performance achieved on a given feed at given conditions. Present systems for evaluation of pig diets do not make this distinction, as they do not sufficiently consider important contributors to biological variation in the utilization of absorbed nutrients and energy.

Therefore, there is a need for a new feed evaluation system for growing pigs. This system should be based on the quantity of truly absorbed nutrients and must be able to predict animal performance and thereby the production value of the diet in question. Mathematical modelling of key digestive and metabolic

processes in pigs seems to be a suitable basis for the development of such a system. This represents a new principle of feed evaluation for farm animals.

From given inputs (diet composition, pig characteristics, environmental temperature), the presented dynamic simulation model can predict rate of food intake, growth rate, composition of growth and production rates of heat and methane, as well as faecal and urinary excretion rates of energy and matter. Simulation results obtained with this model seem to be realistic and biologically meaningful. In one test, the model has proved to be at least as good as the present Danish FU_P system in evaluation of 15 different diets for growing pigs.

Although the current version of the model is quite promising, it needs to be further developed – particularly in the description of the dietary carbohydrate fraction and in the description of nutrient digestion, fermentation and absorption. In the body part of the model, the simulation of amino acid metabolism should be extended from only one pool of total amino acids to include individual essential amino acids. With these and other improvements and after a thorough testing, the model should be ready for incorporation into a new feed evaluation system for growing pigs. It is expected that this new system will be a useful tool for the commercial pig production to increase the efficiency of feed utilization and thereby decrease the excretion of wastes to the environment.

References

Andersen, P.E. and Just, A. (1983) *Tabeller over foderstoffers sammensætning m.m. Kvæg, Svin*. 8. udgave, Det kongelige Danske Landhusholdningsselskab, Landhusholdningsselskabets Forlag, København, 102 pp.

Bergen, W.G., Johnson, S.E., Skjaerlund, D.M., Babiker, A.S., Kent Ames, N., Merkel, R.A. and Anderson, D.B. (1989) Muscle protein metabolism in finishing pigs fed ractopamine. *Journal of Animal Science* 67, 2255–2262.

Blaxter, K. (1989*) Energy Metabolism in Animals and Man*. Cambridge University Press, Cambridge, 336 pp.

Boisen, S. and Fernández, J.A. (1992) *Ny metode til bestemmelse af energiværdien i foderblandinger til svin*. Meddelelse 825, Statens Husdyrbrugsforsøg, Foulum, 6 pp.

Danfær, A. (1990) *A Dynamic Model of Nutrient Digestion and Metabolism in Lactating Dairy Cows*. Thesis. Report 671, National Institute of Animal Science, Foulum, 511 pp.

Dunshea, F.R., Harris, D.M., Bauman, D.E., Boyd, R.D. and Bell, A.W. (1992a) Effect of porcine somatotropin on nonesterified fatty acid and glycerol metabolism in growing pigs. *Journal of Animal Science* 70, 132–140.

Dunshea, F.R., Harris, D.M., Bauman, D.E., Boyd, R.D. and Bell, A.W. (1992b) Effect of porcine somatotropin on *in vivo* glucose kinetics and lipogenesis in growing pigs. *Journal of Animal Science* 70, 141–151.

Emmans, G.C. (1994) Effective energy: a concept of energy utilization applied across species. *British Journal of Nutrition* 71, 801–821.

France, J. and Thornley, J.H.M. (1984) *Mathematical Models in Agriculture*. Butterworths, London, 335 pp.

Graham, N.McC. (1969) The net energy value of artificially dried subterranean clover harvested before flowering. *Australian Journal of Agricultural Research* 20, 365–373.

Just, A. (1982) The net energy value of balanced diets for growing pigs. *Livestock Production Science* 8, 541–555.

Just, A., Jørgensen, H. and Fernández, J.A. (1983) Maintenance requirement and the net energy value of different diets for growth in pigs. *Livestock Production Science* 10, 487–506.

Mulvaney, D.R., Merkel, R.A. and Bergen, W.G. (1985) Skeletal muscle protein turnover in young male pigs. *Journal of Nutrition* 115, 1057–1064.

National Research Council (NRC) (1987) *Predicting Feed Intake of Food-producing Animals*. National Academy Press, Washington, DC, 85 pp.

Nehring, K., Beyer, M. and Hoffmann, B. (1970) *Futtermitteltabellenwerk*. VEB Deutscher Landwirtschaftsverlag, Berlin, 460 pp.

Nielsen, H.E. (1973) Grisenes vækst og udvikling i den præ- og postnatale periode, specielt med henblik på deres senere vækst og slagtekroppens sammensætning [Growth and development in pigs in the pre- and postnatal period with special reference to later growth and carcass composition]. Thesis, Beretning 405, Landøkonomisk Forsøgslaboratorium, København, 152 pp.

Noblet, J., Fortune, H., Dupire, C. and Dubois, S. (1993) Digestible, metabolizable and net energy values of 13 feedstuffs for growing pigs: effect of energy system. *Animal Feed Science and Technology* 42, 131–149.

Sève, B., Reeds, P.J., Fuller, M.F., Cadenhead, A. and Hay, S.M. (1986) Protein synthesis and retention in some tissues of the young pig as influenced by dietary protein intake after early-weaning: possible connection to the energy metabolism. *Reproduction Nutrition Développement* 26, 849–861.

Sève, B., Ballèvre, O., Ganier, P., Noblet, J., Prugnaud, J. and Obled, C. (1993) Recombinant porcine somatotropin and dietary protein enhance protein synthesis in growing pigs. *Journal of Nutrition* 123, 529–540.

Simon, O. (1989) Metabolism of proteins and amino acids. In: Bock, H.-D., Eggum, B.O., Low, A.G., Simon, O. and Zebrowska, T. (eds) *Protein Metabolism in Farm Animals.* VEB Deutscher Landwirtschaftsverlag, Berlin, and Oxford University Press, Oxford and New York, pp. 273–366.

Thorbek, G. (1975) *Studies on Energy Metabolism in Growing Pigs*. Report 424, National Institute of Animal Science, Copenhagen, 159 pp. + appendices.

Tullis, J.B. (1982) Protein growth in pigs. PhD thesis, University of Edinburgh, 183 pp. + appendices.

Index

Note: page numbers in *italics* refer to figures and tables